VOL. 512 JULY 20, 1990
COMPLETE IN ONE ISSUE

9th Int. Symp. on HPLC of proteins, peptides and polynucleotides Philadelphia, PA, November 6–8, 1989

JOURNAL OF

CHROMATOGRAPHY

INTERNATIONAL JOURNAL ON CHROMATOGRAPHY, ELECTROPHORESIS AND RELATED METHODS

SYMPOSIUM VOLUMES

ELSEVIER

JOURNAL OF CHROMATOGRAPHY

Scope. The *Journal of Chromatography* publishes papers on all aspects of chromatography, electrophoresis and related methods. Contributions consist mainly of research papers dealing with chromatographic theory, instrumental development and their applications. The section *Biomedical Applications*, which is under separate editorship, deals with the following aspects: developments in and applications of chromatographic and electrophoretic techniques related to clinical diagnosis or alterations during medical treatment; screening and profiling of body fluids or tissues with special reference to metabolic disorders; results from basic medical research with direct consequences in clinical practice; drug level monitoring and pharmacokinetic studies; clinical toxicology; analytical studies in occupational medicine.

Submission of Papers. Papers in English, French and German may be submitted, in three copies. Manuscripts should be submitted to: The Editor of *Journal of Chromatography*, P.O. Box 681, 1000 AR Amsterdam, The Netherlands, or to: The Editor of *Journal of Chromatography, Biomedical Applications*, P.O. Box 681, 1000 AR Amsterdam, The Netherlands. Review articles are invited or proposed by letter to the Editors. An outline of the proposed review should first be forwarded to the Editors for preliminary discussion prior to preparation. Submission of an article is understood to imply that the article is original and unpublished and is not being considered for publication elsewhere. For copyright regulations, see below.

Subscription Orders. Subscription orders should be sent to: Elsevier Science Publishers B.V., P.O. Box 211, 1000 AE Amsterdam, The Netherlands, Tel. 5803 911, Telex 18582 ESPA NL. The *Journal of Chromatography* and the *Biomedical Applications* section can be subscribed to separately.

Publication. The *Journal of Chromatography* (incl. *Biomedical Applications*) has 37 volumes in 1990. The subscription prices for 1990 are:

J. Chromatogr. (incl. *Cum. Indexes, Vols. 451–500*) + *Biomed. Appl.* (Vols. 498–534):
Dfl. 6734.00 plus Dfl. 1036.00 (p.p.h.) (total *ca.* US$ 3885.00)

J. Chromatogr. (incl. *Cum. Indexes, Vols. 451–500*) only (Vols. 498–524):
Dfl. 5616.00 plus Dfl. 756.00 (p.p.h.) (total *ca.* US$ 3186.00)

Biomed. Appl. only (Vols. 525–534):
Dfl. 2080.00 plus Dfl. 280.00 (p.p.h.) (total *ca.* US$ 1180.00).

Our p.p.h. (postage, package and handling) charge includes surface delivery of all issues, except to subscribers in Argentina, Australia, Brasil, Canada, China, Hong Kong, India, Israel, Malaysia, Mexico, New Zealand, Pakistan, Singapore, South Africa, South Korea, Taiwan, Thailand and the U.S.A. who receive all issues by air delivery (S.A.L. — Surface Air Lifted) at no extra cost. For Japan, air delivery requires 50% additional charge; for all other countries airmail and S.A.L. charges are available upon request. Back volumes of the *Journal of Chromatography* (Vols. 1–497) are available at Dfl. 195.00 (plus postage). Claims for missing issues will be honoured, free of charge, within three months after publication of the issue. Customers in the U.S.A. and Canada wishing information on this and other Elsevier journals, please contact Journal Information Center, Elsevier Science Publishing Co. Inc., 655 Avenue of the Americas, New York, NY 10010. Tel. (212) 633-3750.

Abstracts/Contents Lists published in Analytical Abstracts, ASCA, Biochemical Abstracts, Biological Abstracts, Chemical Abstracts, Chemical Titles, Chromatography Abstracts, Clinical Chemistry Lookout, Current Contents/Life Sciences, Current Contents/Physical, Chemical & Earth Sciences, Deep-Sea Research/Part B: Oceanographic Literature Review, Excerpta Medica, Index Medicus, Mass Spectrometry Bulletin, PASCAL-CNRS, Pharmaceutical Abstracts, Referativnyi Zhurnal, Science Citation Index and Trends in Biotechnology.

See inside back cover for Publication Schedule, Information for Authors and information on Advertisements.

 0021-9673/90/$03.50

This issue is printed on acid-free paper.

Printed in The Netherlands

For contents see p. VII

JOURNAL OF CHROMATOGRAPHY

VOL. 512 (1990)

JOURNAL *of* CHROMATOGRAPHY

INTERNATIONAL JOURNAL ON CHROMATOGRAPHY, ELECTROPHORESIS AND RELATED METHODS

SYMPOSIUM VOLUMES

ELSEVIER
AMSTERDAM — OXFORD — NEW YORK — TOKYO

J. Chromatogr., Vol. 512 (1990)

Philadelphia, Liberty Bell.
(Courtesy of Mrs. Janet Cunningham, President, Barr Enterprises.)

 0021-9673/90/$03.50

This issue is printed on acid-free paper.

Printed in The Netherlands

SYMPOSIUM VOLUME

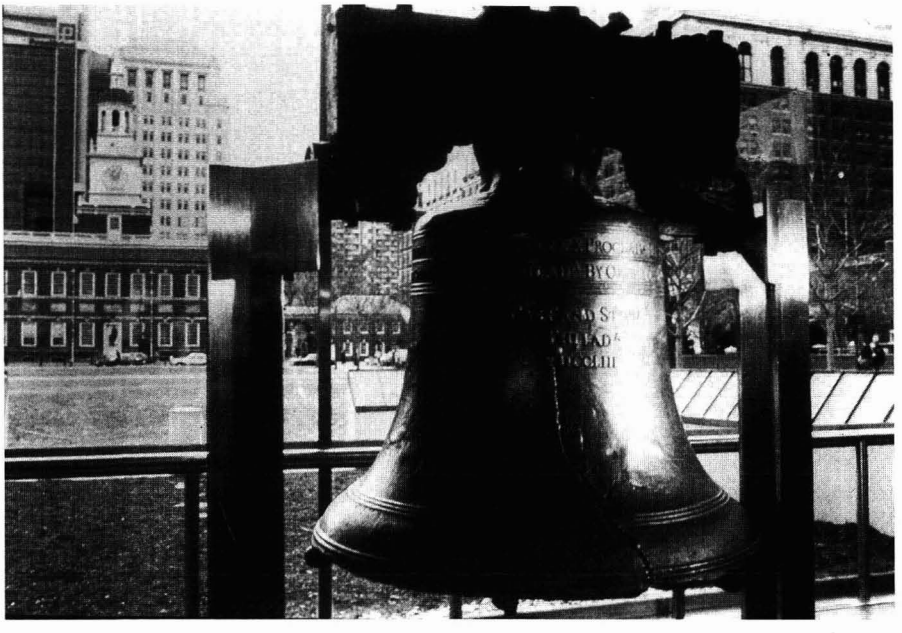

NINTH INTERNATIONAL SYMPOSIUM ON HIGH-PERFORMANCE LIQUID CHROMATOGRAPHY OF PROTEINS, PEPTIDES AND POLYNUCLEOTIDES

Philadelphia, PA (U.S.A.), November 6–8, 1989

Guest Editors

FRED E. REGNIER
(West Lafayette, IN, U.S.A.)

MILTON T. W. HEARN
(Melbourne, Australia)

KLAUS K. UNGER
(Mainz, F.R.G.)

JAN-CHRISTER JANSON
(Uppsala, Sweden)

JOSEPH J. DeSTEFANO
(Wilmington, DE, U.S.A.)

CONTENTS

In articles with more than one author, the name of the author to whom correspondence should be addressed is indicated in the article heading by a 6-pointed asterisk (*)

Journal of Chromatography, 512 (1990) 1–2
Elsevier Science Publishers B.V., Amsterdam

FOREWORD

The *Ninth International Symposium on High-Performance Liquid Chromatography of Proteins, Peptides and Polynucleotides* was held at the Wyndham Franklin Plaza Hotel in Philadelphia, Pennsylvania, U.S.A. from November 6 to 8, 1989. Responding to the call of the Liberty Bell and an outstanding scientific programme, aficionado of modern bioseparation sciences focused their attention on three days of intellectual and sensory stimulation as the pervasive developments of this exciting field were further revealed. Consequently, the essential elements of previous symposia were reinforced and extended, reaffirming once more the observation that modern bioseparation sciences are the powerhouse which technically drives much of biotechnology, protein engineering, molecular biology and the related biomedical sciences as we understand them today.

The format of this symposium followed the successful approach evident in previous meetings, with the scientific programme encompassing the full gambit of research developments related to high-resolution techniques for the analysis and purification of biomacromolecules. Discussion was vigorous and focused, linking together, through detailed evaluation of the concepts and practice, important advances in the modern bioseparation sciences related to column technology and materials; chromatographic retention behaviour of biomacromolecules and its relevance to protein topography, biorecognition and conformation; analytical criteria for defining the purity and quality control of proteins and glycoproteins; purification processes and scale-up requirements; structural analysis of proteins and polynucleotides; analytical application of high-performance electrophoresis; ultramicropreparative techniques and protein sequencing; and new strategies for the characterisation of biomacromolecules. The international basis of this substantial research effort was reflected in over 190 oral and poster presentations from the 450 participants, attracted from 20 countries. Complementing the formal scientific programme were the various well-attended discussion sessions throughout these three stimulating days. Continued dialogues and commentaries persisted well into the evenings, with the scientific exchanges inspired by the Philadelphia Museum of Art, the lilting tones of the Philadelphia String Ensemble, the artistic robustness of the Philadelphia Mummers, as well as the didactic ambience of the various receptions. Keen to exchange information and ideas on recent developments and applications, the attending scientists from academic, commercial and governmental laboratories and organisations gave new meaning to that well-known Aenadian phrase *Felix qui potuit rerum cognoscere causas.*

My symposium cochairmen (J. J. DeStefano, J. C. Janson, F. E. Regnier and K. K. Unger) and myself would like to express our appreciation to all attendees, and particularly the participants in the oral and poster sessions, for their lively and thought-provoking contributions. The smooth running of the symposium was ably orchestrated by Alan Goldberg with the assistance from Janet Cunningham and her staff. Thanks are also due to Dr. Erich Heftmann for his tireless and meticulous efforts in the editorial preparation of this Proceedings Volume. The generous financial sponsorship of the well-attended receptions by E. I. du Pont de Nemours and Co., Inc., Pharmacia LKB Biotechnology AB and Tosoh Corp. is also acknowledged. Finally, we would like to thank again all the scientists who came to Philadelphia,

contributed to the oral, poster and discussion sessions, and through their vigorous participation made this ninth symposium so successful.

Clayton, Melbourne
(Australia)

MILTON T. W. HEARN

Journal of Chromatography, 512 (1990) 3–12
Elsevier Science Publishers B.V., Amsterdam

CHROMSYMP. 1911

Binding of sodium dodecyl sulphate to an integral membrane protein and to a water-soluble enzyme

Determination by molecular-sieve chromatography with flow scintillation detection

MARIA WALLSTÉN* and PER LUNDAHL
Department of Biochemistry, Biomedical Centre, University of Uppsala, P.O. Box 576, 751 23 Uppsala (Sweden)

ABSTRACT

We have determined the binding of sodium dodecyl sulphate (SDS) to the human red cell glucose transporter (polypeptide, M_r 54 117) and to a water-soluble enzyme, N-5′-phosphoribosylanthranilate isomerase–indole-3-glycerol-phosphate synthase (PRAI–IGPS) from *Escherichia coli* (M_r 49 484). [^{35}S]SDS was equilibrated with each protein on molecular-sieve chromatography at a series of SDS concentrations. The binding ratios of SDS to protein were determined by flow scintillation detection and automated amino acid analyses. Unexpectedly the glucose transporter, which is a transmembrane protein, bound about the same amount of SDS per gram of protein as did the enzyme. At 1.6 m*M* SDS, slightly below the critical micelle concentration (CMC) (1.8 m*M*) in the eluent, the binding ratio was 1.6 g SDS/g protein for both the glucose transporter and PRAI–IGPS. At 2.0 m*M* SDS (above the CMC) the glucose transporter showed a binding ratio of 1.7 g SDS/g protein. The corresponding value for the enzyme was about 1.5 g/g. The SDS–glucose transporter complex seems to be more compact than the SDS–enzyme complex as judged by molecular-sieve chromatography and by SDS–polyacrylamide gel electrophoresis. Recent neutron scattering results have shown a protein-decorated triple-micelle structure for the SDS–PRAI–IGPS complex. Hypothetically, the more compact SDS–glucose transporter complex may therefore consist of a dual-micelle structure. The molecular-sieve gel beads bound considerable amounts of SDS. The SDS binding to the gel matrix and to the proteins increased with increasing SDS concentration up to at least 1.6–2.0 m*M* SDS. In the case of the water-soluble enzyme a shoulder was observed in the binding curve at 1 m*M* SDS, probably reflecting a change in the conformation of the complex.

0021-9673/90/$03.50

INTRODUCTION

Recently, a low-resolution structure of the sodium dodecyl sulphate (SDS) complex with a water-soluble enzyme, N-5′-phosphoribosylanthranilate isomerase–indole-3-glycerol-phosphate synthase (PRAI–IGPS), has been elucidated by small-angle neutron scattering analysis[1]. The complex was found to consist of a triple-micelle structure with the polypeptide mainly on the surface of the SDS micelles. The surface location of the amino acid residues is consistent with a model described earlier[2]. The experimentally found structure has been termed the "protein-decorated micelle structure". The change in elution volume of SDS–PRAI–IGPS on molecular-sieve chromatography as the concentration of free SDS is increased has also recently been monitored[3]. In this work, the binding ratio of SDS to PRAI–IGPS and to the human red cell glucose transporter has been determined at a series of SDS concentrations.

Our purpose was to compare the SDS binding to a water-soluble protein with the SDS binding to an amphipathic integral membrane protein (and to support neutron scattering measurements of the formation of SDS–PRAI–IGPS complexes). Some transmembrane proteins bind SDS more extensively than do most water-soluble proteins (*e.g.*, refs. 4–6). In the case of the glucose transporter from the human red cell, the complex with SDS seems to be relatively compact as judged by molecular-sieve chromatography[3,7]. This gives rise to the suspicion that the amount of SDS bound to the glucose transporter is not very large. This protein is thought to contain twelve hydrophobic α-helices spanning the membrane[8].

EXPERIMENTAL

Materials

Human red cell concentrate was supplied by the blood bank of the University Hospital, Uppsala, Sweden. Octyl glucoside (*n*-octyl-β-D-glucopyranoside), Tris (Trizma base) and dithioerythritol were bought from Sigma (St. Louis, MO, U.S.A.). Sodium dodecyl sulphate (AnalaR Biochemical, 99% pure) was purchased from BDH (Poole, U.K.) and sodium dodecyl [^{35}S]sulphate from Amersham International (Little Chalfont, U.K.). Sephadex G-50, Sephacryl HR S-300 HR and a Superose 6 column were obtained from Pharmacia LKB Biotechnology (Uppsala, Sweden). DEAE-cellulose (DE-52) was obtained from Whatman (Maidstone, U.K.). PRAI–IGPS was kindly provided by K. Kirschner and H. Szadkowski (Biozentrum, Basle, Switzerland). Chemicals were of analytical-reagent grade unless stated otherwise. The buffer stock solutions and the samples were filtered through 0.2-μm filters (SM 11107 Sartorius, Göttingen, F.R.G.) and Acrodisc 13 (Gelman, Ann Arbor, MI, U.S.A.), respectively, unless stated otherwise. Flow-Scint III scintillator cocktail was obtained from Radiomatic Instruments (Tampa, FL, U.S.A.).

Molecular-sieve chromatography

Chromatographic experiments were performed at 23–24°C with a 22-ml Sephacryl S-300 HR column (28 × 1 cm I.D.) connected to two precision pumps (P-500), controlled by a gradient programmer (GP-250). The eluent was 50 m*M* sodium phosphate (pH 6.86)–1 m*M* Na_2EDTA–0.2 m*M* dithioerythritol–3.1 m*M* sodium azide

(buffer A) with SDS, including [^{35}S]SDS[3]. The critical micelle concentration (CMC) of SDS is *ca.* 1.8 m*M* in this buffer[1–3]. The chosen SDS concentrations were obtained by combining buffer A and buffer A with 5.0 m*M* SDS (buffer B) from the pumps in appropriate proportions. The flow-rate was 0.4 ml/min. Before sample application, the column was equilibrated with at least 60 ml of eluent for 2.5 h or more until complete or nearly complete equilibration with SDS was achieved, as judged by the scintillation detection. For this purpose the column was by-passed by use of a three-way connection, a tubing and a two-way four-port valve. The samples were applied from 125–2000-μl loops by automatic injection (Act-100). The protein amounts were 0.2–1 mg in each run.

The eluent from the column was passed through a UV detector (UV-1) with measurement at 280 nm and then either collected by a fraction collector (Frac-100) or passed through a flow scintillation detector (Radiomatic A-300 Flo-One Beta; Radiomatic Instruments). The detector cell volume was 0.5 ml and the scintillator cocktail flow-rate was 1.6 ml/min. The protein amounts were determined, in most experiments, by automated amino acid analyses of collected fractions; the amount of bound SDS was determined in a separate run with scintillation detection of the radioactivity (the flow-split function of the detector was not used as it did not function accurately enough for the present purpose). The radioactivity in the eluent was recorded as counts per minute (cpm) for each 20-s sampling time interval. No programmed or manual background subtraction was made as the background was negligible in relation to the [^{35}S]SDS radioactivity level. To determine the amount of SDS bound to the protein, automatic peak integrations (sum of the cpm values for the sampling time intervals, per peak) were done and the values were then corrected for the contribution from the radioactivity in the buffer. The protein amounts according to the amino acid analyses, divided by the areas of the PRAI–IGPS UV peaks, were plotted against the equilibrium concentration of SDS, and from this diagram the protein amounts were determined in a few instances in which no amino acid analyses were made. For the glucose transporter, amino acid analyses were always done for calculation of binding data. All instruments except the scintillation detector were obtained from Pharmacia LKB Biotechnology.

In one experiment with the human red cell glucose transporter at 1.8 m*M* SDS and two experiments at 2.0 m*M* SDS, part of the main protein fractions were collected from two runs, combined and divided into two aliquots. One aliquot was re-run for amino acid analysis and the other was re-run with flow scintillation detection. In this way disturbances from co-purified membrane lipids and, in some instances, octyl glucoside from the transporter sample, could be eliminated or minimized.

At 0.8, 1.2 and 1.5 m*M* SDS, PRAI–IGPS samples pre-equilibrated with SDS by chromatography on Sephacryl S-300 were also applied to the columns (these samples had recently been used for neutron scattering measurements). No significant difference in SDS binding values could be found with these samples compared to native PRAI–IGPS samples. Hence it seems that all bound SDS could be displaced by [^{35}S]SDS. In the case of glucose transporter, the transporter–lipid preparation was solubilized in SDS before application. In experiments at 1.8 and 2.0 m*M* SDS, octyl glucoside-solubilized glucose transporter was also applied.

Samples

The glucose transporter. Human red cell membranes, stripped of peripheral proteins, were prepared as described earlier[9]. Integral membrane proteins were partially solubilized at 2°C at a concentration of 8 mg/ml with 75 m*M* octyl glucoside–70 m*M* Tris–HCl (pH 7.0)–1 m*M* dithioerythritol[10,11]. After centrifugation for 1 h at 160 000 *g* the protein solution was applied to a DEAE-cellulose column at 6°C in the above buffer and the material that passed through the column on isocratic elution was collected as described earlier[10] (sample A). It contained mainly the glucose transporter at a concentration of *ca.* 0.8 mg/ml and some membrane phospholipids[10,11]. In most instances the octyl glucoside was removed by chromatography at 6°C of 2–3-ml samples on a 13-ml Sephadex G-50 column (16 × 1 cm I.D.) in 50 m*M* Tris (pH 7.0, as measured at 23°C)–100 m*M* NaCl–1 m*M* Na_2EDTA at a flow-rate of 0.5 ml/min. The aggregates of lipids and transporter molecules (or proteoliposomes) that were formed were collected by centrifugation at 160 000 *g* for 90 min. The supernatant was removed and the sedimented material was solubilized in buffer A containing 30 m*M* SDS (sample B, protein concentration *ca.* 0.6 mg/ml).

PRAI–IGPS. PRAI–IGPS from *Escherichia coli* was provided as a precipitate in 0.1 *M* potassium phosphate (pH 7.0)–5 m*M* Na_2EDTA–1 m*M* DTE and 42% ammonium sulphate. The preparation had been performed as described in ref. 12. An 0.5-ml aliquot of the enzyme suspension was mixed with 2.1 ml of buffer A and dialysed at 6°C against 4 × 500 ml of buffer A for 48 h. The protein solution was then diluted with buffer A to a concentration of *ca.* 1 mg/ml as estimated by absorbance measurements ($A_{280}^{1\,cm}$ = 0.84). SDS–polyacrylamide gel electrophoresis (SDS-PAGE) showed that the enzyme was nearly pure.

RESULTS

Equilibration of the molecular-sieve gel with SDS

When the SDS concentration in the Sephacryl S-300 HR column was increased in 0.2-m*M* steps up to 2 m*M* SDS, more than three column volumes of eluent were needed to equilibrate the column with SDS at each new concentration. Not until two column volumes of buffer with an increased SDS concentration had passed through the column did the SDS concentration of the eluate increase steeply (Fig. 1), but to a level lower than in the applied buffer (as controlled by flow scintillation detection after by-passing the column). At least one further column volume of buffer was needed for complete equilibration with SDS. A very similar equilibration pattern was found for each 0.2-m*M* SDS concentration increment up to at least 1.6 m*M*. In each 0.2 m*M* step *ca.* 0.22 μmol (about 63 μg) of SDS was adsorbed per millilitre of gel as illustrated in Fig. 2 (probably the binding reaches a constant value at some concentration above 2.0 m*M* SDS). Thus the gel became in principle converted to a cation exchanger. The molecular-sieve properties are retained in the fractionation of SDS–protein complexes, as these are strongly negatively charged, at least at reasonably high SDS concentrations. Superose 6 columns showed slower equilibration with SDS than did Sephacryl S-300 HR at the same flow-rate (and a slow release of SDS on lowering the SDS concentration). We conclude that Superose 6 binds even more SDS than does Sephacryl S-300 HR. For this reason we used the Sephacryl gel in all the final experiments.

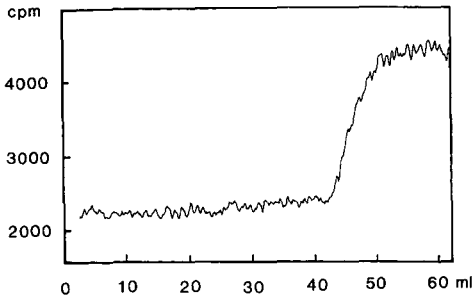

Fig. 1. Equilibration of the Sephacryl S-300 HR column with SDS as monitored by flow scintillation detection of [^{35}S]SDS. In this example the SDS concentration in the buffer applied to the column was increased from 0.2 to 0.4 m*M* at 0 ml elution volume. The SDS concentration in the buffer eluting from the column increased from 0.15 m*M* at 0 ml to 0.30 m*M* at 62 ml, as calculated from the radioactivity levels in the chromatogram. The elution volume, 43 ml, at the beginning of the steep increase in SDS concentration corresponds to 1.95 column volumes. Similar patterns were found for all equilibration steps up to 1.6 m*M* SDS, but for the next two steps up to 2.0 m*M* SDS considerably slower equilibration (greater binding) was observed (*cf.* ref. 3).

Glucose transporter

Examples of the glucose transporter flow scintillation chromatograms are shown in Fig. 3A and B. The lipids present in the SDS-solubilized glucose transporter preparation bind large amounts of SDS (the broad peak after 40 min in Fig. 3A). A re-run is illustrated in Fig. 3B. This experiment corresponds to point d in Fig. 5. In most instances the glucose transporter was applied in the form of an SDS-protein complex with a total SDS concentration of 30 m*M*. The sample included mixed SDS–phospholipid micelles, as some membrane phospholipids co-purify with the transporter[10,11]. As the SDS concentration in the column was increased from 0.4 m*M*

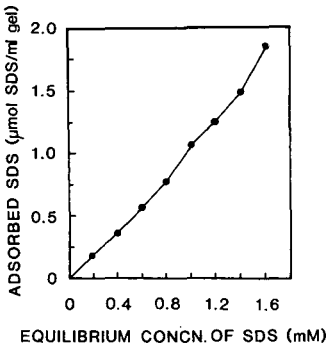

Fig. 2. Minimum amounts of SDS adsorbed to Sephacryl S-300 HR, *versus* equilibrium concentration of SDS. The SDS amounts were calculated from the type of experiments illustrated in Fig. 1. The amount of SDS applied between 22 ml elution volume (one column volume) and the end of each steep SDS concentration increase (50 ml in Fig. 1) was calculated for each 0.2-m*M* SDS concentration increment. The slow increase in SDS concentration after each steep increase (*cf.*, Fig. 1) could not be taken into account owing to lack of complete chromatograms. The values in the diagram are therefore lower limits. Still larger binding increments were observed at 1.6–2.0 m*M* SDS, but owing to the low equilibration complete chromatograms were not collected.

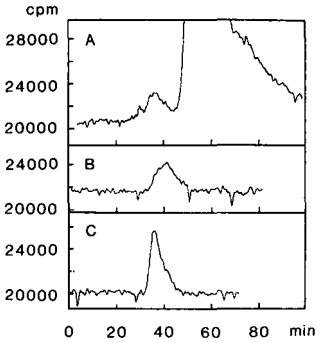

Fig. 3. Flow scintillation chromatograms. (A) SDS-solubilized glucose transporter and lipids from human red cells. Protein amount *ca.* 160 μg; sample volume, 250 μl; SDS concentration, 1.8 m*M*. (B) Re-run of an aliquot of two combined glucose transporter fractions similar to that in (A) at 35–40 min. Protein amount *ca.* 160 μg; sample volume, 2 ml; SDS concentration, 2.0 m*M*. (C), Native PRAI–IGPS. Protein amount, 250 μg; sample volume, 250 μl; SDS concentration, 1.8 m*M*.

SDS, the elution volume of the glucose transporter increased through one main transition between 0.8 and 1.4 m*M* SDS (Fig. 4B). This can be attributed to aggregation of the SDS–transporter complex into multimeric forms of the transporter when the concentration of free SDS, which initially was far above the CMC, is decreased to 0.4–1.2 m*M* as the sample passes into the column. Probably also some lipids aggregate with the transporter multimers. At low SDS concentrations the elution volume was therefore low. At higher SDS concentrations, enough SDS was present to keep

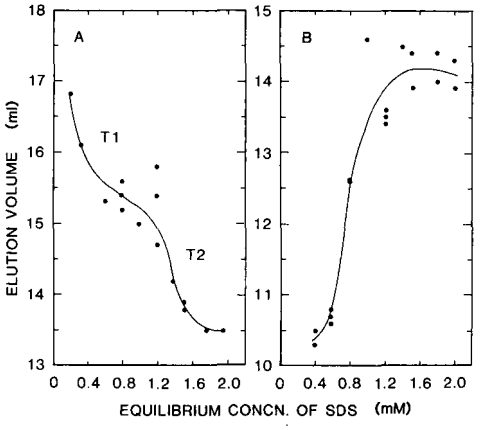

Fig. 4. Elution volume *versus* equilibrium concentration of SDS on molecular-sieve chromatography on Sephacryl S-300 HR of (A) the water-soluble enzyme PRAI–IGPS, applied in native form, and (B) the glucose transporter from human red cells, applied in the form of an SDS complex. For details, see Experimental. The sample volume was 250 μl, except at 2.0 m*M* SDS, where 500 μl of the glucose transporter were applied. The elution volume for PRAI–IGPS (A) decreases with increasing SDS concentration as the SDS binding increases. The elution volume for the glucose transporter (B) increases with increasing SDS concentration, as aggregation occurs at low but not at high SDS concentrations. The experiments were done identically in A and B, so the elution volumes can be compared. Note the difference in elution volume scales.

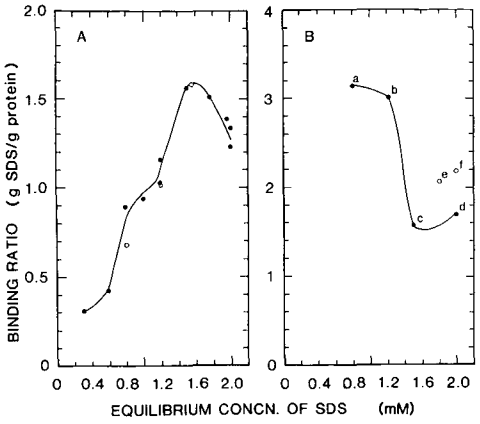

Fig. 5. Binding of SDS to (A) PRAI–IGPS and (B) the human red cell glucose transporter *versus* equilibrium concentration of SDS. For details, see Experimental. The ionic strength of the eluent is 0.1 *M* and the CMC of SDS is 1.8 m*M*. (A) ○ = PRAI–IGPS pre-equilibrated with SDS was applied to the Sephacryl S-300 HR column with [^{35}S]SDS; ● = native PRAI–IGPS was applied. (B) The eluted glucose transporter fraction contained (a) 12%, (b) 9%, (c) 6%, (d) 0% and (f) 0.7% of phosphatidylserine. ● = SDS–glucose transporter complex was applied to the column; ○ = octyl glucoside–glucose transporter was applied. Values d, e and f represent experiments in which eluted material was re-run on the Sephacryl column to remove lipids more efficiently (*cf.*, Fig. 3). The phosphatidylserine values were estimated by use of the known yields of serine from protein (90%) and the experimentally determined yield from phosphatidylserine (79%).

the transporter soluble as a monomer. The elution volume thus reached a large and nearly constant value above 1.4 m*M* SDS.

The binding ratios were very high at 0.8 and 1.2 m*M* SDS (3.1 and 3.0 g SDS/g transporter, respectively). This may be due to the formation of an SDS–transporter–lipid complex. The binding may also be overestimated by overlapping between the SDS–transporter and the SDS–lipids fractions (see Fig. 3A). It decreased to 1.52 g SDS/g transporter at 1.6 m*M* SDS but increased to 1.70 g SDS/g transporter at 2.0 m*M* SDS (Fig. 5B). This is a reliable value as it is obtained from a re-run of SDS-solubilized material that resulted in a transporter fraction free from phosphatidylserine. The value of 2.18 g/g at the same SDS concentration is probably too high as it is based on a re-run of octyl glucoside-solubilized material, and the final fraction was not entirely free from phosphatidylserine. Except at 2.0 mM SDS (point d in Fig. 5B), amino acid analyses showed the presence of an excess amount of serine, probably derived from phosphatidylserine (see the legend to Fig. 5). The protein amounts were corrected for this excess of serine. Phosphatidylserine is negatively charged and may bind by a combination of hydrophobic and electrostatic interactions with the glucose transporter. Presumably other lipids are also present in bound or non-bound form in the transporter fractions in the experiments illustrated in Fig. 5B. As no lipids can be expected to bind more strongly than phosphatidylserine, probably no lipids are present after the re-run at 2.0 m*M* SDS corresponding to point d.

PRAI–IGPS

Native PRAI–IGPS was applied to the Sephacryl S-300 HR column, which had

been equilibrated with buffer A containing SDS. The experiments were done with a series of increasing detergent concentrations in steps of 0.2 m*M* from 0.2 to 2.0 m*M* SDS. PRAI–IGPS is converted into an SDS–polypeptide complex at the top of the column[3]. When the SDS concentration was increased, the elution volume of PRAI–IGPS decreased through two main transitions, the first at 0.2–0.5 m*M* (T1) and the second at 1.2–1.6 m*M* SDS (T2) (Fig. 4A)[3]. The binding ratio of SDS increased with increasing SDS concentration from 0.3 up to 1.6 m*M* SDS (Fig. 5A), with a shoulder around 1.0 m*M* SDS. The SDS–PRAI–IGPS complex thus showed a maximum in SDS binding at 1.6 m*M* SDS, slightly below the CMC. The complex at 1.6 m*M* SDS was found to contain 1.58 g SDS/g PRAI–IGPS. The accuracy can be estimated to be *ca.* ±0.15 g/g (relative error in amino acid analysis 3% and in SDS determination 6%). Earlier determinations[1] with neutron scattering, with methylene blue binding and with a procedure similar to the present one resulted in values of 1.26–1.7 g/g. However, a transition into a complex with a slightly lower SDS-to-protein ratio is indicated by the graph in Fig. 5A at 1.6–2.0 m*M* SDS. The nature of this change in terms of the structure of the complex is not yet known.

Comparison of SDS binding to PRAI–IGPS and to the glucose transporter

Around the CMC of SDS, the maximum SDS binding was found to be about the same for the glucose transporter as for the water-soluble enzyme PRAI–IGPS. However, the binding increased slightly for the glucose transporter as the SDS concentration was increased from 1.6 to 2.0 m*M*, whereas the opposite was true for PRAI–IGPS.

At 2 m*M* SDS the membrane protein bound more SDS than did PRAI–IGPS. In addition, the glucose transporter has a higher molecular mass, M_r (54 117, ref. 8) than PRAI–IGPS (M_r 49 484, ref. 1). Further, the glucose transporter polypeptide also binds a branched oligosaccharide of average M_r *ca.* 9200 (17% of the polypeptide mass[13]). The total molecular mass of the SDS–glycosylated transporter complex (M_r *ca.* 155 000) is thus considerably larger than that of the SDS–PRAI–IGPS complex (M_r *ca.* 127 000) at 2.0 m*M* SDS. However, the glucose transporter was eluted later than PRAI–IGPS on molecular-sieve chromatography in SDS (Fig. 4 in this work, Fig. 6 in ref. 3 and Table II in ref. 7). Either the SDS–glucose transporter complex was retarded on the columns or its SDS complex is more compact (smaller or less elongated) than the SDS–PRAI–IGPS complex. It cannot be excluded that some retardation is caused by the oligosaccharide or by hydrophobic segments of the transporter, but no evidence known to us supports this hypothesis. It seems very likely that the SDS–glucose transporter complex really is more compact (less elongated) compared with SDS complexes of water-soluble proteins, as in SDS-PAGE the deglycosylated glucose transporter migrates with an apparent M_r of *ca.* 44 000–46 000 (refs. 14–16), whereas the true M_r is *ca.* 54 117. The water-soluble protein PRAI–IGPS migrates at a normal rate on SDS-PAGE[17].

DISCUSSION

Sephacryl and Superose

The column materials (Sephacryl S-300 HR and Superose 6) that we used bind SDS. The equilibration thus becomes slow and shows a special behaviour (Fig. 1; *cf.*,

ref. 3). The binding can be explained by hydrophobic and electrostatic interactions in addition to possibly, hydrogen bonding and other weak interactions. It has been shown that SDS also binds to polyoxyethylene[18]. The SDS binding to Superose is probably so high that an electrostatic exclusion effect may explain the lowering of the elution volumes for several proteins with increasing SDS concentration, which was previously observed in the range 5–100 m*M* SDS (Fig. 2 in ref. 7). The special SDS–gel matrix binding properties also caused a considerable retardation of the valleys in SDS concentration after each run with protein or lipid or octyl glucoside. Flow scintillation detection is a valuable tool in monitoring these effects.

SDS–PRAI–IGPS

The SDS binding to PRAI–IGPS at 1.6 m*M* SDS (slightly below the CMC) was found to be 1.58 ± 0.15 g/g. This is higher than the value of 1.26 g/g reported on the basis of neutron scattering measurements[1]. The "normal" binding ratio of two SDS molecules per amino acid residue[2] corresponds to a binding of 1.43 g SDS/g PRAI–IGPS (492 amino acid residues, M_r 49 484). Surprisingly, the SDS binding seems to decrease just above 1.6 m*M* SDS. A similar decrease in the binding above the CMC can be inferred from data for a membrane protein from a *Rhodospirillum rubrum* chromatophore (Fig. 4 in ref. 6). In that case the binding increased again at 3 m*M* SDS[6]. A similar tendency was found for bovine serum albumin, bovine carbonic anhydrase and PRAI–IGPS and the glucose transporter in a preliminary series of experiments on Superose 6 (not shown).

SDS–glucose transporter

Our results show the importance of removing all lipids from membrane protein preparations before attempts to determine SDS binding (or binding of other detergents). Re-runs may be needed in chromatographic procedures. The free lipids and free octyl glucoside (when present) also bind large amounts of SDS in mixed micelles (*cf.*, Fig. 3A). The same certainly applies to other detergents.

PRAI–IGPS forms a protein-decorated triple-micelle structure with SDS just below the CMC[1]. The probably more compact SDS–glucose transporter complex may hypothetically be envisaged as a dual-micelle structure or, possibly, as a short cylinder or ellipsoid. Speculatively, the apparent reduction in size on heating of the SDS–glucose transporter complex[7] may correspond to a transition from a dual-micelle structure to a still more compact cylindrical or ellipsoidal structure. It seems plausible that some or all of the hydrophobic amino acid residue stretches[8] in the glucose transporter traverse the SDS micelle core(s) in the SDS complex[2]. This is not known, however, and these amino acid residues can alternatively be inserted in the complex near its surface with the hydrophobic side-groups pointing inwards. The hydrophilic amino acid residues are probably positioned on the surface of the complex, as is the case for most of the PRAI–IGPS amino acid residues[1].

CONCLUSIONS

Careful equilibration of molecular-sieve columns is needed for the formation of SDS–protein complexes at accurately known detergent concentrations and for accurate determinations of SDS binding. Sephacryl gel beads bind SDS in amounts that

increase with increasing SDS concentration, as probably do Superose gel beads, which makes the equilibration slow. Also, re-equilibration after each chromatographic run needs to be carefully controlled. The use of a radioactive detergent and a flow scintillation counter is thus advantageous for binding studies. Our results indicate that at the CMC the partly hydrophobic glucose transporter protein from human red cells binds SDS in about the same amount per amino acid residue as does the water-soluble enzyme PRAI–IGPS when the membrane protein is properly freed from lipids. The SDS binding to the glucose transporter seemed to increase when the SDS concentration was increased above the CMC.

ACKNOWLEDGEMENTS

We are grateful to Kasper Kirschner and Halina Szadkowski for providing PRAI–IGPS. We thank Eva Greijer for general assistance and help with membrane preparations and manuscript editing, Robert Wallstén for mathematical advice on the scintillation detection-based binding calculations, Erik Mascher for comments on the manuscript, Konrad Ibel and Roland P. May for discussions and neutron scattering measurements (work in progress) and David Eaker for help with phosphatidylserine determinations. We appreciate the loan of an automatic sample applicator system from Hans Lindblom and Kurt Andersson (Pharmacia LKB Biotechnology). This work was supported by the Swedish Natural Science Research Council, the Swedish National Board for Technical Development (89-00519P) and the O.E. and Edla Johansson Science Foundation.

REFERENCES

1 K. Ibel, R. P. May, K. Kirschner, H. Szadkowski, E. Mascher and P. Lundahl, *Eur. J. Biochem.*, (1990) in press.
2 P. Lundahl, E. Greijer, M. Sandberg, S. Cardell and K.-O. Eriksson, *Biochim. Biophys. Acta*, 873 (1986) 20.
3 E. Mascher and P. Lundahl, *J. Chromatogr.*, 476 (1989) 147.
4 S. P. Grefrath and J. A. Reynolds, *Proc. Natl. Acad. Sci. U.S.A.*, 71 (1974) 3913.
5 N. C. Robinson and C. Tanford, *Biochemistry*, 14 (1975) 369.
6 J. Miyake, S. Ochiai-Yanagi, T. Kasumi and T. Takagi, *J. Biochem. (Tokyo)*, 83 (1978) 1679.
7 E. Mascher and P. Lundahl, *Biochim. Biophys. Acta*, 856 (1986) 505.
8 M. Mueckler, C. Caruso, S. A. Baldwin, M. Panico, I. Blench, H. R. Morris, W. J. Allard, G. E. Lienhard and H. F. Lodish, *Science*, 229 (1985) 941.
9 P. Lundahl, E. Greijer, S. Cardell, E. Mascher and L. Andersson, *Biochim. Biophys. Acta*, 855 (1986) 345.
10 E. Mascher and P. Lundahl, *Biochim. Biophys. Acta*, 945 (1988) 350.
11 S. A. Baldwin, J. M. Baldwin and G. E. Lienhard, *Biochemistry*, 21 (1982) 3836.
12 K. Ibel, R. P. May, K. Kirschner, A. N. Lane, H. Szadkowski, M.-T. Dauvergne and M. Zulauf, *Eur. J. Biochem.*, 151 (1985) 505.
13 D. C. Sogin and P. C. Hinkle, *J. Supramol. Struct.*, 8 (1978) 447.
14 M. T. Cairns, D. A. Elliot, P. R. Scudder and S. A. Baldwin, *Biochem. J.*, 221 (1984) 179.
15 G. E. Lienhard, I. H. Crabb and K. J. Ransome, *Biochim. Biophys. Acta*, 769 (1984) 404.
16 F. Y. P. Kwong, S. A. Baldwin, P. R. Scudder, S. M. Jarvis, M. Y. M. Choy and I. D. Yang, *Biochem. J.*, 240 (1986) 349.
17 K. Kirschner, H. Szadkowski, A. Henschen and F. Lottspeich, *J. Mol. Biol.*, 143 (1980) 395.
18 B. Cabane and R. Duplessix, *J. Phys. (Paris)*, 48 (1987) 651.

Journal of Chromatography, 512 (1990) 13–22
Elsevier Science Publishers B.V., Amsterdam

CHROMSYMP. 1951

Systematic optimization of protein separations on high-performance ion-exchange chromatographic media

WILLIAM WARREN, NANCY E. ASTEPHEN and THOMAS E. WHEAT*
Waters Division of Millipore Corp., 34 Maple Street, Milford, MA 01757 (U.S.A.)

ABSTRACT

The options for improving ion-exchange separations of proteins by manipulation of operating conditions on a single column were systematically examined. Manipulation of the slope of the ionic strength gradient involved a compromise between resolution and detection. Improved resolution without loss of sensitivity was obtained by manipulating selectivity. The manipulation of relative retentions by pH adjustment was shown for both anion and cation exchange. Changes in selectivity associated with alternative buffer ions at constant pH were documented. Improvements were also observed with changes in the counterion, and temperature had a direct impact on selectivity. The systematic optimization of these variables was facilitated by incorporation into the Auto-Blend™ Method. The application of this approach to the partial purification of mouse liver lactate dehydrogenase was tested.

INTRODUCTION

Significant improvements in chromatographic protein separations are observed when rigid high-performance anion- and cation-exchange packing materials are used with appropriate instrumentation in place of traditional large particle, compressible packings. The modern, resin-based materials give excellent recoveries of biological activity. In addition, the speed and reproducibility of this chromatography greatly facilitates optimization of the operating conditions. A systematic approach to the several parameters that influence protein separations is required to exploit this potential. Using an automated system, the effect of buffer composition, eluent pH, counter ion species, gradient duration and temperature on the resolution of protein standards will be demonstrated. Adjustments of these parameters is shown to influence the purity and the recovery of an active enzyme from a crude extract of mouse liver. The principles demonstrated in this work can be applied to the optimization of protein separations by ion exchange chromatography.

0021-9673/90/$03.50

EXPERIMENTAL

Chromatography of protein standards was performed on a Waters 650 advanced protein purification system, a refrigerated WISP 712 autosampler, a 484 tunable UV detector at 280 nm, and a 820 data station. Chromatography of mouse liver extracts was performed on a Waters W600 multi-solvent delivery system, a U6K manual injector, a M490 multi-wavelength detector at 280 nm, and a 840 chromatography control and data station.

The Protein-Pak™ columns were from Waters and include DEAE 8HR (100 × 10 mm), SP 8HR (100 × 10 mm), and DEAE 5PW (75 × 7.5 mm). All buffer components and reagents were the highest available commercial grades. Standard proteins were purchased from Sigma (St. Louis, MO, U.S.A.) and were repurified to give a single major peak by ion-exchange chromatography. The standards included hen conalbumin (C-0755), bovine α-chymotrypsinogen (C-4879), horse cytochrome *c* (prepared with TCA; C-2506), hen lysozyme (L7001), hen ovalbumin (A-5503), bovine ribonuclease A (R-5000), human transferrin (T-4515), and soybean trypsin inhibitor (T-9003). Mouse liver extract was prepared by homogenizing fresh mouse liver in 0.02 *M* Tris–HCl, pH 7.5, 5 ml/g, and centrifuging at 48 000 *g* at 4°C for 30 min. The extracts (150 μl/analysis) were chromatographed without further treatment. Lactate dehydrogenase activity was estimated colorimetrically by mixing 100 μl of each fraction with 500 μl of a reaction mixture including 10 mg/ml nicotinamide adenine dinucleotide, 1 mg/ml phenazine methosulfate, 10 mg/ml nitroblue tetrazolium, and 48 mg/ml lithium lactate in 0.1 *M* Tris–HCl, pH 7.5.

RESULTS AND DISCUSSION

Protein separations on ion-exchange media are commonly optimized by adjusting the ionic strength gradient such that the increase is more gradual over the range that the protein of interest is eluted. The power and limitations of the approach were tested over the range of 0.10 *M*/column volume to 0.0125 *M*/column volume. The retention of the protein standards is plotted as a function of gradient duration in Fig. 1, showing that the peaks are further apart with more shallow gradients. The chromatograms at the extreme ends of this test series are compared in Fig. 2. The improved resolution is associated with reduced peak height. When the volume of the

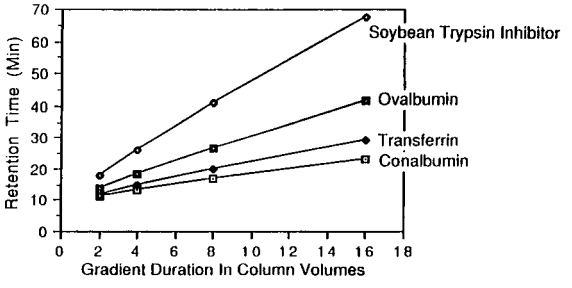

Fig. 1. Retention as a function of peak volume. Protein standards were chromatographed on a Waters Protein-Pak DEAE 8HR (100 × 10 mm) in 0.02 *M* Tris–HCl at pH 7.5. The proteins were eluted with a gradient 0 to 0.2 *M* NaCl over 2, 4, 8 and 16 column volumes.

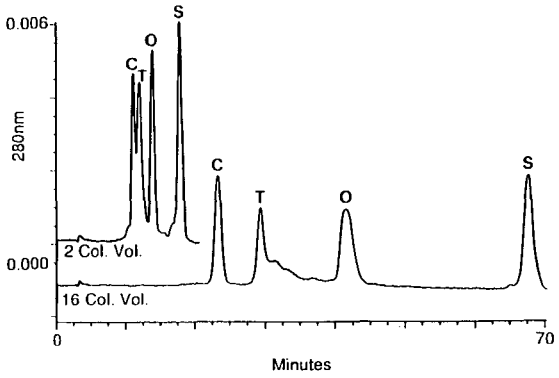

Fig. 2. Effect of gradient duration on resolution. The chromatography of protein standards with a 2- and 16-column volume (Col. Vol.) gradient is compared. Conditions as for Fig. 1. C = Conalbumin; T = transferrin; O = ovalbumin; S = soybean trypsin inhibitor.

ovalbumin peak is plotted as a function of gradient slope (Fig. 3), the increase in sample dilution with more shallow gradients is apparent. With lower protein concentration the sensitivity of UV detection is reduced, and there will be a similar effect on any enzymic or bioassay. In addition, the recovery of biological activity may be compromised by protein denaturation at high dilution. To improve protein separations without the adverse effects associated with extremely shallow gradients, those parameters that control the selectivity of the separation must be exploited. Such options would include a variety of chemical changes, but buffer pH, ionic composition of the buffer, counterion, and temperature are most amenable to systematic optimization.

The retention of protein standards as a function of pH in anion exchange chromatography in shown in Fig. 4. The retentions do change to a different extent for each protein in the mixture as is consistent with modification of chromatographic selectivity. As shown in Fig. 5, the chromatograms reflect significant differences in resolution. Conalbumin and transferrin are better resolved at pH 7.0 than at pH 9.0, while the retention of ovalbumin is virtually unaffected over this pH range. This

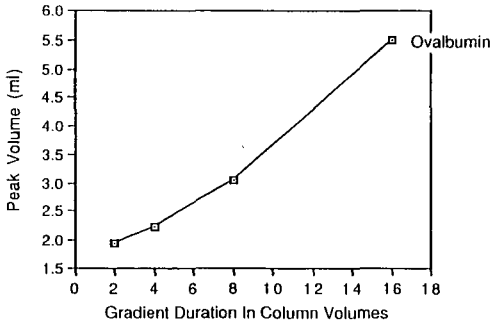

Fig. 3. Effect of gradient duration of peak volume. The volume of the ovalbumin peak when chromatographed as in Figs. 1 and 2 is shown as a function of gradient duration.

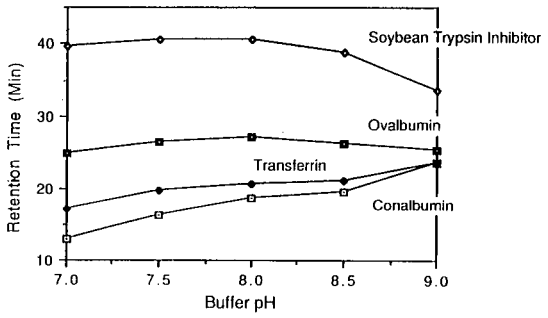

Fig. 4. Retention as a function of buffer pH. A series of protein standards was chromatographed on a Protein-Pak DEAE 8HR (100 × 10 mm) in 0.02 *M* Tris–HCl at selected pH values between 7 and 9. The same ionic strength gradient from 0 to 0.2 *M* NaCl over 8 column volumes was used at each pH.

experiment suggests that it is desirable to optimize empirically the pH to be used for the separation of a particular protein from a complex mixture.

Protein retention as a function of pH in cation exchange chromatography is shown in Fig. 6. Altered selectivity is again observed. The slopes of the retention

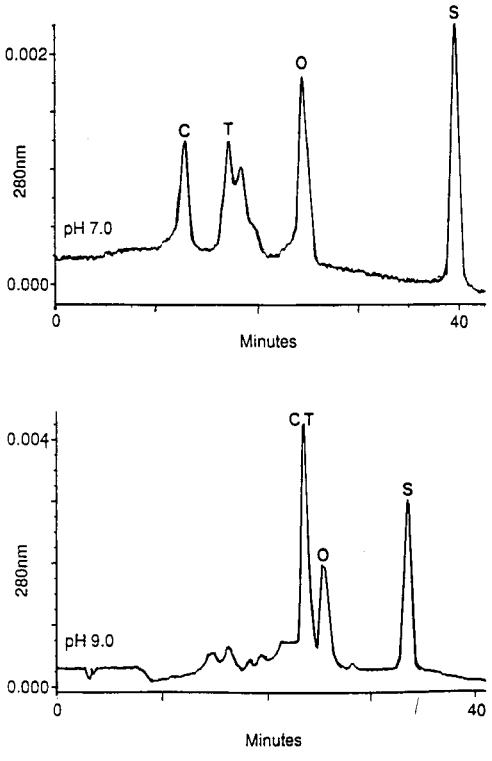

Fig. 5. Resolution as a function of buffer pH. The chromatography of protein standards at pH 7 and 9 is compared. Conditions as for Fig. 4. Abbreviations as in Fig. 2.

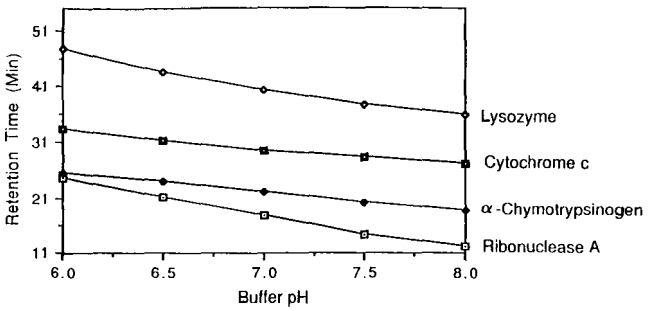

Fig. 6. Retention as a function of buffer pH. A series of protein standards was chromatographed on a Protein-Pak SP 8HR (100 × 10 mm) in 0.02 *M* phosphate at selected pH values between 6 and 8. The same ionic strength gradient from 0 to 0.3 *M* NaCl over 8 column volumes was used at each pH.

curves suggest that there may be an advantage in extending the comparison to lower pH values. Chromatography utilizing the same ionic strength gradient at pH 5.5 shows a change in selectivity compared to the separation at pH 6.0 (Fig. 7). The elution order of ribonuclease and chymotrypsinogen is reversed. The retention of

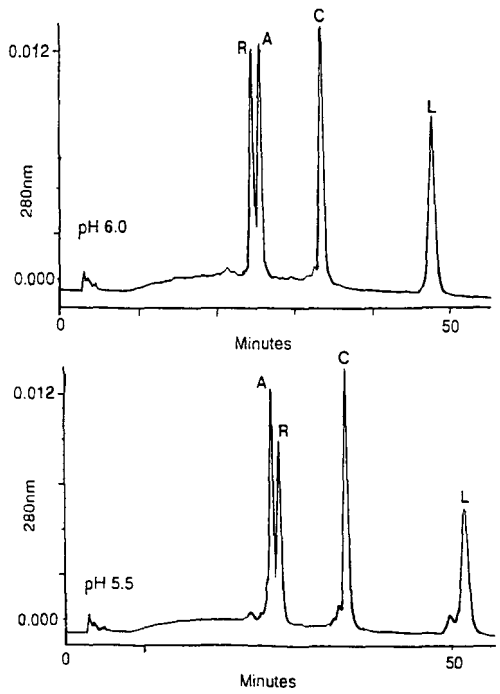

Fig. 7. Selectivity in cation exchange chromatography as a function of buffer pH. The results of cation-exchange chromatography of protein standards at pH 6.0 and 5.5 are shown. Conditions as for Fig. 6. R = Ribonuclease A, p*I* 9.5; A = α-chymotrypsinogen, p*I* 9.1; C = cytochrome *c*, p*I* 10.6; L = lysozyme, p*I* 11.0.

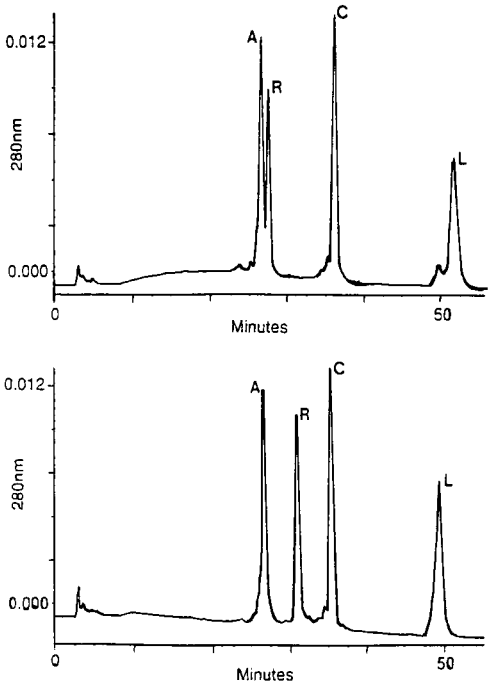

Fig. 8. Selectivity in cation-exchange chromatography as a function of buffer ion. A series of protein standards was chromatographed on a Protein-Pak SP 8 HR (100 × 10 mm) in either 0.02 *M* phosphate (top) or 0.02 *M* acetate (bottom), both at pH 5.5. The same ionic strength gradient from 0 to 0.3 *M* NaCl over 8 column volumes was used with each buffer. Abbreviations as in Fig. 7.

chymotrypsinogen is only sightly affected by this pH change that shifts ribonuclease dramatically. This change in selectivity may reflect the titration of a histidine side chain on the surface of ribonuclease since the change in chromatographic behavior is observed near the p*K* of this amino acid in a protein. Alternatively, since ribonuclease can bind orthophosphate[1], the altered retention may reflect a change in the bound ion. This seems less likely as described below (Fig. 8). The change in selectivity would not have been predicted from the isoelectric points of the proteins. Elution from a cation exchanger should be in order of increasing isoelectric point, and ribonuclease deviates from this rule above pH 5.5[2,3]. It is, in fact, often observed that isoelectric focusing does not accurately predict behavior of a protein sample in ion-exchange chromatography[4–6]. It may, therefore, often be useful to examine a fairly wide pH range, within the limits of protein and column stability, to find the optimum pH for a particular separation. Since such an approach will exceed the useful range of a particular buffer, it is necessary to examine the effect of particular buffer ions on selectivity.

The buffering ion is selected to have a p*K* near the optimum pH for the protein separation. With cation exchangers, phosphate is a suitable buffer from pH 6 to 8, but at lower pH acetate provides better buffering capacity. The effect of these alternative buffer ions was compared at pH 5.5, as shown in Fig. 8. The change in selectivity is most apparent for ribonuclease, but both lysozyme and cytochrome *c* are affected.

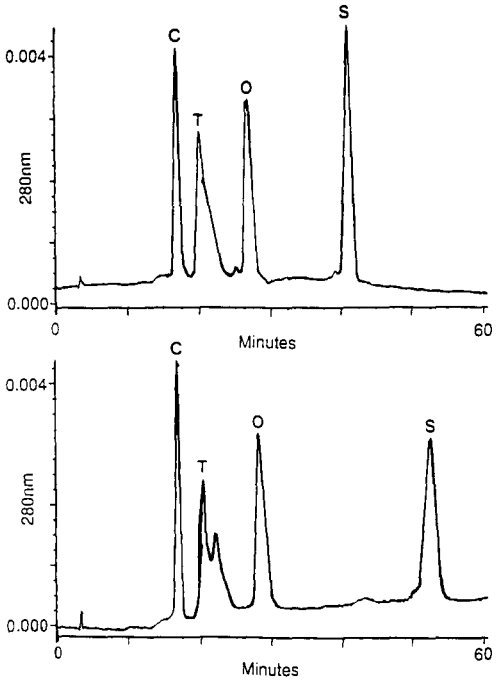

Fig. 9. Selectivity in anion-exchange chromatography as a function of counter ion. A series of protein standards was chromatographed on a Protein-Pak DEAE 8HR (100 x 10 mm) in 0.02 *M* Tris–HCl at pH 7.5. The ionic strength gradient was from 0 to 0.2 *M* sodium chloride (top) or from 0 to 0.2 *M* sodium acetate (bottom) over 8 column volumes. Abbreviations as in Fig. 2.

The increased retention of ribonuclease relative to the other proteins in the mixture may reflect the depletion of orthophosphate that was bound to the protein[1–3], thus exposing cationic amino acid side chains for binding to the packing material.

Since the buffering ion has an effect on selectivity, the counter ion should also profoundly alter the separation. The same ionic strength gradient was compared with chloride and with acetate (Fig. 9). Although conalbumin and ovalbumin are essentially unchanged, resolution of transferrin and its contaminants is improved with acetate. Soybean trypsin inhibitor is eluted much later with acetate, as expected from the elutropic series, but it is surprising that the other standards proteins are not also shifted to longer retention by the same effect.

In addition to the mobile phase components described above, temperature is expected to have an effect on retention. When anion-exchange chromatograms of protein standards at 4 and 25°C are compared (Fig. 10), a change in selectivity is observed. Such alterations are expected but unpredictable since the p*K* of the buffer, the apparent pH, the p*K* of the surface of the ion-exchange resin, the binding constants and the p*K* of each of the ionizable groups of the protein are sensitive to temperature. Commonly, the temperature used for a protein separation is dictated by recovery of biological activity so temperature is not a useful variable for optimizing the separation. However, it may be necessary to readjust other conditions when the chromatographic experiments are shifted between the cold room and the normal laboratory.

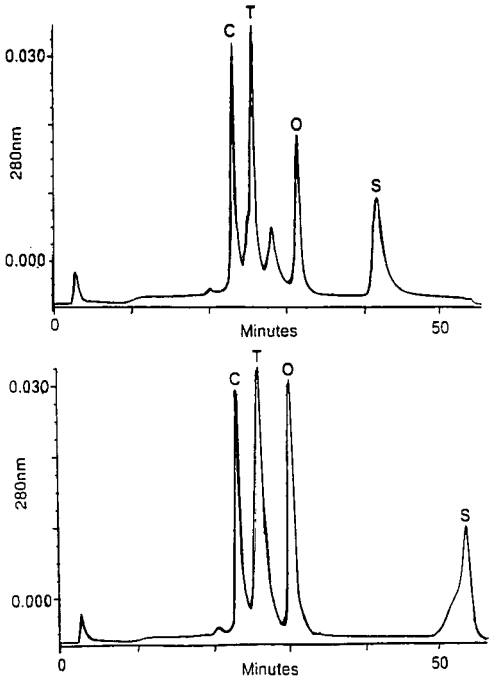

Fig. 10. Selectivity in anion-exchange chromatography as a function of temperature. A series of protein standards was chromatographed on a Protein-Pak DEAE 5PW (75 × 7.5 mm) in 0.02 *M* Tris–HCl at pH 7.5. The same ionic strength gradient from 0 to 0.2 *M* NaCl over 8 column volumes was used at both 4 (bottom) and 25°C (top). Abbreviations as in Fig. 2.

Application of these principles to the development of a particular protein separation involves the preparation of several pairs of buffers. It has proven more convenient and efficient to use the Auto-Blend™ Method[7]. This approach is based on accurate and precise blending of four buffers by the liquid chromatograph. Typically, the A stock is 0.1 *M* acid salt and the B stock is 0.1 *M* basic salt. The relative proportions drawn from the A and B lines determine the pH of the separation. The ionic strength is independently controlled by varying the proportions of the counter-ion stock and the water in the C and D lines, respectively. Both pH and ionic strength are, therefore, determined by entries made in the gradient controller. It is also straightforward to change these parameters independently or simultaneously during the separation.

The Auto-Blend Method was used for the separation of lactate dehydrogenase from crude extracts of mouse liver. As the pH of the buffer was changed, the pattern of protein separation, as judged by the absorbance at 280 nm, also changes. However, the lactate dehydrogenase (LDH) activity was nearly unretained until the pH was raised to 8.6. The retention of LDH relative to the mass of protein in the sample changes dramatically over the narrow range from pH 8.0 to 8.6 (Figs. 11 and 12). Further improvements in the separation can be achieved by reducing the slope of the ionic strength gradient followed by adjustment of the pH in smaller increments. Finally, acetate could replace chloride as the counter ion. These experiments are

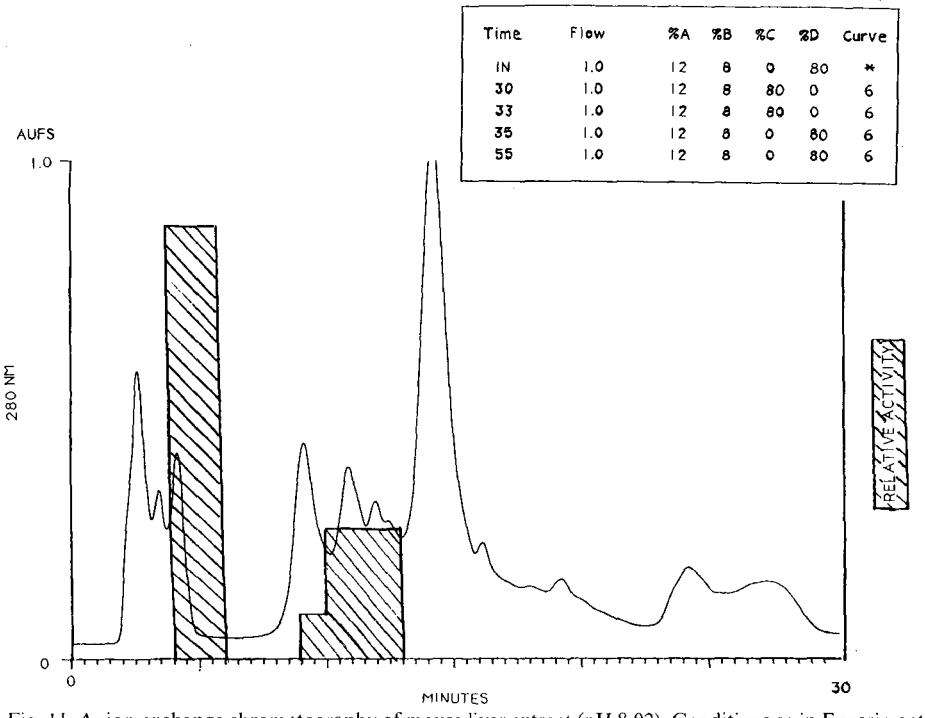

Fig. 11. Anion-exchange chromatography of mouse liver extract (pH 8.02). Conditions as in Experimental section. Enzyme activity (LDH) shown as bars with a diagonal lines and absorbance at 280 nm as continuous tracing.

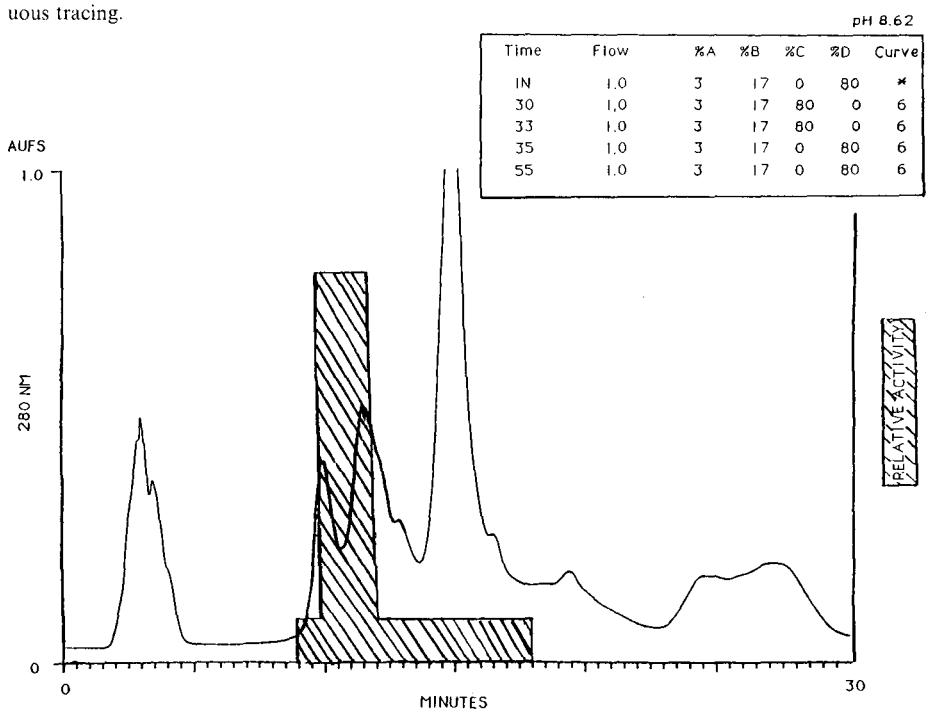

Fig. 12. Anion-exchange chromatography of mouse liver extract (pH 8.62). Conditions as in Experimental section. Enzyme activity (LDH) shown as bars with a diagonal lines and absorbance at 280 nm as continuous tracing.

quickly and conveniently programmed from the keyboard of the gradient controller and can be completely automated by the use of an autosampler.

REFERENCES

1 C. A. Nelson, *J. Biol. Chem.*, 237 (1962) 1575.
2 R. A. Alberty, *J. Phys. Chem.*, 52 (1948) 1345.
3 A. Rothen, *J. Gen. Physiol.*, 24 (1940) 203.
4 A. J. McEvily, B. Holmquist and B. L. Vallee, *Biochromatography*, 5 (1990) 13.
5 L. A. Haff, L. G. Fagerstam and A. R. Barry, *J. Chromatogr.*, 266 (1983) 409.
6 W. Kopaciewicz, M. A. Rounds, J. Fausnaugh and F. E. Regnier, *J. Chromatogr.*, 266 (1983) 3.
7 W. Warren, A. Peterson, T. Wheat, M. P. Strickler, M. J. Stone, M. Dwyer and R. Pfeifer, *Am. Biotech. Lab.*, June (1989) 34.

Journal of Chromatography, 512 (1990) 23–39
Elsevier Science Publishers B.V., Amsterdam

CHROMSYMP. 1932

Evaluation of factors which affect column performance with immobilized monoclonal antibodies

Model studies with a lysozyme–antilysozyme system

MILTON T. W. HEARN* and JEFFREY R. DAVIES[a]
Monash University, Department of Biochemistry and Centre for Bioprocess Technology, Clayton, Victoria 3168 (Australia)

ABSTRACT

Methods are described for the automated evaluation of affinity columns by frontal boundary analysis. These methods were used to evaluate the performance of immunoaffinity columns based on antilysozyme monoclonal antibody–lysozyme immunoaffinity system. This model system enabled the effects of (i) matrix activation and (ii) the density of immobilized antibody on the change in specific activity of immobilized antibody to be quantitatively assessed. Experimental data were accumulated with carbonyldiimidazole-activated Fractogel HW65F and Trisacryl GF2000 resins and cyanogen bromide-activated Sepharose 4B. An increase in the molar ratio between the concentration of the active groups on the activated matrix and the concentration of immobilized antibody ligands did not result in significant change in the specific activity of the immobilized antibody in the immunochromatographic system. However, increased antibody density with the Fractogel HW65F resin resulted in an increase in the apparent heterogeneity of antibody binding sites for lysozyme and a significant decrease in the specific activity of the immobilized antibody. Furthermore, data from size-exclusion studies with these immunoaffinity matrices demonstrated that at high antibody densities, the accessibility of the immobilized antibody was further decreased due to steric resistance as the antigen size increased.

INTRODUCTION

Over the past several years monoclonal antibodies (MAbs) have found application in the purification of a variety of biologically important proteins, including various lymphokines[1–3] and blood coagulation or plasma proteins such as factor VIII[4,5], protein C[6], factor IX[7] and α-fetoprotein[8]. However, the expense of producing

[a] Present address: Commonwealth Serum Laboratories, Poplar Road, Parkville, Victoria 3052, Australia.

bulk (*i.e.* 10–100 g) quantities of MAbs of the correct epitopic specificity and affinity has largely limited their application to laboratory-scale purification studies. From a process automation point of view, one advantage of MAb systems is their potential to allow the development of rational sequential strategies by which large purification factors (*e.g.* > 50-fold) can be achieved. Examples where immunoaffinity chromatographic systems have already been applied at the process scale within biotechnological industries include the biorecovery of interferons[1,2] and the blood coagulation protein factor VIII[5].

Practical experience has demonstrated with both dynamic and static (batch) adsorption conditions that a high percentage of the immobilized antibodies may not bind specific antigens[9–19]. A number of hypotheses can be advanced for this phenomenon. For example, during the synthesis of the immunoaffinity support, the paratope (antigen binding) structure of the MAbs may be destroyed or modified by multisite immobilization due to the presence of high levels of clustered active groups at different patches on the matrix surface[14,19]. Furthermore, lack of control over the orientation of the MAb during immobilization could give rise to functionally inaccessible MAb molecules, *i.e.* the Fab regions are orientated toward the matrix polymer backbone and thus effectively become buried. Alternatively, antigenic binding in a stoichiometric sense may be restricted due to a high density and proximity of immobilized antibody molecules (steric crowding due to antibody clustering). A similar effect can also be expected to arise on steric grounds due to the size and hydrodynamic properties of the antigen (the steric crowding effect due to antigen size). Finally, the issue of ligand leakage will give rise to decreasing capacity with usage. Ligand leakage often necessitates the implementation of further purification stages with high-value therapeutic proteins. Adequate remedy of these current limitations requires quantitative evaluation of the characteristics and performance of the immunoaffinity matrix.

Important concepts in the design of immunoaffinity systems and approaches to optimising and predicting their performance on scale up have previously been described in the scientific literature; for a compendium of recent reviews see refs. 9, 10 and 15–19. In process-scale separations, column chromatographic systems have been preferred because of the ease of automation of these systems compared to batch methods. The capture of antigen by an immobilized antibody in such systems is dependent on a number of factors including: (i) concentration of antigen, (ii) volume of feedstock loaded, (iii) concentration of accessible and active immobilized antibody, (iv) the degree of contaminant fouling and (v) efficiency of regeneration following product desorption and sorbent washing. In order to ensure the greatest capture of antigen, the view has been held by some investigators that the concentration of active immobilized antibody should be as high as possible. However,the studies of Eveleigh and Levy[9] have shown that under such conditions with CNBr-activated Sepharose 4B and porous glass supports a substantial proportion of immobilized antibody will not be functional in immunoaffinity systems. In particular, these investigators have provided data, obtained with supports of equivalent activation levels but different antibody densities, which illustrated that the antibody density effects, rather than the activation levels, played the major role in decreasing the immunoadsorbent capacity with CNBr-activated Sepharose 4B systems. The impact of activation levels on column performace in process biospecific affinity chromatography is nevertheless an im-

portant aspect to study because it is well known that the stability of an immobilized ligand will decrease as the number of immobilized groups per ligand decreases[9,18,20]. Hence for stability and regeneration purposes, high activation levels are desirable. Therefore it is important to establish if the immobilization chemistry *per se* is responsible for decreased specific activity of an immobilized antibody or if the activation chemistry has changed the mass transfer properties of the matrix which in turn results in decreases in the specific activity of the immobilized antibody.

In the present and associated studies we have examined alternative ways to quantitatively evaluate the characteristics of biospecific affinity matrices, including the influence of surface accessibility, ligand density and ligand stability. This manuscript, in particular, examines the influence of matrix activation levels and immobilized antibody density on the specific activity of the immobilized antibody and the binding site heterogeneity, in a model immunoaffinity chromatographic system. A monoclonal immunoaffinity system was used in this study to eliminate polydispersity effects in terms of affinity constants which are an intrinsic feature of polyclonal antibody immunoaffinity systems. Three activated supports were evaluated [carbonyldiimidazole (CDI)-activated Fractogel HW65F and Trisacryl GF2000 and CNBr-activated Sepharose 4B] using a lysozyme–antilysozyme MAb system. The use of Fractogel or Trisacryl in immunoaffinity systems has some practical advantages for large-scale fractionation systems over traditional Sepharose-based supports in that these resins exhibit higher mechanical stability at high flow-rate.

The experimental design was used in our studies based on frontal boundary analysis[21–23]. Experimental data were analyzed in terms of system capacities, binding constants and extent of ligand heterogeneity evaluated from Stewart–Petty (double reciprocal), Scatchard and Sips plots[24–27]. The equations describing these plots assume that near equilibrium conditions prevail for binding of the antigen to both high- and low-affinity binding sites. The Steward–Petty plot is evaluated from the dependency of the total bound antigen $[Ag]_b$ and the initial antigen concentration [Ag], the immobilized antibody concentration [Ab] and the dissociation constant, K_d, namely

$$\frac{1}{[Ag]_b} = \frac{K_d}{[Ag]2[Ab]} + \frac{1}{2[Ab]} \tag{1}$$

The Scatchard plot is given by

$$\frac{r}{[Ag]} = -rK + nK \tag{2}$$

where the ratio, r, corresponds to the number of moles of bound antigen to the total molar concentration of immobilized antibody and is a measure of the extent of saturation of the binding sites: K is the association constant and n is the apparent valency of the antibody. For ideal immunoglobulin G (IgG)–antigen interactions, $n = 2$.

Transformation of eqn. 2 yields

$$\frac{r}{n-r} = K\,[\mathrm{Ag}] \tag{3}$$

which on incorporation of the coefficient "a" (Sips heterogeneity index) yields the Sips plot given by

$$\frac{r}{2-r} = K\,[\mathrm{Ag}]^a \quad \text{or} \quad \log(r/2-r) = \log K + a\log[\mathrm{Ag}] \tag{4}$$

The Sips heterogeneity index is a measure of the non-ideality of the Ab–Ag interaction.

Previous work in this and other laboratories have shown that these equations can readily be adapted for analysis of immunoaffinity and other biospecific affinity systems using frontal boundary data[21–23]. Thus for frontal elution systems eqn. 1 takes the form

$$\frac{1}{[\mathrm{Ag}](V_e - V_{0,\mathrm{ni}})} = \frac{K_d}{[\mathrm{Ag}]2[\mathrm{Ab}]_a} + \frac{1}{2[\mathrm{Ab}]_a} \tag{5}$$

where V_e = elution volume of antigen; $V_{0,\mathrm{ni}}$ = elution volume of a non-interactive]species of similar hydrodynamic characteristics as the antigen and $[\mathrm{Ab}]_a$ = the concentration of accessible antibody assuming a valency of 2.

Similarly the frontal boundary data can also be analysed in terms of the Scatchard and Sips plots (eqns. 2 and 4). However, these numerical derivations require the determination of the variable r. Determination of the concentration of the total antibody immobilized, $[\mathrm{Ab}]_t$, can be achieved by direct measurement of antibody incorporation using ^{125}I labelled antibody, mass difference analysis or amino acid composition of the hydrolysed support. Determination of $[\mathrm{Ab}]_a$ can be achieved from the experimental data by plotting $1/[\mathrm{Ag}](V_e - V_{0,ni})$ *vs.* $1/[\mathrm{Ag}]$ using eqn. 5. Under ideal homogeneous binding conditions with both paratope binding sites of the MAb operating independently (*i.e.* when the association constants for antigen binding to each paratope are identical), the Steward–Petty plot will be linear with the value of the y axis intercept corresponding to $1/(2[\mathrm{Ab}]_a)$; the Scatchard plot will be linear with the numerical value of the x axis intercept being 2 by definition for binding interactions with an IgG class antibody, and the Sips plot will be linear with a slope of 1.

In immunoaffinity systems with MAbs of high ligand densities and close ligand proximity, changes in the binding affinity constants of antibodies may occur due to steric crowding of the immobilized ligand or chemical and physical inhomogeneities of the matrix surface. These effects will result in heterogeneous immunosorbents encompassing several classes of different binding sites with different affinities being generated. Non-ideal interactive behaviour will then be manifested as a boundary set of near equilibrium interactions between the paratope and the (monovalent) antigen such that each paratope, P_i, of the immobilized antibody in each different micro-environment (*e.g.* 1, 2, ...*i*...*n*) on the surface of the stationary phase will exhibit a different affinity constant for the antigen as described in the set of equations below.

$$P_1 + Ag \overset{K_1}{\rightleftharpoons} P_1Ag$$

$$P_2 + Ag \overset{K_2}{\rightleftharpoons} P_2Ag$$

$$\vdots$$

$$P_i + Ag \overset{K_i}{\rightleftharpoons} P_iAg$$

$$\vdots$$

$$P_n + Ag \overset{K_n}{\rightleftharpoons} P_nAg$$

The presence of multiple affinity sites will result in complex dependencies of K_i and the binding kinetics on the ligand density, $[Ab]_t$. In addition as the $[Ab]_t$ increases a proportional increase in the number of binding sites may not result. Such heterogeneity can also theoretically be anticipated to lead to apparent negative cooperativity in the MAb–Ag interaction and be reflected in non-linear Scatchard plots and Sips plots with gradients less than 1. Such interpretation of heterogeneity introduced by the matrix activation chemistry and ligand density effects has previously been complicated by the use of polyclonal antibodies. In order to examine these effects, immunoaffinity sorbents of different MAb ligand densities were prepared using antilysozyme MAbs and the experimental data evaluated in terms of a two component model of binding sites. We have not attempted in the present manuscript to quantify the contribution of third, fourth or higher classes of binding sites in these numerical analyses.

EXPERIMENTAL

Materials

Carbonyldiimidazole, ethanolamine, bovine serum albumin, horse heart cytochrome *c*, hen egg white lysozyme, ovalbumin and bovine γ-globulin, were purchased from Sigma, St. Louis, MO, U.S.A. Fractogel HW65F was purchased from Merck, Darmstadt, F.R.G., Trisacryl GF2000 was from Reactifs IBF, Pointet Girade, France. CNBr-activated Sepharose 4B and Blue Dextran 2000 were obtained from Pharmacia, Uppsala, Sweden. [^{14}C]Lysine and ^{125}Iodine were obtained from Amersham, U.K.

Methods

Purification of monoclonal antibody. Monoclonal antibody against lysozyme was purified from Balb/C mouse ascites fluid using an fast protein liquid chromatographic (FPLC) system with an HR16/10 Mono Q anion-exchange column (Pharmacia). Ascites fluid was diluted two-fold with 20 m*M* Tris · HCl pH 8.0 (buffer A) and loaded onto the column through pump A. The partially fractionated MAb was eluted with a 0–0.5 *M* sodium chloride gradient in buffer A. The flow-rate was 8 ml/min and the gradient time was 60 min. The IgG peak was diluted twofold with buffer A and rechromatographed as described above to ensure resolution of the specific MAb from contaminating proteins. The purified MAb was estimated to be >95% pure from

sodium dodecyl sulphate (SDS)–polyacrylamide gel electrophoresis. Purified IgG was labelled with ^{125}Iodine using a modified chloramine T method[28].

Matrix activation. Acetone was dried by distillation over potassium carbonate and stored under anhydrous conditions. Chromatographic supports were thoroughly washed with dried acetone and then activated with CDI according to the method of Hearn[21]. The concentration of CDI ranged from 0.6 to 4 mmol/g of acetone moist cake of chromatographic gel. Activation levels were assessed by previously described methods[21] and by the quantitative immobilization of [^{14}C]lysine coupled at pH 8.9 in 0.1 *M* sodium borate, 0.5 *M* sodium chloride. Following ligand coupling, the affinity resins were thoroughly washed with 0.1 *M* sodium borate, 0.5 *M* sodium chloride, pH 8.9 and 0.1 *M* sodium acetate, 0.5 *M* sodium chloride, pH 4.5. The amount of [^{14}C]lysine immobilized per ml of resin was determined by hydrolysis of a measured amount of [^{14}C]lysine resin with 6 *M* hydrochloric acid at 60°C for 90 min. The ^{14}C content of the hydrolysate was then determined directly by β-scintillation counting.

Using the above protocols lower levels of activation were achieved with Trisacryl GF2000 resin than found with Fractogel HW65F or agarose-based materials. In order to increase the activation levels, Trisacryl was washed in 100% acetic acid prior to the acetone wash. This treatment resulted in a doubling of the level of CDI-activation when using high ratios of CDI per g moist cake of resin. These results suggest that hydrogen bonding, occurring between hydroxyl groups in this support, plays a significant part in controlling the access of the CDI to the internal surfaces of the porous network and subsequent chemical activation of Trisacryls.

Antibody immobilization. Purified MAb was coupled to activated supports in 0.1 *M* sodium phosphate, 0.1*M* sodium chloride, pH 7.0 in amounts ranging from 1 to 20 mg of antibody per ml of activated resin. Samples were spiked with ^{125}I-labelled antibody with coupling time typically 48 h at 4°C. Following coupling the resins were washed with 0.1*M* sodium borate, 0.5 *M* sodium chloride, pH 8.9 and 0.1 *M* sodium acetate, 0.5 *M* sodium chloride, pH 4.5 then 0.1 *M* phosphate–ethanolamine pH 8.0. The gel was incubated in the phosphate–ethanolamine buffer for 16 h in order to block any unreacted sites. The amount of IgG immobilized was determined by direct measurement of [^{125}I]IgG incorporation.

Calculation of the specific activity of immobilized antibodies. Purified anti-lysozyme IgG was assumed to be 100% pure and specific activities for immobilized IgG systems were expressed as a percentage of the theoretical capacity determined from the amount of IgG immobilized according to the following formula:

$$\text{Specific activity} = 100 \cdot [\text{lysozyme}]_{\text{bound}}\,(M)/2 \cdot [\text{IgG}]_{\text{immobilized}}$$

where the molecular weight of lysozyme was assumed to be 14 300 and IgG 150 000.

Size-exclusion analysis of fractogel matrices. Size-exclusion analysis of Fractogel HW65F resins (native, CDI-activated and bovine IgG Fractogels) was carried out using 0.5-ml bed volume in glass columns (5 mm I.D.). The retention times of hen egg white lysozyme, ovalbumin, bovine serum albumin and bovine γ-globulin were determined from quadruplicate measurements in 8 *M* urea, 0.5 *M* sodium chloride at a flow-rate of 0.2 ml/min. Solute accessibility was determined using the following equation:

$$\text{Solute accessibility} = \frac{V_e - V_0}{V_t - V_0}$$

where V_e = elution volume of solute, V_0 = column void volume (measured using Blue Dextran 2000) and V_t = total column volume (measured using acetone).

Evaluation of regeneration protocols. Desorption and regeneration conditions for the lysozyme–antilysozyme system were determined using several different zonal elution protocols. Protein samples were sequentially injected onto the immunoaffinity supports until a constant peak height was observed for the breakthrough zone, (*i.e.* until the column was saturated with lysozyme). Different reagents were then tested for their ability to restore lysozyme binding capacity of the immunoaffinity support after injection of one column volume pulses of the reagent through the column.

Chromatographic evaluation of MAb-based immunoaffinity gels. The various immunoaffinity chromatographic gels were evaluated using frontal boundary analysis as previously described[21–23], using column bed volumes between 0.2 and 0.5 ml (column internal diameter, 5 mm). The analysis was automated by use of Pharmacia FPLC system equipped with MV7 and MV8 motorized valves. The configuration of the FPLC system used for the frontal analysis is shown in Fig. 1. The system was

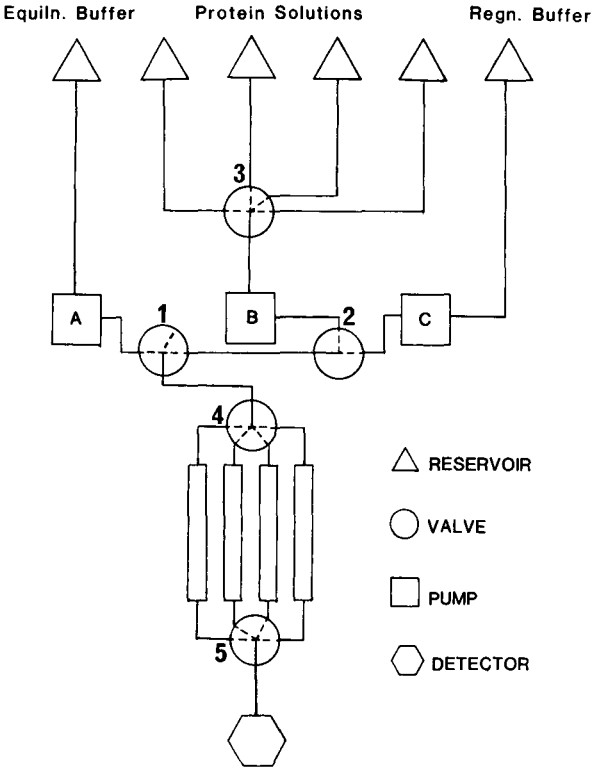

Fig. 1. Automated FPLC system for Frontal Analysis of Immunoaffinity supports. All pump valve and recorder switching was achieved using an LCC500 microprocessor. Sample was applied through pump B (P500) and the recorder (Shimadzu C-R3A Chromatopac) automatically activated when pump B started. Regeneration buffer was applied using pump C (P1 peristaltic) and re-equilibration buffer (20 m*M* sodium phosphate, 0.15 *M* sodium chloride) applied using pump A. Valve 1 was an MV7 valve with the outlet from pump A connected to port 1 and the tubing from valve 2 connected to port 2. All other valves were MV8. (The controlling program can be obtained if required by writing to the authors.)

controlled by a GP500 controller which allowed replicate analyses to be conducted for each measurement. Data were collected and reprocessed using a Shimadzu C-R3A recorder. This data handling feature was necessary for the automated system in order to generate normalised breakthrough curves when samples of different antigen concentrations were being analysed.

Frontal analysis was conducted at a flow-rate of 0.2 ml/min using a lysozyme concentration of 2–100 μg/ml. The $V_{0,ni}$ value used in eqn. 5 was determined using cytochrome *c* at concentrations from 2.5 to 100 μg/ml in 0.1 *M* sodium phosphate, 0.15 *M* sodium chloride, pH 7.0. Cytochrome *c* was chosen beause it has a similar hydrodynamic volume to lysozyme but did not interact with the immunoaffinity support. Measurement of V_c for lysozyme under the different experimental conditions was determined by measuring the volume of eluent corresponding to the $V_{0.5}$ of the breakthrough curve.

Six immunoaffinity chromatographic gels were evaluated. Two Fractogel resins with similar CDI activation but different ligand densities; two Trisacryl resins with different CDI activation levels and similar ligand densities and two CNBr-activated Sepharose derived supports with different ligand densities. With the exception of CNBr-activated resins capacities were determined by evaluation of frontal analysis data. For CNBr systems, biphasic breakthrough curves were obtained complicating interpretation of frontal analysis data. Experimental values of capacities derived from the analysis of the second component of the breakthrough curves exceed the maximum theoretical value. Hence, capacities determined for these experimental systems were obtained from frontal analysis data using 100 μg/ml solutions of lysozyme only and assuming the first front of the breakthrough curve represented saturation of immobilized antibody due to the biospecific interaction and not electrostatic interactions known for systems derived from CNBr activation[29–31].

RESULTS AND DISCUSSION

Influence of buffer conditions on immobilization efficiency

The influence of buffer effects on the efficiency of immobilization of bovine

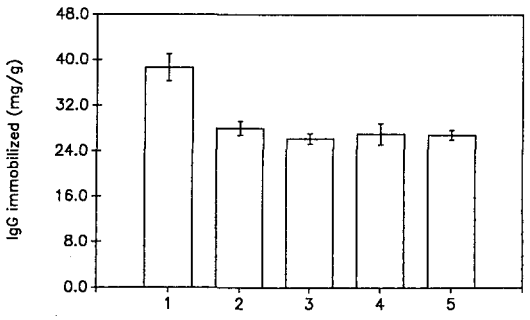

Fig. 2. pH dependence of γ-globulin coupling to CDI-activated Fractogel. The concentration IgG was 40 mg/g of activated Fractogel. All coupling were conducted in 0.5 *M* sodium chloride. IgG immobilizations were determined in triplicate. 1 = 0.1 *M* sodium phosphate, pH 7.0; 2 = 0.1 *M* Tris · HCl, pH 8.0; 3 = 0.1 *M* sodium borate, pH 8.9; 4 = 0.1 *M* Tris · HCl, pH 8.0, 0.2% NaN_3; 5 = 0.1 *M* Tris · HCl, pH 8.0, Brij-35.

polyclonal antibodies to preactivated supports are summarized in Fig. 2. The data show that maximum immobilization efficiency for bovine γ-globulin was achieved at the lowest pH tested, *i.e.* at pH 7.0 (0.1 *M* sodium phosphate) and not at pH 8.0 (0.1 *M* Tris · HCl) or pH 8.9 (0.1 *M* sodium borate). A similar pH effect has also been noted in our earlier investigations on the coupling of various ligands using CDI- and CNBr-activated supports[21,30]. Efficient immobilization of proteins to preactivated matrices could be achieved in the presence of Tris buffer. This result is consistent with the observation that the amino group in Tris is sterically hindered[32] and does not significantly compete with free side chain primary amino groups of proteins at the coupling stage. The presence of the additives NaN_3 (0.2%) and Brij-35 (0.01%), did not interfere with the antibody immobilization. Conditions for the MAb immobilization to preactivated gels were selected on the basis of these observations.

Elution of bound components and column regeneration

For regeneration of the immunochromatographic systems the most effective reagent tested was 2.5 *M* KSCN with complete elution being affected by a single column volume. Glycine 0.1 *M* (pH 2.8)–0.5 *M* sodium chloride was also effective but required 3–4 column volumes to regenerate the immunoaffinity support to equivalent capacity. Column capacity, irrespective of the support matrix, was invariably reduced after the first chromatographic run and thereafter the capacity stabilized. This finding is consistent with previous observations with polyclonal systems[9]. Other reagents tested were 2 *M* solutions of NaCl, $MgCl_2$ and LiCl but these conditions were found to be ineffective in desorbing bound antigen and/or regenerating the column to high capacity. With the KSCN elution system, although the lysozyme zone eluted in a sharp peak, extensive washing was required to remove all KSCN from the column on reequilibration. If this was not affected, earlier breakthrough and decreased capacity was noted with some KSCN-conditioned columns.

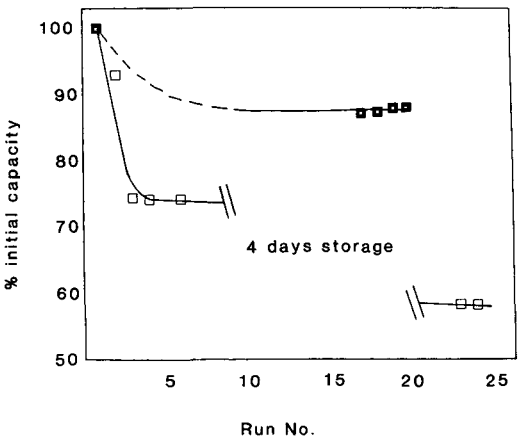

Fig. 3. Comparison of the effect of KSCN and low pH glycine–sodium chloride regeneration systems on antilysozyme–Fractogel columns. Capacities were determined by frontal analysis using a 10-μg/ml solution of lysozyme. The activation level and immobilized antibody concentration was: CDI level = 25 μmol/ml Fractogel; antibody density = 1 mg/ml Fractogel. Regeration with: ■ = 2.5 *M* KSCN, □ = 0.1 *M* glycine–0.5 *M* sodium chloride, pH 2.8.

A comparison of binding capacities (determined by frontal analysis) and the dependence of capacity on the number of runs of two antilysozyme Fractogel HW65F columns regenerated with the glycine and KSCN desorption systems, respectively, is shown in Fig. 3. In both cases a rapid drop in capacity was observed between the first and second runs but in subsequent runs the capacity remained constant with the KSCN elution system providing higher capacities (88% of the initial value) than the glycine system (74%). After 4 days storage at 4°C in 100 m*M* sodium phosphate, 0.1% NaN_3 and 25 adsorption/desorption cycles, the immunoaffinity system regenerated using the glycine system showed a further 20% loss in capacity (Fig. 3). In comparison, analysis of an antilysozyme–Trisacryl GF2000 column (MAb density 1.0 mg of antibody immobilized per ml of resin) regenerated using the KSCN system showed a 45% loss in capacity after 3 months storage at 4°C in 100 m*M* sodium phosphate, 0.1% NaN_3 and 56 cycles of usage.

The influence of immobilized MAb density on lysozyme binding

The influence of the density of immobilized MAb on antigen binding is shown in Table I. A 13-fold increase in MAb density on Fractogel HW65F resulted in only an 8.5-fold increase in the binding capacity. This represents, a decrease of 33% in the specific activity of the immobilized antibody with the high antibody density support. Although frontal breakthrough profiles of immunoaffinity columns with MAb immobilized to CDI-activated gels showed regular asymptotic Langmurian-like isotherm behaviour characteristic of a common retention mechanism, for immunoaffinity gels derived using CNBr-activated Sepharose 4B multimodal adsorption behaviour was evident. This observation is consistent with the well known non-biospecific, coulombic adsorptive properties of the charged isourea linkage generated from the immobilization of ligands onto CNBr-activated matrices[29–31].

Nonetheless with a 10-fold increase in ligand density CNBr-activated Sepharose 4B resulted in an approximately 11-fold increase in antigen binding capacity. Thus

TABLE I

THE EFFECT OF IMMOBILIZED MAb DENSITY ON COLUMN CAPACITIES

The theoretical capacity was determined as 2 · [antibody] (M) immobilized. The molecular weight assummed for antibody was 150 000 and for lysozyme 14 300. The specific activity of immobilized antibody was

$$\frac{100 \cdot \text{experimentally determined capacity}}{\text{theoretical capacity}}$$

Matrix	*Antibody density (mg/ml)*	*Theoretical capacity (μg/ml)*	*Observed capacity (μg/ml)*	*Specific activity of immobilized antibody (%)*
Fractogel	1.0	191	41	21
Fractogel	13.4	2554	350	14
Trisacryl	0.9	172	66	38
Trisacryl	1.2	228	71	31
CNBr-Sepharose	0.73	139	40	29
CNBr-Sepharose	7.3	1391	459	33

TABLE II

ANTIBODY DENSITY EFFECTS ON BINDING SITE HETEROGENEITY

Matrix	*Antibody density (mg/ml)*	*Heterogeneity*				
		Scatchard plot				*Sips plot*
		n (%)	*K (M^{-1}) (10^6)*	*n (%)*	*K (M^{-1}) (10^6)*	*a*
Fractogel	1.0	22	4.2	78	0.36	0.81
Fractogel	13.4	9	11.8	91	0.07	–
Trisacryl	0.9	100	8.4	–	–	0.92
Trisacryl	1.2	100	14.2	–	–	1.04

steric hinderance effects were not apparent for the Sepharose-based matrix consistent with a more open pore structure network for Sepharose compared to the Fractogel matrix. The result with CNBr-activated Sepharose 4B can be compared with the previous study of Eveleigh and Levy[9]. In their study a decrease in the specific activity from 21% to 18% was observed when the polyclonal anti HSA antibody density increased from 0.95 to 8.71 mg immobilized antibody per ml of resin. HSA is significantly larger than lysozyme (molecular weights 67 000 *vs.* 14 300) and hence more susceptible to steric hinderance effects.

The influence of ligand density on binding site heterogeneity

The influence of ligand density on binding site heterogeneity is summarized in Table II. The multi-compartmental influence of ligand density on the performance of antilysozyme–Fractogel HW65F support, was apparent when the extent of heterogeneity of the binding sites was quantitatively examined for the MAb-antigen interaction. In particular, a decrease in the proportion of high-affinity binding sites involved in the interaction was observed with immunoaffinity gels of higher antibody densities. Extrapolation of Steward–Petty and Scatchard plots were used to estimate the magnitude and proportion of high- and low-affinity sites over the investigated regions of the isotherms. These data indicated with an antibody density of 1 mg of immobilized antibody/ml of gel, 22% of binding sites could be classified as "high affinity". However, with an antibody density of 13.4 mg of immobilized antibody/ml of gel, only 9% of the total number of binding sites were of high affinity. This pattern can be clearly seen in Fig. 4A when the Scatchard plots for the Fractogel HW65F matrices are compared. In absolute terms, the total number of high-affinity binding sites of larger association constant(s) is greater with immunoaffinity matrices of higher antibody densities. In relative terms the proportion of high-affinity sites compared to low-affinity sites however become less abundant. Despite the relative change in the ratio of "high"- and "low"-affinity sites, the trend was evident that as the ligand density increased, the respective affinity constants of the high-affinity sites also increased. For example, almost a three-fold increase in the apparent affinity constant was observed for the MAb-based immunoaffinity system with the higher ligand density conditions on Fractogel HW65F. Furthermore, the increase in negative

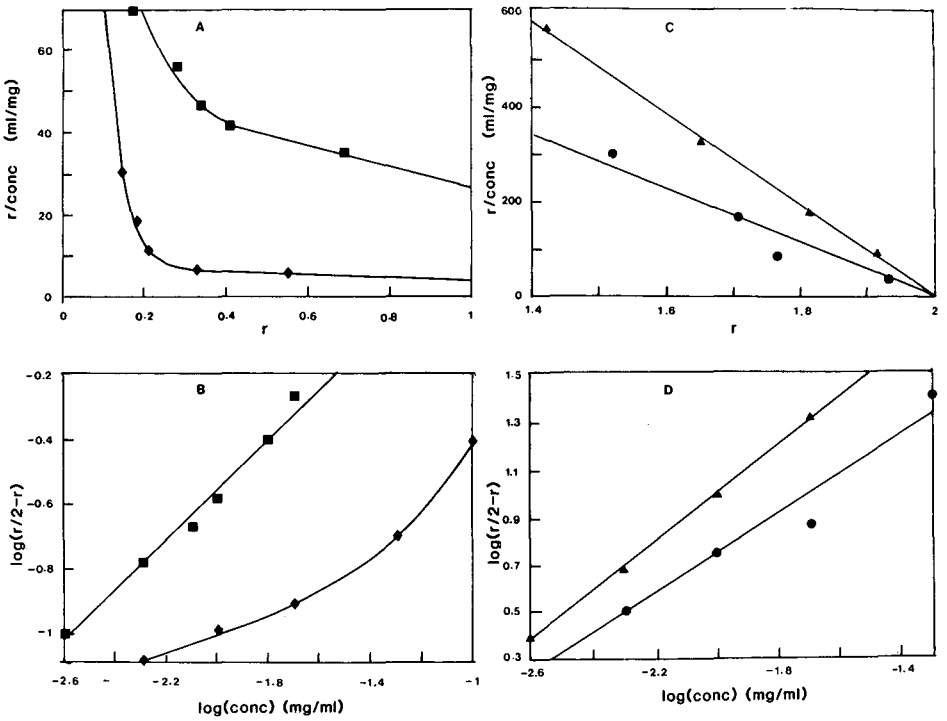

Fig. 4. Scatchard and Sips plots derived from the frontal analysis of antilysozyme immunoaffinity columns. (a) Antilysozyme–Fractogel columns. Scatchard and Sips plots are shown in Panels A and B, respectively. The activation level and immobilized monoclonal antibody concentrations were: ■: CDI per ml of Fractogel = 26 μmol; IgG per ml of Fractogel = 1.0 mg; ◆ = CDI per ml of Fractogel = 22 μmol; IgG per ml of Fractogel = 13.4 mg. (b) Antilysozyme–Trisacryl columns. Scatchard and Sips plots are shown in Panels C and D, respectively. ●: CDI per ml of Trisacryl = 2.0 μmol; IgG per ml of Trisacryl = 0.9 mg; ▲: CDI per ml of Trisacryl = 5.3 μmol; IgG per ml of Trisacryl = 1.2 mg.

cooperativity with the immunoaffinity gel of higher ligand density is clearly demonstrated by the Sips plot (Fig. 4B). With the immunoaffinity gel of low ligand densities (*e.g.* 1.0 mg of immobilized antibody/ml gel), the Sips plot showed slight curvature with the line of best fit having a gradient of *ca.* 0.8. At high ligand density (*e.g.* 13.4 mg immobilized MAb/ml gel) the Sips plot appeared to be curved with gradients ranging from 0.3 to 0.5 over the lysozyme concentration range of 10–50 μg/ml used for the adsorption studies.

Experimental data indicative of homogeneous binding of lysozyme was achieved using the Trisacryl matrix with low ligand density (*ca.* 1.2 and 0.9 mg of immobilized antibody/ml of gel). Scatchard and Sips plots for these low density immunoaffinity matrices are show in Fig. 4C and D. The results achieved using this Trisacryl immunoaffinity gel demonstrate that the negative cooperativity observed for the Fractogel system is not inherent to the interaction of lysozyme with the monoclonal antibody, *i.e.* steric hindrance and inhibition of binding of the lysozyme antigen to one paratope, caused by the prior binding of lysozyme to the other paratope, does not normally occur when the surface is designed to allow adequate spatial distribution of

TABLE III

THE INFLUENCE OF ACTIVATION LEVELS ON ANTIBODY ACCESSIBILITY

Matrix	*Molar excess of CDI to immobilized antibody*[a]	*Ligand density (mg/ml)*	*Specific activity (%)*
Fractogel	3900	1.0	21
Fractogel	250	13.4	14
Trisacryl	330	0.9	38
Trisacryl	660	1.2	31
	Relative excess[b] *of CNBr to immobilized antibody*		
CNBr-Sepharose	10	0.73	29
CNBr-Sepharose	1	7.3	33

[a] Activation levels were measured using ^{14}C-lysine and MAb immobilization was measured by determining incorporation of ^{125}I-MAb as described in the methods section.

[b] CNBr-activated Sepharose 4B was a commercial preparation (Pharmacia). The activation level of this resin was not determined. The difference in the ratio of CNBr groups to immobilized antibody was due to the difference in ligand density.

the immobilized MAb ligands and appropriate volume occupancy of the bound antigen.

The influence of activation levels on the specific activity of immobilized MAbs

The determination of activation levels and immobilization densities allows the calculation of the molar ratio (R) of CDI groups–immobilized antibody where:

$$R = \frac{\text{molar concentration of active CDI groups per ml of gel}}{\text{molar concentration of MAb immobilized per ml of gel}}$$

The influence of matrix activation levels on the subsequent specific activity of the immobilized MAbs is shown in Table III. The results show that for the Fractogel HW65F systems activated with very high levels of CDI prior to immobilization of the antibody (*i.e.* molar excess of CDI groups:immobilized MAb of 3900:1), the amount of antibody subsequently available to bind lysozyme was 21% of the total immobilized antibody concentration compared to 14% when the molar excess of CDI groups to immobilized MAb was 250:1. Data derived from the analysis of Trisacryl GF2000 systems showed that a doubling of the ratio of the concentration of CDI groups available for coupling to the concentration of immobilized antibody resulted in a change in the specific activity of immobilized antibody from 38% to 31%. With the CNBr-activated supports a 10-fold increase in the ratio of the concentration of CNBr activation groups to the concentration of immobilized MAb resulted in a decrease in antibody accessibility from 33% to 29%. Data from the analysis of CNBr-activated Sepharose and CDI-activated Fractogel HW65F resins shows that multisite attachment *per se* plays an insignificant role in the relative decline of the antigen binding capacity as the activation and immobilized antibody concentrations were increased.

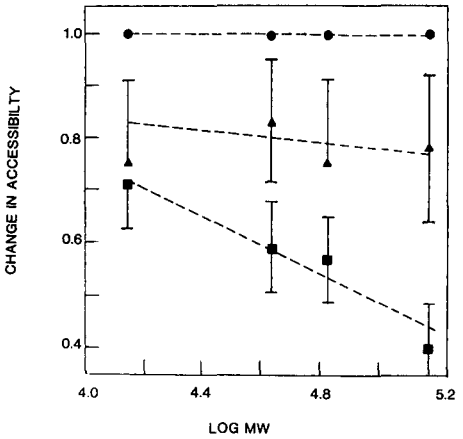

Fig. 5. The influence of CDI activation and IgG immobilization on the size-exclusion properties of Fractogel HW65F. Accessibility (A) was determined using the following formula:

$$A = \frac{V_e - V_0}{V_t - V_0}$$

Change in accessibility (A) was determined by dividing A values by the A value determined for native Fractogel. Analysis was carried out in 0.5 M sodium chloride, 8 M urea. Measurements were done using lysozyme (molecular weight, MW = 14 300), ovalbumin (43 000), bovine serum albumin (67 500) and bovine γ-globulin (150 000). ● = native Fractogel; ▲ = CDI-activated Fractogel (25 μmol/ml resin); ■ = IgG–Fractogel (13 mg/ml resin).

Consequently, other explanations involving MAb orientation at the surface, restricted access of the antigen to the immobilized MAbs due to steric compression or as a result of a decrease in pore volume following the activation or immobilization procedures, must also be considered.

The influence of CDI activation and antibody immobilization on size-exclusion properties of Fractogel HW65F

The above data suggest that significant steric hindrance between the antibody and the antigen occurs with immunoaffinity gels based on Fractogel HW65F and the other gels when antibodies are immobilized to high ligand densities. In order to determine the influence of CDI activation and antibody immobilization on solute accessibility, the size-exclusion properties of native Fractogel HW65F, CDI-activated Fractogel HW65F (25 μmol/ml) and antibody (bovine, 13 mg/ml of gel)-immobilized Fractogel HW65F were compared. Fig. 5 shows that solute accessibility is decreased by CDI activation. This result is in accord with other observations since CDI, and other chemical activation methods, are known to cause gel shrinkage associated with the cross linkage of the polymer chains of the matrix and reduction in pore volume[21]. Solute accessibility to the pores of CDI-activated Fractogel HW65F decreased by about 20% and showed little difference for solute molecules ranging in molecular mass from 14 000–150 000 dalton. A much greater decrease in solute accessibility within the pores was caused following antibody immobilization (at the level of 13 mg MAb/ml

gel) to the hydrophilic porous gels. Furthermore, solute accessibility decreased significantly as solute size increased with the antibody-Fractogel HW65F supports. The decrease in pore accessibility ranged from 30% for solute molecules of 14 000 dalton to between 50 and 60% with 150 000 dalton macromolecules.

SUMMARY AND CONCLUSIONS

The systems and protocols described in this manuscript permit rapid evaluation of the suitability of monoclonal antibodies in immunoaffinity chromatographic systems. Using the approaches which we have outlined, a large amount of experimental information can be derived about a particular immunoaffinity system under evaluation, and criteria for an optimal system determined. The use of mini columns permits pilot evaluations to be carried out with small amounts of valuable antibody and antigen, prior to the final decision being made on the preferred scale-up route. In practice the utility of this approach will depend on the ability to evaluate the concentration of the desired component in the column eluent. This can be achieved using radioactively labelled tracers, on-line assay systems or collection and assay of fractions over the breakthrough regions[10].

The efficiency with CDI-activated Fractogel HW65F of the monoclonal immunoaffinity systems described above, was significantly reduced by high ligand densities. The data indicate that increased ligand density resulted in an increase in the heterogeneity of the immunoaffinity system, and a decrease in the relative proportion of the immobilized antibody available to bind lysozyme. Size-exclusion data, demonstrated that high levels of CDI activation of Fractogel HW65F reduced solute accessibilities and therefore contributed to steric hinderance effects observed at high ligand densities. These data also illustrated that these effects are significantly magnified as the antigen size increases when using this matrix.

A further observation can be made relevant to the high-affinity sites of the two Fractogel supports, namely these sites were present in a lower proportion but exhibited higher affinities in the high-density gel than the low-density support over the same antigen concentration range. The opposite trend was evident observed for the low-affinity sites.

There are at least two explanations for these results both of which may contribute to the observed phenomena.

(i) The Fractogel matrix itself or multiple-site immobilization adversely influences lysozyme binding to the antibody. At higher ligand density externally immobilized antibodies are shielded from these effects by neighboring antibodies. However, within the matrix, crowding and matrix effects serve to lower antibody affinity constants.

(ii) At low ligand density the antibodies will be more evenly distributed throughout the outer region(s) of the matrix and will tend to be immobilized at or near the external surface of the gel. At high ligand densities antibodies are probably immobilized as a decreasing concentration gradient from the outer surface to the inner core of each particle. The theoretical treatments used above, were based on determination of the maximum capacities of the immunoaffinity gels and assumed even distribution of antibodies. If the antibody concentrations were locally higher (or lower) than determined then this would have contributed in the system as apparent heterogeneity of the affinity sites.

Differences in affinity constants for the Trisacryl resins could be measured despite the fact that these resins exhibited no or little apparent heterogeneity as assessed from the linearity of Sips and Scatchard plots. The immunoaffinity gel derived from the procedures using a higher ratio (R) of CDI to antibody immobilized exhibited the higher affinity constant. A possible explanation for this result is that immobilization of the MAb on the more highly activated support resulted in a greater proportion of antibody being externally immobilized. The data also demonstrate that immobilization involving the use of preactivated gels with high proportions of active groups to immobilized antibody will not necessarily lead to a decrease in the proportion of the immobilized antibody available to bind antigen. This finding is consistent with the observations of Eveleigh and Levy[9] for CNBr-activated Sepharose 4B–HSA polyclonal immunoaffinity system. The significance of these results is that highly activated resins (provided the activation has not severely compromised mass transfer properties of the gel as illustrated for Fractogel HW65F) may be suitable for the immobilization of antibodies and indeed may be preferred to low activation levels as increased stability of immobilized antibody can be anticipated using such supports. Under such conditions, a statistically high percentage of immobilized antibody molecules will be immobilized on the exterior surfaces of the support thus generating improved kinetics for antigen adsorption/desorption. The use of highly activated supports should also ensure a more complete reaction of antibody at during the immobilization step.

The experimental results also demonstrate there is little to be gained by attempting to immobilize saturation levels of antibody onto a porous matrix such as Fractogel (*i.e.* to make very high-density immunoaffinity supports), to maximise the use of the active groups and thus reduce the frequency of immobilization sites per MAb molecule, during the coupling step. When antigens with medium to high molecular weights are to be isolated (*e.g.* proteins with molecular mass between 20 000 and 250 000 dalton) such practices are likely to significantly decrease the accessibility of immobilized MAb in the immunoaffinity system. Reduced accessibility to ligands will result in wastage of valuable antibody, and decreased separation performance in terms of resolution and system productivity. The above conclusion is in concordance with previous studies using polyclonal immunoaffinity systems with Sepharose 4B and porous glass supports[9,21] and suggest the need for immunoaffinity systems based on mechanically stable non-porous or pellicular chromatographic medium. Such systems are likely to be of great benefit in the preparation of immunoaffinity supports for large proteins (*e.g.* factor VIII). They should also permit the synthesis of relatively homogeneous systems. This in turn should greatly enhance the predictability of these systems on scale up.

ACKNOWLEDGEMENTS

These studies were supported by the Commonwealth Serum Laboratories (CSL), Parkville, Victoria, Australia and form part of the Ph.D. dissertation of J. Davies. Monoclonal antibody was prepared for this project by Dr. A. McGregor and staff at CSL. The encouragement of the CSL Research Director (Dr. P. Schiff) and associated colleagues is acknowledged.

REFERENCES

1 E. Hochuli, *Chimia*, 40 (1986) 408–412.
2 S. J. Tarnowski and R. A. Liptak, Jr., in A. Mizraki and A. L. van Wezel (Editors), *Advances in Biotechnological Processes*, Vol. 2, A. R. Liss, New York, 1983, pp. 271–287.
3 B. Junming Le, S. Barraclough and J. Vilcek, *J. Immunol. Methods*, 69 (1984) 61–70.
4 H. P. Muller, N. H. Vantilburg, J. Derks, E. Kleinbreteler and R. M. Bertin, *Blood*, 58 (1981) 100–106.
5 T. S. Zimmerman and S. Fulcher, *U.S. Pat.*, 4361 509 (1982).
6 C. T. Esmon, F. B. Taylor, L. B. Hinshaw, A. Chang, P. C. Comp, G. Ferrell and N. L. Esmon, *Dev. Biol. Stand.*, 67 (1986) 51–57.
7 A. H. Goodall, G. Kemble, D. P. O'Brien, E. Rawlings, F. Rotblat, G. C. Russelli, G. Janossy and E. G. D. Tuddenham, *Blood*, 59 (1982) 664–670.
8 U-H. Stenman, M-L. Sutinen, R-K. Selander, K. Tontii and J. Schroder, *J. Immunol. Methods*, 46 (1981) 337–345.
9 J. W. Eveleigh and D. E. Levy, *J. Solid Phase Biochem.*, 2 (1977) 67–80.
10 H. A. Chase, *Chem. Eng. Sci.*, 39 (1984) 1099–1125.
11 A. Lundbland, K. Schroer and D. Zopf, *J. Immunol. Methods*, 40 (1984) 297–301.
12 R. M. E. Parkhouse, *Br. Med. Bull.*,40 (1984) 297–301.
13 C. Schneider, R. A. Newman, D. R. Sutherland, V. Asser and M. F. Greaves, *J. Biol. Chem.*, 257 (1982) 10766–10769.
14 P. Crautrecases and C. B. Anfinsen, *Methods Enzymol.*, 34 (1974) 345–378.
15 H. A. Chase, *J. Biotechnol.*, 1 (1984) 67–80.
16 G. J. Calton, in I. M. Chaiken, M. Wilchek and I. Parikh (Editors), *Affinity Chromatography and Biological Recognition*, Academic Press, London, 1983, pp. 383–391.
17 J. W. Eveleigh, in T. C. J. Gribrau, J. Visser and R. J. F. Nivard (Editors), *Affinity Chromatography and Related Techniques*, Elsevier, Amsterdam, 1982, pp. 293–303.
18 A. L. van Wezel and P. van der Marel, in T. C. J. Gribrau, J. Visser and R. J. F. Nivard (Editors), *Affinity Chromatography and Related Techniques*, Elsevier, Amsterdam, 1982, pp. 283–292.
19 J. W. Goding, *Monoclonal Antibodies—Principles and Practice*, Academic Press, Orlando, FL, 1983, pp. 188–207.
20 R. Kowal and R. G. Parsons, *Anal. Biochem.*, 102 (1980) 72–76.
21 M. T. W. Hearn, *J. Chromatogr.*, 376 (1986) 245–257.
22 K-I. Kasai, Y. Oda, M. Nishikata and S-I. Ishii, *J. Chromatogr.*, 376 (1986) 33–47.
23 F. L. de Vos, D. M. Robertson and M. T. W. Hearn, *J. Chromatogr.*, 392 (1987) 17–32.
24 M. W. Steward and R. E. Petty, *Immunology*, 23 (1972) 881.
25 M. W. Steward and J. Stensgaard, *Antibody Affinity —Thermodynamic Aspects and Biological Significance*, CRC Press, Boca Raton, FL, 1983, pp. 1–9.
26 G. Scatchard, *Ann. N.Y. Acad. Sci.*, 51 (1949) 660.
27 R. Sips, *J. Chem. Phys.*, 16 (1948) 490.
28 W. M. Hunter and F. C. Greenwood, *Nature (London)*, 194 (1962) 495.
29 M. Wilchek, T. Oka and Y. J. Topper, *Proc. Natl. Acad. Sci. U.S.A.*, 72 (1975) 1055–1058.
30 M. T. W. Hearn, *Methods Enzymol.*, 135 (1987) 102–107.
31 G. S. Bethall, J. S. Ayres, W. S. Hancock and M. T. W. Hearn, *J. Biol. Chem.*, 254 (1979) 2572–2576.
32 C. Longstaff, in P.D. G. Dean, W. S. Johnson and F. A. Middle (Editors), *Affinity Chromatography—A Practical Approach*, IRL Press, Oxford, 1985, pp. 31–32.

Journal of Chromatography, 512 (1990) 41–56
Elsevier Science Publishers B.V., Amsterdam

CHROMSYMP. 1933

High-performance liquid chromatography of amino acids, peptides and proteins

XCVIII[a]. The influence of different displacer salts on the bandwidth properties of proteins separated by gradient elution anion-exchange chromatography

A. N. HODDER, M. I. AGUILAR and M. T. W. HEARN*
Department of Biochemistry and Centre for Bioprocess Technology, Monash University, Clayton, Victoria 3168 (Australia)

ABSTRACT

The influence of eight different displacer salts on the bandwidth properties of four globular proteins separated by a high-performance anion-exchange chromatography has been investigated. Proteins were eluted under gradient conditions with a range of alkali metal halide salts, in which the anion and cation were varied in the series F^-, Cl^- and Br^- and Li^+, Na^+ and K^+, respectively. The experimentally observed bandwidths ($\sigma_{v,exp}$) were found to deviate significantly from peak widths ($\sigma_{v,calc}$) predicted on the basis of plate theory for small molecules. For data accumulated under conditions of varied gradient time and constant flow-rate the solute bandwidth ratios ($\sigma_{v,exp}/\sigma_{v,calc}$) increased in the order $Br^- < Cl^- < F^-$ at low values of the gradient steepness parameter, *b*, or increasing column residence times. In addition, systematic changes in the cation influenced the bandwidth ratios ($\sigma_{v,exp}/\sigma_{v,calc}$) in the order $K^+ < Na^+ < Li^+$. Significant deviations between predicted and observed bandwidth values were also observed under elution conditions of constant gradient time and varied flow-rate. The results of the present study further demonstrate the complex nature of the interaction between protein solutes and coulombic chromatographic surfaces.

INTRODUCTION

Our understanding of the physicochemical basis of the high-performance ion-exchange chromatography (HPIEC) of proteins has increased significantly over recent years due to the availability of retention models to assess protein chromato-

[a] For part XCVII, see ref. 23.

0021-9673/90/$03.50

graphic behaviour. In particular, the application of stoichiometric displacement models[1,2] and the linear solvent strength (LSS) model[3], have considerably facilitated the quantitative evaluation of the influences on protein retention of the mobile phase pH, displacer salt concentration, the type of displacer salt and the elution mode[1,4–9].

Despite the widespread application of HPIEC in the purification of biomacromolecules, relatively little work has focused on mobile phase factors contributing to bandbroadening or methods to characterise the origin of zone spreading due to stationary phase induced phenomena. Recently, the LSS model has incorporated the general plate-height theory to provide a quantitative, descriptive model to estimate solute bandwidths associated with the elution conditions employed in HPIEC[9]. This approach has provided a useful basis for selecting criteria to optimise protein separations and enables investigations into the chromatographic behaviour of the HPIEC of proteins to assume quantitative, rather than qualitative details. This paper further investigates the application of these theoretical approaches for predicting protein bandwidth behaviour in gradient high-performance anion-exchange chromatographic systems. In particular, the effects of mobile phase composition and the gradient elution mode on peak widths associated with the mass transport of the globular proteins, lysozyme, myoglobin, carbonic anhydrase and ovalbumin as they migrate along a quaternary ammonium sorbent were investigated.

MATERIALS AND METHODS

All chromatographic experiments were performed with a Pharmacia (Uppsala, Sweden) fast protein liquid chromatographic (FPLC) system, as previously described[6]. All chemicals and reagents used and experimental chromatographic procedures have also been given in detail in previous studies[5,7,8]. Gradient bandwidth parameters ($\sigma_{v,calc}$, $\sigma_{v,exp}/\sigma_{v,calc}$, G, C, B, D_m and N) were calculated using the Sigma programme written in this laboratory in Basic language for IBM AT computers. The input values required for this programme were T, η, t_o, MW, d_p, a', log C_f/C_o, F, Z_c, b, t_G and $\sigma_{v,exp}$.

RESULTS AND DISCUSSION

Theoretical gradient bandwidth relationships

The general plate-height theory provides a basis for assessing the diffusional behaviour of small molecules in chromatographic systems. Snyder and co-workers[3,10] have extended the use of retention parameters derived from the LSS model[3] in conjunction with the plate-height theory to provide a method for predicting solute bandwidths so that overall chromatographic resolution can be evaluated and optimised. Using this elegant method of approach, reversed-phase high-performance liquid chromatographic (HPLC) studies (see for example ref. 4) with small peptides and some small proteins have shown good correlations between the experimentally and theoretically derived solute bandwidths. Recently, this approach has been adapted by Stout *et al.*[10] for the analysis of high-performance ion-exchange bandbroadening data. In these studies, good correlations were observed between the experimental and calculated bandwidths for lysozyme and ribonuclease A eluted using sodium acetate as the displacer salt with the DuPont Zorbax Bio-Series SCX, WCX, SAX and WAX strong and weak cation and anion exchangers.

While different salts have been known for many years to strongly influence protein retention in HPIEC, their influence on protein bandwidths has not generally been as fully assessed. The present paper specifically addresses the important issue of choice of monovalent salts. Associated studies to be reported from this laboratory have also examined the effect of di- and polyvalent ions on bandbroadening of proteins in HPIEC. Under ideal HPIEC conditions of gradient elution, the relationship between peak width, represented by $4\sigma_v$, and the median capacity factor, $\bar{k}$, for linear solvent systems can be expressed[3] as

$$\sigma_{v,calc} = [(\bar{k}/2) + 1]\, G V_m N^{-1/2} \tag{1}$$

where V_m is the column void volume ($V_m = t_o F$, t_o is the retention time of an unretained compound, F is the flow-rate), N is the plate number and G is the band-compression factor[3,10] which arises from the increase in solvent strength across the solute zone as the gradient develops along the column. The parameter G is given by the expression

$$G^2 = [1 + 2.3b + 1/3(2.3b)^2]/(1 + 2.3b)^2 \tag{2}$$

where b is the gradient steepness parameter. Under flow-rate conditions typically used in gradient elution HPLC, N can be approximated to

$$N = D_m t_o \,/\, C d_p^2 \tag{3}$$

where d_p is the particle diameter. The diffusion coefficient, D_m, of the solute in the mobile phase can be expressed in terms of solute molecular weight (MW) as

$$D_m = 8.34 \cdot 10^{-10} T \,/\, \eta\, (\mathrm{MW})^{1/3} \tag{4}$$

where T is the absolute temperature and η is the eluent viscosity. The Knox equation parameter, C, which accounts for resistance to mass transfer at the stationary phase surface can be estimated from

$$C = \frac{[(1 - x + \bar{k}) \,/\, (1 + \bar{k})]^2}{15\rho^* a' + 15\rho^* b'\bar{k} - 19.2\rho^* x} \tag{5}$$

where x is the interstitial column fraction, found to be 0.62 for the Mono-Q anion exchange sorbent in well packed columns[12], a' is assumed to equal 1.1, and the term b' is the surface diffusion parameter, calculated from the relationship

$$B = a' + b'k \tag{6}$$

The Knox equation constant, B, which arises from zonal dispersion due to longitudinal diffusion, was previously determined[9] in this laboratory from isocratic bandwidth data at different flow-rates and substituted into eqn. 6 to obtain a value of b' equal to

0.72. The restricted diffusion parameter, ρ^*, a molecular-weight-dependent term, was calculated by using the Renkin relationship so that

$$\rho^* = 1 - 2.104\rho + 2.09\rho^3 - 0.95\rho^5 \quad (7)$$

where ρ is equal to the ratio of the solute diameter to the sorbent pore diameter (s_d/p_d). The linear logarithmic relationship (correlation coefficient, $r^2 = 0.99$) found[9] experimentally between ρ^* and solute MW for a Mono-Q column, assuming an average pore size of 800 Å and a protein molecular-weight range between 12 000 and 69 000 daltons was

$$\log \rho^* = 0.19 - 0.06 \log \mathrm{MW} \quad (8)$$

The use of the general plate height theory to derive the above bandwidth relationships, and in particular eqns. 1–5, assumes that the solute migrates as a unique, conformationally rigid molecule. With a particular sorbent, fixed salt and defined set of elution conditions the influences of secondary multimodel retention processes due to the interplay of coulombic and hydrophobic effects on bandbroadening are anticipated to make essentially constant contributions to σ_v over the linear operational range of $\bar{k}$ values. In addition, it is generally accepted that peptides and proteins can explore a variety of conformations in solution. These secondary equilibria processes can also be further enhanced or inhibited by the presence of either chaotropic or kosmotropic salts in the chromatographic eluent. If it is assumed that these conformational processes or any additional secondary phenomena, such as monomer–oligomer, or subunit association–dissociation, are extremely rapid compared to the chromatographic separation time, then the ratio between the experimentally observed bandwidth $\sigma_{v,exp}$ and the bandwidth $\sigma_{v,calc}$, determined by eqn. 1, should approach unity over the normal operational range or retention values commonly used in optimisation studies, *i.e.* $1 < \bar{k} < 10$. Similar considerations will also apply when these secondary processes are relatively slow with regard to chromatographic mass transfer. Under these conditions, the protein or peptide solute will effectively migrate as a single time averaged conformer. Such migratory behaviour can be considered "ideal", although divergence from the small molecule plate theory can still be anticipated due to differences in the hydrodynamic shape of various biosolutes, *e.g.* differences arising between globular and ellipsoidal proteins in terms of their intrinsic radii of gyration and molecular weights and their consequences for the calculation of effective D_m values (*cf.* eqn. 5).

However, if time-dependent, mobile or stationary phase induced changes in the secondary, tertiary or quaternary structure of the protein or peptide solute occur with similar time scales as the chromatographic migration, the resulting changes in the diffusional and interactive properties of the solute will lead to a pattern of differential zone migration which is more complex than that anticipated by conventional plate height theory. Two cases of such complex bandbroadening behaviour can be especially identified. The first relates to significant alteration in the molecular dimensions of the peptide or protein solute in the bulk mobile phase due to specific ion interactions affecting the solvated structure, *e.g.* congruent and non-congruent mobile phase unfolding–refolding processes which also have similar half-lives to the separation trans-

port time. The second case relates to changes in the shape and surface topography of the solute as it binds, re-orientates or subsequently desorbs from the sorbent surface, *e.g.* stationary phase induced processes where the apparent time for interconversion is similar to the mass transfer time. These types of kinetic changes in the macroscopic properties of the biosolute will ultimately be revealed as experimental bandwidths which deviate from the values predicted by eqn. 1 with $\sigma_{v,exp}/\sigma_{v,calc}$ becoming significantly greater than unity.

The influence of displacer salt type on solute bandwidth behaviour under conditions of varied gradient time and constant flow-rate

It is well known that many characteristics of the mobile phase can be altered to influence protein retention behaviour in HPIEC[1–10,12–14]. However, there have been relatively few systematic investigations into the effects of the mobile phase composition on protein bandwidth behaviour. Such studies are of importance for the optimisation of sample resolution as well as the preservation of the native structure of the biosolute through minimisation of adverse mobile or stationary phase induced secondary equilibria.

Recently, the LSS theory has been utilised to analyse bandwidth data obtained for several proteins eluted with sodium chloride from a Mono-Q strong anion-exchange column under conditions of varied gradient time and constant flow-rate[9]. In this earlier investigation, variation in the rate of change of the displacer salt, associated with differences in gradient time, was found to dramatically affect the kinetic processes for several protein solutes, *e.g.* ovalbumin, bovine carbonic anhydrase and sperm whale myoglobin. In particular, increased column residence times resulted in significant deviations from the calculated bandwidths, obtained using eqns. 1–8. The divergencies from the predicted peak width were attributed to solute-specific physicochemical phenomena, (the so-called column "dwell" effect) associated with solute solvation or changes in the approach depth of the penetration of the protein at or near the Stern double layer.

In the present study, the effect of systematic changes in the displacer salt composition on protein bandwidth behaviour has been investigated under elution conditions of varied gradient time and constant flow-rate. The proteins listed in Table I were eluted from a Mono-Q strong anion-exchange column by salt gradients (0 to 300 m*M*) varying in time from 8.6 to 171.4 min at a constant flow-rate of 1 ml/min. Eluents A (20 m*M* piperazine) and B (20 m*M* piperazine and 300 m*M* displacer salt)

TABLE I

PROTEIN PHYSICAL PROPERTIES

Protein	*MW*	D_m[a] (m^2/min)
Ovalbumin	43 000	4.24
Carbonic anhydrase	30 000	4.80
Myoglobin	17 500	5.74
Lysozyme	14 300	6.12

[a] Calculated from eqn. 5.

were adjusted to pH 9.6 by the addition of either HF, HCl or HBr as appropriate for the salt type. Theoretical bandwidth values were calculated, using eqn. 1, over the range of experimental conditions used to elute each protein solute. These values were then compared to the corresponding experimental bandwidths and plotted as a function of the reciprocal of the gradient steepness parameter, b.

Figs. 1–6 show plots of $\sigma_{v,exp}/\sigma_{v,calc}$ as a function of $1/b$ for (a) carbonic anhydrase, (b) myoglobin, (c) ovalbumin and (d) lysozyme eluted with LiCl, LiBr, NaF, NaCl, NaBr, KF, KCl and KBr. These figures reveal that each salt type influences protein mass transfer in a unique manner, with the largest deviations from unity for the $\sigma_{v,exp}/\sigma_{v,calc}$ ratio occuring with decreasing b values or increased column residence times. At higher b values, associated with relatively large rates of change in the displacer salt (*i.e.* 17.5 and 35 mM/min) and decreased residence times, the $\sigma_{v,exp}/\sigma_{v,calc}$ ratios were generally found to approach unity as the participation of secondary equilibria effects were reduced. In some instances, for example, carbonic anhydrase eluted with NaF or KCl (Figs. 2a and 3a) or ovalbumin eluted with NaF or KF (Figs. 2c and 3c) the $\sigma_{v,exp}/\sigma_{v,calc}$ values initially decrease with decreasing b values then passed through a minimum at or near unity before increasing again with smaller b values.

The bandwidth ratios for lysozyme shown in Figs. 1–6d were much larger than those observed for the other three proteins evaluated in this study. These values were in the order of magnitude of $5 \leqslant \sigma_{v,exp}/\sigma_{v,calc} \leqslant 60$. Currently, LSS theory has no

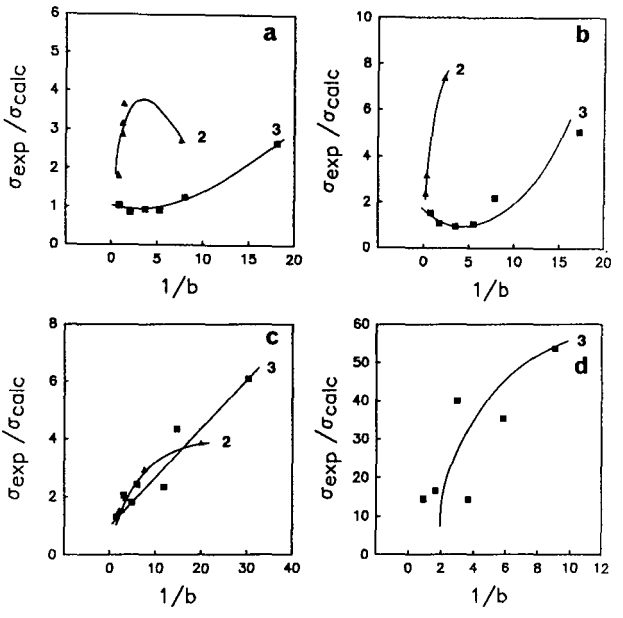

Fig. 1. The influence of anion type on the dependence of $\sigma_{v,exp}/\sigma_{v,calc}$ *versus* $1/b$ for (a) carbonic anhydrase, (b) myoglobin, (c) ovalbumin and (d) lysozyme. Bandwidth data were derived as a result of systematic changes in the anions of lithium salts where ▲ or 2 = LiCl and ■ or 3 = LiBr. Data were acquired under conditions of varied gradient time at a flow-rate of 1 ml/min as described in the Materials and Methods section, $\sigma_{v,calc}$ was evaluated using eqn. 1.

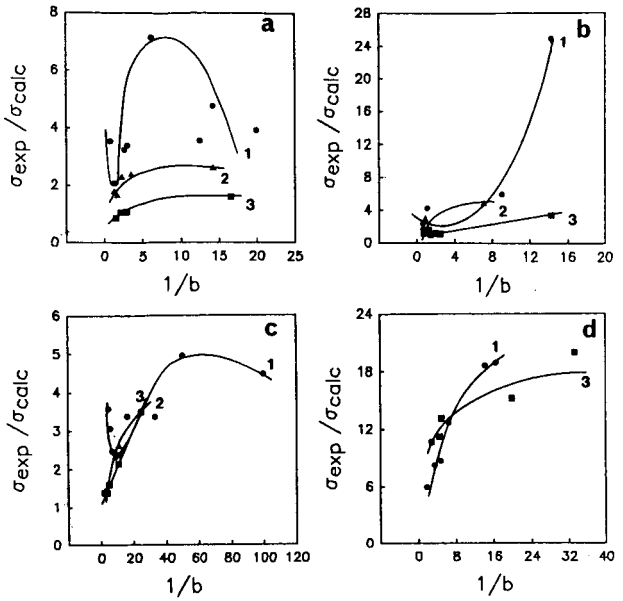

Fig. 2. The influence of anion type on the dependence of $\sigma_{v,exp}/\sigma_{v,calc}$ *versus* $1/b$ for (a) carbonic anhydrase, (b) myoglobin, (c) ovalbumin and (d) lysozyme. Bandwidth data were derived as a result of systematic changes in the anions of sodium salts where ● or 1 = NaF, ▲ or 2 = NaCl and ■ or 3 = NaBr. See Fig. 1 for other details.

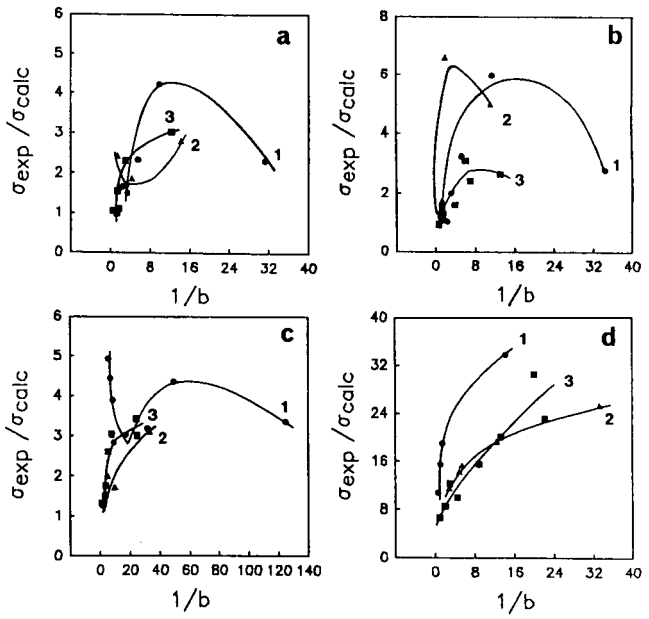

Fig. 3. The influence of anion type on the dependence of $\sigma_{v,exp}/\sigma_{v,calc}$ *versus* $1/b$ for (a) carbonic anhydrase, (b) myoglobin, (c) ovalbumin and (d) lysozyme. Bandwidth data were derived as a result of systematic changes in the anions of potassium salts where ● or 1 = KF, ▲ or 2 = KCl and ■ or 3 = KBr. See Fig. 1 for other details.

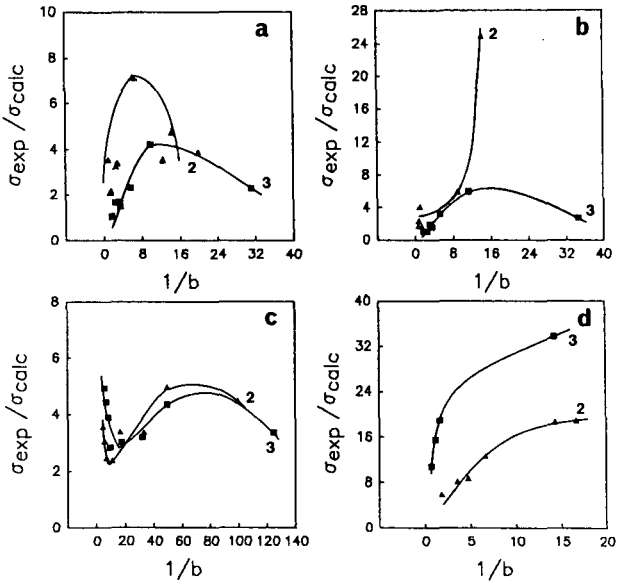

Fig. 4. The influence of cation type on the dependence of $\sigma_{v,exp}/\sigma_{v,calc}$ *versus* $1/b$ for (a) carbonic anhydrase, (b) myoglobin, (c) ovalbumin and (d) lysozyme. Bandwidth data were derived as a result of systematic changes in the cations of fluoride salts where ▲ or 2 = NaF and ■ or 3 = KF. See Fig. 1 for other details.

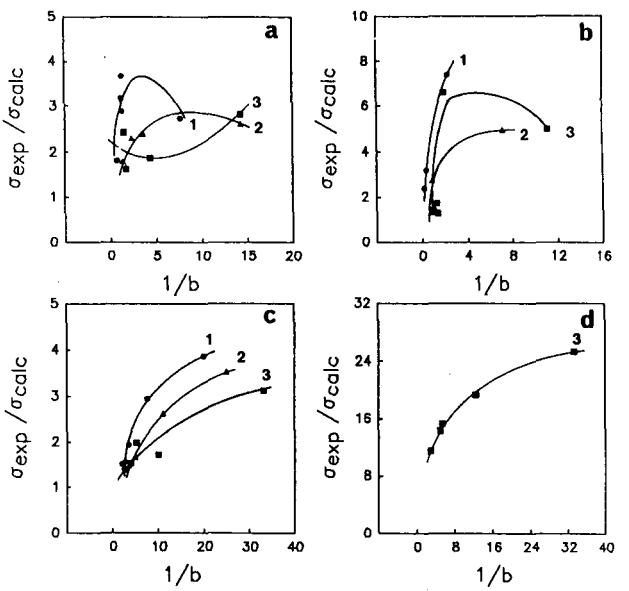

Fig. 5. The influence of cation type on the dependence of $\sigma_{v,exp}/\sigma_{v,calc}$ *versus* $1/b$ for (a) carbonic anhydrase, (b) myoglobin, (c) ovalbumin and (d) lysozyme. Bandwidth data were derived as a result of systematic changes in the cations of bromide salts where ● or 1 = LiBr, ▲ or 2 = NaBr and ■ or 3 = KBr. See Fig. 1 for other details.

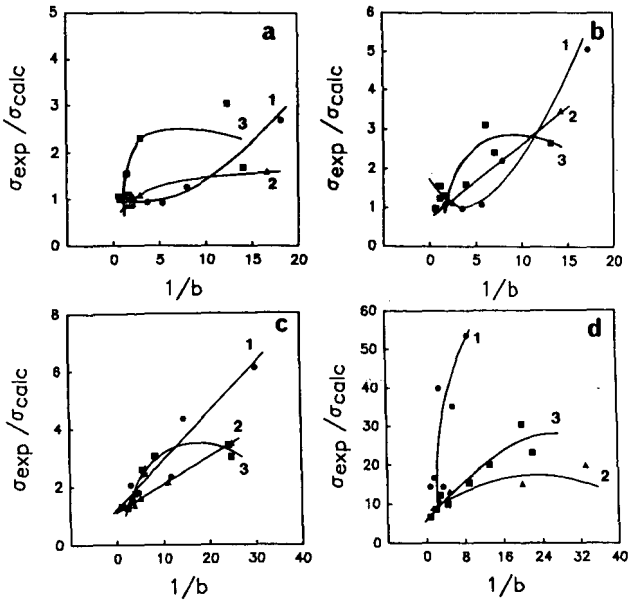

Fig. 6. The influence of cation type on the dependence of $\sigma_{v,exp}/\sigma_{v,calc}$ *versus* $1/b$ for (a) carbonic anhydrase, (b) myoglobin, (c) ovalbumin and (d) lysozyme. Bandwidth data were derived as a result of systematic changes in the cations of bromide salts where ● or 1 = LiCl, ▲ or 2 = NaCl and ■ or 3 = KCl. See Fig. 1 for other details.

provision to account for secondary equilibrium processes such as the hinge motion of the lysozyme domains[15,16] or the dimerisation/polymerisation of lysozyme reported[17–19] to occur at high pH values. Participation of these effects would result in the predicted bandwidth values being much smaller than the experimental bandwidths due to the errors in the calculation of, for example, the diffusion coefficient, D_m and the Knox parameter C.

The data in Figs. 1–6 demonstrate that changes in both the anion or cation species of the displacer salt can dramatically influence protein bandwidths under otherwise identical settings of chromatographic parameters. These data demonstrate that the selection of the most appropriate displacer salt to minimise secondary equilibria effects is clearly essential if optimisation of the resolution behaviour of proteins is to be achieved. For example, salt systems could be empirically selected which provide apparently equivalent behaviour under one set of chromatographic parameters, *e.g.* gradient time, gradient shape, etc., but which generate dramatically different resolution behaviour under another set. This type of behaviour is demonstrated in the band broadening effects of the displacer anion type, *i.e.* F^- to Cl^- to Br^-, with the selected proteins. Under the elution conditions used with high b values, the plots of $\sigma_{v,exp}/\sigma_{v,calc}$ *versus* $1/b$ for the various proteins were frequently coincidental with no apparent preference for a particular salt system evident. However, when small b values or increased column residence times were used, salt specific trends in protein bandwidth behaviour emerged. For example, it was found for the anion series with the lithium, sodium and potassium salts that the bandwidth ratios for each protein

increased in the order $Br^- < Cl^- < F^-$. Systematic changes in the cation species as the fluoride, chloride and bromide salts also influenced protein bandwidth ratios, which increased in the order $K^+ < Na^+ < Li^+$. These results also indicate that the influence of the anion or cation series on the $\sigma_{v,exp}/\sigma_{v,calc}$ ratio was independent of the type of counter ion species present in the displacer salt.

These dependencies of σ_v on salt type can be contrasted to the results observed for anion and cation effects on the value of the slope term Z_c derived from plots of log k' *versus* log $1/c$ (where c = displacer salt concentration) for the same proteins reported previously[6,7]. The effects of various combinations of anions and cations on Z_c values were found to be additive in terms of their position in the lyotropic series. Significant changes in Z_c represent structural variations in the chemical composition or charge density of the solute binding site(s) [the ionotope(s)]. Thus, the two fundamental chromatographic parameters, namely average retention or k', and peak variance σ_v^2, which reflect changes in the thermodynamic and kinetic properties of the ionotopic structure of the solute during column migration respond differently to the type of anion and cation species present in the displacing salt.

The influence of displacer salt type on solute bandwidth behaviour under conditions of varied flow-rate and constant gradient time

As evident from the preceding data, longer gradient times promoted experimental bandwidths which were larger than predicted by eqn. 1. Inspection of the same

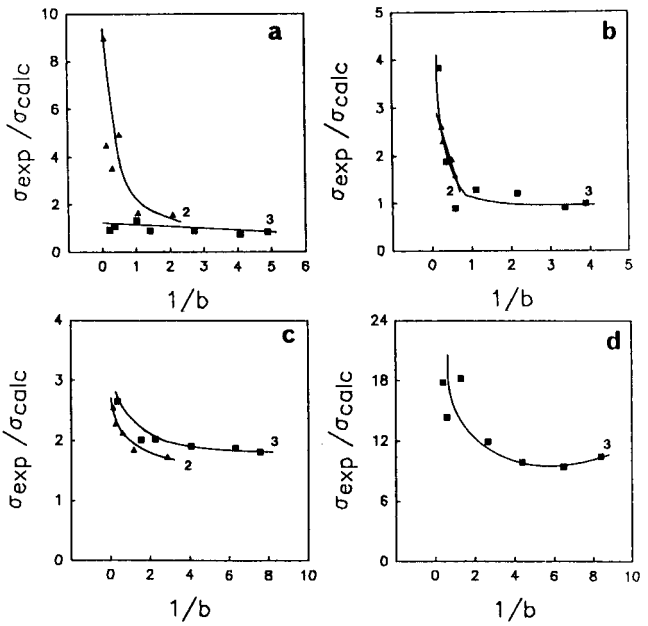

Fig. 7. The influence of cation type on the dependence of $\sigma_{v,exp}/\sigma_{v,calc}$ *versus* $1/b$ for (a) carbonic anhydrase, (b) myoglobin, (c) ovalbumin and (d) lysozyme. Bandwidth data were derived as a result of systematic changes in the cations of lithium salts where ▲ or 2 = LiCl and ■ or 3 = LiBr. Data were acquired under conditions of varied flow-rate at a gradient time of 17.1 min as described in the Materials and Methods section. $\sigma_{v,calc}$ was evaluated using eqn. 1.

data also revealed that peak broadening, presumably due to secondary equilibria effects influencing protein diffusional properties, could be minimised by reducing the column residence time, such that the gradient time (t_G) < 20 min. To gain further insight into this phenomenon, the influence of displacer salt type on protein bandwidth behaviour was investigated using varied flow-rate and constant gradient time conditions with t_G set at 17.1 min.

Figs. 7–12 show comparisons of the ratio of experimental solute bandwidth, $\sigma_{v,exp}$, to the predicted solute bandwidth, $\sigma_{v,calc}$, as a function of the reciprocal of the gradient steepness parameter, b. Plots of $\sigma_{v,exp}/\sigma_{v,calc}$ *versus* $1/b$ were found to decrease with increasing flow-rate or decreasing b values. With myoglobin, carbonic anhydrase and ovalbumin these curves generally approached unity as the flow-rates became $\geqslant$ 0.5 ml/min. The bandwidth curves for lysozyme were an exception to this observation. Figs. 7–12d show bandwidth ratios in the order of $5 < \sigma_{v,exp}/\sigma_{v,calc} < 20$ for lysozyme eluted with various salts. The known[15–19] polymerisation or hinge motion of lysozyme at high pH values could account for this behaviour and significantly influence the diffusional properties of this protein resulting in larger than predicted experimental bandwidths. These observations are consistent with those in the previous section and further exemplify the inability of the plate theory of small molecules to accommodate for these types of secondary equilibria with proteins such as lysozyme.

Large $\sigma_{v,exp}/\sigma_{v,calc}$ ratios were also observed for ovalbumin eluted with either NaF or KF (Figs. 8c, 9c and 10c). The poor displacing ability of these fluoride salts results in very small b values and the slow desorption kinetics. Consequently, oval-

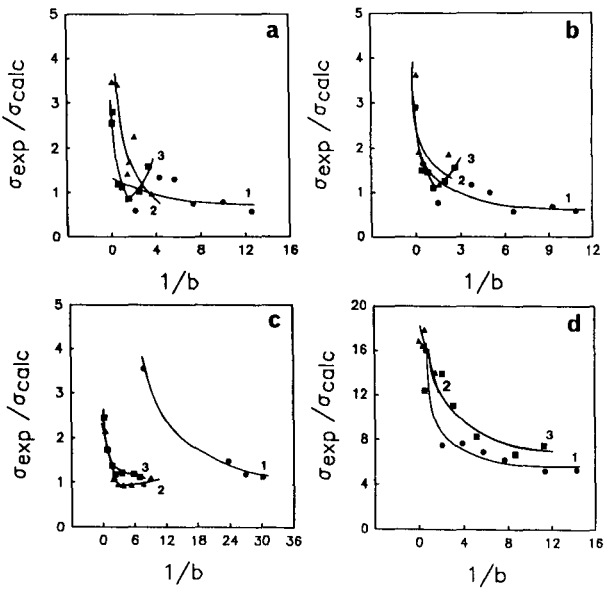

Fig. 8. The influence of cation type on the dependence of $\sigma_{v,exp}/\sigma_{v,calc}$ *versus* $1/b$ for (a) carbonic anhydrase, (b) myoglobin, (c) ovalbumin and (d) lysozyme. Bandwidth data were derived as a result of systematic changes in the cations of sodium salts where ● or 1 = NaF, ▲ or 2 = NaCl and ■ or 3 = NaBr. See Fig. 7 for other details.

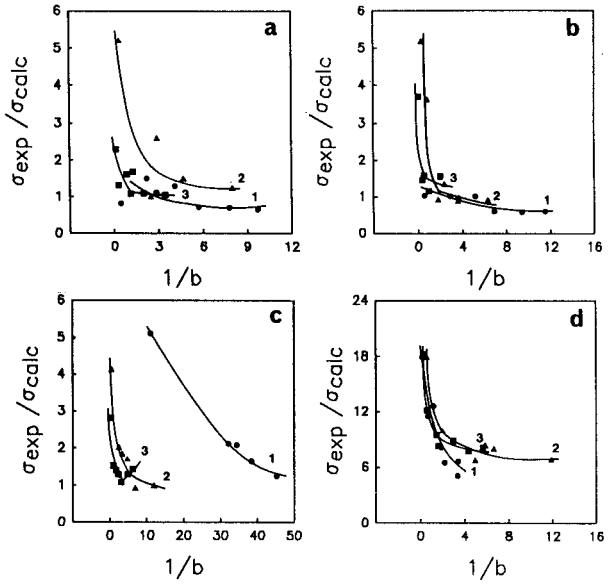

Fig. 9. The influence of cation type on the dependence of $\sigma_{v,exp}/\sigma_{v,calc}$ *versus* $1/b$ for (a) carbonic anhydrase, (b) myoglobin, (c) ovalbumin and (d) lysozyme. Bandwidth data were derived as a result of systematic changes in the cations of potassium salts where ● or 1 = KF, ▲ or 2 = KCl and ■ or 3 = KBr. See Fig. 7 for other details.

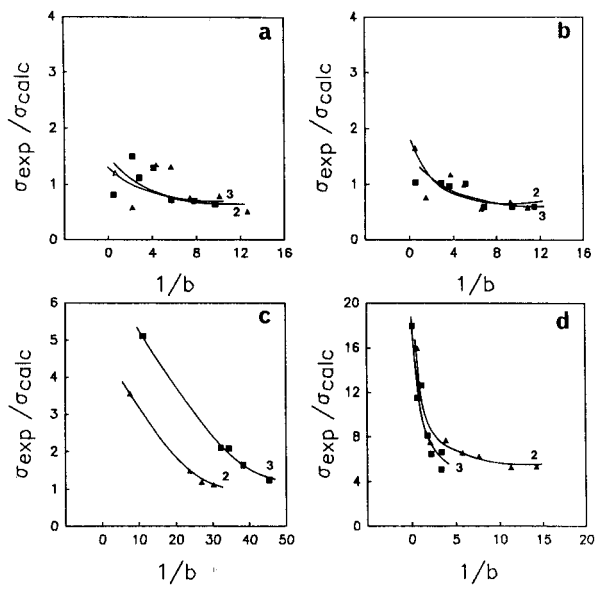

Fig. 10. The influence of cation type on the dependence of $\sigma_{v,exp}/\sigma_{v,calc}$ *versus* $1/b$ for (a) carbonic anhydrase, (b) myoglobin, (c) ovalbumin and (d) lysozyme. Bandwidth data were derived as a result of systematic changes in the cations of fluoride salts where ▲ or 2 = NaF and ■ or 3 = KF. See Fig. 7 for other details.

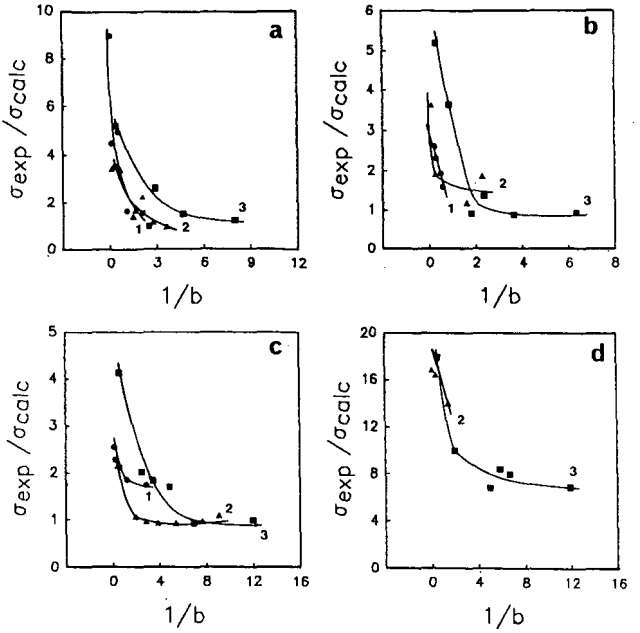

Fig. 11. The influence of cation type on the dependence of $\sigma_{v,exp}/\sigma_{v,calc}$ *versus* $1/b$ for (a) carbonic anhydrase, (b) myoglobin, (c) ovalbumin and (d) lysozyme. Bandwidth data were derived as a result of systematic changes in the cations of chloride salts where ● or 1 = LiCl, ▲ or 2 = NaCl and ■ or 3 = KCl. See Fig. 7 for other details.

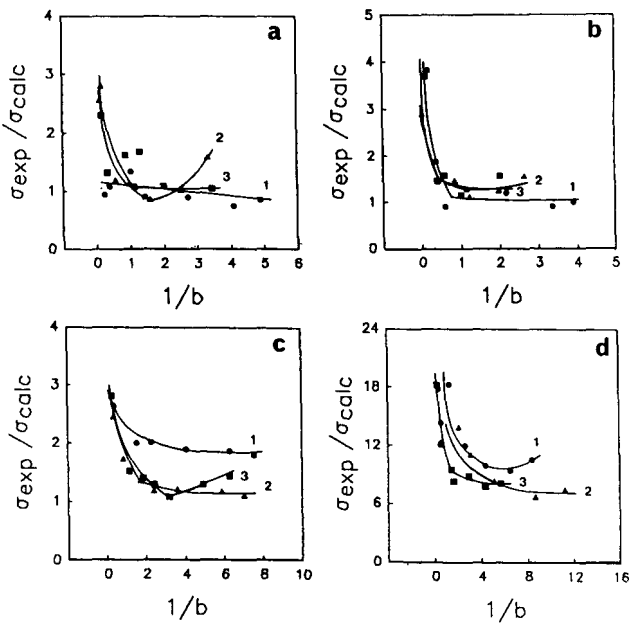

Fig. 12. The influence of cation type on the dependence of $\sigma_{v,exp}/\sigma_{v,calc}$ *versus* $1/b$ for (a) carbonic anhydrase, (b) myoglobin, (c) ovalbumin and (d) lysozyme. Bandwidth data were derived as a result of systematic changes in the cations of bromide salts where ● or 1 = LiBr, ▲ or 2 = NaBr and ■ or 3 = KBr. See Fig. 7 for other details.

bumin bandwidth data for the NaF and KF salts are displaced to the right, causing increased $\sigma_{v,exp}/\sigma_{v,calc}$ values over the normal $1/b$ range, *i.e.*, $0 < 1/b < 10$.

Influence of different salts on the J effect

In RP-HPLC systems, the initial decrease in a solute's $\sigma_{v,exp}/\sigma_{v,calc}$ ratio at large b values has been referred to as the "J effect"[3,4]. Solutes eluted by steep gradients have reduced column residence times and their elution behaviour is therefore influenced predominantly by mobile phase parameters. Differential zone migration resulting from this occurrence is believed to generate this effect. To date, very little information has been reported[8–10] on the occurence or significance of this phenomenon in HPIEC systems. For many of the protein–salt systems examined in this study most bandwidth curves were observed to increase at high b values. Eqn. 9 shows that the calculation of the J value, as derived by Stadalius *et al.*[4], is dependent solely upon the gradient steepness parameter such that

$$J = 0.99 + 1.70b - 1.35b^2 + 0.48b^3 - 0.062b^4 \quad (9)$$

The origin of the phenomenon, numerically described by the J value, has not been fully elucidated. The J effect, however, is thought to arise from non-LSS gradient conditions associated with steep gradients and the increasingly important effect of the gradient elapse time, t_e, at low flow-rates resulting in almost stepwise elution[20–22]. The experimental bandwidth data were consequently used to further investigate anomalous bandbroadening at high b values.

As illustrated in Fig. 9b, a change in displacer salt from KF to KCl or KBr generates different J effects for myoglobin. Similarly in Fig. 7a there is a large difference in the $\sigma_{v,exp}/\sigma_{v,calc}$ ratio for carbonic anhydrase eluted with LiCl and LiBr. Examples such as these demonstrate that the J effect is influenced by the mobile phase composition. With low flow-rates and small gradient times, protein solutes will spend relatively longer periods in the bulk mobile phase than orientated at the stationary phase surface. Therefore, the J effect appears to reflect mobile phase compositional effects, as opposed to stationary phase–double layer effects on the solute's bandbroadening behaviour.

When zone broadening occurs with increasing b, the J value can be used to numerically compensate for the deviation of $\sigma_{v,exp}/\sigma_{v,calc}$ from unity[22]. Initial studies by Stout *et al.*[10] with HPIEC using sodium acetate to elute several proteins from a strong cation exchanger have shown good correlation between experimental and predicted bandwidths calculated from eqn. 1 compensated with a J value derived from eqn. 9. However, the utility of eqn. 9 has yet to be extensively verified over a range of IEC elution conditions. Theoretically, eqn. 9 permits bandwidth ratios which deviate from unity to be adjusted by a particular J factor which is solely dependent on the b value and independent of the type of displacer salt. For example, at $b = 0.5$ eqn. 9 predicts the J value will have a magnitude of $J = 1.6$. When the b value is $b = 2.0$ the J value will increase to $J = 1.8$, *i.e.* over a typical range of slope conditions for gradient elution of $0.5 < b < 2$, the J values will range between 1.6 and 1.8. Table II was derived from data in Figs. 7–11 and shows the effect of displacer salt type on protein bandwidth ratios at $b = 0.5$ and $b = 2.0$. Inspection of the data in Table II reveals that the J factor required to normalise the experimental bandwidth ratios to a value equal

TABLE II

BANDWIDTH RATIOS ($\sigma_{v,exp}/\sigma_{v,calc}$) AT SELECTED b VALUES

Using eqn. 9: $J_{b=0.5}$ = 1.6 and $J_{b=2.0}$ = 1.8.

Protein	*b Value*	$\sigma_{v,exp}/\sigma_{v,calc}$							
		Displacer salt							
		LiCl	*LiBr*	*NaF*	*NaCl*	*NaBr*	*KF*	*KCl*	*KBr*
Carbonic anhydrase	2.0	3.5	1.1	1.2	3.6	1.4	1.4	5.1	1.7
	0.5	1.2	0.9	1.0	1.0	1.0	1.0	1.6	1.0
Ovalbumin	2.0	2.1	2.5	>5	2.0	2.7	>5	3.3	4.1
	0.5	1.7	1.8	>5	1.0	1.2	>5	1.7	1.1
Myoglobin	2.0	1.8	1.3	1.7	1.9	1.5	1.4	4.9	1.5
	0.5	NE[a]	1.0	1.0	1.5	1.2	1.0	1.0	1.5
Lysozyme	2.0	ND[a]	20.0	>15	16.3	>15	12.5	18.0	12.5
	0.5	ND[a]	9.9	7.7	12	9.6	5.6	8.4	8.1

[a] ND = Not determined; NE = solute not eluted at this b value.

to one would vary significantly from those predicted by eqn. 9 for each value of b. The data for each protein in Table II indicates that salt-induced secondary equilibria can influence protein diffusional behaviour at higher b values. Provisions for these secondary equilibria have yet to be incorporated into eqn. 9 and are clearly required in order to permit such empirical adjustment routines to find general applicability for characterising protein bandbroadening in high-performance anion-exchange systems.

CONCLUSION

This study has shown that the bandbroadening behaviour of proteins in HPIEC can be regulated by the nature of the displacing salt in addition to other operating parameters such as the gradient time or flow-rate. The effect of displacer anions and cations on the magnitude of protein bandwidths was found to be dependent upon the relative position of the ions in the lyotropic series.

Increased column residence times associated with longer gradient times were found to lead to aberrant bandbroadening presumably as a consequence of secondary equilibria effects on protein structure. These results demonstrate that the associated decrease in mass transfer efficiency can be eliminated, by selecting experimental elution conditions which reduced the solute residence time at the stationary phase surface.

Anomalous bandbroadening was also observed at high b values. The J value derived from LSS theory, was unable to satisfactorily account for such HPIEC bandwidth behaviour. However, the J effect was demonstrated to be influenced by the salt composition in a solute specific manner. This information clearly has a bearing on the selection of different salts in the optimisation of preparative HPIEC separations which often incorporate steep gradient or step-wise elution conditions.

Overall, this study demonstrates that mathematical models currently used to

describe bandbroadening behaviour require further development to incorporate the influence of mobile phase composition, stationary phase type and solute solvation effects on protein kinetic behaviour in HPIEC. Experimental parameters defining the origin of such complex phenomena need to be established before current models can be adapted to achieve general predictive applications. This will only occur as additional systematic studies exploring the mechanistic basis linking solute structure to chromatographic behaviour, find their way into the scientific literature.

ACKNOWLEDGEMENTS

The support research grants to M.T.W.H. from the National Health and Medical Research Council of Australia, Australian Research Grants Committee and Monash University Special Research fund are gratefully acknowledged.

REFERENCES

1 W. Kopaciewcz, M. A. Rounds, J. Fausnaugh and R. E. Regnier, *J. Chromatogr.*, 266 (1983) 3.
2 R. Matsuna, K. Nakanishi and S. Yamamoto, *Ion Exchange Chromatography of Proteins*, Marcel Dekker, New York, 1988, p. 24.
3 L. R. Snyder, in Cs. Horváth (Editor) *HPLC–Advances and Perspectives*, Vol. 1, Academic Press, New York, 1980, pp. 208.
4 M. A. Stadalius, H. S. Gold and L. R. Snyder, *J. Chromatogr.*, 327 (1985) 27.
5 W. Kopaciewcz and R. E. Regnier, *Anal. Biochem.*, 13 (1983) 251.
6 A. N. Hodder, M. I. Aguilar an M. T. W. Hearn, *J. Chromatogr.*, 476 (1989) 391.
7 M. T. W. Hearn, A. N. Hodder, P. G. Stanton and M. I. Aguilar, *Chromatographia*, 24 (1987) 769.
8 M. T. W. Hearn, A. N. Hodder and M. I. Aguilar, *J. Chromatogr.*, 443 (1988) 97.
9 M. T. W. Hearn, A. N. Hodder and. M. I. Aguilar, *J. Chromatogr.*, 458 (1988) 27.
10 R. W. Stout, S. I. Sivakoff, R. D. Ricker and L. R. Snyder, *J. Chromatogr.*, 353 (1986) 439.
11 M. T. W. Hearn and M. I. Aguilar, in A. Neuberger and L. L. M. van Deenen (Editors), *Modern Physical Methods in Biochemistry*, Elsevier, Amsterdam, 1989, p. 107.
12 M. T. W. Hearn, M. I. Aguilar and A. N. Hodder, in preparation.
13 J. K. Duncan, A. J. C. Chen and C. J. Siebert, *J. Chromatogr.*, 397 (1987) 3.
14 K. N. Gooding and M. N. Schmuck, *J. Chromatogr.*, 296 (1984) 321.
15 J. A. McGammon, B. R. Gelin, M. Karplus and P. G. Wolynes, *Nature (London)*, 262 (1976) 325.
16 J. Janin and M. G. Hamilton, *Biochim. Biophys. Acta.*, 915 (1987) 157.
17 A. J. Sophianopoulos and K. E. Van Holde, *J. Biol. Chem.*, 239 (1964) 2576.
18 A. J. Sophianopoulos, *J. Biol. Chem.*, 244 (1969) 3188.
19 P. R. Willis, L. W. Nichol and R. J. Siezen, *Biophys. Chem.*, 11 (1980) 71.
20 M. T. W. Hearn and M. I. Aguilar, *J. Chromatogr.*, 352 (1986) 35.
21 M. T. W. Hearn and M. I. Aguilar, *J. Chromatogr.*, 359 (1986) 31.
22 M. A. Stadalius, M. A. Quarry and L. R. Snyder, *J. Chromatogr.*, 327 (1985) 93.
23 K. D. Lork, K. K. Unger, H. Bruckner and M. T. W. Hearn, *J. Chromatogr.*, 476 (1989) 135.

Journal of Chromatography, 512 (1990) 57–75
Elsevier Science Publishers B.V., Amsterdam

CHROMSYMP. 1934

High-performance liquid chromatography of amino acids, peptides and proteins

XCIX[a]. Comparative study of the equilibrium refolding of bovine, porcine and human growth hormone by size-exclusion chromatography

M. FRIDMAN, M. I. AGUILAR and M. T. W. HEARN*
Department of Biochemistry and Centre for Bioprocess Technology, Monash University, Clayton, Victoria 3168 (Australia)

ABSTRACT

The equilibrium refolding of bovine, porcine and human growth hormone and ovine prolactin in guanidine hydrochloride has been investigated using high-performance size-exclusion chromatography (HPSEC). It was found that bovine and porcine growth hormones exhibited very similar refolding behaviour. However, the renaturation of human growth hormone followed a different pathway. In particular, the folding transition of human growth hormone occured at 4.7 *M* guanidine hydrochloride compared to 3.8 and 3.5 *M* for the bovine and porcine molecules, respectively, and 3.5 *M* for ovine prolactin. The refolding mechanism of an internally clipped fragment derived from partial tryptic digestion, exhibited similar folding properties to the corresponding intact molecule. The internally clipped analogue existed as a relatively larger molecule under fully denaturing conditions. Reduction followed by carboxymethylation resulted in growth hormone molecules with significantly reduced stability and altered folding properties. The results have been correlated with differences in structure to further demonstrate the utility of HPSEC in the study of protein folding and stability.

INTRODUCTION

The mechanism by which nascent polypeptide chains adopt their native three-dimensional structure remains a fundamental problem in biology. It is generally considered[1,2] that the protein folding process involves the early formation of

[a] For part XCVIII, see ref. 27.

0021-9673/90/$03.50

hydrogen-bonded secondary structures associated with specific nucleation sequences. These events are then followed by reorganisation to yield tightly packed domains constituting the tertiary structure. However, the precise role of the primary amino acid sequence in directing protein folding pathways is not yet understood. As a consequence, the current state of understanding does not allow tertiary structures to be predicted *de novo* solely from the knowledge of the primary amino acid sequence, although useful predictive algorithms which indicate preferred regions of α- or 3_{10}-helical content, β-sheet, or β-turn structures have found wide application over the past decades[3,4].

The reversible denaturation/renaturation pathways of proteins in bulk solution have generally been studied using a combination of techniques including ultraviolet and fluorescence spectroscopy, two-dimensional nuclear overhauser spectroscopy, circular dichroism and sedimentation velocity measurements. These approaches allow the detection and characterisation of specific equilibrium intermediates which are formed during the folding process. In addition, comparison of the unfolding pathways of closely-related proteins with modified sequences derived from different species[5,6] or through recombinant DNA site-directed mutagenesis[7] has been used to provide further characterization of specific amino acid residues which influence protein conformation.

Size-exclusion chromatography (SEC) has also been utilised as an experimental tool for studying protein folding pathways[8–10]. Recent advances in the development of column packing materials for SEC have resulted in higher levels of performance in analytical systems in terms of resolution and separation speed. As a result, high-performance SEC (HPSEC) methods can now be used to monitor relatively minor changes in protein hydrodynamic volumes, apparent equilibrium constants and Gibbs free energy of stabilisation associated with the unfolding or refolding of a protein under different conditions.

In the present study, HPSEC has been used to investigate the equilibrium renaturation pathway in guanidine hydrochloride (Gdn · HCl) of a series of growth hormones (GHs), namely porcine (pGH), bovine (bGH) and human (hGH) and the ovine lactogenic protein, prolactin (oPrl). These proteins are members of the somatotrophic family of structurally conserved pituitary and placental proteins involved in the regulation of growth and lactogenesis in mammals. These proteins are comprised of approximately 190 amino acid residues with molecular weights of about 22 000. In addition to their well-established growth-promoting activity, the GHs are also known to exhibit several other important physiological properties which include significant effects on protein, lipid and carbohydrate metabolism. For example, within the GH molecule, the somatotrophic, lactogenic, diabetogenic and insulin-like action are mediated by specific regions defined by both the topographical and primary structural features. The three-dimensional low resolution 2.8 Å X-ray crystal structure of recombinant pGH has been reported[11] and indicates the presence of four anti-parallel amphipathic helices arranged in a left twisted helical bundle. Alignment of the amino acid sequence of pGH with that of other growth hormones reveals that the residues located within the α-helices are predominantly invariant[12]. This observation suggests that these amino acid residues are necessary for the maintenance of structural integrity of these proteins. The present paper presents results on the refolding behaviour of bGH, pGH, hGH and oPrl and provides insight into the

relationship between amino acid sequence, the mechanism of protein folding and the conformational stability of this protein superfamily.

MATERIALS AND METHODS

Chemicals and reagents

Water was quartz distilled and deionised in a Milli-Q system (Millipore, Bedford, MA, U.S.A.). Acetonitrile (HPLC grade) was obtained from Mallinckrodt (Paris, KE, U.S.A.) and trifluoroacetic acid (TFA) was obtained from Pierce (Rockford, IL, U.S.A.). Gdn · HCl (enzyme grade) was purchased from Bethesda Research Labs. (Gaithersburg, MD, U.S.A.). Human prolactin, recombinant bovine growth hormone (r-bGH) and recombinant porcine growth hormone (r-pGH) were available through associated studies with the Centre for Bioprocess Technology whilst the pituitary derived human growth hormone was kindly provided by Commonwealth Serum Laboratories (Melbourne, Australia). Automated Edman sequence analysis on the carboxymethylated proteins and derived enzymic fragments has confirmed the sequence veracity of these proteins. Dithiothreitol, iodoacetic acid and L-1-Tosylamide-2-phenylethylchloromethyl ketone (TPCK) trypsin were purchased from Sigma (St. Louis, MO, U.S.A.), Fluka (Buchs, Switzerland) and Worthington (Freehold, NJ, U.S.A.), respectively.

Partial tryptic digests

Digestion was carried out by the addition of TPCK trypsin (1%, w/w, in 1 m*M* hydrochloric acid) to a solution of growth hormone (1 mg/ml in 0.15 *M* sodium chloride, 0.05 *M* Na_2HPO_4, pH 8.0) and the mixture was incubated for 6 min at room temperature. Digestion was stopped by acidification with 2 *M* hydrochloric acid.

Reductive alkylation

Dithiothreitol [300 μg in 30 μl of 200 m*M* trishydroxymethylaminomethane (Tris) (pH 8.0) containing 6 *M* Gdn · HCl and 2 m*M* EDTA] was added to pre-incubated solutions (30 min at 37°C) of growth hormone and the mixture was heated at 100°C for 5 min. After cooling, iodoacetic acid (600 μg in 60 μl Tris · HCl, pH 7.9) was added and the sample was incubated in the dark for 15 min, after which 10 μl 2-mercaptoethanol was added.

HPSEC

All HPSEC experiments were performed with a Pharmacia (Uppsala, Sweden) fast protein liquid chromatographic (FPLC) system consisting of two P-500 syringe pumps, a V-7 injector coupled to a Waters M450 variable-wavelength UV detector (Waters Assoc., Milford, MA, U.S.A.). All measurements were routinely monitored at 215 nm and recorded using a Perkin-Elmer (Norwalk, CT, U.S.A.) LCI-100 integrator.

Isocratic elution was controlled with a Pharmacia GP250 solvent programmer, using Pharmacia Superose 12 columns (300 × 10 mm I.D.). All injections were made with SGE (Melbourne, Australia) syringes, and pH measurements were performed with an Orion (MA, U.S.A.) SA520 meter, equipped with a combination glass electrode.

The Superose 12 columns were pre-equilibrated at each guanidine concentration by mixing the appropriate proportions of buffers A and B which both contained 0.01 *M* Tris at pH 8.0 with buffer B also containing 6 *M* Gdn · HCl. Chromatography was carried out isocratically at 0.4 ml/min. The protein molecular weight calibration curve was obtained in 1 *M* Gdn · HCl using cytochrome *c* (11 000 dalton), ribonuclease (13 700 dalton), sperm whale myoglobin (17 000 dalton), ovine growth hormone (22 000 dalton), human carbonic anhydrase (29 000 dalton) and bovine serum albumin (67 000 dalton). V_o and V_t were determined using thyroglobulin (670 dalton) and sodium azide, respectively. Distribution coefficient (K_d) values were determined using the relationship $K_d = (V_e - V_o)/(V_t - V_o)$, see also eqn. 1. Growth hormone samples were dissolved in 100% buffer B at concentrations of 300 μg/ml unless otherwise specified. All solutions were filtered through a 0.45-μm filter prior to injection.

Characterization of growth hormone derivatives

Following partial tryptic digestion and/or reductive alkylation, all derivatives were purified by reversed-phase chromatography on a Waters Assoc. liquid chromatograph consisting of two Model 6000A solvent delivery pumps, a U6K universal injector, and a M660 gradient programmer. Detection was carried out using a Lambda-Max Model 481LC variable-wavelength monitor operating at 215 nm, coupled to a Model M730 data module.

Purification was carried out with a Bakerbond widepore butylsilica stationary phase (Baker, Phillipsburg, NJ, U.S.A.) with nominal particle diameter of 5 μm and average pore size of 30 nm packed into a 25 cm × 0.46 mm I.D. column). Mobile phases TFA–water (0.1:100, v/v) (buffer A) and TFA–water–acetonitrile (0.1:25:75, v/v/v) (buffer B). Elution was carried out using a linear gradient from 100% buffer A to 100% buffer B over 60 min at a flow-rate of 1 ml/min.

The volume of HPLC fractions was reduced on a Savant (Hicksville, NY, U.S.A.) SpeedVac Concentrator at ambient temperature. Automated Edman amino acid sequencing of the derivatives was carried out on an Applied Biosystems (Foster City, CA, U.S.A.) Model 470A Sequencer.

RESULTS AND DISCUSSION

Equilibrium renaturation of growth hormones and prolactin

Under ideal conditions of gel filtration when the sample volume is negligible compared to the chromatographic bed volume and where there is no interaction between the protein solute and the stationary phase, solute elution is characterised by a distribution coefficient, K_d, according to the relationship

$$K_d = \frac{V_e - V_o}{V_t - V_o} \quad (1)$$

where V_e is the solute elution volume. The term V_o is the occluded volume represented by elution volume of molecules totally excluded from entering the largest pores in the gel, and V_t represents the elution volume of a solute which will distribute freely between the mobile phase and all of the pores of the stationary phases. Thus, in the

absence of interactive effects, the only factors which contribute to the elution behaviour of solute molecules are steric effects based on the hydrodynamic size and shape of the solute.

Geometrically, a macromolecule can be described by the axial ratio as a measure of its asymmetry, its volume which is a function of partial specific volume and molecular weight, and the degree of hydration. Formal relationships between a number of specific geometrical factors and HPSEC elution data have been derived[13,14] in the development of universal calibration methods for HPSEC columns. For example, the solution properties of proteins can be characterised by the dependence of K_d on molecular weight, Stokes radius, or an intrinsic viscosity radius. According to Porath[15], the K_d value for a spherical or ellipsoid protein is proportional to the radius of gyration, R, of a hypothetical sphere of equivalent hydrodynamic properties to that manifested by the protein. The dependence of K_d on R can thus be described according to the relationship

$$K_d^{1/3} = a - bR \tag{2}$$

As the volume of a sphere is linearly related to R^3, the chromatographic K_d value for a particular protein is therefore proportional to its hydrodynamic volume, V. HPSEC has been shown to be a considerably more rapid technique for the study of the hydrodynamic properties of proteins under a wide range of solvent conditions than other transport techniques such as intrinsic viscosity measurements and sedimentation techniques. In particular, the ability to characterise solvent and temperature induced conformational changes in protein structure in terms of the degree of associated molecular expansion has provided significant insight into the unfolding pathways of several proteins[8,10]. It should be noted that the derivation of eqns. 1 and 2 assumes a two-state model for the chromatographic process and is not related to the protein refolding process which will be approximated by a more complex model.

Several recent studies[10,16,17] on the equilibrium denaturation of bovine growth hormone (bGH) have utilised HPSEC as a probe for changes in the molecular volume during unfolding of this protein in Gdn · HCl and urea. The non-coincidence of the denaturation transitions as detected chromatographically and spectroscopically, indicated the presence of several unfolded intermediates. Furthermore, while the native and fully unfolded species of bGH are monomeric, the intermediate unfolded forms were found to exist as both monomeric and associated structures. In the present study, similar methods have been extended to the equilibrium refolding behaviour from the fully unfolded state, of different members of the somatotrophic family of proteins. To characterise the refolding behaviour of these growth hormones, experimental studies have been carried out with bovine, porcine and human growth hormone in Gdn · HCl at different concentrations using a Superose 12 column. In particular, the Gdn · HCl concentration was varied between 1 and 6 M in solvents containing 0.1 M Tris buffered at pH 8.0. A typical molecular calibration curve of proteins of different molecular weight separated on the Superose 12 support obtained in 1 M Gdn · HCl is shown in Fig 1. It can be seen from the data that a linear relationship between K_d and log molecular weight (MW) was observed with this elution system.

The chromatographic profiles of bGH eluted under different concentrations of

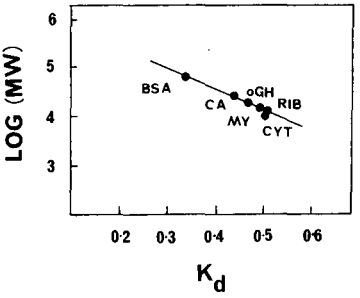

Fig. 1. Protein molecular weight (MW) calibration curve for the Superose 12 column in 1 *M* Gdn · HCl plus 0.1 *M* Tris. Proteins used are listed in the Materials and Methods section. The correlation coefficient, r^2, for the linear regresion analysis was 0.971. BSA = Bovine serum albumin, CA = human carbonic anhydrase, oGH = ovine growth hormone, MY = sperm whale myoglobin, RIB = ribonuclease and CYT = cytochrome *c*.

Gdn · HCl are shown in Fig. 2. Protein solutions were unfolded in 6 *M* Gdn · HCl and then loaded onto the column which was pre-equilibrated at different Gdn · HCl concentrations. While reasonably symmetrical peaks were observed for bGH at each Gdn · HCl concentration examined, the renaturation transition was clearly apparent between 3–4 *M* Gdn · HCl where there was a singnificant change in both the elution volume and the bandwidth of the solute peak. As employed previously, the parameters

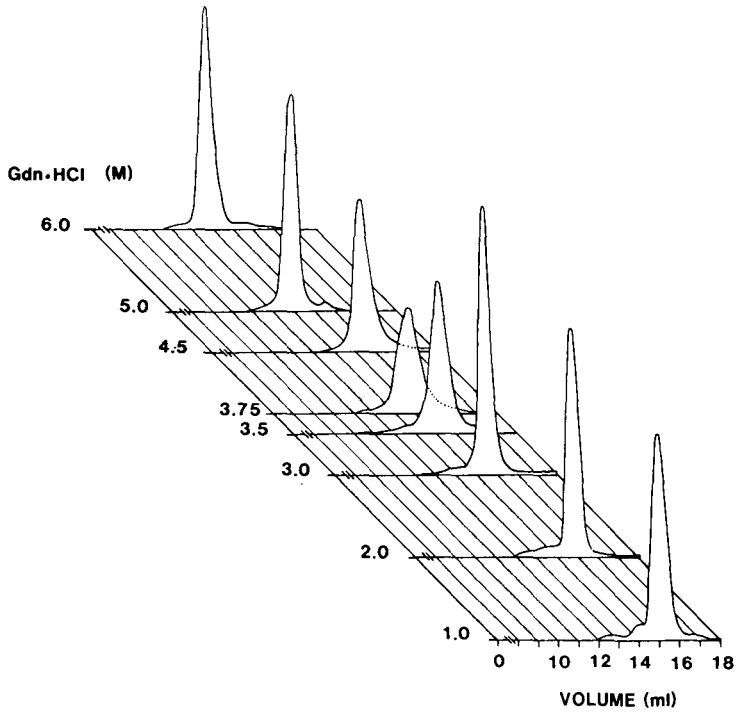

Fig. 2. Chromatographic elution profile of bGH as a function of Gdn · HCl concentration using HPSEC.

most useful to monitor the equilibrium refolding of the bGH molecules were the changes in apparent molecular volume relative to the native conformation and changes in the chromatographic peakwidth calculated at half peak height ($PW_{1/2}$) or from the second centralised moment for grossly asymmetric peaks. Since the kinetics of mass transport in a chromatographic sense will be similar for the different GH proteins, we have for the purposes of the present analysis used the $PW_{1/2}$ as a useful parameter to monitor the refolding pathway. The renaturation curves for bGH as monitored by these parameters are shown in Fig. 3a and b, respectively. In Fig. 3a, the relative change in K_d is represented by the ratio

$$\tau_D = \frac{K_{d,refolded}}{K_{d,native}} \tag{3}$$

where $K_{d,refolded}$ is the distribution coefficient of the refolded form at a particular Gdn · HCl concentration while $K_{d,native}$ is the distribution coefficient of bGH in 1 *M* Gdn · HCl, and is equivalent to the native conformation in neat buffer. The midpoint of refolding for bGH which is listed in Table I occurred at 3.8 *M* Gdn · HCl, while the τ_D ratio at 6 *M* Gdn · HCl corresponded to a 3.5-fold expansion in apparent molecular volume of the solute relative to its native conformation.

Changes in molecular volume during refolding were derived from the elution volume measured at the peak apex. This parameter therefore represents the average hydrodynamic properties of the most abundant conformational species at a particular Gdn · HCl concentration. In comparison, the peakwidth of the solute zone includes contributions from a number of different conformational species involved in the

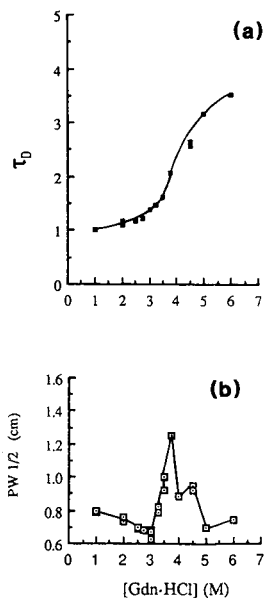

Fig. 3. (a) Equilibrium refolding of bGH as monitored by relative changes in K_d, *i.e.* τ_D with Gdn · HCl concentration. (b) The dependence of peak width at half peak height, $PW_{1/2}$ on Gdn · HCl concentration during the equilibrium refolding of bGH.

TABLE I

REFOLDING TRANSITIONS AND RELATIVE EXPANSION FACTORS OF PROTEINS AND FRAGMENTS USED IN THIS STUDY

	Transition (Gdn · HCl)	τ_D
bGH	3.8	3.5
pGH	3.5	3.6
hGH	4.7	4.1
oPrl	3.5	3.6
TD-bGH[a]	3.9	4.2
TD-pGH	3.3	4.3
TD-hGH	4.5	4.8
RA-bGH[b]	2–3	5.4
RA-pGH	2–3	5.5
RA-hGH	3.4	5.7

[a] TD: partial tryptic digest fragment.
[b] RA: reduced and alkylated.

eluting band, as well as the diffusional properties of these conformers. It is apparent from the data provided in Fig. 3b that there are significant changes in the experimental bandwidth as the Gdn · HCl concentration is increased. In particular, the presence of two distinct bandwidth maxima observed at *ca.* 3.8 and 4.5 *M* Gdn · HCl suggests the formation of at least two stable intermediates. Previous studies[15,17] on the equilibrium unfolding of bGH have demonstrated the reversible formation of a self-associated form of partially denatured bGH at *ca.* 3.7 *M* Gdn · HCl. The identity of the intermediate species, derived from the unfolding and refolding studies at 3.8 *M* Gdn · HCl was further investigated by monitoring the influence of protein concentration on the relative molecular volume of bGH at 3.8 *M* Gdn · HCl. The relative changes in K_d and peak width were assessed by chromatographing solutions of bGH ranging in protein concentration between 0.2 and 2 mg/ml. The results are shown in Fig. 4a and b, respectively, and demonstrate that while the K_d ratio exhibits an almost linear increase with protein concentration, the chromatographic peakwidth reaches a plateau at protein concentrations of *ca.* 1 mg/ml. The data indicate that at 0.3 mg/ml bGH exhibits a K_d value consistent with a monomeric structure. A value of $\tau_D = 4$ for the relative changes in molecular volume at a protein concentration of 2 mg/ml is consistent with the formation of a bGH species, under these partially-renaturing conditions, with a relative molecular volume corresponding to at least two monomer units. From the chromatographic data it is not immediately evident why there is a linear increase in the relative molecular volume rather than a discrete transition between the monomeric and dimeric species. However, the elution profiles obtained at 1 mg/ml exhibited solute peaks which tailed towards the lower molecular weight region. This observation suggests that the dilution of the bGH sample upon injection onto the Superose column results in interconversion of the monomer/dimer equilibrium during the separation, which then induces the formation of a small proportion of monomer. In the present study, the non-coincidence of the dependence of τ_D values and $PW_{1/2}$ on protein concentration suggests that these two parameters may be

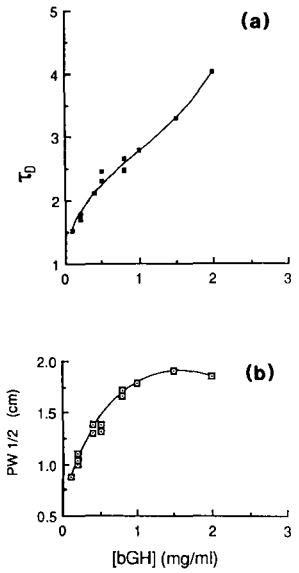

Fig. 4. The influence of bGH concentration on (a) relative molecular volume, τ_D, and (b) $PW_{1/2}$ at 3.7 *M* Gdn · HCl.

a measure of different aspects of this aggregation process. Thus, while the apparent molecular volume of the most abundant species gradually increased with increased protein concentration, the bandwidth reflects the extent of interconversion of the monomer–oligomer species.

It has previously been postulated by Brems *et al.*[18] that the self-association of bGH occurs through specific intermolecular interactions between the exposed hydrophobic face of the amphipathic helix encompassing amino acid residues 107–127. If the mechanisms of unfolding and refolding of GHs involve the formation and interaction of the same or similar structural intermediates, then porcine growth hormone (pGH), which exhibits 90% sequence homology with bGH and also contains an identical sequence between amino acid residues 107–127 except for a Gln/Leu substitution at position 121, should manifest very similar renaturation curves and concentration-dependent aggregation. In Fig. 5a and b, the relative molecular volume and $PW_{1/2}$ of pGH eluted on the Superose column are plotted against the Gdn · HCl concentration. The midpoint of renaturation occurred at 3.5 *M* Gdn · HCl which indicates that pGH is slightly less stable than bGH under these denaturing conditions. However, at 6 *M* Gdn · HCl, pGH increased in molecular volume by a factor of 3.6, which is very similar to the final extended molecular volume of bGH. The peak width data shown in Fig. 5b also shows a similar pattern to bGH with two maxima formed at 3.3 and 3.8 *M* Gdn · HCl, respectively. These results indicate that while at least two stable intermediates are formed during the renaturation of pGH, they also exhibit slightly diminished stability relative to the analogous bGH intermediates. This finding suggests that the intermolecular forces which are responsible for the existence of the transient conformers are also weaker in pGH than in bGH.

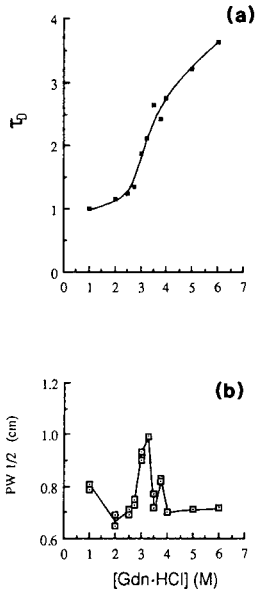

Fig. 5. (a) Equilibrium refolding of pGH as monitored by relative changes in molecular volume, τ_D, with Gdn · HCl concentrations. (b) The dependence of $PW_{1/2}$ on Gdn · HCl concentration during the equilibrium refolding of pGH.

hGH exhibits a 65% sequence homology with bGH and 74% homology with pGH, and displays marked differences in biological activity. The refolding behaviour of hGH in Gdn · HCl is shown in Fig. 6. Changes in relative molecular volume of hGH show the same sigmoidal shape as observed for both bGH and pGH. However, hGH was considerably more stable with a midpoint of refolding at 4.7 *M* Gdn · HCl compared with 3.8 and 3.5 *M* for bGH and pGH, respectively. Another difference in the behaviour of hGH was the tendency to form a small proportion of associated dimers at all Gdn · HCl concentrations, shown in Fig. 7 as a small peak eluting before the main monomeric species. Collection and reinjection of this dimer fraction resulted in identical elution profiles, which indicates that the dimeric form existed as a non-covalent aggregate in equilibrium with monomeric hGH. The renaturation curve of the hGH dimer is also shown in Fig. 6. While the relative molecular volume of the hGH dimer is larger in magnitude, the refolding behaviour appears to mimic that of the monomer. The persistence of the dimer even at 1 *M* Gdn · HCl also suggests that the molecular region involved in the intermolecular bonding may be located within relatively hydrophobic sections of the protein, which are known to be surface exposed in the native protein.

A further difference in the folding behaviour of hGH compared to bGH and pGH is illustrated by the pattern of bandwidth changes. Fig. 6b shows the influence of Gdn · HCl concentration on the monomer bandwidth which increased in a sigmoidal fashion with a midpoint value which corresponded to the transition value in the relative molecular volume. This result is in contrast to the existence of two bandwidth maxima observed for bGH and pGH which occurred in partially denaturing concentrations of Gdn · HCl. It is therefore apparent that hGH, compared to bGH or

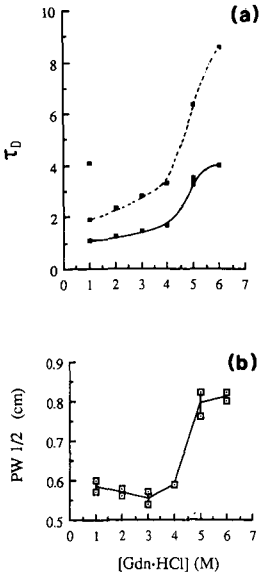

Fig. 6. (a) Equilibrium refolding of hGH as monitored by relative changes in molecular volume, τ_D. (b) The dependence of $PW_{1/2}$ on Gdn · HCl concentration during the equilibrium refolding of hGH.

pGH, follows a significantly different refolding pathway which reflects differences in the overall structural hierarchy within the molecule. These apparent differences between hGH and bGH or pGH in terms of the macroscopic secondary and tertiary structures may also be related to regional susceptibility of the three GH molecules to

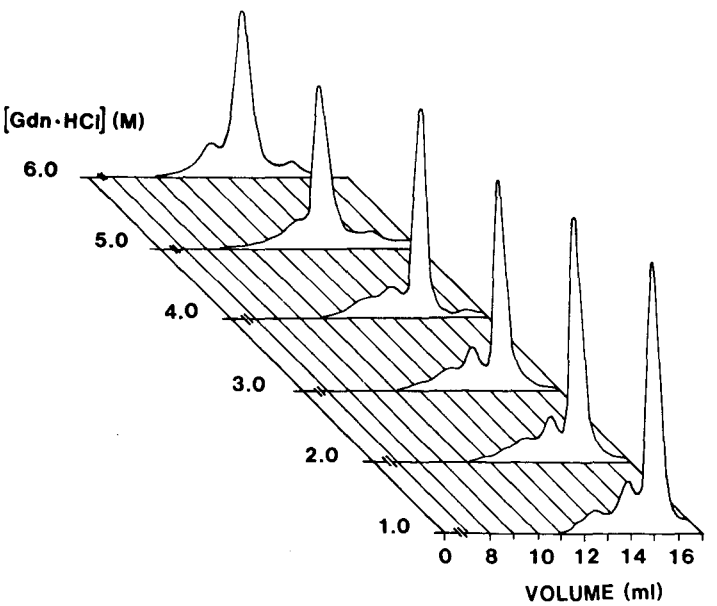

Fig. 7. HPSEC elution profiles of hGH as a function of Gdn · HCl concentration.

tryptic digestion[19]. For example, Fridman *et al.*[19] have found that bGH and pGH exhibited very similar surface structures while hGH exhibited a significantly different pattern of surface accessibility. In addition, recent studies by other workers[20] on the ultraviolet, resonant Raman and fluorescence spectroscopy of GHs, following acid-induced structural alterations, indicated the presence of a different environment around the single conserved tryptophan residue at position 86 in hGH compared to bGH and pGH. The results of the present study provide further confirmation of the overall differences in the structure and stability of the human growth hormone molecule compared to other structurally and functionally related proteins.

The hormone prolactin (Prl) is structurally related to the GHs but exhibits only lactogenic activity[12]. To further investigate the relationship between proteins of similar structure, the renaturation properties of ovine Prl (oPrl) were compared to the refolding behaviour of the three GHs. Fig. 8a shows the changes in relative molecular volume of oPrl as a function of Gdn · HCl concentration, and indicates a renaturation pattern similar to bGH and pGH rather than hGH. Thus, the midpoint of unfolding occurred at 3.5 *M* Gdn · HCl compared with 3.8, 3.5 and 4.7 *M* for bGH, pGH and hGH, respectively. The pattern of bandwidth changes during the unfolding of oPrl is shown in Fig. 8b. In contrast to bGH, pGH and also hGH, oPrl bandwidths increased between 5–6 *M* Gdn · HCl which correspond to the conditions in which the molecule was fully unfolded. Furthermore, there were no bandwidth maxima as observed for bGH and pGH which suggests that similar structural intermediates were not formed during the refolding process. The Prls exhibit approximately 20% sequence homology with hGH. While physicochemical studies have previously indicated[22] that Prls and GHs adopt similar conformations with approximately equivalent α-helical content, the present results indicate that there are significant differences in the intramolecular factors which control the refolding pathways of these proteins.

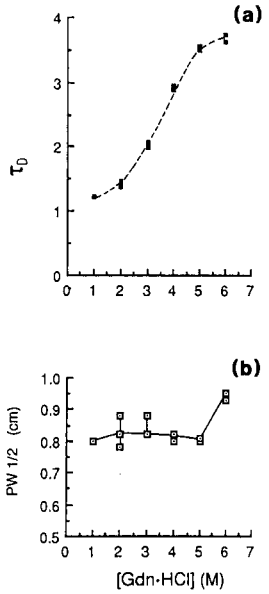

Fig. 8. Equilibrium refolding of oPrl in Gdn · HCl as monitored by (a) changes in τ_D and (b) changes in $PW_{1/2}$.

Chemically modified growth hormones

Limited tryptic digestion. Early reports have documented[21] that hGH, following partial digestion with chrymotrypsin, retains significant somatotrophic activity. Subsequently there has been considerable effort in numerous laboratories directed towards identifying smaller fragments of GHs which retain potent biological activity (for recent review see ref. 22). To date, these approaches have not led to the successful molecular dissection of the somatotrophic and lactogenic activities within the sequential structure of hGH. However, it is known that significant biological activity can be maintained using two types of chemical modification of the GH molecule, namely (i) reduction followed by alkylation and (ii) limited proteolytic cleavage with trypsin[22,23]. The influence of these processes on the folding behaviour and relative stability of bGH, pGH and hGH was therefore investigated using analogous HPSEC methods to those described above.

Partial tryptic digestion of bGH produces a large fragment (TD-bGH) from which the segment encompassing amino acid residues 140–150 has been excised[19]. It is known from Chou-Fasman analyses[24] that this region of bGH is relatively unstructured with significant random coil features. This random coil region of bGH is also present in an analogous region in pGH[11]. Inspection of the X-ray crystal structure of pGH[11] reveals that this portion of the sequence is located within an extended random coil which connects helices 3 and 4. The resulting GH partial tryptic fragment therefore consists of two polypeptide chains corresponding to residues 1–139 and 151–191 which are connected by two disulphide bonds between Cys-53 and Cys-164 and between Cys-181 and Cys-189, respectively. The renaturation curve of TD-bGH which is shown in Fig. 9a shows a similar folding pattern to intact bGH with a refolding

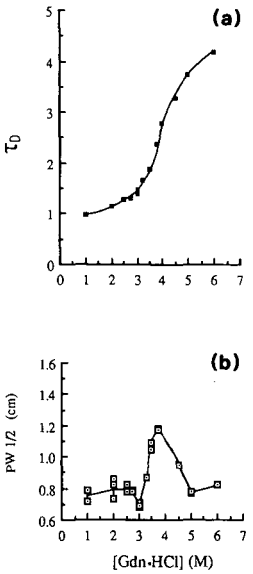

Fig. 9. Equilibrium refolding of TD-bGH in Gdn · HCl as monitored by (a) changes in τ_D and (b) changes in $PW_{1/2}$.

midpoint corresponding to 3.9 *M* Gdn · HCl reflecting a slightly more stable molecule. However at 6 *M* Gdn · HCl the apparent K_d of TD-bGH expanded by a factor of τ_D = 4.2 compared to τ_D = 3.5 for the intact bGH and is consistent with the properties of a more flexible molecule. The excision of residues 140–150 also resulted in a greater propensity of TD-bGH to polymerise which was evidenced by the presence of components of apparently larger molecular weight in the elution profiles. The excision site is adjacent to helix 3, *i.e.* residues 106–129, in the three-dimensional structure and this may result in the increased accessibility of the hydrophobic faces of this helix thereby facilitating aggregation. The dependence of bandwidth on Gdn · HCl concentration is shown in Fig. 9b and exhibits a maximum at 3.8 *M* Gdn · HCl which corresponds to the concentration value for the molecular volume transition.

The renaturation properties of the analogous tryptic derivative of pGH (TD-pGH) are shown in Fig. 10a and b. The midpoint of refolding occurred at 3.3 *M* Gdn · HCl which reflects a less stable structure than intact pGH. However, in 6 *M* Gdn · HCl, TD-pGH also existed as a more expanded open structure with a relative change in molecular volume of τ_D = 4.3 compared to τ_D = 3.6 for pGH. The pattern of bandwidth changes which was observed for bGH and pGH was also evident with TD-pGH. Thus, the presence of two peak maxima at 3 and 3.8 *M* Gdn · HCl in Fig. 10b, indicates the formation of two stable intermediates during the refolding of TD-pGH.

The partial tryptic fragment of hGH (TD-hGH) was also prepared and found to involve an analogous excision region between residues 135 and 145. The results of the Gdn · HCl induced renaturation are shown in Fig. 11a and b. The curves depicted in Fig. 11a correspond to different aggregates present at each concentration of

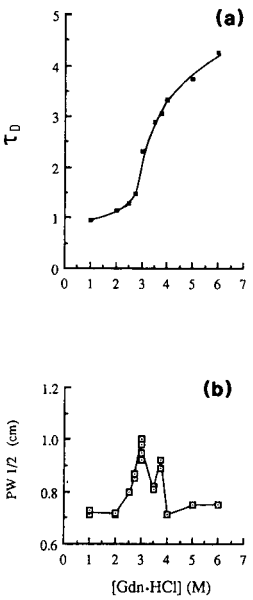

Fig. 10. Equilibrium refolding of TD-pGH in Gdn · HCl as monotired by (a) changes in τ_D and (b) changes in $PW_{1/2}$.

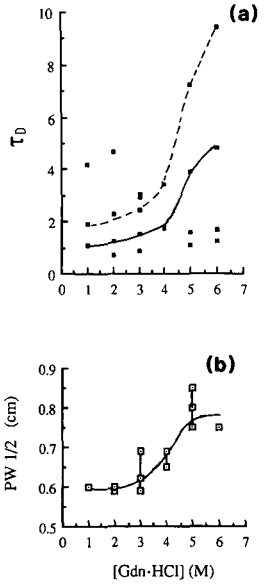

Fig. 11. Equilibrium refolding of TD-hGH in Gdn · HCl as monitored by (a) changes in τ_D and (b) changes in $PW_{1/2}$.

Gdn · HCl. Thus, the tendency of hGH to self-associate was not affected by tryptic cleavage. The bandwidth data also increased in a manner which reflects the changes in relative molecular volume of TD-hGH with Gdn · HCl concentration. These data also indicate that a more complex range of conformational and aggregational species occur with hGH derivatives in solution under denaturing conditions, compared to the bGH or pGH derivatives. Overall, therefore, the loss of a small fragment of the hGH protein from within a random coil section of the molecule does not appear to significantly alter the stability or the folding behaviour, but only influences the extent by which the hGH molecule can unfold in fully denaturing conditions. These conclusions are consistent with the results of other studies which have demostrated that this tryptic fragment of hGH maintains full biological activity[22]. This observation suggests that the region encompassing residues 135–150 is not important in the maintenance of structure and/or the biological function.

Reduction and alkylation. The role of the disulphide bonds in the maintenance of conformation and structural stability of growth hormones was investigated by studying the renaturation behaviour of reduced and carboxymethylated derivatives of bGH, pGH and hGH. This process results in the disruption of the two disulphide bonds between Cys-53–Cys-164 and Cys-181–Cys-189 and also introduces a negative charge on each cysteine through a carboxymethylation reaction.

The chromatographic profiles obtained for the elution of reduced and alkylated bGH (RA-bGH) in different concentrations of Gdn · HCl are shown in Fig. 12. Between 0–4 *M* Gdn · HCl, complex multicomponent elution profiles were obtained, indicative of the presence of various aggregated forms of RA-bGH. While the elution volume for each form was constant at each concentration of Gdn · HCl, the relative

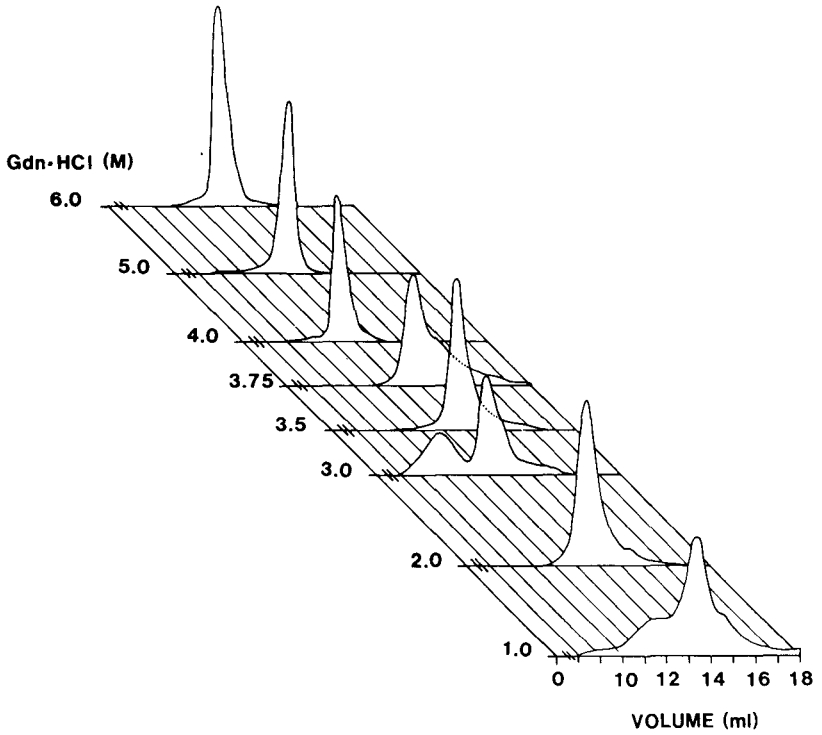

Fig. 12. HPSEC elution profiles of RA-bGH as a function of Gdn · HCl concentrations.

proportion of each aggregate varied with consecutive injections in a protein concentration dependent manner. Under the conditions of these experiments where the protein is refolding from 6 *M* Gdn · HCl, the variation in experimental peak heights corresponding to each aggregate/conformer suggests that they may represent kinetic intermediates along a relatively slow refolding or aggregation pathway. The renaturation curve for RA-bGH is shown in Fig. 13 and shows the refolding pathway of a monomer, dimer, trimer and a decamer. Between 1–3 *M* Gdn · HCl, the predominant form corresponded to an apparent dimer with a relative molecular volume of τ_D = 1.8–2.2 (compared to monomer). Between 4–6 *M* Gdn · HCl, a reproducible single peak was observed with a relative molecular volume of $\tau_D = 5.4$ units. When compared to values of $\tau_D = 3.5$ and $\tau_D = 4.2$ for bGH and TD-bGH, respectively, it thus appears that the monomer is the major species for carboxymethylated bGH under fully denaturing conditions. Similar results were also obtained for the reduced and alkylated derivative of pGH (RA-pGH). While it is not possible from the experimental data to fully delineate the renaturation curve for the monomeric species (because of the presence of higher aggregates), the disruption of the intermolecular forces involved in the formation of the dimer and the transition point for the monomer refolding coincided in the range between 2–3 *M* Gdn · HCl. This value is significantly lower than the midpoint of refolding for both bGH and TD-bGH. Previous studies on the equilibrium unfolding of bGH[25] have indicated that the large loop formed between

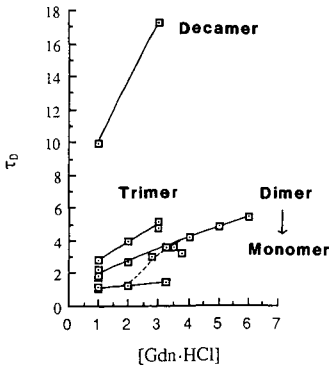

Fig. 13. Equilibrium refolding of RA-bGH as monitored by changes in τ_D.

Cys-53 and Cys-164 plays a major role in secondary structure stabilisation, while the small section between Cys-181 and Cys-189 does not impart any significant stability to the native structure. The results of the present study indicate that reduction and alkylation of bGH and pGH leads to a diminished stability of the tertiary structure presumably due to the exposure of the hydrophobic interior of the molecule which promotes dimerisation through intermolecular interaction between the exposed amphipathic helices.

The chromatographic profiles of RA-hGH are shown in Fig. 14. In 6 *M* Gdn · HCl the relative molecular volume of RA-hGH corresponded to $\tau_D = 5.7$ which demonstrates a significantly larger and more flexible molecule than intact hGH. In contrast to the results observed for RA-bGH and RA-pGH, under non-denaturing

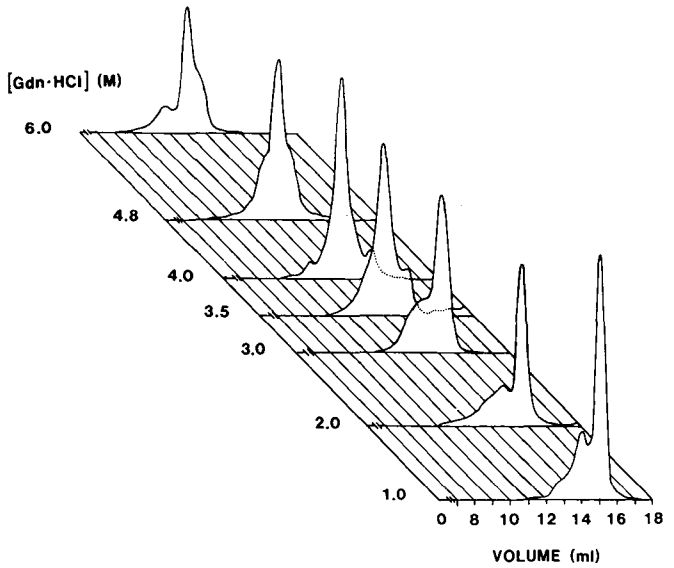

Fig. 14. HPSEC elution profiles of RA-hGH as a function of Gdn · HCl concentrations.

conditions RA-hGH chromatographed predominantly as a monomer, with only a very small proportion of a dimeric form present. The stability of the RA-hGH monomer was significantly decreased relative to hGH, with a midpoint of refolding of 3.4 *M* Gdn · HCl compared to 4.7 *M* for unmodified hGH. This result also provides further insight into the origin of the differences in the folding stability of bGH and pGH compared to hGH, and can be correlated with the influence of reductive alkylation procedures on the biological activity of GHs. For example, reduction and carboxymethylation of hGH causes a loss of growth promoting activity but not lactogenic activity[23]. In contrast, RA-pGH is totally inactive. The disulphide bridge formed between Cys-53 and Cys-164 results in the covalent linkage of a random coil segment and helix 4. Disruption of this disulphide bond alters the topographical arrangement of the amino acid residues within the microenvironment of this region, which may in turn lead to significant effects on the growth promoting activity. While the present study investigates the propensity of the GHs to refold, the unfolding pathway may not necessarily involve the same intermediate steps. Studies into the relationship between the unfolding and refolding of the GHs and the specific role of each helical segment in the aggregation process will be presented in a future paper.

CONCLUSION

The results of the present study further demonstrate the utility of HPSEC in the characterization of protein folding and stability. In particular, the experimental differences observed between the stability and refolding behaviour of hGH and the non-primate molecules bGH, pGH and oPrl confirms other observations that the human molecule is unique in terms of its three-dimensional structure and stability. Previous studies from our laboratories have demonstrated the potential of interactive modes of chromatography, such as reversed-phase[26] and ion-exchange[27], to probe the surface topography and characterise the relative stability of peptides and proteins. The present study further documents HPSEC as an additional dimension in the chromatographic repertoire which can be employed in combination with other techniques for the investigation and characterization of structure–retention-function relationships of medically important proteins.

ACKNOWLEDGEMENT

The project grant support to M.T.W.H. from the National Health and Medical Research Council, the Australian Research Council and the Monash University Special Research Fund is gratefully acknowledged.

REFERENCES

1 J. King, *Chem. Eng. News*, 67 (1989) 35.
2 P. S. Kim and R. L. Baldwin, *Ann. Rev. Biochem.*, 51 (1982) 459.
3 P. Y. Chou and G. D. Fasman, *Biochemistry*, 13 (1974) 222.
4 W. L. Mattice and R. M. Robinson, *Biochem. Biophys. Res. Com.*, 101 (1981) 1311.
5 D. N. Brems, R. Case and E. Stellwagen, *Biochemistry*, 21 (1982) 1488.
6 H. Krebs, F. X. Schmid and R. Jaenicke, *Biochemistry*, 24 (1985) 3846.
7 G. K. Ackers and F. R. Smith, *Ann. Rev. Biochem.*, 54 (1985) 597.

8 R. J. T. Corbett and R. S. Roche, *Biochemistry*, 23 (1984) 1888.
9 J. Withka, P. Moncuse, A. Baziotis and R. Maskiewicz, *J. Chromatogr.*, 398 (1987) 175.
10 D. N. Brems, S. M. Plaisted, H. A. Havel, E. W. Kauffman, J. D. Stodda, L. C. Eaton and R. D. White, *Biochemistry*, 24 (1985) 7662.
11 S. S. Abdel-Megiud, H.-S. Shieh, W. W. Smith, H. E. Dayringer, B. N. Violand and L. A. Bentle, *Proc. Natl. Acad. Sci.*, 84 (1989) 6434.
12 C. S. Nicoll, G. L. Mayer and S. M. Russell, *Endocr. Rev.*, 7 (1986) 169.
13 N. Ui, *Anal. Biochem.*, 97 (1979) 65.
14 M. Potschka, *Anal. Biochem.*, 162 (1987) 47.
15 J. Porath, *Pure Appl. Chem.*, 6 (1963) 233.
16 H. A. Havel, E. W. Kauffman, S. M. Plaisted and D. N. Brems, *Biochemistry*, 25 (1986) 6533.
17 M. T. W. Hearn, M. I. Aguilar, T. Nguyen and M. Fridman, *J. Chromatogr.*, 435 (1988) 271.
18 D. N. Brems, S. M. Plaisted, E. W. Kauffman and H. A. Havel, *Biochemistry*, 25 (1986) 6539.
19 M. Fridman, M. I. Aguilar and M. T. W. Hearn, in preparation.
20 E. W. Kauffman, T. J. Thamann and H. A. Havel *J. Am. Chem. Soc.*, 111 (1989) 5449.
21 A. C. Paladini, C. Pena and E. Poskus, *CRC Crit. Rev. Biochem.*, 15 (1983) 25.
22 C. H. Li, *Fed. Proc., Fed. Am. Soc. Exp. Biol.*, 16 (1957) 775.
23 U. J. Lewis, *Ann. Rev. Physiol.*, 46 (1984) 33.
24 C. H. Chen and M. Sonenberg, *Biochemistry*, 16 (1977) 2111.
25 T. F. Holzman, D. N. Brems and J. J. Dougherty, Jr., *Biochemistry*, 25 (1986) 6907.
26 M. T. W. Hearn and M. I. Aguilar, in A. Neuberger and L. L. M. van Deenen (Editors), *Modern Physical Methods in Biochemistry*, Part B, Elsevier, Amsterdam, 1988, p. 107.
27 A. N. Hodder, K. J. Machin, M. I. Aguilar and M. T. W. Hearn, *J. Chromatogr.*, in press.
28 A. N. Hodder, M. I. Aguilar and M. T. W. Hearn, *J. Chromatogr.*, 512 (1990) 41.

Journal of Chromatography, 512 (1990) 77–87
Elsevier Science Publishers B.V., Amsterdam

CHROMSYMP. 1900

Predicting the performance of gel-filtration chromatography of proteins

SHUICHI YAMAMOTO*, MASAKI NOMURA[a] and YUJI SANO
Department of Chemical Engineering, Yamaguchi University, Tokiwadai, Ube 755 (Japan)

ABSTRACT

A method for determining the column and operating variables for the preparative separation of proteins by gel-filtration chromatography (GFC) of proteins is presented. The recovery of bovine serum albumin monomer from its dimer and higher molecular weight aggregates on high-performance GFC columns of various dimensions (column diameter $d_c = 0.75$–10.8 cm, column length $Z = 10$–80 cm, particle diameter $d_p = 10$–17 μm) was chosen as a model separation system.

In the calculation method, the maximum sample feed volume $V_{F,M}$ that satisfies a specified purity ratio Q_P and recovery ratio Q_R for a given column length Z and particle diameter d_P at a certain linear mobile phase velocity u was sought. The productivity P, defined as the amount of the recovered protein per unit column volume per unit time, was then calculated. The effects of Z and d_P on the P–u relationship were examined. It was found that in general P increases with increasing u and the slope of the P–u curve becomes steep with decreasing d_P and/or Z. A maximum in the P–u relationship was observed when the separation was difficult.

The results show that it is not advantageous to employ larger particle diameter packings and/or a longer column in scaling-up. It is rather recommended that a short column packed with small gels be operated at relatively low flow-rates in the preparative GFC of proteins. It is also suggested that the calculation method presented is useful for scaling up GFC columns.

INTRODUCTION

Gel-filtration (also called size-exclusion or gel-permeation) chromatography (GFC)[1] is an efficient method not only for analytical separations but also for preparative (large-scale) separations of proteins and other biological products[2,3]. GFC is classified as linear isocratic elution liquid chromatography (LC), in which the composition of the mobile phase (elution buffer) is constant and the distribution coefficient of a solute between the mobile and stationary phases (K) is not dependent on the solute concentration. In this type of LC the elution curve is nearly Gaussian

[a] Present address: Tosoh Corporation, Tonda, Shinnanyo 746, Japan.

0021-9673/90/$03.50

when the sample feed volume V_F is small, as in the analytical separation. Such an elution curve can be easily characterized by the HETP–u relationship (u = linear mobile phase velocity) and the K value measured experimentally at small V_F values.

However, in preparative separations, V_F is increased in order to maximize the productivity at a specified purity. This results in a change in the Gaussian-shaped elution curve and overlap of the elution curves. Therefore, the calculation of the whole elution curves by a model which considers the effect of V_F in addition to the other operating and column variables is needed in order to predict the performance of GFC.

Many researchers have reported on the optimization, the maximization of the throughput and the scaling rules (*e.g.*, refs. 4–7), but it seems that the development of a "user-friendly" computer program that can be run on a personal computer is needed for this purpose.

In this paper, a method for determining the column and operating variables for preparative separations of proteins by GFC is presented. The recovery of bovine serum albumin (BSA) monomer from its dimer and higher molecular weight aggregates on high-performance (HP) GFC columns of various dimensions (column diameter d_c = 0.75–10.8 cm; column length Z = 10–80 cm; particle diameter d_p = 10–17 μm) was chosen as a model separation system.

The elution curves for large sample volumes were calculated numerically on the basis of the HETP–u data and the K values obtained at small sample volumes. The calculated curves were compared with the experimental curves for various V_F values. Such a calculation procedure is used for searching for the maximum sample feed volume $V_{F,M}$ that satisfies a specified purrity ratio Q_P and recovery ratio Q_R for a given column length Z and particle diameter d_p at a certain u. The experimental data for HETP–u and K values obtained at small V_F values are used in the calculation. The productivity P, defined as the amount of the recovered protein per unit column volume per unit time, was then calculated.

This calculation method was coded in FORTRAN and BASIC so that it can be run on a personal computer. The program can also search for the V_F and u values that can give the maximum productivity P_M at a certain Z and d_p. The effects of d_p, Z, Q_P and Q_R on P were examined.

THEORETICAL

Calculation of the elution curve

Although GFC is modelled most rigorously by a set of partial differential equations that consider axial dispersion, stationary (gel) phase diffusion, fluid-film mass transfer and distribution of a solute[8,9], the analytical solution is complicated and difficult to calculate owing to its oscillating nature[10]. For the HPGFC columns employed here, the following solution can be employed (the details of the comparison of various models and the validation of the use of the following solution will be described elsehwere[11]):

$$C/C_0 = f(N,T) - f(N,T - T_0) \tag{1}$$

where $f(x,y) = \mathrm{erfc}[(x/2y)^{1/2} - (xy/2)^{1/2}]/2$, $T = tu/[Z(1 + HK)]$ and $T_0 = t_0u/[Z(1 + HK)]$; erfc is the error-function complement, C is the solute concentration

at the outlet of the column, C_0 is the initial concentration, t is the time from the start of the sample injection, $t_0 = V_F/F$ is the sample injection time, F is the volumetric flow-rate and is related to u as $u = F/(A_c\varepsilon)$, A_c is the column cross-sectional area and ε is the void fraction of the column. $H = (1 - \varepsilon)/\varepsilon$ is the parameter describing the ratio of the column gel volume to the void volume. The total number of theoretical plates N (= Z/HETP) in eqn. 1 is considered to be the sum of the contributions of various parameters affecting the zone spreading, such as the axial dispersion, the stationary phase diffusion and the fluid-film mass transfer. This concept has already been propounded by many researchers (*e.g.*, refs. 12–17). The HETP equation derived from the moment equations of the Kubin–Kucera model[8,9] is given with reduced variables as[17]

$$h = A^* + B^*/v + C^*v + D^*v \tag{2}$$

where h = HETP/d_p is the reduced HETP and $v = ud_p/D_m$ is the reduced velocity (D_m is the molecular diffusion coefficient). This has the same form as the van Deemter equation[15]. Under the conditions employed here, the contribution of the second (molecular diffusion) and the fourth (fluid-film mass transfer) terms to the total h value can be ignored[17]. Then eqn. 2 becomes

$$h = A^* + C^*v \tag{3}$$

where A^* is the (constant) axial dispersion term and C^*v is the stationary phase diffusion term. The experimental results were predicted well by this equation, as shown previously[18].

Another important parameter in eqn. 1, K, can be related to the peak retention time of the elution curve t_M at small V_F:

$$t_M - V_F/(2F) = (Z/u)(1 + HK) = (Z/u)(1 + k') \tag{4}$$

Once the elution curves at small V_F have been measured as a function of u, the HETP–u relationship and the K values can be obtained from the peak width and t_M.

Calculation of the productivity

We adopted the following definition for the productivity P:

$$\begin{aligned} P &= [(\text{recovery ratio})(\text{sample feed volume})]/[(\text{column void volume})(\text{cycle time})] \\ &= Q_R V_{F,M}/[V_0(V_0/F)] \end{aligned} \tag{5}$$

where $V_{F,M}$ is the maximum V_F value that satisfies a specified purity ratio Q_P and recovery ratio Q_R. Q_P and Q_R are defined as follows:

$$Q_R = m_d/(V_F C_{0,d}) \tag{6}$$

$$Q_P = m_d/(m_d + m_c) \tag{7}$$

where m is the amount of the recovered fraction. The subscripts c and d imply

a contaminant and desired solutes, respectively. The cycle time in eqn. 5 is the time needed for eluting one column void volume. If we multiply $(1 + H)$ by V_0/F, it will be the time needed for eluting one column volume.

If we consider repetitive injections, the cycle time should be modified[5]. When the zone spreading is ignored (ideal case), $Q_R = 1.0$ and $V_{F,M}$ is the difference in the elution volumes of the two substances, which is equal to $V_{F,M} = [V_0 + K_d(V_t - V_0)] - [V_0 + K_c(V_t - V_0)] = (V_t - V_0)(K_d - K_c)$. Then, inserting the above two relatioships into eqn. 5 yields the ideal P value P_I (here, $K_d > K_c$ is assumed. If $K_d < K_c$, then $K_d - K_c$ should be read as $K_c - K_d$):

$$P_I = [(V_t - V_0)(K_d - K_c)]/[V_0(V_0/F)] = H(K_d - K_c)u/Z \quad (8)$$

This equation implies that P is proportional to u and the inverse of Z.

We search for the maximum sample feed volume $V_{F,M}$ that satisfies a specified purity ratio Q_P and recovery ratio Q_R for a given Z and d_p at a certain u. The calculation scheme is summarized as follows (the experimental results for the h–v relationships and K values are used; the subscript t means a tentative value):

(1) Set K_c, K_d, ε, d_p, $D_{m,c}$, $D_{m,d}$ and Z, and specify Q_R and Q_P.

(2) Set u and determine N_c and N_d from the h–v curves.

(3) Set a tentative value of the sample volume $V_{F,t}$.

(4) Calculate the elution curves by eqn. 1.

(5) Calculate $Q_{P,t}$ as a function of $Q_{R,t}$ for the desired substance. [The elution curves of the target protein and the contaminant are integrated from the rear or the front end of the curve to give m_c or m_d as a function of time (in this study, from the rear end of the BSA monomer curve). Q_P and Q_R are then calculated from these values on the basis of eqns. 6 and 7. Then, from the Q_P–time and Q_R–time relationships, the $Q_P - Q_R$ relationship is obtained (see Fig. 3).]

(6) Compare $Q_{P,t}$ with Q_P at $Q_{R,t} = Q_R$.

(7) If $Q_{P,t} > Q_P$, increase $V_{F,t}$; if $Q_{P,t} < Q_P$, decrease $V_{F,t}$.

(8) Repeat (4)–(7) until $(1 - V_{F,old}/V_{F,new}) < 0.01$.

(9) Set this V_F to be $V_{F,M}$ and calculate P by eqn. 5.

Although the above scheme treats the two elution curves, it can be extended to more than two curves. This program is now commercially available from Nihon Kagaku Gijyutu Kensyusyo (Tokyo, Japan) as JUSE-BIOLC[19].

EXPERIMENTAL

TSK G-3000SW HPGFC columns of various dimensions were employed: column A, $Z = 30$ cm, $d_c = 0.75$ cm, $d_p = 10$ μm; column B, $Z = 67.5$ cm, $d_c = 0.75$ cm, $d_p = 10$ μm; column C, $Z = 67.5$ cm, $d_c = 2.15$ cm, $d_p = 13$ μm; column D, $Z = 60.0$ cm, $d_c = 5.5$ cm, $d_p = 17$ μm; column E, $Z = 80$ cm, $d_c = 10.8$ cm, $d_p = 17$ μm; column F, $Z = 10$ cm, $d_c = 4.5$ cm, $d_p = 17$ μm.

The apparatus used was a CCPE pump (Tosoh) and a UV-8010 UV detector (Tosoh) for columns A, B, C and F and a CCP-8070 pump (Tosoh) and a UV-8070 UV detector (Tosoh) for columns D and E.

The mobile phase (elution buffer) was 10 mM phosphate buffer (pH 6.8) containing 0.3 M sodium chloride or 0.2 M phosphate buffer (pH 6.8). Bovine serum

albumin (BSA) (Cohn Fraction V, Sigma, A8022) dissolved in the buffer solution was used as a sample. The concentration of BSA was 0.2–0.5% in most experiments. The experiments were carried out at 20–25°C.

The peak retention time, t_M, and the peak width at $C = 0.368\ C_M$, w, were measured from the elution curve at small V_F values (C_M = the maximum peak height in the elution curve). The HETP values were calculated according to the equation

$$\text{HETP} = Z[(w^2/8 - t_0^2/12)/(t_M - t_0/2)^2] \tag{9}$$

The HETP–u relationships were then converted to h–v relationships with the d_p value and the D_m value calculated using the equation presented by Young *et al.*[20]. The void fraction of the column, ε, was determined from the t_M of Blue Dextran 2000 pulses. The Q_P and Q_R values and the initial concentration of each component contained in the sample (C_0) were determined from the area of the analytical chromatogram using a TSK G-3000SWXL HPGFC column (30 × 0.75 cm I.D.) with $F = 0.4$ ml/min and $V_F = 0.1$ ml.

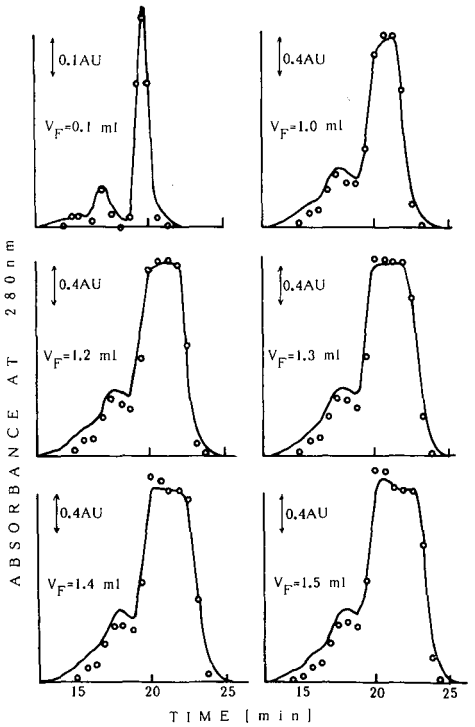

Fig. 1. Experimental and calculated elution curves for various sample volumes (V_F). Curves, experimental elution curves (detector response at 280 nm). Column A (30 × 0.75 cm I.D., d_p = 10 μm); BSA concentration, 0.5%; F = 0.4 ml/min. ○, Calculated results (the sum of monomer, dimer and aggregate curves). Data used for the calculation: $\varepsilon = 0.37$, $K_{monomer} = 0.35$, $K_{dimer} = 0.22$, $K_{aggregates} = 0.14$, $C_{0,monomer}$:$C_{0,dimer}$:$C_{0,aggregates}$ = 1:0.22:0.08 (determined from the chromatogram by analytical HPGFC). N values for monomer, dimer and aggregates were determined from the h–v relationship; $h = 4 + 0.09v$ shown in Fig. 2. The calculated Q_R value at $Q_P = 0.99$ is 0.97 at V_F = 1.0 ml, 0.88 at V_F = 1.2 ml, 0.82 at V_F = 1.3 ml, 0.77 at V_F = 1.4 ml and 0.72 at V_F = 1.5 ml.

RESULTS

Elution curves and h–v relationships

Experimental and calculated elution curves on a small-scale column at various V_F values are shown in Fig. 1. The HETP values of BSA monomer were determined from the peak width of the elution curve at small V_F. Then, the HETP–u relationships were converted to h–v relationships. As shown in Fig. 2, the h–v relationships can be described by the equation

$$h = 4 + 0.09v \tag{10}$$

regardless of the particle size, d_p, as shown in a previous study[18]. This is the basis for examining the effect of d_p on P in the following section.

When V_F is increased, the elution curve of BSA monomer becomes flat-topped, as shown in Fig. 1. It is interesting that the shape of the elution curves varies markedly with a small change in V_F in the range 1–1.5 ml.

No substantial difference is found in the experimental elution curves at different sample concentrations (0.25–1%), as shown in Fig. 3.

We calculated the elution curves with eqn. 1 based on the assumption that they can be described by the sum of the three components, monomer (mol.wt. 69 000), dimer (mol.wt. 150 000) and higher molecular weight aggregates (mol.wt. 300 000), although there may be several different molecular weight aggregates and other contaminants such as globulins. A further assumption is that the h–v relationships are similar for the three components. The calculated points are in fairly good agreement with the experimental curves in Figs. 1 and 3. The calculation shows that the small peak maximum observed on the left-hand side of the monomer curve in Fig. 3 is caused by the sum of the three peaks and is not the true peak. The calculated Q_P–time and Q_R–time curves in Fig. 3 and the calculated Q_R values at $Q_P = 0.99$ given in the legend of Fig. 1 clearly illustrate the general relationship between Q_P and Q_R. For example, in Fig. 1 when $Q_P = 0.99$ and $Q_R = 0.90$ are required, the $V_{F,M}$ value may be between 1.0 and 1.2 ml. This is the principle of the present method of determining P, which will be shown in the next section.

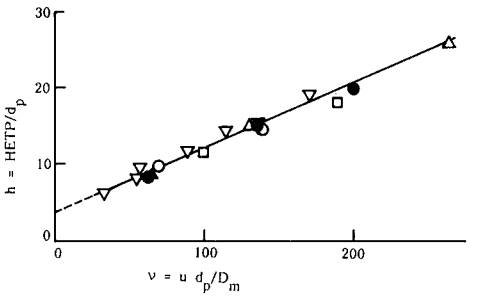

Fig. 2. Relationship between h and v for BSA monomer on columns of various dimensions. ▽ = Column A (30 × 0.75 cm I.D., d_p = 10 μm); ○ = column B (67.5 × 0.75 cm I.D., d_p = 10 μm); □ = column C (67.5 × 2.15 cm I.D., d_p = 13 μm); △ = column D (60.0 × 5.5 cm I.D., d_p = 17 μm); ● = column E (80 × 10.8 cm I.D., d_p = 17 μm). BSA concentration, 0.2–0.5%; V_F = 0.003–0.01 V_t. For other conditions, see Experimental.

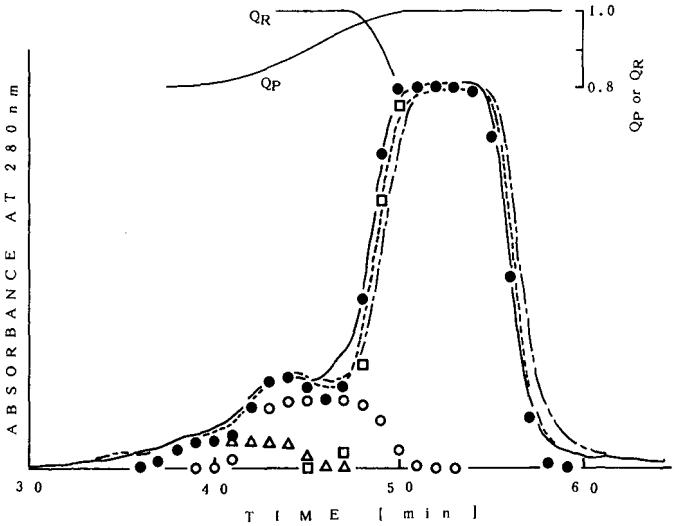

Fig. 3. Experimental and calculated elution curves for various sample concentrations on a large-scale column. Column E (80 × 10.8 cm I.D., d_p = 17 μm); V_F = 695 ml; F = 93 ml/min. — = Experimental results, 0.25% BSA; --- = experimental results, 0.5% BSA; -·- = experimental results, 1.0% BSA; ● = calculated results for the sum of monomer, dimer and aggregate curves; △ = calculated results for aggregates; ○ = calculated results for dimer; □ = calculated results for monomer. Data used for the calculation: ε = 0.36, $K_{monomer}$ = 0.39, K_{dimer} = 0.26, $K_{aggregates}$ = 0.17, $C_{0,monomer}$:$C_{0,dimer}$:$C_{0,aggregates}$ = 1:0.18:0.07. Note that these values are different from those used in Fig. 1 owing to the inter-lot variation of GFC packings and BSA samples. N values were determined by the same procedure as that in Fig. 1. The calculated Q_P–time and Q_R–time curves are also shown.

Relationship between P and u

Fig. 4 shows the calculated relationship between P and u for various combinations of Z and d_p at $Q_R = Q_P = 0.99$. Let us examine the P–u curve for the shortest column, *i.e.*, 17 μm particle size and 10 cm long column. P increases with increasing u in the range u = 0 to 0.6 cm/min and shows a maximum value P_M at u = 0.6 cm/min (hereafter, this u is called u_M). Above u_M, P drops rapidly to zero (the u value at which P is almost equal to zero is designated u_c). This is explained as follows: N decreases with u as predicted by eqn. 3. Therefore, when u is increased V_F should be reduced in order to satisfy Q_P and Q_R. Below u_M the decrease in cycle time (V_0/F) is larger than that in V_F/V_0. This results in an increase in P with u. On the other hand, P decreases with u above u_M as V_F/V_0 decreases much more rapidly than V_0/F. Above u_c, a specified Q_P is not obtained even at the limit of V_F = 0.

Although no substantial P_M is observed for the other three P–u relationships, the slope of the curve decreases gradually with increasing u. For the same d_p, P for a shorter column is higher than that for a longer one in the range $u < u_M$. It should be also noted that P is markedly increased with decrease in d_p.

The filled circles in Fig. 4 are the experimental results obtained with column F (d_c = 4.5 cm, Z = 10 cm and d_p = 17 μm). The Q_P and Q_R values were obtained from the HPGFC trace for the recovered fraction. Fig. 5 shows the elution curves obtained with column F, which corresponds to P_M in Fig. 4. Although the Q_P and Q_R values are

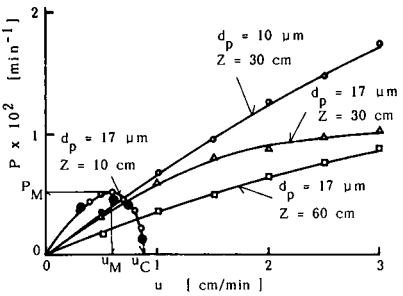

Fig. 4. Relationship between P and u. The data used in the calculation are the same as in Fig. 3; ●, experimental results with column F (10 × 4.5 cm I.D., d_p = 17 μm). Q_R = 0.94–0.95 and Q_P = 0.95–0.96 for these experimental results determined from the chromatogram obtained by analytical HPGFC.

lower than those in Fig. 4, it is seen that such a short column can separate BSA monomer fairly well.

Fig. 6 shows the calculated relationship between P_M and Q_P at Q_R = 0.99 and P_M and Q_R at Q_P = 0.99 for Z = 10 cm and d_p = 17 μm. P_M increases with decreasing Q_P or Q_R, but P_M is more sensitive to Q_P.

Fig. 7 shows the calculated relationship between P_M and Z at $Q_P = Q_R$ = 0.99. The slope of the P_M–Z relationship decreases with increasing Z.

DISCUSSION

The recovery of protein monomer from its aggregates is a very important process in biotechnology[2]. As this process is usually performed in the last stage of purification, the amount of monomer is much larger than that of the aggregates and other contaminants. Therefore, in the production process, the overloading conditions can be

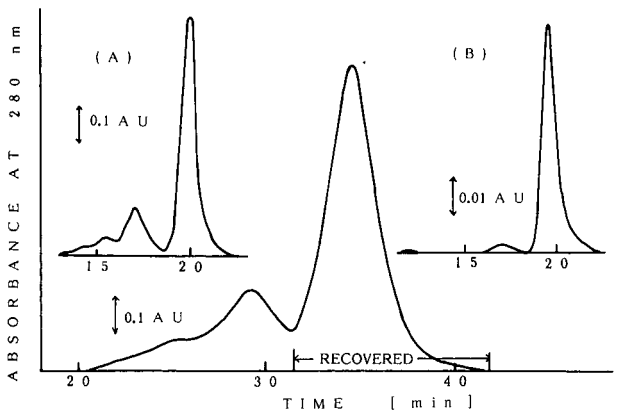

Fig. 5. Experimental elution curves on a 10.0 × 4.5 cm I.D. column (d_p = 17 μm) and the purity of the recovered fraction checked by the analytical column. Column F; 0.5% BSA; V_F = 3.73 ml; F = 2.7 ml/min. The insets show the chromatograms of (A) the sample and (B) the recovered fraction by the analytical column (30 × 0.75 cm I.D. TSK G-3000SW XL); F = 0.4 ml/min; V_F = 0.1 ml. From the analytical chromatogram, Q_P and Q_R of the recovered fraction were determined as 0.95 and 0.96, respectively.

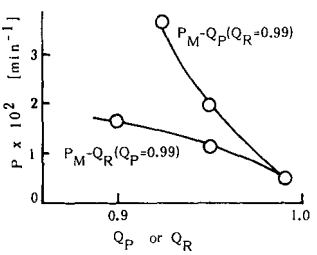

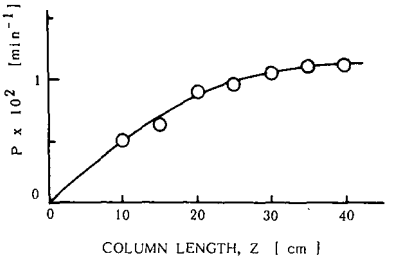

Fig. 6. Calculated relationships P_M–Q_R at $Q_P = 0.99$ and P_M–Q_P at $Q_R = 0.99$. $d_p = 17\ \mu m$; $Z = 10$ cm; $\varepsilon = 0.36$; other data used in the calculation as in Fig. 3.

Fig. 7. Calculated relationship between column length and P_M. $d_p = 17\ \mu m$; $\varepsilon = 0.36$; $Q_P = Q_R = 0.99$; other data used in the calculation as in Fig. 3.

chosen as shown in ref. 2. For the determination of the column dimensions and operating variables for such conditions, the method presented here is considered useful.

The HETP–u relationship for BSA dimer and aggregates were not determined easily from the experimental elution curves as each curve contains the other components. We assumed that the h–ν relationships for BSA dimer and for aggregates are the same as that for BSA monomer. This may be a crude approximation, although the calculated elution curves on the basis of this approximation are in fairly good agreement with the experimental curves shown in Figs. 1 and 3.

The purpose of this work was not to determine the optimum conditions for the system chosen in this study but to present a method for calculating the productivity at a specified purity and recovery. By using such a calculation program, we can survey the general trends of the effect of the column dimensions and particle diameter on the P–u relationship with the HETP–u relationship and K values obtained with a given small-scale column. This will reduce the number of experiments that are needed in scaling up GFC columns.

Although it is difficult to establish a general strategy for maximizing P from the present results, some interesting findings were obtained. P_M exists in the P–u relationship when the separation is difficult, *i.e.*, with columns of small N. In general, when Z is increased, F must be increased in order to obtain a similar P value. However, F cannot be increased beyond a certain F_c value, especially in the case of soft GFC gel columns owing to compression of the gels[3]. Even for rigid gel columns such as HPGFC columns, F_c is designated by the manufacturer. In some instances there is a pressure limit for the apparatus. Hence, even when the calculated P–u relationship has no maximum as shown in Fig. 4, the P value at $F = F_c$ becomes P_M.

Hence, P_M for a given separation system (solutes–gel media) becomes:

$$P_M = f(Q_P, Q_R, d_p, Z, F_c) \tag{11}$$

It is known[3] that F_c decreases with increase in d_c and Z:

$$F_c = f(d_c, Z) \tag{12}$$

These equations indicate that P_M for a specified Q_P and/or Q_R is a complicated function of d_p, d_c and Z. However, as the present calculation method is easily performed on a personal computer, the user may determine the column and operating variables so that the specifications are fulfilled.

It is often said that d_p should be increased in scaling up GFC columns. However, both Z and F must be increased in order to compensate for the loss in P due to the increase in d_p. As stated above, an increase in Z sometimes conflicts with an increase in F. Hence it is desirable that the column with small d_p be operated at low flow-rates in order to increase P.

As GFC is linear isocratic LC, the solute concentration C_0 has no effect on P in the calculation. In this study, the effect of C_0 was not observed for the experimental elution curves with C_0 = 0.25–1.0%, as shown in Fig. 3. However, it should be borne in mind that the separation efficiency often decreases drastically when the sample concentration is so high that the viscosity of the sample is much higher than that of the mobile phase[1,21].

SYMBOLS

A_c	column cross-sectional area (cm^2)
A^*	axial dispersion term in eqn. 2
B^*/v	molecular diffusion term in eqn. 2
C	solute concentration at the column outlet (% or M)
C_M	maximum peak concentration of the elution curve (% or M)
C_0	initial concentration (% or M)
C^*v	stationary phase diffusion term in eqn. 2
D^*v	fluid (stagnant)-film mass transfer term in eqn. 2
D_m	molecular diffusion coefficient (cm^2/s)
d_c	column diameter (cm)
d_p	particle diameter (μm)
F	volumetric flow-rate (ml/min)
H	$= (1 - \varepsilon)/\varepsilon = (V_t - V_0)/V_0$
HETP	height equivalent to a theoretical plate (plate height) (cm)
h	$=$ HETP$/d_p$, reduced plate height
K	distribution coefficient (see eqn. 4 for the definition)
k'	capacity factor
m	amount of recovered fraction (g or mol)
N	$= Z/$HETP, total number of theoretical plates
P	$= Q_R V_{F,M}/[V_0(V_0/F)]$, productivity ($min^{-1}$)
P_M	maximum productivity in the P–u relationship (min^{-1})
Q_P	$= m_d/(m_d + m_c)$, purity ratio
Q_R	$= m_d/(V_F C_{0,d})$, recovery ratio
T	$= t/[(Z/u)(1 + HK)]$
T_0	$= t_0/[(Z/u)(1 + HK)]$
t	time from the start of the sample injection (min or s)
t_M	peak retention time (min or s)
t_0	sample injection time (min or s)
u	$= F/(A_c\varepsilon)$, linear mobile phase velocity (cm/min or cm/s)

V_F = Ft_0, sample feed volume (ml)
$V_{F,M}$ maximum V_F value that satisfies Q_P and Q_R (ml)
V_0 = $V_t\varepsilon$, column void volume (ml)
V_t = A_cZ, total column volume (ml)
w peak width measured at $C = 0.368C_M$ (min or s)
Z column length (cm)
ε void fraction of column
ν = ud_p/D_m, reduced velocity

REFERENCES

1 H. Determann and J. E. Brewer, in E. Heftmann (Editor), *Chromatography*, Van Nostrand Reinhold, New York, 3rd ed., 1975, p. 362.
2 J. M. Curling (Editor), *Methods of Plasma Protein Fractionation*, Academic Press, Oxford, 1980.
3 J. C. Janson and P. Hedman, *Adv. Biochem. Eng.*, 25 (1982) 43.
4 E. Glueckauf, *Trans. Faraday Soc.*, 51 (1955) 34.
5 J. R. Conder and M. K. Shingari, *J. Chromatogr. Sci.*, 11 (1973) 525.
6 J. H. Knox and H. M. Pyper, *J. Chromatogr.*, 363 (1986) 1.
7 P. C. Wankat and Y.-M. Koo, *AIChE J.*, 34 (1988) 1006.
8 M. Kubin, *Collect. Czech. Chem. Commun.*, 30 (1965) 1104.
9 E. Kucera, *J. Chromatogr.*, 19 (1965) 237.
10 A. Rasmuson, *AIChE J.*, 31 (1985) 518.
11 S. Yamamoto, M. Nomura and Y. Sano, in preparation.
12 H. R. Halvorson and G. K. Ackers, *J. Polym. Sci., Part A-2*, 9 (1971) 245.
13 E. N. Lightfoot, R. J. Sanchez-Palma and D. O. Edwards, in H. M. Schoen (Editor), *New Chemical Engineering Separation Techniques*, Interscience, New York, 1962, p. 99.
14 G. Houghton, *J. Chromatogr.*, 15 (1964) 5.
15 J. J. van Deemter, F. J. Zuiderweg and A. Klinkenberg, *Chem. Eng. Sci.*, 5 (1956) 271.
16 S. R. Rudge and M. R. Ladisch, *Biotechnol. Prog.*, 4 (1988) 123.
17 S. Yamamoto, K. Nakanishi and R. Matsuno, *Ion-Exchange Chromatography of Proteins*, Marcel Dekker, New York, 1988.
18 S. Yamamoto, M. Nomura and Y. Sano, *J. Chromatogr.*, 394 (1987) 363.
19 *User's Manual for JUSE-BIOLC Software*, Nihon Kagaku Gijyutsu Kensyujyo, Tokyo, 1989 (in Japanese).
20 M. E. Young, P. A. Carroad and R. L. Bell, *Biotechnol. Bioeng.*, 22 (1980) 947.
21 S. Yamamoto, M. Nomura and Y. Sano, *J. Chem. Eng. Jpn.*, 19 (1986) 227.

Journal of Chromatography, 512 (1990) 89–100
Elsevier Science Publishers B.V., Amsterdam

CHROMSYMP. 1820

Preparative chromatography of proteins

Design calculation procedure for gradient and stepwise elution

SHUICHI YAMAMOTO*, MASAKI NOMURA[a] and YUJI SANO
Department of Chemical Engineering, Yamaguchi University, Tokiwadai, Ube 755 (Japan)

ABSTRACT

A method is presented for determining stepwise elution chromatographic conditions on the basis of the data obtained from linear gradient elution experiments. The separation of crude β-galactosidase by medium-performance (an)ion-exchange chromatography (MPIEC) was chosen as a model separation system. Some factors affecting the purification such as the column dimensions and the residence time were investigated. Large-scale MPIEC was carried out and its performance was compared with that of a small scale-column. The effect of sample loading was also examined.

INTRODUCTION

Stepwise elution, in which a discontinuous change in the salt concentration of the elution buffer is introduced into a column, is one of the elution (separation) methods for proteins in ion-exchange chromatography (IEC), hydrophobic interaction chromatography (HIC) and affinity chromatography. The attraction of this method is that the apparatus and the operating procedure are simple. However, there are several disadvantages with stepwise elution, as pointed out previously[1–3]. One of the most serious disadvantages is an artificial peak due to a discontinuous change in the elution buffer. For example, when all the proteins contained in the sample are desorbed completely by the elution buffer, they will be eluted as a single peak[1]. On the other hand, when a protein is not eluted completely by the first elution buffer, the subsequent second elution buffer may cause an artificial, peak frequently called a 'false peak'[1]. These phenomena make it difficult to interpret the experimental results and may lead to a misunderstanding regarding the homogeneity of the eluted fraction.

In ideal-affinity chromatography, only the desired protein is adsorbed on the

[a] Present address: Tosoh Corporation, Tonda, Shinnanyo 746, Japan.

0021-9673/90/$03.50

column biospecifically and subsequent desorption yields the purified product. In contrast, a number of contaminant proteins present in the sample are adsorbed on IEC or HIC columns and the desired protein must be resolved during the desorption (elution) process. For example, the desired protein is desorbed while the other contaminants are retained or the contaminants are washed out while the desired protein is retained. For this purpose, a knowledge of the salt concentration dependence of the distribution coefficients, $K(I)$, of the contaminant proteins and of the desired protein is required[1,4,5]. However, the measurement of $K(I)$ for the contaminant proteins by a batch experiment is usually impossible unless a specific detection method for individual contaminant proteins is available. Moreover, the measurement of $K(I)$ is time consuming and laborious.

We previously reported a method for determining $K(I)$ from linear gradient elution experiments and verified the method experimentally[1,6]. In this study, this method was applied to the design of the stepwise elution of crude β-galactosidase with medium-performance IEC (MPIEC) columns. Some factors affecting the purification were investigated. Large-scale MPIEC was carried out and its performance was compared with that of a small scale-column. The effect of sample loading was also examined.

EXPERIMENTAL

The enzyme used was crude β-galactosidase from *Aspergillus oryzae*, obtained from Amano Pharmaceutical (Japan) as Lactase F. The enzyme activity of β-galactosidase was determined spectrophotometerically by measuring the change in the absorbance at 420 nm of the substrate (*o*-nitrophenylgalactoside) with time[7].

The MPIEC packings used are anion-exchange gels having diethylaminoethyl (DEAE) groups, distributed by Tosoh (Tokyo, Japan): DEAE Toyopearl 650S ($d_p = 40$ μm) for columns of 15 × 1.6 cm I.D., 30 × 1.6 cm I.D., 2 × 2.2 cm I.D. and 2 × 10.8 cm I.D.; DEAE Toyopearl 650M ($d_p = 65$ μm) for columns of 15 × 1.4 cm I.D. and 40 × 31 cm I.D.; and DEAE Toyopearl 650C ($d_p = 87$ μm) for columns of 15 × 1.4 cm I.D. All were employed as closed columns. Details of the design of the large column are described elsewhere[8]. The apparatus and the operating method are similar to those in our previous studies[6,9,10]: for small columns, peristaltic pumps, an Altex 153 UV detector and a Horiba (Kyoto, Japan) DS-8M conductivity meter for the measurement of sodium chloride concentration; for large columns, a CCP-8070 pump (Tosoh) and a UV-8070 UV detector (Tosoh).

The elution was performed by an increase in sodium chloride concentration from 0.03 *M* either continuously (linear gradient elution) or discontinuously (stepwise elution) at a fixed pH (7.7) and 25°C. The buffer solution was 14 m*M* Tris–HCl (pH 7.7). The initial buffer contained 0.03 *M* sodium chloride. As Blue Dextran 2000, commonly used for the determination of the column void volume, V_o, in gel filtration chromatography, is adsorbed on DEAE IEC columns, we employed Dextran T-2000 (Pharmacia) pulses for determining V_o. The eluted fractions were collected with a fraction collector and the protein concentration and the enzyme activity were determined.

As a measure of the degree of purification, the purification factor, defined as $(\text{enzyme activity/protein amount})_{\text{recovered}}/(\text{enzyme activity/protein amount})_{\text{sample}}$, was used.

The protein concentration in the recovered fraction and in the sample were determined from the absorbance at 280 nm or by the biuret method. HPIEC was employed to test the homogeneity of the fractionated sample by the MPIEC columns. The sample (the peak fraction from the MPIEC columns) was dialysed against the initial buffer (the same as that for the MPIEC) before it was applied to the HPIEC column (TSK-gel DEAE 5PW, 7.5 × 0.75 cm I.D.).

RESULTS

Determination of K(I)

The elution curve for the sample used (crude β-galactosidase), obtained by linear gradient elution on an MPIEC column, is shown in Fig. 1. Although a number of peaks including a peak having the enzyme activity (peak B) are observed, we focus our attention on the three large peaks A, B and C shown in Fig. 1. Peak A is eluted at very low salt concentrations, so, this peak can be washed out with the starting buffer in the stepwise elution. Therefore, the chromatographic conditions should be such that peak B, the desired enzyme, is eluted whereas peak C is retained. The linear gradient elution experiments were carried out with different slopes of the gradient, g, then the salt concentration at the peak position, I_R, was measured (the experimental results are summarized in Table I). The GH *vs.* I_R plots for peaks B and C are shown in Fig. 2 [GH is the slope of the gradient normalized with respect to the column gel volume; $GH = g(V_t - V_o)$]. The GH–I_R relationship is not dependent on the flow-rate, the column dimensions, the sample volume or the particle diameter. The elution position of peaks B and C in the linear gradient elution experiments can be predicted from these GH–I_R curves[1,4,5,8]. It should also be noted that the slope of the GH–I_R curve corresponds to the number of charges involved in the adsorption equilibria[1,4–6].

In the design of the stepwise elution, the K–I relationship is needed[1,4,5]. We have also shown that the K–I relationship can be obtained from the GH–I_R curve on the basis of the following equation[1,6]:

$$d(GH)/dI = 1/[K(I) - K']$$

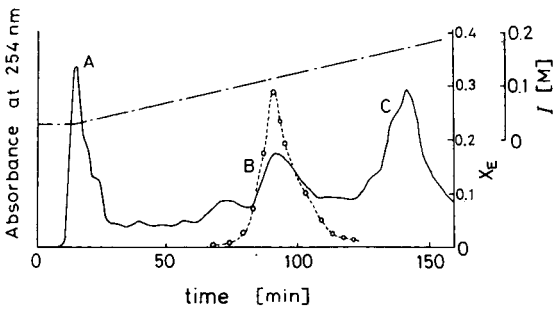

Fig. 1. Elution curve of crude β-galactosidase obtained by linear gradient elution on a MPIEC column. The linear gradient elution experiment was performed with a linear increase in NaCl concentration in the buffer (14 mM Tris–HCl, pH 7.7) from 0.03 M at 25°C. Column DEAE Toyopearl 650S ($d_p = 40$ μm), 15 × 1.6 cm I.D. Slope of NaCl gradient, $g = 6 \cdot 10^{-4}$ M/ml; $F = 2$ ml/min. Sample (crude β-galactosidase), 10 ml of 1% solution. (O) X_E = ratio of the enzyme activity to that of the sample. (— · —) I = NaCl concentration.

TABLE I

EXPERIMENTAL DATA PLOTTED IN FIG. 2.

Sample (crude β-galactosidase) concentration 1%; packing DEAE Toyopearl 650; pH, 7.7; initial salt (NaCl) concentration, 0.03 *M*.

d_p (μm)	d_c (cm)	Z (cm)	F (ml/min)	$g \times 10^3$ (M/ml)	$GH \times 10^2$ (M)	I_R for peak B (M)	I_R for peak C (M)	Sample volume (ml)
40	1.6	15	2.0	2.3	4.0	0.123	0.181	5
				1.1	2.0	0.117	0.177	2
				0.56	1.0	0.101	0.159	10
				0.40	0.71	0.100	ND[a]	2
	1.6	30	1.4	0.87	2.9	0.128	0.195	5
65	1.4	15	1.1	1.5	2.1	0.112	0.166	8
			2.0	0.66	0.91	0.108	0.159	2
				2.9	4.0	0.125	0.182	2
87	1.4	15.	0.9	2.3	3.0	0.131	0.195	8
			2.0	1.6	2.1	0.123	0.188	2
				0.72	0.95	0.115	0.174	2

[a] ND = Not determined.

where K' is the distribution coefficient of the gradient substance (in this instance sodium chloride). The $K(I)$ values for peaks B and C thus obtained are shown in Fig. 3. The K values obtained by isocratic elution experiments with the purified fraction of peaks B and C as a sample (symbols in Fig. 3) are in good agreement with the $K(I)$ values determined from the GH–I_R curve.

Effect of the salt concentration of the elution buffer, I_E

The elution behaviour in the stepwise elution can be grouped into two types, as explained previously[1,4,5]. One is the case where a protein is desorbed completely in

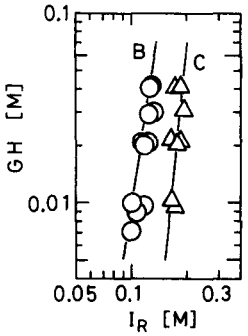

Fig. 2. Relationship between GH and salt concentration at the peak position I_R for peaks B and C in Fig. 1. Linear gradient elution experiments were carried out with various slopes of the gradient g under the experimental conditions shown in Fig. 1. Then the salt (NaCl) concentration at the peak position I_R was measured. $GH = g(V_t - V_o)$; V_t = the total column volume; V_o = the column void volume. Peak B has the enzyme activity and peak C is the contaminant (see Fig. 1). See Table I for the details of the experimental conditions for the points.

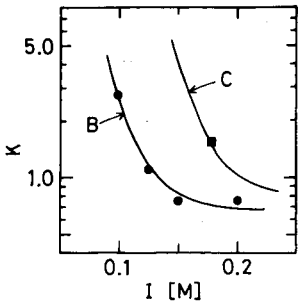

Fig. 3. Relationship between distribution coefficient K and salt (NaCl) concentration, I. The solid curves were obtained from differentiation of the corresponding GH *vs.* I_R curve in Fig. 2[1,6]. The symbols are the experimental results from the isocratic elution experiments with the peak fraction of the linear gradient elution as the sample.

the elution buffer and therefore is eluted in (or near) the spreading front boundary of the elution buffer as a very sharp peak (type I elution). In this case, the K value at $I = I_E$, K_E is less than or nearly equal to K'. The shape of the front boundary of the elution buffer from I_o to I_E plays a similar role to the steep slope of the gradient. In another case, the protein peak appears after the concentration of the composition of the elution buffer at the exit of the column reaches its initial value (type II elution).

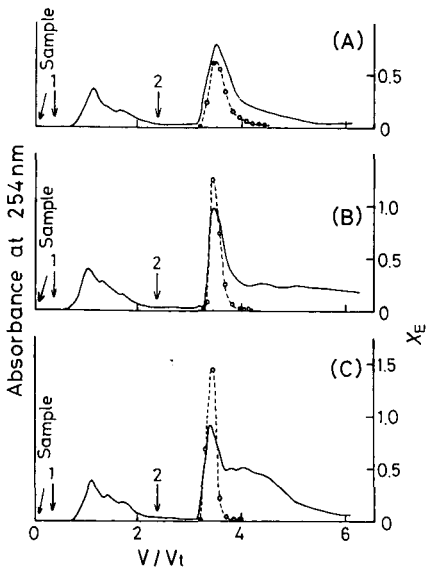

Fig. 4. Effect of the salt concentration of the elution buffer I_E in the stepwise elution. V = the volume from the start of the experiment and V_t is the total column volume. (o) X_E = the ratio of the enzyme activity to that of the sample. Sample = 1% crude β-galactosidase dissolved in the starting buffer [14 mM Tris–HCl (pH 7.7) containing 0.03 M NaCl], 10 ml. Column, DEAE Toyopearl 650S (d_p = 40 μm), 15 × 1.6 cm I.D. The arrows indicate the change in the elution buffer: 1, starting buffer (washing); 2, elution buffer, 14 mM Tris–HCl (pH 7.7) containing (A) 0.13, (B) 0.15 and (C) 0.17 M NaCl. F = 1.3 ml/min; 25°C. The purification factor is (A) 2.6, (B) 2.3 and (C) 2.0. The recovery was 90–93%.

The peak is diluted considerably compared with those in type I elution. K_E in this case is greater than K'. Obviously, it is desirable that the required protein is eluted by type I elution. From Fig. 3, I_E was determined as 0.15, where peak B is eluted by type I elution and the K of peak C is large enough for peak C to be retained in the column. After the sample (1% β-galactosidase, 10 ml) was applied, the column was washed with the initial starting buffer until the UV detector response fell almost to zero. Subsequently, the elution buffer was applied. The elution curves obtained with different I_E values are shown in Fig. 4.

The shape and peak position of the elution curves are markedly influenced by small changes in I_E. The peak elution volume at $I_E=0.13$ is larger than that at $I_E=0.15$. The peak height at $I_E=0.13$ is much lower than that at $I_E=0.15$ and $I_E=0.17$. This is typical of type II elution behaviour. Although the peak height at $I_E=0.17$ is larger than that at $I_E=0.15$, the purification factor is low. In order to check the homogeneity of the fractions, linear gradient elution of the fractions from the MPIEC column was carried out with an HPIEC column. The resulting chromatograms (Fig. 5) indicate that peak A is eliminated in any of the three stepwise elution experiments but the removal of peak C is dependent on I_E. At $I_E=0.17$, considerable amounts of peak C still remain although the ratio of the area of peak B to the total area increased from that in the starting sample. Peak C was removed to a great extent at $I_E=0.13$ and 0.15. The choice of $I_E=0.15$ from Fig. 3 is therefore suitable for the purification of the present sample.

Effect of residence time

The column productivity, *e.g.*, amount of protein recovered per unit column volume in unit separation time, can be increased by decreasing the residence time.

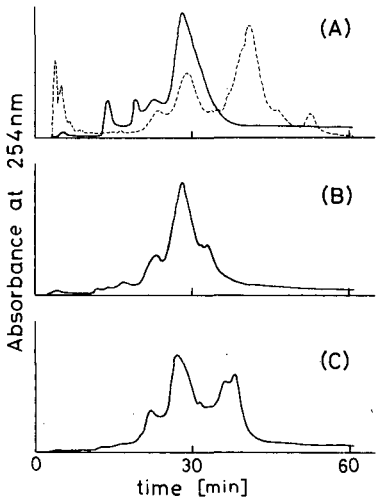

Fig. 5. HPIEC of the purified fraction of β-galactosidase shown in Fig. 4. The linear gradient elution experiment was performed with a linear increase in NaCl concentration in the buffer [14 mM Tris–HCl (pH 7.7)] from 0.03M at 25°C. Column, TSK-gel DEAE 5PW (7.5 × 0.75 cm I.D.); $g=4.7\cdot10^{-3}$ M/ml; $F=1$ ml/min. The sample used is (A) the fraction in Fig. 4A, (B) the fraction in Fig. 4B and (C) the fraction in Fig. 4C. The dashed curve (A) is the elution curve of the crude sample.

This can be done by increasing the flow-rate or by decreasing the column length. Two experiments were carried out in one instance the superficial velocity was increased by a factor of 2.3 and in the other case the column length was decreased by a factor of 7.5 (Fig. 6). Although the X_E values were lowered on decreasing the residence time, the purification factor values and the HPIEC results (Fig. 7) are similar. This suggests that the column productivity can be increased by using a short column and/or high flow-rates if we ignore the concentration factor.

Effect of sample loading

The next task was to determine the sample loading. Unfortunately, this had to be done by preliminary column experiments as it is difficult to measure the $K(I_o)$ values for the contaminants. The elution curves at $I_E = 0.15$ with different sample volumes and sample concentrations are shown in Fig. 8. Although the elution pattern during the wash out is different, the enzyme peak shapes are similar. The peak for the sample of 1% and 75 ml is markedly concentrated. However, the HPIEC results (Fig. 9) indicate that the ratio of the area of peak C in the fraction at a sample volume of 75 ml (1%) is higher than that at a sample volume of 10 ml (1%). This corresponds to a decrease in the purification factor. It is interesting that both the purification factor values and the chromatograms are similar for equal amounts of the sample, *i.e.*, 10 ml of 1% and 100 ml of 0.1% solution. The sample loading for 75 ml of 1% solution is 25 mg of crude enzyme per ml of column. This value is high for protein separation by liquid chromatography[1,11].

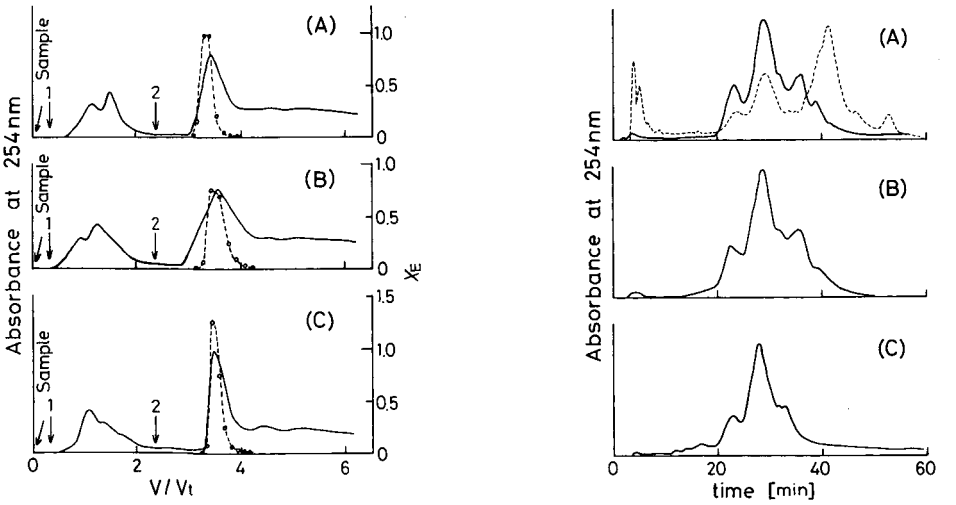

Fig. 6. Effect of residence time. Arrows and symbols as in Fig. 4. Columns DEAE Toyopearl 650 MPIEC ($d_p = 40\mu m$), (A) 15 × 1.6 cm I.D., $F = 3$ ml/min, sample 10 ml of 1% solution, residence time $V_t/F = 10$ min; (B) 2.0 × 2.2 cm I.D., $F = 2.4$ ml/min, sample 2.5 ml of 1% solution, $V_t/F = 3.2$ min; (C) 15 × 1.6 cm I.D., $F = 1.3$ ml/min, sample 10 ml of 1% solution, $V_t/F = 23$ min. Elution buffer, 14 m*M* Tris–HCl (pH 7.7) containing 0.15 *M* NaCl. Other conditions as in Fig. 4. The purification factor is (A) 2.1, (B) 2.0 and (C) 2.3. The recovery was 90–93%.

Fig. 7. HPIEC of the purified fraction of β-galactosidase shown in Fig. 6. Conditions as in Fig. 5. The sample used is (A) the fraction in Fig. 6A, (B) the fraction in Fig. 6B, (C) the fraction in Fig. 6C. The dashed curve is the elution curve of the crude sample.

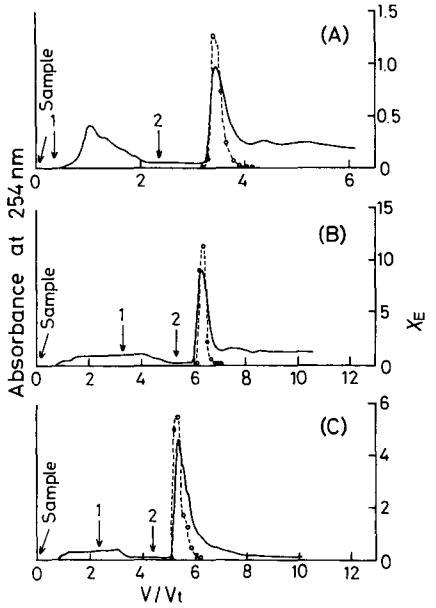

Fig. 8. Effect of the sample loading. Arrows and symbols as in Fig. 4. Column DEAE Toyopearl 650 S (d_p = 40 μm), 15 × 1.6 cm I.D.; elution buffer, 14 mM Tris–HCl (pH 7.7) containing 0.15 M NaCl; F = 1.3 ml/min; 25°C; sample, (A) 10 ml of 1% solution, (B) 100 ml of 0.1% solution and (C) 75 ml of 1% solution. Other conditions as in Fig. 4. The purification factor is (A) 2.2, (B) 2.5 and (C) 1.7. The recovery was 90–93%.

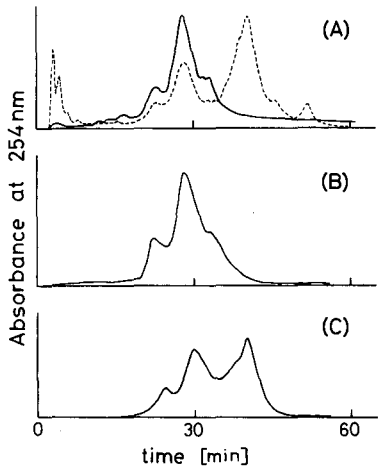

Fig. 9. HPIEC of the purified fraction of β-galactosidase shown in Fig. 8. Conditions as in Fig. 5. The sample used is (A) the fraction in Fig. 8A, (B) the fraction in Fig. 8B and (C) the fraction in Fig. 8C. The dashed curve is the elution curve of the crude sample.

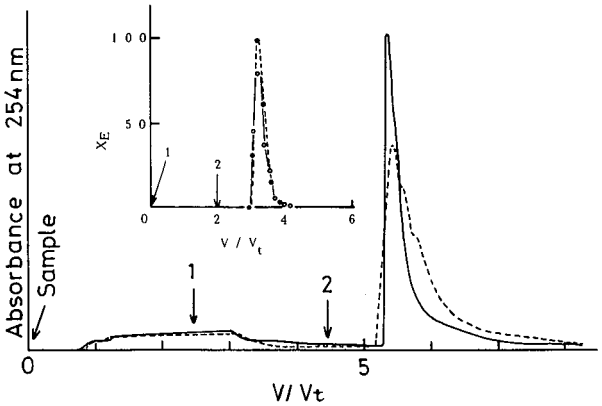

Fig. 10. Comparison of the elution curves of β-galactosidase obtained by stepwise elution with small and large MPIEC columns. Arrows and symbols as in Fig. 4. Columns DEAE Toyopearl 650; elution buffer, 14 m*M* Tris–HCl (pH 7.7) containing 0.15 *M* NaCl. Solid curve, $d_p = 65$ μm, column 40 × 31 cm I.D., $F = 528$ ml/min (superficial velocity $u_0 = 0.7$ cm/min), sample 73.5 l of 1% solution; dashed curve, $d_p = 40$ μm, column 15 × 1.6 cm I.D., $F = 1.5$ ml/min ($u_0 = 0.75$ cm/min), sample 75 ml of 1% solution. Other conditions as in Fig. 4. Inset: sample 30 column volumes of 0.1% solution; superficial velocity 1.8 cm/min for the sample application and washing and 0.32 cm/min for the elution; (○) $d_p = 40$ μm, column 2 × 10.8 cm I.D.; (●) $d_p = 40$ μm, column 2 × 2.2 cm I.D. Other conditions as in Fig. 4.

Large-scale application

Fig. 10 shows a comparison of the elution curve at $I_E = 0.15$ for analytical and large-scale columns. The superficial velocity and the ratio of the sample volume to the total column volume were set equal for the two columns, but the particle diameter in the large column is larger and the column is longer. As can be seen, the elution profiles for the two columns are similar. The peak height for the large column is higher, owing to the longer column. As the superficial velocity is the same, the number of the theoretical plates N increases with increasing column length Z at the same particle diameter d_p. On the other hand, N is proportional to the $1/d_p$ at low flow-rates and to $1/d_p^2$ at high flow-rates[1]. Consequently, an increase in Z from 15 to 40 cm and in d_p from 40 to 65 μm will result in a 1.3-fold increase in N, if we assume that N is proportional to $d_p^{-1.5}$. This increase in N is responsible for the higher peak concentration of the large column. However, the separation time for the large column was 2.67 times longer than that for the small one. It should be noted that when the N value of the two columns are set equal, the resulting peak heights are the same.

The inset in Fig. 10 shows the results obtained with a very short column (length 2 cm) with small (2 cm) and large (10.8 cm) diameters. The enzyme activity profiles are similar. In this case, a large volume of sample containing the enzyme at a relatively low concentration was applied. As a large volume must be processed, the flow-rate during the sample application was high, but was reduced at the elution stage because the concentration factor of the target enzyme in this type of stepwise elution is strongly dependent on the flow-rate[12].

DISCUSSION

Several strategies are possible for increasing the column productivity[1,13,14]. Displacement and/or frontal chromatography may be alternative methods for preparative separations of proteins. Liao and Horváth[15] examined the frontal and displacement IEC of an enzyme similar to that used in this study and found that the contaminant itself can be used as a displacer. They also claimed that the productivity is much higher than that shown in linear gradient elution experiments in our previous study[9].

In fact, the frontal and displacement mode can be applied to the present system. Fig. 11 shows the breakthrough curve (the profiles in frontal chromatography). It is seen that the concentrated and purified enzyme can be recovered by this method. However, during this experiment clogging of the column and a resulting increase in pressure drop were observed. Moreover, it is difficult to monitor the target protein with a UV detector. In the work of Liao and Horváth[15], a large amount of the target enzyme was discarded and the recovery was relatively low (the final recovery was 33%).

Although several theoretical and experimental studies have been reported recently[14–17], it seems that more studies are needed to perform frontal and displace-

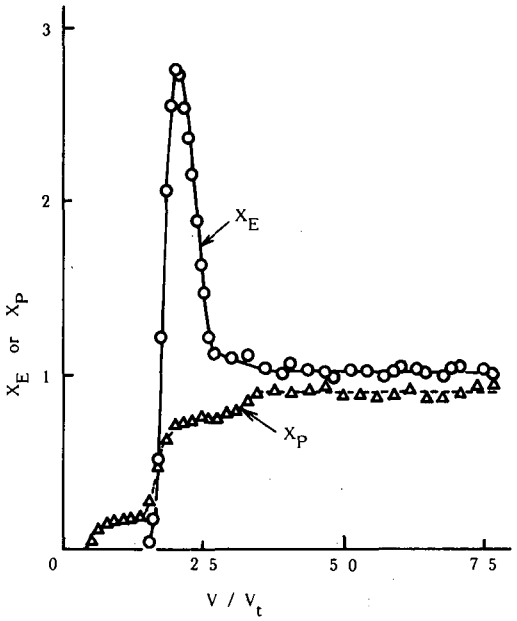

Fig. 11. Breakthrough curve (frontal chromatography). The sample (1% β-galactosidase) dissolved in the buffer [14 mM Tris–HCl (pH 7.7) containing 0.03 M NaCl] was applied to the column (DEAE Toyopearl 650, 7.5 × 0.75 cm I.D., d_p = 40 μm) equilibrated with that buffer at F = 1 ml/min and 25°C until V/V_t = 77 (V = 250 ml). The eluted fraction was collected by a fraction collector and the protein concentration and the enzyme activity were assayed. When the fractions between V/V_t = 16 and 27 are recovered, the purification factor is 2.0 and the recovery is 70%. (○) X_E = ratio of the enzyme activity to that of the sample; (△) Xp = ratio of the protien concentration to that of the sample.

ment chromatography as an efficient method for the preparative separation of proteins.

The purification factor values obtained with the stepwise elution in this study are lower than those in linear gradient elution reported previously[9]. The elution volume used (about four column volumes as shown in Fig. 4) was almost the same for linear gradient elution at $GH = 0.029$ M and $u = 1.7$ cm/min (see Fig. 7 in ref. 9). Moreover, the determination of the chromatographic conditions is not easy, as shown in this study, while the scaling-up of linear gradient elution is easily designed on the basis of the GH–I_R relationship shown in Fig. 2[1,6,9] and the dimensionless variable $[(D_m I_a Z)/(GHud_p^2)]^{1/2}$ (ref. 10).

The most attractive feature of the stepwise elution is the simple operation and the highly concentrated fraction. It is not advantageous to search for chromatographic conditions such that the desired protein is purified to homogeneity. Rather it is advisable to use stepwise elution as a fast purification and concentration method for proteins.

Usually, a very large volume of liquids containing a desired protein must be processed at an early stage of the purification (downstream) process. This might be done by, for example, ultrafiltration. However, the use of liquid chromatography is advantageous as it not only concentrates but also purifies the desired protein. For this purpose, a column of large diameter and short length packed with small particles such as that shown in Fig. 10 is suitable as it can permit high volumetric flow-rates and process a sample of large volume in a short cycle time. The productivity, defined as (amount of the recovered enzyme)/[(column volume)(separation time)], is 0.05 mg enzyme/(ml column)·min and the concentration factor is about 50-fold for the experimental results shown in the inset in Fig. 10. This means that, for example, a 5-l IEC column (10 cm × 25 cm I.D.) can process 150 l of solution of 0.01% enzyme used in this study within 60 min.

SYMBOLS

D_m	molecular diffusion coefficient (cm^2/s)
d_c	column diameter (cm)
d_p	particle diameter (μm)
F	volumetric flow-rate (ml/min)
GH	$g(V_t - V_o)$, slope of the gradient normalized with respect to the column gel volume (M)
g	slope of the linear gradient (M/ml)
I_a	dimensional constant having a numerical value of 1 (M)
I	salt concentration (M)
I_E	salt concentration of the elution buffer (M)
I_R	salt concentration at peak position (M)
I_0	salt concentration of the starting buffer (M)
K	distribution coefficient of proteins as a function of I, $K(I)$
K'	distribution coefficient of a salt
K_E	K at $I = I_E$
u	u_0/ε, linear mobile phase velocity (cm/min)
u_0	$F/(\pi d_c^2/4)$, superficial velocity (cm/min)

V elution volume from the start of elution (ml)
V_o εV_t, column void volume (ml)
V_t total column volume (ml)
X_E ratio of the enzyme activity to that of the sample
X_P ratio of the protein concentration to that of the sample
Z column length (cm)
ε void fraction of the column

REFERENCES

1 S. Yamamoto, K. Nakanishi and R. Matsuno, *Ion Exchange Chromatography of Proteins*, Marcel Dekker, New York, 1988.
2 C. J. O. R. Morris and P. Morris, *Separation Methods in Biochemistry*, Pitman, London, 2nd ed., 1964, p. 93.
3 D. L. Saunders, in E. Heftmann (Editor), *Chromatography*, Van Nostrand-Reinhold, New York, 3rd ed., 1975, p. 84.
4 S. Yamamoto, K. Nakanishi, R. Matsuno and T. Kamikubo, *Biotechnol. Bioeng.*, *25* (1983) 1465.
5 S. Yamamoto, K. Nakanishi, R. Matsuno and T. Kamikubo, *Biotechnol. Bioeng.*, *25* (1983) 1373.
6 S. Yamamoto, M. Nomura and Y. Sano, *AIChE J.*, 33 (1987) 1426.
7 E. Steers, P. Cuatrecasas and H. Pollard, *J. Biol. Chem.*, 246 (1971) 196.
8 K. Nishimoto, Y. Nakahara, K. Matsubara and K. Sakamoto, *Toyo Soda Kenkyu Hokoku*, 31 (1987) 45.
9 S. Yamamoto, M. Nomura and Y. Sano, *J. Chromatogr.*, 396 (1987) 355.
10 S. Yamamoto, M. Nomura and Y. Sano, *J. Chromatogr.*, 409 (1987) 101.
11 J.-Ch. Janson and P. Hedman, *Adv. Biochem. Eng.*, 25 (1982) 43.
12 S. Yamamoto, T. Suehisa and Y. Sano, *AIChE Annual Meeting, San Francisco 1989*, paper No. 180f.
13 I. Mazsaroff, R. Bischoff, P. Tice and F. E. Regnier, *J. Chromatogr.*, 437 (1988) 429.
14 L. Velayudhan and Cs. Horváth, *J. Chromatogr.*, 443 (1988) 13.
15 A. Liao and Cs. Horváth, *Ann. N.Y. Acad. Sci., Biochemical Engineering VI*, 589 (1990).
16 M. W. Philips, G. Subramanian and S. M. Cramer, *J. Chromatogr.*, 454 (1988) 1.
17 V. Svoboda, *J. Chromatogr.*, 464 (1989) 1.

Journal of Chromatography, 512 (1990) 101–114
Elsevier Science Publishers B.V., Amsterdam

CHROMSYMP. 1967

High-performance liquid chromatography of amino acids, peptides and proteins

CIII[a]. Mass transfer resistances in ion-exchange and dye-affinity chromatography of proteins

A. JOHNSTON and M. T. W. HEARN*
Department of Biochemistry and Centre for Bioprocess Technology, Monash University, Clayton, Melbourne, Victoria 3168 (Australia)

ABSTRACT

Adsorption equilibria and rate kinetics have been investigated for the binding of several proteins, with different molecular geometries, to several ion-exchange and dye-affinity chromatographic resins with varying pore size and protein accessibilities. The pore geometry was shown to play a significant role in the protein capacity and loadability of both the ion-exchange and dye-affinity resins. For example the Fractogel HW75–Cibacron Blue F3GA affinity sorbent had the greatest capacity for the small protein, lysozyme, compared to the other Fractogel HW-Cibacron Blue F3GA sorbents, and similarly, the ion-exchange resins, such as DEAE-Fractogel 65, bound more human serum albumin (HSA), as opposed to the larger protein, ferritin.

The apparent diffusion of protein from the bulk phase to the ligands/ionic sites was calculated to be considerably restricted when the pore to protein size ratio was small, as is the case of DEAE Fractogel 65/ferritin system, and the dye-affinity Fractogel HW55/HSA system. In these circumstances, pore diffusivity was calculated to be up to 100-fold smaller than bulk diffusivity.

INTRODUCTION

The purification of a specific protein involves a cascade of chromatographic processes, each step harnessing a unique biological or chemical property to separate the desired component from its contaminants in the crude mixture. Ion-exchange chromatography (IEC) is predominantly used in the initial stages as a reliable method of volume reduction and sample clean up, separating proteins on the basis of their surface charge differences[1]. It is well known that a protein can adopt a local charge

[a] For Part CII, see ref. 29.

0021-9673/90/$03.50

distribution at its surface, depending on the ionic strength and pH of the feed buffer, and is steered towards the ion-exchange resin containing complimentary charges by, amongst others, electrostatic forces. Biospecific and biomimetic chromatography represent highly tuned separation processes, often used at the latter stages of the chromatographic cascade for their high resolution. These chromatographic methods rely on distinct protein recognition of chemical or biological ligands, with the protein being driven by biospecific attractions that mimic *in vivo* phenomena observed, for example, in antigen–antibody or enzyme–substrate interactions.

Selectivity and efficiency in all chromatography modes depend strongly on the type of resin, the appropriate choice of sample buffer, water content, pH, displacing ions and ionic strength. Currently there are several hundred different ion-exchange resins now commercially available, from the traditional celluloses (Whatman diethylaminoethyl cellulose DE-52), cross-linked dextrans and agaroses (Pharmacia QAE-Sephadex A-25 and CM-Sepharose CL-6B), new synthetic methacrylate polymers (IBF Q-Trisacryl M), to various silica-based sorbents (Merck DEAE-LiChrospher 1000), designed for increased chemical and physical stability. In preparative chromatography, selection of the resin rests on the operational capabilities of the resin, its capacity for binding protein, its stability under high flow-rates and its cost. Ultimately, the criteria of resin productivity and throughput, for example, in terms of kilograms per hour per invested dollar, will dictate the use of a particular ion-exchange sorbent in process-scale purification of proteins. This requirement is in direct contrast to the criteria used for selecting resins for analytical purification, where demands of high selectivity and resolution are paramount. Bed compression, for instance, is a serious drawback in using the soft gels, such as the Sephadex based resins[2]. Most optimization studies have to date concentrated on these operational characteristics[3–5], and examined how these parameters influence the efficiency of the resin to adsorb protein.

It has been recently shown that the sorbent–protein interaction harnessed in the chromatographic purification also plays an important role in adsorption efficiency, in transport phenomena and in the binding kinetics[6,7]. At a process scale, effects such as (i) slow diffusion of the protein through the porous network of the sorbent, (ii) by tortuosity of the pore chambers, (iii) rotational masking of the protein affected by steric hindrance, and (iv) non-specific adsorption onto heterogeneous ligand/ionic sites, are exaggerated. The interplay of these effects can become detrimental to overall purity and throughput of the desired protein product[8–10]. Thus, the efficiency of the performance of different ion-exchange and dye-affinity sorbents, in terms of how quickly they adsorb the maximum amount of protein, and their kinetic behaviour towards biosolutes with different molecular features are characteristics that need to be optimized. This can be achieved only through a more lucid and complete understanding of their respective adsorption kinetics and mass transfer phenomena.

The experiments reported here have been designed to study the adsorption kinetics of dye-affinity gels and several ion-exchange resins, to allow a direct comparison of two different systems of selectivity that have similar association constants[11]. Mathematical models and literature correlations were also used to extract physicochemical parameters from the experimental results of two system modes, namely batch ion-exchange and affinity chromatography.

THEORY

Adsorption of protein to a porous ion-exchange or dye-affinity sorbent entails the following macroscopic steps: (1) protein movement from the bulk, mobile phase to the sorbent surface layer; (2) protein transfer across a stagnant film layer surrounding the sorbent particles; (3) protein diffusion into the pores of the particles; (4) adsorption of protein to the solid phase.

Each of these steps contributes to the overall adsorption but the slowest and most significant step will be the rate-governing mechanism. External, bulk diffusion is often considered infinitely fast, resistance to film mass transfer can be minimal provided mixing is adequate, whilst pore diffusion can actually hinder adsorption, particularly if the protein size is large and the pore openings small[10].

The diffusion of complex species, such as proteins, which can change conformation and characteristics[12] is an intricate process. The transportation of a protein from the bulk fluid to the ligands inside the pores can be described mathematically, provided certain assumptions are made. For example, conformational changes of the protein are assumed to be negligible, both in the mobile and stationary phase. Secondly, the adsorption is often assumed to be highly specific, that is, no non-specific binding occurs to secondary sites. In addition, the flow of protein through the chromatographic bed is assumed to be ideal, with well distributed bulk flow, no channelling or no stagnant fluid around the resin particles or within its porous interior. Finally, the concentration of the protein is presumed to be same in the bulk, mobile phase and in the pores of the resin, that is, instantaneous equilibrium is achieved between the phases.

The mass balance equation for adsorption of protein to the stationary phase can then be written in the form,

$$\frac{\partial C}{\partial t} = D_a \frac{\partial C}{\partial x} - u\frac{\partial C}{\partial t} - \frac{\partial q}{\partial t} \tag{1}$$

where

D_a = axial diffusion
C = free protein concentration within solution
u = superficial velocity
q = protein concentration bound to the resin
t = time
x = distance along the bed

Analytical solutions to this equation have yet to be achieved. However, numerical techniques have been implemented to achieve a theoretical solution that is considered to simulate transport within the constraints of the previously stated assumptions. To achieve numerical solutions to equation 1, further assumptions from those mentioned above, have to be made. Firstly, axial diffusion is assumed to be infinitely fast[10,13] ($\partial C/\partial t = 0$) and secondly, mass transfer resistances are often considered to be negligible. Collectively the application of these assumptions thus permits the rate of change of adsorbed protein to be reduced to

$$\frac{dq}{dt} = k_1 C(q_m - q) - k_2 q \tag{2}$$

Eqn. 2, upon integration, yields

$$C(t) = C(\text{in}) - \frac{v(b + a)[1 - \exp(-2a(v/V)k_1 t]}{V[(b + \text{a})/(b - a)] - \exp(-2a(v/V)k_1 t)} \tag{3}$$

where

a^2 $= b^2 - C(\text{in})V/(vq_m)$
b $= 1/2(\text{C(in)}V/v + q_m + K_D V/v)$
V = total buffer volume
v = volume of resin
k_1 = first order rate constant
q_m = maximum protein capacity
$C(t)$ = concentration of protein at any time
$C(\text{in})$ = initial protein concentration in bulk fluid
k_2 = reverse rate constant
K_D = dissociation constant

The Langmuir isotherm has been derived for the most simple case where equilibrium exists at all points within and around the sorbent particles, so that $\partial q/\partial t \rightarrow 0$. Under these conditions, the equilibrium parameters are defined according to the familiar form

$$q = \frac{K_a q_m C}{1 + K_a C} \tag{4}$$

where K_a = the association constant, k_1/k_2.

Inherent to eqn. 4, this approach has been earlier used by Chase[14] for kinetic studies on biospecific affinity adsorption. It should be kept in mind that eqns. 3 and 4 represent a very simplistic picture of a protein binding to an immobilized ligand. This approach takes no account of non-equilibrium effects, such as diffusional restrictions and film mass transfer. In addition, this model assumes unique protein binding to specific ligand, disregarding any heterogeneities, that may be more prevalent at a process level. Furthermore, as presented by Chase[14], the rate constants derived from eqn. 3 represent "lumped" parameters, that underestimate the speed with which protein will bind to the resins[15]. Arnold *et al.*[16], for example, have found that these constants are artificially small if the rate of mass transfer becomes comparable to the rate of binding. Sportmann *et al.*[17] and Hethcote and Delisi[28] have suggested that the rate of biospecific adsorption may be rate limiting, so that the kinetic rate constant measured by eqn. 3 may also not be indicative of the actual adsorption rate constant.

Development of kinetic equations for the binding of protein to an ion-exchange resin has followed similar approaches. Tsou and Graham[8] have developed a solution to the mass balance equations from the two-phase diffusion model[19]. This model assumes there are two effective films contributing to the overall resistance to solute diffusion. The overall flux of a protein is presumed to be concentration driven, a gradient existing between the concentration that would finally be in equilibrium, C^*, and the bulk concentration at any time, $C(t)$. The rate equation then becomes

$$\frac{dq}{dt} = \frac{3K}{r_0}[C(t) - C^*] \tag{5}$$

for which the final kinetic solution for the fractional obtainment of equilibrium, $F(t)$, becomes,

$$\ln[1 - F(t)] = -3\frac{Kt}{r_0}\left[\frac{V}{v} + \frac{1}{m''}\right] \tag{6}$$

where

K = overall mass transfer coefficient

r_0 = radius of resin particle

$F(t) = \dfrac{(q^* - q)}{[q^* - q(\text{in})]}$

$m'' = \dfrac{(q^* - q)}{(C - C^*)}$

Thus, eqn. 6 predicts that the slope of $\ln[1 - F(t)]$ *versus* time, t, will be linear, with a slope proportional to K, and, depending on the rate controlling mechanism, the appropriate diffusivity can be calculated. Two cases are important here, namely when

(1) film diffusion controls adsorption where $D_p \propto \text{slope} \cdot r_0 \cdot (V/v)$ (7)

(2) pore diffusion controls adsorption where $D_f \propto \text{slope} \cdot r_0^2$ (8)

where

D_p = pore diffusion

D_f = film diffusion

Although eqns. 7 and 8 clearly oversimplify the mechanism of adsorption of proteins (species that are amphoteric and structurally diverse) to the charged ion-exchange resins, experimental values of protein diffusivities obtained[18,19] with this approach concur with the values of bulk diffusivities calculated from correlation.

Arve and Liapis[20] have produced a more sophisticated model of protein adsorption to affinity sorbents, by numerically solving the mass balance equation, eqn. 1, and incorporating mass transfer resistances and diffusional characteristics. Three cases of adsorption are applicable with this model.

Case 1: Local equilibrium exists, with Langmuirean behaviour prevailing, (*e.g.* eqns. 3 and 4). The adsorption is thus described solely by the equilibrium parameters, K_a, q_m and the bulk diffusivity, D_m.

Case 2: Adsorption is described by a second order reversible rate equation, as in affinity adsorption, and pore diffusion is controlling.

Case 3: Adsorption is governed by an irreversible rate constant, for example, by very high affinity interactions with biometic and ion-exchange sorbents, and diffusion is again pore controlled.

The numerical solutions in this model are obtained from computational integration, using literature correlations[21,22] for initial parameter estimates, followed by an iterative procedure to obtain theoretical values for the protein diffusivity and rate constants. Solutions to cases 1 and 2 have previously been described using dye-affinity and biospecific affinity systems[23,24].

The applicability and adequacy of each model equation will depend on the

complexity of the crude mixture, the structural and conformational integrity of the protein to be purified and the homogeneity of the sorbents' macro- and micro-structure.

EXPERIMENTAL

Human serum albumin (HSA), as a 21% solution, was kindly donated by Commonwealth Serum Laboratories (C.S.L., Melbourne, Australia). Lysozyme from hen egg white (dialysed and lyophilized), and ferritin, from horse spleen (isoelectrically isolated), were purchased from Sigma (St. Louis, MO, U.S.A.). Cibacron Blue F3GA was obtained from Serva (Heidelberg, F.R.G.). Buffer salts were obtained from Aldrich (Milwaukee, WI, U.S.A.). The Fractogels HW55, HW65 and HW75 were obtained from Merck (Darmstadt, F.R.G.); the Trisacryl M was from Australia Chemical Company (Melbourne, Australia); the Fast Flow Sepharose and the ion-exchange Sephadex resins were a gift from Pharmacia (Uppsala, Sweden). The properties of the chromatographic resins as given by the manufacturer are listed in Table I.

The experimental apparatus included a Model 2238 UV Spectrophotometer and a Model 2210 two-pen chart recorder from Pharmacia. Experimental data were analysed using an IBM PC with linkage to a VAX mainframe.

Batch experiments were performed using the bath system as previously described in our associated studies[7,24]. Typically, protein solutions ranging from 20 to 220 mg/ml were injected into a bath containing 20 ml of buffer and 0.1 g resin for IEC or 1.0 g for dye-affinity (dried on sintered funnel by vacuum). The bath was continuously stirred to maintain good mixing. The buffer used for IEC experiments was 5 m*M* phosphate, and a pH 6.0 was selected so that albumin would adsorb to the anion-exchanger (p*I* of HSA, 4.9). For the dye-affinity experiments, the buffer was 20 m*M* Tris–HCl, pH 7.8. In both cases the concentration of protein in solution was

TABLE I

PROPERTIES OF ANION EXCHANGE AND AFFINITY RESINS

Support	*Particle size (μm)*	*Capacity for albumin (mg/ml)*[b]	*Exclusion limit (dalton)*
DEAE-Sephadex A-25	40–125[a]	31[1]	30 000
Q-Sephadex A-25	40–125	–	30 000
DEAE-Sephadex A-50	40–125[a]	102[2]	200 000
DEAE-Sepharose FF	45–165	110[3]	4 000 000
Q-Sepharose FF	45–165	120[4]	4 000 000
DEAE-Fractogel 65	45–90	25[5]	5 000 000
DEAE-Trisacryl M	40–80	105[6]	10 000 000
Q-Trisacyl M		145[7]	10 000 000
Fractogel HW55	32–63	–	1 000 000
Fractogel HW65	32–63	–	5 000 000
Fractogel HW75	32–63	–	50 000 000

[a] Dry bead diameter.

[b] 1 = Determined in 0.01 *M* Tris–HCl buffer pH 8.0; 2 = determined in 0.01 *M* Tris–HCl buffer pH 8.3; 3 = determined in 0.05 *M* phosphate buffer pH 9.0; 4 = determined in 0.05 *M* phosphate buffer pH 7.0; 5 = determined in 0.05 *M* Tris–HCl buffer pH 8.3; 6 = determined in 0.05 *M* Tris–HCl buffer pH 8.0; 7 = determined in 0.01 *M* Tris–HCl buffer pH 9.5.

measured continuously by UV spectrophotometry (280 nm), giving a concentration profile from the time protein was injected into the bath until steady state was achieved.

The porosities of the resins were measured using a Pharmacia FPLC LCC 500 system. Columns were packed with the sorbents and the elution volumes of (i) acetone, a suitable molecular weight analyte able to penetrate the pores of the resins, and (ii) thyroglobulin, a large globular protein, that should be partially excluded, were measured. The difference between the volumes provided data on the voidage of the columns, and hence a measure of the porosity of the resins, a physical property that can change with buffer conditions and therefore affect the exclusion property of the different sorbents. The densities of the swollen ion-exchange resins were measured in 5 m*M* sodium dihydrogenphosphate buffer, pH 6.0. The properties for the weak ion-exchange resins are listed in Table II.

TABLE II

POROSITY OF THE DEAE RESINS

Support	*Porosity*	*Density (mg/ml)*
Sephadex A-25	0.39	1.5
Sephadex A-50	0.75	1.1
Sepharose FF	0.65	1.4
Fractogel HW65	0.28	1.3
Trisacryl M	0.49	1.2

RESULTS AND DISCUSSION

Equilibrium measurements

Adsorption isotherms were obtained from serial loading of protein solution onto the sorbents, in a batch, well mixed, system, as described previously[5]. These plots reflect the amount of protein bound to a resin once equilibrium with the protein solution is established. Fig. 1, taken from lysozyme and HSA adsorption experiments

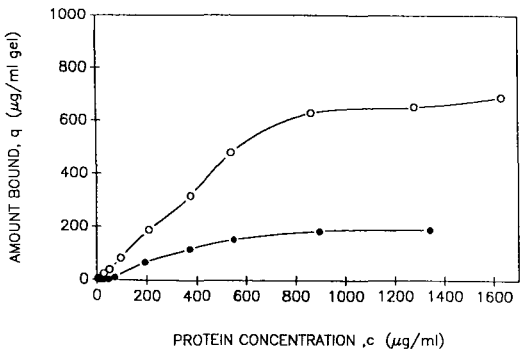

Fig. 1. Adsorption isotherm for the binding of lysozyme (○) and HSA (●) to the Fractogel HW65–Cibacron Blue F3GA support. Results generated from bath experiments with 1.0 g resin suspended in 20 ml of a 50-m*M* solution of Tris–HCl buffer, pH 7.8, temperature 35°C.

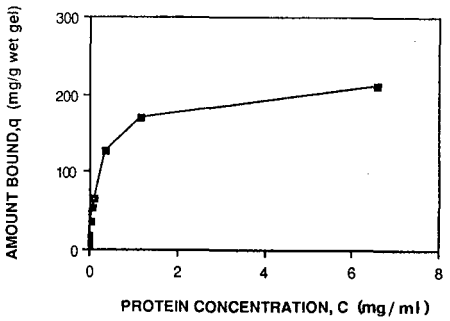

Fig. 2. Adsorption isotherm for the binding of HSA to Q-Sepharose FF resin. Results generated from bath experiments with 0.1 g resin suspended in 20 ml of a 5-m*M* solution of phosphate buffer, pH 6.0, temperature 25°C.

with the dye-affinity resin, Fractogel HW65–Cibacron Blue F3GA, demonstrates the effect of the ratio of pore to protein size. The smaller protein, lysozyme, with a hydrodynamic radius of 27 Å is anticipated to have easier access to the pores within the resin (exclusion limit of 5 000 000 dalton, and pore size approximately 190 Å, Table I), whilst the protein, HSA, with a larger molecular geometry (radius of 45 Å) should have restricted movement. Fig. 1 confirms this difference in accessibility, with the capacity of the Fractogel HW65–Cibacron Blue F3GA for HSA being significantly less. In addition, the adsorption curves of Fig. 1 suggest that the data approximately conform to Langmuirean behaviour. This adsorption behaviour allows estimation of the equilibrium parameters, such as the association constant, K_a, and the maximum capacity, q_m, parameters that are used as initial estimates of adsorption behaviour when equilibrium no longer prevails.

Figs. 2 and 3 show rectangular isotherms for the binding of HSA to the ion-exchange resin Q-Sepharose FF (Fast Flow) DEAE-Sephadex. As is evident from Fig. 2, the maximum capacity of Q-Sepharose FF for HSA was 170 mg/ml (compare with 0.18 mg/ml for Fractogel HW65–Cibacron Blue F3GA). The steeper initial slope reflects the higher affinity of interaction. Fig. 3 compares the capacity of two

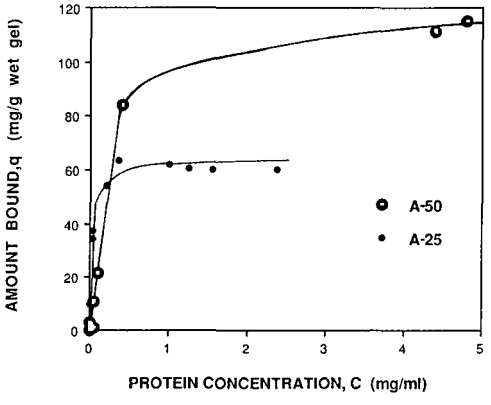

Fig. 3. Adsorption isotherm for the binding of HSA to DEAE-Sephadex A-25 and DEAE-Sephadex A-50 resin. Results generated from bath experiments with 0.1 g resin suspended in 20 ml of a 5-m*M* solution of phosphate buffer, pH 6.0, temperature 25°C.

DEAE-Sephadex-based resins with different pore sizes. DEAE-Sephadex A-25, with an exclusion limit of *ca.* 30 000 dalton will exclude albumin (molecular weight of 67 000 dalton) and thus adsorption is limited to the bead surface, whilst DEAE-Sephadex A-50, with the larger pores and higher surface area available to the protein, clearly binds more.

It is important to note here, that the maximum capacity calculated by this static, batch system, is much higher than that quoted by the manufacturer, see Table I (*e.g.* approximately 60 and 115 mg/ml, respectively). It should be kept in mind that experimental capacities depend on buffer conditions, pH, ionic strength (two conditions that are actually manipulated to affect elution) and mode of operation. Lower capacities are expected for packed beds where mixing is inferior, promoting a large film thickness and a resistance to mass transfer. That is, dynamic loadability (packed beds) is considered lower than static loadability (mixed baths). The soft gels, and in particular the Sephadex based resins, are known to compress under high flowrates in a packed bed, thus reducing their total surface area[2], and this pattern has also been seen in the Fractogel sorbents[24].

Kinetic measurements

Dye-affinity experiments. Concentration profiles of HSA binding to the Fractogel–Cibacron Blue F3GA, for varying pore size, are given in Fig. 4. The fastest rate and the greatest capacity are apparent for the Fractogel HW75, a matrix with large pores. The models of Arve and Liapis, Tsou and Graham, outlined in the theory were utilized and further validated here. Non-linear regression analysis, fitting eqn. 3, yielded first order rate constants, k_1, whilst iteration and parameter estimation are used to fit the solutions to cases 1 and 2 of Arve and Liapis, thus generating the apparent pore diffusivity and second order reversible rate constants. Fig. 5 compares the experimental concentration profile with the fitted theoretical curve of case 2, for the adsorption of HSA to the DEAE-Fractogel 65 resin.

The results for these two approaches are listed in Table III. The rates derived from eqn. 3 are comparable with those published by Chase[14] for the binding of HSA to Sepharose CL-6B Cibacron Blue F3GA. ($k_1' = 0.09$–0.02 *vs.* $k_1 = 0.02$ ml/mg · s). These rate constants appear to decrease with decreasing pore size, in the case of HSA,

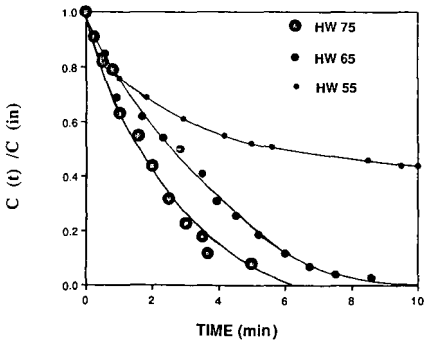

Fig. 4. Concentration time profiles of HSA adsorbing to the Fractogel HW55–, HW65– and HW75–Cibacron Blue F3GA supports. C(in) = 8, 9, 22 μg/ml respectively, for 1.0 g resin in 20 ml of a 50-mM solution of Tris–HCl buffer, pH 7.8, temperature 35°C.

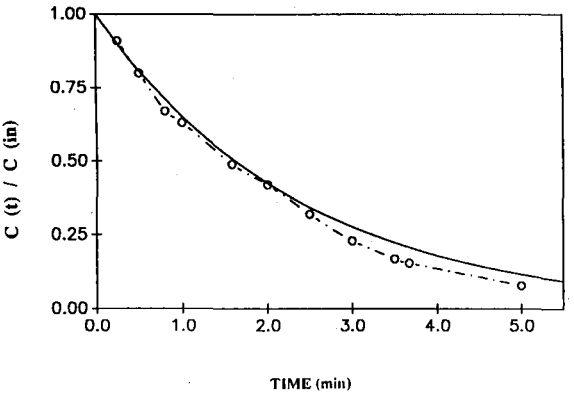

Fig. 5. Theoretical (———) and experimental (O- - -O) concentration curves of HSA adsorbing to the Fractogel HW65–Cibacron Blue F3GA supports. C(in) = 22 μg/ml, D_p = 0.07 m^2/s, k_1 = 0.1 ml/mg · s.

whilst lysozyme follows the opposite trend, indicating that the simple Chase model inadequately accounts for pore restrictions to mass transfer. It must be recognised that the rate constant as proposed by Case is a "lumped" parameter, incorporating all the factors that contribute to the overall adsorption process[15,16,24], and thus masks the true interaction rate. The adsorption process can be considered as a series of steps (see Theory), all of which should be accounted for in calculating the true interaction rate. The model of Arve and Liapis, on the other hand, gives rate constants that are higher than those of the Chase model, (see Table III) suggesting that they are more realistic representations of the rate of protein binding to an affinity resin. The rate constants, *per se*, arise from the interaction of protein with ligand, and therefore, should depend only on the class of protein and the type of ligand. Although diffusional restrictions have been accounted for in this model, there still appears a pore dependency.

Ion-exchange experiments. Proteins of different molecular sizes were used to study the effect of protein size on the kinetics of adsorption to the weak ion exchanger DEAE-Fractogel 65. The concentration profiles of Fig. 6 reflect the differences in

TABLE III

KINETIC PARAMETERS OF DYE-AFFINITY ADSORPTION

Protein	*Support (Fractogel)*	*C (μg/ml)*	*k_1 (ml/mg · s)*		
			Eqn. 3	*Arve and Liapis*[20]	*Chase*[14]
Lysozyme	HW55	5.0	0.096	5.0	0.020[a]
	HW65	7.0	0.041	1.8	0.020
	HW75	11.6	0.023	–	0.020
HSA	HW55	10.4	0.0008	0.10	0.012[a]
	HW65	4.9	0.0033	0.25	0.012
	HW75	9.8	0.0100	0.50	0.012

[a] Adsorption of lysozyme in 50 m*M* Tris–HCl, pH 7.2, onto Sepharose CL-6B.

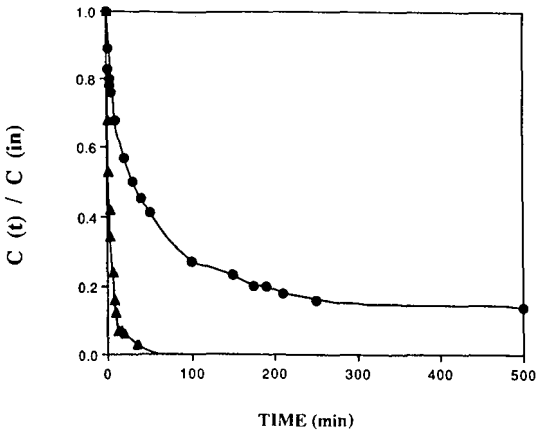

Fig. 6. Concentration–time profiles of HSA (▲) and ferritin (●) adsorbing to DEAE-Fractogel 65. $C(\text{in}) = 104$ μg/ml, for 0.1 g resin suspended in 20 ml of a 5 m*M* solution of phosphate buffer, pH 6.0, temperature 25°C.

molecular characteristics. For example, ferritin, with a molecular diameter two-fold larger than HSA (84:45 Å) adsorbs considerably slower, and because access to the Fractogel pores is expected to be more limited, less ferritin will bind [*i.e.* $C(t)/C(\text{in})_{\text{ferritin}} \rightarrow 0.2$, $C(t)/C(\text{in})_{\text{HSA}} \rightarrow 0.0$]. Experimental parameters, describing the kinetics of adsorption, can be extracted from these concentration profiles, using two mathematical approaches[18,20].

Following the approach of Tsou and Graham[18], concentration profiles such as shown in Fig. 6 were measured, with Figs. 7 and 8 being logarithmic transformation of these profiles. For both the DEAE-Fractogel 65 and the Q-Sephadex A-25, exponential behaviour is apparent from these transformed data. Since the exclusion limit of the Sephadex resin indicates that HSA will not penetrate the pores, it is likely that film diffusion will control the rate at which protein binds. If this behaviour is

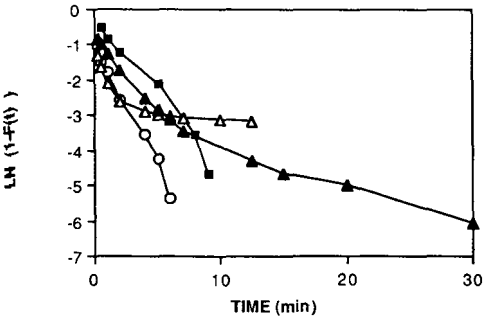

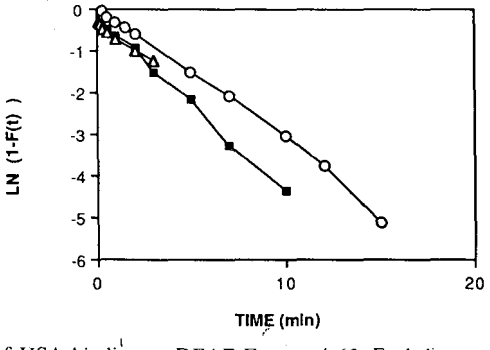

Fig. 7. Logarithmic plots of concentration profiles of HSA binding to DEAE-Fractogel 65. Each line represents sequential injection of a 200 mg/ml solution of HSA into the bath, containing 0.1 g resin in a 5-m*M* solution of phosphate buffer, pH 6.0, temperature 25°C.

Fig. 8. Logarithmic plots of concentration profiles of HSA binding to Q-Sephadex A-25. Each line represents sequential injection of a 200 mg/ml solution of HSA into the bath, containing 0.1 g resin in a 5-m*M* solution of phosphate buffer, pH 6.0, temperature 25°C.

TABLE IV

MODEL COMPARISONS FOR DEAE-FRACTOGEL 65

Protein	*C* (*mg/ml*)	D_p ($\times 10^{-11}$ m^2/s)		k_1 (*ml/mg · s*)
		Ref. 18	*Ref. 20*	
Ferritin[a]	1	0.48	3.20	0.07
	104	0.10	0.05	0.30
	248	0.03	0.10	0.50
HSA[b]	22	0.06	6.0	0.5
	55	0.11	6.0	0.5–1.0
	104	0.08	6.0	0.5

[a] Bulk diffusivity = $3.4 \cdot 10^{-11}$ m^2/s.
[b] Bulk diffusivity = $6.1 \cdot 10^{-11}$ m^2/s.

occurring, then eqn. 7 is applicable for the binding of HSA to Q-Sephadex A-25, where slope $\propto D_p \cdot r_0$, whilst eqn. 8 will be appropriate for the DEAE-Fractogel 65/HSA system.

Using the model of Arve and Liapis[20], on the other hand, entails an iterative procedure, as opposed to a simple transformation, which yields theoretical estimates of the pore diffusivity and irreversible rate constants from experimental results. Table IV compares the results of the models. The model of Arve and Liapis predicts that the small protein, HSA, and low concentrations of the large protein, ferritin, are not pore restricted, their movement within the pore chambers simulating that in the bulk. It is likely that at low protein levels, the majority of ferritin binds exclusively to the surface of the resin. Thus, when iteratively fitting theoretical values to the experimental curve, bulk diffusivity remained unchanged. For higher concentrations of ferritin, the pore diffusivities as calculated from Tsou and Graham, Arve and Liapis are within the same orders of magnitude and are up to 30-fold smaller than the corresponding bulk diffusion. Similar results have been obtained for affinity binding of HSA to Fractogel HW65–Cibacron Blue F3GA, in which the pore to protein size ratio was comparable[6]. Furthermore, a trend is evident in the case of the model of Tsou and Graham, towards a decrease in protein diffusion with increasing concentration of protein injected into the bath. This trend has previously been predicted for adsorbent binding to carbon particles[25]. This behaviour is not however apparent for HSA. In examining the results for HSA, it appears that the effective diffusivities predicted by the two models differ. The model of Tsou and Graham indicates a 100-fold decrease in protein diffusivity, as calculated from eqn. 8, whilst the model of Arve and Liapis model predicts no change in diffusion from the original estimate of the bulk diffusion. In addition, the treatment of Tsou and Graham results in little difference in pore diffusion between the geometrically different proteins, however further experimental results from the adsorption of carbonic anhydrase and ferritin to various ion-exchange resins have demonstrated otherwise[26].

Table IV shows a comparison of the irreversible rate constants, k_1, extracted from the solutions to case 3 of Arve and Liapis. The results for ferritin binding to DEAE-Fractogel 65 for various concentrations, show that this irreversible rate constant increases with increasing protein concentration. This behaviour is consistent

with enzyme kinetic theory which predicts an increase in the rate of binding to the sorbent as more protein is added to the feedstock solution[27]. The equilibrium model of Tsou and Graham for ion exchange, in contrast, has predicted much slower diffusion for HSA binding to the DEAE-Fractogel 65, than the model of Arve and Liapis.

CONCLUSIONS

The above results, demonstrating adsorption capacities and binding kinetics of two different chromatographic systems, have confirmed that protein movement into the porous sorbent particles commonly used in analytical chromatography, can lead to significant restrictions in ligand accessability in preparative applications. Ion-exchange resins, with greater capacities for protein than the dye-affinity resins, show very fast kinetics for the smaller proteins as demonstrated from the measurement of the overall rates of adsorption. Kinetic rate constants have also been calculated in attempt to ascertain the efficiency of the resins. The equilibrium model of Chase was found to underestimate the rate constants of the affinity adsorption process, whilst the pore diffusion models of Arve and Liapis gave rate constants that were higher, yet pore dependant. In addition, rate constants describing the ion-exchange process were found to be concentration dependent with the large protein, ferritin.

ACKNOWLEDGEMENTS

The support of the Australian Research Council and the Monash University Research Committee is gratefully acknowledged. A.J. is a post-graduate scholar associated with the Commonwealth Serum Laboratories.

REFERENCES

1 A. Hodder, M. T. W. Hearn and M. I. Aguilar, *J. Chromatogr.*, 443 (1988) 97.
2 K. K. Unger and R. Janzen, *J. Chromatogr.*, 373 (1986) 227.
3 G. Ganetsos, *J. Chromatogr.*, 411 (1987) 81.
4 S. Ghodbane and G. Guiochon, *J. Chromatogr.*, 452 (1988) 209.
5 T. S. Katoh, T. Kambayashi, R. Deguchi and F. Yoshida, *Biotechnol. Bioeng.*, 20 (1978) 267.
6 F. B. Anspach, A. Johnston, H.-J. Wirth, K. K. Unger and M. T. W. Hearn, *J. Chromatogr.*, 476 (1989) 205.
7 Cs. Horváth and J.-M. Engasser, *Biotechnol. Bioeng.*, 16 (1974) 900.
8 A. M. Lenhoff, *J. Chromatogr.*, 384 (1987) 285.
9 V. Kasche and B. Galunsky, in T. C. J. Gribrau, J. Visser and R. J. F. Nivard (Editors), *Affinity Chromatography and Related Techniques*, Elsevier, Amsterdam, 1982, pp. 93–111.
10 I. A. Webster, *Biotechnol. Bioeng.*, 25 (1983) 2479.
11 Y. S. Ghim and H. N. Chang, *Ind. Eng. Chem. Fundam.*, 21 (1982) 369.
12 M. T. W. Hearn, A. Hodder and M. I. Aguilar, *J. Chromatogr.*, 448 (1988) 95.
13 W. Kopaciewicz, S. Fulton and S. Y. Lee, *J. Chromatogr.*, 409 (1987) 111.
14 H. A. Chase, *J. Chromatogr.*, 297 (1984) 179.
15 H. A. Chase, in A. I. Liapis (Editor), *Proceedings of the 2nd International Conference on Fundamentals of Adsorption, Santa Barbara, CA, 1986*, Engineering Foundation, New York, 1987, pp. 155–165.
16 F. H. Arnold, H. W. Blanch and C. R. Wilke, *Chem. Eng. J.*, 30 (1985) 25.
17 J. R. S. Sportmann, J. D. Liddil and G. S. Wilson, *Anal. Chem.*, 55 (1983) 771.
18 H-S. Tsou and E. E. Graham, *AIChE J.*, 31 (1985) 1945.
19 E. E. Graham and C. H. Fook, *AIChE J.*, 28 (1982) 245.
20 B. H. Arve and A. T. Liapis, *AIChE J.*, 33 (1987) 179.

21 R. E. Treybal, in J. V. Brown and M. Eichberg (Editors), *Mass Transfer Operations*, McGraw-Hill, Tokyo, 1981, p. 144–152.
22 M. E. Young, P. A. Carroad and R. L. Bell, *Biotechnol. Bioeng.*, 12 (1980) 947.
23 F. B. Anspach, A. Johnston, H.-J. Wirth, K. K. Unger and M. T. W. Hearn, *J. Chromatogr.*, 476 (1989) 205–225.
24 A. Johnston, *M.(Sc.) Thesis*, Monash University, Melbourne, 1988.
25 E. Furya, H. Ikeda and Y. Takeucha, in A. I. Liapis (Editor), *Proceedings of the 2nd International Conference on Fundamentals of Adsorption, Santa Barbara, CA, 1986*, Engineering Foundation, New York, 1987, pp. 235–240.
26 A. Johnston and M. T. W. Hearn, in preparation.
27 J. E. Bailey and D. F. Ollis, in B. J. Clark, B. Tokay and J. W. Bradley (Editors), *Biochemical Engineering Fundamentals*, McGraw-Hill, Tokyo, 1977, pp. 92–100.
28 H. W. Hethcote and C. Delisi, *J. Chromatogr.*, 248 (1982) 183.
29 M. T. W. Hearn, in J. Rivier and G. Marshall (Editors), *Peptides '90*, ESCOM Publ., San Diego, CA, 1990, in press.

Journal of Chromatography, 512 (1990) 115–121
Elsevier Science Publishers B.V., Amsterdam

CHROMSYMP. 1869

Ion-exchange high-performance liquid chromatographic isolation of the major allergen of parietaria pollen extract

IB SØNDERGAARD
Royal Veterinary and Agricultural University, 40 Thorvaldsenvej, DK-1871 Frederiksberg C, Copenhagen (Denmark)
PAOLO FALAGIANI
Lofarma Allergeni, Reparto Ricerche, Viale Cassala 40, 20146 Milan (Italy)
and
EZIO BOLZACCHINI, PAOLA CIVAROLI, GIUSEPPINA DI GREGORIO, VALERIA MADONINI, AMEDEA MORELLI and BRUNO RINDONE*
Dipartimento di Chimica Organica e Industriale, Università di Milano, Via Venezian 21, 20133 Milan (Italy)

ABSTRACT

The analysis and purification of a parietaria pollen extract were attempted using an ion-exchange high-performance liquid chromatographic method on a preparative scale. A homopolymerization equilibrium was observed to occur in solution. A combination of electrophoretic methods and immunoelectrophoretic methods was also used and showed that a small amount of the major allergenic component was isolated.

INTRODUCTION

Parietaria (*Parietaria judaica*) allergenic extracts are used therapeutically in the Mediterranean area. Therefore, standardization of the extracts and studies of their chemical composition are needed. In previous papers we reported attempts to purify parietaria pollen extracts with the use of high-performance size-exclusion chromatography (HPSEC)[1] or of a combination of HPSEC and high-performance ion-exchange chromatography (HPIEC)[2]. Other groups used HPSEC[3], gel chromatography[4] and ammonium sulphate precipitation followed by HPSEC[5].

Electrophoretic methods have also been used for the isolation of minute amounts of parietaria allergens, involving sodium dodecyl sulphate–polyacrylamide gel electrophoresis (SDS-PAGE)[6], immunochemical methods[7] or crossed radioimmunoelectrophoresis (CRIE)[8]. In these attempts, low-molecular-weight allergens were also isolated[9], and a pure allergen was obtained in a very low amount[10] and was named Par j I, using the new allergen nomenclature[11].

Chromatographic methods may lead to small-scale purification of allergens if combinations of techniques is used. This has been performed with timothy (*Phleum*

0021-9673/90/$03.50

pratense), where gel chromatography and IEC[12] or HPIEC and SEC[13] were used. With parietaria pollen extract we suggested the use of HPSEC and HPIEC[2] and, more recently[14,15], ultrafiltration and HPIEC. This method was further developed on a micropraparative scale[16].

The molecular weight of the major allergen from parietaria obtained by chromatographic purification experiments seemed to be different from that obtained from small-scale electrophoretic or immunochemical purification experiments, suggesting that the purification technique modified the composition of the allergenic mixture orginally present in parietaria pollen extract. Hence clarification of this point was important both for the standardization of parietaria pollen extracts to be used in therapy and for chemical studies.

EXPERIMENTAL

Parietaria pollen extract

A 10-mg amount of dry pollen obtained from Allergon (Engelholm, Sweden) was extracted with 200 ml of 0.15 *M* phosphate buffer (pH 7.2) for 24 h at 4°C. The pollen grains were filtered and the extract lyophilized (2-ml aliquots). Other samples were dialysed for 48 h against water, using a Spectra/Por 3 membrane (Spectrum Medical Industries, Los Angeles, CA, U.S.A.) with a molecular weight cut-off of 3500, then filtered through a 0.45-μm membrane (Millipore, Bedford, MA, U.S.A.) and lyophilized (2-ml aliquots).

High-performance liquid chromatographic analyses

The lyophilized material was dissolved in a 10 m*M* Tris–acetic acid buffer (pH 7.0)–20 m*M* sodium acetate (eluent A) to obtain a concentration of 6 mg/ml and injected into a Rheodyne 5.1-ml loop. The instrument was a Waters Deltaprep 3000 high-performance liquid chromatograph (Waters Assoc., Milford, MA, U.S.A.) equipped with a DEAE-5PW ion-exchange column (15 cm × 21.5 mm I.D.) (Toyo Soda, Tokyo, Japan) eluting with a 45-min gradient from A to B of a mixture of eluents A and B [10 m*M* Tris–acetic acid buffer (pH 7.0) containing 500 m*M* sodium acetate] at a flow-rate of 6m ml/min. A second linear gradient to 800 m*M* sodium acetate was then added. The detector was a Hewlett-Packard (Palto Alto, CA, U.S.A.) Model 1040 diode-array detector. The eluate was then divided into four pools (A, 72 ml; B, 132 ml; C, 84 ml; D, 204 ml). Pools A–C were analysed by HPIEC under the same conditions, then tested by radio allergo sorbent test (RAST) inhibition for allergenic content. Pool D was analysed with a curvilinear ionic strength gradient.

Radio allergo sorbent test

The fractions were bound to cyanogen bromide-activated paper discs and RAST inhibition was performed according to Yman *et al.*[17] using a pool of sera from patients with high sensitivity to parietaria pollen.

Isoelectric focusing (IEF)

A 5% polyacrylamide gel (18 × 9 cm) containing 2 *M* urea, 0.5 mm thick, was used. Ampholine (LKB, Bromma, Sweden), pH range 3–10, was used. The anodic solution was 1 *M* phosphoric acid and the cathodic solution was 1 *M* sodium

hydroxide. The samples were allowed to migrate at 15°C for 1.5 h at 2500 V and 7 W. Detection was performed by silver staining[18,19].

SDS-PAGE

A 9–27% linear gradient gel was used. The samples were treated with 10% β-mercaptoethanol, 2% SDS and Tris–HCl buffer (pH 6.7) containing glycerol for 1 h, then boiled for 10 min. The electrophoresis was performed using a Tris–glycine buffer (pH 8.3) containing SDS at 200 V for 17 h at 15°C[20]. Detection was performed by silver staining[18,19].

Fused rocket immunoelectrophoresis (FRIE)

A 1% (w/v) agarose gel (10 cm × 10 cm × 1.5 mm) containing 11 $\mu l/cm^2$ of a Lofarma anti-parietaria rabbit antibody (Lofarma Allergeni, Milan, Italy) was used. The buffer was Tris–tricine (pH 8.6, $I = 0.1$). Electrophoresis was performed at 2 V/cm for 18 h at 15°C[21]. Detection was performed by the Coomassie Brilliant Blue R-250 method (0.5% in water–ethanol–acetic acid, 45:45:10).

Crossed immunoelectrophoresis (CIE)

A 1% (w/v) agarose gel (10 cm × 10 cm × 1.5 mm) was used. The buffer was Tris–tricine (pH 8.6, $I = 0.1$). Electrophoresis in the first dimension was performed at 10 V/cm for 25 min and in the second dimension using 3.75 ml of a 1% agarose gel containing 14 $\mu l/cm^2$ of Lofarma anti-parietaria rabbit antibody and operating at 15°C and 2 V/cm for 18 h[22]. Detection was performed with the Coomassie Brilliant Blue R-250 method [0.5% in water–ethanol–acetic acid (45:45:10)].

CRIE

The incubation buffer for the monoclonal CRIE was freshly prepared[23] by addition of 5 g of bovine γ-globulin and 100 ml of normal rabbit serum to 900 ml of glycine buffer containing 0.1 *M* glycine, 0.65 *M* NaCl, 10 ml/l Tween 20 and 15 m*M* NaN_3 at pH 9.2. The washing solution contained 0.65 *M* NaCl, 1 ml/l Tween 20 and 20 mg/l chlorohexidine acetate in distilled water.

The rabbit anti-mouse immunoglobulin was purified by immunosorption against Sepharose-coupled polyclonal human immunoglobulin G (IgG) and by affinity chromatography on Sepharose-coupled mouse IgG[24]. Labelling with ^{125}I was done using a modification of the chloramine-T methods[24,25]. The specific activity of the labelled antibody was *ca.* 4 mCi/mg.

A CIE experiment was performed[26] using 1% agarose in Tris–barbital buffer (0.024 *M* sodium barbital, 0.073 *M* Tris and 0.01 *M* NaN_3, pH 8.6). The first dimension was run for 30 min at 10 V/cm and the second for 18 h at 2 V/cm. The plates were washed, pressed and dried in cold air, then incubated[27,28] for 3 h with the monoclonal antibodies against Par j I obtained as reported in ref. 10, diluted 1 + 1000. The plates were then washed four times and incubated overnight with ^{125}I-labelled rabbit anti-mouse IgG ($4 \cdot 10^5$ cpm), then washed four times, dried in hot air and placed in a X-ray cassette for autoradiography.

RESULTS AND DISCUSSION

The chromatographic purification of a parietaria pollen extract was performed using an anionic preparative HPIEC column eluting with a pH 7 linear ionic strength gradient. The results are shown in Fig. 1. The fractions were then collected in four pools (A, fractions 1–6; B, fractions 7–18; C, fractions 19–24; and D, fractions 25–41) and evaluated by RAST inhibition (RAST-I) for allergenic activity. This was spread all over the chromatogram, suggesting that allergen purification could not be followed simply monitoring the elution profile.

These pools were analysed using the same HPIEC column and the same pH 7 ionic strength gradient. In order to perform this, the material was dialysed with a cut-off membrane 3500 dalton. RAST-I analysis showed that dialysis gave a loss of a small amount of low-molecular-weight allergenic material, probably formed by some protease activity in the fractions.

The HPIEC profiles of pools A–C (Fig. 2a–c) suggested equalization of the fractions. Hence a modification of the composition of the fractions had occurred during the chromatography or while in solution. Pool D, analysed with a different ionic strength gradient, showed the same effect (Fig. 2d). This behaviour could derive from the occurrence of a homopolymerization equilibrium of allergenic and non-allergenic proteins. This had been recently suggested to occur with Par j I purified HPIEC[29] or by immunoaffinity chromatography[30] and is a general behaviour with glycoproteins, owing to hydrophobic interactions[31].

The interpretation of this HPIEC required electrophoretic and immunochemical analysis of the individual chromatographic fractions. Thus, scaling-up of HPIEC purification was performed and a FRIE experiment with all the chromatographic fractions, using antibodies anti-total parietaria extract, showed the presence of several

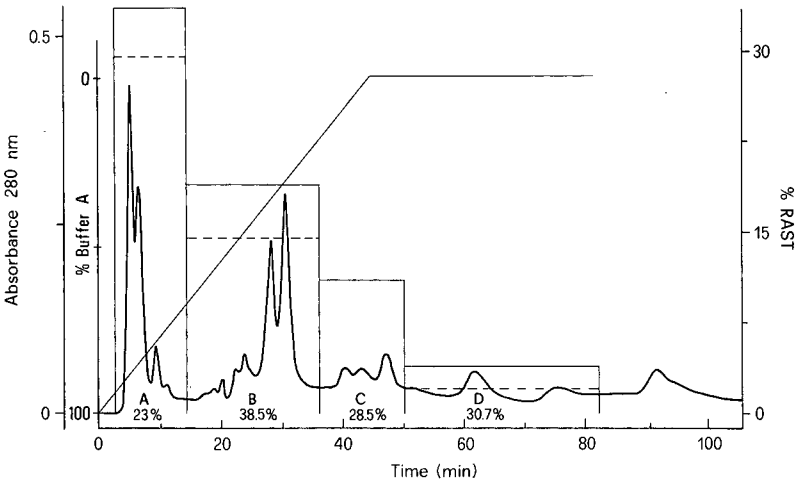

Fig. 1. Preparative HPIEC separation of parietaria pollen extract and RAST-I analysis of the fractions before (solid line) and after (dashed line) dialysis. Column, DEAE-5PW; ionic strength gradient, 10 m*M* Tris–acetic acid buffer (pH 7.0)–20 m*M* sodium acetate (eluent A); 10 m*M* Tris–acetic acid buffer (pH 7.0) containing 500 m*M* sodium acetate (eluent B).

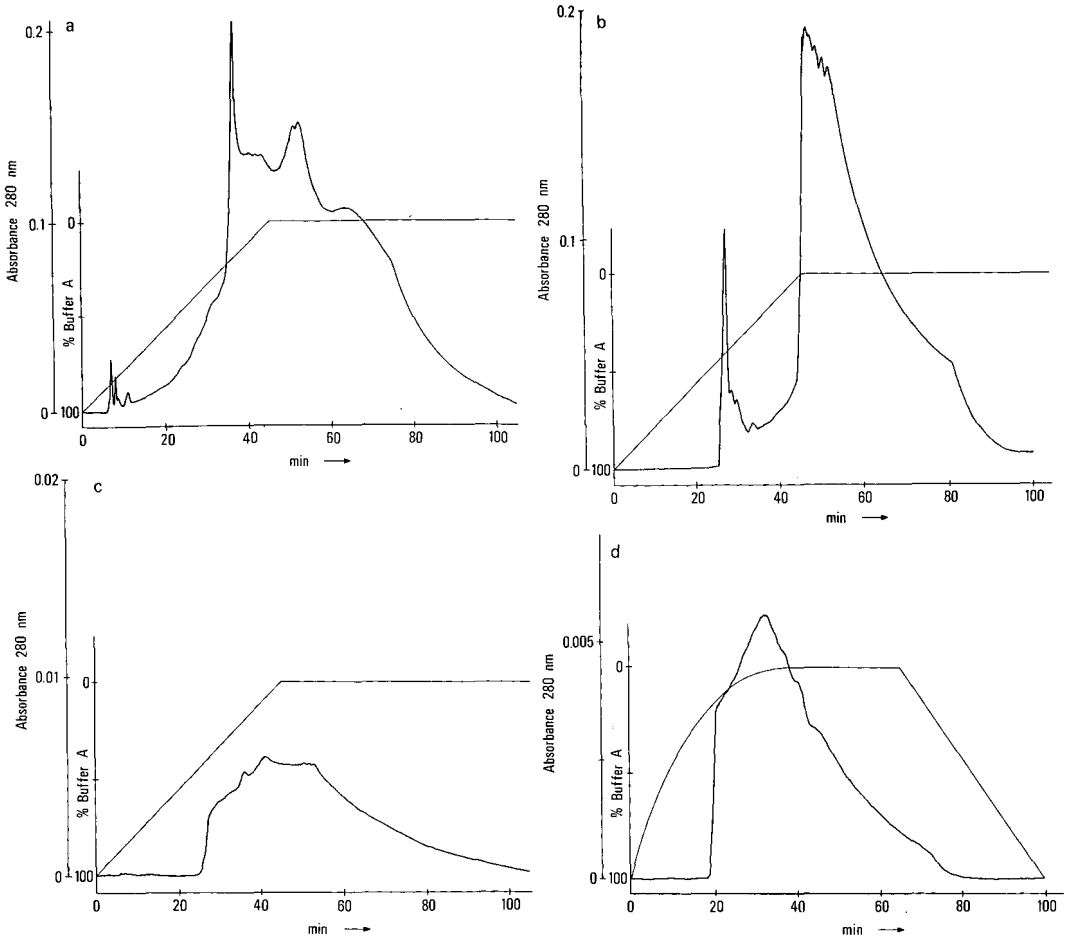

Fig. 2. HPIEC analysis of pools (a) A, (b) B, (c) C and (d) D, collected in the run shown in Fig. 1. Conditions as in Fig. 1.

antigens. One of these was present in all the fractions and was accompanied by a band with very similar characteristics. These two antigens were present as the only components of fraction 31.

An CIE experiment on fraction 31 using the same anti-parietaria antibody confirmed that two precipitation arcs were present in this fraction. A check of the purity of fraction 31 was obtained using a diode-array detector as the UV spectrum recorded by this detector did not change during elution. IEF analysis in the pH range 3.0–10.0 showed that fraction 31 had a single band located at the isoelectric point value of 3.5. An SDS-PAGE experiment was performed and showed that fraction 31 contained a single component which had a molecular weight of 11 000 dalton.

Thus, fraction 31 had a single band in IEF and SDS-PAGE and two precipitation arcs in CIE and FRIE. IEF was performed in the presence of urea and SDS-PAGE in the presence of the surfactant and β-mercaptoethanol, which are

conditions that dissociate homopolymeric material, whereas CIE and FRIE were run in the absence of dissociating agents. Hence, the two components of fraction 31 giving one band in IEF and SDS-PAGE and two in CIE and FRIE could be the monomeric protein and an oligomer.

A CRIE experiment performed on parietaria pollen extract using a monoclonal antibody against Par j I showed that the major allergens were two components with very similar characteristics, which were very similar to the components contained in fraction 31. Their reactivity toward the monoclonal antibody suggested that they had the same allergenic determinant. This fact was in line with the suggestion that they were Par j I and one oligomer.

These observations explain the uncertainty in the molecular weight of Par j I. Geraci and co-workers suggested valus of 10 000 (ref. 6), 22 000 (ref. 7) and 26 000 (ref. 10) dalton; the first value resulted from the allergen obtained from SDS-PAGE effected under dissociating conditions and could be attributed to the monomeric form. Corbi and Carreira[8] suggested that Par j I had a molecular weight of 10 000 dalton and gave a dimer under non-reducing conditions. Our results confirmed the early report[2] that Par j I is an 11 000-dalton protein which has a tendency to give homopolymers. Homopolymerization of this allergen has been also reported by another group[5], and the microhetereogeneity of Par j I has been suggested recently[30].

The HPIEC behaviour of parietaria pollen extract is probably due to the fact that the increase in the ionic strength of the eluent during the chromatography gradually results in dissociation of oligomers. Hence the composition of the mixture to be separated changes during elution.

In conclusion, preparative HPIEC followed by diode-array detection allowed the isolation of the major allergenic component shown to be in equilibrium with its homopolymer. Scaling-up of this technique is expected to allow the isolation of enough material for the solution of the uncertainty about its molecular weight and for chemical studies.

ACKNOWLEDGEMENTS

We thank our students C. Fantoni, D. Feretti and E. Gervasini for their collaboration. This work was supported by a CNR grant.

REFERENCES

1 P. Falagiani, E. Cavallone, M. Nali, B. Rindone, S. Tollari and G. Crespi, *J. Chromatogr.*, 328 (1985) 425.
2 E. Bolzacchini, G. Di Gregorio, M. Nali, B. Rindone, S. Tollari, P. Falagiani, G. Riva and G. Crespi, *J. Chromatogr.*, 397 (1987) 299.
3 N. Rubio and A. Brieva, *J. Chromatogr.*, 407 (1987) 408.
4 S. Feo, R. Cocchiara and D. Geraci, *Mol. Immunol.*, 21 (1984) 25.
5 A. Giuliani, C. Pini, S. Bonini, N. Mucci, L. Ferroni and G. Vicari, *Allergy*, 42 (1987) 434.
6 S. A. Ford, B. A. Baldo, D. Geraci and D. Bass, *Int. Arch. Allergy Appl. Immunol.*, 79 (1986) 120.
7 D. Geraci, K. B. Billesbolle, R. Cocchiara, R. Løwenstein and H. Ispen, *Int. Arch. Allergy Appl. Immunol.*, 78 (1985) 421.
8 A. L. Corbi and J. Carreira, *Int. Arch. Allergy Appl. Immunol.*, 74 (1984) 318; 76 (1985) 156.
9 A. Ruffilli, U. Oreste, V. Santonastaso, A. Scotto D'Abusco and G. Sacerdoti, *Mol. Immunol.*, 2 (1987) 305.

10 R. Cocchiara, G. Locorotondo, A. Parlato, G. Guarnotta, S. Ronchi, G. Albeggiani, S. Amoroso, P. Falagiani and D. Geraci, *Int. Arch. Allergy Appl. Immunol.*, 90 (1989) 84.
11 D. G. Marsh, L. Goodfriend, T. P. King, H. Løwenstein and T. A. Platts-Mills, *Int. Arch. Allergy Appl. Immunol.*, 85 (1988) 194.
12 E. Puttonen and H. J. Maasch, *J. Chromatogr.*, 242 (1982) 153.
13 S. Haavik, B. Smestad Paulsen and J. K. Wold, *J. Chromatogr.*, 321 (1985) 199.
14 E. Bolzacchini, G. Di Gregorio, M. Nali, B. Rindone, S. Tollari, P. Falagiani, G. Riva and G. Crespi, *Allergy*, 42 (1987) 743.
15 A. Bassoli, E. Bolzacchini, F. Chioccara, G. Di Gregorio, B. Rindone, S. Tollari, P. Falagiani and G. Riva, *J. Chromatogr.*, 446 (1988) 179.
16 A. Bassoli, F. Chioccara, G. Di Gregorio, B. Rindone, S. Tollari, P. Falagiani, G. Riva and E. Bolzacchini, *J. Chromatogr.*, 444 (1988) 209.
17 L. Yman, G. Ponterius and R. Brand, *Dev. Biol. Stand.*, 29 (1975) 151.
18 C. R. Merril, D. Goldman, S. A. Sedman and M. H. Ebert, *Science (Washington, D.C.)*, 211 (1981) 1438.
19 J. Guevara, Jr., D. Johnston, L. S. Rawagali, B. A. Martin, S. Capetillo and L. K. Rodiguez, *Electrophoresis*, 3 (1982) 197.
20 U. K. Laemmli, *Nature (London)*, 277 (1970) 580.
21 N. M. G. Harboe and P. J. Svendsen, *Scand. J. Immunol.*, 17, Suppl. 10 (1983) 107.
22 P. J. Svendsen, B. Weeke and B. G. Johansson, *Scand. J. Immunol.*, 17, Suppl. 10 (1983) 3.
23 R. Djurup, I. Søndergaard, U. Minuva and B. Weeke, *J. Immunol. Methods*, 62 (1983) 283.
24 R. Djurup, I. Søndergaard, C. G. M. Magnusson and B. Weeke, *Allergy*, 34 (1984) 51.
25 F. C. Greenwood, W. M. Hunter and J. S. Glower, *Biochem. J.*, 89 (1963) 114.
26 B. Weeke, *Scand. J. Immunol.*, 2, Suppl. 1 (1973) 47.
27 I. Søndergaard, R. Djurup and B. Weeke, *Allergy*, 39 (1984) 622.
28 B. Weeke, I. Søndergaard, P. Lind, L. Aukrust and H. Løwenstein, *Scand. J. Immunol.*, 17, Suppl. 10 (1983) 265.
29 P. Falagiani and B. Rindone, in R. Curto (Editor), *Proceedings of the Internationl Symposium on Pollinosis in the Mediterranean Area, Naples, March 16–18*, 1989, p. 95.
30 J. Carreira, R. Ayuso and F. Polo, in R. Curto (Editor), *Proceedings of the International Symposium on Pollinosis in the Mediterranean Area, Naples, March 16–18*, 1989, p. 91.
31 D. H. Calam and J. Davidson, *J. Chromatogr.*, 218 (1981) 581.

Journal of Chromatography, 512 (1990) 123–129
Elsevier Science Publishers B.V., Amsterdam

CHROMSYMP. 1954

High-performance liquid chromatographic approach to the separation of antiviral and immunostimulant fractions in Neuramide

NICCOLÒ MIRAGLIA and BRUNO RINDONE*
Dipartimento di Chimica Organica e Industriale, Università di Milano, Via Venezian 21, I-20133 Milan (Italy)
GIANCARLO FOLCHITTO
DIBE–Consorzio Ricerca, Via della Cancelliera 60, Ariccia (Italy)
PAOLA AMICUCCI and GUIDO ANTONELLI
Istituto di Virologia, Università di Roma, Via di Porta Tiburtina 28, I-00185 Rome (Italy)
and
ARNALDA LANFRANCHI and MARGHERITA MASSA
Istituto di Clinica Pediatrica, Università di Pavia, Piazza Golgi 2, 27100 Pavia (Italy)

ABSTRACT

Neuramide, a tissue extract having antiviral action against influenza A virus and immunostimulant action, was analyzed by preparative size-exclusion high-performance liquid chromatography (HPLC) and a low-molecular-weight fraction responsible for the antiviral action was isolated after reversed-phase HPLC. Four fractions having immunostimulant activity were also isolated, as evidenced by their potentiating action in the human lymphocyte proliferation induced by phytohaemagglutinin.

INTRODUCTION

Neuramide (NMD) (Difa Cooper, Caronno Pertusella, Italy), a viral inhibitor that is present in crude preparations of tissue extracts which is active against herpes viruses, has been described previously[1,2]. It is also active against a wide range of viruses which are not herpes viruses, and one inhibitory activity of NMD act to block the adsorption of a variety of viruses[3,4]. NMD is also active against influenza A viruses *in vitro* via a block in the replication cycle after the virus has been adsorbed, and ultrafiltration experiments showed that the anti-influenza virus activity was concentrated in the material of molecular weight below 500 Da[5]. During these studies, an immunostimulatory activity was also shown[6,7].

Here we report the preparative high-performance liquid chromatographic (HPLC) analysis of the antiviral and the immunostimulant fraction in NMD.

0021-9673/90/$03.50

EXPERIMENTAL

Neuramide (NMD) preparations were obtained from Difa Cooper.

Ultrafiltration experiments

NMD was fractionated by molecular sieving through Amicon type UM, YM and PM membranes. Markers were actinomycin D (MW = 1225); eosin yellow (MW = 691) and bromphenol blue (MW = 173).

HPLC analyses

Preparative size-exclusion chromatography (SEC) was performed by dissolving the lyophile in distilled water to obtain a concentration of 70 mg/ml. Samples were injected through a 1.1-ml loop. The instrument was a Varian 5000 HPLC system (Varian, Palo Alto, CA, U.S.A.) equipped with a TSK G2000 SWG size-exclusion column (60 cm × 21.5 mm I.D.) (Toyo Soda, Tokyo, Japan) eluted with a two-step gradient (45 min distilled water and 45 min 0.1 *M* sodium chloride solution) at a flow-rate of 6 ml/min. The detector was a Model 1040 diode-array detector (Hewlett Packard, Palo Alto, CA, U.S.A.). Fractions were tested for antiviral activity against the influenza virus and for immunostimulant activity by observing the enhancement of the human lymphocyte proliferation induced by phytohaemagglutinin.

Analytical reversed-phase HPLC of fractions from preparative runs was performed by dissolving the lyophilized material in 0.05 *M* ammonium acetate buffer (pH 6.5) and injecting through a 10-μl loop (30 μg per injection). The instrument was a Model SP8800 system (Spectra-Physics, San Jose, CA, U.S.A.), equipped with a Supelcosil PLC-18 reversed-phase column (25 cm × 4.6 mm I.D.) (Supelco, Bellefonte, PA, U.S.A.), eluted with 0.05 *M* ammonium acetate buffer (pH 6.5) at a flow-rate of 1 ml/min. The detector was a Model 484 tunable absorbance detector (Waters Assoc., Milford, MA, U.S.A.).

Isocratic reversed-phase HPLC purification of fractions from size-exclusion HPLC preparative runs was performed by dissolving the lyophilized material in water–acetonitrile (1:9) and injecting the solution through a 10-μl loop. The instrument was a Spectra-Physics SP8800 system equipped with a Waters Assoc. μBondapak-NH_2 column (30 cm × 3.9 mm I.D.), eluted with water–acetonitrile (1:9) at a flow-rate of 0.8 ml/min. The detector was a Waters Assoc. Model 484 tunable absorbance detector.

Extraction of antiviral components with methylene chloride

An aliquot of 252 mg of the mixture A + B + sodium chloride obtained by ultrafiltration–size exclusion HPLC (Fig. 1) was dissolved in 50 ml of water and extracted three times with 50-ml portions of methylene chloride. The organic extracts were collected, dried over sodium sulphate and the solvent was evaporated under reduced pressure to give 9 mg of the mixture A + B.

Elemental analysis

Carbon and nitrogen contents were measured using a Perkin-Elmer 240 elemental analyser.

Antiviral assay

Influenza A virus strains H_0N_1 and H_2N_2 were grown in chicken embryos and maintained at −70°C until they were used. Titration of the anti-influenza virus effects of NMD or chromatographic fractions was carried as follows. Serial dilutions of the samples in 0.1-ml volumes were added in triplicate to 96-well microtitre cultures of canine kidney cells (MDCK cells), then 0.025 ml of influenza A virus was added to give an input multiplicity of infection of 10 PFU per cell. Supernatants were collected and virus yields were determined after 48 h by a haemagglutination assay, which was performed in triplicate[8]. The end-point activity was defined as the last dilution that was capable of inhibiting the haemagglutination yield four-fold, compared with the virus control yield.

The standard assay was adapted to study the effect of the chromatographic fractions on influenza A virus replication by addition of the inhibitor to the MDCK cell monolayers after the virus challenge. At the high multiplicity of infection which we used, all the cells were infected after 1 h of incubation at 37°C.

Fractions diluted 1:32 and 1:64 in Eagle minimum essential medium, containing 2% foetal calf serum, which were well within the active range of the material, were tested to evaluate the possible toxic effects of NMD or the fractions. The viability of the monolayers after incubation for 48 h in the presence of NMD or the fractions was evaluated by Blue Dye exclusion and by current criteria.

Proliferation assay

Lymphocytes were isolated from heparinized peripheral blood of healthy donors, as described previously[9].

Mononuclear cells were resuspended at a final concentration of $1 \cdot 10^6$ cells/ml in RPMI 1640 medium, supplemented with 10% foetal calf serum, glutamine (2 m*M*) and gentamicin (50 μg/ml). Each sample was stimulated in triplicate microwell cultures in the presence of phytohaemagglutinin (PHA-M, Gibco) at a concentration of 12.5 μg/ml and at three different dilutions (1:100, 1:500 and 1:10 000) of NMD fractions. After incubation for 48 h at 37°C in a humidified atmosphere of 5% carbon dioxide in air, the cultures were labelled for 21 h with 0.5 μCi/well of tritiated thymidine (2 Ci/mmol, Amersham) and were then harvested onto glass-fibre strips with a multiple automated harvester (Skatron), included in scintillation fluid and counted.

RESULTS AND DISCUSSION

The first chromatographic enrichment procedure was performed with material having both antiviral and immunostimulating activity. The antiviral activity had been found in the ultrafiltered fraction containing components of MW less than 500 Da[5] and the immunostimulant activity in the ultrafiltered fraction below 5000 Da[6,7]. Hence, ultrafiltered material with a 5000-Da cut-off was used. In the SEC–HPLC procedure, the components were first eluted with water, then with 0.1 *M* sodium chloride solution and the fractions were tested for biological activity. The immunostimulating activity was tested by monitoring the potentiating effect of the fractions in the human lymphocyte proliferation, induced by phytohaemagglutinin. Several controls were used in this test, owing to the possibility of differences in the

responsiveness of individuals. For the fraction eluted with saline, this was dialysed and lyophilized before the biological test. Fig. 1 shows the chromatographic profile and the histogram of the immunostimulating activity for three dilutions of the chromatographic fractions. Four chromatographic regions of biological activity appear in most controls. The most prominent region (23% of the original amount of material) is the first to be eluted, and is composed of material at MW $\approx$5000 Da. A second, less well defined region (13% recovery) appears in the bulk of the chromatographic peak, and the third region occurs in the tail of the peak (6% recovery) and probably contains a small amount of active low-molecular-weight material. Some active material is retained by the column and is eluted with 0.1 *M* sodium chloride solution. These results suggest that several families of components in the extract have immunostimulating activity.

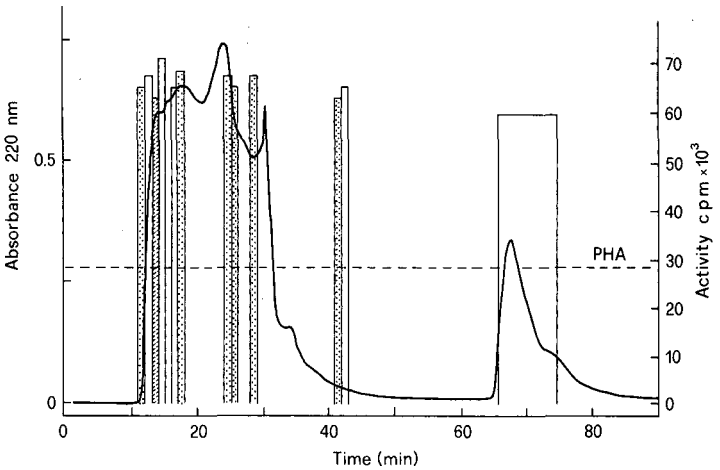

Fig. 1. SEC–HPLC analysis of NMD ultrafiltered with a 5000-Da cut-off membrane and histogram of the enhancement of the human lymphocyte proliferation induced by phytohaemagglutinin at three dilutions (white, 1:100; dotted, 1:500; dashed, 1:10 000).

All fractions were also tested against influenza virus in order to evaluate the presence of antiviral components. It could be shown that these were concentrated in the material eluted by 0.1 *M* sodium chloride.

The fact that the antiviral components were eluted after the V_t value suggested that some effect other that size exclusion was occurring, *i.e.*, some interaction of these components with silica. This observation could be used to improve the purification procedure by elution of non-antiviral components with water before the elution of the antiviral fraction with 0.1 *M* sodium chloride solution.

As antiviral components had MW below 500 Da, the ultrafiltrate below 500 Da having a specific activity of 2.28–4.57 activity units[5,8]/mg was injected into a preparative SEC–HPLC column; the result is shown in Fig. 2. All chromatographic fractions were lyophilized, dissolved in methanol and filtered and the methanolic extract was evaporated to dryness, weighed and submitted to evaluation of the antiviral activity. This was concentrated in the fraction eluted with 0.1 *M* sodium chloride. The specific

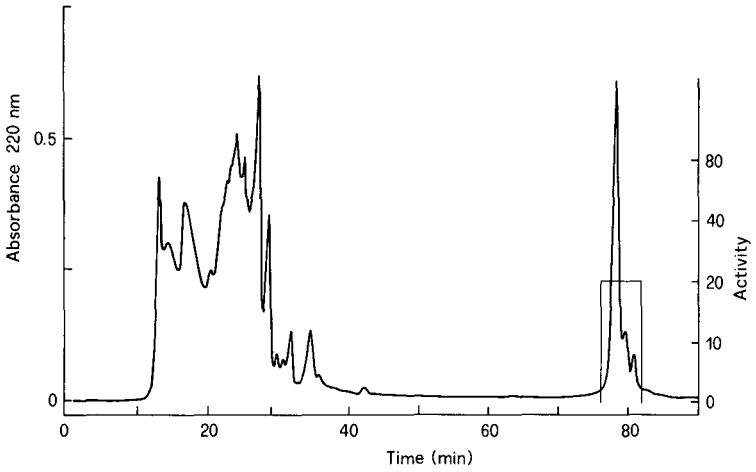

Fig. 2. SEC–HPLC analysis of NMD ultrafiltered with a 500-Da cut-off membrane.

activity of this material was 6.25–12.5 activity units[5,8]/mg with a six-fold increase in comparison with the original ultrafiltrate. Much sodium chloride was present in mixture with the organic material.

The biologically active fraction consisted of two peaks. The diode-array spectrophotometric analysis of these showed a strong absorption at 220 nm and had a very low absorption at 254 nm. Thus, the active fraction seemed not to contain nucleic bases or aromatic amino acid-containing peptides but to be constituted of sugars, non-aromatic amino acid-containing peptides or glycopeptides.

The material containing the two peaks in SEC–HPLC was then analysed with a different chromatographic procedure. Reversed-phase HPLC on a C_{18} column (RP-HPLC-C_{18}) with elution by 0.05 *M* ammonium acetate buffer (pH 6.5) and monitoring at 220 nm gave the result shown in Fig. 3. Again, two components were

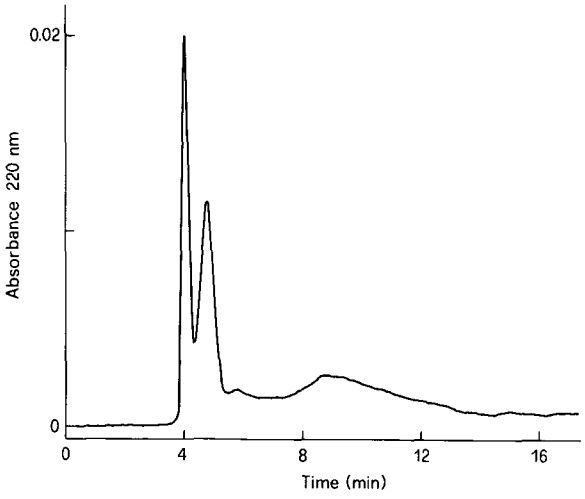

Fig. 3. RP-HPLC-C_{18} analysis of the antiviral fraction from the SEC–HPLC separation.

eluted after a short retention volume. This indicated that they were very polar products.

Reversed-phase HPLC was a good separation procedure for these two components. A better resolution was obtained using an amino-bonded RP-HPLC column (RP-HPLC-NH_2) eluted with water–acetonitrile (1:9). The elution profile typical of very polar material obtained by monitoring at 220 nm is shown in Fig. 4.

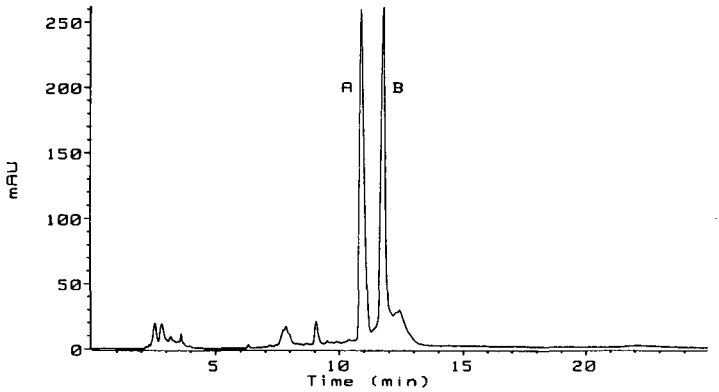

Fig. 4. RP-HPLC-NH_2 analysis of the antiviral fraction from the SEC–HPLC separation.

SEC was repeated fourteen times and the antiviral fraction was collected; 639 mg of material were obtained from 980 mg of NMD ultrafiltered below 500 Da. As this material was shown by the elemental analysis to contain only 4% of organic matter and much sodium chloride, an aliquot of this was used for the solvent extraction procedure intended to eliminate the salt and calculate the enrichment obtained.

Further 3-mg aliquots were injected into the RP-HPLC-NH_2 column and this procedure was repeated twenty times, which made it possible to obtain enough material for the characterization of the individual antiviral components. The lyophiles obtained from both peaks (compounds A and B) were submitted to elemental analysis. The high content of sodium chloride allowed only the carbon to nitrogen ratio in these samples to be obtained; this was 3:2 for compound A and 5:2 for compound B. These data and the UV absorption spectra suggested a polar aliphatic peptidic nature for these compounds.

Compounds A and B could be obtained from their mixtures with sodium chloride by extraction with methylene chloride. This allowed it to be calculated that a nearly equimolecular mixture of compounds A and B was present in a 2% amount in the original NMD ultrafiltrate below 500 Da.

In conclusion, enrichment of the antiviral activity of NMD against the influenza A virus may be obtained by an ultrafiltration and preparative SEC–HPLC sequence. This allows the isolation of two very polar components which may be further purified by RP-HPLC and solvent extraction for future structure determination studies. Four chromatographic fractions having immunostimulant activity have been also obtained by preparative SEC–HPLC.

ACKNOWLEDGEMENTS

We thank Professor C. Scolastico, Dr. M. G. Beretta and V. Frattini for helpful discussions, and our students Dr. S. Giacobbe and Mr. A. Cremonesi. This work was supported by a CNR grant.

REFERENCES

1 T. B. Albrecht, N. Cole, D. Speelman, F. Dianzani and S. Baron, *Chemioterapia*, 2 (1983) 255.
2 T. B. Albrecht, M. Zucca and F. Dianzani, *G. Ital. Chemioter.*, 27 (1980) 103.
3 S. Baron and M. L. McKerlie, *Infect. Immun.*, 32 (1981) 449.
4 S. Kumar, M. L. McKerlie, T. B. Albrecht, A. S. Goldman and S. Baron, *Proc. Soc. Exp. Biol. Med.*, 177 (1984) 104.
5 G. Antonelli, F. Dianzani, D. H. Coppenhaven, S. Baron, P. Calandra and G. Folchitto, *Antimicrob. Agents Chemother.*, 29 (1986) 49.
6 C. M. Alberini, M. De Amici, D. Montagna, S. Guarnaccia, L. Nespoli and A. G. Ugazio *G. Ital. Chemioter.*, 29 (1982) 1.
7 M. De Amici, C. M. Alberini, D. Montagna, S. Guarnaccia, A. Avanzini, L. Nespoli and A. G. Ugazio, *Rec. Prog. Med.*, 78 (1987) 354.
8 L. Rosen, in K. Habel and N. P. Salzman (Editors), *Fundamental Techniques in Virology*, Academic Press, New York, 1969, p. 276.
9 R. Maccario, L. Nespoli, G. Mingrat, A. Vitiello, A. G. Ugazio and G. R. Burgio, *J. Immunol.*, 130 (1983) 1129.

Journal of Chromatography, 512 (1990) 131–137
Elsevier Science Publishers B.V., Amsterdam

CHROMSYMP. 1818

Purification of a amylase–pullulanase bifunctional enzyme by high-performance size-exclusion and hydrophobic-interaction chromatography

CHEORL-HO KIM* and DONG-SOO KIM
Laboratory of Biochemistry, Department of Agricultural Chemistry, University of Tokyo, 1-1-1 Yayoi, Bunkyo-ku, Tokyo 113 (Japan)
HAJIME TANIGUCHI
Laboratory of Bioconversion, National Food Research Institute, 2-1-2 Kannodai, Tsukuba 305 (Japan)
and
YOSHIHARU MARUYAMA
Laboratory of Biochemistry, Department of Agricultural Chemistry, University of Tokyo, 1-1-1 Yayoi, Bunkyo-ku, Tokyo 113 (Japan)

ABSTRACT

A novel bifunctional enzyme, amylase–pullulanase enzyme (APE), which is produced by *Bacillus circulans* F-2, was separated and purified in only two steps by high-performance size-exclusion (HPSEC) and high-performance hydrophobic-interaction chromatography (HPHIC) with 50 m*M* phosphate buffer (pH 7.3) containing 5 m*M* Co^{2+}. About a 90% recovery of the total enzyme activity was achieved, together with a 1821-fold increase in specific activity. APE activity recovered from the column decreased rapidly in the absence of Co^{2+}, which acts as an activator and stabilizer. However, most of the activity was restored on the addition of Co^{2+}. When a descending salt gradient (1 to 0 *M* ammonium sulphate in 60 min) and a mobile phase containing Co^{2+} were used in HPHIC, the APE characteristics were altered, resulting in earlier elution of the enzyme. The results indicate that the hydrophobic properties of APE can be altered by the addition of Co^{2+}, and that the application of HPSEC and HPHIC with cations such as Co^{2+} results in the effective purification of a high-molecular-weight enzyme.

INTRODUCTION

There are two kinds of enzymes that can hydrolyse the α-1,6-glucano binding site on starch materials: an isoamylase (E.C. 3.2.1.68) and a pullulanase (E.C. 3.2.1.41). Whereas pullulanase hydrolyses only the α-1,6-glucano bonds of pullulan and amylopectin, isoamylse can hydrolyse the α-1,6-glucano bonds of amylopectin and glycogen, but not pullulan. These enzymes have been called debranching enzyme or

0021-9673/90/$03.50

debranching amylase[1]. Pullulan, a very highly ordered and branched polysaccharide with a 2:1 ratio of α-1,4-glucano to α-1,6-glucano bonds, is usually produced by the bacterium *Pullularia pullulans*. There have been some reports of the enzymatic application and production of pullulanase[2–7], but the work was focused only on the enzymatic characteristics and the utilization of the pure pullulan molecules. The bifunctional enzyme which has an ability to digest starch (α-1,4-glucano linkage) and pullulan (α-1,6-glucano linkage) has become important in fermentation processes and academic fields.

Amylase–pullulanase enzyme (APE) (α-1,4-and α-1,6-glucanohydrolase) is a high-molecular-weight (*ca.* 220 kDa) extracellular protein of *Bacillus circulans* F-2[8]. Although APE is an abundant protein, it has proved difficult to isolate and purify because it is inactivated in the process of purification. Analysis of the purified APE showed that cobalt chloride activated and stabilized the APE activity.

In previous work[8], several extensive purification steps involving ammonium sulphate fractionation, starch adsorption, DEAE-Toyopearl chromatography and high-performance hydrophobic-interaction chromatography (HPHIC) were utilized to purify APE. These methods are time consuming and produce low yields of purified APE, necessitating the use of large amounts of starting material.

The purification scheme illustrated in this study provides a simple rapid and quantitative method of isolating APE from bacterial culture supernatants. Further, it is shown that application of HPHIC with reagents such as cobalt chloride permits separation.

EXPERIMENTAL

Isolation of amylase–pullulanase enzyme

The bacterial strain used was described previously[9]. The strain was cultivated in a 5-l jar fermenter (Marubishi, Tokyo, Japan) containing 1 l of the medium with the composition described previously[8]. Cultivation was carried out for 4 days at 37°C while rotating the vessel at 150 rpm. The bacterial culture supernatant was concentrated with ammonium sulphate (0–80%) and the resulting enzyme was injected onto high-performance liquid chromatographic (HPLC) columns.

Chemicals

Soluble starch purchased from E. Merck (Darmstadt, F.R.G.) was reduced with sodium borohydride and used in amylase assays as the substrate. Pullulan (MW 50 000) was purhased from Hayashibara Biochemical Labs. (Tokyo, Japan), cobalt chloride and sodium borohydride from Fisher Scientific (Louisville, KY, U.S.A.), TSK gel G3000 SW-XL and TSK gel phenyl 5PW from Tosoh (Tokyo, Japan) and HPLC-grade ammonium sulphate and protein standards for molecular weight measurement from Bio-Rad Labs. (Richmond, CA, U.S.A.).

Protein assay

The protein concentration of the column eluates was monitored by measuring the absorbance at 280 nm, and those of the enzyme solution and other proteins were measured by the method of Lowry *et al.*[10] using bovine serum albumin as the standard.

Assay of amylase and pullulanase activities

Amylase and pullulanase activities were measured by the method used previously[8] and that of Somogyi[11]. One unit of the enzyme was defined as the amount of enzyme that produced reducing sugars corresponding to 1 mmol of glucose from soluble starch or pullulan in 1 min under the assay conditions. Specific activity was expressed as the units per milligram of protein.

Gel electrophoresis

Zymograms of amylase activity staining were obtained with a previously reported method[1]. Native slab polyacrylamide gel electrophoresis (PAGE) was carried out by the method of Davis and Ornstein[12] with 7.5% polyacrylamide gel at pH 8.3. Sodium dodecyl sulphate (SDS) PAGE was done by the procedure of Weber and Osborn[13] with 12.5% polyacrylamide gel. For relative molecular mass measurement, myosin (M_r 205 000), β-galactosidase (M_r 116 000), phosphorylase B (M_r 97 400), bovine serum albumin (M_r 66 000) and egg albumin (M_r 45 000) were used as standards.

High-performance size-exclusion chromatography (HPSEC)

An analytical size-exclusion column (TSK gel G3000 SW-XL), particle size 10 μm (300 × 7.5 mm) (Tosoh), was used for amylase–pullulanase separation, as described previously[8]. HPLC was performed at ambient temperature with a Shimadzu (Tokyo, Japan) solvent-delivery module, including a Model LC-4A system controller and injector block. Concentrated culture broth was applied in 250–500-μl volumes with a Hamilton syringe. The elution buffer (pH 6.5) was 50 m*M* phosphate buffer–0.3 *M* sodium chloride. All buffers were filtered through a 0.45-μm filter (Millipore). Elution was carried out at a flow-rate of 0.5 ml/min. Fractions were collected at 0.5-min intervals in 75 × 12 mm tubes. Recoveries were in the range 95–100%.

HPHIC

Chromatography was performed at ambient temperature. All buffers were vacuum filtered through Millipore (Bedford, MA, U.S.A.) 0.45-μm HAWP filters before use. A volume of 300 μl of the APE activity eluted from the HPSEC, to which 1.0 *M* ammonium sulphate had been added, was pumped at 1 ml/min into a hydrophobic-interaction HPLC column (21.5 × 150 mm) of TSK gel phenyl 5PW (Tosoh) previously equilibrated with 1.0 *M* ammonium sulphate–50 m*M* sodium phosphate (pH 7.3) (buffer A). Elution was carried out with a Shimadzu solvent-delivery module including a Model LC-4A system controller and injector block. All samples were adjusted to 1.0 *M* ammonium sulphate prior to injection.

Unless stated otherwise, the gradient programme consisted of a preliminary wash with buffer A at a flow-rate of 1 ml/min, then, following sample injection, a descending salt gradient was developed with 50 m*M* sodium phosphate (pH 7.3) (buffer B) in 60 min. Buffer B was then maintained at a flow-rate of 1 ml/min for the next 20 min before re-equilibration with buffer A. In experiments that required cobalt chloride in the mobile phase, both buffers A and B contained 5 m*M* cobalt chloride.

Fractions of 0.4 ml were collected and the amylase and pullulanase activities were determined. The recoveries of total enzyme activity and injected protein were almost always 90–100%.

RESULTS AND DISCUSSION

APE, a bifunctional enzyme produced by *Bacillus circulans* F-2, possesses two active sites which hydrolyse α-1,4-and α-1,6-glucosdic linkages at the same rate[8]. APE is a very minor component of the *B. circulans* F-2 amylase system and its physiological function is not known[1,8]. Thus, a sensitive method is required for its purification in studies of its structure–function relationship.

A previous study of the purification of APE from culture broth included fractonation with ammonium sulphate, DEAE ion-exchange chromatography and chromatofocusing[8]. It was shown that the purified APE activity was high and stabilized in the presence of cations such as Co^{2+}. In this study, HPSEC and HPHIC methods were selected to optimize the recovery of purified APE, as the ammonium sulphate fractionation greatly reduced the activity of the crude enzyme and APE is a high-molecular-weight (220 kDa) protein. In this paper data are presented to show the influence of an enzyme-modifying and -stabilizing reagent on APE.

HPSEC

The first step in the purification of APE from culture broth was HPSEC. The procedure not only gave a 66-fold (amylase) and 844-fold (pullulanase) purification of the specific activity, but also yielded 7.4% (amylase) and 94.1% (pullulanase) recoveries of total activity.

Fig. 1 is a representative HPLC elution pattern of the concentrated crude enzyme obtained under the conditions described above and the zymogram of APE on the native PAGE after successful HPSEC, demonstrating the purification achieved. As shown in Fig. 1A, the resolution obtained by HPLC was excellent, indicating satisfactory separation of APE from other proteins.

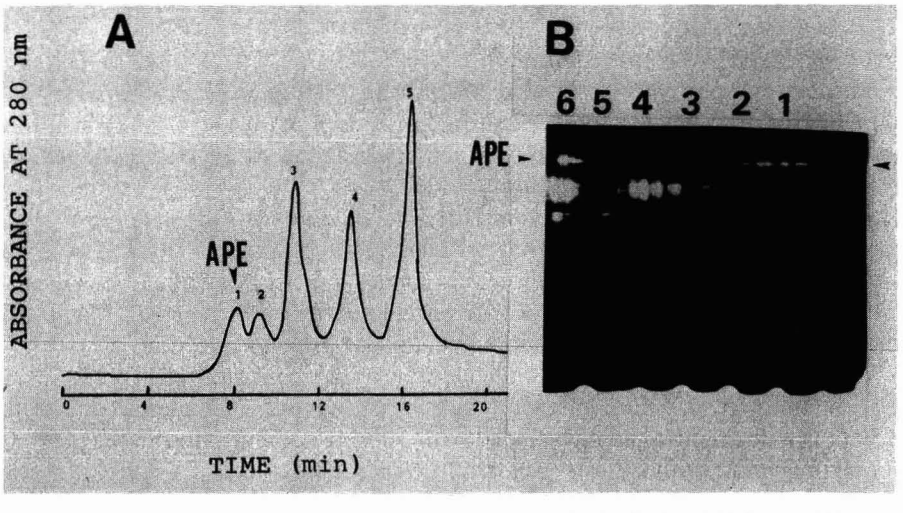

Fig. 1. Separation of APE (peak 1) from culture supernatant by HPSEC. (A) Column, TSK gel G3000 SW-XL; eluent, 50 m*M* sodium phosphate–0.3 *M* sodium chloride (pH 6.5); flow-rate, 0.5 ml/min; temperature, 25°C. (B) Native PAGE zymogram of samples (A) from HPSEC of bacterial culture supernatant; lane 1 = peak 1 (arrow denotes position of APE); lane 2 = peak 2; lane 3 = peak 3; lane 4 = peak 4; lane 5 = peak 5; lane 6 = starting material.

After collection of the peaks the APE activity was determined. Peak 1 was found to contain catalytically active APE. For comparion, lane 6 in Fig. 1B contains the crude enzyme solution before chromatography. Activity-stained PAGE showed that peak I has a single activity band. Peaks 3, 4 and 5 show no APE band, and peak 2 shows a small APE band. The APE-containing peak shows a retention time of 8.10 min, corresponding to a molecular weight of 200–220 kDa, consistent with that found for ADE isolated using DEAE ion-exchange chromatography in our laboratory and with the value reported previously[8]. This result indicates that the successful separation of APE from other carbohydrases can be achieved by HPSEC even though some impurities were still present.

HPHIC

The active APE (300 μl) from the above step was applied to a hydrophobic interaction column of TSK gel phenyl 5PW previously equilibrated with 1 *M* ammonium sulphate and 50 m*M* phosphate buffer (pH 7.5). APE was eluted from the HPHIC column at 22.32 min (corresponding to fraction No. 45), and was a single peak based on activity and protein measurements (Fig. 2A).

In previous work[8] we observed that cobalt chloride enhanced the APE activity.

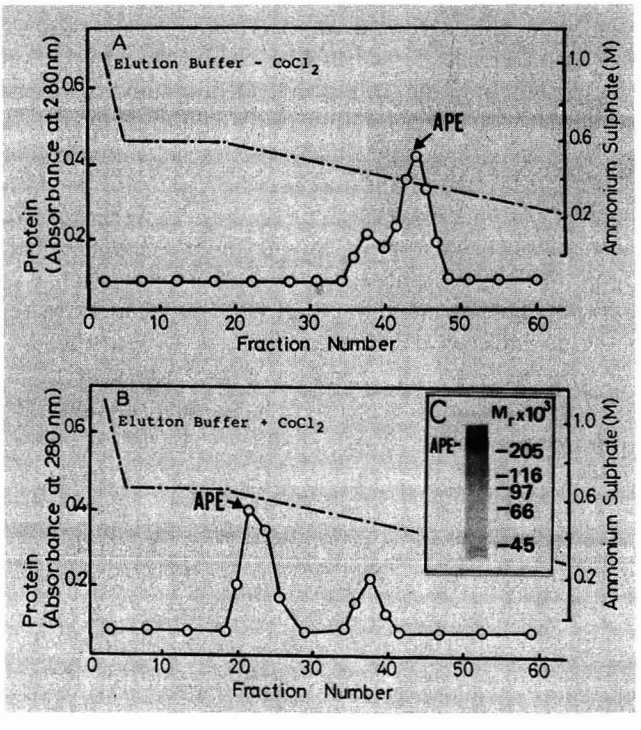

Fig. 2. Isolation of APE by HPHIC and influence of cobalt chloride on the hydrophobic characteristics of APE. Peak 1 of HPSEC was prepared in elution buffer A, as described in under Experimental. One set of aliquots was then made 5 m*M* with respect to cobalt chloride. The elution buffers in each instance are indicated. Purified APE of B was subjected to SDS-PAGE (12.05% gel) with molecular-weight markers. A, Without cobalt chloride; B, with cobalt chloride; C, SDS-PAGE of APE from B. M_r = Molecular weight.

TABLE I

EFFECT OF COBALT CHLORIDE ON APE ACTIVITY

APE samples were stored at 4°C for up to 14 days after HPHIC in the appropriate buffer with or without cobalt chloride as described under Experimental.

Days after HPHIC	*APE activity (%)*[a]	
	Without $CoCl_2$	*With $CoCl_2$ (5-mM)*
0	100	100
1	80	100
2	50	98
3	40	95
7	20	90
14	10	80

[a] The APE activities given are the means of the amylase + pullulanase activities.

In contrast to the chromatogram shown in Fig. 2A (peak of APE, in the presence of cobalt chloride we observed a new peak (peak APE in Fig. 2B), which is eluted at 10.08 min (corresponding to fraction No. 21). When the APE-containing solution was adjusted to 5 m*M* cobalt chloride and chromatographed with cobalt chloride containing buffer, there was a sharp increase in isoform APE in Fig. 2B. The APE in Fig. 2B was a less hydrophobic protein than that in Fig. 2A. Additionally, there was a decrease in isoform APE in Fig. 2A with a concomitant increase in isoform APE in Fig. 2B when chromatograhed with increasing concentrations of cobalt chloride (0 to 10 m*M*) (data not shown). This indicates that, in the absence of cobalt chloride, APE attached to the stationary phase was influenced by cobalt cloride. When cobalt chloride-containing APE solution was chromatographed with buffers lacking cobalt chloride, using extensive column washing in the absence of cobalt chloride, there was little conversion (data not shown). These results imply that APE may contains sites that are sensitive to cobalt chloride and may indicate that isoform APE in Fig. 2A,

TABLE II

PURIFICATION OF APE FROM *BACILLUS CIRCULANS* F-2

Details of the purification procedure and measurement of enzyme activity and protein concentration are given under Experimental.

Purification step	*Total protein (mg)*	*A*[a] *(units)*	*P*[a] *(units)*	*A/P*	*Specific activity (units/mg protein)*		*Yield of activity (%)*	
					A	*P*	*A*	*P*
Culture broth	2250	2025.4	168.2	12.1	0.90	0.075	100	100
TSK gel G3000 SW-XL	2.5	149.1	158.2	0.94	59.6	63.3	7.4	94.1
TSK gel phenyl-5 PW	0.87	143.8	153.6	0.93	125.1	133.6	7.1	91.3

[a] *A* = Amylase activity; *P* = pullulanase activity.

which is modified by cobalt chloride, may be changed to a new conformation (isoform APE in Fig. 2B) resulting in different hydrophobicity.

Fig. 2C is an SDS-PAGE pattern demonstrating the purification achieved. The molecular weight of the APE band is about 220 kDA, which is the same as reported previously[8]. The specific activities (125.1 units/mg for amylase and 133.6 units/mg for pullulanase) of the HPSEC- and HPHIC-purified APE compare favourably with previously reported values (81.7 units/mg for amylase and 84.2 units/mg for pullulanase)[8]. Within 2 days after elution from the HPHIC column, the total enzyme activity recovered from the column, which eluted in the absence of cobalt chloride, decreased from 98% to 50% of the applied sample. However, the enzyme activity was maintained without any decrease in the total activity in the presence of 5m*M* $CoCl_2$, an activator and stabilizer of APE (Table I). Therefore, the loss of activity may be due to the absence of cobalt chloride. The results of these simpler and improved purification procedures are summarized in Table II.

CONCLUSIONS

Purification of APE by HPSEC and HPHIC avoids the use of ammonium sulphate fractionation, which greatly reduces the activity of the crude enzyme. The method is rapid and the enzyme can be recovered in good yield. It is remarkable that the enzyme activity recovered (93%) in the final purification stage is about three times higher than the previous level (31%)[8]and is 1780-fold purified (as pullulanase) from the crude culture supernatants of *B. circulans* F-2. The present study also suggests that two isoforms are separated on the basis of different hydrophobic properties.

ACKNOWLEDGEMENTS

This research was supported in part by Toyobo Biotechnology Research Foundation (Tokyo, Japan).

REFERENCES

1 H. Taniguchi, in H. Taniguchi, S. Ohnish and Y. Sakano (Editors), *Amylase, Its Biotechnological Approach*, Japanese Academic Press Centre, Tokyo, 1986, p. 303.
2 H. Bender and K. Wallenfels, *Biochem. J.*, 79 (1961) 334–340.
3 M. Abdullah and D. French, *Arch. Biochem. Biophys.*, 137 (1970) 483–493.
4 S. Ueda and R. Ohba, *Agric. Biol. Chem.*, 36 (1972) 2381–2391.
5 G. J. Waker, *Biochem. J.*, 108 (1968) 33–40.
6 N. Nakamura, K. Watanabe and K. Horikoshi, *Biochim. Biophys. Acta*, 397 (1975) 188–193.
7 Y. Sakano, M. Higuchi and T. Kobayashi, *Arch. Biochem. Biophys*, 153 (1972) 180–185.
8 H. Sata, M. Umeda, C.-H. Kim, H. Taniguchi and Y. Maruyama, *Biochim. Biophys. Acta*, 991 (1989) 3388–394.
9 H. Taniguchi, C. H. Jae, N. Yoshigi and Y. Maruyama, *Agric. Biol. Chem.*, 47 (1983) 511–519.
10 O. H. Lowry, N. J. Rosebrough, A. L. Farr and R. J. Randall, *J. Biol. Chem.*, 193 (1951) 265–275.
11 M. J. Somogyi, *J. Biol. Chem.*, 195 (1952) 19–23.
12 B. J. Davis and L. Ornstein, *Ann. N.Y. Acad. Sci.*, 121(1964) 404–427.
13 J. Weber and M. Osborn, *J. Biol. Chem.*, 244 (1969) 4406–4412.

Journal of Chromatography, 512 (1990) 139–147
Elsevier Science Publishers B.V., Amsterdam

CHROMSYMP. 1875

Purification of immunomodulatory factors in human peripheral blood leukocytes

P. C. MONTECUCCHI*, R. CALDARINI, M. SANSÓ and A. M. BERTOLASO
Sclavo SpA, DE.BI., Padana Superiore Km 160, 20060 Cassina de' Pecchi (Italy)
and
V. E. M. ROSSO DI SAN SECONDO, G. PICCOLO and G. SIRCHIA
Centro Trasfusionale e di Immunologia dei Trapianti, Ospedale Policlinico, via F. Sforza 35, 20122 Milan (Italy)

ABSTRACT

Procedure is described for purifying low-molecular-weight factors with antigen-aspecific properties from a dialysate of human leukocyte extract. It includes gel chromatography on Sephadex G-25 and G-15, ion-exchange chromatography, reversed-phase high-performance liquid chromatography (HPLC) on a C_{18} hydrophobic column and gel permeation HPLC. The immunosuppressive factor (mol.wt. 800–1000) was purified to near homogeneity. It is probably of peptidic nature, although it is pronase resistant. The enhancer factor (mol.wt. 300–600) is eluted from chromatographic columns together with a hypoxanthine-like substance. Nevertheless, the biological activity cannot be attributed to the purine derivative. Identification of this amplifier activity is still lacking.

INTRODUCTION

A number of immunomodulators from human leukocytes have been described that either enhance or suppress immune functions[1–10]. The characterization of these factors and their reproduction by synthesis is of practical importance in view of their potential use *in vivo* in various clinical disorders and after tissue and organ transplantation.

The presence in leukocyte extracts of *in vitro* and *in vivo* immunosuppressive and immunostimulating activity has been reported previously[3,4,7,11]. This paper deals with the isolation of some of these molecules from peripheral blood leukocytes that exhibit activity on *in vitro* lymphocyte transformation to phytohaemagglutinin (PHA).

0021-9673/90/$03.50

EXPERIMENTAL

Preparation of the leukocyte extract

The leukocyte extract was obtained according to the method of Reymond and Grob[12]. Briefly, ten buffy-coats, containing 40% mononuclear cells and 60% polymorphs, represented the starting material for the purification of the immunosuppressor and enhancing factor. They were obtained from units of 450 ml of blood, collected in plastic bags in citrate dextrose from regular blood donors and separated from red blood cells and platelet-rich plasma after centrifugation of the blood unit at 400 *g* for 15 min at 22°C. After three washes in saline solution, the packed leukocytes were disrupted by adding ten volumes of distilled water, followed by twelve freezing–thawing cycles.

Cellular debris was discarded and the leukocyte extract was ultrafiltered through membranes (molecular weight cut-off 10 000 dalton) (Sartorius, Göttingen, F.R.G.). The leukocyte extract obtained was designatedd DLE (dialysate leukocyte extract). One unit was arbitrarily defined as the material prepared from 10^9 leukocytes (40% mononuclear, 60% polymorphonuclear).

PHA-induced lymphocyte transformation

The assay was performed as described previously[13,14]. Human peripheral blood lymphocytes used for the test were obtained as follows. A 10-ml volume of blood was drawn by venipuncture from healthy donors and defibrinated at 37°C in silica-coated tubes containing polystyrene granules. The lymphocytes were isolated in a gradient of Ficoll-Urovison (1.077 g/ml density) (Flow Labs., McLean, VA, U.S.A.) layering 7 ml of defibrinated blood, diluted 1:4 with Hanks' balanced salt solution (HBSS) (Flow Labs.) onto 3 ml of gradient solution and centrifuging at 400 *g* for 30 min. The cell suspension removed from the interface was washed three times with HBSS and suspended at a concentration of 10^5 cells/ml in RPMI-1640 (Flow Labs.), supplemented with 0.20 m*M* N-(2-hydroxyethyl)piperazine-N′-(2-ethanesulphonic acid) (HEPES), penicillin (100 IU/ml), streptomycin (50 μg/ml) and 10% serum AB. Lymphocyte transformation was obtained in round-bottomed microtitre tissue-culture plates with increasing concentrations of PHA (0.1–10 μg/ml) (Flow Labs.) and various concentrations of DLE or its fractions from the purification steps. The plates were incubated in a 37°C humidified atmosphere for 72 h. Eight hours before the end of incubation the cells were labelled with 1 μCi of [^{3}H]thymidine (2 Ci/mmol; Amersham, Aylesbury, U.K.) per culture, collected on filters and the radioactivity was measured in 10 ml of Picofluor (Packard, Meriden, CT, U.S.A.) in a scintillation spectrometer.

Purification procedures and analytical methods

All reagents and solvents were of analytical-reagent grade form Merck (Darmstadt, F.R.G.). Methanol and the other solvents were of LiChrosolv grade from Merck. Sephadex G-15 and Sephadex G-25 Super Fine were obtained from Pharmacia LKB (Uppsala, Sweden), Dowex 50W-X8 (H^+) (50–100 mesh) from BDH (Poole, U.K.), Dowex 1-X2 (Cl^-) (50–100 mesh) from Bio-Rad Labs. (Richmond, CA, U.S.A.); μBondapak C_{18} column (300 × 39 mm I.D.) from Millipore–Waters (Milford, MA, U.S.A.); LiChrosorb RP-18 (10 μm) column (250 × 4 mm I.D.) from

Merck and TSK 3000 SW Spherogel column (600 × 7.5 mm I.D.) from Beckman (Altex Division, San Ramon, CA, U.S.A.). The efficiency of the columns was monitored using gel permeation (GP) and reversed-phase (RP) high-performance liquid chromatographic (HPLC) peptide standards, obtained from Synthetic Peptides (Department of Biochemistry, University of Alberta, Alberta, Canada). The data from size-exclusion HPLC were analysed using the Autolab Software GPC/PC program (Spectra-Physics, San Jose, CA, U.S.A.). Synthetic peptides were obtained from Peninsula Labs. (Europe) (Merseyside, U.K.) and bradykinin (triacetate salt) and bovine insulin chain B oxidized from Sigma (St. Louis, MO, U.S.A.).

Dialysis was performed at 5°C, using wet cellulose dialysis tubing with a molecular weight cut-off of 1000 dalton[a] (Spectrum 6, 38 mm; Medical Industries, Los Angeles, CA, U.S.A.). The enzymatic digestion with pronase (Boehringer, Mannheim, F.R.G.) (enzyme: substrate ratio from 1:20 to 1:100) was performed in 0.05 *M* ammonium acetate (pH 8.0) at 37°C. At different times, the samples were acidified with 1% trifluoroacetic acid, boiled for 1 min, centrifuged and then injected into the RP-HPLC column. The degradation with xanthine oxidase (XOD) (xanthine:oxygen oxidoreductase, EC 1.2.3.2) (X4500, Sigma) was performed at room temperature in 0.005 *M* phosphate buffer at pH 7.0[15]; the reaction products were analysed by RP-HPLC using the μBondapak column.

Total acid hydrolysis was performed as previously described[16]. The Edman degradation was carried out in an automatic version using a gas-phase sequencer (Applied Biosystems, Foster City, CA, U.S.A.)[16]. The *o*-phthalaldehyde (OPA) derivatives and the 9-fluorenylmethyloxycarbonyl chloride (FMOC) derivatives of the amino acids were separated on Knauer OPA or Knauer FMOC columns (250 × 4 mm I.D.) respectively, according to the method of Kamp[17]. Protein was determined by the method of Lowry *et al.*[18] with bovine serum albumin (Sigma) as a reference standard; in the presence of very small amounts, the quantification was carried out by amino acid analysis.

Instrumentation

HPLC was carried out using the modular Applied Biosystems apparatus, consisting of two pumps (Model 400 solvent-delivery system), two pulse dampers Model LP-21-LO-Pulse (Scientific Systems, State College, PA, U.S.A.), a Spectraflow 491 dynamic mixer/Rheodyne sample injector, a Model 900 programmable fluorescence detector, a Model 1000S diode-array detector (version 1.0A), a derivatizer/autosampler (Knauer, Berlin, F.R.G.), a high-temperature oven with temperature control unit (Waters–Millipore) and an Applied Biosystems 490 A data processor connected to an Epson FX-800 printer.

The eluents were degassed in an Ultrasonic Degass-Branson 2200 (Branson Europe, Soest, The Netherlands). Before injection, the samples were centrifuged in a Biofuge A from Heraeus Sepatech (Am Kalkberg, Osterode, F.R.G.). A single-path UV-1 monitor control unit and optical unit (Pharmacia, Uppsala, Sweden) were employed for monitoring the effluent from chromatography on open columns; a sample cell with a path length of 1.0 mm was used.

---

[a] The synthetic peptide physalaemin (mol.wt. 1265 dalton) was recovered in the retentate, confirming the cut-off value.

RESULTS

Purification

Gel chromatography of the starting material on Sephadex G-25 (Fig. 1) was useful for the separation of the two biological activities. In fact, the leukocyte immunosuppressor factor (LsF) is eluted from the column with V_e/V_t (elution volume/total column volume) = 0.5–0.6 (mol. wt. *ca.* 800–1000 dalton) and the leukocyte enhancer factor (LeF) with V_e/V_t = 1.2 (mol. wt. *ca.* 300–600 dalton).

In each experiment an aliquot corresponding to 10 units (0.66 g of lyophilized material) was dissolved in 4 ml of 0.05 *M* ammonium hydrogencarbonate and applied to the column. The active pools were lyophilized to yield a dry residue containing the biological activities.

The purification on Sephadex G-25 could be replaced by chromatography on Dowex 50W-X8 (Fig. 2), using distilled water as eluent; 1 *M* ammonia solution was employed for recovery of the enhancer activity.

The LsF from Sephadex G-25 was fractionated on a column of Sephadex G-15 and then purified by gel and reversed-phase HPLC. The last RP-HPLC trace (corresponding to step vi in Table I) showed a single sharp peak at a retention time of 4.60 min. The UV spectrum of this fraction did not show any significant absorbance at 280 nm. The first-order derivative of the chromatographic peak had a shape "resembling

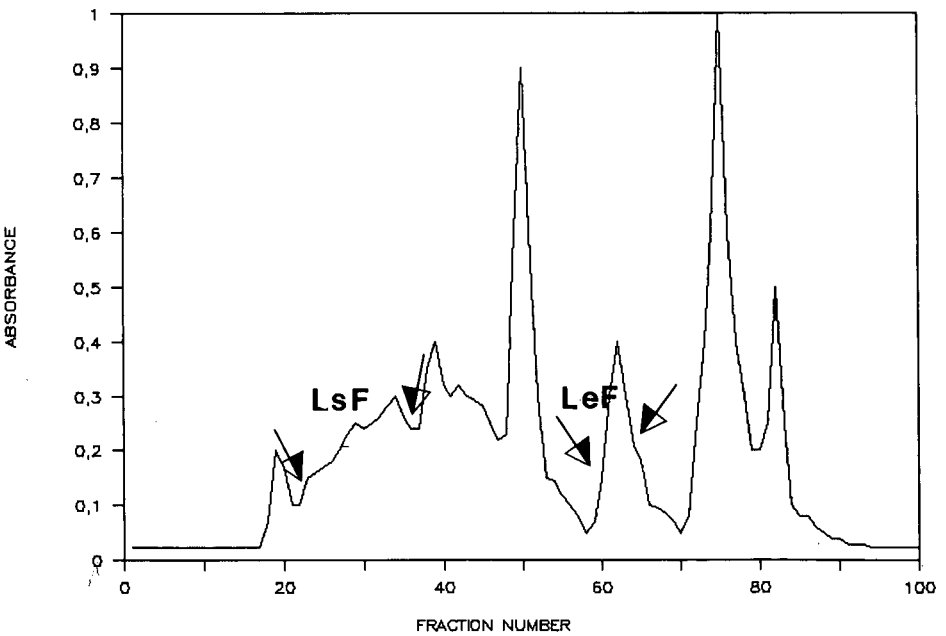

Fig. 1. Gel chromatography on Sephadex G-25 of the dialysate of the leukocyte extract. Column, 1000 mm × 26 mm I.D., stored at 15°C; eluent, 0.05 *M* ammonium hydrogencarbonate; flow-rate, 60 ml/h (one fraction in 10 min); detection, 280 nm (UV-1 sensitivity, 1); recorder, 20 mV, chart speed, 0.1 mm/min; sample size, 10 units. The arrows indicate the pooled fractions containing the LsF and LeF activities, which were subsequently rechromatographed.

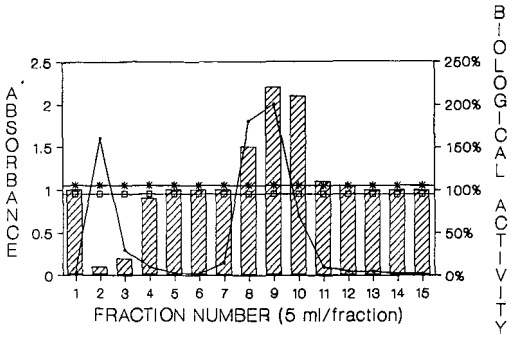

Fig. 2. Ion-exchange chromatography on a Dowex 50W-X8 (H^+) column of the dialysate of the leukocyte extract. Column, 100 mm × 10 mm I.D.; eluents, distilled water (25 ml) and then 1 *M* ammonium hydroxide; flow-rate, 1 ml/min; detection, 280 nm (UV-1 sensitivity, 2); recorder, 20 mV; chart speed, 2 mm/min; sample size, 2 units. The hatched areas represent the biological activity of the fractions; the area between ★——★ and □——□ corresponds to the PHA effects on human leukocytes without the addition of the examined fraction and is considered the reference value. ■——■ = absorbance.

a single cycle of a sine wave" (Users' Manual, Applied Biosystems), indicating that this sample was probably pure.

The immunostimulating activity from the Sephadex G-25 (Table II) or Dowex columns was directly purified by RP-HPLC. In the first HPLC purification step the biological activity was located in the region of the chromatogram between 8 and 10 min. When the collected material was rechromatographed on the same column, LeF activity was associated with the peak with a retention time of 8.89 min. By comparison with a synthetic sample of hypoxanthine, the natural LeF and the synthetic

TABLE I

RECOVERY OF THE IMMUNOSUPPRESSIVE ACTIVITY DURING THE PURIFICATION PROCEDURE

Gel chromatography on Sephadex G-25; conditions as Fig. 1. Gel chromatography on Sephadex G-15: column, 1000 mm × 16 mm I.D., stored at 15°C; eluent, 0.05 *M* ammonium hydrogencarbonate; flow-rate, 10 ml/h; detection, 280 nm. GP-HPLC: column, Spherogel TSK (SW 3000); eluent (isocratic): 0.01% acetic acid; flow-rate, 1 ml/min; detection, 220 nm. RP-HPLC (steps iv and v): column, LiChrosorb RP-18; eluent (isocratic), 0.05% trifluoroacetic acid; flow-rate, 1 ml/min; detection, 220 nm. RP-HPLC (step vi): column, μBondapak C_{18}; eluent (isocratic), 0.005 *M* ammonium acetate; flow-rate, 1 ml/min; detection, 220 nm. ND = Not determined.

Step	*Lyophilized material (LM) (g)*	*Proteins (P) (g)*	*Biological activity*		
			U	*U/LM*	*U/P*
Starting material	13.2	4.400	200	15	45
Sephadex G-25 (step i) active pool	6.7	0.960	200	30	208
Sephadex G-15 (step ii) active pool	1.6	0.155	100	62	645
GP-HPLC (step iii) active pool	0.2	0.015	50	250	3334
RP-HPLC (steps iv and v) active pool	0.01	0.003	50	5000	16 667
RP-HPLC (step vi) active pool	ND	0.0001	25	ND	250 000

TABLE II

RECOVERY OF ENHANCER ACTIVITY DURING THE PURIFICATION PROCEDURE

Gel chromatography on Sephadex G-25: conditions as Fig. 1. RP-HPLC: column, μBondapak C_{18}; eluent A, 0.1% trifluoroacetic acid; eluent B, acetonitrile–water (80:20) containing 0.085% trifluoroacetic acid; flow-rate, 1 ml/min; detection, 220 nm; gradient elution, 1–5 min, 100% eluent A; 6–20 min, 80% eluent B; 21–23 min, 80% eluent B; 24–26 min, 100% eluent B; 27–29 min, 100% eluent B; 30 min, 100% eluent A. The enhancer activity corresponds to the amount (μg) of lyophilized material necessary to produce a 50% increase in lymphocyte response to PHA at various concentrations of the material tested.

Step	*Lyophilized material (g)*	*Proteins (g)*	*Biological activity (μg)*
Starting material	13.2	4.400	516
Sephadex G-25 (step i) active pool	0.078	0.016	50
RP-HPLC (step ii) active pool	0.002	ND	2

purine derivative were unresolved in our HPLC system; in addition, they showed the same UV spectrum (with a maximum at 251 nm at pH 2.7) and identical derivatives. Their sensitivity to total acid hydrolysis and their amino acid analyses appeared to be very similar (see below).

The recoveries of the biological activities attributed to LsF and LeF are reported in Tables I and II.

Preliminary characterization

Enzymatic treatment. Both activities were completely resistant to treatment with pronase. The hypoxanthine-like molecule present in the LeF preparation and hypoxanthine were transformed by xanthine oxidase. The new UV-absorbing peak detected in the RP-HPLC elution profile showed (at pH 2.7) two characteristic maxima in the UV spectrum at 232 (or 231) and 286 nm. The biological activity attributed to LeF was resistant to XOD treatment.

Molecular weight determination. LsF and LeF were linked to chemical entities with molecular weights < 1000 dalton, as deduced by dialysis experiments. In fact, all the material capable of enhancing or inhibiting the response to PHA-treated lymphocytes was in the dialysate.

By size-exclusion HPLC the immunosuppressor showed a molecular weight of *ca.* 1000 dalton and the enhancer activity 300–600 dalton in accordance with the values obtained from chromatography on the Sephadex G-25 column calibrated with synthetic peptides. Nevertheless, these data should be treated with caution. In fact, the elution order of small molecules is not always correlated with their respective molecular weights, probably as a consequence (i) of aspecific interactions between the solutes and the stationary phase and (ii) of the effect of the mobile phase (with reference in particular to the pH values and salt concentrations) on the tertiary structure of the molecules.

The LsF sample obtained by GP-HPLC showed a specific biological activity five times greater than that after Sephadex G-15 (Table I); consequently, this purification step was included in our protocol. The LeF sample obtained in the same way did not show any increase in its specific activity.

Charge detection

The immunosuppressive activity was not retained on a cation exchanger (Dowex 50W-X8, H^+) (Fig. 2) and it co-eluted with an acid molecule, whereas the enhancer factor remained linked to Dowex 50W-X8, because of its basic character, and it was eluted with 1 *M* ammonia solution. The opposite results were obtained by chromatography on an anion-exchange resin (Dowex 1-X2, CH_3COO^-).

Amino acid analysis and primary structure determination

The deduced amino acid composition of the LsF sample with a specific activity of 250 000 A units/g protein after total acid hydrolysis, was 1 Asp, 1 Glu, 1 Ser, 1 Thr, 1 Ala, 1 Gly and 1 Arg. When LsF was analysed by the Edman degradation method, no phenylthiohydantoin derivative could be identified; this indicated that the N-terminus of the peptide material present in the sample was blocked.

The amino acid analysis of the hydrolysed sample of enhancer factor from RP-HPLC showed a peak of glycine and traces of lysine. We assume glycine to originate from the degradation of the hypoxanthine-like molecule present in the sample. In fact, an equivalent amount of hypoxanthine showed the same result, but in this instance the lysine peak was absent[a].

DISCUSSION

Two biological activities have been separated from the DLE obtained by human leukocytes, using gel filtration on a Sephadex G-25 column or ion-exchange chromatography on Dowex 50W-X8. These activities can be defined as antigen-independent, considering the bioassay employed[b]. The former possesses inhibitory properties and the latter enhancing activities (both *in vitro* and *in vivo*)[1–11]. The immunosuppressive agent appears to correspond to a chemical entity with an apparent molecular weight of *ca.* 1000 dalton.

The purification step on a Spherosyl SW 3000 column is useful for obtaining a product with an increase in the specific activity (417% with respect to TsF obtained by Sephadex G-15). Using 0.01% acetic acid as mobile phase, TsF elutes from the Spherosyl column before the peak due to a 0.1-*M* solution of sodium citrate (which is present in the crude starting material). Consequently, the detected biological activity is not due to an aspecific effect induced by salts.

The dificulty in purifying the immunosuppressive factor arises from its properties as follows: (i) LsF is very hydrophilic and does not bind tightly to a C_{18} reversed-phase column; therefore, elution was performed isocratically with water (containing 0.05% trifluoroacetic acid) or a solution of ammonium acetate; and (ii) the factor must be concentrated by lyophilization or evaporation because it is lost by either dialysis or ultrafiltration using the membranes with the smallest pore size commercially available. This is the main reason for the use of volatile buffers as mobile phases in our chromatographic systems.

---

[a] A different oxypurine analogue, xanthine, was resistant to hydrolysis with 6 *M* hydrochloric acid (110°C, 15 h).

[b] In the crude DLE there are also antigen-dependent activities able to transfer the delayed-type hypersensitivity (transfer factors).

LsF was purified 5500-fold; the recovery of the biological activity is 25% (Table I). It appears sufficiently pure as judged by the UV spectra of the single peak in RP-HPLC. Considering the behaviour in ion-exchange chromatography and RP-HPLC, the immunosuppressive activity is linked to an acid molecule with very hydrophilic character. A preliminary amino acid analysis has shown that the preparation contains peptidic material, with the N-terminus blocked; nevertheless, the biological activity is resistant to pronase treatment. This result does not exclude the possible identification of LsF with an amino acid chain. The tetrapeptide recently isolated by Lenfant *et al.*[9] and dermorphins[19] are examples of active natural peptides resistant to proteases treatment. LsF structure analyses, now in progress, will clarify this problem, which is unsolved at present.

The suppressive activity cannot be attributed to cell death, as about 90% of the cells in culture were still viable at the end of the incubation with the suppressive factor. Further, (i) the effect is reversible when cells incubated with the suppressive factor are washed before the addition of PHA and (ii) the factor has to be added within 24 h of the addition of PHA in order to manifest the suppressive effect, suggesting that its action is essentially restricted to the early phase of the cell cycle, after the activation process.

It has been reported[5,6] that the immunosuppressive factor is able to inhibit DNA and RNA synthesis on isolated nuclei and in a cell-free system. The effect on cells and on DNA polymerization is dose dependent.

The data suggest that this factor may act directly at the level of DNA polymerization processes with a mechanism similar to those of cyclosporin A[20], although an indirect route through intracellular mediators cannot be excluded[21].

The apparent molecular weight of the enhancer factor is the range 300–600 dalton. This activity coelutes from the chromatographic columns with the peak of a hypoxanthine-like molecule[a].

The enhancer activity is not due to hypoxanthine itself because (i) the synthetic purine derivative is inactive in the employed bioassays and (ii) the biological activity still remains after treatment of the LeF preparation with xanthine oxidase and it is not attributable to the new UV-absorbing peak detected in RP-HPLC. Consequently, we assume that LeF is linked to a compound that co-elutes with the hypoxanthine in our chromatographic system. LeF was purified only 258-fold (Table II) with a recovery of 4%, probably as a possible denaturation of the active molecule during the purification steps. Moreover, the loss of biological activity could also be due to the chromatographic separation of compounds that act synergistically in the crude material.

The biological activity of the LeF does not correspond to that attributed by Sihna *et al.*[7] to the peptides Tyr–Gly and Tyr–Gly–Gly, isolated from a fraction of DLE. In fact, the di- and tripeptides (which are identical with the amino terminal ends of enkephalins) are eluted later than the enhancer activity in the same chromatographic system[b]. Therefore, DLE contains enhancer compound(s) not yet com-

[a] The identification was made by comparison of the UV spectra, from the HPLC behaviours of the natural and synthetic samples and by their amino acid analyses after total acid hydrolysis.

[b] Analysis of *in vitro* PHA-induced transformation by Tyr–Gly, Tyr–Gly–Gly and the DLE shows that the two peptides are not responsible for all the enhancer activity of DLE. In fact, whereas DLE is able to increase the lymphocyte response by about 70%, the two peptides never increase it by more than 20%, at concentrations equivalent to those used for DLE.

pletely identified, acting on cells different from those on which the two enkephalin fragments exert their activity.

ACKNOWLEDGEMENTS

The authors express their gratitude to A. Henschen and W. Schaefer (Max Planck Institute for Biochemistry, Martinsried b. München, F.R.G.) for stimulating discussions and S. Silvestri (Sclavo, Research Centre, Siena, Italy) for constant encouragement and support in the course of this work.

REFERENCES

1 M. B. Zucker, I. R. Katz, G. J. Thorbecke, D. C. Milot and J. Holt, *Proc. Natl. Acad. Sci. U.S.A.*, 86 (1989) 7571.
2 M. H. Heulin, J. Rajoelina, A. Lasbennes, C. Geschier, F. Lamotte, J. Straczek, M. A. Gelot, M. Arthur, F. Belleville and P. Nabet, in J. F. Stoltz and C. Rivat (Editors), *Biotechnology of Plasma Proteins, Colloque INSERM*, Vol. 175, John Libbey Eurotext, London, Paris, 1989, p. 129.
3 A. A. Gottlieb, J. L. Farmer, C. T. Matzura, R. B. Hester and J. S. Rosenberg, *J. Immunol.*, 132 (1984) 256.
4 H. S. Lawrence and W. Borkowsky, *Immunol. Lett.*, 21 (1989) 75.
5 V. E. M. Rosso di San Secondo, G. Lugaro, G. Sirchia, *J. Exp. Pathol.*, 3 (1987) 425.
6 V. E. M. Rosso di San Secondo, G. Lugaro, F. Tedesco, G. Bernasconi and G. Sirchia, *Basic Appl. Histochem.*, 31 (1987) 325.
7 S. K. Sihna, C. R. Sizemore and A. A. Gottlieb, *Bio/Technology*, 6 (1988) 810.
8 F. Mazerolies, A. Durandy, D. Piatier-Tonneau, D. Charron, L. Montagnier, C. Auffray and A. Fischer, *Cell*, 55 (1988) 497.
9 M. Lenfant, J. Wdzieczak-Bakala, E. Guittet, J. C. Prome, D. Sotty and E. Frindel, *Proc. Natl. Acad. Sci. U.S.A.*, 86 (1989) 779.
10 J. C. Cornelius and S. J. Norman, *J. Immunol.*, 141 (1988) 2174.
11 V. E. M. Rosso di S. Secondo, G. Lugaro, F. Tedesco, A. M. Isetta, P. C. Montecucchi and G. Sirchia, presented at the *XXVI World Congress of the International College of Surgeons, Milan, July 3–9, 1988*, Lecture Book 1, p. 32.
12 J. F. Reymond and P. J. Grob, *Vox Sang.*, 29 (1975) 338.
13 V. E. M. Rosso di San Secondo, P. L. Meroni, C. Fortis and F. Tedesco, *J. Immunol.*, 122 (1979) 1658.
14 G. Sirchia, F. Mercuriali, C. Pizzi, V. E. M. Rossi di San Secondo, P. Borzini and A. Aniasi, *Transplant. Proc.*, 14 (1982) 263.
15 F. Heinz and S. Reckel, in H. U. Bergmeyer (Editor), *Methods of Enzymatic Analysis*, Vol. III, 3rd ed., Verlag Chemie, Weinheim, Deerfield Beach, FL, Basle, 1983, p. 210.
16 P. C. Montecucchi, A. M. Lazzarini, L. Barbieri, F. Stirpe, M. Soria and D. Lappi, *Int. J. Pept. Protein Res.*, 33 (1989) 263.
17 R. M. Kamp, *Amino Acid Analysis*, Knauer Users' Manual.
18 H. Lowry, N. J. Rosebrough, A. Lewis Farr and R. J. Randall, *J. Biol. Chem.*, 193 (1951) 265.
19 P. C. Montecucchi, R. de Castiglione, S. Piani, L. Gozzini and V. Erspamer, *Int. J. Pept. Protein Res.*, 17 (1981) 275.
20 C. Brack, I. W. Mattai, J. Gautschi and S. Cammisuli, *Exp. Cell Res.*, 151 (1984) 314.
21 N. Talal, *Transplant. Proc.*, 20 Suppl. 4 (1988) 11.

Journal of Chromatography, 512 (1990) 149–155
Elsevier Science Publishers B.V., Amsterdam

CHROMSYMP. 1798

Oligosaccharide mapping of therapeutic glycoproteins by high-pH anion-exchange high-performance liquid chromatography

R. KUMARASAMY
Protein Analysis Section, Physical and Analytical Chemisry R & D, Schering-Plough Corporation, 2000 Galloping Hill Road, Kenilworth, NJ 07033 (U.S.A.)

ABSTRACT

The Asn-linked oligosaccharides of four different glycoproteins were cleaved by N-glycanase and analysed by high-pH anion-exchange high-performance liquid chromatography coupled with a pulsed amperometric detector. Each glycoprotein produced unique sets of oligosaccharides. Sialic acid-containing oligosaccharide peaks were readily identified by their large decrease in retention time following neuraminidase digestion. The use of this HPLC technique for tentatively identifying unknown oligosaccharide peaks by retention time comparison with reference standards and for monitoring the consistency of N-glycosylation of recombinant DNA-derived glycoprotein was demonstrated.

INTRODUCTION

Analysis of carbohydrate-mediated heterogeneity of therapeutic glycoproteins is important in clinical evaluation since oligosaccharides may influence biological activity, pharmacokinetics and immunogenicity of proteins[1]. High-performance liquid chromatography (HPLC) techniques for the separation of oligosaccharides, in general, offer speed and resolution, but sensitive detection often requires pre- or post-column derivatization[2–7]. Recently it has been shown that an accurate and sensitive analysis of monosaccharides and oligosaccharides including the glycoprotein-derived structures could be performed without derivatization using high-pH anion-exchange HPLC coupled with pulsed amperometric detection (PAD)[8–13]. N-Glycanase is known to cleave a wide range of Asn-linked oligosaccharides with bi- tri- and tetraantennary chains[7,14–16]. This enzymatic hydrolysis has been shown to be a simple and practical alternative to hydrazinolysis for obtaining N-linked oligosaccharide with an intact di-N-acetylchitobiose on the reducing end[7,14]. In this report, we investigated the utility of this HPLC technique for comparative analysis of N-glycanase-released oligosaccharides from different glycoproteins and for monitoring consistency of glycosylation of recombinant DNA (rDNA)-derived glycoprotein produced in mammalian cell culture.

0021-9673/90/$03.50

EXPERIMENTAL

Materials

The glycoproteins, human serum transferrin, human immunoglobulin G (IgG), human α_1-antitrypsin, N-acetylneuraminic acid (NeuAc), neuraminidase (type x) were obtained from Sigma (St. Louis, MO, U.S.A.). N-Glycanase was purchased from Genzyme (Boston, MA, U.S.A.). rDNA-derived glycoprotein used in this study was human interleukin-4 expressed in Chinese hamster ovary cells. NMR-verified glycoprotein-derived oligosaccharide standards, asialo diantennary, asialo triantennary, sialylated diantennary and sialylated triantennary oligosaccharides (structures I to IV in Fig. 1) were from Dionex (Sunnyvale, CA, U.S.A.) and from Biocarb (Lund, Sweden). 50% (w/w) sodium hydroxide solution was from Fisher Scientific (Rockville, MD, U.S.A.) and sodium acetate was reagent grade from J. T. Baker (Philipsburg, NJ, U.S.A.). Eluents and buffers were prepared with distilled water further purified on a Millipore water system (Milli-Q) or HPLC-grade water from J. T. Baker.

Methods

Enzymatic removal of N-linked oligosaccharides from glycoproteins. Asn-linked oligosaccharides were released by incubating the glycoproteins (100–500 μg) with 0.01–0.05 units of N-glycanase in 50–200 μl of 50 m*M* sodium phosphate buffer, pH

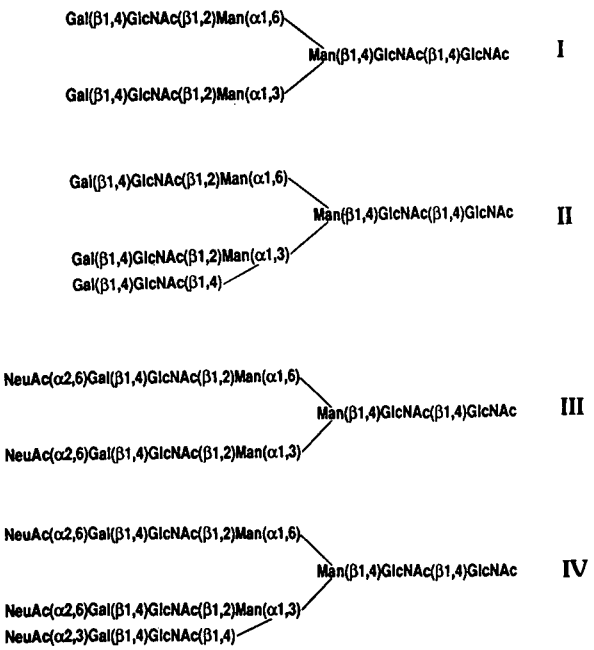

Fig. 1. Oligosaccharide standards used in HPLC analysis, NMR-verified, glycoprotein-derived oligosaccharide standards. (I) Asialo diantennary, (II) asialo triantennary, (III) sialylated diantennary, (IV) sialylated triantennary.

8.3 at 37°C for 18–36 h. In some cases, the glycoproteins were denatured by heating at 100°C for 2–5 min in the sodium phosphate buffer containing 0.1% sodium dodecyl sulfate (SDS) and 0.1% mercaptoethanol.

Deglycosylation of glycoproteins was evaluated by SDS-polyacrylamide gel electrophoresis and by binding to concanavalin A-peroxidase[14]. Following N-glycanase digestion, deglycosylated protein was removed by precipitation with three volumes of ice-cold ethanol and centrifuged at 12 000 *g* for 15 min at room temperature. The supernatant containing oligosaccharides was evaporated to dryness in a Speed-Vac and redissolved in 100–200 μl of distilled water and filtered using Millipore HV filters.

Removal of sialic acids from glycoproteins and N-glycanase-released oligosaccharides was performed by enzymatic digestion with *Clostridium perfringens* neuraminidase (0.05 units) in 50 μl of 50 m*M* sodium acetate buffer (pH 5.5) at 37°C for 4 h[17].

Chromatography. The HPLC system used for the analysis of oligosaccharides was Dionex Bio-LC set up with a pellicular anion-exchange column (Carbopac, PA-1; 250 × 4.6 mm I.D.) and a pulsed amperometric detector (Model PAD 2, Dionex). The Dionex eluent degas module was used to sparge and pressurize the eluents. For a linear gradient, eluent A was 100 m*M* sodium hydroxide and eluent B contained 100 m*M* sodium hydroxide and 200 m*M* sodium acetate. Samples were injected manually using a 50-μl-volume sample loop. Oligosaccharides were separated by a linear gradient elution with eluent A and B over the period of 40 min. A Carbopac (PA) guard column (25 × 3 mm) was used in all experiments. Sodium hydroxide (500 m*M*) was added to the post-column effluent via a mixing tee at 0.2 ml/min using a Dionex Auto-Ion reagent pump. Detection of oligosaccharides was accomplished by PAD with a gold working electrode[8,9]. The following pulse potential and durations were used E_1 = 0.05 V (t_1 = 360 ms), E_2 0.80V (t_2 = 120 ms), E_3 = −0.60V (t_3 = 420 ms). The response time of the PAD system was set to 3 s.

RESULTS AND DISCUSSION

Four different glycoproteins were digested with N-glycanase and the released oligosaccharides were separated by high-pH anion-exchange HPLC using 0–200 m*M* sodium acetate gradient in 100 m*M* sodium hydroxide. Fig. 2 shows the N-linked oligosaccharide profile of human IgG, human serum transferrin, human α_1-antitrypsin, and rDNA-derived glycoprotein produced in cell culture. Human IgG oligosaccharides were eluted as a cluster of multiple peaks (Fig. 2A). Both α_1-antitrypsin and transferrin produced one major peak each with identical retention time along with several minor peaks while rDNA-derived glycoprotein showed two major peaks (Fig. 2A). Under the conditions used, *ca.* 70–90% of N-linked oligosaccharides in glycoproteins were released by N-glycanase digestion as estimated by the carbohydrate analysis of deglycosylated protein and in the case of transferrin and rDNA-derived glycoprotein, by blotting with concanavalin A-peroxidase following SDS-gel electrophoresis[14]. Denaturation of glycoproteins with either SDS or mercaptoethanol did not enhance the release of oligosaccharides by N-glycanase. Comparison of elution profile of oligosaccharides in human serum transferrin and α_1-antitrypsin suggests that both may contain similar oligosaccharide structures (Fig. 2A). Both

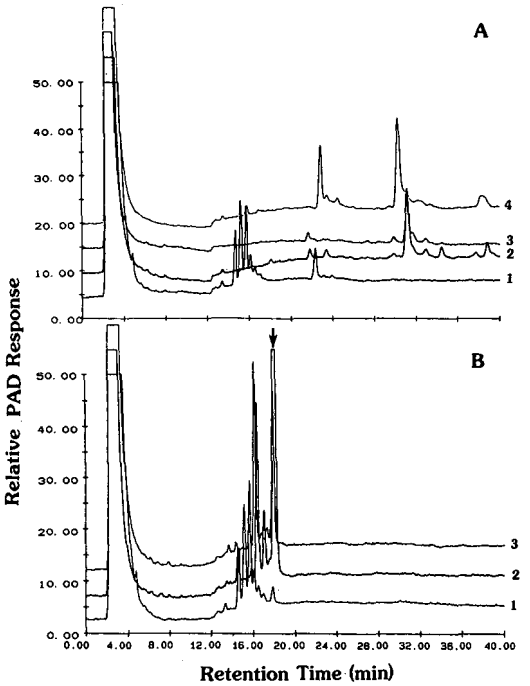

Fig. 2. HPLC separation of N-linked oligosaccharides released from glycoproteins by digestion with N-glycanase alone (A), followed by neuraminidase treatment (B). Oligosaccharide profiles were from (1) 150 μg of human IgG, (2) 100 μg of human α_1-antitrypsin, (3) 100 μg of human transferrin, (4) 25 μg of rDNA-derived glycoprotein. Oligosaccharides were separated on an anion-exchange column with a linear gradient of 0–200 m*M* sodium acetate in 100 m*M* sodium hydroxide over a period of 40 min and detected by PAD. The arrow indicates the elution position of NeuAc standard (1 nmol).

glycoproteins were shown previously by various analytical techniques[18,19] to carry two oligosaccharide chains each with common sialylated diantennary structures, and α_1-antitrypsin, in addition to two diantennary oligosaccharides, also carried an oligosaccharide with triantennary structure[18]. rDNA-derived glycoprotein contained predominantly diantennary structure, but unlike α_1-antitrypsin and serum transferrin, its oligosaccharides carried fucose residues[20].

In order to find out sialylated oligosaccharides in the chromatographic profile in Fig. 2A, N-glycanase released oligosaccharides were digested with neuraminidase and rechromatographed. Neuraminidase treatment converted most of the oligosaccharide peaks in α_1-antitrypsin, transferrin and rDNA-derived glycoprotein (data not shown) into faster eluting species while the majority of oligosaccharides in IgG remained unaffected (Fig. 2B). The release of NeuAc in the digest was confirmed by coelution experiments with authentic NeuAc standard. Under similar chromatographic conditions, glycoprotein-derived sialylated oligosaccharide standards were well separated from their asialo forms (Figs. 2 and 3). These experiments confirm the earlier finding that the oligosaccharides with sialic acid moieties interact strongly with the column and elute progressively later[12]. This HPLC technique has been shown to

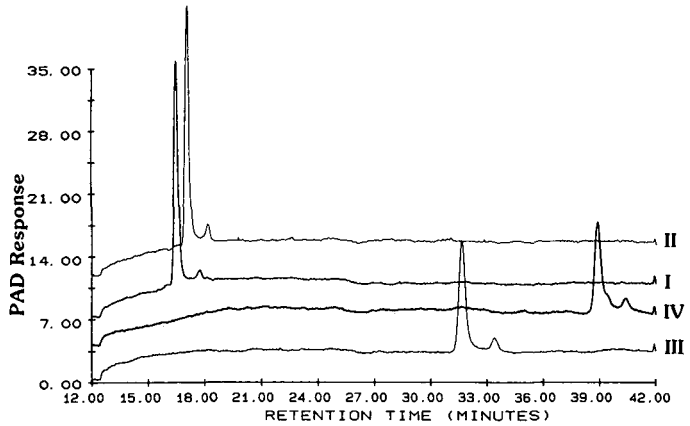

Fig. 3. Separation of NMR-verified oligosaccharide standards in Fig. 1 (5 nmol each) by anion-exchange HPLC under identical conditions as in Fig. 2.

separate positional isomers in both sialylated and neutral oligosaccharide structures[11,12]. In the case of neutral oligosaccharides, separation appears to be dependent on the relative acidity of sugar hydroxyl groups at alkaline pH and also their accessibility to the column matrix[11–13]. The molar response factor for desialylated oligosaccharides in Fig. 3 was found to be two-fold higher compared to sialylated oligosaccharides. Such differences in the electrochemical responses between synthetic neutral and sialylated oligosaccharides were observed previously[12,13]. During quantitative analysis of monosaccharides, molar response for aminosugars was found to be 20–30% higher than that obtained for neutral sugars such as glucose[10]. Hence, for

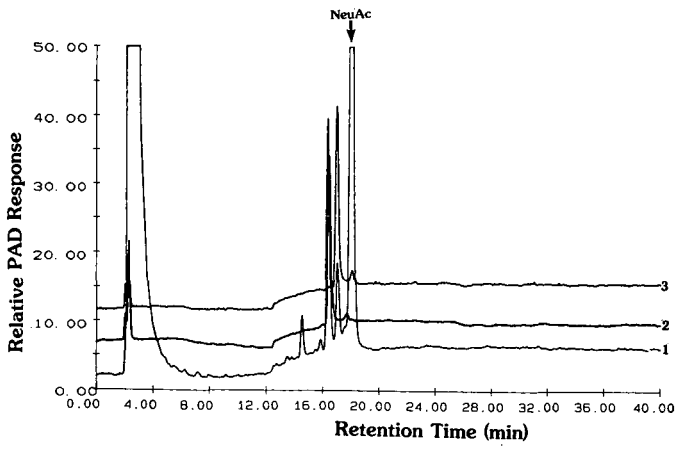

Fig. 4. HPLC analysis of oligosaccharides of α_1-antitrypsin and oligosaccharide standards. (1) Oligosaccharides from α_1-antitrypsin following digestion with neuraminidase and N-glycanase, (2) and (3) NMR-verified asialo biantennary and asialo triantennary standards (5 nmol each), respectively. Arrow indicates the elution position of NeuAc standard. Chromatographic conditions as in Fig. 2.

quantitative analysis of oligosaccharides in glycoprotein, response curves for each standard oligosaccharide must be obtained.

The ultility of the HPLC method for identifying unknown peaks in the sample was investigated using α_1-antitrypsin as a model glycoprotein with NMR-verified oligosaccharide standards. α_1-Antitrypsin contains three N-glycosylation sites carrying mostly two sialylated biantennary and one sialylated triantennary chains[18]. α_1-Antitrypsin was digested with neuraminidase and N-glycanase, sequentially and chromatographed. Fig. 4 shows the elution profile of N-glycanase-released, desialylated oligosaccharides of α_1-antitrypsin. Four major chromatographic peaks were seen in the enzyme digest (Fig. 4); three of them coeluted with asialo biantennary, asialo triantennary and NeuAc standards, respectively (Fig. 4). The identity of the fastest eluting peak was not known (Fig. 4). The relative proportion of biantennary and triantennary chains in α_1-antitrypsin as calculated from peak areas in Fig. 4. corresponded to the relative number of these structures present in the molecule[18], suggesting that this technique can be used to tentatively identify unknown oligosaccharides in the glycoproteins with previously characterized authentic standards. However, post-column analysis of oligosaccharide peaks by techniques such as fast atom bombardment mass spectrometry and high-field NMR spectroscopy may be needed to confirm unknown oligosaccharide structure since structural isomers and other unrelated oligosaccharides might have identical chromatographic retention time.

The elution time characteristics of N-glycanase released oligosaccharides from glycoproteins in Fig. 2 was highly reproducible. This led us to investigate whether this HPLC technique could be used to monitor the consistency of glycosylation of rDNA-derived therapeutic glycoprotein produced in cell culture. This glycoprotein was shown previously to carry Asn-linked oligosaccharides at a single glycosylation site in the molecule and contained predominantly fucosylated, mono/disialylated, biantennary structures[20]. Fig. 5 shows N-glycanase-released oligosaccharide profile of five

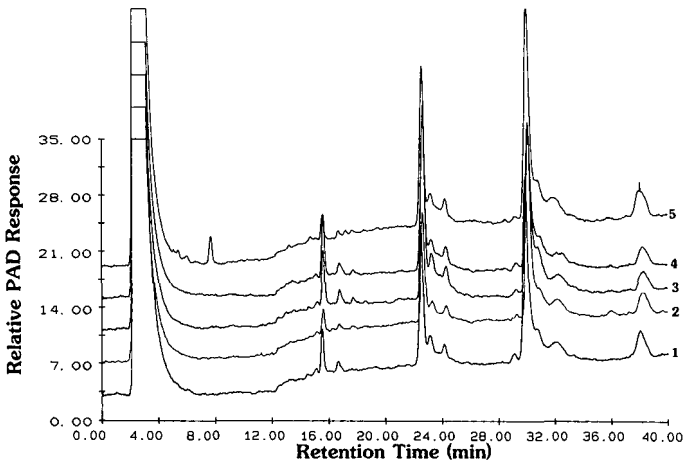

Fig. 5. Anion-exchange HPLC analysis of N-glycanase-released oligosaccharides from rDNA-derived glycoprotein batches. Approximately 25 μg of glycoprotein from each batch (1–5) following N-glycanase digestion was analysed under identical conditions as in Fig. 2.

different batches of glycoproteins. The enzymatic digestion released more than 90% of carbohydrate in each of five glycoprotein batches as estimated by SDS-gel electrophoresis. There are two oligosaccharide peaks and several minor species (Fig. 5). Qualitatively, the chromatographic profiles of five batches are similar (Fig. 5) except for batch number five which showed an additional peak (Fig. 5). Once the structure of the oligosaccharide in the glycoprotein is established, the consistency and identity of N-linked oligosaccharides in the glycoprotein can be monitored by comparing the chromatographic profile of N-glycanase digest of production batches *versus* the reference standard chromatographed in parallel. The structures of oligosaccharides are heterogenous even at single glycosylation sites on the polypeptide chain. HPLC techniques are increasingly being used to analyse the microheterogeneity of oligosaccharides in glycoproteins[3,7,13,15]. The chromatographic selectivity and specificity of the high-pH anion-exchange HPLC with pulsed amperometry offer a rapid and sensitive analysis of oligosaccharide distribution in glycoproteins.

ACKNOWLEDGEMENTS

The author thanks Dr. J. Bausch for his support for this investigation and Laurel Gray for typing the manuscript.

REFERENCES

1 T. W. Rademacher, R. B. Parekh and R. A. Dwek, *Ann. Rev. Biochem.*, 57 (1988) 785.
2 S. Hase, T. Ikenaka and Y. Matsushima, *J. Biochem.*, 90 (1981) 407.
3 S. Honda, *Anal. Biochem.*, 140 (1984) 1.
4 W. T. Wang, N. C. LeDone, B. Ackerman and C. C. Sweeley, *Anal. Biochem.*, 141 (1984) 366.
5 W. M. Blanken, M. L. E. Bergh, P. L. Koppen and D. H. van den Eijnden, *Anal. Biochem.*, 145 (1985) 322.
6 G. R. Her, S. Santikarn, V. N. Reinhold and J. C. Williams, *J. Carbohydr. Chem.*, 6 (1987) 129.
7 N. Tomiya, M. Kurono, H. Ishihara, S. Tejima, S. Endo, Y. Arata and N. Takahashi, *Anal. Biochem.*, 163 (1987) 489.
8 R. D. Rocklin and C. A. Pohl, *J. Liq. Chromatogr.*, 6 (1983) 1577.
9 S. Hughes and D. C. Johnson, *Anal. Chim. Acta*, 149 (1983) 1.
10 M. R. Hardy, R. R. Towensend and Y. C. Lee, *Anal. Biochem.*, 170 (1988) 54.
11 M. R. Hardy and R. R. Townsend, *Proc. Natl. Acad. Sci. U.S.A.*, 85 (1988) 3289.
12 R. R. Townsend, M. R. Hardy, O. Hindgaul and Y. C. Lee, *Anal. Biochem.*, 174 (1988) 459.
13 R. R. Townsend, M. R. Hardy, D. A. Cumming, J. P. Carver and B. Bendiak, *Anal. Biochem.*, 182 (1989) 1.
14 S. Hirani, R. J. Bernasconi and J. R. Rasmussen, *Anal. Biochem.*, 162 (1987) 485.
15 E. D. Green, R. M. Brodbeck and J. U. Baenziger, *Anal. Biochem.*, 167 (1987) 62.
16 F. Maley, R. B. Trimble, A. L. Tarentino and T. H. Plummer, Jr., *Anal. Biochem.*, 180 (1989) 195.
17 R. Kumarasamy and H. A. Blough, *Arch. Biochem. Biophys.*, 236 (1985) 693.
18 L. Vaughan and R. Carrell, *Biochem. Int.*, 2 (1981) 461.
19 G. Spik, B. Bayard, B. Fournet, G. Strecker, S. Bouquelet and J. Montreuil, *FEBS Lett.*, 50 (1975) 296.
20 G. R. Her, A. Tsarbopoulos, R. Kumarasamy, P. P. Das, B. N. Pramanik, T. L. Nagabhushan, P. P. Trotta and S. H. Tindall, *Abstracts of the Third Symposium of Protein Society, Seattle, WA, 1989*, F 172.

Journal of Chromatography, 512 (1990) 157–163
Elsevier Science Publishers B.V., Amsterdam

CHROMSYMP. 1879

Isolation of isoproteins from monoclonal antibodies and recombinant proteins by chromatofocusing

ALOIS JUNGBAUER*, CHRISTA TAUER, ELISABETH WENISCH, KAROLA UHL, JUTTA BRUNNER, MARTIN PURTSCHER, FRANZ STEINDL and ANDREA BUCHACHER

Institute of Applied Microbiology, University of Agriculture and Forestry and Biotechnology, Peter Jordanstrasse 82, A-1190 Vienna (Austria)

ABSTRACT

A fast protein liquid chromatographic method for the preparative separation of the various isoproteins is described. Highly purified human monoclonal antibodies, recombinant human superoxide dismutase and human superoxide dismutase from erythrocytes were used as starting material. The isoproteins were separated by chromatofocusing on Mono P columns. A very narrow pH gradient was applied to achieve complete separation of the isoproteins. The prepurification steps and the pretreatment of the samples to achieve optimum resolution are described in detail. The method is also applicable to extremely basic monoclonal antibodies (p*I* = 9). The successful separation was checked by isoelectric focusing in immobilized pH gradients (Immobilines). The future of these methods is discussed, because for many different biochemical and biophysical investigations pure and homogeneous isoproteins are necessary.

INTRODUCTION

Monoclonal antibodies[1–3] and many enzymes[4] exhibit strong microheterogeneity. Up to ten different isoproteins are observed by isoelectric focusing (IEF) in a monoclonal antibody sample. To investigate the microheterogeneity and the reasons for this biological phenomenon, the proteins must be separated into the various isoproteins. Owing to the separating power required, only a few methods are applicable for this separation problem. The most popular method is preparative isoelectric focusing[1]. The isoproteins are easily resolved. After staining part of the gel, the proteins must be extracted from the gel and often the yield of the extraction process is very low. Ion-exchange chromatography is also applicable to this separation problem, but its resolving power is inadequate for the complete separation of isoproteins with similar isoelectric points.

Chromatofocusing, first described by Slyterman and co-workers[5,6], separates proteins in order of their isoelectric points (p*I*). The column is filled with a weak ion exchanger. On tritrating the ion-exchange matrix with an amphoteric buffer, a linear

0021-9673/90/$03.50

pH gradient is formed in the column. Focusing takes place and results in peak sharpening. The samples are eluted in high concentration and are highly resolved.

A human monoclonal antibody exhibiting as very high p*I* and a native and recombinant superoxide dismutase (SOD) exhibiting a low p*I* were used as model substances. All three model substances displayed a characteristic microheterogeneity pattern in IEF. The human monoclonal antibody and the SOD were highly purified. This material was used for chromatofocusing on Mono P columns. The successful separation was demonstrated by IEF.

EXPERIMENTAL

Starting material

As starting material human monoclonal antibodies were prepared as described by Jungbauer *et al.*[7]; human recombinant SOD and human SOD from erythrocytes, as described by Weselake *et al.*[8], were used. The proteins were highly purified, with at least 99% purity. The samples were lyophilized from volatile buffers (10 m*M* ammonium formate, pH 8.0).

Chromatofocusing

Mono P chromatofocusing columns (Mono HR 5/20 and HR 10/30) from Pharmacia (Uppsala, Sweden) were used. The columns were connected to a fast protein liquid chromatographic (FPLC) system and chromatography was performed at flow-rates of 0.1 ml/min (HR 5/20) and 1.0 ml/min (HR 10/30).

For chromatofocusing of the human monoclonal antibody, 25 m*M* diethylenamine (pH 9.5) was used as the starting buffer and Polybuffer 96 (pH 7.0) (Pharmacia) as the elution buffer. For chromatofocusing of the native SOD, 25 m*M* histidine buffer (pH 6.2) was used as the starting buffer and Polybuffer 74 (pH 4.0) as the elution buffer. For chromatofocusing of recombinant SOD, 25 m*M* histidine buffer (pH 6.2) was used as the starting buffer and Polybuffer 74 (pH 5.0) as the elution buffer. The buffers were prepared according the manufacturer's recommendations (Pharmacia). In all experiments the gradient volume was at least 10 total column volumes. A linear gradient was applied.

Additionally, the FPLC system was equiped with a pH ion monitor (LKB, Bromma, Sweden) to record the pH gradient during elution.

Isoelectric focusing

IEF was performed in Immobiline gels. At low pH, ready-to-use Immobiline dry plates (Pharmacia LKB, Uppsala, Sweden) were used. At high pH, a gel was cast, as described by Wenisch *et al.*[1] using immobilized pH gradients (Immobiline II). The eluted fractions were applied directly to the gel and focused. The gel was stained with Coommassie Blue R 250.

RESULTS

To cover the high and low pH ranges, different proteins were chosen. A human monoclonal antibody exhibiting p*I* between 9.0 and 9.7 was chosen for the basic range and SOD for the acidic range. Highly purified proteins were used as starting

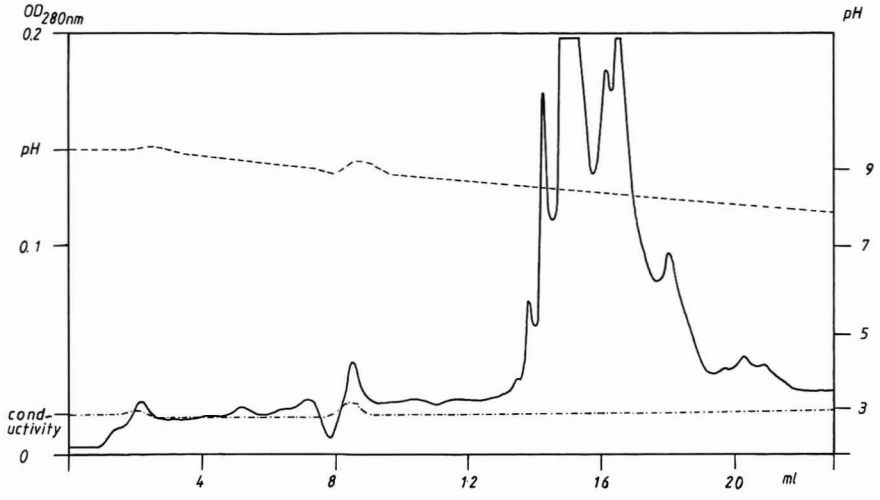

Fig. 1. Separation of isoproteins of a human monoclonal antibody by chromatofocusing on a Mono P column (HR 5/20). Sample: 1 mg of lyophilized monoclonal antibody dissolved in 500 μl of equilibration buffer and loaded onto a 3.4-ml column. Elution was effected with a linear pH gradient from 9.5 to 7.0 at a flow-rate of 0.1 ml/min.

material. A purity of more than 99% was determined by sodium dodecyl sulphate–polyacrylamide gel electrophoresis and silver staining. The highly purified material was chromatographed in a volatile buffer (10 m*M* ammonium formate, pH 8.0) on Sephadex G-25 and lyophilized. The lyophilized material was dissolved in equilibration buffer at a concentration of 4 mg/ml. The sample was injected into the equili-

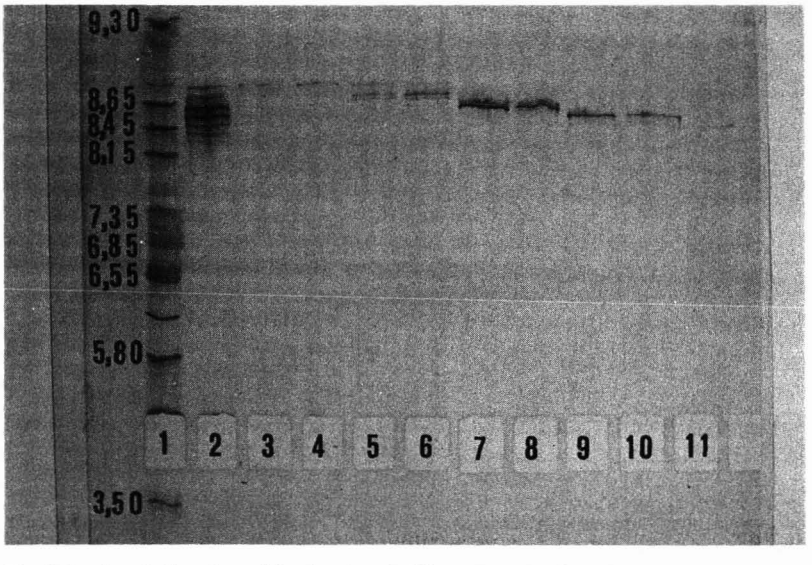

Fig. 2. Isoelectric focusing of the fractions in Fig. 1. Samples: lane 1 = p*I* marker 3–10; lane 2 = starting material (human monoclonal antibody); lanes 3–11 = isoprotein fractions.

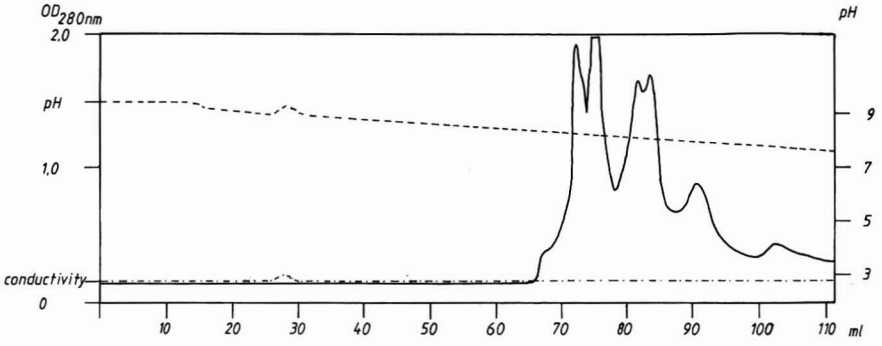

Fig. 3. Separation of isoproteins in a human monoclonal antibody by chromatofocusing on a Mono P column (HR 10/30). Sample: 10 mg of lyophilized human monoclonal antibody dissolved in 2 ml of equilibration buffer and loaded onto a 23-ml column. Elution was effected with a linear pH gradient from 9.5 to 7.0 at a flow-rate of 1 ml/min.

brated and prefocused column. To obtain optimum resolution the linear pH gradient should last for 10–15 column volumes. The isoproteins were eluted by the pH gradient according to their p*I* values. The formation of the gradient was observed with an on-line pH monitor. The peaks were fractionated and the separation was checked by IEF on immobilized pH gradients.

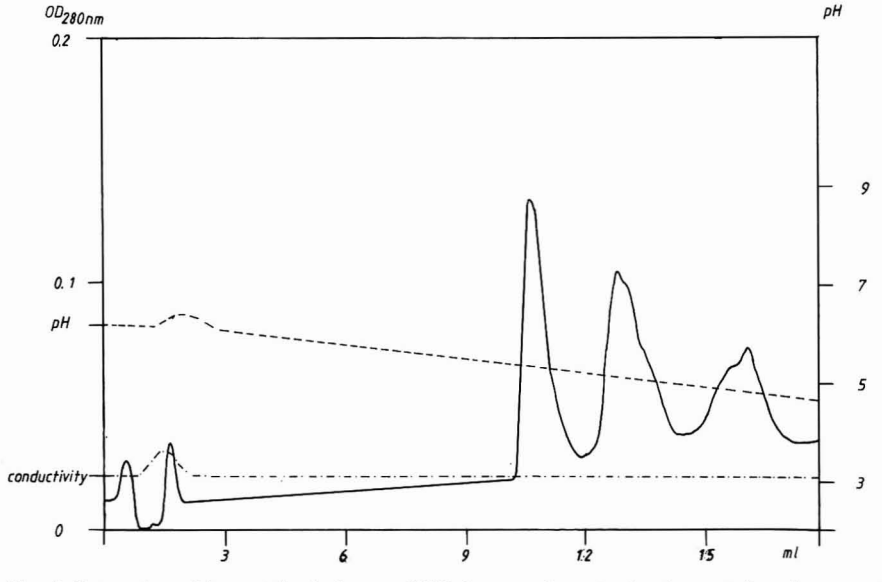

Fig. 4. Separation of isoproteins in human SOD from erythrocytes by chromatofocusing on a Mono P column (HR 5/20). Sample: 1 mg of lyophilized human SOD from erythrocytes dissolved in 500 μl of equilibration buffer and loaded onto a 3.4-ml column. Elution was effected with a linear pH gradient from 6.2 to 4.0 at a flow-rate of 0.1 ml/min.

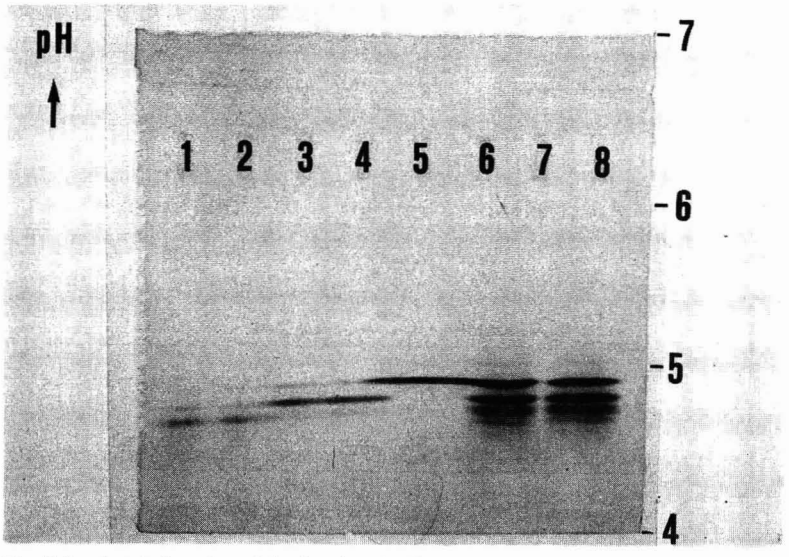

Fig. 5. Isoelectric focusing of the fractions in Fig. 4. Samples: lanes 1–6 = isoprotein fractions; lanes 7 and 8 = starting material (human SOD from erythrocytes).

Focusing of the human monoclonal antibody

The human monoclonal antibody was chromatofocused on two columns, an analytical column and a preparative column. The isoproteins could be resolved on both columns (Figs. 1–3). The number of peaks corresponded to the protein bands in IEF. As a baseline separation could not be obtained, a few fractions were contaminat-

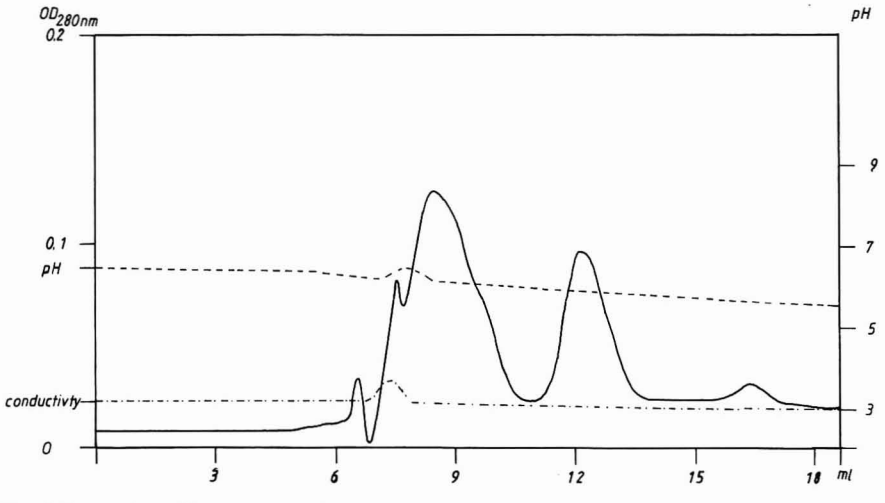

Fig. 6. Separation of isoproteins of human recombinant SOD by chromatofocusing on a Mono P column (HR 5/20). Sample: 1 mg of recombinant human SOD dissolved in 500 μl of equilibration buffer and loaded onto a 3.4-ml column. Elution was effected with a linear pH gradient from 6.2 to 5.0 at a flow-rate of 0.1 ml/min.

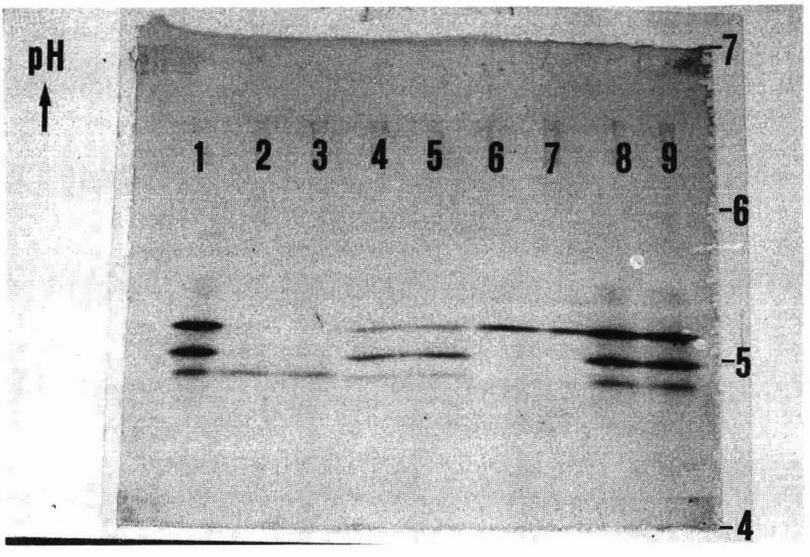

Fig. 7. Isoelectric focusing of the fractions in Fig. 6. Samples: lanes 1, 8 and 9 = starting material (recombinant human SOD); lanes 2–7 = isoprotein fractions.

ed with neighbouring isoproteins. However, the ratio of isoproteins in the antibody samples could easily be determined from the chromatogram.

Focusing of the SOD

Human SOD from erythrocytes and recombinant human SOD were chromatofocused on an analytical column. The native and recombinant SOD differ in the first amino acid, the native enzyme being acetylated.[9] This difference results in a p*I* difference of *ca.* 0.5 pH unit. Both enzymes could be separated into the three isoenzymes and a baseline separation could be achieved (Figs. 4 and 5). IEF also indicated that the separation was nearly complete (Figs. 6 and 7). Arai *et al.*[4] observed this heterogeneity in a highly purified SOD sample by slab gel IEF.

DISCUSSION

Regulations for recombinant proteins and proteins from transformed animal cells to be used as injectable therapeutics require extensive quality control. The potency, purity, identity and consistency must be proved[10,11]. The isoprotein pattern is a valuable method for testing the consistency of different production lots. Generally, IEF is used for this purpose, but there is no exact correlation between concentration and intensity of the stained protein. Therefore, an exact quantitative comparison of different lots is not possible. In qualitative comparisons, chromatographic differences in band patterns can easily be detected. There is an exact relationship between protein concentration in the eluent and detector response. Using various statistical models, the areas of partially overlapping peaks can be calculated with acceptable accuracy. A quantitative measurement of the isoprotein composition of a protein displaying microheterogeneity can be carried out.

For further investigations, such as peptide mapping or the determination of carbohydrate moieties, the separation of the isoproteins is essential. In this paper an attempt has been made to show that chromatofocusing could be an alternative to conventional preparative IEF[12–14]. The various isoproteins could be partially separated, as shown by IEF.

ACKNOWLEDGEMENTS

This project was supported by the Innovations- und Technologiefond of the Federal Ministry of Science and Research (project number 7/62) and CL-Pharma (Austria).

REFERENCES

1 E. Wenisch, A. Jungbauer, C. Tauer, M. Reiter, G. Gruber, F. Steindl and H. Katinger, *J. Biochem. Biophys. Methods.*, 18 (1989) 309.
2 R. G. Hamilton, M. Roebber, C. B. Reimer and L. S. Rodkey, *Hybridoma*, 6 (1987) 206.
3 A. Jungbauer, F. Unterluggauer, K. Uhl, A. Buchacher, F. Steindl, D. Pettauer and E. Wenisch, *Biotechnol. Bioeng.*, 32 (1988) 326.
4 K. Arai, S. Iizuka, A. Makita, K. Oikawa and N. Taniguchi, *J. Immunol. Methods*, 91 (1986) 139.
5 L. A. Æ. Slyterman and O. Eglersma, *J. Chromatogr.*, 150 (1978) 17.
6 L. A. Æ. Slyterman and J. Wijdenes, *J. Chromatogr.*, 150 (1978) 31.
7 A. Jungbauer, C. Tauer, E. Wenisch, F. Steindl, M. Purtscher, M. Reiter, F. Unterluggauer, A. Buchacher, K. Uhl and H. Katinger, *J. Biochem. Biophys. Methods*, 19 (1989) 223.
8 R. Weselake, S. L. Chesney, A. Petkau and A. D. Friesen, *Anal. Biochem.*, 155 (1986) 193.
9 D. Barra, F. Martini, J. Bannister, M. Schinina, G. Rotilio, W. Bannister and F. Bossa, *Biochemistry*, 19 (1980) 2310.
10 Guidelines on the production and quality control of monoclonal antibodies of murine origin intended for use in man, *Trends Biotechnol.*, 6 (1988) G5.
11 Guidelines on the production and quality control of medicinal products derived by recombinant DNA technology, *Trends Biotechnol.*, 5 (1988) G1.
12 B. Radola, *Biochim. Biophys. Acta*, 386 (1974) 181.
13 B. Radola, *Biochim. Biophys. Acta*, 295 (1973) 412.
14 G. Ebers, G. Rice and H. Armstrong, *J. Immunol Methods*, 37 (1980) 315.

Journal of Chromatography, 512 (1990) 165–176
Elsevier Science Publishers B.V., Amsterdam

CHROMSYMP. 1877

Separation of fragments from human serum albumin and its charged variants by reversed-phase and cation-exchange high-performance liquid chromatography

PAOLO IADAROLA*, MARIA CARLA ZAPPONI, LORENZO MINCHIOTTI, MARIA LAURA MELONI, MONICA GALLIANO and GIUSEPPINA FERRI
Dipartimento di Biochimica, Università di Pavia, Via Taramelli 3B, Pavia (Italy)

ABSTRACT

Reversed-phase high-performance liquid chromatography (RP-HPLC) and ion-exchange chromatography on poly(2-sulphoethylaspartamide)–silica (SCX) were compared as alternative approaches in characterizing charged genetic variants of human serum albumin. The chromatographic behaviour of cyanogen bromide (CNBr), tryptic and V8 protease digests from normal and mutant albumins were examined. The results showed that substituted site-containing CNBr fragments are successfully resolved by RP-HPLC; in most instances SCX and RP-HPLC are equally adequate in identifying the modified tryptic peptides from CNBr fragments; although generally useful, SCX chromatography is specifically needed in all instances where amino acid replacement is occurring in a small hydrophilic tryptic fragment and choosing *Staphylococcus aureus* V8 protease instead of tryptic digestion is advantageous.

INTRODUCTION

More than 100 genetic variants of human serum albumin (HSA) have been identified by routine clinical electrophoresis or during population surveys and classified as slow or fast with respect to the electrophoretic behaviour of the normal protein[1,2]. The structural characterization of these variants has recently been stimulated by interest in protein genetics and evolution and by the knowledge of the complete protein[3] and genomic[4] sequence of HSA. The availability of high-resolution chromatographic techniques has so far allowed the identification of the molecular defects causing more than twenty different abnormal albumins (alloalbumins)[5–10].

A procedure suggested by Takahashi *et al.*[11] consists in the peptide mapping of the whole HSA tryptic digest through an automated tandem high-performance liquid chromatographic (HPLC) system, which is a combination of anion-exchange (IE) and reversed-phase (RP) column chromatography. Although applied to the structural studies of some variants, this method seems inadequate for identifying the substitution

0021-9673/90/$03.50

site in all mutants, as only 80% of tryptic peptides can be properly characterized[11]. Another method is based on the separation of all the seven fragments obtained after cyanogen bromide (CNBr) digestion of the whole protein, by high-performance size-exclusion chromatography (HP-SEC) combined with peptide mapping of the tryptic digest of the modified fragment by RP-HPLC[7]. The resolving power of SEC seems poor, however, and is probably limited either by the similarity in size of the cleavage products or by their interaction with the matrix.

The strategy we have developed also involves cleavage of the fully alkylated albumins by CNBr, but the isolation of CNBr produced fragments is achieved by RP-HPLC[12]. Despite the large number and size of the components (ranging between 31 and 175 residues), the complete resolution of the CNBr digest is easily accomplished. Moreover, the fragment containing the amino acid substitution may be immediately identified as the retention time of most fragments on the RP support used can be correlated with their amino acid composition[13]. Sequential analysis of the abnormal peptide isolated from the tryptic digest of the modified CNBr fragment allowed us to elucidate the molecular lesion of all the variants studied in our laboratory[5,8,9]. However, the separation by RP-HPLC of tryptic peptides was sometimes difficult, especially when small and extremely hydrophilic peptides are involved. In these cases RP-HPLC is not sufficient to resolve these peptides, so an alternative chromatographic method is needed that provides the required selectivity.

A relatively new material, poly(2-sulphoethylaspartamide)–silica, has been reported to possess good selectivity and efficiency in the purification of peptides as a strong cation-exchange (SCX) packing material[14]. As suggested by Alpert and Andrews[15], retention of peptides on this material is proportional to the number of basic residues; moreover, the selectivity can be affected by addition of various levels of organic solvents to the mobile phases. This material thus displays a selectivity complementary to that of reversed phases and has also been successfully used to resolve peptides containing modified amino acids[14,15].

This paper describes the application of cation-exchange chromatography to the resolution of tryptic and *Staphylococcus aureus* V8 protease digests obtained from CNBr fragments of normal and abnormal albumins. Also, data are presented which show that SCX chromatography in some instances may be a unique means for the unambiguous identification of the molecular defect of HSA charged variants. The results obtained may indicate general utility of the sulphoethylaspartamide sorbent for the routine characterization of proteins containing charged amino acid substituents.

EXPERIMENTAL

Apparatus

The chromatographic system consisted of two Waters Assoc. (Milford, MA, U.S.A.) Model M 6000 pumps equipped with one M 680 automated gradient controller and a U6K sampling valve with a 2-ml sample loop. A Jasco (Japan Spectroscopic, Tokyo, Japan) Uvidec 100-III variable-wavelength UV detector was used to monitor the column effluent at 220 nm. Chromatograms were recorded with an Omni Scribe chart recorder (Houston Instruments, Austin, TX, U.S.A.).

Columns

Peptide mixtures were separated on RP- and SCX-HPLC columns. For RP-HPLC the following columns were used: an Aquapore RP-300 (10 μm) column (25.4 cm × 7 mm I.D.) from Brownlee Labs. (Santa Clara, CA, U.S.A.), a μBondapak C_{18} (10 μm, 100 Å pore size) column (30 cm × 3.9 mm I.D.) from Waters Assoc. and a Vydac (10 μm, 300 Å pore size) column (25 cm × 4.6 mm I.D.) from Separation Group (Hesperia, CA, U.S.A.). For cation-exchange chromatography a poly-(2-sulphoethylaspartamide) column (20 cm × 4.6 mm I.D.) was used, purchased from Nest Group (Southborough, MA, U.S.A.).

Chemicals

Acetonitrile of HPLC grade was obtained from Carlo Erba (Milan, Italy) and filtered through a 0.45-μm Millipore filter prior to use. Doubly distilled water was purified by passage through an UHQ Elgastat purification system (Elga, High Wycombe, U.K.). Trifluoroacetic acid (TFA) of sequenal grade was purchased from LKB (Bromma, Sweden) and CNBr from Sigma (St. Louis, MO, U.S.A.). The reagents used for automated sequential analyses were supplied by Beckman (Palo Alto, CA, U.S.A.). All other reagents were of analytical-reagent grade and were obtained from Carlo Erba. Trypsin [L-1-tosylamido-2-phenylethylchloromethyl ketone (TPCK-treated] was supplied by Worthington Biochemicals (Freehold, NY, U.S.A.) and *Staphylococcus aureus* V8 protease by Boehringer (Mannheim, F.R.G.).

Sample preparation

CNBr fragments from HSA and its charged variants (Roma, Verona, Castel di Sangro) were obtained as previously described[12]. Digestion of these peptides with TPCK-treated trypsin was performed according to Swenson *et al.*[16]. *Staphylococcus aureus* V8 protease digestion was carried out on CNBr VI from normal and Castel di Sangro albumins for 24 h at room temperature under conditions in which this enzyme is specific for glutamic acid residues (enzyme-to-substrate ratio, 1:20, w/w; 0.05 *M* NH_4HCO_3, pH 7.8)[17].

Identification and nomenclature of peptides

All peptides were identified by their amino acid composition or amino acid sequence. Amino acid analyses were carried out by ion-exchange chromatography with post-column ninhydrin derivatization according to Moore[18] on a Cromakon 500 automatic analyser (Kontron, Zurich, Switzerland). The amino acid sequences were determined by liquid-phase sequence degradation on a Beckman System 890 M instrument using the fast-protein Quadrol program with precycled Polybrene. Amino acid derivatives were identified by RP-HPLC on a Beckman Ultrasphere ODS column as described by Pucci *et al.*[19].

Tryptic and V8 protease peptides are designated T and S, respectively, and numbered consecutively in their predicted order in the sequence[20].

RESULTS AND DISCUSSION

In our previous structural studies of HSA mutants, both recognition and preparative isolation of the substituted-site-containing fragments have been successfully

obtained by comparatively mapping on RP-HPLC CNBr digests from S-carboxymethylated normal and variant albumins[12,13]. Unlike all other cases, identification of the molecular defect of a new variant named Castel di Sangro has required a modification of our strategy. Castel di Sangro is a fast-migrating albumin which arises from a point mutation occurring at position 536 (Lys → Glu), in CNBr VI (residues 447–548)[21].

Under the conditions that we proposed previously, amino acid substitution appears to be related to the retention time of the abnormal fragment on RP-HPLC[13]; in accordance with the loss of a hydrophilic Lys residue, fragment CNBr VI from Castel di Sangro albumin is eluted 2 min later than the normal counterpart, partially overlapping CNBr III fragment. However, its resolution was obtained by slightly changing the gradient slope, as shown in Fig. 1. Identification of the recovered fragments was checked by N-terminal and amino acid analyses; the amino acid composition of Castel di Sangro CNBr VI, showing a decrease of one lysine and the presence of an additional glutamic acid residue, confirms this as the variant fragment.

Purified CNBr VI from the normal and Castel di Sangro albumins were then cleaved with trypsin and the digests were mapped by RP-HPLC on an Aquapore RP-300 column. This procedure was ineffective in identifying the variant peptide; as shown in Fig. 2A and B, the elution patterns of the two digests are indistinguishable. Analyses of the recovered material showed that only seven of the fourteen peptides

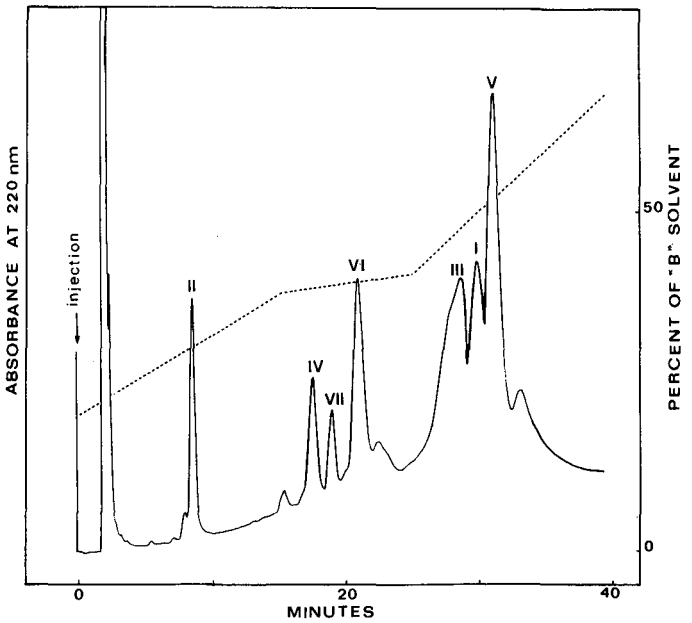

Fig. 1. Elution pattern of CNBr fragments of Castel di Sangro albumin. The digest was dissolved in 0.05% TFA (pH 2.3) (solvent A); samples of 100 μl (corresponding to *ca.* 10 nmol of protein) were injected into a Vydac C_{18} (10 μm, 300 Å pore size) column (25 cm × 4.6 mm I.D.), equilibrated with 80% solvent A and 20% acetonitrile–2-propanol (2:1, v/v) containing 0.05% TFA (solvent B). Elution was performed at room temperature using the gradient indicated by the dashed line. Flow-rate, 2 ml/min; absorbance range, 0.64 full-scale.

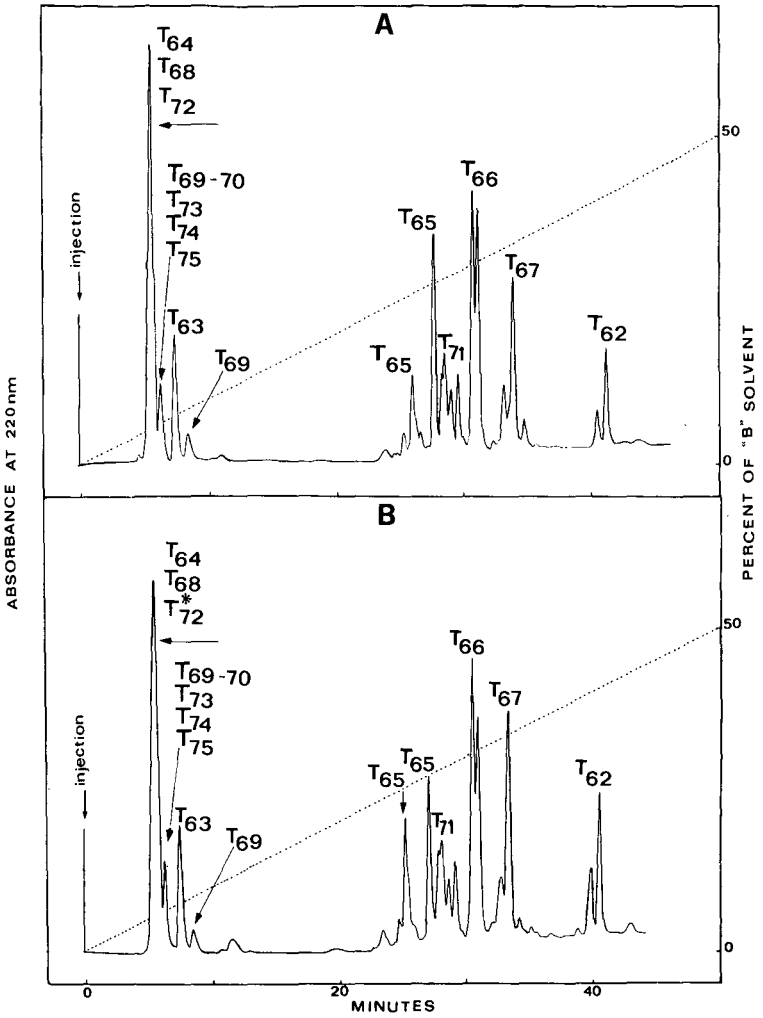

Fig. 2. Comparative tryptic peptide maps of CNBr VI from normal human serum albumin (A) and Castel di Sangro variant (B). 5 nmol of each CNBr digest were chromatographed on an Aquapore RP-300 (10 μm) column (25 cm × 7.5 mm I.D.) under the following conditions: eluent A, 0.05% aqueous TFA; eluent B, 0.05% TFA in acetonitrile. Elution was performed at room temperature and at a flow-rate of 1.5 ml/min using the gradient indicated by the dashed line. Absorbance range, 0.64 full-scale. T = tryptic peptides. Peptides are designated by arabic numerals following the predicted order in the albumin sequence[20]. Abnormal peptides are marked with asterisks. The presence of two peptides with the same amino acid composition is due to different extents of cysteine alkylation.

expected on the basis of the known sequence of CNBr VI (Table I) are obtained as homogeneous species, all the others, including the modified one, T^*_{72}, being eluted unresolved under the first two peaks. The use of a μBondapak C_{18} column and of supports with short-chain bonded phases did not substantially improve the resolution of the small fragments.

TABLE I

AMINO ACID SEQUENCE OF TRYPTIC FRAGMENTS FROM CNBr VI OF HSA

T_{62}:	P–C–A–E–D–Y–L–S–V–V–L–N–Q–L–C–V–L–H–E–K (450, 460)
T_{63}:	T–P–V–S–D–R (470)
T_{64}:	V–T–K
T_{65}:	C–C–T–E–S–L–V–N–R (480)
T_{66}:	R–P–C–F–S–A–L–E–V–D–E–T–Y–V–P–K (490, 500)
T_{67}:	E–F–N–A–E–T–F–T–F–H–A–D–I–C–T–L–S–E–K (510)
T_{68}:	E–R (520)
T_{69}:	Q–I–K
T_{70}:	K
T_{71}:	Q–T–A–L–V–E–L–V–K (530)
T_{72}:	H–K[a]–P–K
T_{73}:	A–T–K (540)
T_{74}:	E–Q–L–K
T_{75}:	A–V–M

[a] Lys 536 is substituted by Glu in Castel di Sangro variant.

As an alternative method to achieve purification of the peptide mixture, we submitted the two tryptic digests to ion-exchange chromatography. The strong cation exchanger poly(sulphoethylaspartamide) was chosen; in agreement with its excellent selectivity[14,15], this sorbent allowed the identification of the variant peptide. Profiles obtained by SCX chromatography are compared in Fig. 3A and B. Normal and CNBr VI tryptic patterns show the same number of peaks, and all but one eluted with similar retention times. The shift of T^*_{72} relative to T_{72} indicates the former to be the variant peptide. This was confirmed by sequence analysis of the two fragments: T^*_{72} gave the sequence H–E–P–K, instead of H–K–P–K as determined for the normal fragment T_{72}. The elution order was as expected on the basis of the nominal net positive charge, T_{72} (+4) being eluted about 8 min later than the modified T^*_{72} (+3).

Owing to their similarity in net positive charge, many of the tryptic peptides from

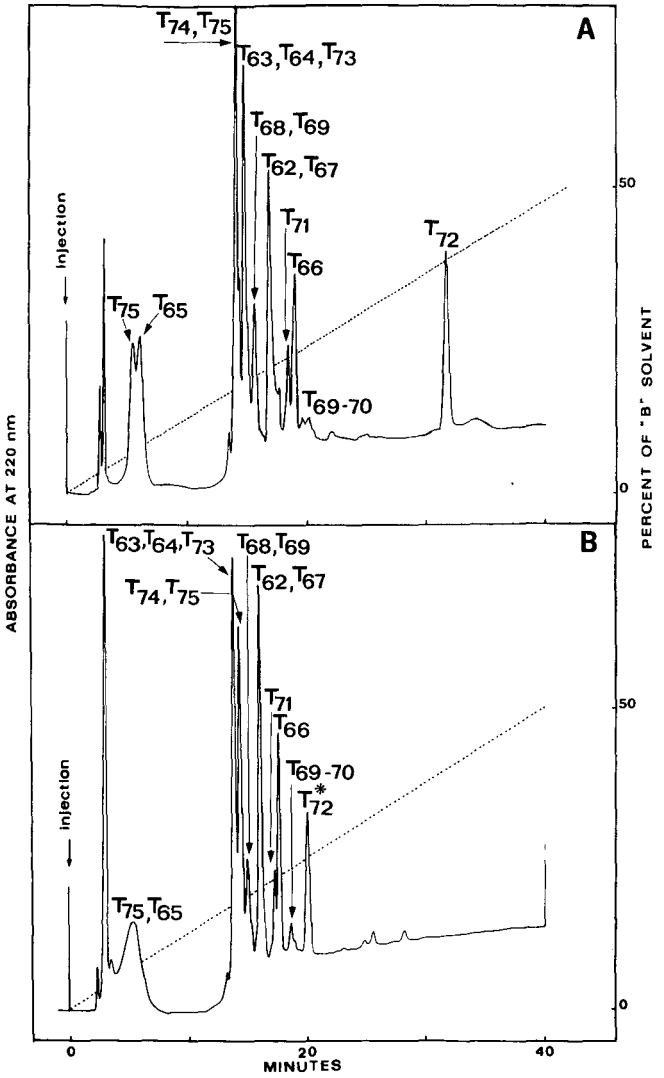

Fig. 3. Comparative tryptic peptide maps of CNBr VI from normal (A) and Castel di Sangro (B) human serum albumins. 5 nmol of each CNBr digest were chromatographed on a poly(sulphoethylaspartamide) SCX column (20 cm × 4.6 mm I.D.) under the following conditions: eluent A, 5 m*M* potassium phosphate (pH 3.0)–acetonitrile (75:25); eluent B, 5 m*M* potassium phosphate +0.5 *M* KCl (pH 3.0)–acetonitrile (75:25). Elution was performed at room temperature and at a flow-rate of 1 ml/min using the gradient indicated by the dashed line. Absorbance range, 0.64 full-scale. The presence of two peptides with the same amino acid composition is due to homoserine–homoserine lactone equilibrium.

CNBr VI are coeluted, but by examining the elution profiles of Fig. 3 it is of interest to stress the different selectivity of the exchanger toward fragments of the same size and net positive charge. Tetrapeptides Q–I–K–K (T_{69-70}) and H–E–P–K (T^*_{72}) are in fact eluted under different peaks, the first about 1 min earlier than the second, thus suggesting a positional effect of charged residues.

Although reliable identification and excellent resolution of the substituted peptides was obtained, SCX chromatography was inadequate in resolving many of the remaining components of the tryptic mixture. The failure to obtain all tryptic peptides in homogeneous form prompted us to experiment with a different enzymatic cleavage of CNBr VI, in order to characterize the complete primary structure of the variant fragment.

Both recognition of the abnormal fragment and complete resolution of the mixture components were achieved by submitting *S. aureus* V8 protease digests of normal and variant CNBr VI to SCX chromatography. Fig. 4 shows the elution

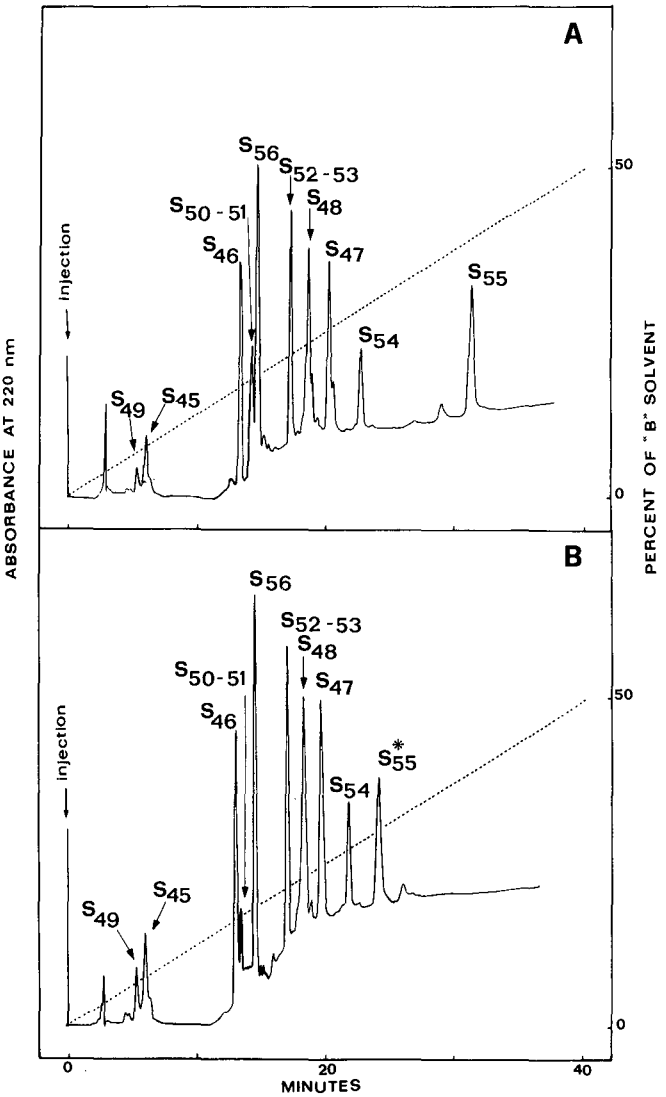

Fig. 4. Comparative peptide maps of *Staphylococcus aureus* V8 protease digests from CNBr VI of normal (A) and Castel di Sangro (B) human serum albumins. HPLC was performed with the stationary and mobile phases described in Fig. 3.

patterns of the *S. aureus* fragments. The total number of *S. aureus* fragments is not modified by Lys 536 → Glu replacement because the Glu 536–Pro 537 bond is not cleaved by *S. aureus* V8 protease. All the fragments expected on the basis of the listed sequence (Table II) are recovered in a homogeneous form. Peptides, indicated as S_{50-51} and S_{52-53} in Fig. 4, result from lack of the cleavage at the bonds Glu 501–Phe 502 and Glu 518–Lys 519, respectively.

TABLE II

AMINO ACID SEQUENCE OF *S. AUREUS* V_8 PROTEASE FRAGMENTS FROM CNBr VI OF HSA

	450
S_{45}:	P–C–A–E
	460
S_{46}:	D–Y–L–S–V–V–L–N–Q–L–C–V–L–H–E
	470
S_{47}:	K–T–P–V–S–D–R–V–T–K–C–C–T–E
480	490
S_{48}:	S–L–V–N–R–R–P–C–F–S–A–L–E
S_{49}:	V–D–E
	500
S_{50}:	T–Y–V–P–K–E
S_{51}:	F–N–A–E
	510
S_{52}:	T–F–T–F–H–A–D–I–C–T–L–S–E
520	
S_{53}:	K–E
	530
S_{54}:	R–Q–I–K–K–Q–T–A–L–V–E
	540
S_{55}:	L–V–K–H–K[a]–P–K–A–T–K–E
S_{56}:	Q–L–K–A–V–M

[a] Lys 536 is substituted by Glu in Castel di Sangro variant.

Because of the difference in their net positive charge, the substituted fragment S^*_{55} (+5) is eluted about 8 min earlier than the normal S_{55} (+6). The elution order of S_{46} (13 min) and S_{56} (15 min), both possessing the same net positive charge (+2), can be explained by the presence in the former of three additional acidic groups which, as previously suggested[14,15], may affect the chromatographic behaviour. However, the difference in additional acidic residues[15] (four *versus* two) does not prevent fragment S_{47} from being eluted later than S_{48}. Again, the positional effect of charged residues seems clear, as the presence of two adjacent arginine residues in S_{48} may cause it to interact loosely with the exchanger.

The greater selectivity of SCX chromatography for *S. aureus* than for tryptic fragments is obviously dependent on a more favourable distribution of positive charge in the former species. In fact, because of the enzyme specificity, most of the fragments originating from tryptic cleavage share the same positive net charge at pH 3, being distinct in two main families, the larger one consisting of the peptides which have the N-terminal and the C-terminal basic residue (Arg or Lys) as positively charged groups, and the second containing those which possess additional positive charges, namely

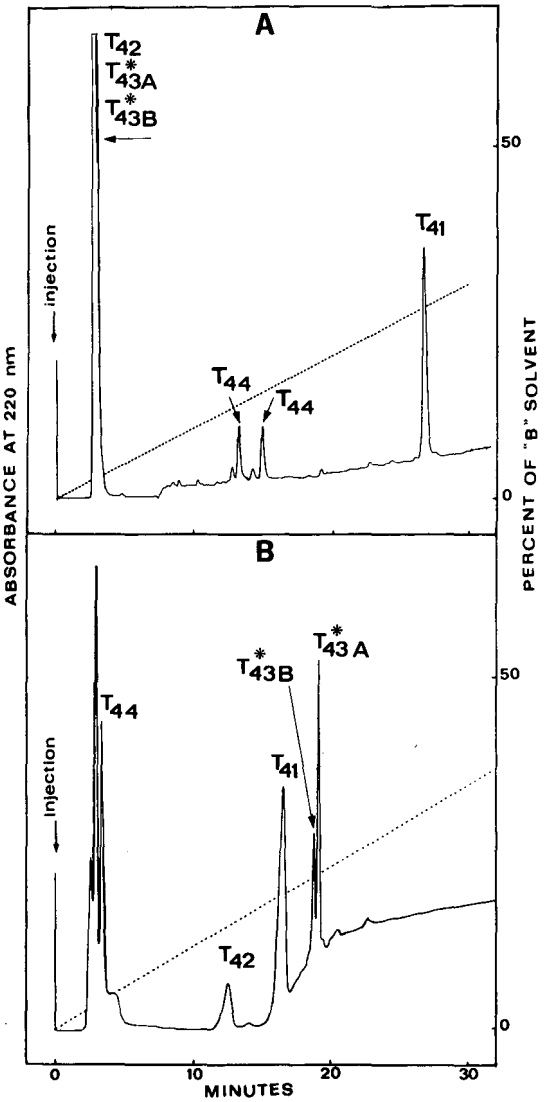

Fig. 5. (A) RP-HPLC profile of CNBr IV tryptic digest from Roma albumin. Column and chromatographic conditions as in Fig. 2. The presence of two peptides with the same amino acid composition is due to homoserine–homoserine lactone equilibrium. (B) SCX-HPLC profile of CNBr IV tryptic digest from Roma albumin. Column and mobile phase as in Fig. 3.

hystidine residues or Lys/Arg–Pro uncleaved bonds. On the other hand, the number and distribution of arginine and lysine residues through the sequence, resulting in a greater charge differentiation of *S. aureus* fragments, make them suitable to interact more selectively with the exchanger.

SCX chromatography has also been used to resolve tryptic digests from CNBr IV and CNBr VII of two slow variants, namely Roma (Glu 321 → Lys)[8] and Verona (Glu 570 → Lys)[5]. Because of the amino acid replacement, the total number of the expected tryptic peptides from the variant fragments is increased in both instances by one unit (five from Roma CNBr IV and seven from Verona CNBr VII). Both RP and SCX chromatography were equally efficient in resolving the tryptic digest of Verona CNBr VII, giving all peptides in a homogeneous form. Three modified fragments were formed because of the known incomplete cleavage at the Lys–Glu bonds; all of these are separately eluted in both RP and SCX chromatography (data not shown).

As a consequence of the Glu 321 → Lys replacement occurring in Roma CNBr IV, two small peptides are formed: the tetrapeptide N–Y–A–K (T^*_{43A}) and the dipeptide A–K (T^*_{43B}). Both fragments were resolved by RP-HPLC on a μBondapak C_{18} column, T^*_{43B} being eluted as a shoulder of the signal peak[8]. As shown in Fig. 5, the two modified fragments and T_{42}, the tetrapeptide D–V–C–K, were coeluted in the void volume when the tryptic digest was passed through an Aquapore RP-300 column (Fig. 5A). As expected, SCX chromatography allowed the separation of these fragments, and also that of all the other components of the tryptic mixture (Fig. 5B).

The results reported here lead to the conclusion that in all instances, characterization of variant tryptic fragments from charged mutants of human serum albumin may be usefully approached through SCX chromatography. In fact, ion-exchange chromatography may offer an additional advantage over the RP mode in identifying substituted-site-containing fragments, as all of these differ in charge from the normal counterpart. In most instances, as in Roma and Verona mutants, RP and SCX chromatography may be equally selective and efficient: however, situations may arise where, as with Castel di Sangro albumin, ion-exchange chromatography should be the method of choice for isolating the modified fragments. The demonstrated utility of poly(sulphoethylaspartamide) in characterizing serum albumin charged variants suggests a more general use of this sorbent in structural studies of abnormal proteins.

ACKNOWLEDGEMENTS

This work was supported by grants from the Ministero della Pubblica Istruzione (Rome, Italy). The authors thank Dr. M. Frezza for amino acid analyses and Mr. A. Mortara for skilful technical assistance.

REFERENCES

1 L. M. Schell and B. S. Blumberg, in V. M. Rosenoer, M Oratz and M. A. Rothschild (Editors), *Albumin: Structure, Function and Uses*, Pergamon, New York, 1977, pp. 113–141.
2 L. R. Weitkamp, E. M. McDermid, J. V. Neel, J. M. Fine, C. Petrini, L. Bonazzi, V. Ortali, F. Porta, R. Tanis, D. J. Harris, T. Peters, G. Ruffini and E. Johnson, *Ann. Hum. Genet.*, 37 (1973) 219.
3 J. R. Brown and P. Shockley, in P. Jost and O. H. Griffith (Editors), *Lipid–Protein Interactions*, Vol. 1, Wiley, New York, 1982, pp. 25–68.
4 P. P. Minghetti, D. E. Ruffner, W. J. Kuang, O. E. Dennison, J. W. Hawkins, W. G. Beattie and A. Dugaiczyk, *J. Biol. Chem.*, 261 (1986) 6747.

5 L. Minchiotti, M. Galliano, P. Iadarola, M. Stoppini, G. Ferri and A. A. Castellani, *Biochim. Biophys. Acta*, 916 (1987) 411.
6 N. Takahashi, Y. Takahashi, T. Isobe, F. W. Putnam, M. Fujita, C. Satoh and J. V. Neel, *Proc. Natl. Acad. Sci. U.S.A.*, 84 (1987) 8001.
7 O. Sugita, N. Endo, T. Yamada, M. Yakata and S. Odani, *Clin. Chim. Acta*, 164 (1987) 251.
8 M. Galliano, L. Minchiotti, P. Iadarola, M. C. Zapponi, G. Ferri and A. A. Castellani, *FEBS Lett.*, 233 (1988) 100.
9 L. Minchiotti, M. Galliano, P. Iadarola, M. L. Meloni, G. Ferri, F. Porta and A. A. Castellani, *J. Biol. Chem.*, 264 (1989) 3385.
10 K. Arai, J. Madison, K. Huss, N. Ishioka, C. Satoh, M. Fujita, J. V. Neel, I. Sakurabayashi and F. W. Putnam, *Proc. Natl. Acad. Sci. U.S.A.*, 86 (1989) 6092.
11 N. Takahashi, Y. Takahashi, N. Ishioka, B. S. Blumberg, F. W. Putnam, *J. Chromatogr.*, 359 (1986) 181.
12 P. Iadarola, G. Ferri, M. Galliano, L. Minchiotti and M. C. Zapponi, *J. Chromatogr.*, 298 (1984) 336.
13 P. Iadarola, M. C. Zapponi, M. Stoppini, M. L. Meloni, L. Minchiotti, M. Galliano and G. Ferri, *J. Chromatogr.*, 443 (1988) 317.
14 D. L. Crimmins, J. Gorka, R. S. Thoma and B. D. Schwartz, *J. Chromatogr.*, 443 (1988) 63.
15 A. J. Alpert and P. C. Andrews, *J. Chromatogr.*, 443 (1988) 85.
16 R. P. Swenson, C. H. Williams, Jr., V. Massey, S. Ronchi, L. Minchiotti, M. Galliano and B. Curti, *J. Biol. Chem.*, 257 (1982) 8817.
17 G. R. Drapeau, *Methods Enzymol.*, 47 (1977) 189.
18 S. Moore, *J. Biol. Chem.*, 243 (1968) 6212.
19 P. Pucci, G. Sannia and G. Marino, *J. Chromatogr.*, 270 (1983) 371.
20 K. Huss, J. Madison, N. Ishioka, N. Takahashi, K. Arai and F. W. Putnam, *Proc. Natl. Acad. Sci. U.S.A.*, 85 (1988) 6692.
21 L. Minchiotti, M. Galliano, P. Iadarola, E. Zepponi and G. Ferri, *Biochim. Biophys. Acta*, in press.

Journal of Chromatography, 512 (1990) 177–188
Elsevier Science Publishers B.V., Amsterdam

CHROMSYMP. 1845

Immobilized metal ion affinity chromatography for the purification of *Fel d* I, a cat major allergen, from a house-dust extract

J.-P. DANDEU*, J. RABILLON, M.-J. BELTRAND, M. LUX, R. DUVAL and B. DAVID
Unité d'Immuno-Allergie, Institut Pasteur, Paris (France)

ABSTRACT

Although the efficient isolation and purification of the major feline allergen have previously been achieved using polyclonal or monoclonal antibody affinity chromatography, these methods lead to a relatively low yield of pure allergen. Therefore, attempts were made to establish a process involving ion-exchange chromatography followed by immobilized metal ion affinity chromatography. Although slightly more time consuming than the immunological methods, it gives a higher yield. It consists of four steps. From a crude house-dust extract, precipitation of a *Fel d* I enriched fraction is obtained by addition of acetone. After dissolution in water, exhaustive dialysis takes place against a citric acid solution to eliminate divalent metal ions. This gives the whole house-dust extract. Then partial isolation and purification are obtained by ammonium sulfate precipitation. The resulting precipitate is dissolved in and dialysed against water to remove ammonium salts. This partially purified house-dust extract can be submitted to chromatography on an anion exchanger and then on a copper ion charged chelating gel. All steps of the isolation and purification were controlled by immunochemical analyses using a crossed immuno-electrophoretic method and enzyme-linked immunoadsorbent assays. The HD75 Q2 Cu2 fraction so obtained can be considered to be a pure cat major allergen *Fel d* I preparation. Its homogeneity was demonstrated using physico-chemical and immunochemical methods.

INTRODUCTION

Allergens are immunogenic and antigenic molecules, generally proteins or glycoproteins, which give rise to an immunoglobulin E (IgE) antibody response in genetically predisposed humans. Most of these allergens have a very high biological potency and an apparent molecular weight (MW) between 10 000 and 50 000 daltons.

The isolation and purification of allergens, whatever their origin, house-dust mites, pollens, moulds or foods, are currently performed in many laboratories. The availability of a pure allergen from any source and a knowledge of its amino acid composition and sequencing of the protein part can be useful for the study of hyper- and hyposensitization processes in animal models and in man.

0021-9673/90/$03.50

Some allergens derived from the domestic cat (*Felis domesticus*) frequently cause severe allergic reactions. One of these allergens is found in the saliva and can be transferred to the cat pelt by licking. It can be considered as the major cause of these reactions, designated Cat 1 allergen, and more recently *Fel d* I, first described by Leitermann and Ohman[1]. It has a native MW of *ca.* 35 000 daltons[1,2] and is composed of two chains which can be easily dissociated as they are not covalently linked. *Fel d* I has been defined as a homodimer, each monomer (17 000 daltons) having an equivalent allergenic and antigenic potency[1,2].

The presence of cat allergens in house dust has been shown by Ohman and co-workers[1,3]. To extract all soluble and allergenic components from the house dust, harvested during house vacuum cleaning, we followed the method originally described by Guibert and Causse-Combes[4].

Fel d I was first isolated by biochemical processes with some success but immunochemical methods of purification with immunosorbents, prepared with either polyclonal or monoclonal antibodies, were more efficient, although they gave a poor yield[1,2]. The biochemical method described here leads not only to a higher yield but could easily be scaled up for various purposes.

EXPERIMENTAL

Whole house-dust extract (WHDE)

The whole extract from a pool of house dusts harvested with a vacuum cleaner was essentially prepared according to Guibert and Causse-Combes[4]. Briefly, it consists of two steps, an aqueous extraction followed by two acetone precipitations at 25% and 75%, the last precipitate being termed the WHDE (Scheme 1).

Partially purified extract from house dust

From the whole house-dust extract, a partially purified extract was obtained by precipitation at 75% ammonium sulphate saturation in order to concentrate medium- and high-molecular-weight proteins and leave small molecules in the supernatant. After solubilization of the resulting precipitate, a dialysis against distilled water was performed to eliminate ammonium sulphate and other coprecipitated and dialysable molecules, using a dialysis bag with a 6000–8000-dalton MW cut-off. The resulting brownish solution was named HD75 and lyophilized (Scheme 1).

Fractionation methods

Ion-exchange chromatography. As preliminary experiments showed that the majority of HD75 antigenic components were negatively charged and *Fel d* I was shown to have a p*I* 3.8, an anion exchanger was used. A Mono Q HR 10/10 column (Pharmacia, Uppsala, Sweden) controlled by a fast protein liquid chromatographic (FPLC) system (Pharmacia) was loaded after equilibration with 0.02 *M* Tris–HCl buffer (pH 8.6)–0.125 *M* sodium chloride with a batch dissolved in the same buffer. A stepwise elution was performed; an isocratic run with the equilibration buffer was carried out followed by a second and a third step with the same buffer containing 1 and 2 *M* sodium chloride, respectively.

Immobilized metal ion affinity chromatography. Chelating Sepharose Fast Flow (Pharmacia) was used to pack an empty HR 10/10 column after being washed

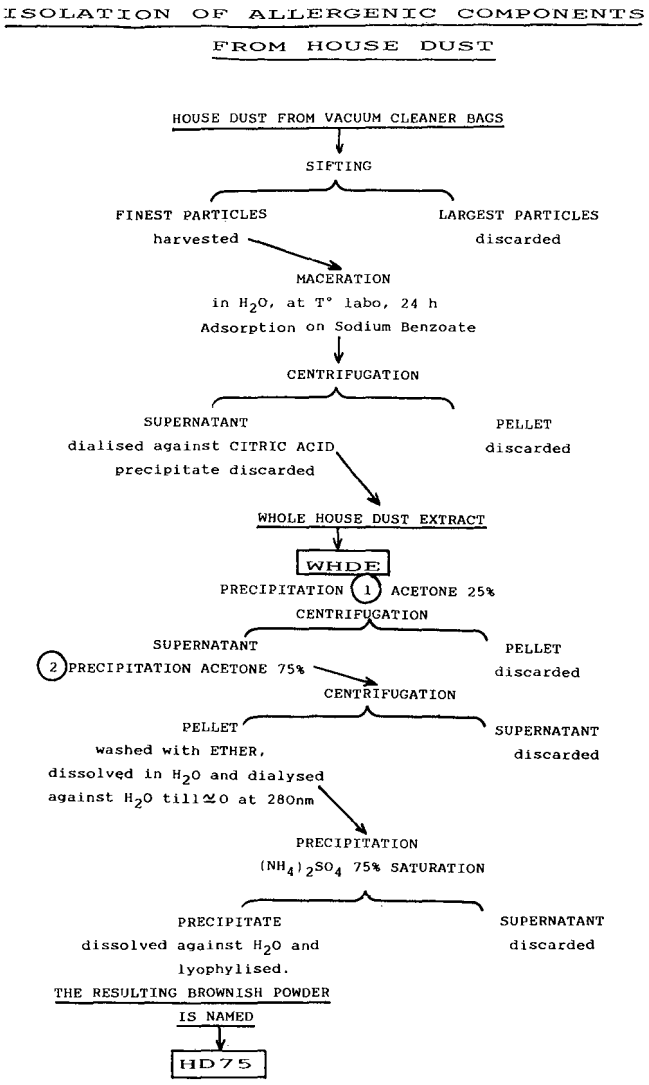

Scheme 1.

according to the manufacturer. It was charged, at saturation, with Cu^{2+} ions from aqueous copper(II) chloride solution (5 mg/ml). Unbound copper ions were washed out by a run with water. Before use, a blank run at a flow-rate of 3 ml/min was performed. The process was as follows: we began with a 15-min run with the equilibration buffer (solution A, 1 *M* sodium chloride in 0.02 *M* sodium phosphate buffer, pH 7.0), then a short 5-min linear gradient of molarity was applied to reach 100% B (solution B, 1 *M* ammonium chloride in 1 *M* sodium chloride–0.02 *M* sodium phosphate buffer, pH 7.0). A 15-min plateau at this concentration of B was followed by a decreasing linear gradient (5 min) to 0% B, then after a further run of 15-min with A the column was ready for use. The fractionation process was controlled by an FPLC

system, UV detection was done at 280 nm and events were recorded on a three-way recorder. A pre- and a post-column packed with the chelating gel without metal ions were inserted in the system to remove any free metal ions that might interfer with the chelating process; the columns used were of the HR 5/5 type.

Immunoelectrophoresis

To follow the purification steps of the cat major allergen *Fel d* I, crossed immunoelectrophoresis (CIE) methods were used as described by Axelsen *et al.*[5] and a rocket line experiment (RLIE) as described by Rabillon and co-workers[6,7] using a hyperimmunized rabbit sera pool against the partially purified house-dust extract HD75. The immunization process was as described by Le Mao *et al.*[8]. Each fraction obtained by chromatographic techniques was tested in a crossed-line rocket immunoelectrophoresis (CLIE) where the intermediate gel is lengthened on the right-hand part of the CLIE, allowing us to perform an RLIE leading to the easy identification of each antigen.

Allergenicity of these antigens can be previously challenged, before Coomassie blue staining, in applying the crossed radioimmunoelectrophoresis process described by Weeke and Lowenstein[9], using a cat-sensitized patient sera pool.

Enzyme-linked immunosorbent assay (ELISA)

To specifically detect the presence of the major cat allergen *Fel d* I in the different fractions obtained, ELISAs were performed using monoclonal antibodies (anti *Fel d* I), Mab 6F9 and biotinylated Mab 3E4 from Charlottesville University (VA, U.S.A.), Martin Chapman Laboratory and the two-site immunoassay described by Chapman *et al.*[2].

A CEB Immunoplate (Centre Européen de Biotechnologie, France) was coated with 1 μg per well of Mab 6F9 (anti *Fel d* I) in 0.1 *M* hydrogen carbonate buffer (pH 9.6) overnight at 4°C. The plate was then washed twice with phosphate-buffered saline (PBS) (pH 7.4), containing 1% Tween 20 and treated for 1 h with 100 μl per well of a bovine serum albumin (BSA) solution at 1% in the same buffer.

The wells were then incubated for 1 h at room temperature with 100 μl of diluted fractions (from 10^2 to 10^7), using double dilutions of a reference *Fel d* I fraction (Q2 Cu2, 10–0.04 μg/ml of PBS) to obtain a calibration graph.

After washing five times, the wells were incubated for 1 h at room temperature with 100 μl of a 10 μg/ml solution of biotinylated Mab 3E4 (anti *Fel d* I). The plate was then washed a further five times and the wells were incubated for 30 min with 1/1000 streptavidin–peroxidase (Sigma S-5512, 0.25 mg of protein reconstituted in 1 ml of distilled water).

Finally, the assays were developed by adding 100 μl per well of 1 m*M* 2,2′-azino-di(3-ethylbenzthiazoline sulphonate) (ABTS)–5% hydrogen peroxide in 70 m*M* citrate–phosphate buffer (pH 4.2) (ABTS Sigma A-1888). The reaction was stopped after 10 min by adding 100 μl per well of 2 m*M* sodium azide solution. The absorbance was read at 414 nm in an ELISA microplate reader.

Sodium dodecyl sulphate–polyacrylamide gel electrophoresis (SDS-PAGE)

SDS-PAGE was performed on a PHAST apparatus (Pharmacia) according to the procedure described by the manufacturer; after electrophoretis silver staining was used.

Gel filtration

A 50 cm × 1.6 cm I.D. column was packed with Superose 12 by the Chromatography Department of Pharmacia. The column was used after connection to an FPLC system with two pumps providing precise and accurate flow at relatively low back-pressure. It was equilibrated with 0.02 *M* Tris–HCl buffer (pH 8.6) containing 1 *M* sodium chloride to avoid ionic interactions. Buffer and protein samples were filtered through 0.45-μm membranes in order to eliminate foreign particles and dissolved gas.

Calibration of the column using protein molecules of known molecular weight was performed. To control the exclusion limit, Blue Dextran 2000 (MW $2 \cdot 10^6$ daltons) was added to the following mixture: ferritin, MW = $4.4 \cdot 10^5$, bovine γ-globulin, MW = $1.6 \cdot 10^5$, bovine serum albumin, MW = $6.9 \cdot 10^4$, α-chymotrypsin, MW = $2.35 \cdot 10^4$, egg lysozyme, MW = $1.75 \cdot 10^4$, bovine approtinin, MW = $6.5 \cdot 10^3$, and mellitin from honey bee venom, MW = $2.5 \cdot 10^3$ daltons. A 500-μl volume of the mixture was loaded onto the column.

RESULTS

Immunochemical analysis of HD75 by CIE

Homologous reactions between HD75 and the anti HD75 rabbit sera pool revealed at least eight antigens, the allergenicity of wich was demonstrated by CRIE using a cat-sensitized human patient sera pool. The results of these experiments are shown in Fig. 1a and b. In these experiments (Fig. 1a and b) a very marked uptake of radioactivity on the precipitin line corresponding to the antigens numbered 1, 2, 5 and 8 was obtained with cat-specific human IgE.

Identification of *Fel d* I among the HD75 antigens and allergens and discrimination from cat albumin, a potent allergen, were performed using a monoclonal immunosorbent-purified *Fel d* I and cat albumin purified by gel filtration from a whole cat serum, in one CIE and two CLIE, Fig. 1c, d and e.

Fractionation of HD75

Anion-exchange chromatography. This was carried out on a Mono Q HR 10/10 column equilibrated with 0.02 *M* Tris–HCl buffer (pH 8.6)–0.125 *M* sodium chloride. A sample of lyophilized HD75 (100 mg) previously dissolved in the same buffer was loaded onto the column. A stepwise elution was performed, beginning with an isocratic run during which one peak was eluted (Q1), and followed by elution with 1 *M* sodium chloride of almost all the remaining components of the extract (Q2). Finally, the column was eluted with 2 *M* sodium chloride, giving a third peak (Q3), essentially composed of pigmented material (Fig. 2). Immunochemical analysis using the rabbit sera pool against HD75 in CLIE and RLIE showed that only fraction Q2 contained *Fel d* I in a partially purified form (Fig. 4).

Application of a linear gradient of molarity between 0 and 1 *M* sodium chloride did not give a better purification but it allowed us to define the correct concentration, *i.e.*, 0.125 *M*, in the first run leading to the elution of the house-dust component of interest.

Copper chelate Sepharose chromatography. A 50-mg amount of the HD75 Q2 fraction from the Mono Q column dialysed against water and then lyophilized was

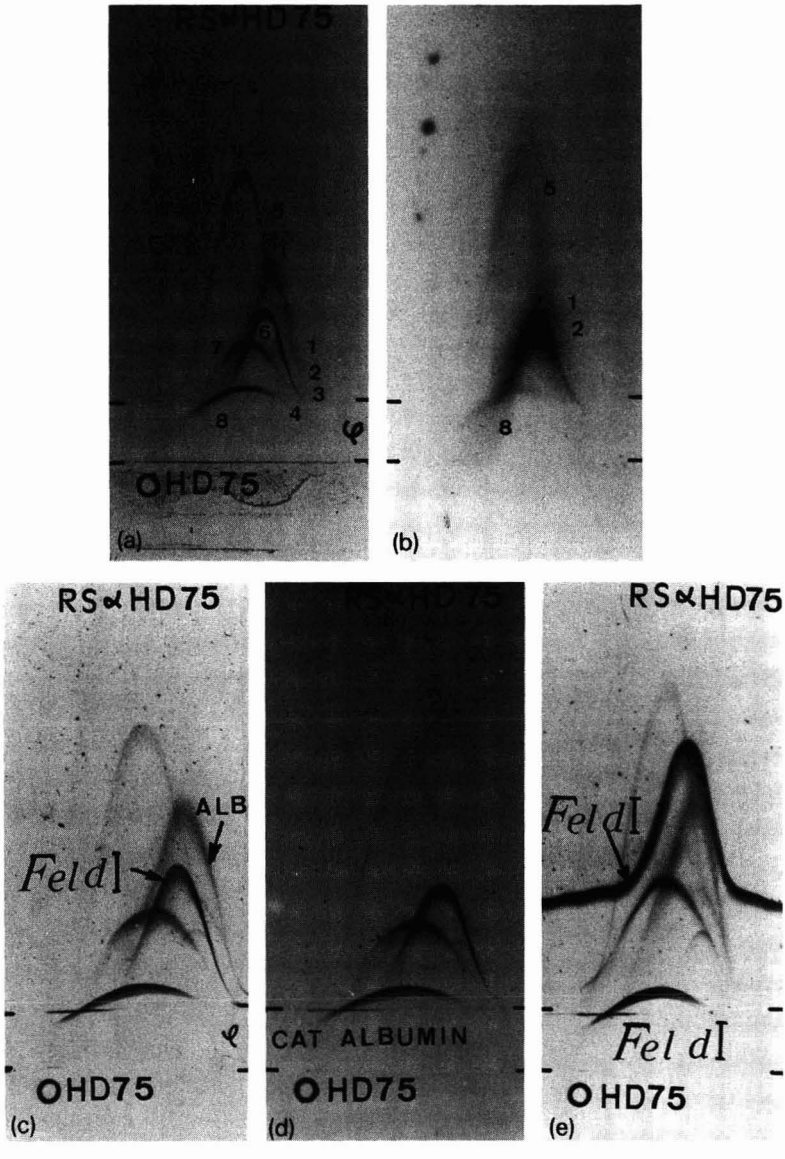

Fig. 1. Immunochemical analysis of HD75 by CIE, CRIE and CLIE. (a and b) CIE and CRIE where HD75 reacts with homologous rabbit antibodies, allergens are revealed by human IgE from a pool of cat-sensitized human sera. Autoradiography. (c, d and e) CIE and CLIE where cat albumin and *Fel d* I are identified by using their respective standards.

dissolved in 500 μl of the equilibration buffer and loaded onto the copper column prepared as described under Experimental.

The following elution programme was controlled by the FPLC system. The first step was a 60-min isocratic run with solution A in order to remove unbound material and to desorb proteins weakly bound to the immobilized copper ions. The second step

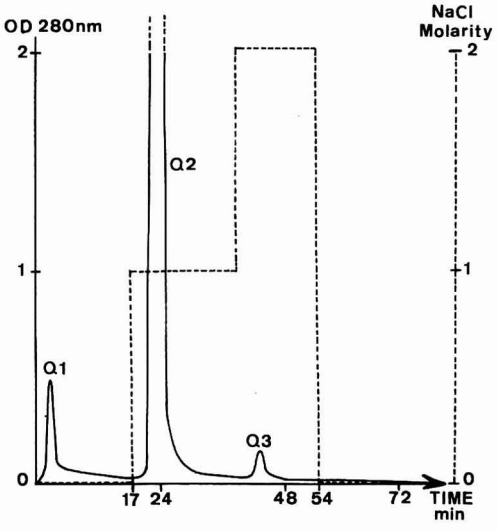

Fig. 2. Chromatogram of HD75 on a Mono Q HR 10/10 column equilibrated with 0.125 *M* NaCl in 0.02 *M* Tris–HCl buffer (pH 8.6) (solution A). Elution is carried out with 1 *M* NaCl in 0.02 *M* Tris–HCl buffer (pH 8.6) (solution B). Flow-rate, 1 ml/min. UV detection at 280 nm.

was a 30-min run using 50% solution B and the third a 30-min run at 100% solution B to desorb strongly bound protein molecules. All these runs were performed at a flow-rate of 0.5 ml/min. Finally, a 30-min run at a flow-rate of 3 ml/min with an injection of 20 ml of a 50 m*M* EDTA solution in solution A was carried out to elute all the material for which all other attempts had failed. The chelating Sepharose elution profile is shown in Fig. 3. Five peaks were obtained, and the last one, Cu5, was essentially composed of brown pigments. The other four fractions, Cu1, Cu2, Cu3 and Cu4, were immunochemically tested in the same system as used above and the results

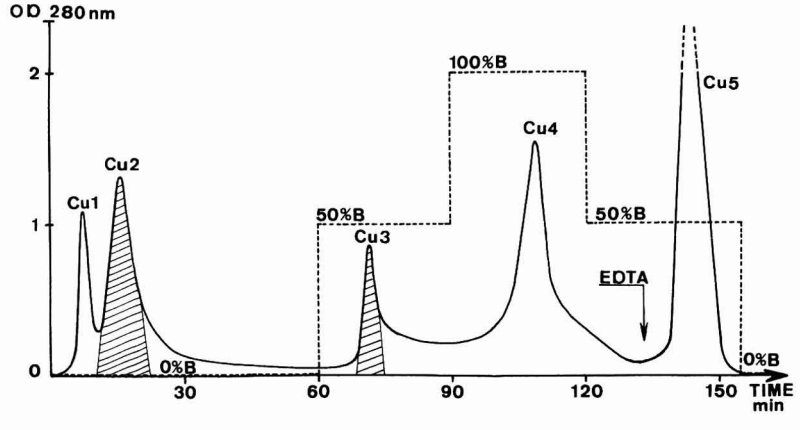

Fig. 3. Chromatogram of HD75 Q2 on a chelating Sepharose fast flow HR 10/10 column, charged with Cu^{2+} ions equilibrated with 1 *M* NaCl in 0.02 *M* sodium phosphate buffer (pH 7.0) (solution A). Elution is carried out with 1 *M* ammonium chloride in solution A (solution B). Flow-rate, 0.5 ml/min. UV detection at 280 nm.

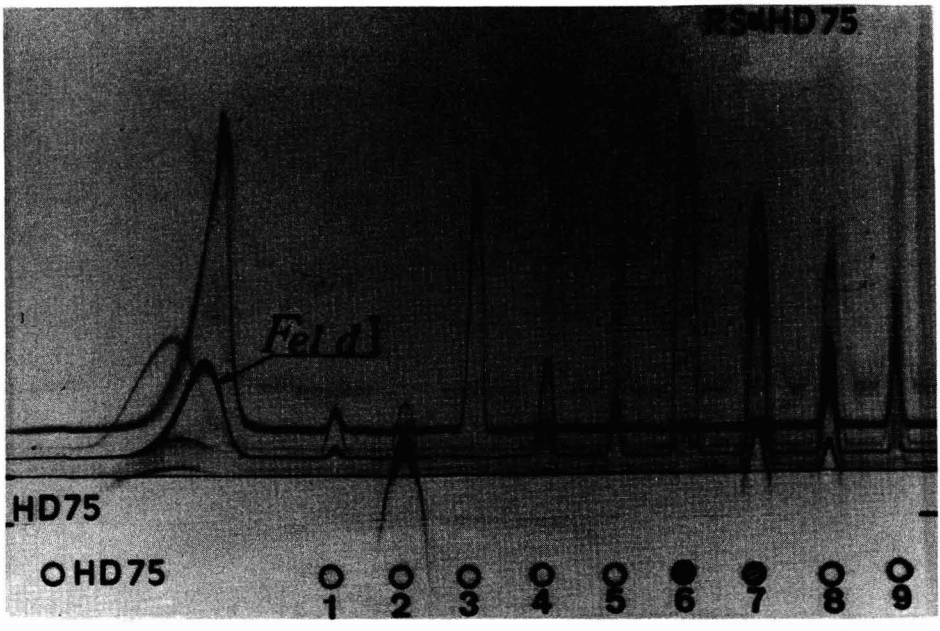

Fig. 4. Immunochemical analysis of chromatographic fractions by CLIE and RLIE using rabbit antibodies against HD75. Only HD75 is submitted to the first-zone electrophoresis. HD75 is present in the whole intermediate gel. Each fraction is tested in a contiguous RLIE. 1 = Cat saliva; 2 = HD75 Q1; 3 = cat albumin; 4 = HD75 Q2; 5 = Q2 Cu1; 6 = Q2 Cu2; 7 = Q2 Cu3; 8 = Q2 Cu4; 9 = Q2 Cu5.

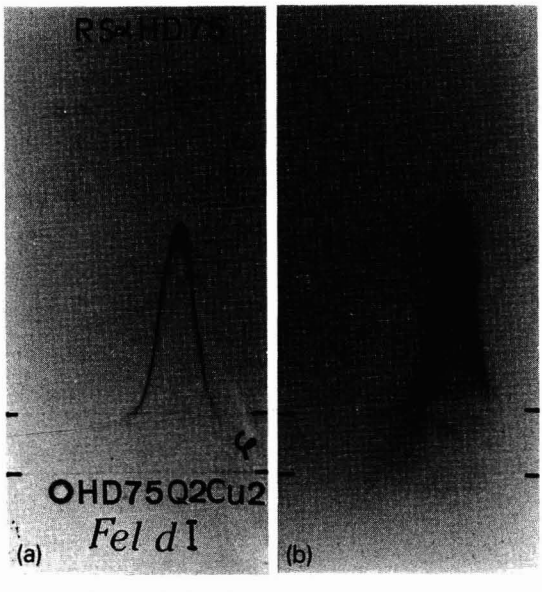

Fig. 5. CIE and CRIE where pure *Fel d* I (Q2 Cu2) reacts with rabbit antibodies against HD75. Allergenic activity is revealed by specific human IgE. Autoradiography.

are shown in Fig. 4. Fraction Q2 Cu2 appears as an immunologically pure allergen *Fel d* I and more particularly when tested in CIE, its allergenic activity being challenged by CRIE using a pool of cat-sensitized patient sera (Fig. 5a and b). Q2 Cu3 does contain *Fel d* I but a lower concentration and rather contaminated.

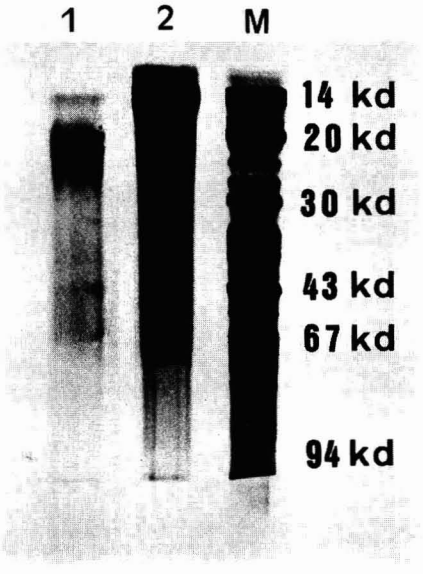

Fig. 6. Physico-chemical analysis o *Fel d* I enriched fractions. SDS-PAGE performed in a PHAST system (Pharmacia) according to the manufacturer. Phast gel gradient 8–25. A 1-μl sample of each native proteinic fraction is deposited, corresponding to 10 μg dry weight. The gel was silver stained. M = protein markers of known molecular weight; 1 = Q2 Cu2; 2 = Q2 Cu3. kd = kilodaltons.

SDS-PAGE

An SDS-PAGE experiment performed under non-dissociating conditions showed that the fraction Q2 Cu2 gives a homogeneous band but a minor one around 14 000 daltons and a second band, more diffuse, between 17 000 and 20 000 daltons. Fraction Q2 Cu3 gives a highly stained and very homogeneous band at 14 000 daltons (Fig. 6).

Gel filtration

In a gel filtration experiment performed on a Superose 12 column as described under Experimental, we showed that the Q2 Cu2 fraction appears as a peak with one shoulder, the main peak corresponds to a molecular species with MW = 14 000 daltons and the first-eluted shoulder to one with MW = 30 000 daltons. The Q2 Cu3 fraction is eluted from the column as a homogeneous peak essentially composed of three proteinic molecules with MW of 20 000, 30 000 and 50 000 daltons. All these results are shown in Fig. 7a and b.

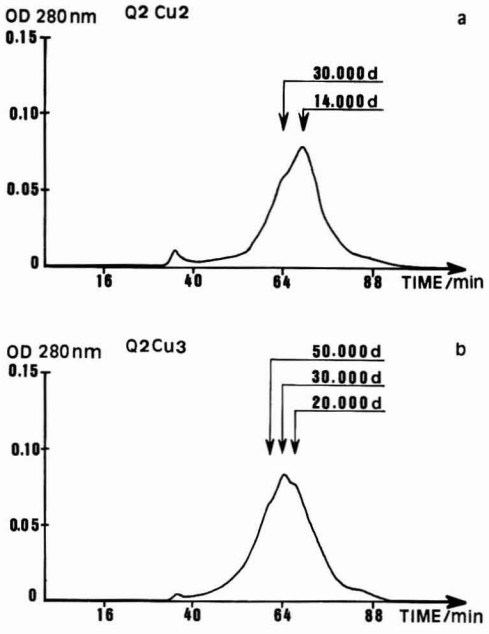

Fig. 7. Gel filtration experiments performed on a Superose 12 HR 16/50 column, equilibrated in 1 *M* NaCl–0.02 *M* Tris–HCl buffer (pH 8.6). Flow-rate, 1 ml/min. UV detection at 280 nm. (a) Q2 Cu2 analysis; (b) Q2 Cu3 analysis. d = daltons.

Increase in purity over the purification process

This was assayed using ELISA (a two-site assay) with two different specificity monoclonal antibodies against *Fel d* I: Mab 6F9 for coating of the plate wells and the biotinylated Mab 3E4. Fraction Q2 Cu2, since it was demonstrated by all other methods to be pure *Fel d* I, was used as a standard reference to challenge the presence of *Fel d* I allergen in every fraction obtained during its purification process. The results are shown in Table I.

House dust (kindly provided by the Allergens Department, Institut Pasteur) contains 8 μg/g of *Fel d* I as tested in the first aqueous extract, WHDE. Thus, from

TABLE I

CONCENTRATION OF *Fel d* I AS DETERMINED BY A TWO-SITE IMMUNOASSAY (ELISA)

Fraction	*Fel d I (%)*
WHDE	0.8
HD75	8.0
HD75 Q2	75.0
Q2 Cu1	17.0
Q2 Cu2	100.0
Q2 Cu3	62.0
Q2 Cu4	21.0
Q2 Cu5	4.2

35 kg of house dust containing *ca.* 300 mg of active *Fel d* I molecules only 10% were obtained in a pure and homogeneous form as Q2 Cu2 fraction.

DISCUSSION

In order to purify the cat major allergen *Fel d* I from house dust, we developed a procedure combining two chromatographic techniques. The first is a stepwise elution process which gives three fractions from HD75, the partially purified house dust extract when it has been loaded on an anion-exchange column. Of these fractions only the second, Q2, contained *Fel d* I allergen as assayed by RLIE and ELISA (a two-site immunoassay)[2]. Thus for further purification, immobilized copper ion affinity chromatography was used.

Immobilized metal ion affinity chromatography (IMAC) is certainly one of the most powerful methods available for fractionating protein mixtures. First described about 15 years ago by Porath *et al.*[10], is is not currently used. A knowledge of the protein to be isolated is generally necessary as binding of protein(s) to divalent metal ions depends on the presence of certain amino acid residues, whereas for ion-exchange chromatography and gel filtration only charge and/or size characteristics have to be known. Amino acids form stable chelates with metal ions[11], but many workers have demonstrated that exposed imidazole and thiol groups on the protein molecules are the most important binding sites for copper-containing adsorbents[12]. Therefore, peptides containing histidine and/or cysteine residues bind more stably with the immobilized copper ions. Nevertheless, arginine residues can also bind metal ions via their guanidinium group[11].

From the amino acid composition of *Fel d* I published by other workers[2], we could only presume a relatively weak affinity of this allergenic protein for copper ions. Cysteine was not determined and histidine was totally absent. However, it could be useful in any case to challenge divalent metal ions bound to any available support in order to choose either a biochemical or an immunochemical method of purification for the protein of interest. Preliminary experiments led us to use a chelating Sepharose fast flow column, charged with copper ions. A four-step elution process was performed. All buffers contained 1 *M* sodium chloride which increases the adsorption capacity of the solid phase as shown by Porath and Olin[13]. Ammonium, considered to be a competitive ligand, was used (as ammoniom chloride) to achieve displacement of the highly adsorbed proteinic molecules.

From the *Fel d* I enriched fraction Q2, among the five fractions so obtained, only two contain *Fel d* I: Q2 Cu2, a highly pure monomeric form of *Fel d* I, with MW = 17 000 daltons and slightly contaminated by a proteinic component with MW = 14 000 daltons, and Q2 Cu3, which shows a higher affinity for copper ions and contains cat major allergen contaminated by a proteinic component with MW = 14 000 daltons.

In a gel filtration experiment, pure *Fel d* I as present in Q2 Cu2 seemed to undergo a dimerization as described previously[1,2]. In this homodimer, monomers are not engaged in covalent interactions and can be easily dissociated in the SDS-PAGE experiment without reduction. Aggregation could be evoked to explain the behaviour of Q2 Cu3 in a similar gel filtration process.

Our results are consistent with those obtained by other workers[1,2], who stated

that *Fel d* I exists as two molecular species a monomer of MW *ca.* 17 000–19 000 daltons and an homodimer of MW 35 000–39 000 daltons.

It must be emphasized that our process for purification from the crude house-dust extract is fairly drastic and could lead to some denaturation of the allergenic molecules. Nevertheless, antigenic and allergenic activities are totally preserved. Allergenic activity was challenged by CRIE and skin tests.

In conclusion, the results confirm IMAC to be a powerful tool not only for protein purification but also for the study of their native or post-synthetic molecular structure. In the case of allergen purification we can conclude that combination of anion-exchange chromatography and IMAC provides a very efficient biochemical process which may certainly benefit from subsequent scale-up.

REFERENCES

1 K. Leitermann and J. L. Ohman, *J. Allergy Clin. Immunol.*, 74 (1984) 147.
2 M. Chapman, R. C. Aalberse, M. J. Brown and T. A. E. Platts-Mills, *J. Immunol.*, 140 (1988) 812.
3 J. L. Ohman, J. R. Lorusso and S. Lewis, *J. Allergy Clin. Immunol.*, 79 (1987) 955.
4 L. Guibert and R. Causse-Combes, *Ann. Inst. Pasteur*, 108 (1965) 579.
5 N. H. Axelsen, J. Kroll and B. Weeke, *Scan. J. Immunol.*, 2 (Suppl. 1) (1973) 47.
6 J. Rabillon, J.-P. Dandeu and B. David, *J. Allergy Clin. Immunol.*, 79 (1987) 32.
7 B. David, G. Peltre, J. P. Dandeu, J. Rabillon and X. Desvaux, *Proceedings of the 13th Congress of Allergology and Clinical Immunology*, 1989, p. 422.
8 J. Le Mao, J.-P. Dandeu, J. Rabillon, M. Lux and B. David, *Immunology*, 44 (1981) 239.
9 B. Weeke and H. Lowenstein, *Scand. J. Immunol.*, 2 (1973) 149.
10 J. Porath, J. Carlsson, I. Olsson and G. Belfrage, *Nature (London)*, 258 (1975) 598.
11 F. R. N. Gurd and P. E. Wilcox, *Adv. Protein Chem.*, 11 (1956) 311.
12 E. Sulkowski, K. Vastola, D. Oleszek and W. Muenchenhausen, *Anal. Chem. Symp. Ser.*, 9 (1982) 313.
13 J. Porath and O. Olin, *Biochemistry*, 22 (1983) 1621.

Journal of Chromatography, 512 (1990) 189–202
Elsevier Science Publishers B.V., Amsterdam

CHROMSYMP. 1892

Chromatography and generation of specific antisera to synthetic peptides from a protective *Boophilus microplus* antigen

PHILLIP J. SHARP*, BERNIE V. McINERNEY and DONALD R. J. SMITH
Biotechnology Australia Pty. Ltd., P.O. Box 20, Roseville, N.S.W. 2069 (Australia)
IAN F. TURNBULL
Department of Microbiology, University of Melbourne, Parkville, Victoria 3052 (Australia)
DAVID H. KEMP
CSIRO, Division of Tropical Animal Production, PMB 3, Indooroopilly, QLD 4068 (Australia)
and
KEITH N. RAND and GARY S. COBON
Biotechnology Australia Pty. Ltd., P.O. Box 20, Roseville, N.S.W. 2069 (Australia)

ABSTRACT

Four oligopeptides corresponding to predicted antigenic regions of the protective Bm86 glycoprotein of the cattle tick *Boophilus microplus* were synthesized and purified. Three were conjugated to carrier proteins and antisera raised in rabbits and cows. All elicited antipeptide antibodies that recognized Bm86 and recombinant derived products in Western blots; however, only one produced antiserum capable of recognizing native Bm86 in an indirect immunofluorescence assay. Ticks fed *in vitro* on this antiserum showed no obvious gut damage.

INTRODUCTION

Antibodies directed against synthetic peptides which react with the intact protein are useful in the detection of gene products, the study of functionally active regions of proteins and the development of synthetic vaccines.

The cattle tick *Boophilus microplus* is a major ectoparasite of cattle in many parts of the world. Bm86 is a gut epithelial cell surface glycoprotein isolated from the tick which, when used to vaccinate cattle, stimulates an immune response which protects cattle against subsequent tick infestation[1]. The DNA sequence of the cloned gene[2], shows that Bm86 has 650 amino acids, 10% of which are cysteines. The cysteine residues are organized into eight domains each containing six cysteines with the spacing characteristic of the epidermal growth factor (EGF) precursor and several other proteins. Previous studies with synthetic peptides have shown that receptor binding of both murine EGF[3] and urokinase-type plasminogen activator (uPA)[4]

0021-9673/90/$03.50

occurs within the "B loop" of the 6-Cys units. The intra-chain disulphide bonded peptide of uPA has a higher receptor binding affinity than the reduced form[4]. Since the "B loop" region of these molecules is functionally active it is not unreasonable to speculate that these regions within Bm86 may be also functionally important. Antibodies directed to these regions may inhibit the function of this molecule and confer a protective response.

We report here the synthesis and purification of two "B loop" oligopeptides from Bm86 which were used to generate reagents to help define the epitopes that may elicit protective antibody. We also report the use of two other linear oligopeptides from the NH_2- and COOH-terminal regions of Bm86 in the characterisation of recombinant products.

EXPERIMENTAL

Materials and equipment

All reagents used were of analytical grade. Ovalbumin, bovine serum albumin, keyhole limpet hemocyanin, fish gelatin, *m*-maleimidobenzoyl-N-hydroxysuccinimide ester, Coomassie Brilliant Blue R, Freund's complete and incomplete adjuvant were from Sigma (St. Louis, MO, U.S.A.). Glutaraldehyde was from BDH (Kilsyth, Australia). Western blotting reagents were from Promega (Rozelle, Australia). Immulon 2 microtitre plates were purchased from Dynatech (Alexandria, VA, U.S.A.). Peroxidase-conjugated antibodies were from Dakopatts (Glostrup, Denmark). Fluorescein-labelled rabbit anti-bovine Ig was a gift from R. Pearson (CSIRO, Division of Tropical Animal Production). Purified Bm86 (ref. 1) was a gift from CSIRO Division of Tropical Animal Production. Sephadex G-25 was obtained from Pharmacia (Uppsala, Sweden). N^{α}-Butyloxycarbonyl (tBoc)-L-amino acid derivatives and 4-methylbenzhydrylamine polystyrene resin were from Applied Biosystems (Foster City, CA, U.S.A.). N-Methylmercaptoacetamide was purchased from Fluka (Buchs, Switzerland).

The high-performance liquid chromatography (HPLC) system consisted of two pumps with extended flow heads (Model 510, Waters Chromatography Division, Millipore, Milford, MA, U.S.A.), a gradient controller and data system (Model 840, Waters), a sample injection valve (Model U6K, Waters) and a multiwavelength detector (Model M-490, Waters). Reversed-phase (RP) HPLC columns were obtained from The Separations Group (Hesperia, CA, U.S.A.).

Peptide synthesis

The protected peptide was assembled by solid-phase synthesis[5] on a cross-linked polystyrene support using an Applied Biosystems 430A automated peptide synthesiser. tBoc-amino acids were coupled sequentially to a 4-methylbenzhydrylamine polystyrene resin. A cysteine was added to the COOH terminal of pep 2 to facilitate coupling to the carrier protein. Internal cysteines present in pep 3 and pep 4 (Cys^{37} and Cys^{307} respectively) were replaced by alanine residues to avoid undesired disulphide-bonded loop formations. After assembly the protected peptide–resin was cleaved and the protecting groups were removed by anhydrous hydrogen fluoride in the presence of scavengers: HF–anisole–dimethylsulphide–*p*-thiocresol (10:1:1:0.2, v/v) for 1 h at −5°C to 0°C. The cleaved peptide was washed with diethyl ether then dissolved in 10% aqueous acetic acid and lyophilised.

Reduction of methionine sulphoxide in pep 4

After HF treatment the crude pep 4 (5 mg/ml in 10% aqueous acetic acid) was reduced by the addition of 10% (v/v) N-methylmercaptoacetamide (MMA) and the reaction was allowed to proceed for 26 h at 37°C (ref. 6). The reduced peptide was purified by size-exclusion chromatography followed by preparative RP-HPLC.

Chromatography

Analytical RP-HPLC was performed on a wide-pore, octadecyl silica column (Vydac 218TP 54; 250 × 4.6 mm I.D.). Pep 1 and pep 2 were eluted with a linear gradient of 5–60% acetonitrile in 0.1% aqueous trifluoroacetic acid (TFA) in 30 min. The flow-rate was 1 ml/min and the absorbance was monitored at 220, 254 and 280 nm using a multiwavelength detector. Pep 3 and pep 4 were eluted with a 10–60% gradient of acetonitrile in 0.1% TFA. The separation of the linear and folded forms of pep 3 was achieved using a 17.5–30% gradient.

Preparative RP-HPLC was also performed on an octadecyl column (Vydac 218TP 1022; 250 × 22 mm I.D., 10 μm particle size). Elution gradients were identical to those used for the analytical RP-HPLC using a flow-rate of 16 ml/min. All fractions were lyophilised after collection.

After MMA treatment, pep 2 and pep 4 were chromatographed on Sephadex G-25 gel filtration media to remove reagents and low molecular weight contaminants. The column (100 × 1.6 cm I.D.) was eluted with 5% aqueous acetic acid at a flow-rate of 3 ml/min and monitored at 254 nm.

Disulphide loop formation

RP-HPLC-purified pep 3 was allowed to fold and oxidise by stirring for 20 h at a concentration of 0.1 mg/ml in 100 m*M* Tris–HCl, pH 7.9. The reaction was monitored by RP-HPLC and Ellman's assay[7]. The reaction products were desalted by preparative RP-HPLC.

Peptide analysis

Amino acid analysis was performed on a Waters Picotag system with pre-column formation of the phenylthiocarbamyl derivatives[8]. NH_2-terminal sequence analysis was carried out on an Applied Biosystems Model 470A gas phase sequencer.

Coupling of peptides to carrier proteins

Pep 1 and pep 2 were coupled to ovalbumin (OVA) and bovine serum albumin (BSA) respectively with *m*-maleimidobenzoyl-N-hydroxysuccinimide ester (MBS)[9]. Pep 3 was coupled to keyhole limpet hemocyanin (KLH) with glutaraldehyde using a modification of the described method[10]. Carrier proteins and conjugates were subjected to amino acid analysis (Waters Picotag) to monitor coupling efficiency.

Immunization

(i) New Zealand White rabbits were immunized with 0.5 mg of either pep 1–OVA or pep 2–BSA conjugate in Freund's complete adjuvant by subcutaneous injection. Two booster injections were given on days 21 and 38 in Freund's incomplete adjuvant. Venous blood was collected by standard procedures, usually 14 days after each injection.

(ii) Three *Bos taurus* cows were vaccinated on two occasions four weeks apart. A 1-mg amount of a pep 3-KLH conjugate in saline was emulsified with an equal volume of Montanide/Marcol and delivered by intramuscular injection. Blood was collected 14 days after the second vaccination.

Western blotting

Proteins were transfered to nitrocellulose paper as described[11] and blocked for 1 h at room temperature in 0.5% fish gelatin–TBST (10 m*M* Tris–HCl, pH 8.0, 150 m*M* NaCl, 0.05% Tween 20). The blots were then incubated in antisera diluted in TBST overnight at 4°C, washed four times in TBST, and then incubated in alkaline phosphatase conjugated goat anti-rabbit or rabbit anti-bovine immunoglobulin at room temperature. After washing four times in TBST the blots were developed by incubation in 10 m*M* Barbital–acetate buffer (pH 10.0) containing 0.35 mg/ml nitro-blue tetrazolium and 0.17 mg/ml 5-bromo-4-chloro-3-indoyl phosphate.

Titration of antisera

Antisera were titred by an indirect enzyme-linked immunosorbent assay (ELISA)[12]. Microtiter plates were coated overnight at room temperature with 0.1–1 μg/well of free peptide or protein antigen in 100 m*M* sodium carbonate buffer (pH 9.6). Pre-immune serum from each animal served as a negative control. Optical density (OD) at 414 and 490 nm was measured after 10–20 min with a multiscan photometer (Bio-Tek Instruments).

Bm86 expression vectors

BTA1696, under control of the pL promoter, encodes a "full-length" protein consisting of 610 amino acids of Bm86 (residues 20–629). An insert encoding amino acids 1–629 (including the leader sequence consisting of residues 1–19 which are post-translationally cleaved) was also transformed into *Aspergillus nidulans* strain VH, under control of the *amdS* promoter[13]. BTA1753, also under control of the pL promoter, encodes a truncated Bm86 protein consisting of 264 amino acids of Bm86 (residues 97–360).

Expression tests

BTA1696, BTA1753 and N4830/pBTA 602 (which is the host–vector combination that lacks an insert) were grown in tryptone soybroth medium (TSB) containing Ampicillin (100 μg/ml) overnight at 28°C, diluted 1/10 in fresh TSB and grown a further 3 h before induction for 2 h at 40°C. Cell culture (0.1 ml) was centrifuged and the cell pellet was resuspended in 20 μl sodium dodecyl sulphate (SDS) boiling buffer (2% SDS, 0.5 *M* urea and 1% β-mercaptoethanol) and boiled for 5 min. The proteins were resolved on a 10% SDS–polyacrylamide gel and either stained with Coomassie Brilliant Blue or Western blotted.

Culture media from a *A. nidulans* transformant expressing a full-length Bm86 molecule was concentrated by ultrafiltration using a Centricon-30 microconcentrator and secreted proteins were prepared in SDS boiling buffer. The proteins were resolved on a 10% SDS–polyacrylamide gel and either stained with Coomassie Brilliant Blue or Western blotted.

Indirect fluorescent antibody binding to tick gut cells

This was performed by the method of Willadsen *et al.*[1]. Briefly, semi-engorged adult female ticks were dissected and small pieces of gut everted, reacted with bovine or rabbit antisera for 2 h at 4°C, washed, then reacted with the appropriate second antibody conjugated to fluorescein. The pieces of gut were then examined under a Zeiss fluorescence microscope.

Tick feeding in vitro

Adult ticks were fed *in vitro*[14] on antisera from cows vaccinated with pep 3 conjugate. Ticks were assumed to have suffered gut damage if they showed evidence of excessive leakage of bovine serum proteins into the haemolymph.

RESULTS

Selection criteria for synthetic peptides

Pep 1 and pep 2 (Table I) were chosen on the basis of hydrophilicity and terminal location. Hydrophilicity analysis[15] allows prediction of protein determinants that are likely to be surface-oriented and, therefore likely to be antigenic. Pep 1 and pep 2 had hydrophilicity indices of +0.33 and +0.94 respectively. A secondary consideration was the terminal location of both peptides; Walter *et al.*[16] found that sera against both the NH_2- and COOH-terminal peptides of the large T-antigen of SV40 precipitated the protein from extracts of infected cells. Terminally directed antibodies also reacted strongly with native gp70 of Friend murine leukaemia virus[17]. The flexibility of many chain termini presumably allows a greater chance of a "fit" with an antibody produced to a relatively short peptide that can adopt several confirmations in solution.

Bm86 is similar to EGF precursor and several other extracellular proteins[18]; the homology is mainly due to the conserved cysteine spacing in their growth factor

TABLE I

PROPERTIES OF SYNTHETIC PEPTIDES

Single-letter amino acid code used.

Peptide	*Amino acid sequence*[a]	*Position*[b]	*Hydrophilicity*[c]	*Location*
pep 1	E S S I C S D F G N E F C R N A E C	20–37 (1–18)	+ 0.33	NH_2-term.
pep 2	T T T K A K D K D P D P G K S S A A (C)	612–629 (593–610)	+ 0.94	COOH-term.
pep 3	F C R N A E A E V V P G A E D D F V C K	31–50 (12–31)	+ 0.41	B-loop
pep 4	K C H E E F M D A G V Y M N R Q S C Y	299–317 (280–298)	+ 0.08	B-loop

[a] Amino acid sequence predicted from nucleotide sequence of Bm86 cDNA[2]. The residue in parentheses was added to facilitate coupling. Underlined residues are substitutes to prevent formation of unwanted disulphide-bonded products.

[b] Residue numbers in parentheses refer to primary sequence position in mature Bm86 assuming processing of a 19 amino acid leader sequence.

[c] Calculated according to Hopp and Woods[15].

modules. The presence of this conserved module in many proteins may mean that it is a part of a receptor–ligand system responsible for defined biological functions[2]. Synthetic peptide studies[3] showed that murine EGF residues 20–31 (resident in the so-called B-loop) constituted the primary receptor binding region and also contained the predominant EGF antigenic determinant. The homologous region within human uPA is also responsible for specific receptor binding[4]. By analogy with these proteins it is possible that the B-loop region within the growth factor modules present in Bm86 (Fig. 1) also serves a receptor binding function. Pep 3 and pep 4 (Table I) were chosen to represent the putative receptor binding regions in two EGF modules of Bm86. This strategy was based on the observation that the intra-chain disulphide bonded uPA synthetic peptide 12–32 displayed a stronger receptor binding affinity than did the reduced form[4].

Pep 1 and pep 2 were selected to raise antisera primarily for the purpose of characterizing gene products under denaturing conditions. Pep 3 was selected for the purpose of providing reagents useful in the characterization of the native antigen and to investigate the potential for the development of a synthetic peptide vaccine.

Peptide purification and analysis

The quality of the synthetic peptides was assessed by RP-HPLC analysis of the crude peptides using a wide pore C_{18} column. Crude pep 1, pep 2 and pep 3 contained only a single major peak at 220 nm which accounted for greater than an estimated 75–90% of the crude peptide content (data not shown). This supports the conclusion that each of the syntheses proceeded with high yield at each step and few side-reactions had occurred.

Pep 1 and pep 3 were efficiently purified to homogeneity by RP-HPLC using a wide pore C_{18} column and a standard acetonitrile gradient with TFA as the counter-ion. Pep 2, with a single major peak at 220 nm containing greater than an estimated

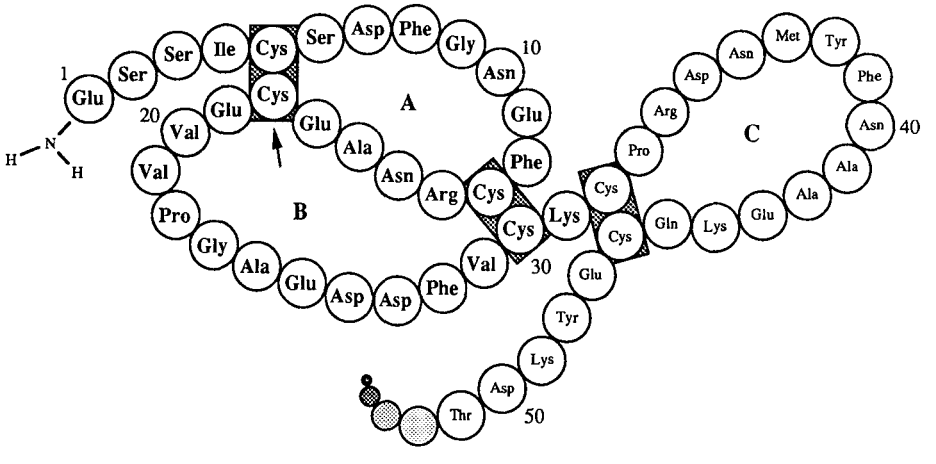

Fig. 1. A working model of the proposed NH_2-terminal EGF-like region of Bm86. The three loops designated A to C are analogous to those present in murine EGF (ref. 3). Pep 1 (residues 1–18) and pep 3 (residues 12–31) were chosen for synthesis; the arrow marks the location of the cysteine substituted by alanine in the synthetic peptide to avoid undesired disulphide bond formations.

90% of the crude peptide content, did not require HPLC purification but was desalted on a Sephadex gel filtration column.

In contrast, the crude pep 4 HPLC analysis showed a profile with multiple peaks when monitored at 220 (Fig. 2a), 254 or 280 nm. Further, the ratio of the peak heights at the different wavelengths was the same, indicating that the multiple impurity peaks were not due to partial deprotection or rearrangements of the benzyl protecting groups during the HF cleavage reaction. Pep 4 contained two methionine residues that were protected during synthesis as the sulphoxide form. It was suspected that this group had been incompletely deprotected during the HF cleavage step. This was confirmed by reduction with MMA; upon treatment there was a dramatic change in the chromatogram (Fig. 2b) with only a single major peak now remaining at 14.3 min. The peak at 11.5 min and the doublet at 12.9 min had disappeared. Methionine sulphoxide (Met[O])-containing peptides elute earlier under RP conditions than the peptides containing reduced methionine as illustrated by Fig. 2a. The peak at 11.5 min is most probably the peptide containing two Met[O] residues and the doublet of peaks at 12.9 min are most probably two peptide isomers each with a single Met[O] residue. The reduced peptide was further purified to homogeneity by RP-HPLC (Fig. 2c).

Peptide refolding

Purified pep 3 was air oxidised and folded in dilute basic solution to form the intra-chain disulphide-bonded loop peptide. An analytical RP-HPLC method was developed to separate the linear and the oxidised forms of pep 3 (Fig. 3). The oxidised form of the peptide (as determined by Ellman's assay[7]) elutes ahead of the linear form. This method allowed the progress of the oxidation to be monitored and ensured complete conversion and high recovery of the desired product.

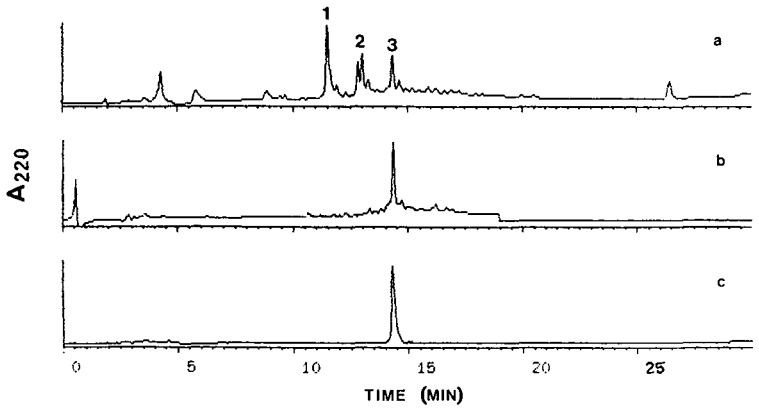

Fig. 2. RP-HPLC analysis of pep 4. (a) Crude pep 4 after HF cleavage from the support resin showing (1) the diMet[O] peptide, (2) two isomer forms of the monoMet[O] peptide and (3) the reduced peptide. (b) Crude pep 4 after MMA reduction. (c) Purified pep 4 after preparative RP-HPLC. Samples were chromatographed on a Vydac 218 TP column (250 × 4.6 mm I.D.) developed with a linear gradient from 10 to 60% acetonitrile containing 0.1% TFA during 30 min. Eluent was monitored at 220 nm and the flow-rate was 1 ml/min.

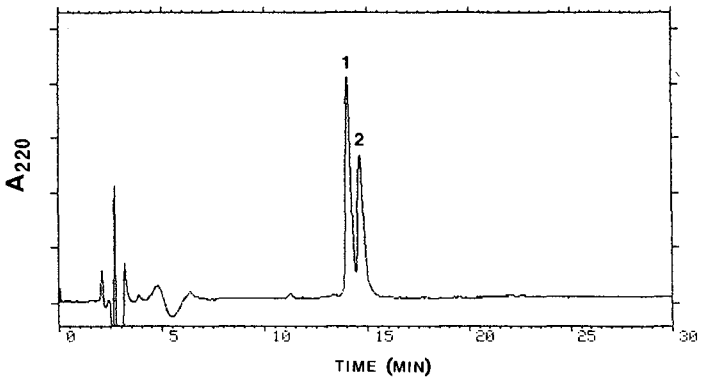

Fig. 3. RP-HPLC analysis of oxidized-refolded pep 3. Purified pep 3 was oxidized and chromatographed to show a shift to a shorter retention time after refolding: (1) oxidized and (2) reduced peptide. Chromatographic conditions were the same as for Fig. 2 with the gradient composition 17.5 to 30% acetonitrile in 0.1% TFA.

Production of peptide antisera

Pep 1 and pep 2 conjugates were analyzed by amino acid analysis and were shown to have coupling efficiencies of 3:1 and 10:1, respectively, on a molar ratio of peptide to carrier protein. The pep 3-KLH conjugate was not analyzed as the carrier had no defined molecular weight and was heterogeneous as judged by SDS–polyacrylamide gel electrophoresis (data not shown). Pep 4 was not conjugated and is the subject of research that will be presented elsewhere.

Rabbits (two per group) were immunized with pep 1 and pep 2 conjugates; three cows were immunized with pep 3 conjugate. Serum obtained 14 days after the second vaccination was titred by ELISA (Table II) and all peptides were shown to be immunogenic. The titres against homologous peptides in rabbits immunized with pep 1 and pep 2 conjugates ranged from 500 to 2500 with the latter conjugate being more immunogenic. Similarly, the titres of the cows immunized with pep 3 conjugate varied significantly with two animals responding relatively poorly and eliciting antibody responses that were an order of magnitude lower than the third animal. At the highest concentration, antisera to the unrelated peptides were not reactive. Antibodies cross-

TABLE II

ANTI-PEPTIDE ANTIBODY TITRES

ELISA titres of the serum from individual animals are defined as the reciprocal of the dilution ($\times 10^{-3}$) providing an OD of 0.5 measured at 414 nm. – = No titre recorded at a 1:10 dilution.

Immunising peptide	*Antiserum titres against*		
	pep 1	*pep 2*	*pep 3*
pep 1	0.5, 2.5	–, –	–, –
pep 2	–, –	1.6, 2.4	–, –
pep 3	–, –, 0.05	–, –, –	0.6, 0.8, 10

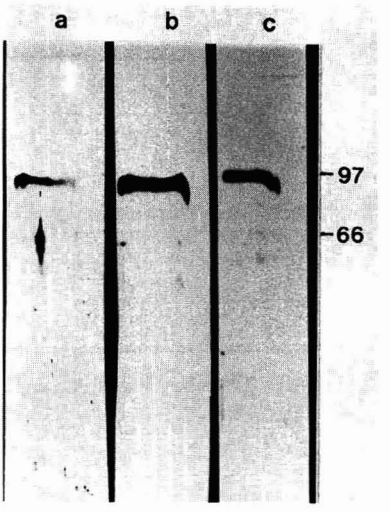

Fig. 4. Antipeptide antibodies recognise denatured Bm86. Purified Bm86 (ref. 1) was electrophoresed on a 10% SDS–polyacrylamide gel and electroblotted onto nitrocellulose. Nitrocellulose replicas were incubated with antiserum directed against pep 1 (a), pep 2 (b) or pep 3 (c). The positions of molecular size markers are given in kilodalton.

reacted poorly with the overlapping pep 1 and pep 3 which suggests that secondary structure may be important. The strongest peptide antiserum of each group was used in subsequent studies.

Recognition of denatured Bm86 by the antipeptide sera

To determine if the antipeptide antibodies were capable of recognising denatured Bm86, sera were diluted 1:1000 and used to probe Western blots. All sera reacted strongly with 100 ng of purified Bm86 (Fig. 4) and this result suggested that the sera would be useful in the characterization of Bm86 and associated recombinant products under denaturing conditions. Pre-immune sera did not react with Bm86.

Characterization of recombinant Bm86 expressed in E. coli

BTA1696 expresses a 70 000-dalton protein at detectable levels upon induction, as shown by Coomassie Blue staining of an SDS–polyacrylamide gel. Uninduced bacteria do not synthesize this protein (data not shown). Two controls were included: (i) the host strain transformed with the expression plasmid without a recombinant insert (N4830/pBTA 602) and (ii) BTA1753 encoding a truncated Bm86 which expresses a detectable protein of 35 000 dalton upon induction (Fig. 5a).

Both controls and the full-length Bm86 were also Western blotted and probed in separate experiments with sera directed against pep 1, pep 2 and pep 3 (Fig. 5b–d). The three antipeptide sera reacted strongly with a band of 70 000 dalton which corresponds to the predicted molecular weight of the full-length Bm86. This band was only present in samples prepared from cells expressing the full length Bm86 (BTA1696). A corresponding band was not detected in samples prepared from cells expressing the truncated Bm86 (BTA1753). This indicates that each antipeptide serum contains

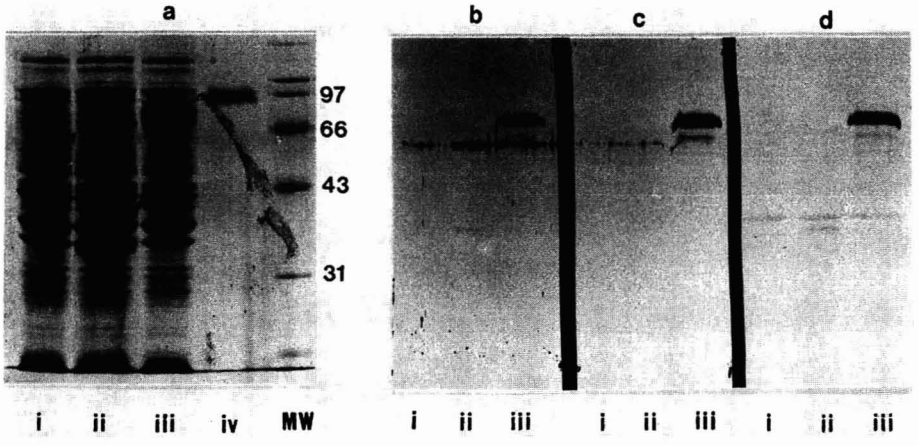

Fig. 5. Characterization of recombinant Bm86 expressed in *E.coli*. Cells were grown in TSB at 28°C and induced at 40°C. Samples were separated on a 10% SDS–polyacrylamide gel and either stained with Coomassie Brilliant Blue (a) or electroblotted onto nitrocellulose (b–d). Samples were from: lane i = host–vector control (N4830/pBTA 602); lane ii = cells expressing a truncated Bm86 (BTA 1753); lane iii = cells expressing full-length Bm86 (BTA1696); lane iv = purified Bm86. Nitrocellulose replicas were incubated with antiserum directed against pep 1 (b) pep 2 (c) and pep 3 (d). Molecular weight (MW) markers are given in kilodalton.

antibodies that are (a) specific for Bm86 and (b) recognise epitopes in both the NH_2 and COOH termini of the Bm86 and not other regions of the protein. All sera reacted, with varying degree, to several *E. coli* proteins present in all samples however pre-immune sera reacted similarly with these bands (data not shown). The sera should therefore be useful as site-directed reagents for the detection and characterization of Bm86 and proteolytically related products expressed by recombinant organisms.

Characterization of recombinant Bm86 expressed in Aspergillus nidulans

Full-length Bm86 expressed in *E. coli*[2] formed insoluble inclusion bodies and was therefore considered unlikely to posses the same tertiary structure as the glycosylated Bm86 present in ticks. It is more likely that Bm86 expressed and secreted by eukaryotic cells would be correctly folded and glycosylated and, as such, antigenically very similar to native Bm86. The filamentous fungus, *Aspergillus nidulans* has proved to be a useful eukaryotic expression system allowing the expression of a number of heterologous proteins[19–22]. Amino acid residues1–629 of Bm86 were expressed in *A. nidulans* under the *amdS* promotor system[13].

Secreted proteins from one transformant and a control were electrophoresed on polyacrylamide gels and stained with Coomassie Blue. A Bm86 standard was run in addition to molecular weight standards. A faint stained band of approximately 85 000 dalton was visible in the secreted products of the transformant (Fig. 6a). To demonstrate that this protein was Bm86 replicate Western blots were probed with antisera against pep 1, pep 2 and pep 3 and all reacted with the 85 000-dalton diffuse band (Fig. 6a–d). The molecular weight of the *Aspergillus* product is smaller than that of the Bm86 standard isolated from ticks (95 000 dalton); the predicted molecular weight from the DNA sequence is 70 000 dalton with the remainder being carbo-

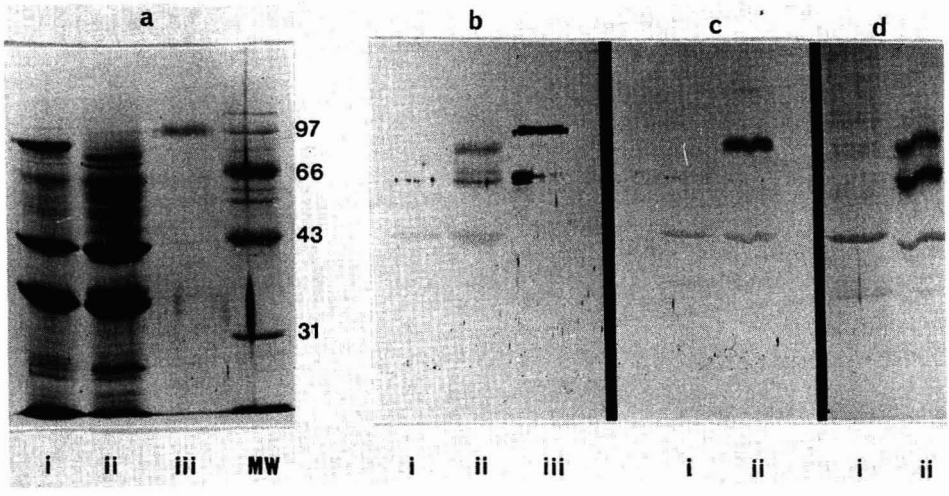

Fig. 6. Characterization of recombinant Bm86 expressed in *A. nidulans*. Culture media from mycelia was concentrated by ultrafiltration and samples were separated on a 10% SDS–polyacrylamide gel and either stained with Coomassie Brilliant Blue (a) or electroblotted onto nitrocellulose (b–d). Samples were from: lane i = wild-type control; lane ii = transformant expressing full length Bm86; lane iii = purified Bm86. Nitrocellulose replicas were incubated with antiserum directed against pep 1 (b), pep 2 (c) and pep 3 (d).

hydrate. As the native Bm86 may have an additional twenty COOH terminal amino acids which are not present in the *A. nidulans* expressed Bm86, it is probable that the latter is glycosylated but perhaps not as extensively as native Bm86. Careful examination of the immunoreactive bands in the *A. nidulans* culture supernatant shows that there are actually three bands bands of nearly identical molecular weight. This is a feature of many glycoproteins and presumably results from a common protein backbone that is differentially glycosylated. An additional band of approximately 55 000 dalton was present in Western blots probed with antiserum to pep 1 and pep 3 but was absent in blots probed with antiserum to pep 2. Such a result suggested the possibility that this band was a COOH terminal degradation product or a product of early termination of translation.

The above data showed that the antipeptide sera were universally reactive with full-length Bm86 when assayed under fully denaturing conditions. The following experiments were carried out to investigate the reactivity of the sera with oxidized recombinant Bm86.

Total secreted protein from cultures of wild-type control and Bm86 transformed *A. nidulans* strains was assayed by ELISA with Bm86 purified from ticks as standard. Antiserum raised against the NH_2-terminal pep 1 failed to react with either the secreted *A. nidulans* Bm86 or the purified, tick-derived Bm86. This may be explained by possible coupling of pep 1 to the carrier protein through the internal cysteines preventing the formation of the appropriate secondary structure. Antisera to pep 2 and pep 3 did recognise both antigens to varying extents (Table III) however the titre of antiserum to pep 2 against recombinant Bm86 was five fold lower than the titre against tick-derived Bm86. This may have been due to some degree of denaturation occurring during the purification of Bm86 from ticks; this was possible since

TABLE III

SPECIFICITY OF PEPTIDE ANTISERA

Abbreviations: W = Western blot; E = ELISA; An = *Aspergillus nidulans*; Bm = *Boophilus microplus*; IFA = Indirect Fluorescent Antibody test.

Immunising peptide	*Reactivity of antiserum with Bm86 produced by*[a]						*Biological Assay*[b]	
	BTA 1753	*BTA 1696*	*An*		*Bm*		*Tick gut IFA*	*In vitro damage*
	W	*W*	*W*	*E*	*W*	*E*		
pep 1	−	+	+	0	+	0	−	−
pep 2	−	+	+	0.1	+	0.5	−	−
pep 3	−	+	+	0.2	+	0.2	+	−

[a] Western blot titre defined as reactivity (+/−) of a 1:1,000 dilution of antiserum with 100 ng Bm86. ELISA titre defined as the OD measured at 414 nm using a 1:1000 dilution of the antiserum. Only antiserum from the most productive animal in each group was titred.

[b] Serum was evaluated for its ability to react in IFA with everted tick gut cells[1] and to elicit gut damage in ticks fed *in vitro*[14].

the use of a detergent was necessary in each step of the purification[1]. Alternatively, detergent molecules may bind to the hydrophobic anchor sequence or phosphatidylinositol linkage[2] present in tick-derived Bm86 (but not in the *A. nidulans*-derived Bm86) and expose epitopes located in the pep 2 region.

Immunofluorescence staining of tick gut cells using antipeptide sera

A previsous study[1] had shown that Bm86 was located on the surface of tick gut digest cells and could be visualized by an indirect fluorescent antibody test (IFA) using polyclonal antisera directed against the whole Bm86 isolated from ticks. Small pieces of everted tick gut were incubated with each of the antipeptide sera and then stained with a second antibody conjugated to fluorescein. Antibodies directed against the B-loop pep 3 bound weakly to the gut cell surface (Table III). The distribution of fluorescence was identical to that previously observed[1] using bovine antiserum directed against native Bm86. Antisera to pep 1 and pep 2 failed to stain significantly above pre-immune background levels. The difference in reactivity of the antiserum to pep 2 with Bm86 in ELISA compared with Bm86 *in situ* may possibly be due to steric interference since the pep 2 region in Bm86 is directly adjacent to the putative hydrophobic anchor sequence. Detergent solubilization would remove the Bm86 from the membrane and expose epitopes that are not accessible when the antigen is bound to the gut cell.

In vitro feeding

Antibodies directed against pep 3 were tested for their ability to produce gut damage in ticks fed *in vitro* on bovine serum. Despite their ability to bind to the cell-bound Bm86, the antibodies directed to pep 3 did not damage any of the ticks fed under standard conditions (Table III).

DISCUSSION

We have succesfully synthesized and purified four peptides for use in the immunological study and characterization of Bm86 and related recombinant products. Pep 1, pep 2 and pep 3 were synthesized in high yields and were readily purified to homogeneity by RP-HPLC or size-exclusion chromatography. In contrast, the crude pep 4 preparation recovered after synthesis was heavily contaminated with multiple methionine sulphoxide containing peptides and only after reduction with MMA was it clear that the peptide was the major product. Purified pep 3, with cysteine[37] replaced by an alanine residue, was oxidized and folded in dilute solution to form the intra-chain disulphide-bonded loop peptide.

Pep 1, pep 2 and pep 3 were coupled to carrier proteins and were immunogenic when used to vaccinate both rabbits and cows although titres varied considerably. All antipeptide sera specifically recognized epitopes within Bm86 or recombinant products (expressed in both prokaryotic and eukaryotic cells) as judged by reaction with reduced and denatured proteins in Western blots. The sera could be used in combination to check for the presence of proteolytically related products during expression testing.

Antisera to pep 2 and pep 3 also recognized Bm86 purified from ticks and Bm86 expressed in *A. nidulans* when tested under physiological conditions. This adds weight to the proposal that Bm86 expressed in *A. nidulans* was antigenically similar to the antigen produced by the tick. The failure of antiserum to pep 1 to recognise Bm86 in ELISA may be explained by possible coupling of pep 1 to the carrier protein through the two internal cysteines thus preventing the formation of the appropriate disulphide bonding present within the native Bm86. Alternatively, the pep 1 region within the native molecule may be concealed and unable to react with specific antibodies. The possibility that carbohydrate may be linked to serine and/or threonine within the pep 2 region of Bm86 (ref. 2) may need modification. As antibodies directed against pep 2 were reactive in both Western blot and ELISA, it is unlikely that the serine/threonine residues within this region are glycosylated.

Only antiserum to pep 3 recognised the native, cell-bound Bm86 as judged by IFA. The failure of antiserum to pep 2 to recognize cell-bound Bm86 may be explained by the extreme COOH-terminal location of this peptide within Bm86, abutting the 23 hydrophobic amino acid residues that presumably span the cell membrane. Antibodies directed to epitopes within this region may not bind the cell-bound Bm86 due to steric interference but are capable of binding upon removal of Bm86 from the membrane as is evident from the ELISA results. Alternatively, it is known that Bm86 is in relatively low abundance in the gut cell plasma membrane[1] so the IFA on whole cells is not likely to be a sensitive assay.

The presence of several EGF-like regions in Bm86 suggested that they may play an important role in the function of this molecule. Since pep 3 was the homologue to the B loop region of EGF responsible for cell binding[3], and could be targeted by antibodies *in vitro*, we speculated that antibodies against pep 3 may induce the gut damage evident when ticks are fed on blood from cows vaccinated with Bm86 (ref. 23) or disrupt an essential function of the molecule resulting in a decrease in the viability of the tick. The results of feeding ticks *in vitro* would seem to suggest that this may not be the case; despite the fact that antiserum to pep 3 bound to cell-bound Bm86 this

binding did not lead to any significant gut damage or reduction in tick viability. However, these effects may be titre dependent and it is known that *in vitro* damage is lost when sera are diluted only 1:5 (unpublished data). The immunofluorescent staining of gut cells with the antipeptide serum was considerably weaker than that seen with antiserum from cows vaccinated with native Bm86 (data not shown), so it is possible that this region may be more efficient if higher titre antibodies can be elicited. It is also possible that EGF-like domains other than the NH_2 terminal one are the targets of the protective immune response. In addition, tick viability can be more accurately assessed by *in vivo* feeding which will be undertaken in future studies.

ACKNOWLEDGEMENT

The authors are grateful to Ross Tellam for his expert advice and assistance.

REFERENCES

1 P. Willadsen, G. A. Riding, R. V. McKenna, D. H. Kemp, R. L. Tellam, J. N. Nielsen, J. Lahnstein, G. S. Cobon and J. M. Gough, *J. Immunol.*, 143 (1989) 1346.
2 K. N. Rand, T. Moore, A. Sriskantha, K. Spring, R. Tellam, P. Willadsen and G. S. Cobon, *Proc. Natl. Acad. Sci. U.S.A.*, 86 (1989) 9657.
3 A. Komoriya, M. Hortsch, C. Meyers, M. Smith, H. Kanety and J. Schlessinger, *Proc. Natl. Acad. Sci. U.S.A.*, 81 (1984) 1351.
4 E. Appella, E. A. Robinson, S. J. Ullrich, M. P. Stoppelli, A. Corti, G. Cassani, and F. Blasi, *J. Biol. Chem.*, 262 (1987) 443.
5 R. B. Merrifield, *J. Am. Chem. Soc.*, 85 (1963) 2149.
6 R. A. Houghton and C. H. Li, *Anal. Biochem.*, 98 (1979) 36.
7 G. L. Ellman, *Arch. Biochem. Biophys.*, 82 (1959) 70.
8 B. A. Bidlingmeyer, S. A. Cohen and T. L. Tarvin, *J. Chromatogr.*, 336 (1984) 93.
9 N. Green, H. Alexander, A. Olsen, S. Alexander, T. M. Shinic, I. G. Sutcliffe and R. A. Lerner, *Cell*, 28 (1982) 477.
10 A. Kagen and S. Glick, in B. M. Jaffe and H. R. Behrman (Editors), *Methods in Hormone Immunoassay*, Academic Press, New York, 1979, p. 327.
11 H. Towbin, T. Staehlin and J. Gordon, *Proc. Natl. Acad. Sci. U.S.A.* 76 (1979) 4350.
12 E. Engvall and P. Perlmann, *Immunochemistry*, 8 (1971) 871.
13 I. F. Turnbull, M. J. Hynes, D. R. J. Smith, G. S. Cobon and P. J. Sharp, *Appl. Environ. Microbiol.*, submitted for publication.
14 D. H. Kemp, R. I. S. Agbede, L. A. Y. Johnston and J. M. Gough, *Int. J. Parasitol.*, 16 (1986) 115.
15 T. P. Hopp and K. R. Woods, *Proc. Natl. Acad. Sci. U.S.A.*, 78 (1981) 3824.
16 G. Walter, K.-H. Scheidtmann, A. Carbone, A. P. Laudano and R. F. Doolittle, *Proc. Natl. Acad. Sci. U.S.A.*, 77 (1980) 5197.
17 H. Bayer, W. Gruber, J. Schneider and G. Hunsmann, *EMBO J.*, 3 (1984) 1925.
18 D. J. G. Rees, I. M. Jones, P. A. Handford, S. J. Walter, M. P. Esnouf, K. J. Smith and G. G. Brownlee, *EMBO J.*, 7 (1988) 2053.
19 D. Cullen, G. L. Gray, L. J. Wilson, K. J. Hayenga, M. H. Lamsa, M. W. Rey, S. Norton and R. M. Berka, *Bio/Technology*, 5 (1987) 369.
20 D. I. Gwynne, F. P. Buxton, S. A. Williams, S. Garven and R. W. Davies, *Bio/Technology*, 5 (1987) 713.
21 A. Upshall, A. A. Kumar, M. C. Bailey, M. D. Parker, M. A. Favreau, K. P. Lewison, M. L. Joseph, J. M. Maraganore and G. L. McKnight, *Bio/Technology*, 5 (1987) 1301.
22 I. F. Turnbull, K. Rand, N. S. Willetts and M. J. Hynes, *Bio/Technology*, 7 (1989) 169.
23 P. Willadsen, R. V. McKenna and G. A. Riding, *Int. J. Parasitol.*, 18 (1988) 183.

Journal of Chromatography, 512 (1990) 203–212
Elsevier Science Publishers B.V., Amsterdam

CHROMSYMP. 1835

Characterization of apolipoproteins from chicken plasma

ELEANOR M. BROWN* and HAROLD J. DOWER
Eastern Regional Research Center, Agricultural Research Service, U.S. Department of Agriculture, 600 E. Mermaid Lane, Philadelphia, PA 19118 (U.S.A.)

ABSTRACT

Although functionally similar, the lipoprotein systems of birds and mammals differ in composition. The major apolipoproteins, apo A-I and apo B, are common to all vertebrates; however apo A-II and apo E, functionally important components of mammalian lipoproteins, are absent from chicken plasma. Chicken apo A-I and apo B have been characterized, and several minor apolipoprotein components have been observed in electrophoretic patterns of chicken lipoproteins. In this study a single density gradient ultracentrifugation was used to isolate and subfractionate chicken lipoproteins into density classes. Isolated lipoproteins were delipidated with hexane–isopropanol (3:2). Apolipoproteins were then solubilized at pH 8.5 in 3 *M* guanidine hydrochloride and chromatographed on a 25 × 0.4 cm C_4 reversed-phase column using 0.1% trifluoroacetic acid in a gradient of acetonitrile in water. Molecular weights estimated by sodium dodecyl sulfate–polyacrylamide gel electrophoresis and amino acid compositions were compared with those of apolipoproteins from other species in a search for functional similarities. Similarities in composition between the major chicken apolipoprotein and several human apolipoproteins were observed.

INTRODUCTION

Plasma lipoprotein particles are the major vehicles for lipid transport in the circulatory systems of vertebrates. Lipoprotein profiles and compositions are important indicators of the nature of lipid metabolism in the organism. The chicken, *Gallus demosticus*, has long been considered a suitable animal model for comparative studies of lipid metabolism[1–4] because in both man and aves liver is the main site of *de novo* fatty acid synthesis. However, differences in lipid biosynthesis and transport between birds and man have been documented[5]. These differences include: porto-microns which transport dietary lipids from the gut directly to the liver[6], and a predominance of high-density lipoproteins (HDL) in the plasma of chickens other than the laying hen[7].

Human serum lipoproteins have been characterized in great detail. The major protein constituents of human HDL, apo A-I and apo A-II, are associated with minor amounts of the apo C proteins (-I, -II and -III), and apo E and apo D, each having

a particular function. Apo B with a molecular weight of about 500 000 dalton is the major protein component of low-density lipoproteins (LDL) and is also found in very-low-density lipoproteins (VLDL) from all species.

In the lower vertebrates, lipoproteins are generally characterized by density class following sequential flotation[8] or density gradient ultracentrifugation[9]. The individual lipoprotein classes are then described in terms of specific lipid moieties and total protein. Either of the commonly used centrifugation methods require at least 48 h of centrifuge time which may allow redistribution of lipoprotein components to occur. Accordingly, more rapid isolation techniques are needed for lipoprotein isolation and analysis.

The present study was undertaken to learn more about the mechanisms of lipid transport and deposition in the chicken where apo A-I and apo B have been characterized. Because counterparts to other human apolipoproteins have not been identified in chicken, it is reasonable to look for proteins which may perform the functions of the minor human proteins. A 4-h centrifugation technique[10], lipid extraction and reversed-phase high-performance liquid chromatography (HPLC) were combined to isolate the water-soluble apolipoproteins from the plasma of broiler chicks. These apolipoproteins were characterized by molecular weight and amino acid composition and compared to apolipoproteins from other species.

EXPERIMENTAL[a]

Materials

Five week old broiler chicks were maintained on a commercial diet at the U.S. Department of Agriculture Poultry Research Laboratory (Georgetown, DE, U.S.A.). After an overnight fast, blood was collected by heart puncture into tubes containing EDTA (1 mg/ml final concentration) and immediately placed on ice. Plasma was prepared from pooled blood of several chicks by centrifugation at 4°C, 2000 *g* for 10 min. To prevent degradation, sodium azide (0.20%), and reduced glutathione (0.5 μg/ml) were added to the plasma[11]. Buffer containing 10 m*M* Tris, 1.5 *M* NaCl, 1 m*M* EDTA, 0.1% NaN_3, 0.5 μg/ml reduced glutathione, and 1 m*M* phenylmethylsulfonyl fluoride at pH 8.5 (density, $d = 1.006$) was used throughout, with modifications as noted.

Lipoprotein isolation

Lipoprotein fractions were isolated from plasma by density gradient ultracentrifugation using the single vertical spin method described by Chung *et al.*[10]. A 10-ml volume of plasma was adjusted to a density of 1.35 g/ml by the addition of 5.94 g KBr and placed in a 40-ml Quickseal polyallomer tube (Beckman, Palo Alto, CA, U.S.A.). A peristaltic pump was used to layer 10 ml of buffer adjusted to 1.20 g/ml by the addition of 0.3265 g/ml KBr over the plasma. The tube was then filled with buffer ($d = 1.006$ g/ml) to a final volume of 40 ml and sealed. Ultracentrifugation was performed at 15°C in a Model L8-70 (Beckman Instruments) preparative ultra-

[a] Reference to a brand or firm name does not constitute endorsement by the U.S. Department of Agriculture over others of a similar nature not mentioned.

centrifuge in the slow acceleration mode using the VTi50 vertical rotor for 3.5 h at 50 000 rpm (242 000 *g*). After completion of the centrifugation, a 2-ml fraction containing VLDL was removed from the top of each tube with a Pasteur pipet, the tops were then cut off and the tubes emptied by upward flow fractionation using an HBI-Haake Buchler (Saddle Brook, NJ, U.S.A.) fraction recovery system. Fractions were separated on the basis of color, the refractive index of each fraction was measured, and the density calculated. Whole plasma and lipoprotein fractions were stained for lipid with Sudan Black, and electrophoresed on a discontinuous polyacrylamide-gel gradient (separating gel, 3.6%, spacer gel 2.5%, sample gel 3.3%) constructed in tubes as described by Naito and Wada[12].

Apolipoprotein preparation

Apoprotein fractions were prepared by extracting 2 ml of a lipoprotein fraction with 5 ml of hexane–isopropanol (3:2) (v/v) followed by 4 ml of hexane alone[13]. Aqueous layers were dialyzed in 3500 molecular weight cutoff tubing against buffer containing 3 *M* guanidinium hydrochloride (GdnHCl) to reduce the salt level while preventing precipitation of the apoproteins. Apolipoprotein fractions in 3 *M* GdnHCl were concentrated to about 4 mg/ml in an Amicon filter cell with a UM2 membrane (Amicon, Danvers, MA, U.S.A.).

Reversed-phase HPLC

A Varian (Sunnyvale, CA, U.S.A.) System 54 liquid chromatograph with a Bio-Rad (Richmond, CA, U.S.A.) Hi-Pore RP-304 reversed-phase column (25 × 0.4 cm I.D.) was operated at 50°C with a flow-rate of 1.2 ml/min. Elution of proteins from the column was monitored at 214 nm with a Varian UV-50 detector. Solvents used were: solvent A, 0.1% trifluoroacetic acid (TFA, Sequanal grade, Pierce, Rockford, IL, U.S.A.) in water; solvent B, 0.1% TFA in acetonitrile (HPLC grade, American Burdick and Jackson, Muskegon, MI, U.S.A.). The composition of the eluent was varied by two linear gradients, initially from 25 to 35% B at 5 min and then to 53% B at 30 min. At 33 min the concentration of B was increased to 75% for 10 min after which the column was reequilibrated to the starting conditions.

Characterization of proteins

Electrophoretic patterns of the apolipoprotein fractions were obtained by polyacrylamide gel electrophoresis in sodium dodecyl sulfate (SDS-PAGE) on an 8–25% gradient gel using the PhastGel System (Pharmacia, Piscataway, NJ, U.S.A.). Estimates of protein molecular weights were made by comparison with a standard protein mixture run at the same time. The composition of protein peaks separated by HPLC were determined by amino acid analysis. Fractions with identical elution times were collected from several HPLC runs, pooled and dried under nitrogen, then hydrolyzed in sealed evacuated tubes at 110°C for 24 h with 5.7 *M* HCl, containing 0.05% phenol[14]. Analyses were performed on a Beckman (Fullerton, CA, U.S.A.) 119 CL amino acid analyzer, using the standard 90-min single-column hydrolyzate protocol. Amino acid compositions of peak materials were compared with published compositions of apolipoproteins of other species using the algorithm of Cornish-Bowden[15] for relating proteins by amino acid composition. Compositions of proteins to be compared were obtained from the Protein Identification Resource (National

Biomedical Research Foundation, Washington, DC, U.S.A.), sequences are available for each of these proteins.

RESULTS AND DISCUSSION

Hermier *et al.*[16] showed that the lipoprotein classes of chicken plasma could be separated by density gradient ultracentrifugation. The single vertical spin technique[10] adapted here proved equally effective. VLDL ($d < 1.016$) formed a thin opalescent film on the top of each centrifuge tube. A layer of clear salt solution separated the VLDL from the LDL ($d = 1.020$–1.046) layer, a pale yellow, slightly turbid band. After a second clear, colorless layer of salt solution, the HDL ($d = 1.052$–1.130) fraction formed a clear deep yellow band. Separation of lipoprotein fractions after ultracentrifugation was aided by the carotenoid pigments associated with the LDL and HDL layers. The electrophoretic pattern (not shown) obtained for prestained whole plasma and fractions from the density gradient on discontinuous gels in tubes confirmed the separation. Electrophoresis was continued until the HDL fraction reached the bottom of the 3.6% separating gel, at this time the VLDL fraction remained at the interface between the sample gel and the spacer gel (2.5% acrylamide), the LDL fraction had entered the separating gel and moved about 10% of its length.

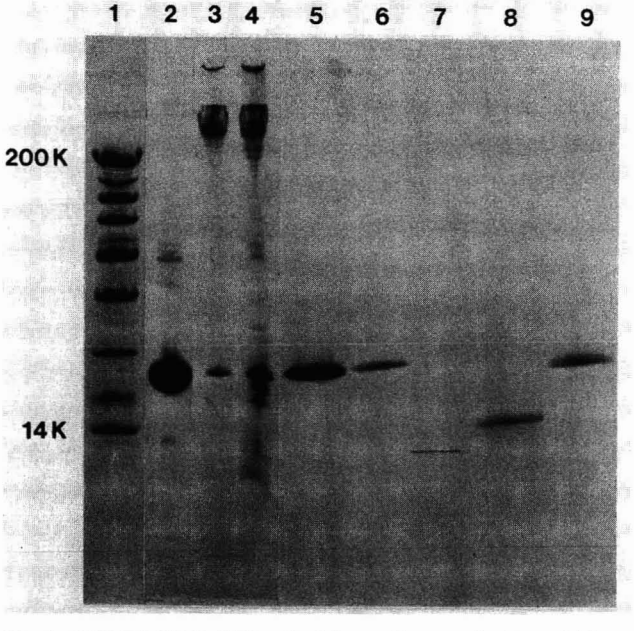

Fig. 1. SDS–PAGE (8–25% gel) of the apolipoproteins from chicken plasma. Molecular weight standards in lane 1 are from the top: myosin, 200 000; β-galactosidase, 116 250; phosphorylase *b*, 97 400; bovine serum albumin, 66 200; ovalbumin, 43 000; carbonic anhydrase, 31 000; soybean trypsin inhibitor, 21 500; lysozyme, 14 400. Lanes 2–4 are HDL, LDL and VLDL fractions after density gradient ultracentrifugation and delipidation. Lanes 5–9 are RP-HPLC fractions of the apolipoproteins: lane 5 is material from peak 5 (Fig. 2); lane 6 = peak 4; lane 7 = peak 3 (a very faint band with molecular weight of about 11 000 dalton; lane 8 = peak 2; lane 9 = peak 1. K = Kilodalton.

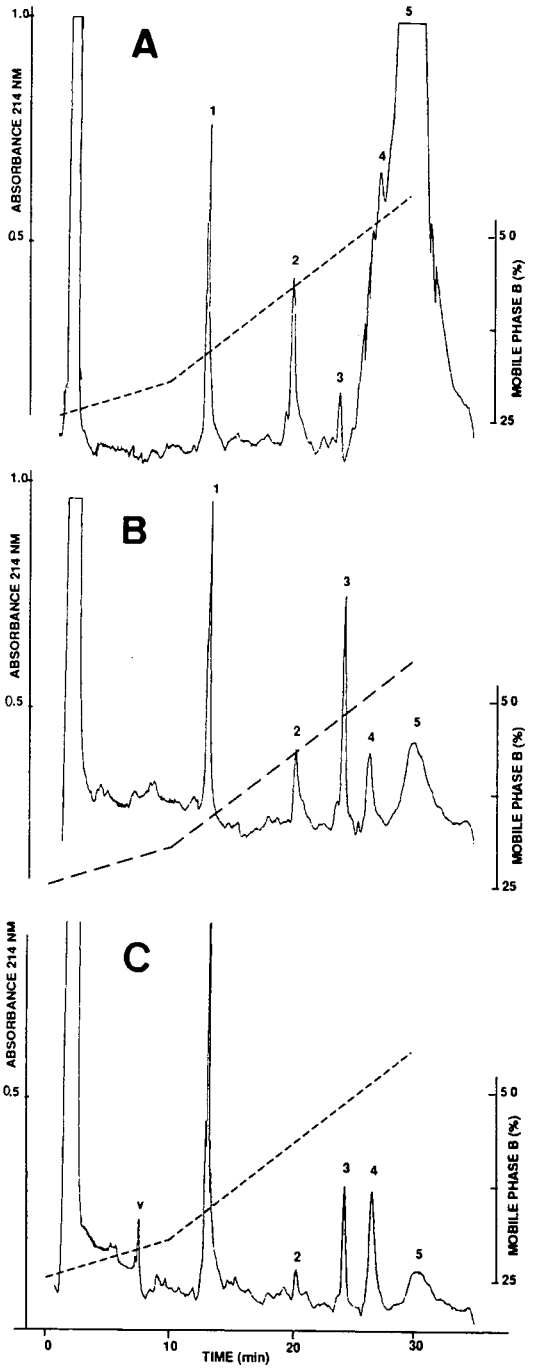

Fig. 2. Separation by RP-HPLC of apolipoproteins from chicken plasma. (A) HDL fraction; (B) LDL fraction; (C) VLDL fraction.

Extraction with lipid solvents removed carotenoid pigments as well, leaving colorless apoproteins in solution. The SDS-PAGE patterns obtained for centrifuged and extracted lipoprotein classes are shown in Fig. 1 (lanes 2–4). The apolipoproteins of chickens, as noted previously[16], are more uniformly distributed throughout the lipoprotein classes than are those of mammals. All fractions had a major band in the 25 000–30 000-dalton molecular weight range; both VLDL and LDL fractions had a smear of proteins or protein fragments with molecular weights greater than 200 000 dalton. HDL fractions had bands between 50 000 and 75 000 dalton which appear to be plasma proteins, not lipoproteins. These bands were more prominent in the electrophoretic patterns of fractions with $d > 1.130$. Several bands with molecular weights lower than 20 000 dalton were also apparent when the gels were heavily loaded.

Fig. 2 shows the HPLC chromatograms of the apolipoproteins from each of the lipoprotein classes. The soluble protein content of HDL and LDL was separated into five peaks eluting between 13 and 29 min. The same five peaks appeared in the chromatogram of VLDL, along with a small additional peak at 8.3 min. Fig. 1 (lanes 5–9) shows the electrophoretic patterns of the peak material from the HPLC experiments. Table I summarizes the molecular weights and relative amounts of the proteins in each class. Apo B and the high-molecular-weight fragments apparent on SDS-PAGE were not sufficiently soluble even in 3 *M* Gdn HCl to be isolated by the HPLC technique.

The amino acid compositions of peak material from each of the five major HPLC bands are given in Table II. Mean residue weights and average hydrophobicities[17] are included to emphasize differences in composition. Larger amino acid residues tend to be more hydrophobic than smaller ones, so it is not surprising that both the mean residue weight and the average hydrophobicity are positively correlated with retention volume on the reversed phase column.

Table III gives $S\Delta n$ values for comparison of the amino acid composition of the protein in each chromatographic peak with lipoproteins of known composition and with each other. The $S\Delta n$ values were calculated with the formula derived by Cornish-Bowden[15]:

TABLE I

DISTRIBUTION OF APOLIPOPROTEINS

Peak[a]	*Elution time (min)*[b]	*Molecular weight*[c]	*Peak area*		
			HDL	*LDL*	*VLDL*
v[d]	8.28				0.055
1	13.37 ± 0.11	22 300	0.021	0.072	0.228
2	20.06 ± 0.51	14 200	0.032	0.091	0.179
3	23.35 ± 0.65	11 400	0.005	0.152	0.196
4	25.92 ± 0.36	25 500	0.132	0.150	0.172
5	29.00 ± 0.42	23 500	0.809	0.535	0.169

[a] Peak numbers are referenced to the chromatograms in Fig. 2.
[b] Elution times are the average for HDL, LDL and VLDL with variation.
[c] Molecular weights are estimated from the SDS-PAGE, see Fig. 1.
[d] Insufficient material to obtain molecular weight or amino acid composition for this peak.

TABLE II

AMINO ACID ANALYSIS

Amino acid	*Mole%*[a]				
	Peak 1	*Peak 2*	*Peak 3*	*Peak 4*	*Peak 5*
Ala	5.9	6.7	8.0	8.8	8.5
Arg	6.9	4.8	2.4	7.6	7.8
Asp	9.9	7.1	8.6	7.1	7.0
Cys	0.0	0.0	0.0	1.7	0.7
Glu	11.8	17.5	14.9	20.8	20.9
Gly	15.5	14.1	9.3	2.8	1.8
His	2.6	3.9	4.7	0.4	0.3
Ile	3.1	2.2	1.8	2.2	2.0
Leu	8.2	9.0	8.1	13.9	14.4
Lys	2.4	4.2	7.5	9.4	9.9
Met	0.0	0.0	0.0	0.1	1.5
Phe	4.1	3.8	4.1	2.2	2.2
Pro	5.8	5.4	0.0	5.6	6.4
Ser	8.5	10.1	11.2	4.3	4.1
Thr	7.0	6.0	8.2	4.9	4.4
Tyr	1.1	2.1	2.3	3.0	2.9
Val	7.2	3.0	7.8	5.2	5.3
mrw[b]	104.69	106.45	108.20	114.59	115.82
Hb[c]	1.00	0.95	0.94	1.20	1.24

[a] Based on the average of three sets of chromatographic experiments.
[b] mrw = the mean residue weight for the protein.
[c] Hb = the average hydrophobicity[17].

$$S\Delta n = 0.5\sum(n_{iA} - n_{iB})^2$$

where n_{iA} *and* n_{iB} are the mole fraction of residue (i) in protein A or B respectively. $S\Delta n < 0.42$ is a strong indication of relatedness for proteins A and B, while $S\Delta n > 0.93$ suggests no relatedness for the two proteins[15]. The requirement that proteins to be compared must be of equivalent size[15] has been relaxed somewhat in the calculations reported here because it is reasonable to anticipate some degree of relatedness among a single class of proteins.

For all three lipoprotein classes, the protein in peaks 4 and 5 is mostly apo A-I[18]. Multiple HPLC peaks for human apo A-I have been attributed to the presence of multiple oxidation states for methionine and considered to be an artifact of preparation[11]. The compositions of these two peaks correlated very strongly with each other (Table IV) and with apo A-I from chicken[18] ($S\Delta n = 0.07$ and 0.05), and humans[19] ($S\Delta n = 0.15$ and 0.17). Peaks 4 and 5 also correlated moderately with human[20] ($S\Delta n = 0.47$ and 0.52) and *Rhesus macaque*[21] ($S\Delta n = 0.58$ and 0.62) apo A-II and with human[22] ($S\Delta n = 0.57$ and 0.63) and rat[23] ($S\Delta n = 0.53$ and 0.57) apo E. These peaks had a very weak correlation with human apo C-II[24] ($S\Delta n = 0.92$ and 0.99). In contrast human apo A-II, apo E and apo C-II are not compositionally related ($S\Delta n = 1.1$ to 1.7). Thus, the functions of these minor HDL apoproteins which are apparently absent in chickens may be incorporated into avian apo A-I.

TABLE III

COMPARISON OF ISOLATED CHICKEN PROTEINS WITH APOLIPOPROTEINS OF OTHER SPECIES

Comparison of the amino acid composition of each HPLC peak from chicken apolipoprotein is with sequenced apolipoproteins. C A-I = chicken apolipoprotein A-I[18]; H A-I = human apo A-I[19]; H A-II = human apo A-II[20]; M A-II = *Rhesus macaque* apo A-II[21]; R A-IV = rat apo A-IV[29]; H A-IV = human apo A-IV[30]; H C-I = human apo C-I[31]; H C-II = human apo C-II[24]; H C-III = human apo C-III[25]; H D = human apo D[32]; H E = human apo E[22]; R E = rat apo E[23]; C Vit = chicken apovitellenin[26].

Peak	*Molecular weight (dalton)*	*SΔn values*[15]												
		C A-I, 28 000	*H A-I, 28 000*	*H A-II, 9000*	*M A-II, 9000*	*R A-IV, 42 000*	*H A-IV, 42 000*	*H C-I, 7000*	*H C-II, 9000*	*H C-III, 9000*	*H D, 21 000*	*H E, 34 000*	*E E, 34 000*	*C Vit 9000*
1	22 000	1.96	1.59	1.86	2.06	1.73	1.98	2.34	1.82	1.53	1.27	2.12	1.71	1.38
2	14 000	1.41	1.05	1.25	1.40	4.26	4.17	1.79	1.21	1.32	1.52	1.50	1.34	1.71
3	11 000	1.28	0.98	0.83	0.89	3.60	3.63	1.17	0.75	0.52	1.15	1.79	1.56	1.11
4	25 000	0.07	0.15	0.47	0.58	4.52	4.51	1.09	0.92	1.55	1.21	0.57	0.53	1.06
5	23 000	0.05	0.17	0.52	0.62	4.06	4.07	1.11	0.99	1.68	1.29	0.63	0.57	1.16

TABLE IV

INTERNAL COMPARISON OF PROTEIN COMPOSITIONS

Peak numbers refer to HPLC traces.

Peak	*SΔn values*[15]				
	Peak 1, 22 000	*Peak 2, 14 000*	*Peak 3, 11 000*	*Peak 4, 24 000*	*Peak 5 25 000*
1	0				
2	0.37				
3	0.77	0.56			
4	1.91	1.30	1.32		
5	2.14	1.51	1.54	0.03	0

The composition of peak 3 correlated weakly with apo A-II ($S\Delta n$ = 0.82 and 0.89) and somewhat more strongly with apo C-II ($S\Delta n$ = 0.75) and apo C-III ($S\Delta n$ = 0.52). As these proteins are all in the 9000–12 000 daltons molecular weight range peak 3 protein may represent a real homologue with apo C-III[25], apo C-II, or apo A-II, and should be examined further. Alternatively, this similarity may imply a lipase activator role for peak 3 protein as has been demonstrated for human apo A-II[26] and apo C-II[24]. Proteins in peaks 1 and 2 were not correlated with any mammalian proteins, yet these two are apparently related to each other (Table IV). No other significant correlations with mammalian apolipoproteins were observed.

The poor correlation ($S\Delta n$ = 1.06 to 1.70) between any of the isolated apolipoproteins from broiler chick plasma and apovitellenin[27] is notable because this egg yolk lipoprotein has been isolated from the lipoprotein fraction of plasma from laying hens[28].

By reducing the time during which the various classes of lipoproteins were in contact with each other, the single vertical spin ultracentrifugation employed in this study should minimize the redistribution of components. Nevertheless, except for apo B which was not detected in the HDL fractions, the apolipoproteins were distributed among all density classes. The relative proportions were in general agreement with previous studies of chicken plasma lipoproteins[16]. The HPLC technique, however, gives a rapid profile of the soluble apolipoproteins in each density class and can generate samples for electrophoresis and amino acid analysis more rapidly than traditional separation techniques. The technique could easily be applied to a comparison of apolipoproteins from a variety of species. It also may provide a rapid, sensitive method for following changes in apolipoprotein distribution as affected by disease or dietary changes.

ACKNOWLEDGEMENT

The authors wish to thank Hein Le for technical assistance.

REFERENCES

1 L. A. Hillyard, H. M. White and S. A. Pangburn, *Biochemistry*, 11 (1972) 511.
2 K. L. Luskey, M. S. Brown and J. L. Goldstein, *J. Biol. Chem.*, 249 (1974) 5939.
3 D. J. Kudzma, J. B. Swaney and E. N. Ellis, *Biochim. Biophys. Acta*, 572 (1979) 257.
4 A. W. Kruski and K. A. Narayan, *Lipids*, 7 (1972) 742.
5 M. J. Chapman, *J. Lipid Res.*, 21 (1980) 789.
6 A. Bensadoun and A. Rothfeld, *Proc. Soc. Exp. Biol. Med.*, 141 (1972) 814.
7 J. Y-L Yu, L. D. Campbell and R. R. Marquardt, *Poult. Sci.*, 55 (1976) 1626.
8 R. J. Havel, H. A. Eder and J. H. Bragdon, *J. Clin. Invest.*, 34 (1955) 1345.
9 M. J. Chapman, *J. Lipid Res.*, 22 (1981) 339.
10 B. H. Chung, T. Wilkinson, J. C. Geer and J. P. Segrest, *J. Lipid Res.*, 21 (1980) 284.
11 T. A. Hughes, M. A. Moore, P. Neame, M. F. Medley and B. H. Chung, *J. Lipid Res.*, 29 (1988) 363.
12 H. K. Naito and M. Wada, in L. A. Lewis and J. J. Opplt (Editors) *Handbook of Electrophoresis*, Vol. 1, CRC Press, Boca Raton, FL, 1980, p. 183.
13 N. S. Radin, *Methods Enzymol.*, 72 (1981) 5.
14 E. M. Brown, H. J. Dower and R. Greenberg, *J. Chromatogr.*, 443 (1988) 247.
15 A. Cornish-Bowden, *Methods Enzymol.*, 91 (1983) 60.
16 D. Hermier, P. Forgez and M. J. Chapman, *Biochim. Biophys. Acta*, 836 (1985) 105.
17 C. C. Bigelow and M. Channon, in G. D. Fasman (Editor), *CRC Handbook of Biochemistry and Molecular Biology, Proteins*, Vol. I, CRC Press, Cleveland, OH, 1976, p. 209.
18 C.-Y. Yang, Z.-W. Gu, W. Patsch, S.-A. Weng, T. W. Kim and L. Chan, *FEBS Lett.*, 224 (1987) 261.
19 H. B. Brewer, Jr., T. Fairwell, A. LaRue, R. Ronan, A. Houser and T. J. Bronzert, *Biochem. Biophys. Res. Commun.*, 80 (1978) 623.
20 S. E. Lux, K. M. John, R. Ronan and H. B. Brewer, Jr., *J. Biol. Chem.*, 247 (1972) 7519.
21 C. Edelstein, C. Noyes, P. Keim, R. L. Heinrikson, R. E. Fellows and A. M. Scanu, *Biochemistry*, 15 (1976) 1262.
22 S. C. Rall, Jr., K. H. Weisgraber and R. W. Mahley, *J. Biol. Chem.*, 257 (1982) 4171.
23 J. W. McLean, C. Fukazawa and J. M. Taylor, *J. Biol. Chem.*, 258 (1983) 8993.
24 A. V. Hospattankar, T. Fairwell, R. Ronan and H. B. Brewer, Jr., *J. Biol. Chem.*, 259 (1984) 318.
25 H. B. Brewer, Jr., R. Shulman, P. Herbert, R. Ronan and K. Wehrly, *J. Biol. Chem.*, 249 (1974) 4975.
26 C. E. Jahn, J. C. Osborn, Jr., E. J. Schaefer and H. B. Brewer, Jr., *FEBS Lett.*, 131 (1981) 366.
27 A. Dugaiczyk, A. S. Inglis, P. M. Strike, R. W. Burley, W. G. Beattie and L. Chan, *Gene*, 14 (1981) 175.
28 R. L. Jackson, H.-Y. Lin, L. Chan and A. R. Means, *J. Biol. Chem.*, 252 (1977) 250.
29 M. S. Boguski, N. Elshourbagy, J. M. Taylor and J. I. Gordon, *Proc. Nat. Acad. Sci. USA*, 81 (1984) 5021.
30 C-y. Yang, Z-W. Gu, I. Chong, W. Xiong, M. Rosseneu, H-x. Yang, B-r. Lee, A. M. Gotto, Jr. and L. Chan, *Biochim. Biophys. Acta*, 1002 (1989) 231.
31 R. L. Jackson, J. T. Sparrow, H. N. Baker, J. D. Morrisett, O. D. Taunton and A. M. Gotto, Jr., *J. Biol. Chem.*, 249 (1974) 5308.
32 D. Drayna, C. Fielding, J. McLean, B. Baer, G. Castro, E. Chen, L. Comstock, W. Henzel, W. Kohr, L. Rhee, K. Wion and R. Lawn, *J. Biol. Chem.*, 261 (1986) 16535.

Journal of Chromatography, 512 (1990) 213–218
Elsevier Science Publishers B.V., Amsterdam

CHROMSYMP. 1785

Rapid high-performance liquid chromatographic protein quantitation of purified recombinant Factor VIII containing interfering substances

WERNER SCHRÖDER
Bayer AG, Wuppertal (F.R.G.)
and
MICHAEL L. DUMAS* and UDO KLEIN
Miles Inc., Cutter Biological, 4th & Parker Streets, P.O. Box 1986, Berkeley, CA 94701 (U.S.A.)

ABSTRACT

A simple and rapid high-performance liquid chromatography method for the quantitative estimation of protein content in highly purified recombinant Factor VIII (rFVIII) solutions containing substances which interfere in other methods has been developed. The method is an adaptation of a procedure [Stoffel *et al.*, *Hoppe-Seyler's Z. Physiol. Chem.*, 363 (1982) 1117] described for separating peptides from tryptic digests. Many detergents, stabilizing reagents, amino acids, or high salts may interfere in the more common protein determination assays, such as the Lowry, Bradford, bicinchoninic acid or A_{280} nm reading. This simple high-performance liquid chromatography method separates protein from interfering substances, such as amino acids, detergents, and high salts by size-distribution chromatography in the presence of 90% formic acid. The 90% formic acid mobile phase is an extremely effective solvent for proteins, including any aggregated protein which may be present. The formic acid dissociates non-covalent bonding and allows the proteins to move in a gel permeation system as a single peak which is well separated from UV interfering substances. Sample preparation is not necessary. Quantitation is based upon UV absorbance at 280 nm using a protein standard similar to the sample being quantitated. When analyzing highly purified proteins, the standard may be assigned a protein content based upon the amino acid composition of that protein. The method is accurate, fast, reproducible and relatively easy to perform.

INTRODUCTION

Protein assays such as the Lowry, Bradford, bicinchoninic acid (BCA) or A_{280} are affected by interfering substances[1]. Plasma-derived Factor VIII of recombinantly engineered Factor VIII (rFVIII) is an inherently unstable protein which requires the addition of stabilizers during its purification. The presence of these stabilizers pre-

0021-9673/90/$03.50

cludes the use of the classical protein quantitation methods. Sample manipulation such as dialysis or gel filtration to remove the interfering substances is unreliable, because of potential diminution of biological activity or absorptive protein losses. In order to assay unaltered rFVIII, it was necessary to develop an alternative method of quantitation which required no sample preparation.

This paper describes the simple and rapid quantification of highly purified rFVIII by high-performance gel chromatography in 90% formic acid. The method described is a high-performance liquid chromatography (HPLC) procedure which separates protein from interfering excipients and stabilizers with a molecular weight $\geqslant$ 12 500 dalton by size distribution. The mobile phase, 90% formic acid, dissociates non-covalent bonding and allows the protein to move in the gel permeation system as a single peak well separated from other UV-absorbing substances. Quantitation is determined by the peak area of the protein as measured at 280 nm and the results are expressed in μg/ml based on a standard curve generated with a rFVIII standard. Although this paper focuses on rFVIII, the procedure should be readily adaptable to other proteins such as human serum albumin and haptoglobin which were used to develop the assay.

MATERIALS AND METHODS

Apparatus and materials

The liquid chromatograph consisted of a Model 114 M constant-flow solvent pump, a Model 160 UV-absorbance detector equipped with a 280-nm filter and low-volume analytical flow cell, and a Model 340 system organizer fitted with a Model 7125 sample injector containing a 10-μl fixed loop (Beckman-Altex, San Ramon, CA, U.S.A.). The sample injector was a product of Rheodyne (Cotati, CA, U.S.A.). The LiChrosorb Si-100, 10 μm column (250 mm $\times$ 7 mm I.D.) was purchased from Alltech (Deerfield, IL, U.S.A.). An Uptight, short column (2 cm $\times$ 4 mm I.D., Upchurch, Oak Harbor, WA, U.S.A.) packed with pellicular silica (Alltech) served as the guard column. A Hewlett-Packard (Palo Alto, CA, U.S.A.) Model HP3393A digital electronic integrator plotted and integrated the signals received from the UV detector. The mobile phase, 90% formic acid, was prepared by diluting 900 ml of GR-grade formic acid (EM Science, Cherry Hill, NJ, U.S.A.) with 100 ml of HPLC-grade water (J. T. Baker, Phillipsburg, NJ, U.S.A.). The 90% formic acid solution was filtered through a 0.2-μm, 47 mm diameter polycarbonate membrane filter (Poretics, Livermore, CA, U.S.A.) using a 1-l ground-glass joint flask equipped with a 300-ml glass funnel and tubulated base (Millipore, Milford, MA, U.S.A.).

Chromatographic conditions

The mobile phase was 90% formic acid in HPLC-grade water. The flow-rate was 1.0 ml/min. The detector sensitivity was set at 0.020 a.u.f.s. (at 280 nm), the chart speed was 0.5 cm/min, and the temperature was ambient. A25-μl volume of sample was injected manually into the 10-μl sample loop using a Hamilton (Reno, NV, U.S.A.) blunt-tipped syringe. Prior to the next injection, the injector loop was rinsed with 250 μl of 90% formic acid to insure that there is no sample carryover.

Proteins

Human serum albumin (Sigma, St. Louis, MO, U.S.A.), 1 mg/ml was prepared by dissolving 10 mg into 10 ml of 50 m*M* sodium phosphate, 150 m*M* sodium chloride pH 7.2 buffer. Human haptoglobin (Sigma), 2 mg/ml was dissolved into 50 m*M* sodium phosphate, 150 m*M* sodium chloride, 1 m*M* EDTA, pH 7.1 buffer (PBS). Horse heart cytochrome *c* (Pierce, Rockford, IL, U.S.A.), 1 mg/ml was prepared by dissolving 1.12 mg into 1.12 ml of PBS. Horse spleen ferritin (Pierce), 10 mg/ml was diluted 1:10 with PBS to attain a 1.0 mg/ml solution. Insulin (Eli Lilly, Indianapolis, IN, U.S.A.), 5 mg/ml was diluted 1:5 with PBS for a final concentration of 1.0 mg/ml. The rFVIII samples were obtained during purification of this product for clinical evaluation[2].

Interfering substances

All of the reagents used in this study were known to interfere with at least one of the following protein assays: Coomassie blue (Bradford), Lowry, Biuret, BCA or A_{280} (refs. 1 and 3). The reagents were all ACS grade or equivalent. The stock solutions were prepared with water suitable for injection (WFI) or the appropriate buffer. The reagents investigated in this study included: Nonidet-P-40 (Sigma), sodium dodecylsulfate (SDS; Bio-Rad, Richmond, CA, U.S.A.), glycerol (Sigma), Thimerosal (Sigma), Tris (Sigma), Guanidine · HCl (Sigma), Tween-80 (Sigma, calcium chloride (J. T. Baker), imidazole (Kodak, Rochester, NY, U.S.A.), and L-tryptophan (Calbiochem, La Jolla, CA, U.S.A.).

Interfering substance study

Human serum albumin (HSA) at 1.0 mg/ml was diluted 1:10 with WFI to serve as the control for this study. HSA was also diluted 1:10 with the various interfering substances. Aliquots (25 μl) of the HSA samples were injected into the 10-μl fixed-loop injector and applied to the column. Injections of the various reagents without HSA were also made. All samples were run in duplicate or triplicate. The mean peak area of the sample containing interfering substances was divided by the mean peak area of the HSA control sample to determine the amount of interference (if any).

Protein retention time study

Aliquots (25 μl) of ferritin, cytochrome *c*, HSA, haptoglobin and insulin were individually injected into the 10μl loop and subsequently injected into the column. A pool of equal amounts of ferritin, cytochrome *c*, HSA and haptoglobin was made and a 25-μl injection of the pool was carried out. A pool of HSA and insulin was also injected into the column. The retention times for all samples in this study were recorded.

Quantitation of rFVIII

A pool of approximately twenty-five 1-ml aliquots of highly purified (>90%) rFVIII was made. A protein concentration value was assigned to the pool by performing amino acid analysis on an aliquot of the pool. The rFVIII standard pool was diluted with buffer to obtain a final concentration of 160 μg/ml. This stock solution is subsequently serially diluted with buffer to generate standards at 80, 40 and 20 μg/ml. A known amount of standard per 10 μl was injected. The peak area is directly related

to the amount of standard injected and is expressed as peak area × 10^4 per μg per 10 μl. Each standard curve point is made in duplicate unless where triplicate may be necessary. The mean ($\bar{x}$) peak area × 10^4 value is plotted *vs.* their respective μg load and calculated according to linear regression. The resulting y intercept and slope are used to calculate the $\bar{x}$ peak area × 10^4 values of the unknowns by the straight line formula $y = ax + b$. Controls are run with each assay to monitor intra-assay variation.

RESULTS AND DISCUSSION

Interfering substances

The combination of 90% formic acid as the mobile phase and LiChrosorb Si-100 as the analytical column allows for the separation of interfering substances from proteins. The formic acid dissociates non-covalent bonding associated with protein–protein interactions or protein–interfering substance interactions. This environment allows for the separation of proteins from low-molecular-weight substances by size-exclusion chromatography. Fig. 1a is a typical chromatogram demonstrating the elution position of the interfering substance, tryptophan. All the interfering substances listed in Table I had a retention time between 6 and 9 min. Fig. 1b shows the separation of tryptophan from human serum albumin. The presence of any of the interfering substances did not alter the chromatographic profile or retention time of HSA. Fig. 1c is a chromatogram of the integrated protein peak only, the plotter/integrator was stopped before the tryptophan eluted from the column. This system of evaluation (*i.e.*, HSA with and without additives) was carried out for each of the interfering substances described in this paper. The results (Table I) indicate that the substances known to interfere in other protein assays do not interfere in this assay. Since there are many substances known to interfere with one or more of the other protein assays, it was beyond the reasonable scope of this paper to evaluate each one. However, the results reported in this paper indicate that this method should be adaptable to many of the other known interfering substances of various protein assays.

Protein retention time

The proteins selected for this study were chosen because they represented a wide molecular weight range of 6 000–450 000 dalton. One of the objectives was to deter-

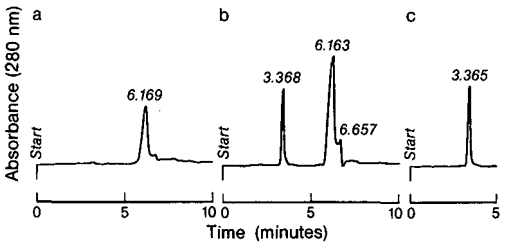

Fig. 1. HPLC chromatograms of (a) tryptophan, (b) human serum albumin and tryptophan and (c) human serum albumin as the only peak integrated and plotted. Mobile phase: 90% formic acid. Flow-rate: 1.0 ml/min. Chart speed: 0.5 cm/min. Detector: 0.02 (280 nm).

TABLE I

LABORATORY REAGENTS KNOWN TO SIGNIFICANTLY INTERFERE IN COMMON PROTEIN ASSAYS

Sample additive[a]	*Deviation from known concentration (%)*[b]
Nonidet-P-40 (0.9%)	− 3.2
SDS (0.9%)	0
Glycerol (13.5%)	+ 2.5
Thimerosal (0.9%)	+ 1.6
Tris (0.9 *M*)	− 5.1
Guanidine · HCl (3.6 *M*)	− 10.2
Tween-80 (0.09%)	+ 10.0
$CaCl_2$ (0.9 *M*)	− 9.9
Imidazole (180 m*M*)	− 8.1
L-Tryptophan (0.9 mg/ml)	− 5.0

[a] HSA sample contained these additives at the listed concentrations.
[b] Deviations ⩽ 10% are considered not significant. The percent deviation was determined by comparing the HSA additive samples with the HSA control which contained no additives.

mine the molecular weight at which separation of proteins occurs. Insulin (6000 dalton) had the only significantly different retention time (Table II). The other proteins shared nearly identical retention times as did a pool of 4 proteins. This information allowed us to conclude that the method is suitable for proteins with a molecular weight greater than 12 500 dalton. The advantage of this system is that the proteins elute as a single peak which allows for easy quantification of the peak area. Since insulin is baseline separated from the HSA (Fig. 2a–c), it is reasonable to assume that one could still quantitate the protein peak and/or the insulin peak. However, that type of assay would require a more complex standard.

Quantitation of rFVIII

The need to determine an accurate specific activity of rFVIII greatly influenced the development of this assay. The essential requirements for the assay included

TABLE II

RETENTION TIMES OF SIX PROTEINS

Protein	*Molecular weight (dalton)*	*Retention time (min)*
Insulin	6000	4.506
Cytochrome *c*	12 500	3.342
HSA	66 500	3.365
rFVIII	220 000	3.350
Haptoglobin	86 000–400 000	3.330
Ferritin	450 000	3.368
Pool of haptoglobin, HSA, ferritin. cytochrome *c*	12 500–450 000	3.348

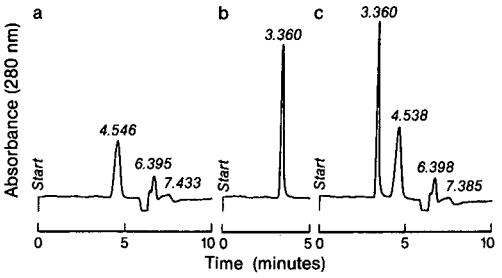

Fig. 2. HPLC chromatogram of (a) insulin, (b) human serum albumin and (c) human serum albumin plus insulin. Chromatographic conditions as in Fig. 1.

accuracy, sensitivity, small sample volume, reproducibility, and no sample preparation. Sample preparation, such as dialysis, can result in absorptive losses of protein and/or loss of biospecific activity of the sample. Such losses result in an inaccurate estimation of the sample's biospecific activity. Because highly purified rFVIII solutions contain substances that interfere with the more commonly used protein assays, it was imperative that the rFVIII sample could be assayed without any type of preparation. To insure that this assay was accurate, we prepared a rFVIII standard that was similar in composition to our rFVIII samples. This standard was subjected to amino acid composition analysis and assigned a protein concentration.

A typical linear regression curve generated by one of our rFVIII standards involving 32 separate experiments resulted in a coefficient of variation (C.V.) for each of the 4 standard curve points of 4.0–11.4%. The correlation coefficient was 0.9999. The C.V. for 26 separate intra-assay control samples was 6.25%, an indication of excellent reproducibility. The standard curve range reported in this paper covers 0.2–1.6 μg/10 μl injection. The range could be adjusted lower or higher to fit individual assay requirements. Typically, less than 100 μl sample is required to run in triplicate.

The HPLC protein assay using formic acid is easy to use, and it generates results quickly. Each run takes only 8 min when the flow-rate is 1 ml/min. The method can be automated. Very accurate sample protein content can be obtained, if a well defined standard similar to the sample of interest is used. Since sample preparation is not necessary, a direct relationship between protein content and protein biological activity can be made. This allows for a highly accurate estimation of biospecific activity.

REFERENCES

1 E. M. Davis, *Am. Biotech. Lab.*, (1988) 28.
2 J. J. Sixma (Editor), *First International Symposium on Recombinant Factor VIII, Proc. XIIth Congress of the International Society on Thrombosis and Haemostasis, Tokyo, August 26, 1989*, Schattauer, Stuttgart, New York, 1989, in press.
3 M. A. Phelan, J. W. Hall and R. E. Mayner, *Biotechniques*, 4 (1986) 130.
4 W. Stoffel, W. Schröder, H. Hillen and R. Deutzmann, *Hoppe-Seyler's Z. Physiol. Chem.*, 363 (1982) 1117.

Journal of Chromatography, 512 (1990) 219–226
Elsevier Science Publishers B.V., Amsterdam

CHROMSYMP. 1812

Purification of membrane protein complexes isolated from a cyanobacterial thylakoid membrane by high-performance liquid chromatography

MATTHIAS RÖGNER
E.I. du Pont de Nemours & Co., Experimental Station, CR&D Department, P.O. Box 80173, Wilmington, DE 19880-0173 (U.S.A.)

ABSTRACT

Reaction centers of photosystem I, photosystem II and a genetically altered photosystem II and the cytochrome b_6f complex have been isolated from the thylakoid membrane of the cyanobacterium *Synechocystis* PCC 6803 and purified by two high-performance liquid chromatography steps. For comparison, both steps (*i.e.* an anion-exchange and a hydroxyapatite column chromatography) have been performed on different columns, including 5-μm-particle-size material. Protein complexes purified according to the optimized high-performance liquid chromatography procedure retained their biological activity and were characterized for homogeneity and apparent molecular mass by gel high-performance chromatography.

INTRODUCTION

The photosynthetic electron transport chain, located in the thylakoid membrane of cyanobacteria, algae and higher plants, consists of three major membrane-spanning protein complexes —the photosystem I reaction center (PS I RC), the photosystem II reaction center (PS II RC) and the cytochrome b_6f complex— which are interconnected by mobile electron carriers. The overall process finally leads to the oxidation of water at the PS II RC and the reduction of $NADP^+$ at the ferredoxin/NADP oxidoreductase. For further elucidation of the complicated structure–function relationships, these three membrane-spanning multisubunit complexes are needed in an isolated and highly purified form. Purification of these complexes from wild-type and specific mutants facilitates their characterization by spectroscopic methods, and should finally lead to a complete resolution of the tertiary structure by crystallization and subsequent X-ray diffraction. In addition to the need for a pure and functionally active starting material, crystallization benefits from a strict homogeneity in the size of the complexes, since smaller-sized particles are easier to analyze than large aggregates.

Until now, few attempts have been made to isolate and characterize PS I and PS

0021-9673/90/$03.50

II RC by high-performance liquid chromatography (HPLC)[1–5], and no HPLC procedure has been published for the purification of the b_6f complex. In this report, a two-step HPLC procedure for the purification of all three components from the cyanobacterium *Synechocystis* PCC 6803 is described. As a demonstration of the versatility of this separation method, the purification of a modified PS II RC present in low amount in the membrane, will also be described.

EXPERIMENTAL

Growing of cells and extraction of isolated membranes

Cells from a glucose-tolerant and phycocyanin-deficient strain of the cyanobacterium *Synechocystis* PCC 6803 (characterized in ref. 6) were grown photo-autotrophically according to ref. 7. In addition, cells from a mutant with a deleted *psb*C gene, which codes for the chlorophyll-binding 43 000-dalton protein (CP-43 subunit) of the PS II RC (a kind gift of D.A. Chisholm), were grown photoheterotrophically in the presence of 5 m*M* glucose. Membranes from both strains were isolated as reported in ref. 6, extracted by 1% dodecyl β-D-maltoside (β-DM), loaded on a sucrose density gradient and centrifuged overnight (150 000 *g*, 16 h 4°C) in the presence of 0.04% β-DM. Out of three bands, the middle (green) band was collected and diluted with buffer A (20 m*M* 4-morpholineethanesulfonic acid (MES) (pH 6.5)–10 m*M* $CaCl_2$–10 m*M* $MgCl_2$–0.5 *M* mannitol–0.03% β-DM) to reduce the residual sucrose concentration to less than 100 m*M*. After concentration to less than 50 ml in a stirred cell (Amicon 8400, equipped with a YM 100 membrane, molecular mass cut-off 100 000 dalton; W. R. Grace & Co.), up to 1 ml was injected for analytical HPLC runs. For (semi-)preparative runs, the sample was applied via a 50 ml superloop (Pharmacia-LKB), which was kept in the oven compartment of the chromatograph.

Apparatus and columns

All HPLC steps were performed on a Hewlett-Packard 1090 M liquid chromatograph, equipped with a diode-array detector and an oven compartment (connected to an external thermostat). Samples were collected in a Gilson FC 203 fraction collector connected to a thermostat (LKB).

For anion-exchange chromatography the following columns were used: TSK DEAE-5PW (75 × 8 mm I.D.; TosoHaas, U.S.A.), Mono Q HR 5/5 (50 × 5 mm I.D.) and HR 10/10 (100 × 10 mm I.D.; Pharmacia-LKB, Sweden), and a LiChrospher 1000 TMAE glass cartridge (50 × 10 mm I.D.; Merck, F.R.G.). Hydroxyapatite HPLC was performed on a MAPS HPHT analytical cartridge (30 × 4.6 mm I.D.; Bio-Rad, U.S.A.), a HAP5-50 column (50 × 7.5 mm I.D.; Toa Nenryo Kogyo K.K., Japan) and a MHAP5-10 (100 × 21 mm I.D.; Toa Nenryo Kogyo K.K., Japan/Syn-Chrom, U.S.A.). Size-exclusion HPLC was performed on a TSK 4000 SW-column (300 × 7.5 mm I.D.; Toyo Soda, Japan); column calibration was carried out, using common standard calibration proteins from Pharmacia. Buffer exchange was achieved via gel chromatography on Econo-Pac 10DG disposable desalting columns (Bio-Rad).

RESULTS

Restrictions on the conditions for separation of the PS I RC, PS II RC and cytochrome b_6f complexes by HPLC

Conditions for separating PS II RC from the other two complexes by anion-exchange chromatography are flawed by the lability of the PS II RC under both acidic and alkaline conditions and the loss of subunits from PS II RC at high-salt concentrations and at elevated temperature. Furthermore, during all steps of purification, detergent at 3–5 times the micellar concentration and an appreciable amount of sugar (0.5–1.0 *M*) must be present to prevent (irreversible) aggregation of these hydrophobic complexes. β-DM proved to be the mildest detergent for the preservation of the activity of both the isolated PS I and PS II RC, and mannitol, having lower viscosity than sucrose at the same concentration, the best-suited sugar for HPLC.

All separations were performed at 10°C, a reasonable compromise between an increase in column backpressure at lower temperatures, and an increase stability of

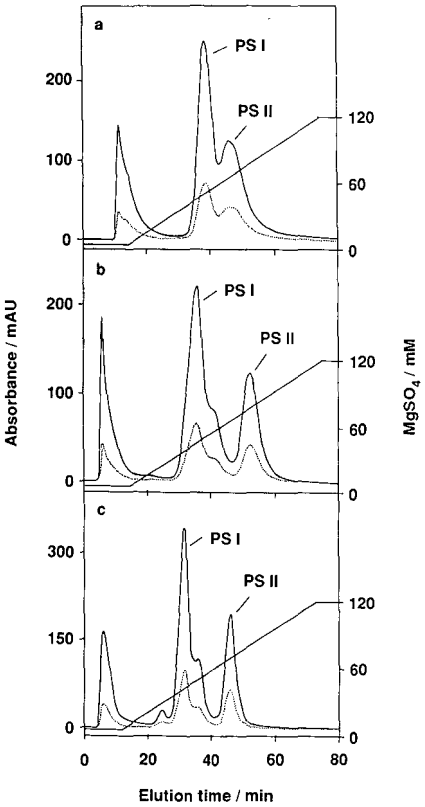

Fig. 1. Chromatogram of an extract of *S.* 6803, pre-purified by sucrose-density-gradient centrifugation, on different HPLC anion-exchange columns: (a) TSK DEAE-5PW column, (b) Mono Q HR 5/5 column and (c) LiChrospher 1000 TMAE glass cartridge. Buffer 20 m*M* MES (pH 6.5)–10 m*M* $MgCl_2$–10 m*M* $CaCl_2$–0.5 *M* mannitol–0.03% (w/v) β-DM; gradient of 5 to 120 m*M* $MgSO_4$; flow-rate 0.4 ml/min (a + b) and 0.8 ml/min (c). Absorbance was recorded at 280 nm (dotted line) and 435 nm (solid line).

the proteins at lower temperatures. Immediately after separation, all fractions were kept at 4°C. Instability at higher salt concentrations, especially of PS II RC, was reduced by desalting the respective protein fractions by gel chromatography and concentrating all samples immediately after separation.

Separation of PS I and PS II RC by anion-exchange HPLC

Three anion-exchange columns were tested for their ability to separate PS I from PS II RC under the conditions described above. Fig. 1 shows elution profiles of the membrane extract (prepurified on a sucrose density gradient) obtained with a linear gradient of $MgSO_4$. All columns show the same sequence of elution of three main components —free pigment (carotene/chlorophyll), the PS I RC, and the PS II RC. The TSK DEAE-5PW column (Fig. 1a) showed a poorer separation of PS I and PS II RC than the Mono Q HR 5/5 column (Fig. 1b). Although run at a higher flow-rate (due to the larger bed volume) and with a larger amount of sample, the LiChrospher TMAE-column (Fig. 1c) yielded the best resolution. Both Mono Q and the LiChrospher column show a minor peak of PS I RC, following the main peak; this peak, containing PS I RC, mixed with a contaminating protein (data not shown), was discarded.

It should be mentioned, that a gradient of monovalent (*i.e.* NaCl) or trivalent (*i.e.* sodium phosphate) ions yielded a similar elution pattern to the $MgSO_4$ gradient on the Mono Q column.

This step was scaled up on a Mono Q HR 10/10 column, applying up to *ca.* 100 mg protein in a volume of up to 50 ml by a "superloop". Additionally, instead of a linear gradient, a multi-stage gradient was applied, yielding a better separation of the PS I and PS II RC peaks.

It should also be mentioned that, relative to the amount of PS I RC, the preparation shown in Fig. 1 (from the phycocyanin-deficient mutant) contains more than double the amount of PS II RC found in preparations from wild-type cells and considerably more PS II RC than most of the engineered mutants with defects in PS II function. This fact stresses the importance of this first HPLC purification step and the requirement of quantitative separation of PS I and PS II RC prior to spectroscopic characterization, as the PS I signal may mask the PS II signal. As an example, Fig. 2 shows a separation of PS I and PS II RC from a mutant in which the gene for one

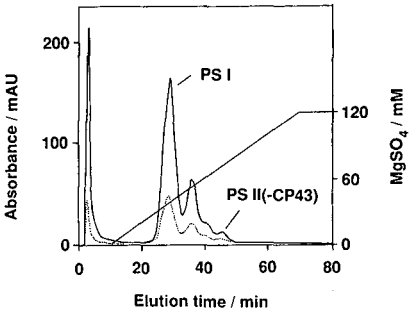

Fig. 2. Chromatogram of an extract from a *S.* 6803 mutant, lacking the CP43 subunit in the PS II RC, from a Mono Q HR 5/5 column; conditions as for Fig. 1b. Absorbance was recorded at 280 nm (dotted line) and 435 nm (solid line).

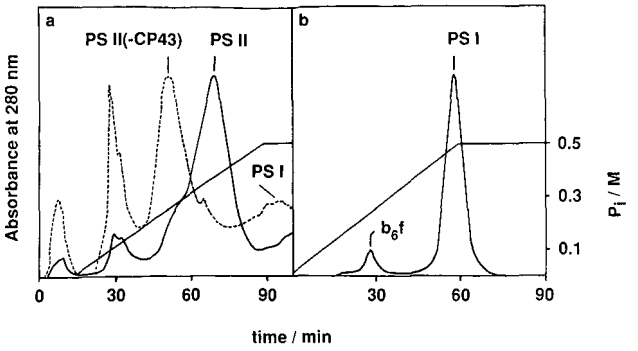

Fig. 3. Chromatogram of PS II(−CP43)RC and PS II RC (a), and for PS I RC and cytochrome b_6f complex (b) from an analytical HPLC hydroxyapatite column (HAP5-50); starting buffer 10 m*M* sodium phosphate (pH 6.8)–10 m*M* $MgCl_2$–13 μM $CaCl_2$–0.5 *M* mannitol–0.03% (w/v) β-DM; gradient up to 0.5 *M* sodium phosphate; flow-rate 0.4 ml/min.

subunit of the PS II RC, the *psb*C gene, has been deleted. Conditions of the separation are identical to those of Fig. 1b. This gene deletion leads to a severely decreased amount of PS II RC in the thylakoid membrane of this mutant and the loss of photo-autotrophic growth. Although the amount of PS II(−CP43)RC extracted from the thylakoid membrane is only about 1% of the amount of extracted PS I RC (on a chlorophyll basis), a higher purity of this impaired PS II RC is still possible by this first HPLC step. However, analysis by sodium dodecyl sulfate–polyacrylamide gel electrophoresis (SDS-PAGE) still revealed the presence of several contaminants among the subunits of the PS I and PS II RCs. To achieve extremely pure preparations, a second HPLC step with different elution characteristics is necessary.

Further purification of the complexes by hydroxyapatite HPLC

Prior to the hydroxyapatite step, the PS I and PS II RC peak fractions of the anion-exchange step were passed twice through an Econo-Pak gel column. With this step, the $MgSO_4$ and Ca^{2+} concentrations were reduced to <10 m*M* and 13 μM, respectively, and MES buffer was exchanged for sodium phosphate buffer (see Experimental). The low calcium concentration turned out to be necessary for the prevention of frequent high-pressure-instrument shutdowns, caused by the formation of salt crystals.

Due to the different sequence of elution from a new ceramic spherical hydroxyapatite column, HAP5-50, the PS II RC could be further purified; the main contaminants were an unpigmented protein, eluted at lower phosphate concentrations than PS II RC (presumably ATPase), and residual PS I RC (see Fig. 3a). Similarly, PS II(−CP43)RC, eluted at somewhat lower phosphate concentrations than PS II RC, could be further purified from these two contaminants.

Further purification of PS I RC on this column (Fig. 3b) by applying a linear gradient of 10 to 500 m*M* sodium phosphate revealed the presence of another protein, which could be identified as the b_6f complex (see below). Repeating the anion-exchange chromatography step on this purified complex showed that it was eluted at the same $MgSO_4$ concentration as the PS I RC (data not shown).

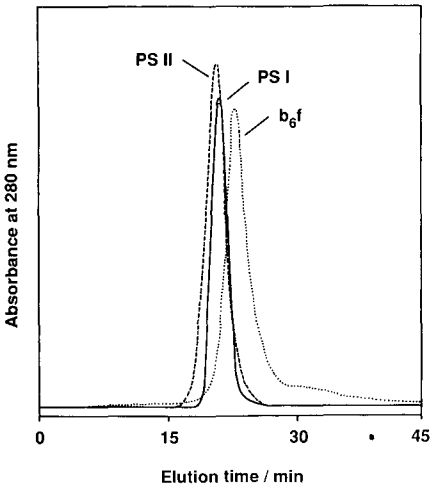

Fig. 4. HPLC gel chromatography of purified PS I RC, PS II RC and cytochrome b_6f complex on a TSK 4000 SW column; buffer 20 m*M* MES (pH 6.5)–10 m*M* $MgCl_2$–30 m*M* $CaCl_2$–0.5 *M* mannitol–0.03% (w/v) β-DM; flow-rate 0.5 ml/min.

The hydroxyapatite purification step could be scaled up by using a larger column of the same type, *i.e.* MHAP5-10. This column was observed to exhibit stable operation at reasonable flow-rate (0.8–1.6 ml/min). In contrast, the hydroxyapatite cartridge, MAPS HPHT, showed frequent pressure fluctuations, and the increase in backpressure with increasing analysis time was much greater than with the ceramic spherical type of HAP5-50 and MHAP5-10. The elution profiles were similar for all three columns.

Characterization of the isolated protein complexes

The homogeneity and molecular mass of the isolated protein complexes was determined by gel chromatography HPLC. The elution profiles of the PS I RC, PS II RC, and the b_6f complex from a TSK 4000 SW column, shown in Fig. 4, yielded apparent molecular masses (including the detergent shell) of $(300 \pm 20) \cdot 10^3$ dalton, $(310 \pm 20) \cdot 10^3$ dalton and $(180 \pm 20) \cdot 10^3$ dalton, respectively. The PS II(−CP43)RC from the *psb*C deletion mutant showed a molecular mass slightly lower than that of the PS I RC. The contribution of the detergent shell in all three cases is *ca.* 50 000 dalton, as estimated from electron micrographs of a similar PS II RC (ref. 3). By SDS-PAGE and immunoblotting, the PS I RC was determined to contain 9 protein subunits (*ca.* 60, *ca.* 60, 18.5, 18.5, 16, 15, 10.5, 9.5 and $6.5 \cdot 10^3$ dalton), the PS II RC 5 subunits (43, 37, 33, 29 and 10–11 $\cdot 10^3$ dalton) and the b_6f complex 4 subunits (38, 24, 19 and $15 \cdot 10^3$ dalton); subunits below 5 000 dalton may not have been resolved in these gels[6]. Analysis by SDS-PAGE and immunoblotting also confirmed that the CP43-apoprotein was absent from the PS II RC isolated from the deletion strain[8]. In addition, determination of the chlorophyll-per-reaction-center ratio yielded values of 70 Chl/PS I, 40 Chl/PS II, and 33 Chl/PS II(−CP43), based on light-flash-induced-charge separation. These values are among the lowest reported for these isolated complexes. A more detailed biophysical and biochemical characterization of these complexes, including a detailed subunit analysis, will be given elsewhere[6,8].

DISCUSSION

HPLC purification of comparatively labile hydrophobic protein complexes imposes severe operating conditions on columns, if the protein is to be kept in its native state, *i.e.* retain its biological activity. The presence of detergent, high sugar and high salt concentrations contribute to increasing column backpressure, as does the lower temperature (< 10°C) at which chromatography must be performed. Therefore, it is worth mentioning that all the columns tested here are usable under these conditions; biological activity of the isolated membrane proteins is retained.

However, comparing the resolution of separation and the stability of experimental conditions major differences between the columns tested became obvious. Within the group of anion-exchange columns, the LiChrospher 1000 TMAE yielded the best separation of PS I and PS II RC and removed some unwanted proteins. Several effects may contribute to the superior resolution of this recently developed column in comparison to the TSK DEAE-5PW and the Mono Q columns:

(1) The ion-exchange groups of the LiChrospher column are not bound to the matrix via short spacer groups, but sit on "tentacle"-like polymer chains, which are claimed to move freely. This should minimize non-specific interactions between the protein and the matrix and avoid irreversible deformations, which may occur if the ionic groups of the ion exchanger were rigidly fixed on the surface.

(2) The support material of hydrophilic silica beads carries untreated silanol groups on their surface, which may cause a difference in the interaction with the proteins.

(3) The smaller size of the particles, 5 μm, may also lead to a much higher mass transfer rate (greater peak sharpness) than with the other ion exchangers, which contain 10-μm particles. This is especially decisive for separating larger macromolecules, which have poorer diffusion.

On the other hand, differences in the chromatograms between the TSK DEAE-5PW and the Mono Q column may be due to different matrices and/or different charge densities of the anion-exchange groups. Considering that a separation of PS I and PS II RC isolated from the same organism was not achieved by conventional anion-exchange chromatography on a TSK DEAE-Toyopearl 650S column[9], the use of HPLC for this first step constitutes a considerable progress in the purification of these two photosystem core complexes.

As in the first HPLC step, the hydroxyapatite step was improved by the use of the 5μm spherical particles of the HAP5-50 column[10] rather than the larger, irregularly shaped particles of the MAPS HPHT cartridge: Besides better resolution, the column used exhibited much more stable chromatographic conditions and lower back-pressure, even after scaling up by a factor of more than 10.

This second HPLC step is very important for obtaining PS I and PS II RCs free of any contaminating proteins. In the case of the PS I RC, the b_6f complex is the only "contaminant" in the main peak of the Mono Q column. As both protein complexes are eluted from the anion-exchange column together, hydroxyapatite chromatography is required for their separation. Much higher yields of the cytochrome b_6f complex can be obtained, if instead of the middle (green) band, the upper yellow-brown band of the sucrose density gradient is taken as the starting material (data not shown). The molecular mass determined by gel HPLC suggests that this is the first

reported isolation of a monomeric cytochrome b_6f complex. The benefit of this additional purification for PS I RC is reflected by the fact that preliminary crystallization attempts using this monomeric particle have been successful[11].

In addition, this hydroxyapatite chromatography is especially valuable for further purifying PS II RC from mutants with low levels of PS II RC in site-directed mutations. In the case of the CP43-less mutant shown above, the amount of extracted PS II(−CP43)RC is only 1% of that of PS I RC (on a chlorophyll basis). The fact that PS II RC is eluted before PS I RC from the hydroxyapatite column (in contrast to the first HPLC step) enables purification of a PS II(−CP43)RC free of PS I RC contamination, despite its low concentration in this mutant. High purity was a prerequisite for absorbance change measurements, which showed that this "minimal core complex" was still capable of a stable charge separation[8].

It should be mentioned that this HPLC method, for the first time, enables the characterization of isolated complexes from genetically engineered PS II RCs. For example, it was shown recently by electron paramagnetic resonance and optical spectroscopy of PS II RCs isolated according to this method that a mutant in which tyrosine 161 of the D1 polypeptide was replaced by phenylalanine had lost the PS II secondary electron donor, Z (ref. 12).

ACKNOWLEDGEMENTS

I am grateful to Bruce A. Diner, Peter J. Nixon, Jim G. Metz, J. Jack Kirkland and Barry E. Boyes for stimulating discussions.

REFERENCES

1 M. Rögner, J. P. Dekker, E. J. Boekema and H. T. Witt, *FEBS Lett.*, 219 (1987) 207.
2 E. J. Boekema, J. P. Dekker, M. G. van Heel, M. Rögner, W. Saenger, I. Witt and H. T. Witt, *FEBS Lett.*, 217 (1987) 283.
3 J. P. Dekker, E. J. Boekema, H. T. Witt and M. Rögner, *Biochim. Biophys. Acta*, 936 (1988) 307.
4 M. Rögner, U. Mühlenhoff, E. J. Boekema and H. T. Witt, *Biochim. Biophys. Acta*, 1015 (1990) 415.
5 D. F. Ghanotakis, J. C. de Paula, D. M. Demetriou, N. R. Bowlby, J. Petersen, G. T. Babcock and C. F. Yocum, *Biochim Biophys. Acta*, 974 (1989) 44.
6 M. Rögner, P. J. Nixon and B. A. Diner, *J. Biol. Chem.*, 265 (1990) in press.
7 J. G. K. Williams, *Methods Enzymol.*, 167 (1988) 766.
8 M. Rögner, D. A. Chisholm and B. A. Diner, *Biochemistry*, submitted for publication.
9 K. Gounaris, D. J. Chapman and J. Barber, *Biochim. Biophys. Acta*, 973 (1989) 296.
10 T. Kadoya, T. Ogawa, H. Kuwahara and T. Okuyama, *J. Liq. Chromatogr.*, 11 (1988) 2951.
11 B. A. Diner and M. Rögner, unpublished results.
12 J. G. Metz, P. J. Nixon, M. Rögner, G. W. Brudvig and B. A. Diner, *Biochemistry*, 28 (1989) 6960.

Journal of Chromatography, 512 (1990) 227–236
Elsevier Science Publishers B.V., Amsterdam

CHROMSYMP. 1844

Simultaneous determination of *Bordetella pertussis* toxin and filamentous haemagglutinin concentrations by hydroxyapatite high-performance liquid chromatography

PELE CHONG*, GAIL JACKSON, WILLIAM CWYK and MICHEL KLEIN
Connaught Centre for Biotechnology Research, 1755 Steeles Avenue West, Willowdale, Ontario M2R 3T4 (Canada)

ABSTRACT

A simple and rapid method for the simultaneous determination of *Bordetella pertussis* toxin (PT) and filamentous haemagglutinin (FHA) concentrations in fermentation broths has been developed. The rapid single-step analysis performed by hydroxyapatite high-performance liquid chromatography using a salt gradient with UV detection allows both the separation of PT from FHA and the measurement of their respective concentrations. The assay is highly reproducible. Over 35 lots of acellular *B. pertussis* vaccine production lots were examined and PT concentrations measured by high-performance liquid chromatography were found to be in good agreement with the values obtained by sodium dodecyl sulphate–polyacrylamide gel electrophoresis densitometry. The chromatographic conditions have been optimized to separate the intact holotoxin from its B-oligomer subunits.

INTRODUCTION

Bordetella pertussis is the microorganism causing whooping cough. *B. pertussis* toxin (PT) and flamentous haemagglutinin (FHA) have been identified as potential protective antigens against *B. pertussis* infection. Antibodies to PT have been shown to protect mice against both intracerebral and respiratory challenges with virulent organisms. On the other hand, FHA protected mice from *B. pertussis* respiratory infection only (For reviews, see refs. 1–3). Both proteins promote adherence of the bacteria to ciliated epithelial cells *in vitro*[4]. Therefore, PT and FHA are prime candidate antigens for inclusion in any new *B. pertussis* vaccine. Pertussis toxin is a hexameric protein (105 000 dalton) composed of five subunits: S1 (28 000 dalton); S2 (23 000 dalton); S3 (23 000 dalton); S4 (12 000 dalton) and S5 (11 000 dalton) assembled in a molar ratio of 1:1:1:2:1, respectively. The holotoxin is an A:B type toxin. The A subunit (S1) catalyzes the ADP-ribosylation of a family of GTP-binding regulatory proteins in eukaryotic cells[5–7]. The other subunits (S2–S5) form a non-covalent B-oligomer which mediates the binding of the toxin to its target-cell

0021-9673/90/$03.50

receptors[8,9]. FHA has an apparent molecular weight of 220 000 dalton and may be spontaneously degraded into 130 000- and 90 000-dalton proteolytic fragments[10,11].

Both antigens are secreted into *B. pertussis* culture supernatants and the relative concentrations of these proteins vary significantly depending on fermentation conditions. To achieve consistency between vaccine production lots, the relative concentrations of PT and FHA must be closely monitored during vaccine preparation. In this report, we describe a hydroxyapatite high-performance liquid chromatography (HPLC) method which allows the simultaneous determination of PT and FHA concentrations in a fermentation broth sample.

EXPERIMENTAL

Chemicals

All buffer reagents were obtained from Fisher. Chemicals for gel electrophoresis and HPLC columns (Bio-Gel HPHT column) were purchased from Bio-Rad Labs., Canada. Water was either HPLC grade (Fisher) or purified through a Milli-Q water purification system (Millipore, MA, U.S.A.).

Preparation of protein standards

FHA was isolated from the culture supernatant of *B. pertussis* strain 10536 by hydroxyapatite chromatography, as described by Sato *et al.*[10]. PT was purified by fetuin-Sepharose 4B affinity chromatography, as previously described[12]. The B-complex of PT was prepared according to Chong and Klein[12]. Both PT and FHA were stored at −20°C in glass vials.

Protein concentration determination

Protein concentrations were determined by amino acid analysis performed by the Department of Biochemistry, University of Toronto, Canada.

Chromatographic apparatus

Chromatography was performed on an analytical Bio-Gel HPHT column using a Pharmacia fast protein liquid chromatography (FPLC) system. The effluent was monitored with a UV detector (Erma Model ERC-7210) at 230 nm, and protein peaks were integrated using a Spectra-Physics SP4270 integrator.

Preparation of samples for HPLC analysis

To achieve accurate determinations of PT, the ionic strength of the sample solution has to be less than 10 m*M* potassium phosphate and 50 m*M* NaCl, since the binding of PT to hydroxyapatite is salt concentration-dependent. All samples were filtered through a 0.22-μm filter before injection. To avoid precipitation of PT at low ionic strength, samples were tested within 2 days of their preparation.

Separation and analysis of PT and its B-oligomer

PT samples and standards (100–500 μl) were subjected to chromatography on an analytical Bio-Gel HPHT column using a phosphate-salt gradient and a flow-rate of 1 ml/min (see below). Fractions (1 ml) were collected and analyzed by sodium dodecyl sulphate–polyacrylamide gel electrophoresis (SDS-PAGE). Buffer A was 10 m*M*

potassium phosphate, pH 8.0. Buffer B was 200 m*M* potassium phosphate containing 1 *M* sodium chloride, pH 8.0. After equilibration of the column in buffer A at room temperature, the holotoxin and its B-oligomer were separated from other *B. pertussis* proteins under the following conditions: after sample injection, buffer A (100%) was run for 5 min, followed by a linear gradient from 0 to 12% buffer B, established in 3 min and held for 5 min to remove any contaminants. In order to elute PT, a second linear gradient from 12 to 35% buffer B was then established in 10 min. Finally, the column was re-equilibrated with buffer A for 15 min before the next injection.

HPLC analysis of PT and FHA mixtures

The chromatographic conditions were essentially as described above except for the addition of a second linear gradient of 35–85% buffer B over 15 min, in order to elute FHA.

SDS-PAGE

Protein samples (10–100 μg protein) were subjected to SDS-PAGE on a discontinuous 13.5% gel according to the method of Laemmli[13]. Two PT standards at different concentrations were included to allow for the quantification of PT in the sample preparations. Protein bands were visualized by Coomassie brilliant blue staining. After destaining, the concentration of PT was determined using a Philips PU8800 densitometer equipped with a computing analysis program.

RESULTS AND DISCUSSION

A method for the purification and separation of FHA and PT from *B. pertussis* culture supernatants using a two-step hydroxyapatite chromatography has been reported by Sato *et al.*[10]. We have modified their approach and designed a single-step hydroxyapatite HPLC method to measure simultaneously the concentrations of PT and FHA in a fermentation broth.

PT (P273) and FHA (P214) standards were prepared by fetuin-affinity and hydroxyapatite chromatography, respectively, as previously decribed[10,12]. SDS-PAGE analysis of these standards (Fig. 1) revealed that both PT (lane 1) and FHA (lane 2) standards were homogeneous. PT was shown to consist of five subunits with molecular weights similar to those reported in the literature[10,14,15]. Typical FHA protein bands at 220 000, 130 000 and 90 000 dalton were detected (Fig. 1, lanes 2 and 3). This observation is consistent with a WHO report indicating that the molecular weight of native FHA is 220 000 dalton whereas the 130 000- and 90 000-dalton bands correspond to spontaneous proteolytic fragments[11,14]. Furthermore, the amino acid analyses of PT and FHA standards (Table I) revealed that their respective amino acid compositions were in agreement with those published in the literature[10,15].

Fig. 2 depicts the typical hydroxyapatite HPLC elution profiles obtained for PT and FHA standards, individually. The HPLC analysis of the PT standard is shown in panel A. A 10-μg amount (200 μl) of PT standard (P273) was injected and the column was washed with the starting buffer (buffer A) for 5 min. A steep gradient (0–12% B in 3 min) was applied to remove any minor contaminants. PT was subsequently eluted with a shallow gradient from 12 to 35% B in 10 min. PT eluted as a sharp peak at 21.6 min which could easily be integrated for PT concentration determination. Since the

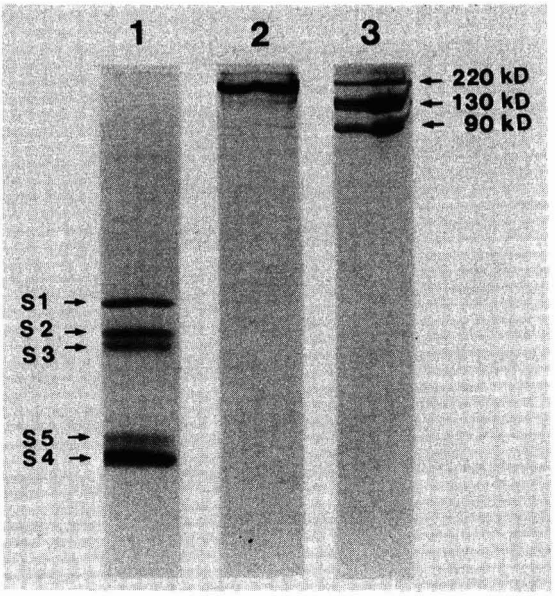

Fig. 1. SDS-PAGE analysis of native PT, native FHA and degraded FHA. Lane 1 = 6 μg of PT standard (P273); lane 2 = 8 μg of FHA standard (P214); lane 3 = 6 μg of degraded FHA sample. kD = Kilodalton.

TABLE I

AMINO ACID COMPOSITION OF PT AND FHA STANDARDS (% OF TOTAL)

Amino acid	*PT*		*FHA*	
	Expected[a]	*P273*	*Expected*[b]	*P214*
Asx	6.9	7.5	10.5	10.8
Thr	7.3	6.4	6.1	6.9
Ser	7.1	6.6	7.6	7.8
Glx	8.6	9.0	9.0	8.8
Pro	5.7	6.2	2.2	2.2
Gly	8.5	9.2	13.7	13.6
Ala	9.2	9.3	15.3	15.1
Cys	2.7	1.1[c]	0.2	0.0[c]
Val	6.9	7.5	8.3	9.1
Met	2.9	2.9	1.1	0.5
Ile	4.1	4.3	3.3	3.5
Leu	7.7	8.8	8.6	8.6
Tyr	6.5	5.3	1.3	1.0
Phe	3.4	4.0	1.4	2.0
Lys	3.4	4.0	4.6	4.9
His	1.8	2.1	1.7	0.5
Arg	6.3	5.9	5.1	4.8

[a] Published amino acid composition of PT[15].
[b] Published amino acid composition of FHA[10].
[c] Cysteine residues were directly measured without any modification.

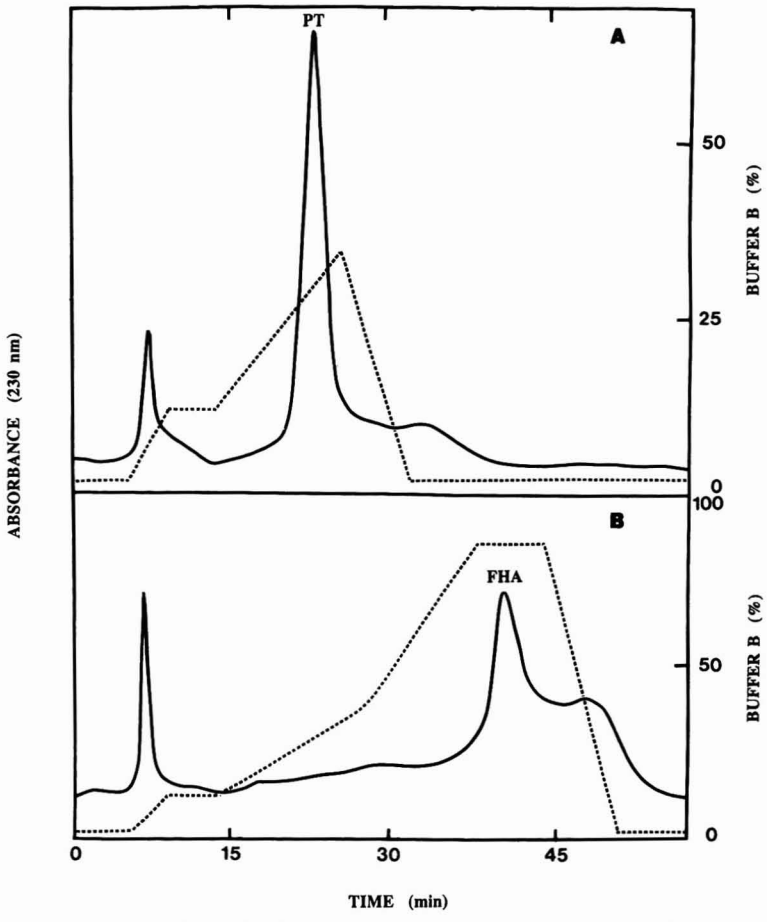

Fig. 2. Elution profile of PT and FHA standards on hydroxyapatite HPLC. Panel A, chromatogram of 15 μg of PT standard. Panel B, chromatogram of 25 μg of FHA standard. Samples were injected at time 0. The gradient program is indicated by the dotted line.

binding affinity of FHA for hydroxyapatite is very high, FHA was eluted with a steep salt gradient from 35 to 85% B within 15 min as indicated in panel B. Native FHA and its proteolytic fragments co-eluted as a single peaks at 41 min. Due to the upwards shift of the baseline, FHA peak areas could not be automatically integrated. Therefore, peak heights were used to calculate FHA concentrations. Since PT and FHA have significantly different retention times, the hydroxyapatite HPLC method allows for the identification of each protein in a sample as well as the calculation of there respective concentrations. A typical run of an FHA–PT mixture is shown in Fig. 3A. A sample (500 μl) containing 10 μg of PT and 25 μg of FHA standards was subjected to hydroxyapatite HPLC analysis. Both the PT and FHA peak were easily separated (Fig. 3A). The binding affinity of PT for hydroxyapatite was found to be salt and phosphate concentration-dependent. Essentially all of the PT binds to the column equilibrated in buffer containing less than 10 m*M* phosphate and 50 m*M* NaCl. Interestingly, we found that most *B. pertussis* proteins had very little binding affinity

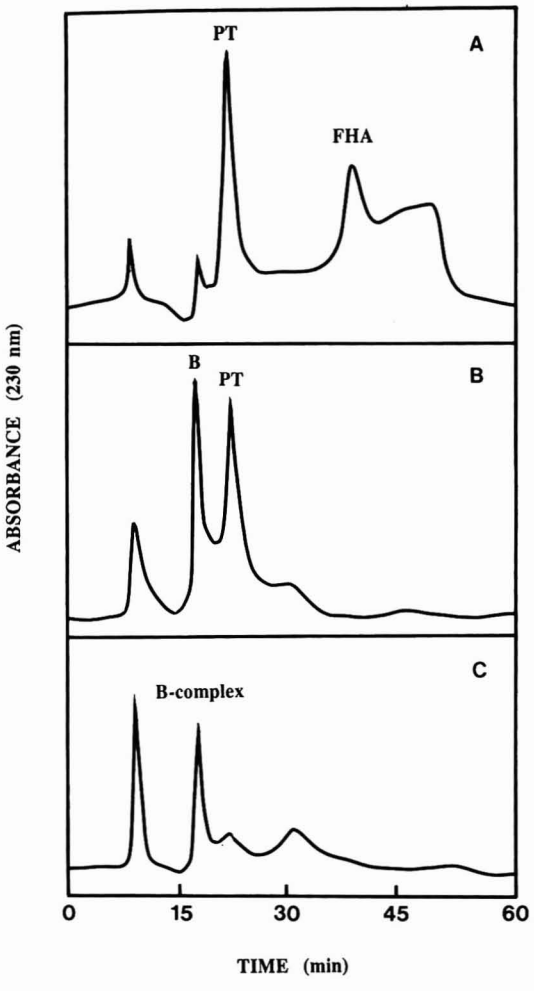

Fig. 3. Chromatographic separation of PT, FHA and B-oligomer of PT by hydroxyapatite HPLC, as described in Experimental. (A) Elution pattern of a mixture containing 10 μg of PT and FHA standards in 0.5 ml; (B) elution profile of 15 μg of a PT sample (P192) stored at 4°C for 2 weeks, peak B was collected for SDS-PAGE analysis (see Fig. 4, lane 2); (C) elution profile of 5 μg of fetuin-Sepharose-purified B-oligomer.

for hydroxyapatite and were eluted during the first 15 min. Thus, they did not interfere with the analysis of HPLC profiles.

During the course of stability studies, it was observed that the S1 subunit of PT purified by fetuin-affinity chromatography was prone to proteolytic degradation during storage at 4°C for a period of 2 weeks. Degradation of S1 and S5 subunits under similar conditions has been previously reported by Peppler *et al.*[16]. The loss of S1 cannot be detected by the conventional fetuin capture enzyme-linked immunosorbent assay (ELISA). The CHO cell clustering and the ADP-ribosyltranferase assays are necessary to demonstrate the loss of PT activity (unpublished results). When PT stored at 4°C for long periods of time was subjected to HPLC analysis, two elution peaks were

observed as shown in Fig. 3B. The first peak (B) eluted at 16.5 min was subjected to SDS-PAGE analysis and found to contain the four subunits of pertussis toxin B-oligomer (Fig. 4, lane 2). The second peak corresponded to intact PT (Fig. 4, lane 1). Fetuin-Sepharose-purified B-component subjected to HPLC analysis eluted as a single peak (Fig. 3C) with a retention time similar to that of peak B of Fig. 3B. These results suggest that the holotoxin and the B-component have different binding affinities for hydroxyapatite and can easily be separated. Thus, HPLC analysis offers a unique advantage over conventional ELISA and protein assays since it allows the simultaneous determination of the concentrations of both the holotoxin and its B-oligomer.

The sensitivity of the hydroxyapatite HPLC method was evaluated by injecting increasing amounts of PT and FHA standards (1–30 μg). The recovery of PT from the column was high (>95%) and a linear dose–response relationship was observed between 1 and 25 μg (Fig. 5). Due to the baseline shift, a linear dose-response curve could only be observed for amounts of FHA above 10 μg (Fig. 5). However, the method could be directly used for measuring PT and FHA concentrations in fermentation broths since they range from 5–20 μg/ml and 20–200 μg/ml, respectively.

To test the reproducibility of the method, PT and FHA standards were subjected to hydroxyapatite HPLC analysis at various time intervals over a 6 months period. The results in Table II show that the assay is reproducible with a variation in retention times of less than 30 s for both proteins. Moreover, less than 10% variation from the mean values was observed for both PT protein peak areas and FHA peak heights.

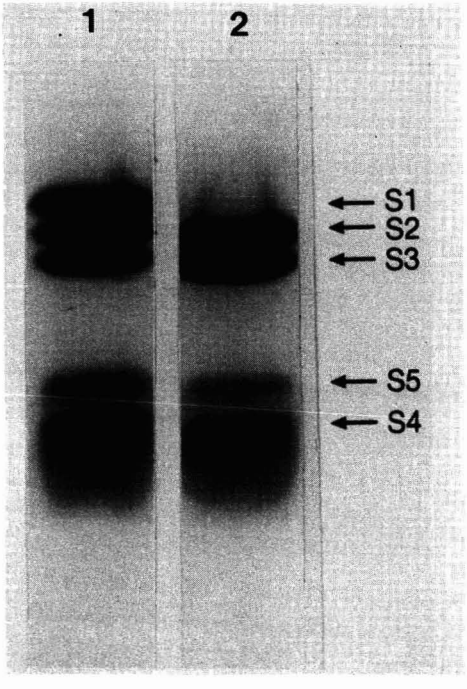

Fig. 4. SDS-PAGE analysis of the intact PT and peak B of Fig. 3B. Lane 1 = 20 μg of the intact PT collected from the HPLC run shown in Fig. 3B; lane 2 = 20 μg of peak B collected from the HPLC run shown in Fig. 3B.

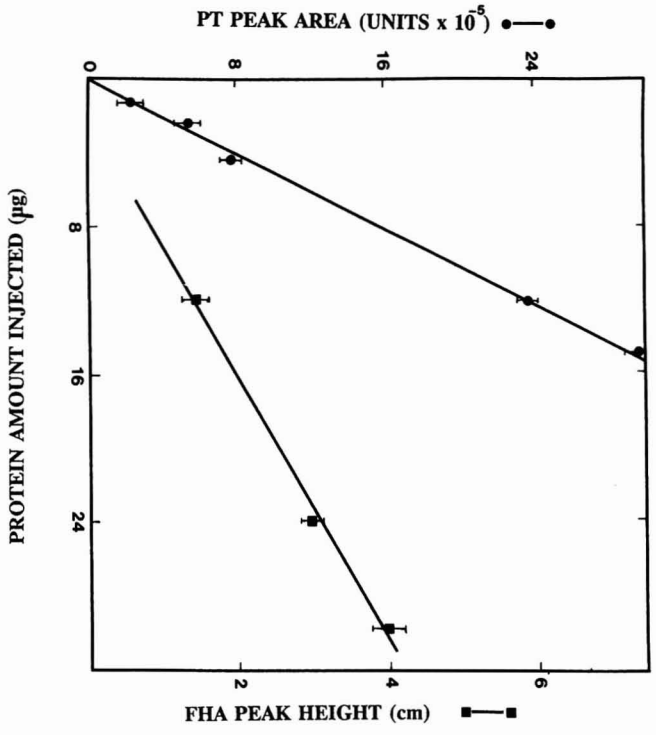

Fig. 5. Standard curves of PT and FHA obtained from hydroxyapatite HPLC analysis. Assays were performed in duplicate. PT is measured as peak area in arbitrary units (●), and FHA was reported as peak height (■).

PT and FHA concentrations were measured by both HPLC and amino acid analysis to determine the accuracy of the hydroxyapatite method. Results summarized in Table III indicate that the values obtained by both methods are in good agreement.

A comparative HPLC and SDS-PAGE analysis of 35 broth concentrates (25%

TABLE II

REPRODUCIBILITY OF THE HYDROXYAPATITE HPLC ASSAY

ND = Not determined.

Time	*Peak area of PT (P273) (mean ± S.D., n=3) (units)*[a]		*Peak height of FHA (P214) (mean ± S.D., n=3) (cm)*
	12 µg	*15 µg*	*30 µg*
0	2397 ± 25	2996 ± 36	3.8 ± 0.1
3 Days	ND	3008 ± 25	3.9 ± 0.1
3 Months	2393 ± 20	2991 ± 22	ND
6 Months	2360 ± 35	ND	4.2 ± 0.1

[a] Arbitrary units.

TABLE III

COMPARATIVE ANALYSIS OF PT AND FHA CONCENTRATIONS OBTAINED BY HYDROXYAPATITE HPLC AND AMINO ACID ANALYSIS

Samples	*Protein concentration (μg/ml)*		*Ratio of values obtained by the two assays*
	HPLC	*Amino acid analysis*	
PT			
P192	678	735	1.08
P261	128	115	0.90
P273[a]	180	180	1.00
P278	327	363	0.98
P280	350	371	1.06
FHA			
P214[b]	114	114	1.00
P258	154	173	1.12
P271	146	152	1.04
FHA-PC8	108	113	1.03

[a] Sample P273 was used as standard for all PT HPLC analyses.
[b] Sample P214 was used as standard for all FHA HPLC analyses.

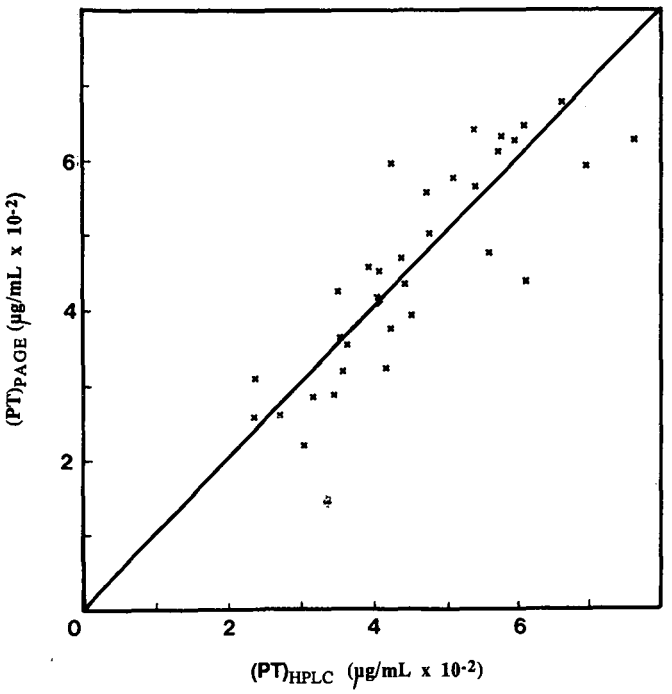

Fig. 6. Linear regression analysis of PT concentration values obtained from 35 lots of fermentation broth concentrates analysed by both hydroxyapatite HPLC and SDS-PAGE densitometry.

ammonium sulfate precipitates) from fermentors which had been optimized for PT secretion was carried out. These precipitates contained significant amounts of PT representing 70–90% of the total proteins, as judged by SDS-PAGE analysis[17]. As shown in Fig. 6, a strong positive correlation was observed between PT concentrations determined by these two methods ($r = 0.84$). Two batches of broth concentrates (lots 012 and 014) contained significant amounts of FHA protein, as judged by SDS-PAGE analysis. To determine whether the hydroxyapaptite HPLC method could be used to measure the relative concentrations of PT and FHA in these samples, a densitometric scanning analysis of SDS gels was performed on samples 012 and 014. The PT–FHA ratio was found to be 85:15 for both samples. Similar PT–FHA ratios were obtained by HPLC analysis (88:12 for lot 012 and 83:17 for lot 014), indicating good agreement between the two methods.

In conclusion, we have developed a simple, rapid and reproducible hydroxyapatite HPLC method for the simultaneous determination of PT and FHA protein concentrations in *B. pertussis* culture supernatants. In addition, the chromatographic conditions have been optimized to separate the holotoxin from its B-component. Since the analysis can be completed within 30 min, this HPLC method can potentially be used as an in-process monitoring of PT levels in fermentation broths.

ACKNOWLEDGEMENTS

We thank Drs. K. J. Dorrington and S. Wilson for the critical review of this manuscript and Mr. R. Robinson for technical assistance.

REFERENCES

1 C. R. Manclark and J. C. Cowell, in R. Germarier (Editor), *Bacterial Vaccines*, Academic Press, Orlando, FL, 1985, pp. 69–106.
2 A. Robinson, L. I. Iron and L. A. E. Ashwoth, *Vaccine*,3 (1985) 11–22.
3 A. A. Weiss and E. L. Hewett, *Ann. Rev. Microbiol.*, 40 (1986) 661–686.
4 E. Tuomanen, A. Weiss, A. Rich, F. Zak and O. Zak, *Dev. Biol. Standards*, 61 (1985) 197–204.
5 M. Tamura, K. Nogimori, S. Murai, M. Yajima, K. Ito, T. Katada, M. Ui and S. Ishii, *Biochemistry*, 21 (1982) 5516–5522.
6 T. Katada and M. Ui, *Proc. Natl. Acad. Sci. U.S.A.*, 79 (1982) 3129–3133.
7 A. G. Gilman, *Cell*, 36 (1984) 577–579.
8 M. Tamura, K. Nogimori, M. Yajima, K. Ase and M. Ui, *J. Biol. Chem.*, 258 (1983) 6756–6761.
9 D. Burns, J. Kenimer and C. Manclark, *Infect. Immun.*, 55 (1987) 24–28.
10 Y. Sato, K. Izumiya, H. Sato, J. Cowell and C. Manclark, *Infect. Immun.*, 31 (1981) 1223–1231.
11 D. R. Relman, M. Domenighni, E. Tuomanen, R. Rappuoli and S. Falkow, *Proc. Natl. Acad. Sci. U.S.A.*, 86 (1989) 2637–2641.
12 P. Chong and M. Klein, *Biochem. Cell Biol.*, 61 (1989) 387–391.
13 J. R. Laemmli, *Nature (London)*, 227 (1970) 680–685.
14 *Report on Meeting on the Results of the WHO Collaborative Study on the Acellular DPT Vaccine*, WHO, Geneva, May 28–30, 1984.
15 C. Locht and J. M. Keith, *Science (Washington, D.C.)*, 232 (1986) 1258–1264.
16 M. Peppler, R. Judd and J. Munoz, *Dev. Biol. Standards*, 61 (1985) 75–87.
17 L. Gordon, D. Stainer, S. Johnson and E. Pearson, *Workhop on Acellular Pertussis Vaccines, September 22–24, 1986.*

Journal of Chromatography, 512 (1990) 237–247
Elsevier Science Publishers B.V., Amsterdam

CHROMSYMP. 1897

High-performance metal chelate interaction chromatography of proteins with silica-bound ethylenediamine-N,N′-diacetic acid

MARIA D. BACOLOD and ZIAD EL RASSI*
Department of Chemistry, Oklahoma State University, Stillwater, OK 74078-0447 (U.S.A.)

ABSTRACT

Wide-pore microparticulate silica gel having surface bound ethylenediamine-N,N′-diacetic acid (EDDA) was developed for the separation of proteins by metal chelate interaction chromatography (MIC). The separation of proteins including glycoproteins was carried out by gradient elution using increasing salt concentration. Different selectivities were obtained when changing the nature of the chelated metal on the surface of the stationary phase, manipulating eluent pH and varying the nature and concentration of the salts in the eluent. The retention–pH dependency of iron-free and holo transferrins suggested that MIC could be used for studying metal–protein complexes provided that the metal binding site in the protein molecule is also involved in the protein interactions with the chelated metal on the surface of the stationary phase. The eluting strength of sodium salts with "hard" metal–EDDA columns increased in the order $Cl^- < CH_3COO^- \leqslant HCOO^- < H_2PO_4^-$, whereas with "soft" metal–EDDA columns it increased in the order $CH_3COO^- < H_2PO_4^- < Cl^-$. Compared to another type of metal interaction column such as silica-bound iminodiacetic acid (IDA), the EDDA column exhibited different selectivity and retentivity toward proteins under otherwise identical elution conditions. Metal–EDDA stationary phases can be viewed as complementary to metal–IDA ones.

INTRODUCTION

High-performance metal chelate interaction chromatography (MIC) is a useful technique for the purification and determination of proteins[1–6]. It offers a selectivity different from that of other biopolymer high-performance liquid chromatography (HPLC) techniques such as ion-exchange and hydrophobic interaction chromatography. Indeed, MIC has been the technique of choice for the isolation of interferons[7,8]. Recently, it has been shown that MIC is a suitable HPLC technique for the separation and purification of human erythrocyte glycophorins[3]; traditional approaches by size-exclusion[9] and ion-exchange chromatography[10] were ineffective in purifying the different forms of the membrane proteins. In addition, MIC has been found to be

0021-9673/90/$03.50

more effective than hydroxyapatite chromatography for the separation of site specific variants of subtilisin[6].

In metal chelate interaction chromatography, a metal ion is immobilized to the stationary phase via chelating functions bound to the surface. Retention and separation is achieved by the interaction of solute molecules with the chelated metal. Side chain groups of amino acid residues on the surface of the protein molecule, such as histidine, cysteine and to a lesser extent tryptophan, are thought to penetrate the outer coordination sphere of the chelated metal and form coordinate bonds.

Selectivity and retention in MIC can be conveniently modulated and adjusted (i) by changing the type of the metal on the stationary phase[11–13], (ii) by varying the eluent pH[5,12], (iii) by the nature and concentration of the salt[3,11,14,15], and (iv) by the nature and concentration of the competing agent in the eluent[11,16]. Thus far, little attempt has been made to manipulate retention and selectivity by the nature of the chelating functions on the surface of the stationary phase[12,17,18]. Indeed, with agarose or rigid microparticulate stationary phases, iminodiacetic acid (IDA) chelating functions have been the most widely used. This indicates that the potential of MIC has not been fully explored so that the technique will have a common place in a wider range of applications.

This report addresses the need for investigating the potential of new chelating functions in MIC of proteins. In this regard, large-pore silica-bound ethylenediamine-N,N′-diacetic acid (EDDA) was developed in our laboratory. The chromatographic behavior of standard proteins and glycosylated proteins was evaluated with metal–EDDA chelates over a wide range of elution conditions including eluent pH, salts and competing agents. A comparison with IDA stationary phases is also presented.

EXPERIMENTAL

Instrumentation

The chromatograph was assembled from an ISCO (Lincoln, NE, U.S.A.) Model 2350 solvent delivery pump and a Model 2360 gradient programmer with a variable-wavelength detector Model V[4]. A Rheodyne (Cotati, CA, U.S.A.) Model 7010 sampling valve with a 100-μl sample loop was used for injection. Chromatograms were recorded with a Shimadzu (Columbia, MD, U.S.A.) Model C-R5A integrator.

Columns

Zorbax PSM 300, a spherical silica, having mean particle and pore diameters of 7.5 μm and 300 Å, respectively, was obtained from DuPont (Wilmington, DE, U.S.A.). The EDDA and IDA stationary phases were made by first reacting Zorbax silica gel with γ-glycidoxypropyltrimethoxysilane in aqueous solution, pH 6.0, for 2 h at 95°C[19]. The products thus obtained were allowed to react with EDDA or IDA using a well established procedure[11]. The surface coverage with EDDA or IDA functions was found to be approximately 2.0–2.2 μmol/m^2, which correspond to 96–105 μmol/ml of packed silica gel, as calculated from the nitrogen content measured by elemental analysis at Galbraith Labs. (Knoxville, TN, U.S.A.). The approximate structures of both stationary phases in metal chelate forms are shown in Fig. 1. The stationary phases thus obtained were packed from an aqueous sucrose–sodium chlo-

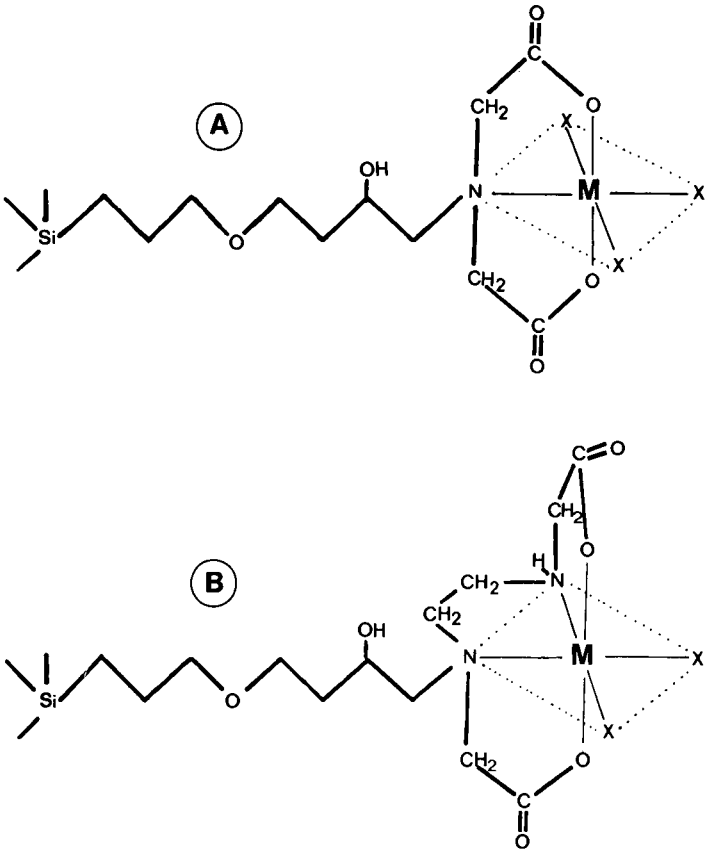

Fig. 1. Schematic illustration of the surface bound metal chelates. (A) Tridentate IDA and (B) tetradentate EDDA. M = Metal; X = protein molecule, salt ion, water molecule or any competing agent.

ride slurry containing 50% sucrose (w/v) at 8000 p.s.i. with 1.0 *M* sodium chloride solution and using a Shandon column packer instrument (Keystone Scientific, Bellefonte, PA, U.S.A.). All columns were made of 100 × 4.6 mm I.D. No. 316 stainless steel tubes (Alltech Assoc., Deerfield, IL, U.S.A.).

Materials

The following materials were purchased from Sigma Chemical (St. Louis, MO, U.S.A.): cytochrome *c* from horse heart; lysozyme from chicken egg white; iron-free (*ca.* 90% substantially iron-free) and holo (*ca.* 98% iron saturated) transferrins from human; lactoferrin from bovine colostrum; β-casein from bovine milk; and EDDA. IDA was obtained from W. R. Grace (Nashua, NH, U.S.A.). Reagent grade sodium hydroxide, ethylenediaminetetraacetic acid (EDTA) disodium salt, acetic acid, ferric chloride, zinc chloride, cupric chloride, cobalt chloride, nickelous nitrate, phosphoric acid, sodium acetate, sodium formate, methanol and acetonitrile (both HPLC grade) were obtained from Fisher (Pittsburgh, PA, U.S.A.). γ-Glycidoxypropyltrimethoxysilane was obtained from Aldrich (Millwaukee, WI, U.S.A.).

Procedures

Freshly packed columns with IDA or EDDA siliceous stationary phases were first conditioned with water and then loaded with the appropriate metal by injecting 10 ml of 50 m*M* metal salt solution using a sampling valve equipped with a 10-ml sample loop. This amount was enough to saturate the column with the desired metal since we have found that the retention of standard proteins did not change for concentrations above 50 m*M*. After loading the column with a given metal, the excess unchelated metal was subsequently removed from the column by washing it with an ample amount of water followed by the equilibrating mobile phase in order to ensure reproducible results during the ensuing chromatographic separation. The column was unloaded from the metal by washing it with 20 ml of 50 m*M* EDTA disodium salt. After regeneration with water, the column regained its naked form (without chelated metal) and was ready for reloading with a different metal.

RESULTS AND DISCUSSION

Columns packed with silica-bound EDDA, chelated with Cu(II), Co(II), Ni(II), Zn(II) or Fe(III) metal ions, were evaluated in protein HPLC over a wide range of elution conditions. These metal–EDDA stationary phases were also compared to metal–IDA stationary phases. Phosphorylated and dephosphorylated β-caseins, lactoferrin, iron-free and holo transferrins, cytochrome *c* and lysozyme were used as model solutes. These proteins, which are well characterized in many aspects, form an attractive set of solutes for elucidation of protein–metal chelate stationary phase associations. Horse heart cytochrome *c* and egg white lysozyme, each having one surface exposed histidine residue, may serve to evaluate the extent to which proteins that have the same histidine content but are slightly different in molecular weights (MW) and p*I* values (cytochrome *c*: MW 12 200, p*I* 10.6; lysozyme: MW 14 000, p*I* 11.0) will interact with different metal chelate sorbents. Phosphorylated and dephosphorylated β-caseins may be useful to ascertain the involvement of phosphate groups in metal chelate interaction chromatography. Human serum transferrins and bovine lactoferrin, which are iron-binding proteins[20] (two ferric ions per molecule of protein) of similar molecular weights (about 80 000 for lactoferrin and 75 000 for transferrin), yet differing in their isoelectric points (about 6.0 for human transferrin and 10.0 for bovine lactoferrin), may be regarded as model proteins to assess the implication of the net charge of protein in MIC.

As expected, metal–EDDA columns exhibited weaker interactions with the proteins investigated than their counterparts metal–IDA columns under otherwise identical elution conditions. As illustrated in Fig. 1 metal–IDA columns provide more coordination sites for interaction with the protein molecule, than do metal–EDDA columns. On the other hand, as a result of one fewer donor atom in the IDA molecule, metal–IDA complexes are less stable than metal–EDDA chelates; *cf.* Table I, which compiles the logarithmic stability constants of both metal complexes as measured in free solution[21]. Indeed, certain metal–IDA stationary phases such as Zn(II)–IDA[5] and Cu(II)–IDA[2] are unstable under most elution conditions and change in retention time from run to run is common. In order to circumvent this problem, Figueroa *et al.*[2] added a small amount of salt of the chelated metal to the mobile phase.

TABLE I

LOGARITHMIC STABILITY CONSTANTS OF METAL–EDDA AND METAL–IDA COMPLEXES IN FREE SOLUTIONS

Data taken from ref. 21.

Metal	*Logarithmic stability constant*	
	EDDA	*IDA*
Zn(II)	11.22	7.24
Ni(II)	13.65	8.13
Co(II)	11.25	6.94
Cu(II)	16.20	10.57
Fe(III)	–	10.72

Particularly noticeable is the strong binding of most proteins to the Cu(II)–IDA column[11,12]. The elution of proteins from the Cu(II)–IDA column necessitated the use of either a linear gradient by increasing both salt and glycine (a bidentate competing agent) concentrations in the eluent or a gradient by decreasing pH and increasing imidazole (a monodentate competing agent) concentration, which often lead to leaching out of the metal and contamination of the separated proteins. It has been demonstrated that the contamination of the protein with metal ions removed by the competing agent from the stationary phase may be avoided by loading the first two-thirds of the column with the metal only[22]. Another alternative may be the use of a naked IDA post column. However, in both cases a metalloprotein may lose its metal to the naked IDA and consequently its biological activity may be reduced as it has been found for holocarboxypeptidase A[23]. In contrast, with the Cu(II)–EDDA column the proteins under investigation were readily eluted and separated with a gradient of increasing sodium chloride concentration in the eluent. On the other hand, the proteins studied could be eluted from both Co(II)–IDA and Co(II)–EDDA columns using the same salt gradient. The retention data obtained on both stationary phases are shown in

TABLE II

COMPARISON OF α-VALUES OF PROTEINS MEASURED WITH Co(II)–IDA AND Co(II)–EDDA COLUMNS

Columns, 100 × 4.6 mm I.D. each; flow-rate 1.0 ml/min; temperature, 25°C. Linear gradient in 15 min from 0 to 1.0 *M* sodium chloride in 10 m*M* acetate buffer, pH 5.5, followed by 5 min isocratic elution with 1.0 *M* sodium chloride in 10 m*M* acetate buffer.

Pair of proteins	*Selectivity, α*	
	Co(II)–EDDA	*Co(II)–IDA*
Iron-free transferrin–holo transferrin	8.79	1.00
Cytochrome *c*–iron-free transferrin	1.23	1.06[a]
Lysozyme–cytochrome *c*	1.15	1.12
Lactoferrin–lysozyme	1.32	1.45

[a] Reversal in elution order.

Table II in terms of selectivity. As can be seen in Table II, the Co(II)-EDDA column exhibited higher selectivity than the Co(II)–IDA column and in particular toward holo and iron-free transferrins. However, the Co(II)–IDA stationary phase yielded higher retention for the proteins than did Co(II)–EDDA. As a result, peaks were broader on the former columns than on the latter.

As stated above, the elution of the different proteins from the various metal–EDDA columns was carried out using a linear salt gradient by increasing the sodium chloride concentration in the eluent. Different selectivities were obtained when going from one metal chelate column to another under otherwise identical elution conditions. Fig. 2, which depicts the separation of five proteins on the Co(II)–EDDA column, demonstrates the high selectivity and high efficiency that can be obtained with such columns.

Fig. 3 illustrates the separation of phospho- and dephosphorylated β-caseins on the Fe(III)–EDDA column using a linear gradient by increasing the sodium chloride concentration in the eluent. Whereas dephosphorylated casein eluted from the Fe(III)–EDDA column with practically little or no retention, phosphorylated casein

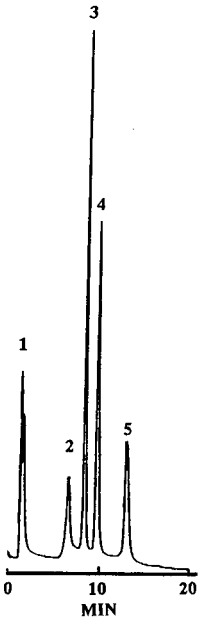

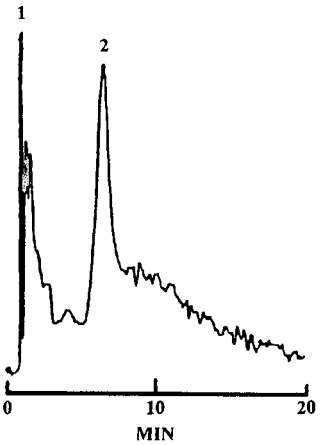

Fig. 2. Chromatogram of standard proteins obtained on Co(II)–EDDA column. Column, 100 × 4.6 mm I.D.; flow-rate, 1.0 ml/min; temperature, 25°C. Linear gradient in 15 min from 0.02 to 1.0 *M* sodium chloride in 10 m*M* sodium acetate buffer, pH 5.5, followed by 5 min isocratic elution with 1.0 *M* sodium chloride in 10 m*M* sodium acetate. Proteins: 1 = holo transferrin; 2 = iron-free transferrin; 3 = cytochrome *c*; 4 = lysozyme; 5 = lactoferrin. UV detection at 280 nm.

Fig. 3. Chromatogram of phosphorylated and dephosphorylated β-caseins. Column, Fe(III)–EDDA; flow-rate, 1.0 ml/min; temperature, 25°C. Linear gradient in 15 min from 0 to 1.0 *M* sodium chloride in 10 m*M* sodium acetate, pH 5.0, followed by 5 min isocratic elution with 1.0 *M* sodium chloride in 10 m*M* sodium acetate. Proteins: 1 = dephosphorylated β-casein; 2 = β-casein. UV detection at 280 nm.

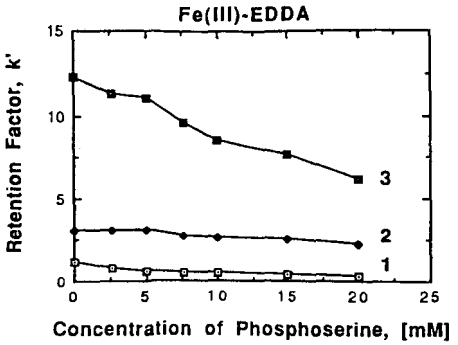

Fig. 4. Plots of retention factor of proteins against phosphoserine concentration in the eluent. Column, 100 × 4.6 mm I.D.; flow-rate, 1 ml/min; temperature, 25°C. Isocratic elution with 10 m*M* acetate containing 0.15 *M* sodium chloride at different phosphoserine concentrations, pH 5.0. Proteins: 1 = iron-free transferrin; 2 = cytochrome *c*; 3 = lysozyme.

was retained by the metal chelate column. This is not unexpected since it is well known that phosphate forms a complex with ferric ions.

In another set of experiments phosphoserine, a phosphorylated amino acid, was added to the eluent and the retention of cytochrome *c*, lysozyme and iron-free transferrin on the Fe(III)–EDDA column was measured using isocratic elution. As can be seen in Fig. 4, a few millimoles of this amino acid were a useful adjunct for modulating protein retention. Indeed, when adding 20 m*M* phosphoserine to the eluent, the retention factors of iron-free transferrin, lysozyme and cytochrome *c* decreased by a factor of 0.2, 0.5 and 0.7, respectively, from their values obtained in the absence of phosphoserine. This is another indication of the predominance of metal interaction with Fe(III)–EDDA stationary phase.

The effect of eluent pH on MIC retention was investigated with various metal–EDDA columns using gradient elution with linearly increasing sodium chloride concentration in the eluent. The results are depicted in Fig. 5 by plots of adjusted retention volumes *versus* eluent pH. As expected, this effect varies from one metal chelate column to another for a given set of proteins[11]. With the exception of the Ni(II)–EDDA column, which did not exhibit an affinity toward holo and iron-free transferrins in the pH range studied, the retention of these two proteins decreased with increasing pH on all other metal–EDDA columns and reached zero at pH values which were different from one column to another. Both transferrins were retained to the same extent on Zn(II)–EDDA at pH 5.0 but eluted with no retention at pH 5.5 and above. On the other hand, on the Fe(III)–EDDA column the holo and iron-free transferrins were only separated at pH 6.25, whereas on Co(II)–EDDA they could be separated at pH values ranging from ca. 5.2 to 6.0 (*cf.* Fig. 5). The decrease in affinity of transferrins toward the chelated metals on the surface of the stationary phase with increasing pH may be explained by the increase in net negative charge of the proteins leading to electrostatic repulsion from the sorbent having the same net charge. The equal affinity of holo and iron-free transferrins toward some of the metal chelate columns at low pH (below or equal to 5.0) may be explained by the dissociation of the iron–protein complex at that pH[20] so that the holo transferrin will lose its iron and

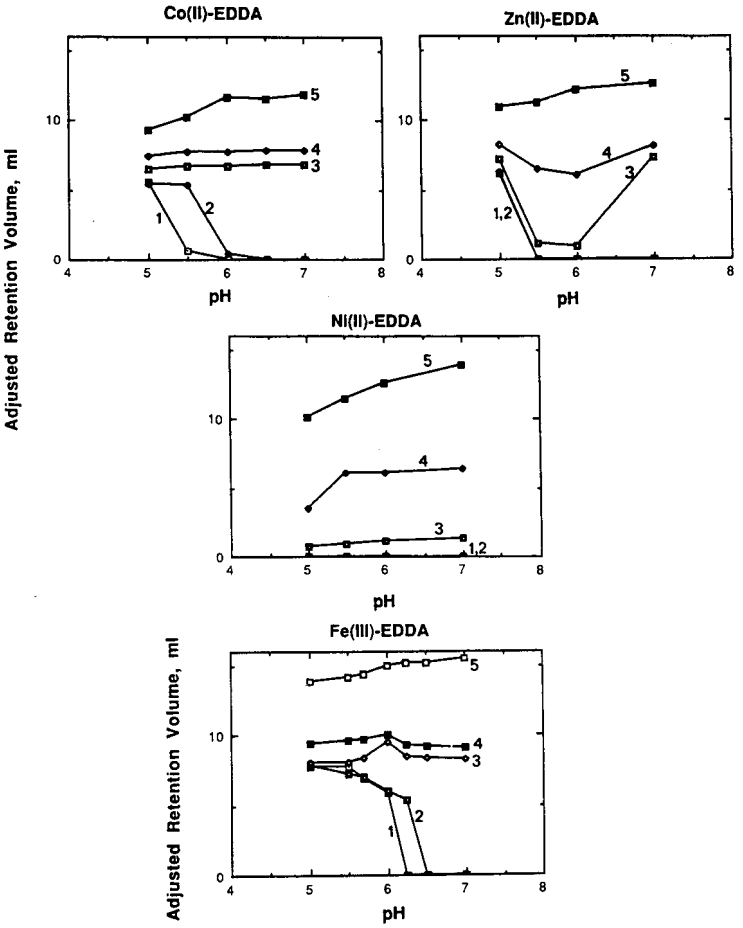

Fig. 5. Plots of adjusted retention volume *versus* pH, measured with different metal–EDDA columns. Column, 100 × 4.6 mm I.D.; flow-rate, 1.0 ml/min; temperature, 25°C. Linear gradient in 15 min from 0 to 1.0 *M* sodium chloride in 10 m*M* acetate or phosphate buffer at different pH values, followed by 5 min isocratic elution with 1.0 *M* sodium chloride in 10 m*M* buffer. 1 = holo transferrin; 2 = iron-free transferrin; 3 = cytochrome *c*; 4 = lysozyme; 5 = lactoferrin.

become an iron-free protein. Therefore, we believe that MIC will find use in studying protein–metal complexes provided that the metal-binding site in the protein molecule is also involved in the interaction process between the protein and the chelated metal on the surface of the stationary phase. The monotonic increase in the retention of lactoferrin with eluent pH on the various metal–EDDA columns (Fig. 5) may reflect the presence of imidazole groups on the surface of the protein molecule. Indeed, with the high histidine content of such a molecule[20] and the high p*I* value (net positive charge over a wide range of pH) an interaction of that kind may be favored. In contrast, due to their net negative charge at pH values above 5.5–6.0, acidic transferrins may be hindered from interacting with the chelated metals of the stationary

phases despite their high content of histidine. The plots of retention *vs.* eluent pH for cytochrome *c* and lysozyme on the Zn(II)–EDDA column are U-shaped curves (see Fig. 5). This may be explained by the presence of both carboxyl and imidazole groups in the binding site to the Zn(II)–EDDA column. These same proteins showed little or no change in retention on other columns when varying the eluent pH. It has been advocated that a cluster of groups rather than a single group[24,25] may be involved in the binding of proteins to the chelated metal on the surface of the stationary phase.

To study the effect of the nature and concentration of the salt in the eluent on MIC retention and selectivity, isocratic measurements were carried out with various salts at pH 5.5. The salts studied were sodium chloride, sodium formate, sodium acetate and sodium phosphate, and the columns examined were Co(II)– and Fe(III)–EDDA. Co(II) is a representative of "soft" metal ions, whereas Fe(III) is somewhat on the borderline of "hard" metal ions[26]. In all cases retention decreased with increasing salt concentration in the eluent in the concentration ranging from 0 to 0.5 *M*. Typical results are shown in Fig. 6 by plots of logarithmic retention factor *versus* the logarithmic salt concentration in the eluent. As shown in Fig. 6 straight lines were obtained for all the proteins under investigation. The intercepts of these lines with the ordinate (*y*-intercept), which are summarized in Tables III and IV, were used to rank the eluting strength of the different salts. A greater negative intercept reflects a stronger eluting salt. According to this empirical consideration the eluent strength with Fe(III)–EDDA column increased in the order of $Cl^- < CH_3COO^- \leqslant HCOO^- < H_2PO_4^-$ (except for lysozyme), whereas with Co(II)–EDDA column it increased in the order $CH_3COO^- < H_2PO_4^- < Cl^-$. These results are in agreement with the observation that "hard" metals such as Fe(III) coordinate preferably with oxygen containing ions (*e.g.* phosphate, acetate, formate), whereas "soft" metal ions such as cobalt have preference for large donor atoms, *e.g.* chloride ions in this study.

Based on the above results, MIC selectivity can be varied by keeping the eluting strength of the salt roughly the same while changing the nature of the salt in the eluent. As shown in Fig. 6 and Table V, different selectivities were achieved on the Fe(III)–EDDA column by exchanging sodium acetate for sodium formate; both salts have about the same eluting strength.

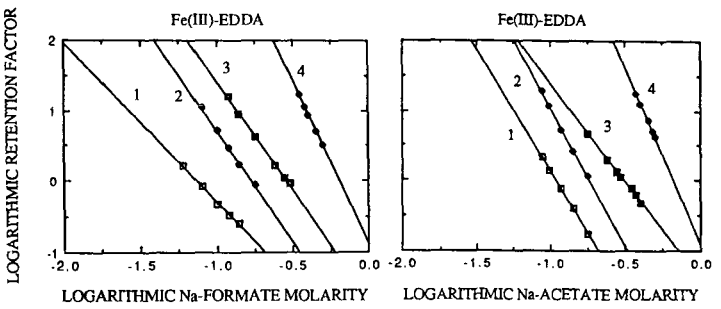

Fig. 6. Plots of logarithmic retention factor of proteins *versus* logarithmic salt molarity. Column, 100 × 4.6 mm I.D.; flow-rate, 1.0 ml/min; temperature, 25°C. Isocratic elution with 10 m*M* acetate buffer, pH 5.5, at different salt concentrations. Proteins: 1 = iron-free transferrin; 2 = cytochrome *c*; 3 = lysozyme; 4 = lactoferrin.

TABLE III

VALUES OF y-INTERCEPT OF PLOTS OF LOGARITHMIC RETENTION FACTOR OF PROTEINS *VERSUS* THE LOGARITHMIC SALT MOLARITY IN THE ELUENT

Column, 100 × 4.6 mm I.D., Co(II)–EDDA; flow-rate, 1.0 ml/min; temperature, 25°C. Isocratic elution with 10 m*M* acetate buffer, pH 5.5, at different salt concentrations.

Protein	*y-Intercept*		
	Sodium acetate	*Sodium phosphate*	*Sodium chloride*
Iron-free transferrin	−3.54	−3.03	−4.73
Cytochrome *c*	−2.05	−2.81	−3.11
Lysozyme	−1.29	−2.10	−2.53
Lactoferrin	−0.97	−1.69	−2.01

TABLE IV

VALUES OF y-INTERCEPT OF PLOTS OF LOGARITHMIC RETENTION FACTOR OF PROTEINS *VERSUS* THE LOGARITHMIC SALT MOLARITY IN THE ELUENT

Column, 100 × 4.6 mm I.D., Fe(III)–EDDA; flow-rate, 1.0 ml/min; temperature, 25°C. Isocratic elution with 10 m*M* acetate buffer, pH 5.5, at different salt concentrations.

Protein	*y-Intercept*			
	Sodium chloride	*Sodium formate*	*Sodium acetate*	*Sodium phosphate*
Iron-free transferrin	−2.07	−2.55	−3.36	−4.00
Cytochrome *c*	−2.04	−2.44	−2.84	−2.78
Lysozyme	−1.94	−1.68	−1.41	−2.15
Lactoferrin	−1.06	−0.88	−0.89	−1.51

TABLE V

SELECTIVITY, α, MEASURED WITH TWO SALTS OF COMPARABLE ELUTING STRENGTH

Column, 100 × 4.6 mm I.D., Fe(III)–EDDA; flow-rate, 1.0 ml/min; temperature, 25°C. Isocratic elution with 0.12 *M* sodium acetate or formate buffer, pH 5.5.

Pair of proteins	*Selectivity, α*	
	Sodium acetate	*Sodium formate*
Cytochrome *c*–transferrin	6.75	8.85
Lysozyme–cytochrome *c*	2.66	5.29

The slopes of the plots of log k' *vs.* log salt molarity, which measure the magnitude of interaction between the protein and the metal chelate stationary phase[11], were also calculated. A greater negative slope reflects a stronger interaction. As determined from these slopes, lactoferrin exhibited the strongest interaction with the Co(II)– and Fe(III)–EDDA columns, while all other proteins, *i.e.* cytochrome *c*, lysozyme and

iron-free transferrin, interacted with the metal chelate columns to a lesser extent than lactoferrin and at slightly different magnitude among each other.

In conclusion, EDDA stationary phases in an appropriate metal form are very suitable for the separation and determination of proteins. Such stationary phases can be viewed as complementary to IDA stationary phases, since they afford different selectivity and retentivity toward proteins. In addition, metal–EDDA stationary phases are stable as manifested by the constancy of the retention of proteins under elution conditions used in this study.

ACKNOWLEDGEMENTS

This work was supported by Grant No. HN9-004 from the Oklahoma Center for the Advancement of Science and Technology, Oklahoma Health Research Program and by The College of Arts and Sciences, Dean Incentive Grant Program at Oklahoma State University.

REFERENCES

1 M. Belew, T. Y. Yip, L. Anderson, R. Ehrnstrom and J. Porath, *Anal. Biochem.*, 164 (1987) 457.
2 A. Figueroa, C. Corradini and B. L. Karger, *J. Chromatogr.*, 371 (1986) 335.
3 D. Corradini, Z. El Rassi, Cs. Horváth, G. Guerra and W. Horne, *J. Chromatogr.*, 458 (1988) 1.
4 D. Matsuo, T. Tanbara, K. Okada, H. Fuko, H. Bando and T. Sukai, *J. Chromatogr.*, 369 (1986) 391.
5 Y. Kato, K. Nakamura and T. Hashimoto, *J. Chromatogr.*, 354 (1989) 511.
6 R. M. Chicz and F. E. Regnier, *Anal. Chem.*, 61 (1989) 1742.
7 E. Bollin and E. Sulkowski, *Arch. Virol.*, 58 (1978) 149.
8 V. G. Edy, A. Billiau and P. Desomer, *J. Biol. Chem.* 252 (1977) 5934.
9 H. Furthmayr, M. Tomita and V. T. Marchesi, *Biochem. Biophys. Res. Commun.*, 65 (1975) 113.
10 D. Blanchard, W. Dahr, M. Hummel, F. Latron, K. Beyreuther and J.-P. Carton, *J. Biol. Chem.*, 262 (1987) 5808.
11 Z. El Rassi and Cs. Horváth, *J. Chromatogr.*, 359 (1986) 241.
12 J. Porath, J. Carlsson, I. Olsson and G. Belfrage, *Nature (London)*, 258 (1975) 598.
13 J. Porath, B. Olin and B. Granstrand, *Arch. Biochem. Biophys.*, 225 (1983) 543.
14 J. Porath, *Biotechnol. Progr.*, 3 (1987) 14.
15 E. Sulkowski, in R. Burgers (Editor), *Protein Purification: Micro to Macro, UCLA Symposium on Molecular and Cellular Biology, Frisco, CO, March 29–April 4, 1987*, New Series, Vol. 68, Alan R. Liss, New York, 1987, p. 149.
16 G. Muszynska, L. Anderson and J. Porath, *Biochemistry*, 25 (1986) 6850.
17 E. S. Hemdan and J. Porath, *J. Chromatogr.*, 323 (1985) 255.
18 E. Hochuli, H. Dobeli and S. Schacher, *J. Chromatogr.*, 411 (1987) 177.
19 S. H. Chang, K. M. Gooding and F. E. Regnier, *J. Chromatogr.*, 125 (1976) 114.
20 F. W. Putnam, in F. W. Putnam (Editor), *The Plasma Proteins*, Vol. IV, Academic Press, Orlando, FL, 2nd ed., 1984, pp. 96–98.
21 A. E. Martell and R. M. Smith, *Critical Stability Constants*, Vol. 1, Plenum Press, New York, 1974, pp. 86–87 and pp. 116–117.
22 H. Kikuchi and M. Watanabe, *Anal. Biochem.*, 115 (1981) 109.
23 G. Muszynska, Y.-J. Zhao and J. Porath, *J. Inorg. Biochem.*, 26 (1986) 127.
24 E. Sulkowski, *Makromol. Chem., Macromol. Symp.*, 17 (1988) 335.
25 F. R. N. Gurd and P. E. Wilcox, *Adv. Protein Chem.*, 11 (1956) 311.
26 R. G. Pearson, *J. Am. Chem. Soc.*, 85 (1963) 3533.

Journal of Chromatography, 512 (1990) 249–254
Elsevier Science Publishers B.V., Amsterdam

CHROMSYMP. 1837

High-performance liquid chromatographic investigations on the cleavage kinetics of side-chain-protected arginine derivatives with a sophisticated post-column reaction detector

GERALD GRÜBLER, FRANK GUTJAHR, HARTMUT F. ECHNER, WOLFGANG VOELTER and HERMAN BAUER*

Abteilung für Physikalische Biochemie des Physiologisch-chemisches Institut, Universität Tübingen, Hoppe-Seyler-Strasse 4, D-7400 Tübingen (F.R.G.)

ABSTRACT

In the field of peptide synthesis, only a few exact data on the behaviour of side-chain-protecting groups and their specific cleavage methods are available. A method is described for the separation and highly specific detection of guanidino-protected and -free arginine residues. The simultaneous determination of the cleavage kinetics of α- and side-chain-protecting groups of arginine becomes feasible. A high-performance liquid chromatographic system with a highly specific post-column reaction detector for the (released) guanidino group in arginine derivatives was developed. The cleavage kinetics of the most important protecting groups for the guanidino residue in arginine derivatives were established.

INTRODUCTION

Various methods in protein chemistry, *e.g.*, classical and solid-phase synthesis and the modification of natural peptides and proteins, require side-chain-protected amino acid derivatives. The aim is to use appropriate protecting groups that resist all the required chemical and biochemical treatments but on the other side can be cleaved under special conditions. One of the most difficult side-chain groups to protect is the guanidino group in arginine, which shows additionally a great tendency to form lactams. To optimize the strategy for the synthesis or chemical modification of peptides or proteins containing guanidino-protected arginine residues it is important to consider the reactivity and the cleavage kinetics of the applied side-chain-protecting groups in relation to the optimum mode of synthesis.

To control the cleavage of guanidino-protecting groups, several methods have been described[1–4]. However, almost no data about the specificity of the reaction, including the side-reactions, are available.

An increase in the overall yield of a synthesis and the minimization of the side-reactions require an exact knowledge of the reaction kinetics of all the important

0021-9673/90/$03.50

steps. In the case of arginine derivatives, almost no data are available. Samples of synthetic peptides which have been submitted to the mostly used cleavage conditions show, on high-performance liquid chromatography (HPLC) numerous peaks resulting from the reaction itself, and from the reagents and solvents. Hence a precise determination of the released guanidino group is virtually impossible. This prompted us to develop a post-column reaction detector with high specificity with respect to the guanidino group in arginine residues.

Phenanthrenequinone reacts with the guanidino group in arginine specifically to form a fluorescent dye[5,6]. Fig. 1 shows the proposed mechanism of the reaction of phenanthrenequione with arginine in alkaline solution and the production of a Schiff base, 2-amino-1*H*-phenanthro[9,10-*d*]imidazole (API). The eluted components are first detected with a standard UV detector. There after an alcoholic solution of phenanthrenequione is added, reacted in alkaline conditions and finally acidified to form the fluorescent compound, which is detected with a fluorescence monitor. High selectivity and sensitivity are found[7,8]. Hence it is possible to determine the cleavage kinetics of allmost all guanidino-protecting groups used in peptide chemistry. The developed separation technique allowed us to investigate and to evaluate the suitability of the most frequently used guanidino protecting groups, *viz.*, 4-methoxy-2,3,6-trimethylbenzenesulphonyl- (Mtr)[9], 2,2,5,7,8-pentamethylchromane-6-sulphonyl- (Pmc)[10], *p*-methoxybenzenesulphonyl- (Mbs)[11], mesitylene-2-sulphonyl- (Mts)[12] and 2,4,6-triisopropylbenzenesulphonyl- (Tip)[13].

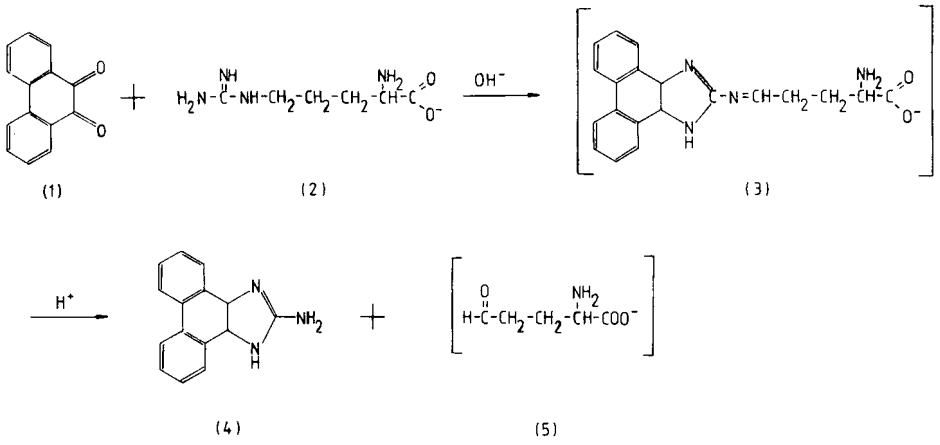

Fig. 1. Formation of the fluorescent dye from 9,10-phenanthrenequinone with the guanidino function of arginine. (1) 9,10-Phenathrenequinone; (2) arginine; (3) 2-(ω-imidoglutamic acid)-1*H*-phenanthro[9,10-*d*]imidazole; (4) 2-amino-1*H*-phenanthro[9,10-*d*]imidazole (API); (5) glutamic-γ-semialdehyde.

EXPERIMENTAL

Apparatus

The investigations were performed with a modified Biotronik BT 3020 liquid chromatograph. The separation was carried out on a 250 × 4 mm I.D. steel column of Nucleosil 100-C_{18}(5 μm). Direct detection was effected with a standard variable-wavelength UV monitor. The effluent from the UV detector was continuously mixed

with 1 mol l^{-1} sodium hydroxide solution and thereafter with a solution of 2.5 mg l^{-1} pheneanthrenequinone in ethanol. The reaction of eluted guanidino residues to give a Schiff base (see Fig. 1) was performed in a 16 m × 0.25 mm I.D. PTFE tube at elevated temperature (95°C). The fluorescent dye was finally formed in a second 4 m × 0.25 mm I.D. PTFE tube on adding 5% sulphuric acid at ambient temperature. Detection was carried out with an F1000 fluorescence monitor (313/395 nm) (Merck–Hitachi, Darmstadt, F.R.G.).

Chemicals and reagents

Amino acid derivatives of the highest available purity were obtained from Novabiochem (Läufelfingen, Switzerland). (*Z*)-Arg(Tip)-OH was synthesized in our laboratory. All other solvents and reagents were of analytical-reagent of HPLC grade from Merck.

Evaluation of the eluent and reagent compositions

The optimization of the post-column reactor was carried out after establishing the appropriate gradient for the HPLC separation. Alinear gradient from acetonitrile–water [0.06% trifluoroacetic acid (TFA) (2:8) to acetonitrile–water (0.5% TFA) (9:1) within 15 min proved to be sufficient for all the cleavage kinetics investigated.

The initial values of the eluent and reagent compositions and the mixing ratio were taken from test-tube experiments. The reagent concentrations and the flow-rate were varied stepwise until optimum values were found. The flow-rate of the eluent was adjusted to 1 ml min^{-1}. The flow-rates of the pheneanthrenequinone reagent and of the sulphuric acid were initially adjusted to 0.5 ml min^{-1} while that of the sodium hydroxide solution was optimized. Thereafter the flow-rates of the other reagents were subsequently optimized. Fig. 2 shows the relationship between the fluorescent yield and the reagent composition.

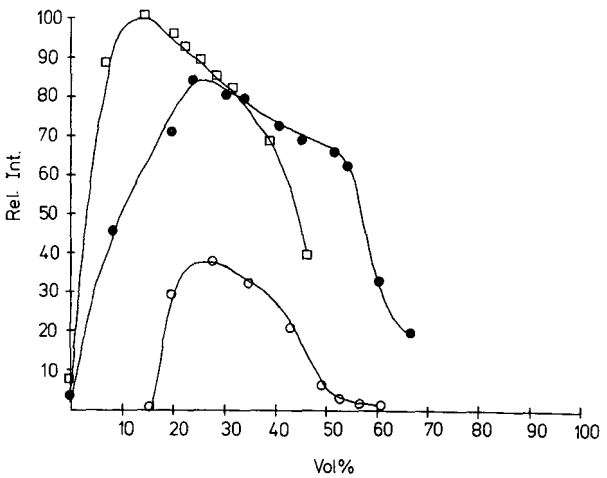

Fig. 2. Dependence of fluorescence yield on reagent composition. Flow-rate of eluent, 1 ml min^{-1}; initial flow-rate of reagents, 0.5 ml min^{-1}; temperature, 95°C (coil I) and ambient (coil II). (○) 0.2 mol l^{-1} NaOH; (●) 2.5 mg l^{-1} 9,10-phenanthrenequinone–ethanol; (□) 5% H_2SO_4.

The appropriate length of the PTFE tubing was determined by cutting pieces successively from over-long tubing. The first reaction step, the formation of 2-(ω-imidoglutamic acid)-1*H*-phenanthro[9,10-*d*]imidazole, under the chosen conditions showed a maximum at a coil length of 16 m, which corresonds to a reaction time of 22 s. The fluorescent dye, 2-amino-1*H*-phenanthro[9,10-*d*]imidazole (API), is formed immediately in a shorter coil only 4 m long, which corresponds to a reaction time of 5 s.

Cleavage conditions

Protected arginine derivatives, *e.g.*, (*Z*)-Arg(Pmc)-OH (5 mmol), were reacted under standard cleavage conditions at 23°C with 1 ml of trifluoracetic acid–thioanisole (4:1). To establish the kinetics, periodically aliquots of 100 μl were drawn and neutralized with 150 μl of triethylamine. Volumes of 20 μl of each of the samples were injected.

RESULTS AND DISCUSSION

All investigations of the cleavage of protecting groups of the guanidino residue in arginine derivatives were made with N-protected arginine derivatives. Such arginine derivatives should be useful models for natural and synthetic peptides. However, as is shown later, the N-α-benzyloxycarbonyl (*Z*) group is also cleaved under the commonly chosen acidic conditions in the presence of thioanisole.

The direct chromatograms (see Fig. 3), which were obtained with UV detection at wavelengths between 200 and 225 nm, show numerous peaks in addition to the expected components, guanidino-protected (*Z*)-α-arginine, free (*Z*)-α-arginine, free arginine and the released protecting groups. The additional peaks are caused

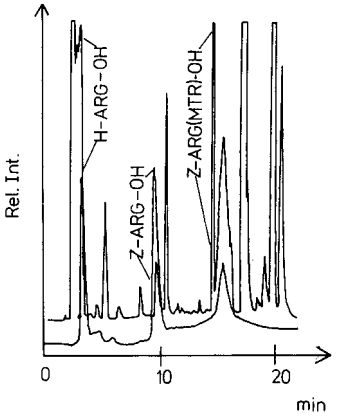

Fig. 3. Chromatogram of (*Z*)-Arg(Mtr)-OH after treatment with TFA–thioanisole for 30 min at 23°C, with UV and fluorescence detection. Column Nucleosil 100-C_{18}, 5 μm (250 × 4 mm I.D.); solvents, (A) acetonitrile–water (0.06% TFA) (2:8) and (B) acetonitrile–water (0.5% TFA) (9:1); gradient, linear from A to B in 15 min; sample volume, 20 μl; direct detection (upper chromatogram), UV, 220 nm; post-column reaction (lower chromatogram); flow-rate of reagent 1 (1 mol l^{-1} NaOH), 0.3 ml min^{-1}; flow-rate of reagent 2 [phenanthrenequinone (2.5 mg l^{-1}) in ethanol], 0.5 ml min^{-1}; flow-rate of reagent 3 (5% H_2SO_4), 0.3 ml min^{-1}; reaction coil 1, 16 m × 0.25 mm I.D., 95°C; reaction coil 2, 4 m × 0.25 mm, ambient temperature; detector, fluorescence, 315/395 nm.

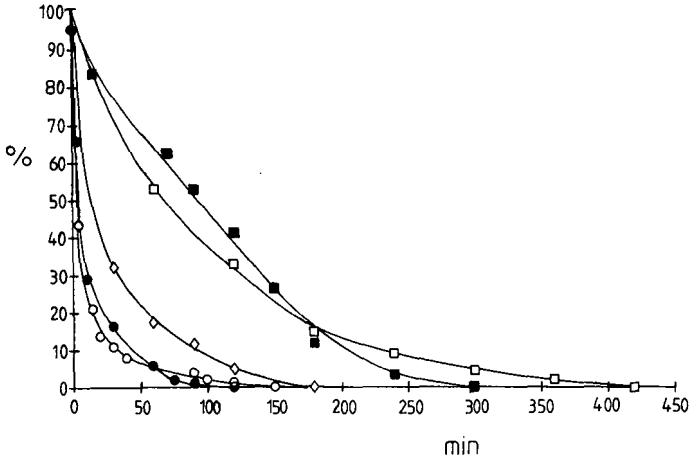

Fig. 4. Decrease in some guanidino-protected arginine derivatives under acidic conditions. Cleavage conditions: 5 mmol of derivative in 1 ml of trifluoroacetic acid–thioanisole (4:1), 23°C. Chromatographic conditions as in Fig. 2. ○ = (*Z*)-Arg(Tip)-OH; ● = (*Z*)-Arg(Pmc)-OH; ◇ = (*Z*)-Arg(Mtr)-OH; □ = (*Z*)-Arg(Mbs)-OH; ■ = (*Z*)-Arg(Mts)-OH.

predominantly by the additon of thioanisole to the acidic reagent and were therefore subsequently not further investigated. The chromatograms resulting from the post-column reactor show a high selectivity for the released arginine derivatives with unprotected guanidino groups. Only one non-specific broad peak was eluted additionally after (*Z*)-Arg(Mtr)-OH, which did not interfere with the interpretation of the chromatograms, however.

The decrease in the fully protected arginine derivatives in the cleavage kinetics of some of the investigated guanidino-protected derivatives is shown in Fig. 4. The reactions are complete within 120 min [(*Z*)-Arg(Pmc)-OH] and 425 min [(*Z*)-Arg(Mtr)-OH]. However, the yields of the expected compounds investigated are in all instances much lower than the theoretical values. Fig. 5 shows, for example, the cleavage kinetics of (*Z*)-Arg(Pmc)-OH. The guanidino-free derivative is released very

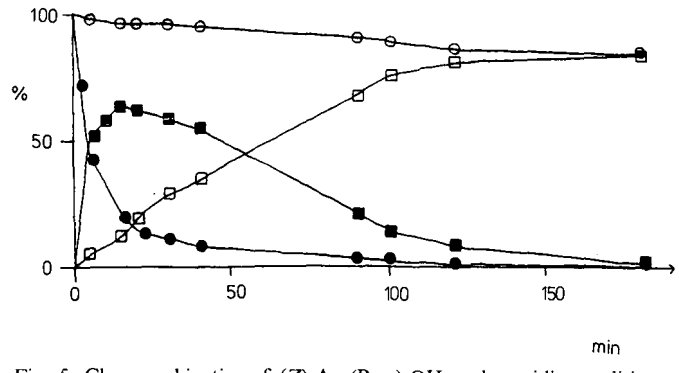

Fig. 5. Cleavage kinetics of (*Z*)-Arg(Pmc)-OH under acidic conditions. Cleavage conditions: 5 mmol (*Z*)-Arg(Pmc)-OH in 1 ml of trifluoroacetic acid–thioanisole (4:1), 23°C. Chromatographic conditions as in Fig. 3. ● = (*Z*)-Arg(PMc)-OH; □ = H-Arg-OH; ■ = (*Z*)-Arg-OH; ○ = sum.

TABLE I

PRODUCT YIELD *VERSUS* REACTION TIME AT REACTION RATES[a] OF 95% AND 99%

Protecting group	*Reaction rate*			
	95%		*99%*	
	Reaction time (min)	*yield (%)*	*Reaction time (min)*	*yield (%)*
(*Z*)-Arg(Tip)-OH	60	78	180	60
(*Z*)-Arg(Pms)-OH	130	88	180	90
(*Z*)-Arg(Mtr)-OH	140	85	175	80
(*Z*)-Arg(Mbs)-OH	225	88	290	85
(*Z*)-Arg(Mts)-OH	310	85	400	82

[a] Decrease in the fully protected arginine derivative. Cleavage conditions: 5 mmol of arginine derivative in 1 ml of trifluoroacetic acid–thioanisole (4:1), 23°C.

fast at the beginning of the reaction. However, after about 10 min the instability of the *Z*-group becomes substantial, and the first formed (*Z*)-Arg-OH is converted to free H-Arg-OH. In Table I the yields and the reaction times for some arginine derivatives are correlated with different reaction rates. The investigated arginine derivatives show different reactivities. The released derivatives are more or less instable and undergo further reactions. Hence the optimum reaction times differ considerably.

In peptide chemistry synthetic strategies have been developed that require the combination of different protecting groups. Therefore, it is very important to correlate these protecting groups according to their reactivity. The investigated derivatives cover a range of optimum reaction times from 60 to 400 min.

The investigations carried out in our laboratory allow the currently most often used protecting groups for the guanidino group in arginine derivatives to be classified according to their reactivity and their overall yield.

REFERENCES

1 R. E. Smith and R. MacQuarrie, *Anal. Biochem.*, 90 (1978) 246.
2 R. Reed and C. MacKay, *Anal. Biochem.*, 84 (1978) 324.
3 H. Yajima, M. Takeyama, J. Kanaki, O. Nishimura and M. Fujino, *Chem. Pharm. Bull.*, 26 (1978) 3752.
4 S. Yamada and H. A. Itano, *Biochim. Biophys. Acta*, 130 (1966) 538.
5 H. A. Itano and S. Yamada, *Anal. Biochem.*, 48 (1972) 483.
6 H. A. Itano, K. Hirota, I. Kawasaki and S. Yamada, *Anal. Biochem.*, 76 (1976) 134.
7 F. Gutjahr, *Diplom Thesis*, Naturwissenschaftliche-Technische Akademie, Isny, 1989.
8 G. Grübler, *Thesis*, University of Tübingen, 1990.
9 M. Fujino, M. Wakimasu and C. Kitada, *Chem. Pharm. Bull.*, 29 (1981) 2825.
10 R. Ramage and J. Green, *Tetrahedron Lett.*, 28 (1987) 2287.
11 O. Nishimura and M. Fujino, *Chem. Pharm. Bull.*, 24 (1976) 1568.
12 Y. Haruaki, H. Yajima, M. Masaharu, J. Kanaki and O. Nishimura, *Chem. Pharm. Bull.*, 26 (1978) 3752.
13 H. Echner and W. Voelter, *Z.Naturforsch. R*, 42 (1987) 1591.

Journal of Chromatography, 512 (1990) 255–263
Elsevier Science Publishers B.V., Amsterdam

CHROMSYMP. 1922

Identification of peptides containing aromatic amino acids, cysteine, iodotyrosine and iodothyronine by high-performance liquid chromatography with photodiode-array detection

JULIO ESCRIBANO
Servicio de Endocrinología, Centro Ramón y Cajal, 28034 Madrid (Spain)
MIRYAM ASUNCIÓN, JUSTA MIGUEL and LUIS LAMAS
Instituto de Investigaciones Biomédicas, CSIC, 28029 Madrid (Spain)
and
ENRIQUE MÉNDEZ*
Servicio de Endocrinología, Centro Ramón y Cajal, 28034 Madrid (Spain)

ABSTRACT

A general method for the identification of peptides containing tyrosine, tryptophan, phenylalanine and cysteine and a preliminary study of the identification of peptides containing monoiodotyrosine, diiodotyrosine, triiodothyronine and thyroxine by high-performance liquid chromatography photodiode-array ultraviolet–visible detection is reported. The technique was tested with an immunoglobulin light chain and with an *in vitro* iodinated urinary human complex-forming glycoprotein, heterogeneous in charge (protein HC), and human thyroglobulin (Tg) after enzymatic digestion. The system continuously monitors wavelengths and collects data that can be analysed by comparison with standard spectra via software routines. This procedure saves sample, time and reagents and avoids the use of radioactive reagents.

INTRODUCTION

The detection of peptides containing specific amino acids or their derivatives is of importance in protein studies in order to proceed to their characterization. Since the introduction of high-performance liquid chromatography (HPLC), many different procedures for the identification of peptides containing aromatic amino acids[1,2] and cysteine[3] have been described. The separation by HPLC of peptides containing monoiodotyrosine (MIT), diiodotyrosine (DIT) and thyroxine (T_4) from *in vivo* iodinated, non-radiactive thyroglobulin (Tg) has been reported[4]; a multi-wavelength detector was used, recording the absorbance at 230 nm to detect peptides, at 325 nm to detect sites of iodination [MIT, DIT, triiodothyronine (T_3) and T_4] and at 350 to detect T_4. More recently, a method for the separation, detection, hydrolysis and storage of

0021-9673/90/$03.50

iodine and fluorine derivatives of thyrosine peptides by reversed-phase (RP) chromatography at various pH levels[5] and a method for the identification of iodoamino acids in peptide sequences of Tg, iodinated *in vitro* with radioiodine[6], has been described. However, none of them is simple and they require a series of separation steps prior to detection.

In the last few years, photodiode-array (PDA) ultraviolet (UV) or ultraviolet–visible (UV–VIS) detectors have been employed as components of HPLC systems. The advantage of these detectors is that they can continuously monitor all wavelengths of the spectrum and collect the data for future processing. After chromatography the data can be analysed via software routines, such as spectral analysis for peak identification and purity confirmation or comparison of absorption spectra of separated peaks, to obtain specific information about the sample. Recently, metabolites of aromatic amino acids[7], mycotoxins and other fungal metabolites[8], protein HC[9] and several chromophores[10,11] have been analysed with this detection system. This study was focused on peptide characterization and a PDA detector was used for identification of peptides containing aromatic amino acids, cysteine, MIT, DIT, T_3 and T_4.

In this paper we report a general procedure that allows the identification of all the above-mentioned peptides, using several simple data processing modes: "spectrum analysis", "second-derivative spectra", "spectrum index plot" and "multichromatogram analysis".

EXPERIMENTAL

Acetonitrile was obtained from Scharlau (Barcelona, Spain), guanidinium chloride, dithiothreitol, pronase, lactoperoxidase, glucose oxidase, MIT, DIT, T_3 and T_4 from Sigma (St. Louis, MO, U.S.A.), 4-vinylpyridine from Aldrich (Milwaukee, WI, U.S.A.) and tetrahydrofuran, 1-tosylamino-2-phenylethyl chloromethyl ketone (TPCK)-treated trypsin, trifluoroacetic acid (TFA) and other compounds from Merck (Darmstadt, F.R.G.). Ultrapure water for HPLC was generated by a Milli-RO4, coupled to a Milli-Q water-purification system (Millipore, Bedford, MA, U.S.A.) and was used in the preparation of all buffers.

The chromatograph consisted of two Waters Assoc. (Milford, MA, U.S.A.) M6000A pumps, a Waters Assoc. 680 automated gradient controller and a Waters Assoc. 990 PDA detector with a dynamic range from the ultraviolet to the visible region (190–800 nm), based on an NEC APC III personal computer. All sample injections were performed with a Waters Assoc. U6K universal injector.

Size-exclusion HPLC was performed on a TSK 3000 SWG column (300 × 21.5 mm I.D.) (Toyo Soda, Tokyo, Japan), fitted with a TSK 3000 SWG guard column, by isocratic elution with 0.1 *M* ammonium acetate buffer (pH 5.0). The column was operated at room temperature at flow-rate of 1 ml/min.

RP-HPLC was performed with a NovaPak column (150 × 3.9 mm I.D.) (Waters Assoc.), protected by a guard column packed with μBondapak C_{18}/Corasil (Waters Assoc.). The column was eluted with acetonitrile gradients containing 0.1% (v/v) TFA (pH 2.0). The TFA-insoluble material was solubilized with 6 *M* guanidinium chloride and eluted with acetonitrile gradients containing 0.7% (w/v) ammonium hydrogencarbonate (pH 8.0). The column was operated at room temperature at a flow-rate of 0.5 ml/min.

The urinary protein HC preparation was provided by Dr. A. O. Grubb (Lund University, Sweden). Protein HC was purified as described earlier[12]. A completely reduced and S-pyridylethylated λ-light chain, isolated from a human monoclonal IgM (ESC), was used for this study.

Iodine-poor (0.01% I) human Tg from a multinodular goitre kindly provided by Dr. Geraldo Medeiros Neto (Laboratorio de Tiroides, Hospital das Clinicas, Facultad de Medicina de Sao Paolo, Brazil) was purified as described previously[13].

Urinary protein HC and Tg were iodinated enzymatically *in vitro* in 0.067 *M* phosphate buffer (pH 7.0) at 37°C with 10^{-4} *M* iodide, labelled with radioiodine (I*, specific activity 1.0 μCi/μat), 1.5 μg/ml lactoperoxidase, 1.0 mg/ml glucose and 1.5 μg/ml glucose oxidase for 1 h and 15 min, respectively. The number of atoms of iodine bound per mole of protein was calculated as described previously[13].

A 3-mg amount of human monoclonal IgM, dissolved in 200 μl of 2 *M* Tris–HCl buffer (pH 8.6) containing 0.002 *M* EDTA and 6 *M* guanidinium chloride, was incubated with 35 m*M* dithiothreitol for 120 min at 37°C. S-Pyridylethylation was achieved by adding 5.0 μl of 4-vinylpyridine and incubating for 15 min at room temperature. The excess of reagents was removed by HPLC on a TSK-3000 SWG column (300 × 21.5 mm I.D.) in 0.1 *M* ammonium acetate buffer (pH 5.0).

Reduced and S-pyridylethylated λ-light-chain immunoglobulin (115 μg) was digested with 1.15 μg of TPCK-trypsin in 250 μl of 0.2 *M* N-methylmorpholine acetate buffer (pH 8.2) for 2 h at 37°C. After digestion, the material was freeze-dried, lyophilized and redissolved immediately before chromatographic analysis in 0.1% (v/v) TFA.

The iodinated Tg was reduced with mercaptoethanol (ME) (100 mol ME/mol S–S in Tg) and subsequently S-cyanoethylated with acrylonitrile (2 mol/mol ME added), stopping the reaction with ME (2 mol/mol acrylonitrile added). The excess of reagents was eliminated by passage through an Econopac 10DG disposable chromatographic column (Bio-Rad Labs., Richmond, CA, U.S.A.). Tg fractions were pooled and digested with TPCK-trypsin (5%, w/w) for 16 h at 37°C.

Aliquots from iodinated protein HC and Tg were digested with pronase and the iodoamino acid distribution was determined as described previously[13].

MIT, DIT, T_3 and T_4 standards were dissolved in 50% aqueous acetonitrile containing 0.1% (v/v) TFA or in 0.7% aqueous ammonium hydrogencarbonate containing 5% acetonitrile, injected into a NovaPak C_{18} column, and eluted with 50% aqueous acetonitrile containing 0.1% (v/v) TFA or with 52.5% aqueous acetonitrile containing 0.35% (w/v) ammonium hydrogencarbonate. The absorption spectrum was obtained using a Waters Assoc. 990 PDA detector.

RESULTS AND DISCUSSION

The conventional way to identify aromatic Tyr- and Phe-containing peptides in HPLC is by acid hydrolysis, followed by amino acid analysis. However, this procedure cannot be used for Trp-containing peptides, as Trp is partly destroyed by the action of the acid, and consequently an additional technique to identify them must be used[14]. The above-described procedures require the use of additional sample- and time-consuming detection techniques. Alternatively, in HPLC the aromatic amino acid-containing peptides can be also localized simply by monitoring the chromatogram at

260 or 280 nm. However, this system itself does not distinguish precisely among the three aromatic amino acid-containing peptides, and consequently further analysis must be employed.

To solve this problem, we have used a routine procedure with a PDA detector adapted to our HPLC system in order to identify immediately after separation each of the Tyr-, Trp- and Phe-containing peptides. Fig. 1A shows a typical chromatogram, monitored at 220 nm by PDA detection and corresponding to a tryptic digest of a λ-light-chain immunoglobulin, chromatographed on an RP-HPLC column. By using the "spectrum index plot" data program, it is possible to obtain automatically the absorption spectrum at any wavelength range in the peak maximum from each peak of the chromatogram (Fig. 1B). By selecting the spectra from 240 to 310 nm, it is possible to recognize unequivocally by inspection of these spectra the three aromatic amino acid-containing peptides. A typical Phe spectrum with a maximum at 254 nm can be observed in peak 1, which corresponds to a Phe-containing peptide. Tyr-containing peptides can also be immediately recognized by inspection of the characteristic spectrum with a maximum around 278 nm and returning to the baseline at around 290 nm in peaks 6, 7, 12, 13, 14 and 15. Trp-containing peptides can be identified in peaks 8, 9, 10, 11, 16 and 17 by their spectrum with a maximum at 280 nm but not returning to baseline until 310 nm.

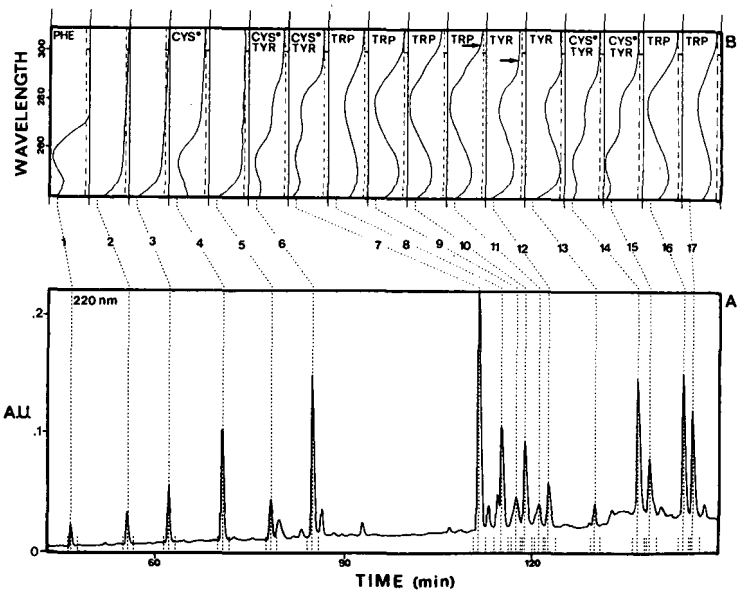

Fig. 1. Separation of a tryptic digest of reduced and S-pyridylethylated λ-light-chain immunoglobulin (ESC). Sample, 5.0 nmol; column, NovaPak C_{18} (300 × 21.5 mm I.D.); flow-rate, 0.5 ml/min. The column was equilibrated with 0.1% (v/v) aqueous TFA, and peptides were eluted at room temperature, using a linear gradient from 0 to 80% of acetonitrile containing 0.1% (v/v) TFA. (A) The chromatogram was analysed by monitoring the absorbance at 220 nm. (B) Automatic spectra were acquired from the peak maxima from 240 to 330 nm. Arrows indicate the end of the spectrum of Trp and Tyr. CYS*, TRP, TYR and PHE correspond to peptides containing S-4PE-cysteine, triptophan, tyrosine and phenylalanine, respectively.

The presence of Phe and Tyr in these peaks was verified by amino acid analysis and Trp was identified by sequence studies (data not shown). The additional use of the program "spectrum analysis" provides a useful help in the comparison of the spectra of the Phe-, Tyr- and Trp-containing peaks and with standard aromatic amino acids, as shown in Fig. 2, which displays the normalized spectra corresponding to peaks 1, 6, 12 and 10 in Fig. 1.

Another amino acid generally considered to be difficult to identify during peptide purification is cysteine. In HPLC, Cys-containing peptides can be identified either by the presence of cysteic acid or carboxymethylcysteine in the amino acid composition of their hydrolysates or by the radioactivity of labelled carboxymethylcysteine-containing peptides. These procedures require the use of an amino acid analyser or scintillation counter, which are both time and sample consuming. More recently, Cys in peptides has been identified as 4-pyridylethylcysteine (4-PE-Cys) from S-pyridylethylated proteins[3]. Based on the fact that this reagent has an extremely high molar absorptivity at 254 nm compared with the three aromatic amino acids, 4-PE-Cys-containing peptides can be easily localized in a HPLC trace by monitoring the absorbance at 254 nm. Fig. 3 shows in the "multichromatogram analysis" program the two patterns at 254 and 220 nm, corresponding to the tryptic digest of reduced and S-pyridylethylated λ-light chains of IgM (Fig. 1). Visual inspection of the chromatogram at 254 nm shows the presence of four major and a few minor peaks. Characterization of the 4-PE-Cys-containing peptides was possible by means of the program "spectrum index" without recourse to amino acid analysis (Fig. 1). As can be seen in Fig. 1B, the spectra corresponding to peaks 4, 6, 7, 14 and 15 shows a characteristic maximum at 254 nm, indicating the presence of 4-PE-Cys-containing peptides. This system also allows the identification of the minor peaks, 16 and 17, detected at 254 nm as Trp-containing peptides instead of 4-PE-Cys derivatives. In both Figs. 1B and 2 these programs allow the easy identification of peptides containing more than one chromophore, such as Cys and Tyr in peaks 6, 7, 14 and 15.

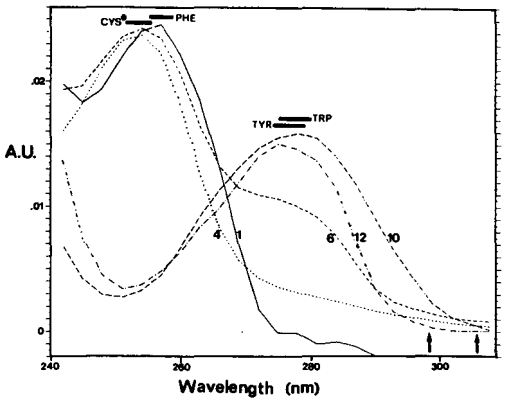

Fig. 2. Comparative spectral analysis from 240 to 310 nm of peaks 1, 4, 6 and 12 from Fig. 1. Spectra were normalized in order to eliminate concentration differences. Arrows show the end of the absorption spectrum of tryptophan and tyrosine. Horizontal bars represent the range around the maxima for S-4PE-Cys, Trp, Tyr and Phe standards.

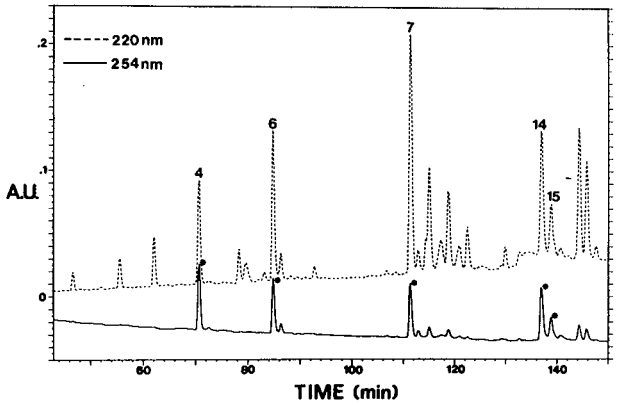

Fig. 3. Multi-chromatographic analysis of the absorbance at 220 and 254 nm of tryptic peptides from Fig. 1. The peaks marked with asterisks represent S-4PE-Cys-containing peptides. The peak numbers correspond to peaks in Fig. 1.

We investigated the direct ditection of iodoamino acid-containing peptides, both in Tg (which is the Tyr-containing protein forming thyroid hormones with the highest efficiency by iodination and coupling of some of its Tyr residues) and in protein HC, which does not form thyroid hormones efficiently after *in vitro* iodination. As a preliminary step to the detection of MIT-, DIT-, T_3- and T_4-containing peptides in both protein HC and Tg, standards were injected into the HPLC system in both TFA (pH 2.0) and ammonium hydrogencarbonate (pH 8.0). Using the "spectrum analysis" program (Fig. 4A), the absorbance maxima in TFA for MIT, DIT, T_3 and T_4 were 284, 290, 298 and 302 nm, respectively. These data agree with those reported earlier[5] and show a gradual shift towards higher wavelengths with increasing number of iodine atoms in the molecule. Although the spectra of T_3 and T_4 have similar maxima around 300 nm, the spectrum of T_3 ends at about 334 nm whereas that of T_4 ends at about 340 nm. The "second-derivative" program (Fig. 4B) shows that for each iodoamino acid there is a characteristic maximum around 304, 310, 320 and 330 nm for MIT, DIT, T_3 and T_4, respectively. The clearly different absorption and second-derivative maxima of each iodoamino acid allow their identification.

Fig. 5 shows the 220 nm and the ^{125}I radioactivity patterns of a partial hydrolysate of *in vitro* iodinated protein HC, chromatographed on an RP-HPLC column. Peaks 47 and 87 contained 85.5% and 92.5% MIT, respectively, whereas peaks 93 and 273 contained 90.0% and 82.2% DIT, respectively, as shown by pronase digestion and paper chromatography (Table I). This was confirmed by using the "spectral analysis" and "second-derivative" programs, as shown in Fig. 6A and B, respectively, as the spectrum of fraction 87 coincided exactly with that of the MIT standard, and the spectra of fractions 93 and 273 coincided with that of the DIT standard. However, peak 47 does not coincide completely with either the MIT or the DIT standard by spectral analysis (Fig. 6A), probably owing to the contribution of aromatic amino acid contaminants, as the absorbance peak and the ^{125}I peak around that fraction do not coincide (Fig. 5). However, when using the "second-derivative"

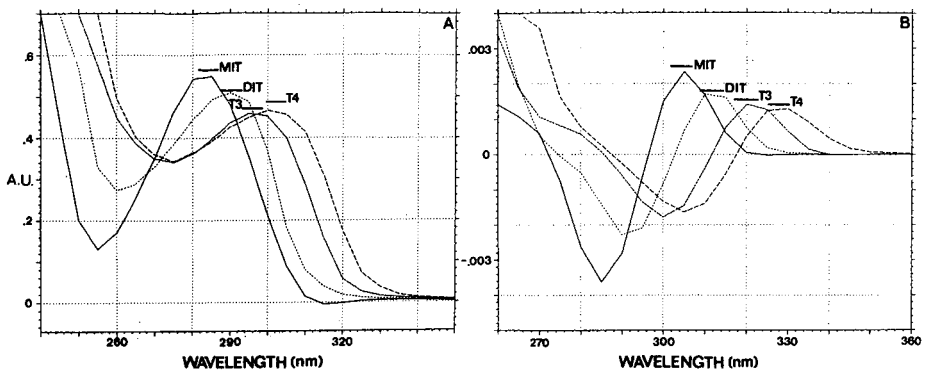

Fig. 4. Comparative spectral analysis from 240 to 350 nm (A) and second-derivative spectra from 260 to 360 nm (B) of MIT, DIT, T_3 and T_4 standards. Horizontal bars represent the range around the spectra maximum. Spectra were normalized in order to eliminate concentration differences.

program, the maximum and the minimum of fraction 47 are closer to those of MIT, strongly suggesting that the main iodoamino acid present is MIT.

Fig. 7A shows the absorption spectra of MIT, DIT, T_3 and T_4 standards and that of a T_4-rich peptide obtained by tryptic digestion of an *in vitro* iodinated Tg containing 23.4 atoms of iodine per mole of protein and 11.7% T_4. After pronase digestion of the fractions, it was seen that peak 137 contained as much as 77.0% T_4 (Table I). Although its maximum was at 285 nm, not coinciding with that of T_4, it absorbed beyond 340 nm as only the T_4 standard does. When using the "second-derivative" program (Fig. 7B), the maximum was closer to that of the DIT standard, but again it absorbed beyond 340 nm. Hence the most specific criterion to detect

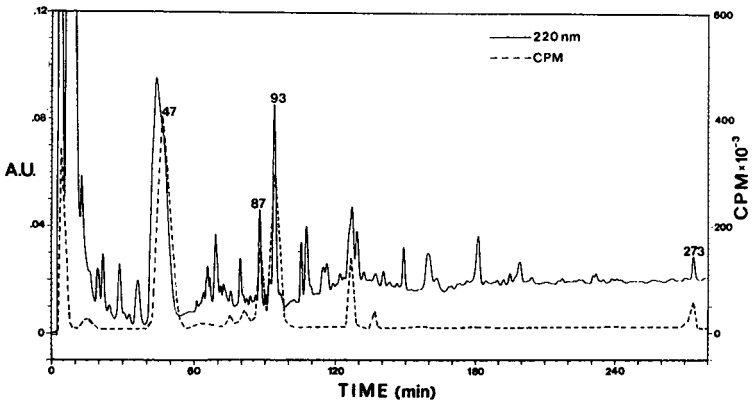

Fig. 5. Fractionation of a pronase digest of urinary ^{125}I-labelled protein HC. Sample, 31.0 nmol; column, NovaPak C_{18} (300 × 21.5 mm I.D.); flow-rate, 0.5 ml/min. The column was equilibrated with 0.1% (v/v) aqueous TFA, and peptides were eluted at room temperature, using a linear gradient from 0 to 80% of acetonitrile containing 0.1% (v/v) TFA. Fractions of 2 ml were collected and the radioactivity was measured.

TABLE I

IODINE ATOMS BOUND AND IODOAMINO ACID DISTRIBUTION OF *IN VITRO* IODINATED PROTEIN HC, THYROGLOBULIN AND PEPTIDES FROM TRYPTIC HYDROLYSIS

Species	*I (atoms/mol)*	*Labelled iodoamino acid distribution (%)*			
		DIT	*MIT*	T_4	T_3
Protein HC	2.0	14.2	62.7	0.8	0
Peptide 47		1.8	85.5	0.3	0.5
87		1.6	92.5	0.4	0.2
93		90.0	3.2	0.8	0.4
273		82.2	4.3	0.6	0.25
Thyroglobulin	23.4	43.5	36.2	11.7	1.5
Peptide 137		6.9	3.5	77.0	1.5

a T_4-containing peptide is the detection of significant absorbance beyond 340 nm. The fact that this T_4-rich peptide has a maximum absorption around 285 nm and a second-derivative maximum around 312 nm could be due to a high aromatic amino acid content. Both the "spectrum analysis" and the "second-derivative" programs seem to be complementary and are helpful in the direct detection of iodotyrosine- and iodothyronine-containing peptides.

In conclusion, we have described a procedure that permits the identification by HPLC of aromatic amino acids (Tyr, Trp and Phe) and cysteine (4-PE-Cys) using a PDA detector. In addition, a prelminary report on the direct detection of iodotyronine (MIT, DIT)- and iodothyronine (T_3, T_4)-containing peptides has been given. The direct detection of these peptides, even when they are still impure, is very useful for the identification and follow-up of the selected peptides during their HPLC purification. In addition to avoiding the need for radioactive compounds, this system permits the identification of peptides immediately after HPLC with corresponding savings of sample, time and reagents.

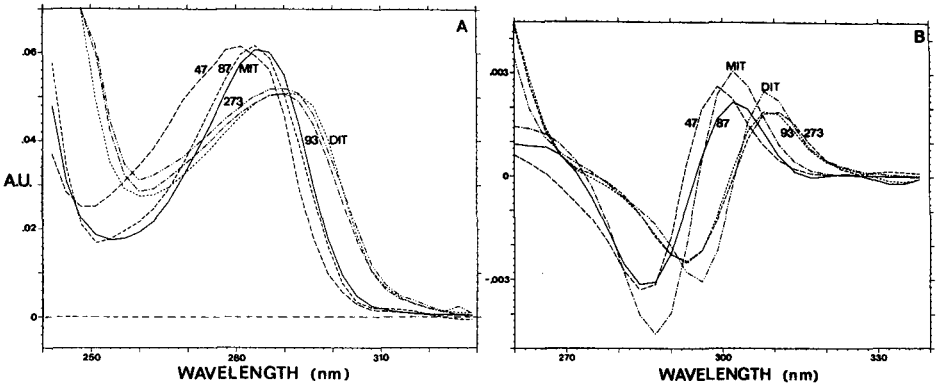

Fig. 6. Comparative spectral analysis from 240 to 330 nm (A) and second-derivative spectra from 240 to 340 nm (B) of protein HC pronase peptides 47, 87, 93 and 273 from Fig. 5. The spectra of MIT and DIT are included for comparison. Spectra were normalized in order to eliminate concentration differences.

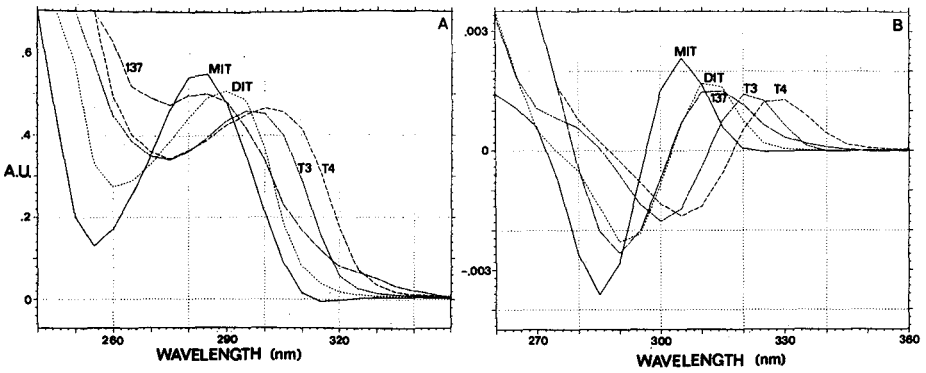

Fig. 7. Comparative spectral analysis from 240 to 350 nm (A) and second-derivative spectra from 260 to 360 nm (B) of a T_4-rich tryptic peptide (137) from *in vitro* iodinated thyroglobulin. The spectra of MIT, DIT, T_3 and T_4 are included for comparison. Spectra were normalized in order to eliminate concentration differences.

ACKNOWLEDGEMENTS

This work was supported by grants from CICYT (PM-880015), FISS (88/1453) and CEE (88300408). J. Escribano is a fellow from the Comunidad de Madrid.

REFERENCES

1 F. Nyberg, C. Pernow, U. Moberg and R. B. Eriksson, *J. Chromatogr.*, 359 (1986) 541.
2 E. Mendez, J. Escribano and G. Gonzalez, in Wittmann-Liebold (Editor), *Methods in Protein Sequence Analysis*, Springer, Berlin, Heidelberg, 1988, p. 293.
3 C. S. Fullner, *Anal. Biochem.*, 142 (1984) 336.
4 A. B. Rawitch, J. Gregg and C. D. Turner, in M. C. Eggo and G. N. Burrow (Editors), *Thyroglobulin —the Prothyroid Hormone, Progress in Endocrine Research and Therapy*, Vol. 2, Raven Press, New York, 1985, p. 43.
5 L. A. Edwards, R. E. Huber and T. J. Carne, in A. W. Kenneth (Editor), *Methods in Sequence Analysis*, Humana Press, Clifton, NJ, 1986, p. 457.
6 J. T. Dunn, L. A. Lamas and J. W. Fox, in A. W. Kenneth (Editor), *Methods in Sequence Analysis*, Humana Press, Clifton, NJ, 1986, p. 451.
7 A. F. Fell, B. J. Clark and H. P. Scott, *J. Chromatogr.*, 297 (1984) 203.
8 J. C. Frisvad and U. Thrane, *J. Chromatogr.*, 404 (1987) 195.
9 J. Escribano, R. Matas and E. Mendez, *J. Chromatogr.*, 444 (1988) 165.
10 W. A. Dark, *J. Chromatogr. Sci.*, 24 (1986) 495.
11 T. Alfredson and T. Sheelan, *J. Chromatogr. Sci.*, 24 (1986) 473.
12 L. Tejler and A. O. Grubb, *Biochim. Biophys. Acta*, 439 (1976) 82.
13 L. Lamas, P. Santisteban, C. Turmo and A. M. Seguido, *Endocrinology*, 118 (1986) 2131.
14 J. Chrastil, *Anal. Biochem.*, 158 (1986) 443.

Journal of Chromatography, 512 (1990) 265–272
Elsevier Science Publishers B.V., Amsterdam

CHROMSYMP. 1852

Reversed-phase high-performance liquid chromatographic separation of synthetic phosphopeptide isomers

LASZLO OTVOS, Jr.*
Wistar Institute of Anatomy and Biology, 3601 Spruce Street, Philadelphia, PA 19104 (U.S.A.)
IBRAHIM A. TANGOREN
Department of Pathology and Laboratory Medicine, University of Pennsylvania, Philadelphia, PA 19104 (U.S.A.)
KRZYSZTOF WROBLEWSKI[a]
Wistar Institute of Anatomy and Biology, 3601 Spruce Street , Philadelphia, PA 19104 (U.S.A.)
MIKLOS HOLLOSI
Department of Organic Chemistry, Eotvos L. University, Budapest (Hungary)
and
VIRGINIA M.-Y. LEE
Department of Pathology and Laboratory Medicine, University of Pennsylvania, Philadelphia, PA 19104 (U.S.A.)

ABSTRACT

Selectively phosphorylated synthetic peptides corresponding to the human neurofilament protein middle-sized subunit, H-Lys–Ser–Pro–Val–Pro–Lys–Ser–Pro–Val–Glu–Glu–Lys–Gly-OH, and its analogues were separated by reversed-phase high-performance liquid chromatography of mixtures consisting of the non-phosphorylated, the diphosphorylated and the two different monophosphorylated isomers. Application of the algorithm for the expected retention times to 4–9 amino acid-long peptide fragments revealed the correct elution order of the monophosphorylated isomers. According to circular dichroism studies, this elution order is also compatible with the possibility of induced conformational orientation on the surface of the bonded phase. Chromatographic analysis of the synthetic phosphorylation reaction indicates that the reaction rates of the two structurally different monophosphorylated peptides are similar, which is in contrast to the *in vivo* site-directed reaction.

INTRODUCTION

Numerous cellular functions are regulated through covalent phosphorylation of proteins[1]. Although protein sequences deduced from cDNA clones have led us to

[a] Present address: Department of Biochemistry and Biophysics, University of Pennsylvania, Philadelphia, PA 19104, U.S.A.

0021-9673/90/$03.50

understand several functions of the unmodified proteins, post-translational modifications, *e.g.*, phosphorylation and glycosylation, can be followed only by isolating phosphorylated protein fragments obtained by chemical or enzymatic cleavage methods, or by using synthetic peptides phosphorylated at the proposed phosphorylation sites. Several phosphoproteins contain more than one phosphorylation site within a short sequence[2,3]. Reversed-phase separation is the method of choice for the purification of both synthetic[4] and isolated[5] phosphopeptides; however, two-dimensional thin-layer chromatography was suggested to have advantages for the separation of phosphorylated insulin-receptor tryptic fragments[6]. Phosphorylated peptides have been shown to elute with decreased retention times compared with their parent non-phosphorylated analogues from reversed-phase high-performance liquid chromatographic (HPLC) columns[7], but the separation of monophosphorylated isomers of the same sequence has not been accomplished[8,9].

Earlier we reported the synthesis and conformation of a perphosphorylated peptide using polyphosphoric acid[10] corresponding to the repeat of the human neurofilament protein middle-sized subunit H–Lys–Ser–Pro–Val–Pro–Lys–Ser–Pro–Val–Glu–Glu–Lys–Gly–OH, where both serine residues carried covalently bound phosphate groups. The peptide, and three repeats thereof in addition to analogues, were used to identify[11] and characterize[12] the multi-phosphorylation repeats of mammalian neurofilaments. Most recently, we reported the solid-phase synthesis of this peptide by site-directed phosphorylation[13], where the serines were phosphorylated individually and together, to result in one diphosphorylated and two monophosphorylated isomers. Purification of the peptides was carried out by reversed-phase HPLC and, on the basis of the observed differences in the retention times, it was suggested that this method allows the separation of the phosphopeptide isomers obtained by a single post-synthetic phosphorylation reaction. In this paper we report the achievement of that separation for the first time.

EXPERIMENTAL

Peptide synthesis

The peptides were synthesized on *p*-alkoxybenzyl alcohol–glycine resin and peptide chain assembly was made with Fmoc-amino acid symmetrical anhydrides[14]. After cleavage with trifluoroacetic acid (TFA) and precipitation with diethyl ether, the peptides were dialyzed briefly in 1000 mol.wt. cut-off tubing (Spectrum, Los Angeles, CA, U.S.A.) against water and then lyophilized. Purity was tested by reversed-phase HPLC, amino acid analysis and positive ion fast atom bombardment mass spectrometry (FAB-MS).

Phosphorylation was carried out with polyphosphoric acid, made *in situ* from P_2O_5 and 85% H_3PO_4[10]. The reaction mixtures were stirred for 12–20 h under vacuum. Warm 2 *M* hydrochloric acid was added to the solidified product and the mixtures were shaken until they redissolved. The solutions were neutralized with 5 *M* sodium hydroxide solution and extensively dialyzed (nine solvent changes in three days) in a 1000 mol.wt. cut-off tubing against doubly distilled water and finally were lyophilized.

Chromatography

The chromatographic system consisted of two Beckman 110A pumps, regulated by a 421A controller, an Altex Ultraphere ODS 25 cm × 10 mm I.D. column, a Beckman 160 fixed-wavelength detector operating at 214 nm, 0.1 a.u.f.s., and a Shimadzu C-R6A integrator. Solvent A was 0.1% aqueous TFA, solvent B was 0.1% TFA in acetonitrile. The samples were loaded in 5% solvent A. The flow-rate was 3 ml/min throughout. A linear gradient of 1.33%/min of solvent B was used for analytical and 1%/min for preparative applications. The analytical loads were 10–100 μg and the preparative loads 2–5 mg. Fractions were collected manually.

Circular dichroism (CD) spectra were taken on a Jobin-Yvon Mark V spectrograph. Spectrograde trifluoroethanol (TFE) and water were used as solvents. All measurements were made in 0.02-cm cells. The peptide concentration was *ca.* 0.1 mg/ml. Details of the CD studies will be reported elsewhere. ^{31}P NMR spectra were taken on a Bruker AM 500 instrument. FAB-MS spectra were taken on a ZAB-E instrument at the Chemistry Department of the University of Pennsylvania by Dr. J. Dykins.

RESULTS

Three sets of peptides were synthesized and phosphorylated by the methods outlined under Experimental. A 13 amino acid-long peptide, H-Lys–Ser–Pro–Val–Pro–Lys–Ser–Pro–Val–Glu–Glu–Lys–Gly-OH (HNFM 1–13), corresponds to the repeat unit found six times in the middle-sized subunit of human neurofilament protein. A fragment four amino acids longer, H-Glu–Glu–Lys–Gly–Lys–Ser–Pro–Val–Pro–Lys–Ser–Pro–Val–Glu–Glu–Lys–Gly-OH (HNFM 1–17), was made to obtain stronger binding to anti-neurofilament antibodies. To verify the structure-determining effect of Lys^6 in HNFM 1–13 through forming intra- and intermolecular salt bridges[10], the lysine residue was replaced with Leu; this resulted in the third peptide, H-Lys–Ser–Pro–Val–Pro–Leu–Ser–Pro–Val–Glu–Glu–Lys–Gly-OH (1–13 L). After phosphorylation with polyphosphoric acid for less than 1 day, the reaction mixtures contained the monophosphorylated peptide, the diphosphate and the monophosphate isomers. The double phosphorylated forms are termed PP; the Ser^2 non-phosphorylated, Ser^7 phosphorylated peptides are termed nPP; the Ser^2 non-phosphorylated, Ser^7 nonphosphorylated peptides are termed PnP; and the HNFM 1–13 and 1–13L peptides without any phosphate are termed nPnP. In HNFM 1–17 the symbols refer to Ser^6 and Ser^{11}, respectively. With site-directed phosphorylation (when phosphorylation was carried out on the resin with dibenzyl phosphochloridate to unprotected serine residues, while the serines not to be phosphorylated were properly protected) we have shown[13] that on reversed-phase HPLC the elution order of phosphorylated and non-phosphorylated HNFM 1–13 and HNFM 1–17 peptides is PP, nPP, PnP, nPnP. Fig. 1 shows the gradient fraction of the preparative chromatogram when the post-synthetic phosphorylation mixture of HNFM 1–13 was loaded. The four peaks, (a) PP, (b) nPP, (c) PnP and (d) nPnP, were identified by comparison of the retention times with those of the corresponding selectively phosphorylated peptides and by undistinguishable binding of the phosphopeptides of different origin to anti-neurofilament antibodies that selectively recognize the different phosphate isomers. These monoclonal antibodies were raised to purified neuro-

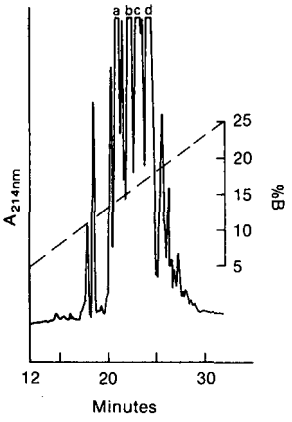

Fig. 1. Preparative reversed-phase chromatography of HNFM 1–13 phosphopeptides. Peaks were later identified as follows: a, PP, b, nPP; c, PnP; d, nPnP. P and nP refer to the presence or absence of the phosphate group on Ser^2 and Ser^7, respectively. Chromatographic conditions as described under Experimental.

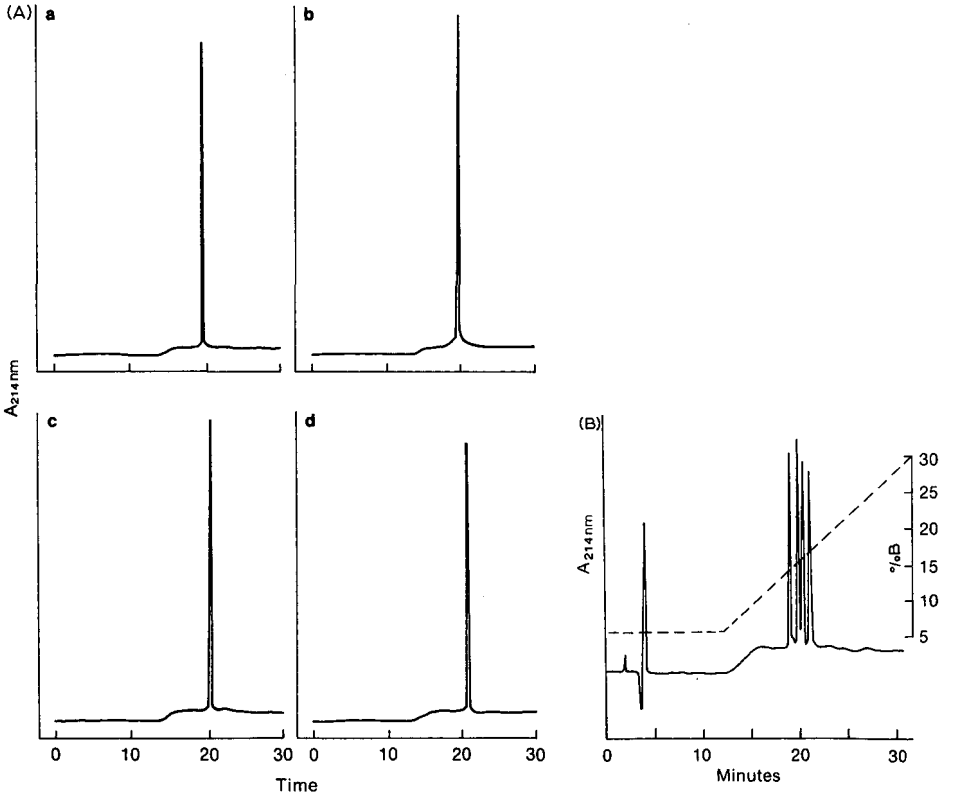

Fig. 2. (A) Chromatographic re-run of each individual peak fraction of HNFM 1–13 phosphopeptide isomers obtained from the preparative chromatography in Fig. 1. (B) Chromatographic re-run of 25 μg of each peak fraction injected together.

TABLE I

METHODS USED FOR VERIFYING THE STRUCTURES OF SEPARATED PHOSPHOPEPTIDES[a]

Peptide	*Retention time (min)*	*Phosphate analysis (%)*[b]	*FAB-MS (m/z)*	*^{31}P NMR (ppm)*	*Other*[e]
HNFM 1–13 a (PP)	19.2	102	M: 1542	n.d.[d]	ELISA[e]
HNFM 1–13 b (nPP)	20.0	96	M+H: 1463	n.d.[d]	ELISA
HNFM 1–13 c (PnP)	20.5	98	M+H: 1463	n.d.[d]	ELISA
HNFM 1–13 d (nPnP)	21.1	–	M: 1382		ELISA
HNFM 1–17 a (PP)	19.5	92	N/A[c]	1.19; 1.21	ELISA
HNFM 1–17 b (nPP)	20.4	106	M: 1905	1.28	ELISA
HNFM 1–17 c (PnP)	20.8	107	M: 1905	1.22	ELISA
HNFM 1–17 d (nPnP)	21.5	–	M: 1825		ELISA
1–13 L a (PP)	23.6	91	M+Na:1550	n.d.[d]	
1–13 L b (nPP)	24.2	109	M: 1447	n.d.[d]	
1–13 L c (PnP)	24.6	101	M: 1447	n.d.[d]	
1–13 L d (nPnP)	25.2	–	M−H: 1366		

[a] All peptides were subjected to amino acid analysis and CD.

[b] Calculation based on theoretical bound phosphate content; method as described[15].

[c] Diphosphorylated peptides sometimes fail to give any FAB-MS spectrum, possibly because of their highly hydrophilic character and intramolecular salt-bridge formation.

[d] Not determined.

[e] ELISA = Enzyme-linked immunoadsorbent assay; peptide recognition by anti-neurofilament antibodies was different, regulated by the location and number of the phosphate group(s).

filament protein subunits (the method of production was described previously[11,12]) and were selected based on their crossreactivity with synthetic peptides. Fig. 2 shows the HPLC profile of an analytical chromatographic re-run of a mixture consisting of 25 μg of each peak fraction. The HNFM 1–17 phosphopeptides were characterized as above. The analogy derived from the previous two sets of peptides was applied to fractions b and c of 1–13 L. Table I reports all parameters analyzed to verify the structure of the three sets of peptides.

To gain an insight into the kinetics of the post-synthetic phosphorylation reaction, we compared the peak integration values of four individual phosphorylations of HNFM 1–17 peptide (Table II). The percentages of the two monophosphorylated isomers were similar and reproducible.

TABLE II

PERCENTAGE OF DIFFERENTIALLY PHOSPHORYLATED HNFM 1–17 PEPTIDES OBTAINED BY FOUR PHOSPHORYLATION REACTIONS DETERMINED FROM REVERSED-PHASE HPLC PEAK-AREA INTEGRATION VALUES

Experiment No.	*PP (%)*	*nPP (%)*	*PnP (%)*	*nPnP (%)*
1	47	24	19	10
2	27	19	15	39
3	20	20	16	44
4	36	21	16	27

CD studies were conducted to characterize the conformation of the peptides carrying the phosphate groups on structurally different serine residues. In water the peptides showed unordered CD spectra. In TFE the phosphorylated fragments of HNFM 1–13 (fractions a, b and c, Fig. 1) exhibited spectra reflecting the equilibrium of unordered and repeating turn conformations, similarly to the CD curve of the non-phosphorylated peptide 1–13 nPnP (studies on the conformation of HNFM 1–13 nPnP have been reported previously[10]).

DISCUSSION

This study is a continuation of our efforts to characterize the conformation of neurofilament fragments important for their recognition by anti-neurofilament antibodies and to reveal the possible effect of neurofilament conformation in neurofibrillary tangle deposition[12]. Our selective phosphorylation procedure, in which the phosphorylation is carried out on the solid-phase synthetic support, provided HNFM 1–13 phosphate isomers in good yield[13] but longer peptides were needed for strong antibody binding and for conformational studies. Similar site-directed phosphopeptide syntheses for HNFM 1–17 = H-Glu–Glu–Lys–Gly–Lys–Ser–Pro–Val–Pro–Lys–Ser–Pro–Val–Glu–Glu–Lys–Gly-OH = Glu–Glu–Lys–Gly–1–13 resulted in low yields, probably owing to steric hindrance on the resin. Earlier, we reported a post-synthetic phosphorylation procedure by which fully phosphorylated peptides are obtained after exposure to polyphosphoric acid for 3 days[10]. On reversed-phase HPLC the resultant perphosphorylated HNFM fragment eluted with the starting 5% acetonitrile in 0.1% aqueous TFA. We obtained large amounts of both sets of peptides when we stopped the post-synthetic phosphorylation reaction after 1 day, when all four phosphate forms (PP, nPP, PnP and nPnP) were present.

Recently we found that the selectively phosphorylated phosphopeptides bound metal ions[16]. Extensive dialysis was needed to remove all residual sodium ions (introduced at neutralization after the phosphorylation reaction) in order to obtain the same retention times in reversed-phase HPLC (11–15% acetonitrile) of phosphopeptides prepared by polyphosphoric acid and selective phosphorylation, respectively. The phosphopeptides separated by reversed-phase HPLC were free from all other peptides with different phosphate forms. Application of the algorithm of Browne *et al.*[17] (based on the algorithm of Meek[18]) to 4–9 amino acid residue-long fragments of HNFM 1–17 surrounding the two structurally different serines revealed correct elution order of the two monophosphorylated isomers, where nPP was eluted with a lower acetonitrile concentration than PnP. The larger decrease in the retention time of nPP than PnP compared with nPnP is probably due to the break of an extended, relatively hydrophobic region around Ser[11] involving the Pro–Val–Pro–Lys–Ser–Pro–Val segment by the incorporation of the hydrophilic phosphate group on the serine residue (the longest similar hydrophobic segment around Ser[6] is Gly–Lys–Ser–Pro–Val–Pro). The decrease in retention times due to phosphate incorporation at the two positions is fairly additive: PP was eluted 2.0 min earlier than nPnP, and addition of the difference for the two monophosphorylated peptides compared with nPnP resulted in a 1.8-min retention time (Table I).

A possible induction of an ordered secondary structure of unoriented peptides on the surface of the stationary reversed-phase is the focus of many studies now[19,20].

Peptides, with a tendency to assume both β-pleated sheets[19] and α-helices[20], were reported to change their conformation during reversed-phase separation. Ostresh *et al.*[20] found that although the secondary structural prediction[21] revealed an amphipathic α-helix, CD studies in water showed a random structure. The observed increase in retention time compared with Meek's prediction[18] suggested induction of an ordered conformation. None of the four HNFM 1–13 isomers exhibited a tendency to form an ordered structure in water. In TFE the CD spectrum of PnP was similar to that of nPnP but the band intensities of the former spectrum were higher. PP exhibited a transitional spectrum between type C and that of unordered polypeptides[22]. Peptide nPP showed a C-like spectrum[10] with low band intensities. Type C spectra are similar to those of an α-helix, except that their band intensities are significantly lower. Type C spectra were measured recently for β-turns with established type I (III) character[23]. Based on our CD data, PnP shows a more pronounced tendency to assume an ordered conformation in TFE than does nPP. The stronger binding of PnP to the bonded phase may reflect this conformational orientation during the reversed-phase separation or just a result of the break of a smaller hydrophobic surface, as we discussed earlier.

The separation of the phosphate isomers by reversed-phase HPLC depends on the sequence around the phosphoserine residue[24]. We observed smaller differences in the retention times between PP and nPnP (1.6 min compared with 1.9 min for HNFM 1–13 and 2.0 min for HNFM 1–17) on peptides 1–13 L (the Lys^6 in HNFM 1–13 was replaced with Leu), when the overall retention times were higher.

Finally, we have some clues to the kinetics of the chemical post-synthetic phosphorylation reaction. Peak integration values of four individual phosphorylation reactions of HNFM 1–17 (Table II) revealed variable amounts for PP and nPnP [the solidification time of the reaction mixture varied (12–20 h), based on the amount of the polyphosphoric acid used and the strength of the vacuum; there were also small differences in the solubility of the lyophilized peptides in the phosphorylating reagent]. The very similar nPP and PnP production suggests reactions in which the concentration of the intermediate products is constant for the examined period. The ratio of the reaction rates for the two monophosphorylated isomers, k_{nPP}/k_{PnP}, is 1.27. We observed that, *in vivo*, phosphorylation of Ser^2 precedes that of Ser^7 in HNFM 1–13[25]. As the chemical phosphorylation rates do not suggest conformation in the solid state, where none of the serines is more accessible than the others to the polyphosphoric acid, the *in vivo* sequence of the phosphorylation is possibly regulated in solution by recognition of a certain part or particular conformation of the neurofilament molecule by the neurofilament-directed kinase(s).

ACKNOWLEDGEMENTS

The authors thank Shirley Peterson for editing the manuscript. This work was supported by National Institutes of Health grant NS 18616 (to V.M.-Y.L.).

REFERENCES

1 E. G. Krebs and J. A. Beavo, *Annu. Rev. Biochem.*, 48 (1979) 923.
2 D. H. Schlesinger, A. Buku, H. R. Wyssbrod and D. I. Hay, *Int. J. Pept. Protein Res.*, 30 (1987) 257.
3 H. Juhl, V. S. Sheorain, C. M. Schworer, M. F. Jett and T. R. Soderling, *Arch. Biochem. Biophys.*, 222 (1983) 518.

4 J. W. Perich, P. F. Alewood ad R. B. Johns, *Tetrahedron Lett.*,27 (1986) 1373.
5 T. R. Soderling and K. Walsh, *J. Chromatogr.*, 253 (1982) 243.
6 J. M. Tavare and R. M. Denton, *Biochem. J.*, 252 (1988) 607.
7 J. Lucas and A. Henschen, *J. Chromatogr.*, 369 (1986) 357.
8 M. R. Munday, D. G. Campbell, D. Carling and D. G. Hardie, *Eur. J. Biochem.*, 175 (1988) 331.
9 C. F. B. Holmes, N. K. Tonks, H. Major and P. Cohen, *Biochim. Biophys. Acta,* 929 (1987) 208.
10 L. Otvos, Jr., M. Hollosi, A. Perczel, B. Dietzschold and G. D. Fasman, *J. Protein Chem.*, 7 (1988) 365.
11 V. M.-Y. Lee, L. Otvos, Jr., M. J. Carden, M. Hollosi, B. Dietzschold and R. A. Lazzarini, *Proc. Natl. Acad. Sci. U.S.A.*, 85 (1988) 1998.
12 V. M.-Y. Lee, L. Otvos, Jr., M. L. Schmidt and J. Q. Trojanowski, *Proc. Natl. Acad. Sci. U.S.A.*, 85 (1988) 7384.
13 L. Otvos, Jr., I. Elekes and V. M.-Y. Lee, *Int. J. Pept. Protein Res.*, 34 (1989) 129.
14 E. Atherton, H. Fox, D. Harkiss, C. J. Logan, R. C. Sheppard and B. J. Williams, *J. Chem. Soc., Chem. Commun.*, (1978) 537.
15 C. W. I. McClare, *Anal. Biochem.*, 39 (1971) 527.
16 M. Hollosi, unpublished results.
17 C. A. Browne, H. P. Bennett and S. Solomon, *Anal. Biochem.*, 124 (1982) 201.
18 J. L. Meek, *Proc. Natl. Acad. Sci. U.S.A.*, 77 (1980) 1632.
19 M. T. W. Hearn and M. I. Aguilar, *J. Chromatogr.*, 392 (1987) 33.
20 J. M. Ostresh, K. Buttner and R. A. Houghten, in R. Hodges (Editor), *HPLC of Peptides and Proteins: Separation, Analysis and Conformation*, CRC Press, Boca Raton, FL, in press.
21 P. Y. Chou and G. D. Fasman, *Adv. Enzymol.*, 47 (1978) 45.
22 R. W. Woody, in E. R. Blout, F. A. Bovey, M. Goodman and M. Lotan (Editors), *Peptides, Polypeptides and Proteins,* Wiley, New York, 1974, p. 338.
23 M. Hollosi, M. Kawai and G. D. Fasman, *Biopolymers,* 24 (1985) 211.
24 R. E. H. Wettenhall and M. J. Quinn, *J. Chromatogr.*, 336 (1984) 51.
25 V. M.-Y. Lee, unpublished results.

Journal of Chromatography, 512 (1990) 273–281
Elsevier Science Publishers B.V., Amsterdam

CHROMSYMP. 1834

Optimization of high-performance liquid chromatographic peptide separations with alternative mobile and stationary phases

PATRICIA M. YOUNG* and THOMAS E. WHEAT
Waters Division of Millipore Corp., 34 Maple Street, Milford, MA 01757 (U.S.A.)

ABSTRACT

Peptides are routinely separated with reversed-phase high-performance liquid chromatography using increasing concentrations of acetonitrile in the presence of trifluoroacetic acid. While these separations may be improved by adjustments of gradient slope or substitutions of different solid-phase chemistries, many mixtures would benefit from systematic optimization of mobile phase components. Tryptic digests of cytochrome *c* from various species were separated on Waters Delta-Pak™ C_{18}. The effects of varying pH as well as the concentration and type of ion-pair reagent were examined. In addition, low pH, ion-suppression/ion-pairing chromatography was inverted using a polymeric reversed-phase column at high pH with alkyl amine ion pairing. Finally, a tryptic digest of cytochrome *c* was resolved by ion-exchange chromatography with a strong cation-exchange high-performance liquid chromatography column. These data suggest a framework for dramatically changing the selectivity of peptide separations, leading to more satisfactory peptide mapping.

INTRODUCTION

Peptide mapping is most commonly performed on silica-based reversed-phase columns using aqueous trifluoroacetic acid (TFA) as a starting eluent. Peptides are retained on the column and eluted as a function of increasing organic solvent, usually acetonitrile containing the same concentration of TFA[1–4]. While this mode of chromatography has proven useful, complex mixtures of peptides commonly obtained in enzymatic digests of high-molecular-weight proteins may include too many different species to provide complete resolution of each peptide. Mixtures of peptides within a single peak are unsuitable for amino acid sequencing or compositional analysis[5]. Alternative reversed-phase packings can provide different selctivities[6], but it may be more practical to optimize the separation by changing the mobile phase operating conditions. Conventional peptide mapping with TFA is performed at approximately pH 2, where the carboxyl functions are largely protonated. In addition, TFA serves as an ion pair to the positively charged amino functions. Alterations in mobile phase components and gradient slope can alter peptide retention and selectivity[7–12];

0021-9673/90/$03.50

however, alternative separation mechanisms may lead to greater resolution of complex peptide mixtures[12].

The ion pairing and ion suppression can be inverted at basic pH using high-resolution, polymeric reversed phase packings. At pH 11, amine groups will have suppressed ionization, while carboxyl groups will be negatively charged. An ion pair with the carboxyl group can be formed using alkyl amines, resulting in dramatically different reversed-phase separations.

Alternatively, it is possible to exploit the charge of peptides in an ion exchange separation[13]. Each peptide has an amino and carboxyl terminus, but more importantly, some of the amino acid residues have charged groups that contribute to the net charge of the peptide. Ion exchange offers an entirely different selctivity than reversed phase and can be used to obtain additional information about a peptide mixture.

MATERIALS AND METHODS

Tryptic digestion

Cytochrome *c* (Sigma, St. Louis, MO, U.S.A.) from bovine, rabbit, chicken and horse heart mitochondria (1 mg/500 μl) were suspended in 0.1 *M* ammonium bicarbonate (Sigma) buffer, pH 8.0. N-Tosyl-L-phenylalanine chloromethyl ketone (TPCK)-treated trypsin (Worthington Biochemical, Freehold, NJ, U.S.A.) was dissolved at a concentration of 0.2 mg/1 ml buffer. Trypsin solution (500 μl) was added to the cytochrome *c* suspensions and incubated for 24 h at 37°C.

Following incubation, trypsin was deactivated by heating at 100°C for 5 min. The digests were separated into aliquots of 100 μl and frozen (−20°C) until chromatographed. Prior to high-performance liquid chromatography (HPLC), digests were diluted 1:10 with aqueous TFA.

HPLC system

Samples were chromatographed on a 625 LC System (Waters Division of Millipore, Milford, MA, U.S.A.) equipped with a column heater and autosampler (Waters Model 712). Samples were analyzed by photodiode array detection (Waters Model 990+) in a wavelength range of 190–425 nm with 1.4 nm resolution. Peptide mixtures were separated on both stainless-steel (150 × 3.9 mm and 150 × 2 mm) and non-metallic (3.9 × 150 mm) columns packed with Delta-Pak™ C_{18}, 300 Å, 5 μm as well as RS-Pak™ DS-613 (150 × 6 mm) and Protein-Pak™ SP-5PW (75 mm × 7.5 mm), all from Waters.

Reagents

Chromatographic eluents were Milli-Q™ water (Millipore, Bedford, MA, U.S.A.) and HPLC-grade acetonitrile (Baker, Phillipsburg, NJ, U.S.A.). Heptafluorobutyric acid and sequanal grades of trifluoroacetic acid and hydrochloric acid were obtained from Pierce (Rockford, IL, U.S.A.). Tetrabutylammonium hydrogen sulfate and sodium chloride were obtained from Sigma.

RESULTS AND DISCUSSION

Gradient slope

Peptide retention times are sensitive to the concentration of organic solvent in the mobile phase, and subtle variations of gradient slope are commonly used to optimize a separation. Reductions in gradient slope or more shallow gradient formation result in greater resolution; however, the peptides elute in a larger volume. A 16 column volume gradient to 60% acetonitrile (1%/min) was compared to a 32 column volume gradient (data not shown). Peak heights were 30–50% greater with the steeper (16 column volume) gradient. The total peak volume was on the order of twice as large with the more shallow gradient (32 column volumes). An optimized chromatogram may be a compromise between resolution and sensitivity. More dilute materials may be difficult to use in subsequent analytical steps because fractions may necessitate concentration. This may result in sample loss with concomitant increase in trace contaminants that may be present in the mobile phase. It is important to consider other options that alter the selctivity of the separation so that resolution can be improved without increasing peak volume.

TFA concentration

TFA is used as a mobile phase modifier in peptide mapping to protonate or ion suppress peptide carboxyl groups at pH 2 while ion pairing to basic functionalities. Changes in TFA concentration primarily affect ion suppression and should alter the selectivity of the separation. The effect of varying TFA concentration can be conveniently tested using the Auto-Blend™ method[14] where one of the four inlet solvent lines contains 1% TFA solution (data not shown). The fraction of the flow taken from the stock TFA solution determined the final concentration blended in the mobile phase without mixing additional starting eluents. Separation of peptides at 0.1% and 0.05% TFA resulted in similar maps with subtle alterations in resolution. Some closely spaced peaks were resolved better with lower concentrations of TFA while other difficult pairs were separated better at higher concentrations of TFA. In addition, the baseline rise was approximately half as great with 0.05% TFA.

Alternative ion-pair reagents

The selective effects of ion-pair reagents were tested by separating a tryptic digest with a linear gradient in the presence of TFA (Fig. 1A), HCl (Fig. 1B), and heptafluorobutyric acid (HFBA, Fig. 1C). Dilute HCl (6 m*M*) maintained suppression of the carboxyl groups without the ion-pairing effect seen with TFA, leading to reduced retention of peptides. In contrast, 6 m*M* HFBA formed a bulky ion pair leading to increased retention of peptides when compared to TFA. Comparison of the HCl (Fig. 1B) chromatogram to TFA (Fig. 1A) indicated the following selectivity changes: (a) region 1 had greater resolution of the more hydrophilic peptides, (b) region 2 resolved an additional peak, (c) region 3 had peak rearrangement, and (d) peak 4 had altered mobility when compared to adjacent peaks. With HFBA (Fig. 1C), all peptides were retained longer with significant selectivity changes seen with the more hydrophilic peptides. The elution of the peaks in regions 3 and 4 was retarded and the elution order of the last two peptides, region 5, was inverted. Also, each modifier had important spectral characteristics. With HFBA, there was a large baseline shift due to

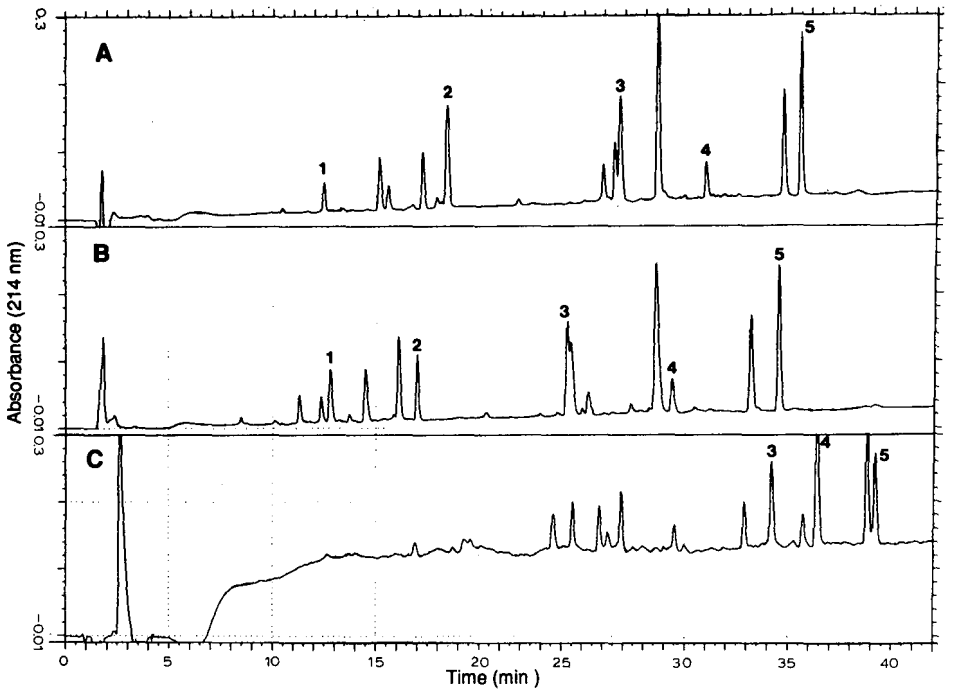

Fig. 1. Effect of mobile phase modifier on reversed-phase separation of tryptic peptides. The selective effects of ion-pair reagents were tested by separating a tryptic digest of chicken cytochrome *c* (1.3 nmol) on a non-metallic Delta-Pak C_{18} column (150 × 3.9 mm) at 35°C with a flow-rate of 1 ml/min with eluent A = water and eluent B = acetonitrile each containing the same concentration of modifier with a linear gradient (0–60% B, 33 column volumes) in the presence of 0.1% TFA (A), 6 m*M* HCl (B), and 6 m*M* heptafluorobutyric acid (C).

the increased extinction coefficient of this acid. Conversely, the baseline shift was diminished with HCl. The relative optical clarity of HCl may facilitate detailed spectral characterization in the low UV where the side chains of non-aromatic amino acids absorb.

Temperature

Peptide mapping at increased temperature led to reduced retention for all peptides (Fig. 2). While there were changes in selectivity, the differences were not as striking as those seen with alternative mobile phase modifiers. At 75°C (Fig. 2B), peaks 3 and 4 eluted closer to peak 5 and farther from peak 2. Also, at higher temperature, the relative distance between peak 6 and peak 7 decreased. In the chromatogram at 30°C (Fig. 2A), peak 1 was a co-elution of two peptides that differ by one Lys residue. At 75°C, peak 1 resolves the two components. However, due to decreased column life, continued operation at 75°C is not recommended.

Inverted ion suppression

Peptide mapping is most commonly performed on silica-based packing materials

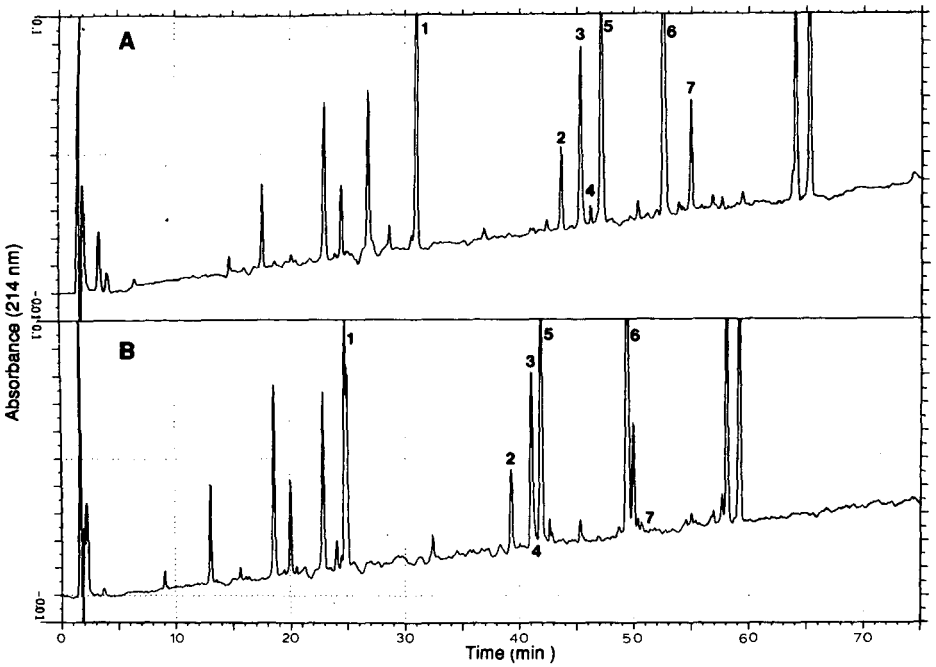

Fig. 2. Effect of temperature on reversed-phase separation of tryptic peptides. A tryptic digest of chicken cytochrome *c* (1.3 nmol) was separated on a stainless-steel Delta-Pak C_{18} column (150 × 3.9 mm) at 30°C (A) and 75°C (B). Chromatographic conditions: eluent A = water–0.1% TFA and eluent B = acetonitrile–0.1% TFA with a flow-rate of 1 ml/min using a linear gradient (0–60% B, 33 column volumes).

having alkyl-bonded phases where chromatography is restricted to a pH range of 2–8. The advent of polymeric or resin-based supports with extended pH ranges has increased the repertoire of the peptide chemist. The Waters RS-Pak DS-613 column performed similarly to Delta-Pak C_{18} when used with a conventional TFA gradient (Fig. 3A). While the maps were comparable (see Fig. 2A), there were marked changes in selectivity. In addition, the RS-Pak DS-613 was used in an inverted ion-pair mode, where the separation was performed at elevated pH (Fig. 3B). This resulted in ionization of the carboxyl groups and suppression of the amine functionalities. The ionized carboxyl group was, in turn, ion-paired with an alkyl amine. As seen, the selectivity was markedly altered.

Selectivity and resolution of inverted peptide mapping

Inverted ion-pair peptide maps were generated for horse, cow and chicken cytochrome *c* (data not shown). Many of the species differences reside in single amino acid residue substitutions that can be distinguished using this method of chromatography. Cytochrome *c* has a covalently bound heme group attached on tryptic peptide 14–22. In the chicken this peptide has a serine (S) residue at position 15, while in the mammalian cytochrome residue 15 is alanine (A). When the tryptic digests were chromatographed using 0.1% TFA (Fig. 4B), the heme-containing peptides could not be resolved on the basis of this single amino acid residue substitution. However, with

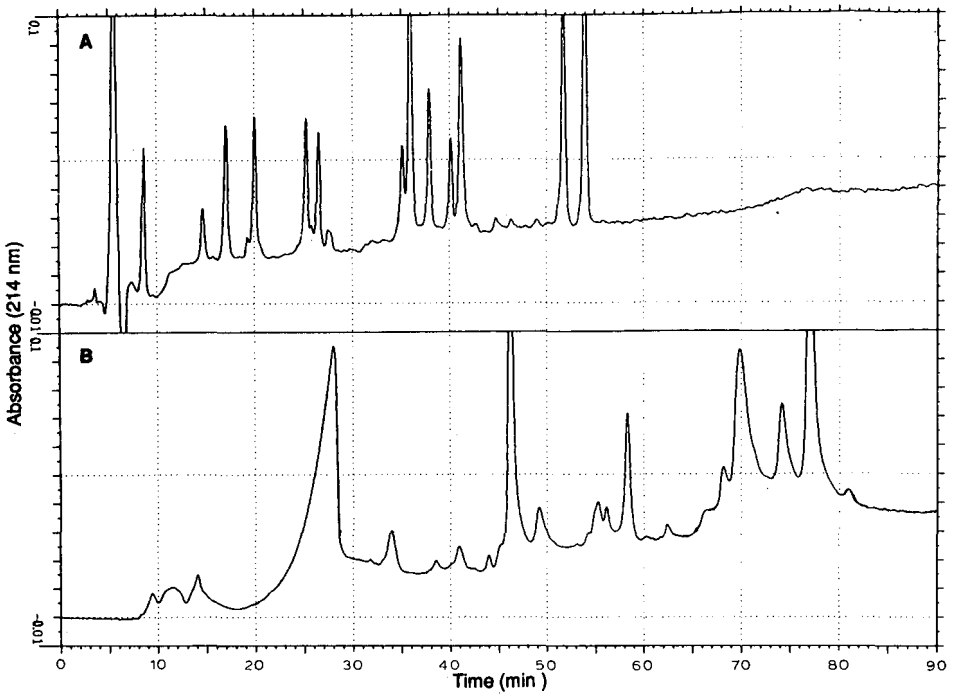

Fig. 3. Separation of tryptic peptides on polymeric reversed-phase supports. A tryptic digest of rabbit cytochrome *c* (2 nmol) was chromatographed at 35°C on a RS-Pak DS-613 (150 × 6 mm). For (A), the digest was separated with 0.1% TFA (pH 2.1) in water (eluent A) and acetonitrile (eluent B) at a flow-rate of 0.5 ml/min with a linear gradient (0–60% B, 14 column volumes). For (B), the digest was separated at with 2.5 m*M* tetrabutylammonium hydrogen sulfate (pH 11) in water (eluent A) and acetonitrile (eluent B) at a flow-rate of 0.3 ml/min with a linear gradient (10–70% B, 9 column volumes).

inverted ion-pair chromatography on the RS-Pak DS-613, these peptides were resolved (Fig. 4A). Thus, inverted ion pairing provided a distinctly different selectivity enabling resolution of the chicken peptide from the mammalian peptides.

Cation-exchange chromatography

It is possible to exploit the charge of peptides in an ion-exchange separation. Cytochrome *c* is a basic protein (p*I* 10), and digestion with trypsin produced several basic peptides. In Fig. 5, chicken tryptic peptides were separated on a Protein-Pak SP-5PW cation-exchange column. The basic peptides were retained on a sulfopropyl column at low ionic strength and acidic pH and separated with a salt gradient. As expected this column generated an entirely different peptide map enabling further characterization of the digest on the basis of net charge.

CONCLUSIONS

Peptide separations are most effectively improved by modification of the operating conditions and the mobile phase. Resolution is better with more shallow

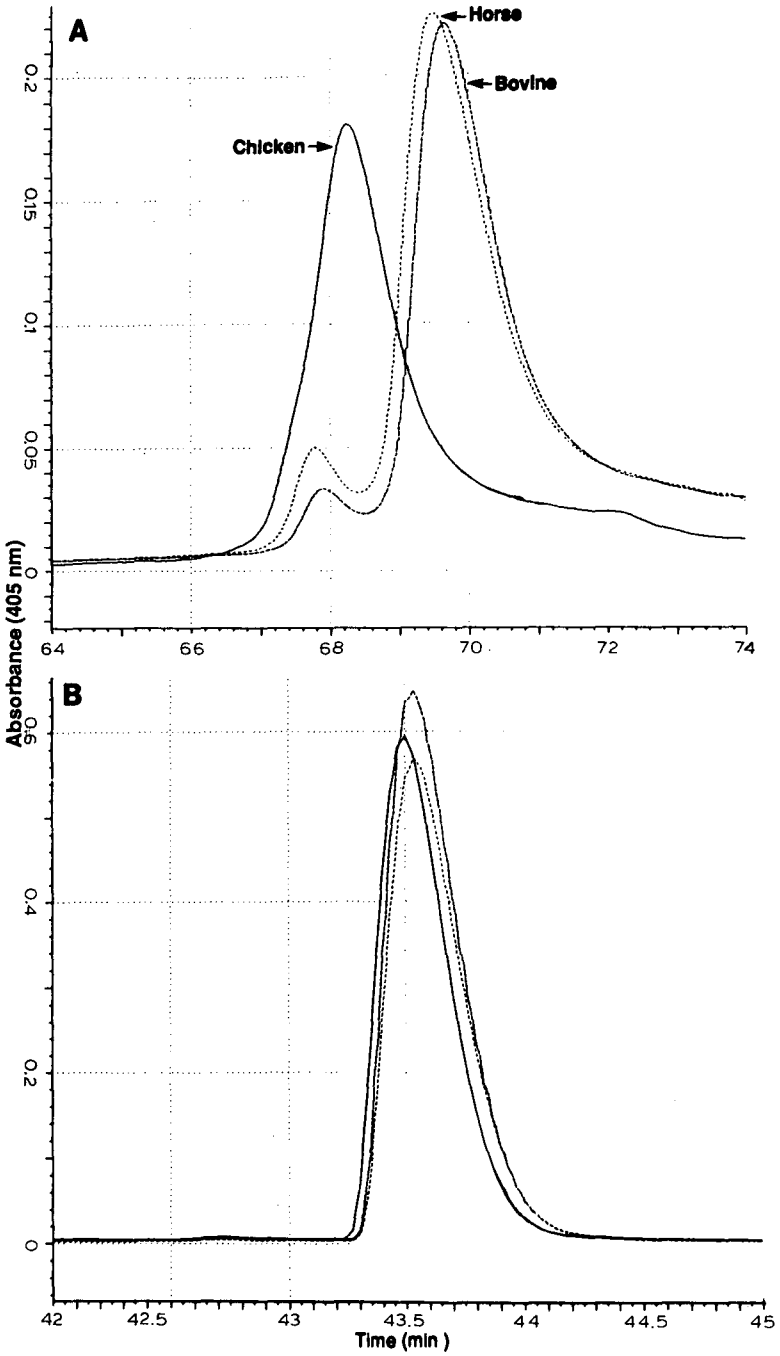

Fig. 4. Resolution in inverted peptide mapping. Tryptic digests of horse, bovine and chicken cytochrome *c* (2 nmol) were chromatographed at 35°C using inverted ion pairing (A) and standard TFA ion pairing (B). A portion of each chromatogram is shown depicting the heme containing peptides at 405 nm: chicken peptide 14–22 (CSQCHTVEK, single-letter amino acid codes) and horse/bovine peptides 14–22 (CAQCHTVEK). For (A), the digests were separated on a RS-Pak DS-613 (150 × 6 mm) with 2.5 m*M* tetrabutylammonium hydrogen sulfate (pH 11) in water (eluent A) and acetonitrile (eluent B) at a flow-rate of 0.3 ml/min with a linear gradient (10–70% B, 9 column volumes). For (B), the digests were separated on a Delta-Pak C_{18} (150 × 2 mm) with 0.1% TFA (pH 2.1) in water (eluent A) and acetonitrile (eluent B) at a flow-rate of 0.25 ml/min with an optimized linear gradient [0 min, A–B (95:5); 3 min, A–B (90:10); 13 min, A–B (87:13); 67 min, A–B (60:40); 77 min, A–B (40:60)].

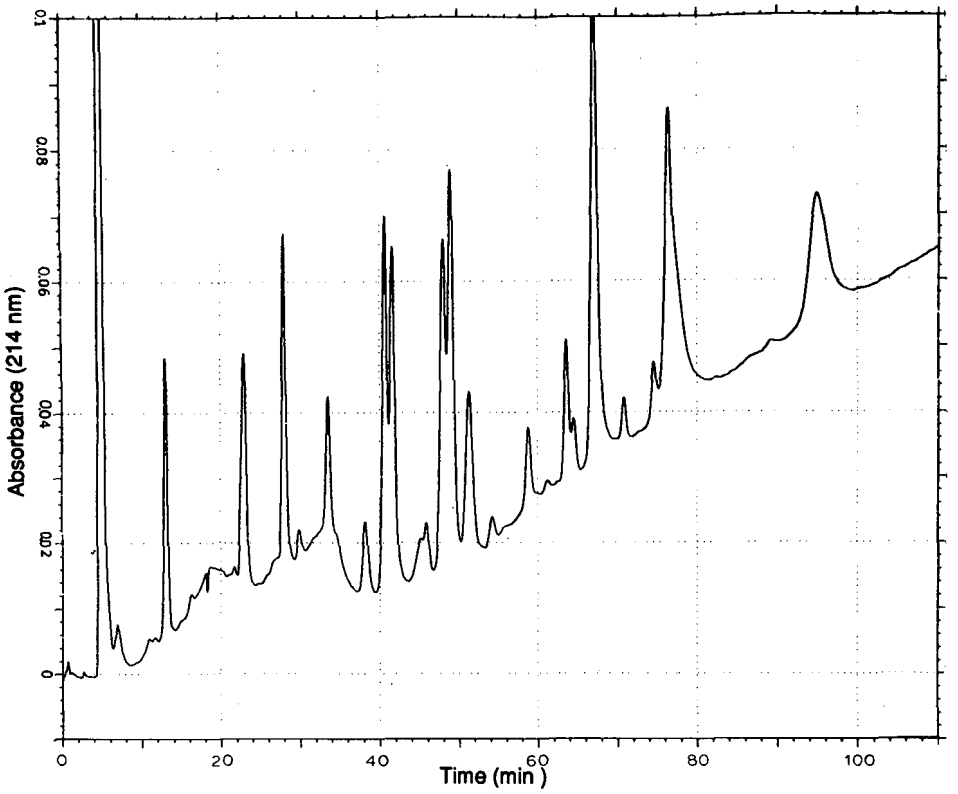

Fig. 5. Cation-exchange chromatography of cytochrome *c* tryptic peptides. Chicken cytochrome *c* (1.2 nmol) was separated on a Protein-Pak SP-5PW column at 30°C at a flow-rate of 0.5 ml/min with eluent A = aqueous HCl (6 m*M*) and eluent B = A + 1.0 *M* sodium chloride with an optimized linear gradient (0 min, 100% A; 40 min, A–B (80:20); 120 min, 100% B).

gradients. However, this approach involves a compromise between resolution and sensitivity as well as peak volume. The selectivity of the separation can be changed by small variations in pH and ion pairing associated with varying the TFA concentration. More extensive changes are observed with alternative mobile phase modifiers. HFBA increases the effect of ion pairing while only ion suppression occurs with HCl. The improved UV transparency of HCl provides enhanced opportunities for spectral characterization of peptides using photodiode array detection. The selectivity of peptide mapping is most dramatically changed by inverting the usual ion pairing and ion suppression. These options in mobile phase modification enhance the ability of the protein chemist to routinely separate all possible peptides.

Ion-exchange chromatography offers an additional mode for peptide separations. Reversed-phase chromatography relies upon ion suppression and ion pairing of the charged amino acid residues, essentially negating the charge of the peptide. For ion-exchange chromatography, it is possible to employ subtle variations of pH and ionic strength to optimize a separation based upon the net charge of the peptides. For peptide mapping, the selection of a cation or anion exchangers may depend on the p*I* of

the intact protein. In the case of a basic protein such as cytochrome *c*, tryptic fragments were separated on a strong cation-exchange column while little resolution was obtained on an anion exchanger (data not shown). Thus, the charge of the peptide becomes a major factor in determining the selectivity of the separation.

In summary, peptide mapping can be optimized on silica-based reversed-phase supports by altering the gradient slope, temperature and ion-pair reagent. Additionally, the use of polymeric supports over a wider pH range with inverted ion-pair reagents further enhances selectivity. Ion-exchange chromatography provides an additional method for peptide mapping having a dramatically different selectivity than reversed-phase techniques.

REFERENCES

1 M. T. W. Hearn and B. Grego, *J. Chromatogr.*, 266 (1983) 75.
2 M. A. Stadalius, M. A. Quarry and L. R. Snyder, *J. Chromatogr.*, 327 (1983) 93.
3 K. L. Stone and K. Williams, *J. Chromatogr.*, 359 (1986) 203.
4 J. J. L'Italien, *J. Chromatogr.*, 359 (1986) 213.
5 C. Y. Yang, E. Pauly, H. Kratzin and N. Hilschmann, *Hoppe-Seyler's Z. Physiol. Chem.*, 362 (1981) 1131.
6 E. C. Nice, M. W. Capp, N. Cooke and M. J. O'Harry, *J. Chromatogr.*, 218 (1981) 569.
7 W. C. Mahoney and M. H. Hermodson, *J. Biol. Chem.*, 255 (1980) 199.
8 H. P. J. Bennett, C. A. Browne and S. Solomon, *J. Liq. Chromatogr.*, 3 (1980) 1353.
9 J. L. Meek and Z. L. Rossett, *J. Chromatogr.*, 211 (1981) 15.
10 K. J. Wilson, A. Honegger, R. P. Stotzel and G. J. Hughes, *Biochem. J.*, 199 (1981) 31.
11 M. J. O'Hare, M. W. Capp, E. C. Nice, N. H. C. Cooke and B. G. Archer, in M. T. W. Hearn, F. E. Regnier and C. T. Wehr (Editors), *High Performance Liquid Chromatography of Proteins and Peptides*, Academic Press, Orlando, FL, 1983, p. 161.
12 W. H. Vensel, V. S. Fujita, G. E. Tarr, G. E. Margoliash and H. Kayser, *J. Chromatogr.*, 266 (1983) 491.
13 N. Takahasi, Y. Takahashi and F. W. Putnam, *J. Chromatogr.*, 266 (1983) 511.
14 W. Warren, A. Peterson, T. Wheat, M. P. Strickler, M. J. Stone, M. Dwyer and R. Pfeifer, *Am. Biotech. Lab.*, June (1989) 34.

Journal of Chromatography, 512 (1990) 283–290
Elsevier Science Publishers B.V., Amsterdam

CHROMSYMP. 1849

Analysis of amino acids by liquid chromatography after pre-column derivatization with 4-nitrophenylisothiocyanate

STEVEN A. COHEN
Waters Division of Millipore, 34 Maple Street, Milford, MA 01757 (U.S.A.)

ABSTRACT

Derivatization of amino acids with the phenylisothiocyanate analogue, 4-nitrophenylisothiocyanate, results in stable thiocarbamyl derivatives which are suitable for analysis via liquid chromatography. Detection limits of *ca.* 1 pmol can be achieved with detection at either 254 or 340 nm. Separation of the normal hydrolyzate amino acids is readily accomplished in less than 25 min using a 30-cm reversed-phase column. Using reaction conditions optimized for derivative yield and minimal reagent interference, the procedure provided reproducible, accurate compositional analyses of hydrolyzed peptide and protein samples.

INTRODUCTION

Improved procedures for pre-column derivatization of amino acids have been the major driving force behind recent advancements in amino acid analysis. Fluorescent reagents such as 9-fluorenylmethyl chloroformate (FMOC)[1], 7-fluoro-4-nitrobenzo-2-oxa-1,3-diazole (NBD-F)[2] and *o*-phthalaldehyde[3] (OPA) have allowed femtomole (10^{-15}) and even attomole (10^{-18}) detection limits by liquid chromatography or capillary zone electrophoresis. Highly absorbing colored derivatives such as those found with 4-dimethylaminoazobenzene-4-sulfonyl (dabsyl) chloride[4] have also been employed to provide low picomole level analysis. One of the more popular procedures has utilized the sequence reagent phenylisothiocyanate (PITC) to form stable phenylthiocarbamyl (PTC) derivatives[5,6]. The isothiocyanate reacts with both primary and secondary amines (a major drawback of OPA[7]) and shows excellent selectivity towards the amine functionality. Reactions of derivatizing reagents with phenolic or imidizole side chains can cause problems with the other reagents but have not been reported for PITC.

Over the past seven years our laboratory has exploited the reaction selectivity of PITC to develop fast, accurate methods for a wide variety of samples including protein hydrolyzates[5], feed samples[8] and physiologic fluids[6]. Detection limits of 1 pmol[5] were achieved using 254-nm detection for the highly absorbing PTC derivatives. Thus, PITC derivatization provides sufficient sensitivity for 100-ng protein samples[9], below

0021-9673/90/$03.50

which level interference from environmental contamination usually precludes accurate analysis even with inherently more sensitive fluorescent tagging reagents.

Recently we have begun to study alternative isothiocyanate derivatives that would potentially offer the same advantages of PITC (*e.g.* selective, rapid reaction with primary and secondary amines) but improve either the sensitivity or detection selectivity. One of these reagents, 4-nitrophenylisothiocyanate (NPITC), has been shown to retain many of the favorable characteristics of PITC, and also allow selective detection at 340 nm. This paper discusses the use of NPITC for amino acid analysis, the first PITC analogue employed successfully for pre-column derivatization amino acid analysis.

MATERIALS AND METHODS

Materials

Amino acids, peptides and proteins were from Sigma (St. Louis, MO, U.S.A.). HPLC-grade acetonitrile was purchased from J T. Baker (Phillipsburg, NJ, U.S.A.). HPLC-grade water was obtained from a Milli-Q® system (Millipore, Bedford, MA, U.S.A.) fed with a reverse osmosis purified supply. Constant-boiling HCl and triethylamine (TEA) were from Pierce (Rockford, IL, U.S.A.). Crude NPITC was purchased from Eastman Kodak (Rochester, NY, U.S.A.). Other chemicals were reagent grade.

NPITC Purification

Crude NPITC was a gummy, orange solid. A 1-g amount of this material was purified by vacuum sublimation. The sample was heated to 96°C and the pressure was 0.13 mm. Approximately 800 mg (80% yield) of a free flowing, pale yellow powder with a sharp melting point at 106.5°C (lit. 107°C)[10] was recovered.

Derivatization

A 50-m*M* stock solution of NPITC in acetonitrile was prepared daily. The working reagent consisted of 490 μl of stock NPITC, 50 μl of 10% TEA in acetonitrile, and 50 μl of water. Amino acid standards were vacuum dried in 50 × 6 mm Pyrex® tubes. Derivatization was initiated by pipetting 10 μl of working reagent into the tubes following by vigorous vortexing. After 10 min, 40 μl of water were added, and excess reagent was removed by a single extraction with 50 μl of hexane, Freon®, ethyl acetate or toluene. Aliquots of 1–10 μl of the aqueous layer were injected for analysis. For extraction studies, 1–2 μl of the organic layer were analyzed.

Separation of NPITC amino acids

The chromatographic system consisted of two M510 pumps, a M712 WISP® autosampler, controlled by an M840 chromatography and data station. Detection was accomplished with a M490 multiwavelength detector or an M440 single-wavelength detector equipped with either a 254 or 340 nm filter kit. Spectra of derivatized samples and NPITC were collected with a 990+ photodiode array detector using a W600 solvent delivery system for the analysis. Column temperature was controlled to 46.0 ± 0.1°C with a temperature control module (all hardware from Waters Chromatography Division of Millipore).

Separations were carried out on a Pico · Tag® free amino acid analysis column (300 × 3.9 mm) from Waters using a linear gradient running from 85% A [94% 0.14 *M* sodium acetate, 0.05% TEA (v/v), pH adjusted to 6.4 with acetic acid, 6% acetonitrile] and 15% B (60% acetonitrile in water) to 40% A and 60% B in 20 min. The flow-rate was 1.0 ml/min. After a 5-min wash with 100% B, the column was equilibrated for 12 min under the initial conditions. Total analysis time (injection-to-injection) was 40 min. For extraction studies and spectral analysis the gradient was extended to 30 min ending at 80% B, 20% A.

Sample hydrolysis

Peptides and proteins were dissolved in water (1–5 mg/ml) and aliquots containing 1–5 μg were vacuum dried in 50 × 6 mm Pyrex tubes. Constant-boiling HCl (200 μl) was added to the bottom of the large vial containing the tubes and the samples were sealed under vacuum after three alternate vacuum-nitrogen purging steps. Hydrolysis was carried out at 112°C for 20–24 h, after which the samples were cooled, vacuum dried, and derivatized as described for standard solutions.

RESULTS

Extraction studies

Unlike PITC, NPITC cannot be easily removed under reduced pressure. The hydrophobic nature of isothiocyanates made solvent extraction a potential alternative to vacuum drying. Hexane (which has been used for PITC extraction[11]), Freon, ethyl acetate and toluene were compared for extraction efficiency. The non-polar solvents hexane and Freon were not as effective as the more polar solvents in removing NPITC. In contrast, ethyl acetate was very effective at reagent removal, but also extracted some of the hydrophobic derivatized amino acids. Extraction with toluene gave an acceptable compromise between reagent removal and recovery of the amino acid analytes. Subsequent experiments all used toluene for extraction.

Reaction optimization

Derivatization of a standard amino acid mixture with PITC is typically carried out using reagent concentrations of 0.5–1.0 *M*. Concentrations ⩽ 300 m*M* can result in less than quantitative yields, particularly for Asp and Glu. In contrast to PITC, NPITC derivatization using 1 *M* reagent results in an enormous artifact peak that is only partially extracted by toluene. Limiting the reagent concentration to 50 m*M* eliminated the great majority of the artifact, and separation of the resulting smaller peak from the NPTC-amino acids was readily accomplished (Fig. 1A). However, with ⩽ 25 m*M* reagent, reduced yields of amino acids were observed.

Chromatography of NPTC-amino acids

The derivatization products of NPITC are the nitro analogues of the PTC-amino acids formed from the reaction with PITC. Consequently, the chromatographic behavior of the NPTC-amino acids is very similar to that observed for PTC-amino acids. The effect of operating parameters such as ionic strength, pH, gradient steepness and column temperature are very similar to that reported for PTC-amino acids[6]. Thus, higher ionic strength increased retention of neutral and acidic amino acids without

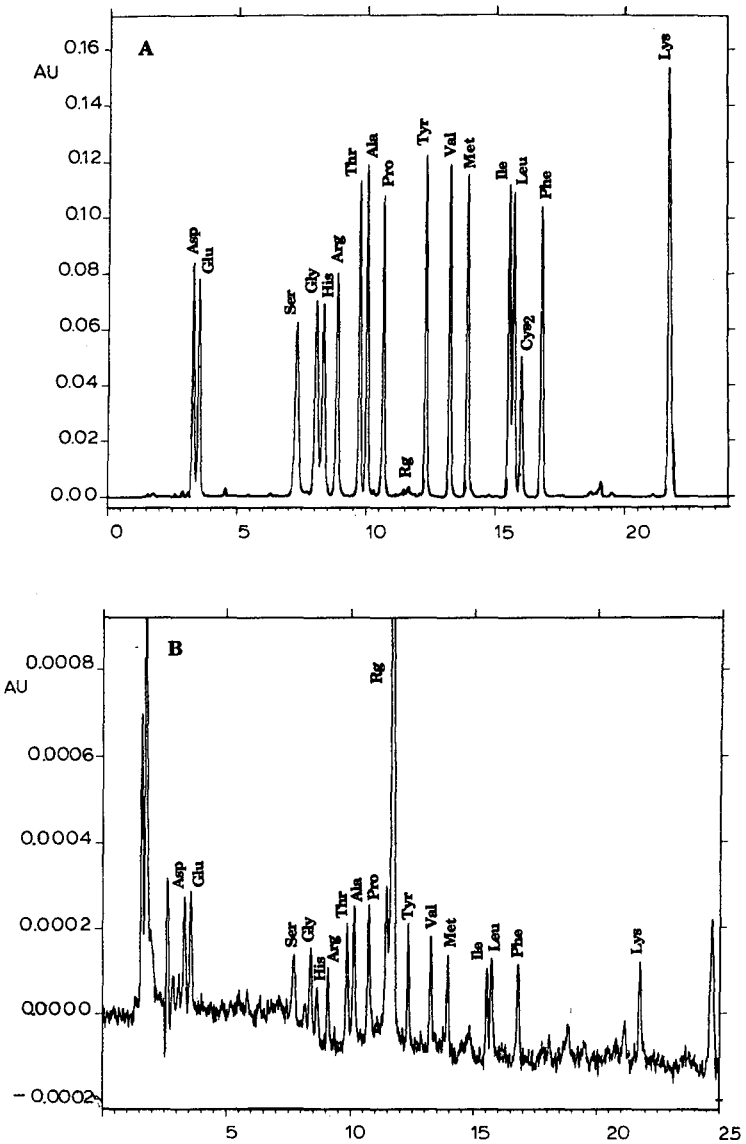

Fig. 1. Separations of NPITC-derivatized amino acids: (A) 833 pmol standard (B) 1.3 pmol standard. Full scale deflections are (A) 0.16 AU, (B) 0.001 AU. Horizontal axis: retention time in min. Chromatographic conditions and sample preparation are described in Materials and Methods.

affecting retention of basic derivatives. In fact, with only changes in gradient shape and initial solvent strength, resolution of all 18 amino acids in a standard mixture was readily accomplished (Fig. 1A) using identical mobile phases and the same column used for PTC-amino acid chromatography. The order of elution was the same except that Cys_2 elutes after Leu instead of before Ile. The optimized conditions also provide

TABLE I

REPRODUCIBILITY OF NPITC-AMINO ACID ANALYSIS

Based on five replicate analyses. C.V. = Coefficient of variation = 100 · standard deviation/average.

Amino acid	*C.V. (%)*	
	Peak area	*Retention time*
Asp	5.6	0.35
Glu	7.2	0.33
Ser	1.2	0.20
Gly	2.6	0.21
His	2.1	0.17
Arg	3.3	0.09
Thr	1.1	0.06
Ala	2.5	0.05
Pro	1.8	0.08
Tyr	0.7	0.07
Val	1.4	0.05
Met	1.5	0.04
Ile	1.4	0.05
Leu	1.9	0.03
Cys	22.6	0.04
Phe	1.5	0.05
Lys	5.9	0.04

TABLE II

COMPOSITIONAL ANALYSIS OF HYDROLYZED SAMPLES

Samples were prepared as described in the Materials and Methods section. Amounts injected were approximately 60 ng per sample. Expected values are given in parentheses.

Amino acid	*Lysozyme*	*Neurotensin*	*Angiotensin II*
Asp	20.0 (21)	1.0 (1)	0.9 (1)
Glu	5.8 (6)	1.9 (2)	0
Ser	8.1 (10)	0	0
Gly	12.1 (12)	0	0
His	0.7 (1)	0.1 (0)	1.1 (1)
Arg	11.0 (11)	2.5 (2)	1.1 (1)
Thr	6.5 (7)	0	0
Ala	12.4 (12)	0	0
Pro	2.4 (2)	2.0 (2)	1.1 (1)
Tyr	2.5 (3)	0.9 (2)	0.6 (1)
Val	5.4 (6)	0	1.0 (1)
Met	1.3 (2)	0	0
Ile	5.4 (6)	0.9 (1)	1.0(1)
Leu	7.9 (8)	1.9 (2)	0
Phe	3.1 (3)	0	1.1 (1)
Lys	5.8 (6)	0	0

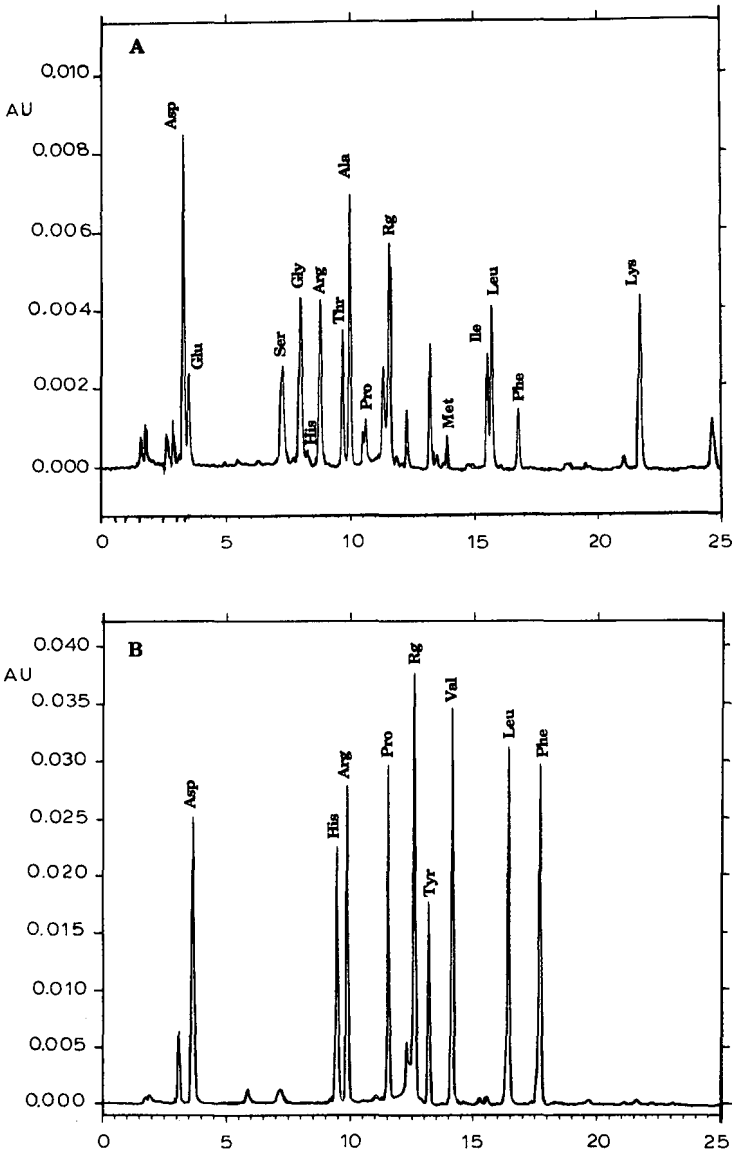

Fig. 2. Analysis of hydrolyzed (A) lysozyme and (B) angiotensin II. Conditions as in Fig. 1 except (A) AUFS = 0.01 and (B) AUFS = 0.04.

excellent resolution of the amino acid derivatives from the two major reagent peaks. Even at very low levels reagent interference is not observed. In general, the NPTC derivatives exhibit greater retention that their PTC analogs, an effect that is enhanced with the diderivatized compounds Lys and Cys_2.

Spectral analysis of eluting peaks with a photodiode array detector showed a peak maximum for NPITC at 335 nm with local maxima at 212 and 239 nm.

Carbamylation increased the relative absorbance of the second local maximum such that the NPTC derivatives exhibited absorption maxima at 236 nm, the longer wavelength maxima ranging from 341–347 nm. Absorbance was strong at 254 nm and detection limits of 0.5–1.0 pmol were estimated using UV detection at this wavelength (Fig. 1B) with a signal-to-noise ratio of 3. This is comparable to that reported for PTC-amino acids[5].

Reproducibility

Six replicate samples containing 12.5 nmol of each amino acid were derivatized and 5 μl out of a total of 75 μl aqueous layer were injected (833 pmol). Table I shows that the relative standard deviations ranged from approximately 1 to 7%, except for Cys_2, which was 23%. The reason for this large deviation has not been determined.

Protein and peptide compositional analysis

Protein and peptide samples (approximately 1 μg) were hydrolyzed with HCl, and aliquots containing 40–200 ng analyzed. Typical hydrolyzate samples are shown in Fig. 2. Compositions experimentally determined for the peptides neurotensin and angiotensin and the protein lysozyme agree very well with the expected values (Table II).

DISCUSSION

In a study on isothiocyanate sequencing reagents, Tarr[12] has recently reported on the reactivity of NPITC with peptides. Although found unsuitable as an alternative to PITC for protein/peptide sequencing, the rate of NH_2-terminal labelling with NPITC was shown to be more rapid than with PITC. The greater electrophilicity of NPITC is also the likely cause of large reagent related peaks that are observed in reactions where the NPITC concentration $\geqslant$ 200 m*M*. Side reactions with water and/or ethanol[13] are the most likely source of these peaks. However, greater reactivity allows the reagent concentration to be reduced more than 10-fold in comparison to standard PITC labelling procedures, thus reducing the reagent peaks to a manageable size.

Tarr also reported that NPITC-labelled peptides were slow to cyclize to the corresponding nitroanilino thiazolinone. Consistent with these findings are data from our lab showing markedly increased stability of the NPTC-amino acids in comparison to their PTC analogues. Thus, while slow cyclization is an unfavorable property for a sequencing reagent, the greater stability of NPTC compounds is very desirable for amino acid analysis.

Using the optimized reaction conditions, no evidence for side chain derivatization was observed with His or Tyr. Each of the amino acids yielded only a single peak, the retention being consistent with reaction at a single site (presumably the free amine). As expected, only Cys_2 and Lys formed disubstituted products. This simplifies the quantitation of these amino acids in comparison to more reactive compounds such as FMOC and NBD-F, which react with the imidazole of His[14] or the phenolic group of Tyr[15], respectively.

This report demonstrates that isothiocyanates besides PITC can be effective reagents for amino acid analysis via precolumn derivatization. Although most of the

data reported herein were obtained via detection at 254 nm, detection at 340 nm could prove very useful, as it is comparably sensitive, the increased absorbance and flatter baselines being offset by increased detector noise at the higher wavelength. Studies on samples such as urine, which contain components that absorb at 254 nm but not at 340 nm would benefit from detection at the higher wavelength and are currently in progress. While such components can pose potential interference problems with PITC analysis of urine amino acids[6], NPITC derivatization with derivative detection at 340 nm should eliminate most if not all interference from non-amine containing components. These studies also have provided guidelines for future work with isothiocyanate analogs. Rapid coupling to form thiocarbamyl derivatives is essential as is slow cyclization to the thiohydantoin. Analogues that are fluorescent or chemiluminescent are commercially available, and could allow the detection of subpicomole amounts of amino acids.

REFERENCES

1 S. Einarsson, B. Josefsson and S. Lagerkvist, *J. Chromatogr.*, 282 (1983) 609–618.
2 Y. Watanabe and K. Imai, *J. Chromatogr.*, 309 (1984) 279–286.
3 D. W. Hill, F. H. Walters, T. D. Wilson and J. D. Stuart, *Anal. Chem.*, 51 (1979)1338–1341.
4 R. Knecht and J.-Y. Chang, *Anal. Chem.*, 58 (1986) 2375–2379.
5 B. A. Bidlingmeyer, S. A. Cohen and T. L. Tarvin, *J. Chromatogr.*, 336 (1984) 93–104.
6 S. A. Cohen and D. J. Strydom, *Anal. Biochem.*, 174 (1988) 1–16.
7 M. Roth, *Anal. Chem.*, 43 (1971) 880–882.
8 B. A. Bidlingmeyer, S. A. Cohen, T. L. Tarvin and B. Frost, *J. Assoc. Off. Anal. Chem.*, 70 (1987) 241–247.
9 B. A. Bidlingmeyer, T. L. Tarvin and S. A. Cohen, in K. A. Walsh (Editor), *Methods in Protein Sequence Analysis*, Humana Press, Clifton, NJ, 1986, pp. 229–243.
10 *Material Safety Data Sheet R-0267.400*, Eastman Kodak Company, Rochester, NY.
11 A. S. Inglis, N. A. Bartone and J. R. Finlayson, *J. Biochem. Biophys. Methods*, 15 (1988) 249–254.
12 G. E. Tarr, in J. E. Shively (Editor), *Methods of Protein Microcharacterization*, Humana Press, Clifton, NJ, 1986, pp. 155–194.
13 L. Drobnica, P. Kristian and J. Augustin, in S. Patai (Editor), *The Chemistry of Cyanates and Their Thio Derivatives*, Part 2, Wiley, New York, 1977, pp. 1003–1221.
14 D. M. Gauside, P. M. S. Monteiro and M. J. Orren, *S. Afr. J. Mar. Sci.*, 6 (1988) 47–53.
15 T. Toyo 'Oka, Y. Watanabe and K. Imai, *Anal. Chim. Acta*, 149 (1983) 305–312.

Journal of Chromatography, 512 (1990) 291–297
Elsevier Science Publishers B.V., Amsterdam

CHROMSYMP. 1928

High-performance liquid chromatographic separation and partial characterization of the α- and β-chains of Alaskan sockeye salmon hemoglobin

LAWRENCE K. DUFFY* and REBECCA A. REYNOLDS
Department of Chemistry and Institute of Arctic Biology, University of Alaska Fairbanks, Fairbanks, AK 99775 (U.S.A.)
and
JOHN P. HARRINGTON
Department of Chemistry, University of South Alabama, Mobile, AL 36688 (U.S.A.)

ABSTRACT

The life cycle of the sockeye salmon (*Oncorhynchus nerka*) includes both fresh water early development and oceanic adult periods. These salmon have multiple hemoglobins whose functional and evolutionary significance is still unresolved. The presence of these various hemoglobins may be advantageous to assuring adequate oxygen transport over a wide variety of environmental conditions. Functional differences between hemoglobin components in oxygen affinity, thermal stability and autoxidation have been reported. In order to better understand the molecular basis of these functional properties of the hemoglobin components, we have identified and characterized several of the polypeptide chains of sockeye salmon hemoglobins. The hemoglobin components were separated by chromatography into cathodal and anodal components. These components were then resolved by reversed-phase high-performance liquid chromatography. A gradient system was developed which could separate seven polypeptide chains. Amino acid compositions and sequence analysis of the polypeptide chains allowed the classification of some of the polypeptide chains as either α- or β-chains.

INTRODUCTION

Over the past decade increased studies of the physical and chemical properties of fish hemoglobins have contributed to a greater understanding of the variability of the structure and function relationships exhibited by these unique oxygen transport proteins as compared to mammalian hemoglobins. Comparative aspects of the structure and function of these proteins have received much attention[1–3]. Fish are unique in that many species possess a large number of hemoglobin components whose functional activity may be altered by a variety of environmental or physiological factors.

0021-9673/90/$03.50

The study of many diverse species of fish have demonstrated that electrophoretically distinct hemoglobin components of individual fish species usually exhibit different oxygen-binding characteristics[4,5]. In addition, recent comparative studies on the thermostability of fish hemoglobins reveal lower resistance to thermal denaturation and oxidation[6,7].

Reversed-phase high-performance liquid chromatography (HPLC) was applied to the separation of human hemoglobin chains[8] and hemoglobin chain variants[9–11]. These methods with modifications have been extended to primates[12,13], other mammals[14–19] and reptiles[20]. In studies of fish hemoglobin, reports of HPLC analysis of the individual α- and β-chains have become more common in the literature. In studies on bluefin tuna, a 0.1 *M* ammonium acetate–formic acid buffer with acetonitrile gradient was used[21], while in Goosefish, with only one component, isocratic elution with a mobile phase of 0.8 *M* sodium perchlorate–methanol–acetonitrile–nonylamine–phosphoric acid (29:5:66:0.1:0.5, v/v) was successful[7]. The single hemoglobin of the Crucian was separated into its chains by using a potassium phosphate (pH 2.5)–acetonitrile–methanol system[22]. In order to study developmental changes during smoltification and aging of fish in a system not prone to produce the artifacts that can accompany electrophoresis, we have worked on developing an HPLC procedure for separating the hemoglobin chains associated with the multi-component systems of fish.

EXPERIMENTAL

Chemicals

HPLC-grade water and acetonitrile were purchased from Fisher (Springfield, NJ, U.S.A.) and trifloroacetic acid (TFA) was sequential grade (Pierce, Rockford, IL, U.S.A.). All other chemicals were purchased from Sigma (St. Louis, MO, U.S.A.).

Apparatus

Ion-exchange chromatography was performed on a Waters 650 fast protein liquid chromatographic (FPLC) system, equipped with a Model 484 variable-absorbance detector and a Spectrophysics Model 9200 integrator. A Waters HPLC system with a Model 441 fixed-wavelength detector and Baseline (Dynamic Solutions, CA, U.S.A.) data processing software was used for the chain separation.

Hemoglobin preparation

Blood samples were obtained from sockeye salmon, *Oncorhynchus nerka,* caught in the Kenai River, Alaska. Individual fish were bled from the caudal vein, and the blood was transferred to flasks containing cold 1% sodium chloride. Red cell suspensions were centrifuged at 4°C, and the supernatant was discarded. Packed red cells were washed at least three times with the above saline solution. After the final wash, the red cells were osmotically lysed by the addition of two volumes of cold deionized distilled water. Cellular debris was removed by centrifugation at low speed for 10 min at 4°C, followed by centrifugation of the hemoglobin supernatant for 30 min at 8160 *g*.

Preparation of globins for HPLC analysis

Globin was precipitated from the hemoglobins at −20°C in acidified acetone.

TABLE I

SUMMARY OF HPLC GRADIENT CONDITIONS FOR SEPARATION OF SALMON HEMOGLOBIN CHAINS

Eluent A = 20% acetonitrile containing 0.1% TFA; eluent B = 80% acetonitrile containing 0.1% TFA. Column: Vydac C_4, 250 mm × 4.6 mm I.D. (300 Å).

Event No.	*Time (min)*	*Flow-rate (ml/min)*	*Composition (%)*	
			Eluent A	*Eluent B*
1	0.0	1.0	100.0	0.0
2	10.0	1.0	99.0	1.0
3	15.0	1.0	60.0	40.0
4	75.0	1.0	75.0	65.0
5	80.0	1.0	0.0	100.0
6	89.0	1.0	100.0	0.0
7	90.0	0.0	100.0	0.0

Hemoglobin α- and β-chains were isolated by reversed-phase HPLC of a solution with 8 *M* urea and 1% mercaptoethanol (pH 3). When using relatively large amounts of hemolysate, we found that urea treatment insures complete dissociation of the hemoglobin molecule. Chains were separated on a Vydac C_4 column using an acetonitrile gradient with 0.1% TFA as a counter-ion at pH 2.1. The flow-rate was 1 ml/min. Peaks were detected by absorbance at either 214 or 254 nm. Table I summarizes the gradient.

Amino acid analysis

Samples were hydrolyzed in constant-boiling hydrochloric acid (Pierce, Rockford, IL, U.S.A.) with 0.1% phenol at 108°C for 24 h and analyzed in a Beckman 6300 analyzer[13].

Protein sequence analysis

Hemoglobin and peptide samples were used for N-terminal sequence analysis on an Applied Biosystems Model 470A gas phase protein sequencer[13]

Isolation of hemoglobin component fractions

Isolation of the anodal and cathodal fractions was carried out by ion-exchange chromatography on DE-52 (diethylaminoethyl cellulose) developed with 0.05 *M* Tris–HCl buffer (pH 8.4). Individual fractions and components were eluted from the column with 0.5 *M* sodium chloride in the same buffer. This procedure was modified by using the Waters advanced protein chromatography system with either a Waters Protein-Pak DEAE column or a Waters Accell QMA column.

RESULTS AND DISCUSSION

The uniqueness and complexity of fish hemoglobins compared to mammalian hemoglobins are well demonstrated by the extensive hemoglobin polymorphism ob-

served in the various species of trout and salmon[23–25]. These electrophoretically distinct hemoglobins appear to provide an adaptive mechanism necesary for the life cycle of these fish. Each species of salmon exhibits a similar life cycle in many respects, with spawning and early development occurring in fresh water, giving way to the highly saline environment of the ocean as adults. An increase in the number of hemoglobin components has been reported to occur during this development[25]. Also differences in thermal stability of the anodal and cathodal hemoglobin components of salmon hemoglobins have been observed[2,5]. Since sockeye salmon can show five to thirteen hemoglobin components[6,26], the chain compositions of the sockeye salmon hemoglobins were analyzed by reversed-phase HPLC.

Fig. 1 shows a representative elution profile of hemoglobin chains from the total salmon hemoglobin preparation. Good separation of the chains was obtained with the Vydac C_4 reversed-phase column within 65 min. Between time 45 to 60 min, seven major peaks and two minor peaks could be resolved. In an attempt to correlate the chains seen in Fig. 1 with the individual hemoglobin components which had been defined by electrophoretic mobility[6,26], individual hemoglobin components which had been partially separated by ion-exchange chromatography on DE-52 (Whatman) were analyzed by HPLC. HPLC analysis of an overlapping triplet of peaks easily demonstrated that the middle component contained hemoglobin chains associated with its neighboring components[5]. The HPLC profile of the first-eluting hemoglobin component of this triplet, in which only single α- and β-chains are seen, is illustrated in Fig. 2. The analysis by this HPLC method of homogeneous fractions separated by either ion-exchange chromatography or by gel electrophoresis will allow us to confirm the hemoglobin chain number and designations proposed by Tsuyuki and Ronald[26].

Preliminary amino acid analysis of the globin peaks in Fig. 2 led to the identification of an α-chain (Table II). Since the α-chains of salmonoid fish usually have

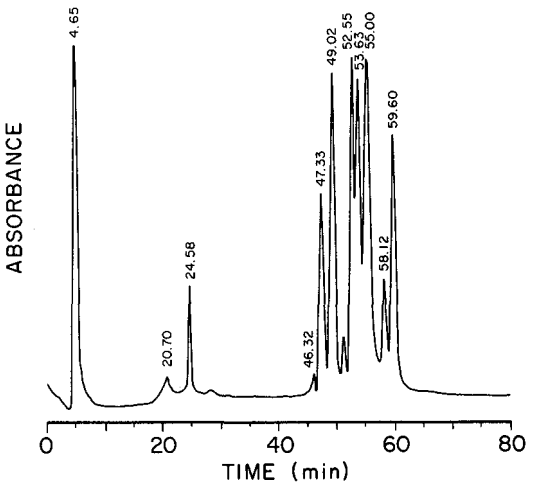

Fig. 1. HPLC separation of the sockeye salmon hemoglobin chains (200 μg) on a Vydac C_4 column (250 mm × 4.6 mm I.D.) in a 0.1% TFA–acetonitrile system. The gradient was from 20 to 80% acetonitrile with detection at 214 nm (see Table I).

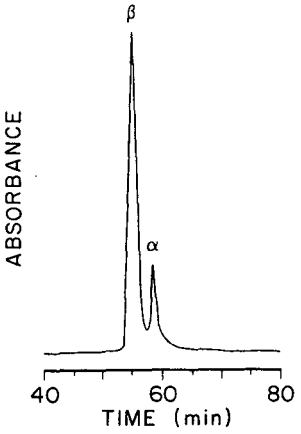

Fig. 2. HPLC separation of the sockeye salmon hemoglobin chains from a column fraction previously eluted from DE-52 cellulose. Elution conditions were the same as in Fig. 1.

TABLE II

COMPARISON OF SALMONOID FISH α-CHAIN AMINO ACID COMPOSITION WITH SOCKEYE HEMOGLOBIN HPLC PEAK

Amino acid	*Trout I*[a]	*Trout IV*[a]	*Carp*[a]	*Atlantic*[a] *salmon I*	*Sockeye*[b] *salmon C1*
Asx	13	15	14	14	13.8
Thr	6	6	3	6	7.6
Ser	11	9	11	9	9.1
Glx	3	9	6	4	6.9
Pro	6	7	8	6	5.8
Gly	14	6	11	14	12.1
Ala	18	16	17	20	20.4
Val	12	10	12	12	13.2
Met	4	3	4	4	3.4
Ile	8	10	8	6	6.9
Leu	13	16	14	15	13.3
Tyr	3	4	4	3	3.4
Phe	7	6	6	7	7.3
Lys	13	13	14	11	11.8
His	6	6	5	5	3.9
Arg	3	3	3	4	3.2
Trp	2	2	2	2	N.D.[c]
Cys	–	1	–		N.D.[c]

[a] References: trout, ref. 23; Atlantic salmon, ref. 27.

[b] Based on a 142 amino acid composition; C1 designation for this component is based on ion-exchange chromatography and electrophoresis[5].

[c] N.D., not determined.

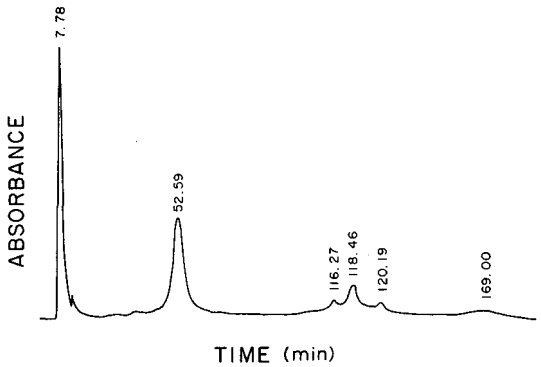

Fig. 3. Component separation of the hemolyzate of the sockeye salmon by ion-exchange chromatography (200 μl). Column: Accell QMA (10 mm × 8 mm I.D.); buffer A, 10 m*M* sodium phosphate, pH 8.0; buffer B, buffer A + 1 *M* sodium chloride. Linear gradient from 1 to 100% B over 200 min. Flow-rate, 0.5 ml/min, detection at 415 nm. Numbers at peaks indicate retention times in min.

acetylated amino terminals, protein sequencing could not be used to identify chain type. However, the amino acid analysis clearly shows that the sockeye salmon hemoglobin component has an α-chain which is homologous to Type I α-chain of Atlantic salmon and trout[20,27], as can be seen in he glycine and valine compositions. Separation and isolation of the globin chains by HPLC has allowed for a partial determination of the amino acid sequences of the β-chains for these components[28]. So far there is 90–100% homology between trout hemoglobin β-chains and sockeye hemoglobin β-chains depending on which hemoglobin components are compared[28]. The HPLC separation of the chains now allows us to see whether all the heterogeneity of the components seen in electrophoresis and isoelectric focusing is directly related to polypeptide gene products or to post-translational events such as non-enzympatic glycosylation.

In an attempt to purify sockeye salmon hemoglobin components for HPLC analysis, we tried ion-exchange chromatography using a Waters Protein-Pak DEAE column. We found that this column, used under conditions identical to those previously used with the DE-52 column[5], bound very little of the hemoglobin components. This may be because an initial pH of 8.4 is not high enough for sockeye salmon hemoglobin binding to this particular column. When we used an Accell QMA column with a sodium phosphate–sodium chloride system, we were able to separate hemoglobin into several fractions. Fig. 3 shows a typical separation. The acidic fraction is eluted first, followed by a more basic fraction. HPLC analysis can be used to identify the homogeneity of these fractions based upon their chain compositions.

Since hemoglobin components change around the time of smoltification[25], the use of this HPLC procedure will allow us to quantitate the amounts of various chains synthesized during this transitional period. It will also allow us to monitor post-translational changes such as glycosylation which may occur during salmon spawning. The use of HPLC analysis of individual fish hemoglobins will obviate the autoxidation artifacts commonly seen in electrophoresis of stored fish hemoglobin samples. The reproducibility and sensitivity associated with HPLC analysis improve the use of the hemoglobin molecule as a monitor of early development in fish.

ACKNOWLEDGEMENTS

Funded in part by NSF Grants CHE-8804238 and DIR 8908016, and the Whitehall Foundation. We also appreciate the assistance and advice of Joackim Luick.

REFERENCES

1 J. Bonaventura, C. Bonaventura and B. Sullivan, *J. Exp. Zool.*, 194 (1975) 155.
2 M. F. Perutz and M. Brunori, *Nature (London)*, 299 (1982) 421.
3 M. F. Perutz, *Mol. Biol. Evol.*, 1 (1983) 1.
4 J. P. Harrington, *Comp. Biochem. Physiol.*, 84B (1986) 111.
5 J. Sauer and J. P. Harrington, *Comp. Biochem. Physiol.*, 91A (1988) 109.
6 J. P. Harrington, *Ann. N.Y. Acad. Sci.*, 435 (1985) 154.
7 T. A. Borgese, J. P. Harrington, I. Ganjian and C. Duran, *Comp. Biochem. Physiol.*, 91B (1988) 663.
8 L. R. Congote, H. P. Bennett and S. Solomon, *Biochem. Biophys. Res. Commun.*, 89 (1979) 851.
9 P. E. Petrides, R. T. Jones and P. Bohlen, *Anal. Biochem.*, 105 (1980) 383.
10 J. R. Strahler, B. B. Rosenbloom and S. M. Hanash, *Science (Washington, D.C.)*, 221 (1983) 860.
11 J. B. Shelton, J. R. Shelton and W. A. Schroeder, *Hemoglobin*, 9 (1985) 325.
12 S. O. Brennan, *Chromatogr. Rev.*, 10 (1983) 11.
13 D. H. Coppenhaver, J. Buettner-Janusk, M. M. Ehrhardt and L. K. Duffy, *Biochim. Biophys. Acta*, 873 (1986) 372.
14 H.-X. Lin, T. Kleinschmidt and G. Braunitzer, *Biol. Chem. Hoppe-Seyler*, 369 (1988) 209.
15 L. K. Duffy, C. T. Genaux and G. L. Florant, *Comp. Biochem. Physiol.*, 83B (1986) 797.
16 H. Chang, K. Rodewald and G. Braunitzer, *Biol. Chem. Hoppe-Seyler*, 370 (1989) 417.
17 H. Lin, T. Kleinschmidt, M. L. Johnson and G. Braunitzer, *Biol. Chem. Hoppe-Seyler*, 370 (1989) 135.
18 W. A. Schroeder, J. B. Shelton, J. R. Shelton, V. Huynk and D. B. Teplow, *Hemoglobin*, 9 (1985) 461.
19 K. Rodewald, W. Oberthur and G. Braunitzer, *Biol. Chem. Hoppe-Seyler*, 368 (1987) 795.
20 A. Abbasi, R. M. G. Wells, T. Brittain and G. Braunitzer, *Biol. Chem. Hoppe-Seyler*, 369 (1988) 755.
21 F. Huber and G. Braunitzer, *Biol. Chem. Hoppe-Seyler*, 370 (1989) 245.
22 F. Hung and Y. Shaoyi, *Zool. Sci.*, 5 (1988) 809.
23 R. Petruzzelli, D. Barra, L. Sensi, F. Bossa and M. Brunori, *Biochim. Biophys. Acta*, 995 (1989) 255.
24 M. A. Giles and D. J. Randall, *Comp. Biochem. Physiol.*, 65A (1980) 265.
25 C. V. Sullivan, W. W. Dickhoff, C. V. M. Mahnken and W. K. Hershberger, *Comp. Biochem. Physiol.*, 81A (1985) 807.
26 H. Tsuyuki and A. P. Ronald, *Comp. Biochem. Physiol.*, 39B (1971) 503.
27 J. P. Wolff and F. Gannon, *Nucleic Acid Res.*, 17 (1989) 4369.
28 L. K. Duffy, R. A. Reynolds and J. P. Harrington, *Comp. Biochem. Phys.*, 96B (1990) 41.

Journal of Chromatography, 512 (1990) 299–314
Elsevier Science Publishers B.V., Amsterdam

CHROMSYMP. 1883

High-performance displacement chromatography–mass spectrometry of tryptic peptides of recombinant human growth hormone

JOHN FRENZ*
Department of Medicinal and Analytical Chemistry, Genentech, Inc., 460 Point San Bruno Boulevard, South San Francisco, CA 94080 (U.S.A.)
JAMES BOURELL
Department of Protein Chemistry, Genentech. Inc., 460 Point San Bruno Boulevard, South San Francisco, CA 94080 (U.S.A.)
and
W. S. HANCOCK
Department of Medicinal and Analytical Chemistry, Genentech. Inc., 460 Point San Bruno Boulevard, South San Francisco, CA 94080 (U.S.A.)

ABSTRACT

The combination of high-performance displacement chromatography with continuous flow fast atom bombardment (FAB)-mass spectrometry (MS) offers a means of overcoming the sample capacity limitations imposed by the low flow-rates tolerated in microbore systems employed for directly coupled liquid chromatography–MS. Displacement chromatography is performed at high concentrations with the same equipment and columns as typically used in chromatography at low concentrations. By using this mode of chromatography with a solution of cetyltrimethylammonium bromide as the displacer, the capacity of a reversed-phase column can be increased 50- to 100-fold for separation of a tryptic digest of biosynthetic human growth hormone. Despite the high load, the use of displacement chromatography allowed high-resolution separation of the complex mixture of eighteen major components. On-line analysis by continuous flow FAB-MS yielded high-quality spectra of these peptides and demonstrated that sharp, single-component bands can be obtained in this separation. Along with the major fragments, the chromatogram showed other peptides originating from protein variants in the sample, from non-specific cleavage in the enzymatic digest or from autolysis of trypsin. On-line analysis also allowed selective ion monitoring of the column effluent for individual peptides and confirmed the high efficiency and resolution obtained by preparative displacement separations on HPLC columns and equipment.

0021-9673/90/$03.50

INTRODUCTION

Continuous growth over the last decade of the segment of the pharmaceutical industry based on the commercialization of therapeutic proteins produced by recombinant DNA technology has spawned other important scientific disciplines, including that of analytical biotechnology. That field has been developed to characterize the purity and identity of recombinant proteins, both as a guide to optimization of manufacturing and recovery processes and to satisfy the requirements for marketing approval by regulatory agencies. Recombinant proteins pose new and particular analytical challenges not encountered in the production of small-molecule drugs or proteins isolated from animal or human tissues. Over the last ten years, the demands of protein characterization have led to continual refinement of the tools of protein chemistry, as well as to the introduction of powerful new techniques.

One of the most useful approaches to characterization is the analysis by high-performance liquid chromatography (HPLC) of the peptide mixture produced by enzymatic digestion of a protein[1]. The specificity conferred by selection of the appropriate enzyme together with the high efficiency and selectivity of modern HPLC united in this approach to yield a sensitive, reproducible method of determining the identity and, to a certain extent, the purity of a protein. Reversed-phase HPLC is the separation system of choice in this application, since it delivers high resolution of such moderately sized analytes, and, with suitable mobile phases, offers the possibility of isolating purified individual peptides for subsequent characterization by amino acid composition analysis or sequencing, or by mass spectrometry (MS). By this strategy nearly the entire sequence of a protein can be confirmed, as has been demonstrated by many recent examples[2–4], including that of recombinant human growth hormone[5].

Fast atom bombardment (FAB) ionization[6] has become the method of choice for MS of peptides. Peptides isolated by reversed-phase HPLC with volatile mobile phases are eminently suited for transfer to the FAB matrix and deposition onto the probe tip for analysis. By this procedure highly accurate, sensitive molecular weight determinations and sequence information can be obtained for peptides up to 10 000 dalton in size. The analysis and characterization of complex mixtures can be made more efficient by coupling HPLC directly with MS[7,8]. Such an on-line analysis minimizes sample handling losses and reduces the time required for analysis of the entire mixture to little more than the time for the chromatographic separation. One constraint imposed on the HPLC in continuous FAB applications is the limitation on flow-rates due to the solvent removal capacity of the vacuum pumps in the mass spectrometer. In practice, the eluent flow is split either before[9] or after[10] the column in order to attain flow-rates in the range of 10 μl/min or less. Pre-column splitting requires the use of capillary columns and has the advantage that the entire sample passing through the column is introduced into the mass spectrometer.

The chief limitation of current LC–MS interfaces is due to the relatively low flow-rates tolerated by conventional vacuum systems. The restriction on flow-rate also effectively limits the mass load of the mass spectrometer, since the concentration of individual peptides in the traditional elution mode is governed by the sample concentration and by the dilution characteristics of the chromatographic system employed. One way to enhance the capacity of the system is to select an operating mode that results in increased concentration of the peptides in the column effluent and

more efficient utilization of the column capacity. High-performance displacement chromatography (HPDC)[11] meets certain of these requirements. Displacement chromatography (DC) was developed by Tiselius[12] as a means of efficiently resolving complex mixtures at high concentrations in order to facilitate detection by optical detectors. Although subsequently rendered obsolete for most analytical applications by the development of more sensitive detectors and the dominance of linear elution chromatography, DC carried out in columns and equipment developed for HPLC has enjoyed a renaissance recently as a preparative technique[13–22]. The displacement mode allows high-resolution separations to be carried out at concentrations and column loads that are one or two orders of magnitude higher than in conventional gradient or isocratic elution. The increased capacity afforded by the displacement mode is achieved by employing a displacer solution to mobilize the feed components after they are loaded into the column. Unlike the eluents employed in conventional elution chromatography the displacer solution contains a component that is more strongly retained than the feed components. The displacer thus saturates the stationary phase surface, displacing the feed mixture and causing the individual components to move down the column at a constant velocity and to separate into adjacent single-component bands. The mathematical description of the separation process in displacement chromatography is more involved than for the elution mode[23], but operationally the process is no more complex once the separation conditions have been established.

HPDC may offer significant advantages for micro-analytical techniques, such as capillary LC–MS, since it increases the amount of a mixture that can be separated on a given column, and thus, that can be analyzed by the mass spectrometer. In an analogous fashion, the advantages of isotachophoresis as the operating mode for capillary electrophoresis–MS have been described[24]. By increasing the sample load of the instrument, the detectability of minor components of the sample can be enhanced. The displacement of tryptic peptides of recombinant human growth hormone has been demonstrated[25] on columns and equipment identical to that employed for the gradient elution tryptic mapping procedure[5]. In this example, the displacement mode allowed an approximately 50-fold increase in the capacity of the reversed-phase column for preparative isolation of tryptic peptides. DC thus allowed the purification and recovery of relatively large amounts of minor components of the enzymatic digest. This paper describes the extension of those studies to DC–MS in a capillary HPLC system.

EXPERIMENTAL

Materials

Trifluororacetic acid (TFA) was from Applied Biosystems (Foster City, CA, U.S.A.). Recombinant methionyl human growth hormone (met-hGH) was produced as described previously[26]. L-1-Tosylamide-2-phenylethyl chloromethyl ketone (TPCK)-treated trypsin was obtained from Worthington (Freehold, NJ, U.S.A.). Water was purified with a Milli-Q system from Millipore (Bedford, MA, U.S.A.). Spectrometric-grade glycerol, hydrochloric acid and cetyltrimethylammonium bromide (cetrimide) were from Aldrich (St. Louis, MO, U.S.A.). HPLC-grade acetonitrile (ACN) was from Burdick & Jackson (Muskegon, MI, U.S.A.). Fused-

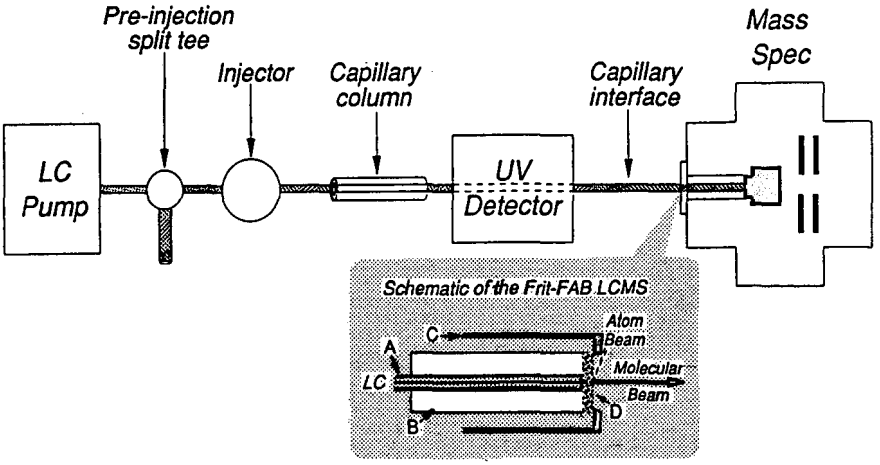

Fig. 1. Schematic diagram of the continuous flow FAB-LC–MS. The effluent from the dual syringe pump is split ahead of the injector so that 5% of the mobile phase delivered by the pump flows through the column. The UV absorbance detector and mass spectrometer are arranged in series to monitor the composition of the column effluent. Inset: Detail of the Frit-FAB target: (A) fused-silica capillary, (B) support guide, (C) cap and (D) stainless-steel frit. As the column effluent emerges from the frit, the volatile solvent components evaporate and the glycerol matrix spreads annularly towards the edge of the frit, exposing peptides to the atom beam. Reprinted with permission from ref. 9.

silica capillary tubing was obtained from Polymicro Technologies (Tucson, AZ, U.S.A.).

Instrumentation

Conventional HPLC. The conventional analytical-scale tryptic map of met-hGH was produced with a Hewlett-Packard (Palo Alto, CA, U.S.A.) Model 1050 HPLC system with data analysis by a Nelson Analytical (Cupertino, CA, U.S.A.) Model 6000 software package. The reversed-phase tryptic map employed a 150 × 4.6 mm I.D. Nucleosil C_{18} column obtained from Alltech Assoc. (Deerfield, IL, U.S.A.), heated in a Flatron Laboratory Systems (Oconomowoc, WI, U.S.A.) Model CH-30 column heater.

Micro-bore HPLC. The capillary-column HPLC system is shown schematically in Fig. 1. As described previously[9], the instrument was assembled from a Brownlee (Sunnyvale, CA, U.S.A.) Model 120 dual-syringe pump and Model 783 UV absorbance detector and Rheodyne (Berkeley, CA, U.S.A.) Model 8125 injector, directly coupled to the 150 × 0.32 mm I.D. capillary column (LC Packings, Zürich, Switzerland) packed with 3-μm RP-18 silica. The pump was operated at 100 μl/min and the eluent was split before the injector to deliver approximately 5 μl/min to the column. The outlet of the column was connected to a length of 50-μm I.D. fused-silica capillary. For detection, a downstream segment of the capillary was stripped of its polyimide coating and secured in a focusing support within the detector.

LC–MS interface. Capillary tubing exiting the detector was connected to a JEOL USA (Peabody, MA, U.S.A.) Frit-FAB probe, shown schematically in the insert to Fig. 1, and consisting of a 50-μm I.D. fused-silica tubing (A) passing through an insulated support (B) and pressed against a 0.25-mm-thick sintered stainless-steel frit

(D). The column effluent passed through the frit and was bombarded with a xenon atom beam at 6 keV in the mass spectrometer source at a temperature of *ca.* 50°C.

Mass spectrometer. Mass spectra were acquired with a JEOL HX110/110 tandem mass spectrometer at a resolution of 3000 and an accelerating voltage of 10 kV. Spectra were acquired at a rate of 12 s per scan, with a mass range of 500 to 4000 mass units (m.u.).

Methods

Tryptic digest. Tryptic digestion was carried out by reconstituting 10 mg of met-hGH in 10 ml of 100 m*M* tris–acetate buffer (pH 8.3), warming the sample to 37°C, and adding 100 μg of trypsin. After 2 h, a second aliquot of 100 μg of trypsin was added. Digestion was stopped at the end of 4 h by lowering the pH of the solution below 3 with 1 *M* hydrochloric acid. The digest mixture was stored at 5°C until analyzed.

Conventional tryptic map. The tryptic map with the conventional analytical system was produced by injecting 200 μl of the digest mixture into the Nucleosil C_{18} column, equilibrated at 35°C with 0.12% aqueous TFA at a flow-rate of 1 ml/min. After a 5-min hold, a linear gradient to 38% ACN over 60 min was started. At the end of the gradient, the ACN content was increased to 57% over 10 min. The column effluent was monitored at 214 nm. Peaks were identified by comparison of retention times with previously characterized maps[5].

LC–MS tryptic map. The elution-mode tryptic digest was chromatographed by

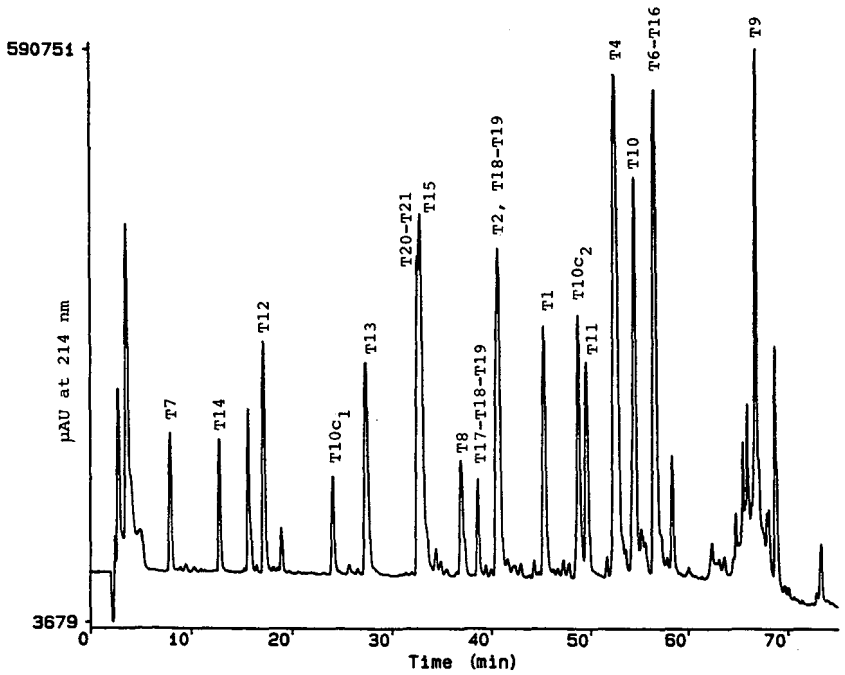

Fig. 2. Tryptic map of 200 μg of the biosynthetic human growth hormone digest mixture. Chromatographic conditions are given in the text. Peaks are labeled according to the identifiers given in Table I.

injecting 25 pmol of digested protein into the capillary column, equilibrated with a mobile phase consisting of 2% ACN, 1% glycerol and 0.1% TFA in water. After an initial 10-min hold, the gradient was started to linearly reach 60% ACN in 65 min. Detection was by absorbance at 195 nm.

DC–MS tryptic map. The displacement separation was carried out by injecting 10 nmol of the digest mixture into the capillary column, equilibrated with a mobile phase consisting of 1% glycerol and 0.1% TFA in water. After a 5-min hold, the displacer solution consisting of 2 mg/ml cetrimide, 1% glycerol and 0.1% TFA in water was pumped into the column. The switch from starting eluent to displacer solution occurred within a 1-min period. The absorbance detector monitored the column effluent at 195 nm. Data collection by the mass spectrometer commenced 150 min after flow of the displacer solution was started.

RESULTS AND DISCUSSION

The chromatogram shown in Fig. 2 represents a typical analysis of the tryptic

TABLE I

PEPTIDES PRODUCED BY DIGESTION OF METHIONYL HUMAN GROWTH HORMONE WITH TRYPSIN

$[M + H]^+$ is the calculated molecular weight for the most abundant monoisotopic species. Single-letter code for amino acids used.

Identifier	*Residues*	*$[M + H]^+$*	*Sequence*
T1	1–9	1061.58	MFPTIPLSR
T2	10–17	979.50	LFDNAMLR
T3	18–20	383.21	AHR
T4	21–39	2342.14	LHQLAFDTYQEFEEAYIPK
T5	40–42	404.22	EQK
T6[a]	43–65	2616.24	YSFLQNPQTSLCFSESIPTPSNR
T7	66–71	762.36	EETQQK
T8	72–78	844.49	SNLELLR
T9	79–95	2055.20	ISLLLIQSWLEPVQFLR
T10	96–116	2262.13	SVFANSLVYGASDSNVYDLLK
T11	117–128	1361.67	DLEEGIQTLMGR
T12	129–135	773.38	LEDGSPR
T13	136–141	693.39	TGQIFK
T14	142–146	626.32	QTYSK
T15	147–159	1489.69	FDTNSHNDDALLK
T16[a]	160–168	1148.55	NYGLLYCFR
T17	169	147.11	K
T18–T19	170–179	1253.62	DMDKVETFLR
T20[b]	180–184	618.34	IVQCR
T21[b]	185–192	785.31	SVEGSCGF
Non-tryptic cleavages			
$T10c_1$	96–100	537.27	SVFAN
$T10c_2$	100–116	1743.90	LWGASDSNVYDLLK
T17–T18–T19	169–179	1381.71	KDMDKVETFLR

[a] T6 and T16 are disulfide-linked, with a total $[M + H]^+$ of 3762.8.
[b] T20 and T21 are disulfide-linked, with a total $[M + H]^+$ of 1401.4.

digest of met-hGH obtained using the conventional-scale HPLC mapping procedure. The identity, amino acid sequence, position in the intact protein and $[M + H]^+$ of the predominant peptides in the map are given in Table I. The high resolution afforded by reversed-phase HPLC allows collection of individual peaks so that the identity of the major peaks can be determined by subsequent analysis. The identification of minor peaks is more problematic, however, since the low abundance of these peptides often demands scaling up the separation in order to obtain a sufficient quantity for further analysis. Under the chromatographic conditions shown, resolution of individual peptides is largely independent of the column load up to about 10 nmol of digested protein. Higher loads than this seriously impair resolution of certain peptides in this chromatographic system.

In order to establish the efficacy of the displacement mode for scale-up of the separation of the tryptic digest mixture, the HPLC system employed for the chromatogram shown in Fig. 2 was run in the displacement mode with cetrimide as the displacer[25]. The displacement purification was performed without modification of the analytical instrument, using 0.1% aqueous TFA or 10 m*M* aqueous phosphoric acid as the carriers. By this procedure, up to 500 nmol of digested protein were separated on the analytical column. These results demonstrated the applicability of this approach to

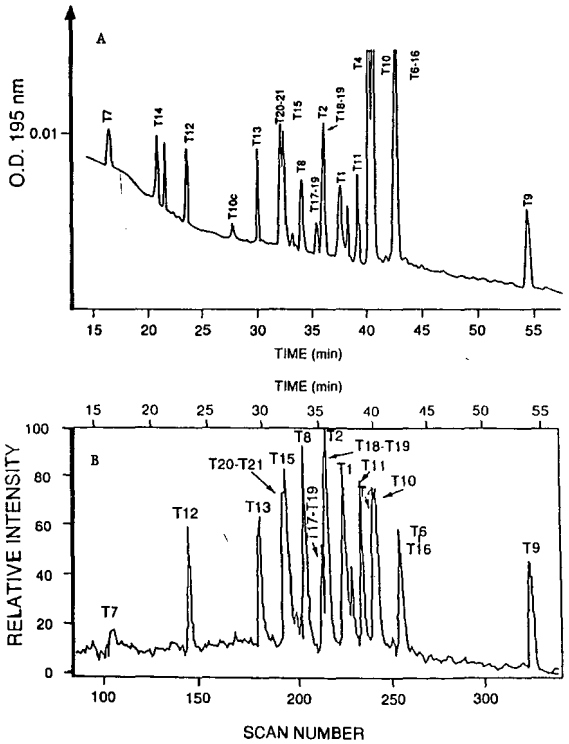

Fig. 3. Tryptic maps of 25 pmol monitored by (A) absorbance of light at 195 nm and (B) the total-ion current in the mass spectrometer. Peaks are labeled as in Fig. 2 and Table I. Experimental conditions are given in the text. Reprinted with permission from ref. 9.

the scale-up of the peptide separation, although certain of the most strongly retained hGH tryptic peptides, including T4, T10, T6–T16 and T9 were not recovered in the displacement train. Nevertheless, the remaining components of the mixture were isolated in high yield, indicating the potential of the displacement mode as an alternative in the scale-up of chromatographic purification.

As discussed above, LC–MS has an enormous potential for rapidly separating and characterizing the components of a tryptic map. The capillary LC–MS system described earlier[9] exhibits high sensitivity and resolution and, by diverting the entire column effluent into the mass spectrometer, it avoids the losses that typically accompany the handling steps associated with fraction collection and off-line FAB-MS analysis. Fig. 3 shows the total ion current (TIC) and UV absorbance chromatograms of a tryptic map of met-hGH run on the capillary system in the gradient elution mode. The small physical dimensions of the capillary LC system prevent untoward dilution of the sample components during analysis, and thereby allow high-sensitivity separations of complex mixtures, as evidenced by the analysis in Fig. 3 that was carried out on 25 pmol of digested protein. The similarity of the chromatograms in Figs. 2 and 3 despite the different provenances of the stationary phases supports the validity of the "down-scaling" of the separation to the capillary LC.

The displacement separation was also scaled down to the dimensions of the capillary LC. Fig. 4 shows the displacement chromatograms for separation of 10 nmol of digested met-hGH. The chromatogram in Fig. 4A was made by UV-absorbance detection, while that in Fig. 4B is the TIC chromatogram obtained by MS detection. Both chromatograms illustrate the "stair-case" pattern expected in displacement-mode separations. The plateau heights measured by UV absorbance of the tryptic peptides generally increase across the displacement train, as expected, since the

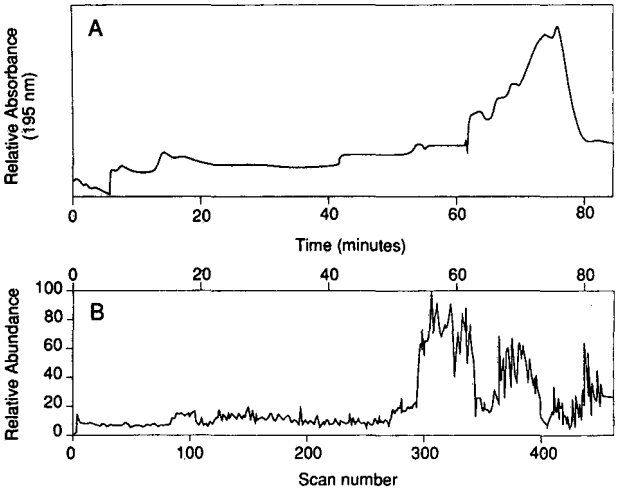

Fig. 4. Column effluent profile during displacement chromatography of 10 nmol of digested biosynthetic human growth hormone monitored by (A) absorbance of light at 195 nm and (B) the total-ion current in the mass spectrometer. Spectra were acquired in 12-s scans, and data collection commenced 150 min after the displacer solution started flowing into the column.

extinction coefficients of the peptides typically increase with increasing size. The TIC chromatogram in Fig. 4B exhibits a converse behavior, with the plateau heights decreasing in size across the displacement train. This behavior reflects the relatively poorer ionization properties of the larger, more hydrophobic peptides that is a feature of the FAB process. In addition, little ion signal was observed at the end of the displacement train, just ahead of the displacer front, so this portion of the column effluent was not analyzed in the mass spectrometer. The cause of this disruption in the

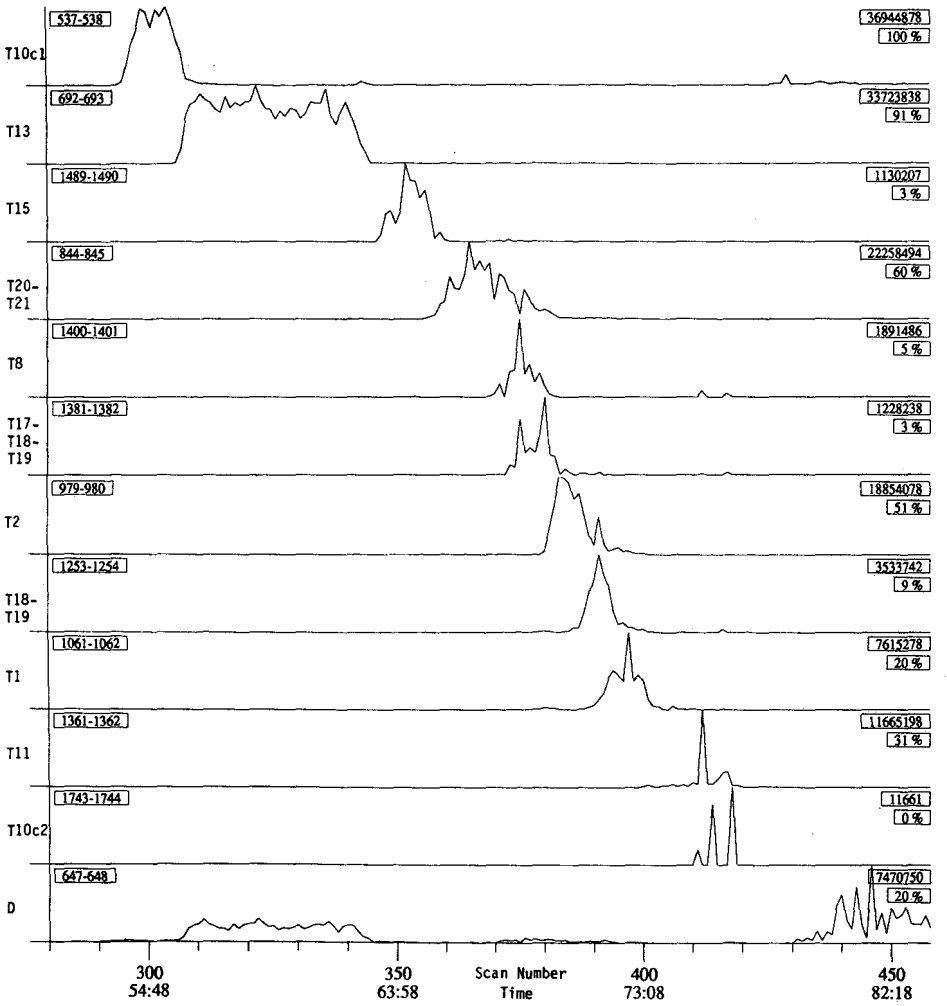

Fig. 5. Reconstructed ion-current chromatograms of the ions corresponding to the predominant peptides comprising the tryptic digest of biosynthetic hGH. The RIC chromatograms were produced by monitoring the abundance of ions within a narrow mass window measured by the mass spectrometer during the run. Each RIC thus selectively monitors a single species in the effluent. The mass range employed in the RIC and peptide identity are indicated on the left side of each chromatogram. The abundance of ions relative to that of the $T10c_1$ RIC maximum is given on the right. "D" indicates the RIC of the brominated dimer of cetyltrimethylammonium, used to monitor the displacer front.

ion current is under investigation. It may be related to the high concentrations of peptides in the glyerol at the probe tip. The TIC chromatogram also shows instability in the ion current under these conditions. Both of these untoward effects may be meliorated by optimization of the choice of ionic modifier and glycerol content in the carrier. The relatively sharp rear boundary of the UV chromatogram indicates that cetrimide, which exhibits little UV absorbance, efficiently displaces peptides under these conditions.

As has been demonstrated[13,23], interpretation of the course of the displacement separation of complex mixtures requires selective analysis of the composition along the displacement train. Such a requirement has been met previously by fraction collection and subsequent analysis of the fractions by HPLC[13,15] or thin-layer chromatography[14], or by a tandem HPLC–HPLC system[17], in which the first chromatograph performed the displacement separation and the second acted as an on-line analyzer for fast HPLC analysis of the column effluent. The results of these analyses in either case were then employed to reconstruct displacement chromatograms that defined the boundaries between components of the mixture in the displacement train. The mass spectrometer provides the opportunity to monitor the masses of peptides in the displacement train and thereby reconstruct individual species displacement chromatograms that yield the information required for interpretation of the displacement separation. Fig. 5 shows the reconstructed ion current (RIC) profiles for the predominant peptides in the tryptic digest. The RIC chromatograms demonstrate that each peptide occupies a distinct band in the displacement train that in most cases is well separated from adjacent bands. Fig. 5 also illustrates the narrowing of bands that occurs near the displacer front, where peptide concentrations are highest. The earliest-eluted peptides are at the lowest concentrations and therefore form wider bands. The more strongly retained peptides form extremely narrow, concentrated bands and, in the cases of T11 and $T10c_2$, the band is little more than one scan wide in the RIC chromatograms. The most hydrophobic peptides, as noted above, were not identified in the displacement train, owing to the interruption in ion current in the latter part of the displacement train. The displacer was monitored by the mass at 647.5 m.u., which corresponds to a brominated cetrimide dimer, since the cetrimide monomer ($[M + H]^+ = 285$) was below the mass range scanned in this experiment. The displacer ion appeared upon resumption of the ion current, evidently after the disturbance at the probe tip had been removed. All of the peptides eluted before T4 in the tryptic map shown in Fig. 2 were observed in the displacement train, although certain pairs of peptides reversed their elution order at the high concentrations employed in this mode of chromatography. Thus, T20–T21 is eluted before T15 in the chromatogram of Fig. 2, but these peptides exit the column in the reversed order in the displacement train of Fig. 5. This reversal of affinity for the stationary phase at high concentrations has previously been observed in the measurement of adsorption isotherms of proteins[27,28], but has not been reported for molecules of the size employed here.

The mass range from 500 to 4000 m.u. was scanned every 12 s, providing a "snapshot" of the composition of the column effluent at 12-s intervals. Subsequent scans can be compared to provide insight into the dynamics of the displacement process, in a manner analogous to the tandem HPLC–HPLC arrangement described previously[17]. Fig. 6 shows sequential mass spectra, starting with scan 305, which was

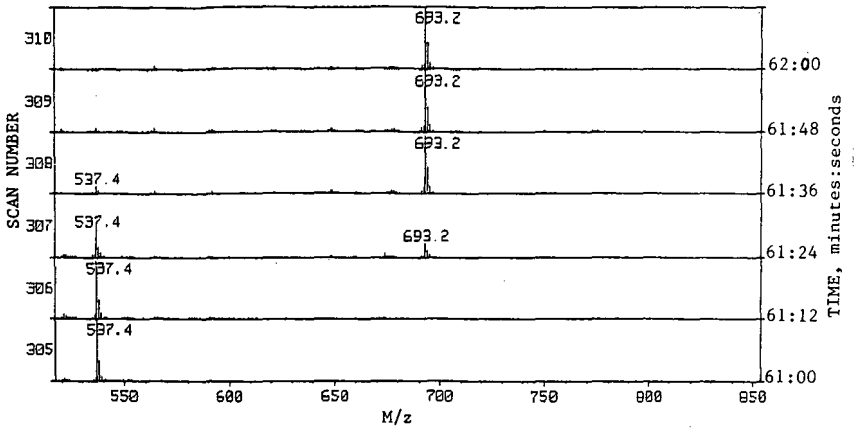

Fig. 6. Mass spectra acquired as scans 305–310 during the displacement separation. The time corresponding to the start of each scan is indicated on the right side of the figure and the scan number on the left.

started at 61 min. The dominant ion in scan 305 has a molecular mass of 537.4 m.u. and corresponds to residues 96–99 in met-hGH. This peptide arises from a chymotryptic-like clip in the T10 peptide, has been observed previously[2], and is dubbed the "T10c$_1$" peptide. Scan 306 is also dominated by the T10c$_1$ peptide, while scans 307 and 308 represent the boundary between the zone of this peptide and the next in the displacement train, an ion with a mass of 693.2 m.u. This peptide corresponds to the T13 fragment of the tryptic digest of met-hGH, as seen in Table I. Fig. 6 thus shows the small extent of overlap between bands in displacement chromatography, *i.e.*, less than two scans or 24 s wide. Few on-line or off-line analytical techniques can monitor the effluent compositon at higher scan rates than mass spectrometry, demonstrating the power of this approach in studies of the displacement process.

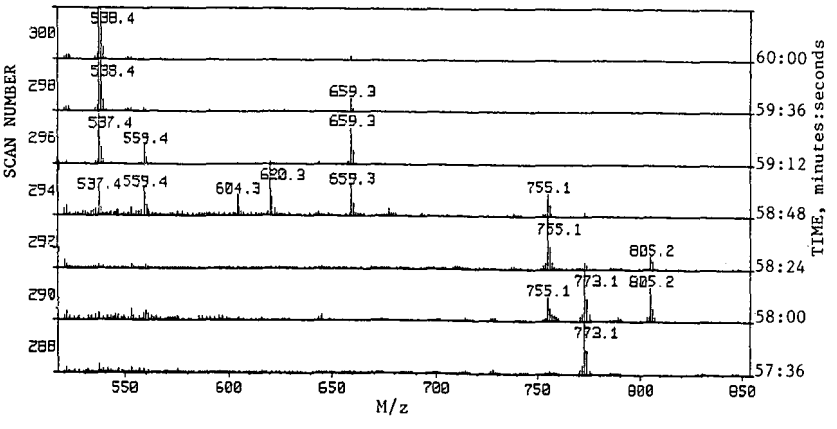

Fig. 7. Mass spectra acquired during the displacement separation by summation of pairs of scans. The spectrum labeled 288 is thus the sum of scans 288 and 289. The time corresponding to the start of the scan is indicated on the right side of the figure and the beginning scan number on the left.

In contrast to the clean transition from T10c$_1$ to T13 observed in Fig. 6, the boundary at the front of the T10c$_1$ band, which marks the transition from T12 to T10c$_1$, contained several small fragment ions, as shown in Fig. 7. The serial spectra shown in Fig. 7 illustrate that minor components of the digest, such as the 559.4 ion, which can be assigned to a non-specific cleavage of the T15 peptide, concentrate between the bands of the predominant peptides and yield intense ions in individual scans that unambiguously indicate their presence and allow precise determination of their mass. This concentrating effect illustrates the power of the displacement mode for accumulation and characterization of minor components of a complex mixture. The other ions identified in Fig. 7 are included, with their assignments, in Table II. The relative amounts of individual species in the digest mixture could be estimated roughly from the width of the zones occupied in the displacement train, as indicated by Tiselius[12]. Optimization of the FAB process may allow more accurate quantification of the peptides in the displacement train, as has been reported for other applications[8].

The dominant peptides shown in Figs. 2 and 5 include both expected tryptic cleavages, *i.e.*, peptides containing terminal arginine and lysine residues, along with the expected incomplete cleavages around T18 and the non-specific cleavage in T10. Other

TABLE II

MOLECULAR IONS OBSERVED IN DISPLACEMENT CHROMATOGRAPHY–MASS SPECTROMETRY OF METHIONYL HUMAN GROWTH HORMONE

Sequence assignments were made by comparison of the observed mass with that calculated for the most abundant isotopes of each peptide.

Observed $[M + H]^+$	*Calculated* $[M + H]^+$	*Residues*	*Sequence*
609.3	609.7	102–107	LVYGAS
773.1	773.4	129–135	LEDGSPR
805.2	804.5	98–105	trypsin fragment T7
755.1	755.3	106–112	ASDSNVY
604.3	604.3	13–17	NAMLR
620.4	620.3	13–17	NAMLR (sulfoxide)
559.4	559.4	155–159	DALLK
659.3	659.3	48–53	NPQTSL
537.4	537.3	96–100	SVFAN
693.2	693.4	136–141	TGQIFK
707.2	?	?	?
1012.1	1012.5	151–159	SHNDDALK
892.3	892.3	173–179	KVETFLR
764.2	764.4	174–179	VETFLR
1489.8	1489.7	147–159	FDTNSHNDDALLK
844.2	844.5	72–78	SNLELLR
618.3	618.3	180–184	IVQCR
785.1	785.3	185–192	SVEGSCGF
1401.4	1401.4	180–192	IVQCR-SVEGSCGF
1381.4	1381.7	169–179	KDMDKVETLR
979.3	979.5	10–17	LFDNAMLR
1253.3	1253.6	170–179	DMDKVETLR
1061.3	1061.6	1–9	MFPTIPLSR
1361.5	1361.7	117–128	DLEEGIQTLMGR
818.2	818.6	1–7	MFPTIPL

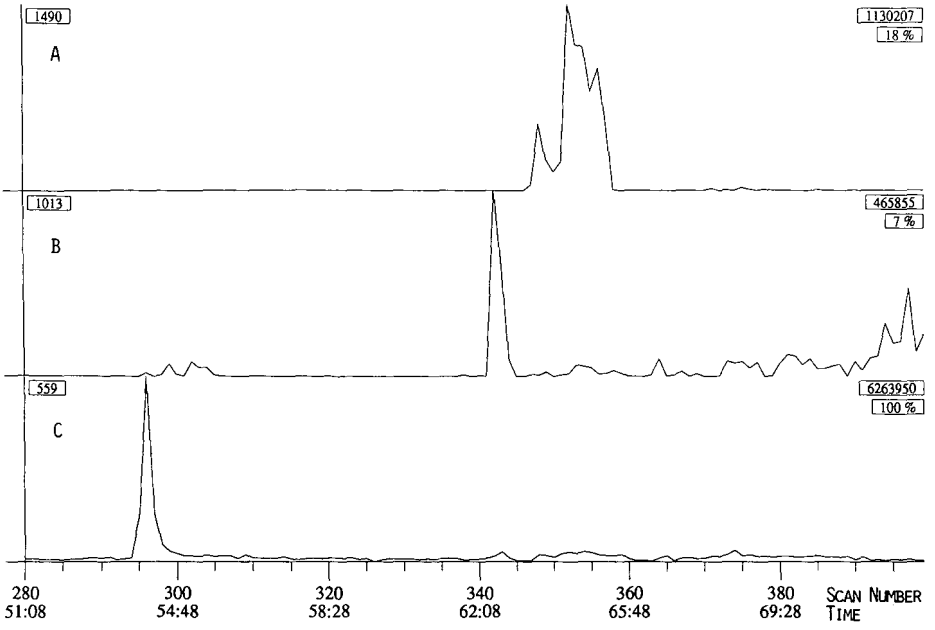

Fig. 8. (A) RIC chromatogram of T15 (residues 147–159, $[M + H]^+ = 1489.7$ m.u.), along with the chromatograms of two fragments formed by non-specific cleavage of T15 during digestion. The fragments correspond to residues (B) 151–159 ($[M + H]^+ = 1012.5$) and (C) 155–159 ($[M + H]^+ = 559.4$). The individual chromatograms are all normalized to the same scale. The relative abundance of ions is given alongside each chromatogram.

non-specific cleavages occurring during the digest were also observed as indicated above. Fig. 8 shows the RIC chromatogram of T15 (residues 147–159, predicted $[M + H]^+ = 1489.7$) in the displacement train, together with two other peptides that formed very narrow bands at earlier positions within the train. A mass spectral analysis program developed in-house at Genentech assigned the observed molecular weights of these peptides to the sequences comprising residues 151–159 (predicted $[M + H]^+ = 1012.5$) and 155–159 (predicted $[M + H]^+ = 559.4$). Thus, the two peptides arise from a non-tryptic cleavage of the T15 peptide. The relatively high abundance of these ions within their narrow bands in Fig. 8 further demonstrates the utility of displacement chromatography for concentrating minor components of a complex mixture in order to obtain a high-quality signal in on-line mass-spectrometry. Many ions were observed in the displacement separation that were assigned to other non-specific cleavages in the digest, and are summarized in Table II. Certain of these peptides have not been reported previously, owing to their relatively low abundance in the mixture that hampers their collection and characterization by conventional approaches.

Aside from non-specific cleavage arising during the enzymatic digestion, fragmentation of ions can also occur during bombardment in the continuous-flow FAB interface. Fig. 9A shows the RIC chromatograms of the T20–T21 peptide ($[M + H]^+ = 1401.4$), which contains the T20 and T21 peptides linked by a disulfide bond. The individual RIC chromatograms of T20 ($[M + H]^+ = 618.3$) and T21

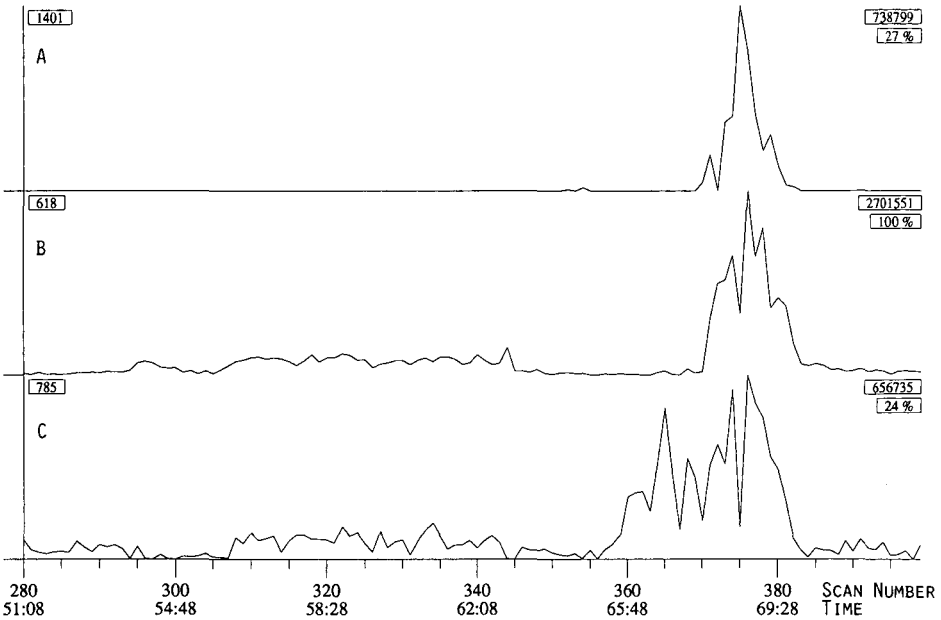

Fig. 9. (A) RIC chromatogram of T20–T21 ($[M + H]^+ = 1401.4$ m.u.), along with the chromatograms of the two fragments formed by breakage of the disulfide bond contained in this peptide. The fragments correspond individually to (B) T20 ($[M + H]^+ = 618.3$ m.u) and (C) T21 ($[M + H]^+ = 785.1$ m.u.). The individual chromatograms are all normalized to the same scale. The relative abundance of ions is given alongside each chromatogram.

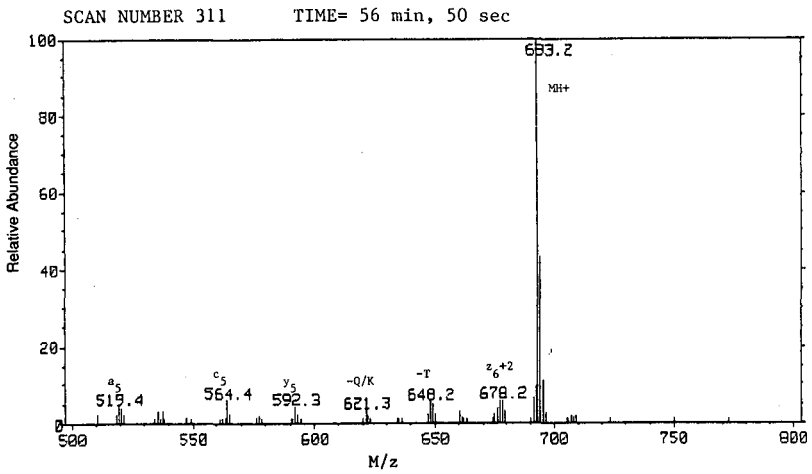

Fig. 10. Mass spectrum acquired at scan 311 during displacement chromatography. The dominant ion corresponds to T13, and smaller ions to fragments generated during xenon fast-atom bombardment on the probe. The assignment of daughter ions is indicated by the standard nomenclature[30].

($[M + H]^+ = 785.1$) are shown in Fig. 9B and C, respectively. The disulfide bond in T20–T21, like that in the other disulfide linked peptide, T6–T16, is relatively labile, so ions corresponding to the two fragments are observed together with the ion of the intact peptide. Fragmentation of other bonds within a peptide is also known to occur in the FAB ionization process[29]. Fig. 10 shows the spectrum collected at scan 311, which is dominated by the ion corresponding to the T13 peptide, with an $[M + H]^+$ of 693.2 m.u. As in the case for T20–T21 and its fragments, the fragment ions occur in the same position within the displacement train as the "parent" ion, suggesting that they arise as artifacts of the ionization process, in contrast to the peptides arising from non-specific enzymatic cleavages discussed above that appear in a different position within the displacement train. The daughter ions in Fig. 10, however, arise from breakage of bonds along the peptide backbone, or from loss of a residue side chain. The resulting ions can be assigned to fragments that are known to occur during FAB ionization[31].

CONCLUSIONS

Columns and equipment developed for reversed-phase HPLC are well suited to displacement separation of the mixture resulting from tryptic digestion of met-hGH with cetyltrimethylammonium bromide as the displacer. By this means, the capacity of the column can be increased 50-fold. Preparative purification of relatively large amounts of tryptic peptides can thus be carried out on the high efficiency equipment. Useful amounts of minor components of the digest mixture can be isolated for subsequent characterization.

Displacement chromatography offers a means of increasing the sample load in microbore LC–MS, thereby obviating some of the limitations imposed by the low flow-rates tolerated in on-line mass spectrometry, and extending the dynamic range of the analysis. In addition, the mass spectrometer acts as a highly selective detector that permits the reconstruction of the band profiles of individual species in the displacement train. It can thus aid in rapid description of the performance of the chromatographic system, to optimize the conditions for preparative and process applications.

Analysis by DC–MS of 10 nmol of recombinant human growth hormone digested with trypsin revealed the presence of most of the major expected peptides along with many smaller peptides associated with non-specific proteolysis and autolysis of trypsin. High-quality spectra were obtained for peptides present in extremely low amounts in the sample. Fragmentation of peptides in the FAB process was also observed, but could be distinguished from proteolysis arising during enzymatic digestion.

Instability in the ion signal late in the displacement train may be associated with the high concentrations characteristic of DC, and may be meliorated by optimization of chromatographic and FAB experimental conditions.

ACKNOWLEDGEMENTS

The authors wish to express their thanks to Professor Csaba Horváth of Yale University for valuable discussions and encouragement in the DC–MS concept.

Thanks are also due William Henzel of Genentech for help in optimizing the LC–MS performance and John Stults of Genentech for assistance in interpretation of the mass spectra.

REFERENCES

1 W. S. Hancock, C. A. Bishop, R. L. Partridge and M. T. W. Hearn, *Anal. Biochem.*, 89 (1978) 203.
2 W. G. Bennett, R. Chloupek, R. Harris, E. Canova-Davis, R. Keck, J. Chakel, W. S. Hancock, P. Gellefors and B. Pavlu, in E. E. Miller, D. Cocchi and V. Locatelli (Editors), *Advances in Growth Hormone and Growth Factor Research*, Pythagora Press, Rome-Milan, and Springer-Verlag, Berlin-Heidelberg, 1989, p. 28.
3 W. P. Blackstock, R. J. Dennis, S. J. Lane, J. I. Spards and M. P. Weir, *Anal. Biochem.*, 175 (1988) 319.
4 P. Gellerfors, K. Axelsson, A. Helander, S. Johansson, L. Kenne, S. Lindqvist, B. Pavlu, A. Skottner and L. Fryklund, *J. Biol. Chem.*, 264 (1989) 11444.
5 W. J. Kohr, R. Keck and R. N. Harkins, *Anal. Biochem.*, 122 (1982) 348.
6 M. Barber, R. S. Bordoli, R. D. Sedgwick and A. N. Tyler, *J. Chem. Soc., Chem. Commun.*, (1981) 325.
7 T. Mizuno, T. Kobayashi, Y. Ito and D. Ishii, *Mass Spectrom.*, 35 (1987) 9.
8 R. M. Caprioli, W. T. Moore and T. Fan, *Rapid Comm. Mass Spectrom.*, 1 (1987) 15.
9 W. J. Henzel, J. H. Bourell and J. T. Stults, *Anal. Biochem.*, submitted for publication.
10 R. M. Caprioli, W. T. Moore, B. DaGue and M. Martin, *J. Chromatogr.*, 443 (1988) 355.
11 J. Frenz and Cs. Horváth, in Cs. Horváth (Editor), *HPLC —Advances and Perspectives*, Vol. 5, Academic Press, New York, 1989, p. 212.
12 A. Tiselius, *Ark. Kemi Mineral Geol.*, 16A (1943) 1.
13 Cs. Horváth, A. Nahum and J. H. Frenz, *J. Chromatogr.*, 218 (1981) 365.
14 H. Kalász and Cs. Horváth, *J. Chromatogr.*, 215 (1981) 295.
15 Cs. Horváth, J. Frenz and Z. El Rassi, *J. Chromatogr.*, 255 (1983) 273.
16 G. E. Veress, Cs. Horváth and E. Pungor, in H. Kalász (Editor), *New Approaches in Liquid Chromatography*, Akadémiai Kiadó, Budapest, 1984, pp. 45–56.
17 J. Frenz, Ph. van der Schrieck and Cs. Horváth, *J. Chromatogr.*, 330 (1985) 1.
18 Cs. Horváth, in F. Bruner (Editor), *The Science of Chromatography*, Elsevier, Amsterdam, 1985, pp. 179–203.
19 S. M. Cramer and Cs. Horváth, *Prep. Chromatogr.*, 1 (1988) 29.
20 S. M. Cramer, Z. El Rassi and Cs. Horváth, *J. Chromatogr.*, 394 (1987) 305.
21 A. W. Liao, Z. El Rassi, D. M. LeMaster and Cs. Horváth, *Chromatographia*, 24 (1987) 881.
22 G. Viscomi, S. Lande and Cs. Horváth, *J. Chromatogr.*, 440 (1988) 157.
23 J. Frenz and Cs. Horváth *Am. Inst. Chem. Eng. J.*, 31 (1985) 400.
24 R. D. Smith, J. A. Loo, C. J. Barinaga, C. G. Edmonds and H. R. Udseth, *J. Chromatogr.*, 480 (1989) 211.
25 J. Frenz, unpublished results.
26 K. C. Olson, J. Fenno, N. Lin, R. N. Harkins, C. Snider, W. J. Kohr, M. J. Ross, D. Fodge, G. Prender and N. Stebbing, *Nature (London)*, 293 (1981) 408.
27 J.-X. Huang and Cs. Horváth, *J. Chromatogr.*, 406 (1987) 275.
28 J.-X. Huang and Cs. Horváth, *J. Chromatogr.*, 406 (1987) 285.
29 D. H. Williams, C. V. Bradley, S. Santikarn and G. Bojeses, *Biochem. J.*, 201 (1982) 835.
30 P. Roepstorff and J. Fohlman, *Biomed. Mass Spectrom.*, 11 (1984) 601.
31 S. Naylor and G. Moneti, *Biomed. Environ. Mass Spectrom.*, 18 (1989) 405.

Journal of Chromatography, 512 (1990) 315–323
Elsevier Science Publishers B.V., Amsterdam

CHROMSYMP. 1861

Tryptic fingerprinting on a poly(styrene–divinylbenzene) reversed-phase column

JOEL K. SWADESH
Polymer Laboratories, Inc., 160 Old Farm Road, Amherst, MA 01002 (U.S.A.)

ABSTRACT

The properties of poly(styrene–divinylbenzene) (PS–DVB) in gradient reversed-phase peptide separations have not been fully explored. Comparisons of selectivity and fraction capacity with silica alkyl bonded phases remain to be established. Investigation of the effects of gradient rate and flow-rate on separation are desired. The present work examines separations of synthetic peptides and of tryptic fragments of three species of cytochrome *c* and reduced, carboxymethylated human plasminogen. Fingerprinting is a means to localize the position of one or more variant amino acids within the sequence of a large polypeptide. Reproducibility of separation is a dominant issue, potentially affected by variability in pump performances. The susceptibility of the peptide fingerprint to changes in pump performance can be examined by systematic variation of the flow-rate and gradient rate. PS–DVB exhibited predictable separations equivalent to those of alkyl bonded phases. The selectivity parallelled that observed for bonded phases. Two observations made in the course of these studies may be of interest to the theory of reversed-phase liquid chromatography. First, the peak capacity was found to be a simple function of the gradient rate. Also, the resolution was observed to increase with increasing flow-rate in a separation of horse cytochrome *c* tryptic fragments at fixed gradient rate.

INTRODUCTION

There have been many elegant demonstrations of applications of peptide mapping by various separations techniques, particularly reversed-phased liquid chromatography[1–3]. Reversed-phase high-performance liquid chromatography (RP-HPLC) is presently perhaps the most widely used technique, combining high reproducibility and resolving power with low sample requirements and easy post-separation recovery. Poly(styrene–divinyl benzene) (PS–DVB) has become widely accepted as a high-performance reversed-phase material only recently[4–6], so many of its applications in separations remain to be demonstrated. PS–DVB is known to exhibit a number of properties relevant to ruggedness in fingerprinting, among which are pH stability and ease of cleaning. The present work examines PS–DVB selectivity and peak capacity, using as probes a series of synthetic peptides, tryptic digests of cytochrome *c* from three species, and the tryptic digest of human plasminogen.

0021-9673/90/$03.50

EXPERIMENTAL

Materials

The HPLC system consisted of two Model 364 pumps, a Model 50 HPLC Programmer, and a Model 87.00 UV detector equipped with a 3-mm 0.8-μl flow-cell (Knauer, Berlin, F.R.G.). High-pressure mixing was accomplished with a 10-μl Model TCMA 0120113T Visco-Jet mixer (Lee Co., Westbrook, CT, U.S.A.). Injection was performed with a Model 231 autoinjector (Gilson, Middleton, WI, U.S.A.) equipped with a 100-μl sample loop. Separations were accomplished on a 25 × 0.46 cm I.D. 100 Å PLRP-S column (Polymer Labs.), Church Stretton, U.K.). Solvents were degassed and maintained under a positive pressure of helium.

Oxalic acid, sodium iodoacetate, ammonium bicarbonate, cytochrome *c* species variants (horse type VI, tuna type XI and rabbit type XV) and the synthetic peptides (single-letter code for amino acids used) GFL, YY, YF, GYG, GLY, YGGFM, YG, YV, PY, GY, YA, YGGFL, YAGFM, YGGFLK, YGG, GGFM, FV, YL, YE, RVYIHPF and DRVYIHPF were obtained from Sigma (St. Louis, MO, U.S.A.). Benzoic acid was from Chem Service (West Chester, PA, U.S.A.). Trishydroxymethylaminomethane (Tris), dithiothreitol (DTT), disodium ethylenediaminetetraacetic acid (EDTA) and guanidine hydrochloride (GuHCl) were from ICN Biomedicals (Costa Mesa, CA, U.S.A.). Acetonitrile, 2-propanol and trifluoroacetic acid were from Baker (Phillipsburg, NJ, U.S.A.). Dialysis membrane with a 3500 molecular weight cutoff was from Spectrum Medical (Los Angeles, CA, U.S.A.). Glu-plasminogen from human serum was from Serva (Westbury, NY, U.S.A.). Sequencing grade bovine pancreatic trypsin was from Boehringer Mannheim (Indianapolis, IN, U.S.A.).

Methods

Reversed-phase separations were conducted at a flow-rate of 1 ml/min unless otherwise specified. The aqueous mobile phase was prepared from 990 ml water, 10 ml 2-propanol and 1 ml trifluoroacetic acid. The organic mobile phase was 990 ml acetonitrile, 10 ml 2-propanol and 1 ml trifluoroacetic acid. For separations of the synthetic peptides, oxalic acid was added to the sample as an injection marker and benzoic acid was used as a gradient marker. About 5–25 μg of each synthetic peptide was injected.

A stock solution of 0.5 *M* Tris, pH 8.86 was prepared. Reduction of 10 mg plasminogen was performed at 37°C in 1 ml 100 m*M* Tris, 1 m*M* EDTA, 6.3 *M* GuHCl. Incubation with 4.9 mg DTT proceeded for 1 h. The reaction was quenched with 2.7 mg sodium iodoacetate in 210 μl water and allowed to stir 45 min. Then, the sample was dialyzed three times against 0.5 *M* ammonium bicarbonate (200 ml; 1 h) and once against 4 l of 0.1 *M* ammonium bicarbonate. The species of cytochrome *c* were also dialyzed into 0.1 *M* ammonium bicarbonate.

Trypsin digestion of 5 mg of plasminogen and 5 mg of each of the cytochrome *c* variants was performed at 37°C in 1.4 ml 0.1 *M* ammonium bicarbonate. Aliquots of 20 μg of trypsin (1 μg/μl) were added at 0, 1, 2, 4 and 8 h. The progress of the digestion was monitored by RP-HPLC to ensure completion. About 35 μg of trypsinized cytochrome *c* and 350 μg trypsinized plasminogen were injected in 100 μl. In all cases, chromatography was performed at ambient temperature (24 ± 2°C).

RESULTS AND DISCUSSION

Illustration of fingerprinting

Fig. 1 shows tryptic fingerprints of three species of cytochrome *c*. The peptides containing the protoporphyrin IX heme moiety were established by detection at 400 nm (data not shown) and are marked with an asterisk in the figure. Despite 85–95% homology between the species, the fingerprints are distinctive. Tryptic fingerprints of horse cytochrome *c* on several alkyl bonded phases are available in the literature[2].

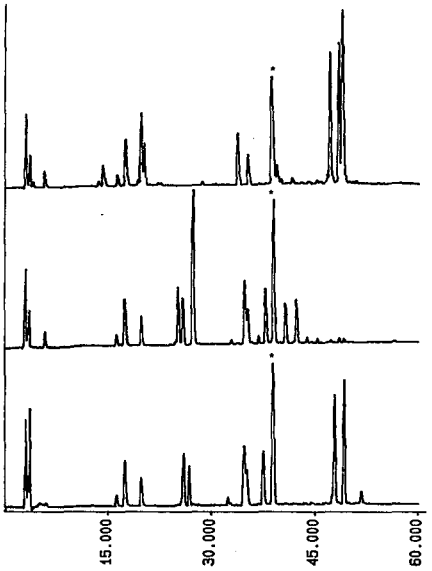

Fig. 1. Tryptic fingerprints of species of cytochrome *c*. Reversed-phase separation of tryptic fragments of about 35 μg tuna (upper panel), horse (middle panel) and rabbit (lower panel) cytochrome *c* on a 25 × 0.46 cm I.D., 5-μm, 100-Å PLRP-S column, using acetonitrile–water–0.1% trifluoracetic acid–2-propanol as the mobile phase. Gradient conditions were aqueous-organic mobile phase (95:5) (0–5 min) to aqueous–organic (60:40) (5–55 min), 1 ml/min. The ordinate is the absorbance at 220 nm, while the abscissa is retention in minutes. The peaks marked with an asteriks exhibited absorbance at 400 nm and were therefore assigned as peptides containing heme.

Selectivity

Fig. 2 is a graph of the peptide retention times observed on PLRP-S, shown on the *y*-axis, *versus* the retention times predicted by a theory developed for alkyl.bonded phases[7,8], shown on the *x*-axis as the sum of retention coefficient ($\sum R_c$) corrected for gradient rate (4.5% min) and for gradient delay effects (5.9 min). The gradient delay effects include the programmed gradient delay, the column void volume and the pre-column void. Therefore, Fig. 2 is a direct and simple comparison of the retention order of small peptides on PLRP-S with that on silica-based alkyl-bonded phases. No corrections are made for such effects as molecular weight[9] or changes in retention due to gradient rate, because for small peptides on relatively large pore materials, the effects of molecular weight are known to be far less dominant than hydrophobicity[9],

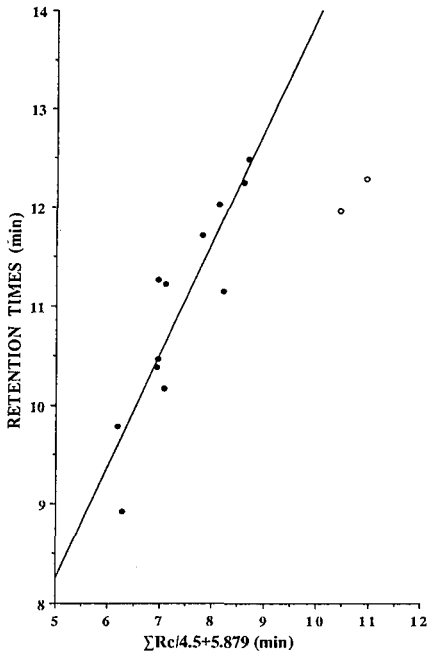

Fig. 2. Peptide retention on poly(styrene–divinyl benzene) *versus* alkyl-bonded phases. The retention (in minutes) predicted by the theory of Hodges and co-workers[9–11] is indicated by $\sum R_c/4.5 + 5.879$ and graphed on the abscissa, while the observed retention (in minutes) is graphed on the ordinate. Twelve peptides, including GFL, YY, YF, GLY, YGGFM, YV, YGGFL and YAGFM, YGGFLK, GGFM, FV and YL, appear to correlate well with the theory of Hodges and co-workers, and are indicated with filled circles (●). Two peptides which do not correlate well with the theory, RVYIHPF and DRVYIHPFHL, are indicated with hollow circles (○).

as are the effects of gradient rate[8]. Also, a mixture of GYG, PY, YV, YY, GLY, YF, GFL, YGGFM and benzoic acid was chromatographed at gradient rates of 2.25–9% acetonitrile/min and no inversions of retention were observed. The theory of Hodges and co-workers[7–9] assumes that the hydrophobicities of peptide side chains and termini contribute additively to retention time and that effects of alkyl chain length, column length, particle size and carbon loading can all be accounted for by the inclusion of a single standard. Fig. 2 shows that, to a first approximation, the same assumptions hold for PLRP-S and that retention can be predicted by additive retention coefficients.

Of the 21 peptides tested, seven (GYG, YG, PY, GY, YA, YGG and YE) are predicted by the theory of Hodges and co-workers not to be retained on column and these peptides do elute either isocratically or very early in the gradient, Fourteen (GFL, YY, YF. GLY, YGGFM, YV, YGGFL, YAGFM, YGGFLK, GGFM, FV, YL, RVYIHPF and DRVYIHPFHL) are predicted to be retained on column. Of these fourteen, all except the latter two appear to obey the linear behavior predicted in the theory of Hodges and co-workers. The peptides RVYIHPF and DRVYIHPFHL are slightly less strongly retained than predicted by theory. So, PLRP-S appears to exhibit the same general pattern of selectivity observed in alkyl bonded

phases, although it may be desirable to recalculate retention coefficients specifically for PS–DVB.

Another aspect of selectivity is the dependence of the capacity on the conditions of elution. Modern gradient theory[10–13] describes this dependence by means of graphs of the logarithm of the median solute capacity factor, log $\bar{k}$, on the median organic modifier mole fraction, $\bar{\varphi}$. The data required for such plots can be obtained by measurement of retention time on systematic variation of the gradient rate at constant flow-rate. The tryptic digest of horse cytochrome *c* was chromatographed at 1 ml/min on a gradient from aqueous–organic (95:5) (0–3 min) to aqueous–organic (60:40) mobile phase over a period of 40, 20, 10, 5 and 2,5 min. The data obtained from the plot of log $\bar{k}$ *vs.* $\bar{\varphi}$ are given in Table I.

TABLE I

DATA OBTAINED FROM THE PLOT OF log $\bar{k}$ *VS.* $\bar{\varphi}$

Cytochrome c peptide	*Retention time (min)*[a]	*Intercept*	*Slope*
1	16.3	0.34	−3.6
2	17.4	0.43	−3.8
3	19.9	0.53	−4.0
4	25.2	0.72	−5.3
5	25.9	0.76	−5.3
6	27.3	0.88	−4.8
7	34.8	1.3	−6.1
8	35.1	1.3	−5.8
9	37.8	2.2	−9.0
10[b]	38.9	1.6	−7.1
11	40.7	1.7	−7.2
12	42.3	1.8	−6.9

[a] Retention times (min) obtained from Fig. 1 (middle panel).
[b] Heme-containing peptide.

At gradient rates greater than 7% min, curvature was seen in the plots. The magnitudes of the slopes (and intercepts) are smaller than those generally seen in studies of peptide separations on bonded phase materials[12,13] and closer to the values seen for small organic molecules[14]. For YGGFM, values of −4.8 and 1.1 were obtained for the slope and intercept; these values are likewise smaller than those reported for separation on C_{18}-bonded phases[12,13]. Since the magnitude of the slope is believed to be related to the molecular weight[12,13], the implication would seem to be that peptides are less tightly and less cooperatively adsorbed to PS–DVB than to C_{18}-bonded phases.

Peak capacity

Plasminogen, comprised of 790 amino acids and bearing sites of glycosylation, is one of the most complex single-chain proteins. Fig. 3 shows the separation of plasminogen tryptic fragments as a function of gradient rate. There are noticeable changes in the fingerprint at different gradient rates, although careful examination reveals that common features are preserved.

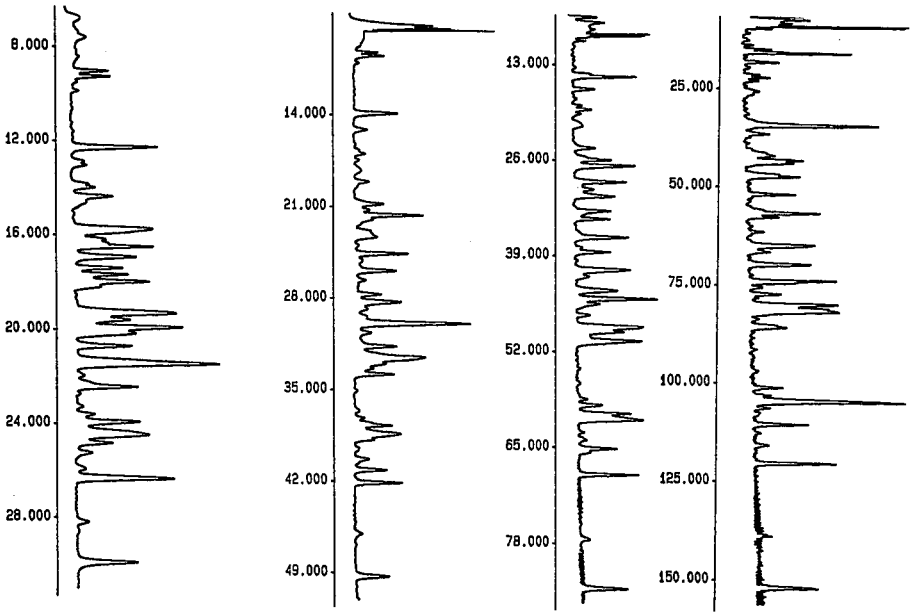

Fig. 3. Gradient rate dependence of tryptic fingerprints of human Glu-plasminogen. Reversed-phase separation of tryptic fragments of about 350 μg human plasminogen on a 25 × 0.46 cm I.D. 5-μm 100-Å PLRP-S column, using acetonitrile–water–0.1% trifluoroacetic acid–2-propanol as the mobile phase. Gradient conditions were aqueous-organic (95:5) (0–3 min) to aqueous–organic (90:10) (3–5 min), to aqueous–organic (50:50) over a variable period. From upper to lower panels, the gradient times were 4 h, 2 h, 1 h, and 30 min. Flow-rate was, in all cases, 1 ml/min. The ordinate is absorbance at 220 nm and the abscissa is retention time in minutes.

The peak capacity, which is a measure of the resolving power of a separation system, is usually defined as the maximum number of peaks which can be resolved to baseline over the gradient range. In fingerprinting, the peak capacity must exceed the number of expected proteolytic fragments to maximize the probability that all peaks will be resolved. The peak capacities of the gradient separations examined were esti-

TABLE II

PEAK CAPACITIES AT TYPICAL GRADIENT RATES

Tryptic digest	*Gradient rate (%/min)*	*Peak capacity*
Cytochrome *c*	14	31
	7	44
	3.5	55
	1.75	73
	0.88	87
Plasminogen	1.33	81
	0.67	112
	0.33	130
	0.17	137

mated according to the usual definition[2], but subtracting the gradient delay time (Table II). The peak capacities at typical gradient rates are about those observed for typical alkyl bonded silica phases[2,12,15]. In Fig. 4 is graphed the peak width as a function of gradient rate. A simple relationship, $W_{0.5} = 0.19(\Delta\psi/t_G)^{0.55}$, where $W_{0.5}$ is the peak width at half height and $\Delta\psi/t_G$ is the gradient rate, appears to hold over a regime of gradient rates spanning separations lasting 2.5 min to 4 h.

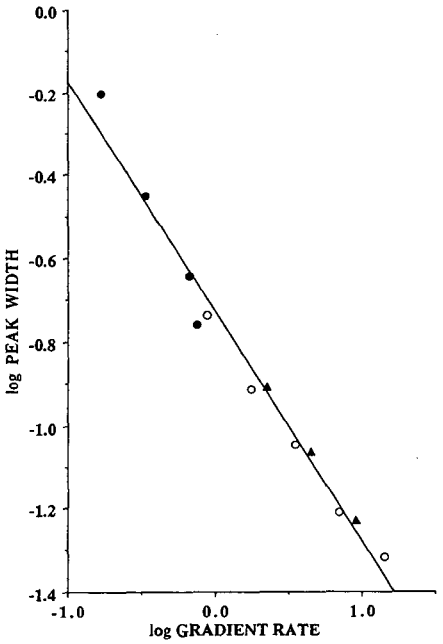

Fig. 4. Dependence of peak width on gradient rate. The peak widths at half height were measured for I: a mixture of PY, YV, YY, GLY, YF, GFL and YGGFM chromatographed at gradient rates of 2.25–9% acetonitrile per minute, II: those tryptic digest fragments of horse cytochrome *c* pictured in Fig. 1 which elute on the gradient and III: four well-resolved peaks of the tryptic digest of Glu-plasminogen pictured in Fig. 3 (retention items on the 4 h gradient 34.0, 56.6, 120.1 and 151.8 min). The logarithms of the average peak width are plotted against the logarithm of the gradient rate for the separation. I = △; II = ○; III = ●.

As is shown in Fig. 5, under conditions of high gradient rate, the performance of the PLRP-S column appears to improve slightly with an an increase in flow-rate. At 1.5 ml/min, the column pressure is at the maximum recommended by the manufacturer, *i.e.*, 3000 p.s.i., but still well below the column packing pressure. If one were to interpret this observation according to the Knox equation[16], it would seem to indicate that band broadening in fingerprint mapping on PLRP-S might not be dominated by mass transfer effects, but rather by diffusional broadening, presumably in the mobile phase. At present the effect is merely noted as an empirical observation and it is recommended that users investigate increased flow-rate as a means of improving resolution.

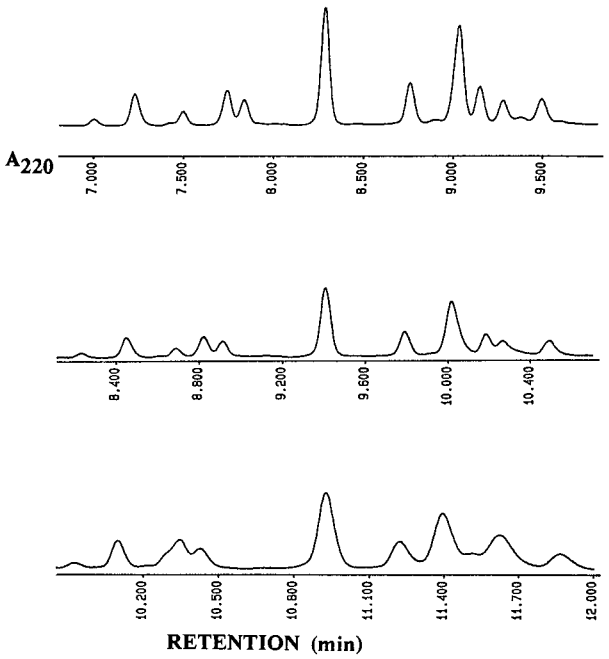

Fig. 5. Separation of tryptic fragments of horse cytochrome *c* as a function of flow-rate. Separation was performed on a 25 × 0.46 cm I.D. 5-μm 100-Å PLRP-S column, using acetonitrile–water–0.1% TFA–2-propanol as the mobile phase. Gradient conditions were aqueous-organic (95:5) (0–3 min) to aqueous–organic (60:40) over a variable period, with the gradient rate being 5% acetonitrile/min. Flow-rate was 1.5 (upper panel), 1.0 (middle panel) or 0.7 ml (lower panel). The ordinate is absorbance at 220 nm and the abscissa is retention time in minutes.

CONCLUSIONS

A number of factors may contribute to variability in reversed-phase fingerprint mapping. Among these factors are deamidation and peptide bond hydrolysis, both of which processes are time-dependent and accelerated at low pH and high temperature. Some of the recent approaches to rapid fingerprinting, which may require high temperatures and the addition of surfactants for optimal performance[3] may not be appropriate if fractions are to be collected and analyzed.

Pump performance, due to variation in flow-rate or gradient formation, is also an important factor in obtaining reliable fingerprints. The present manuscript has shown that small changes in gradient rate cause only small changes in fraction capacity and order of elution, but small changes in flow-rate can cause notable changes in the peptide fingerprint. The present study has shown that 100-Å, 5-μm PLRP-S exhibits selectivity equivalent to that of alkyl-bonded phases. The retention order is relatively insensitive to changes in gradient rate or flow-rate, making this phase suitable for rapid fingerprints of simple proteins. The peak capacity is about the same as that of other alkyl bonded phases. Although additional peak capacity is certainly desirable for complex fingerprints, such as plasminogen, PLRP-S is an excellent material for peptide mapping.

ACKNOWLEDGEMENTS

K. D. Nugent and F. P. Warner are thanked for review of this manuscript.

REFERENCES

1 R. F. Ebert and C. H. Schmelzer, *J. Chromatogr.*, 443 (1988) 309.
2 A. J. Banes, G. W. Link and L. R. Snyder, *J. Chromatogr.*, 326 (1985) 419.
3 K. Khalgati and Cs. Horváth, *J. Chromatogr.*, 443 (1988) 343.
4 D. P. Lee, *J. Chromatogr. Sci.*, 20 (1982) 203.
5 J. V. Dawkins, L. L. Lloyd and F. P. Warner, *J. Chromatogr.*, 352 (1986) 157.
6 F. Nevejans and M. Verzele, *J. Chromatogr.*, 406 (1987) 325.
7 D. Guo, C. T. Mant, A. K. Taneja, J. M. R. Parker and R. S. Hodges, *J. Chromatogr.*, 359 (1986) 499.
8 D. Guo, C. T. Mant, A. K. Taneja and R. S. Hodges, *J. Chromatogr.*, 359 (1986) 519.
9 C. T. Mant, T. W. L. Burke, J. A. Black and R. S. Hodges, *J. Chromatogr.*, 458 (1988) 193.
10 P. J. Schoenmakers, H. A. H. Billiet, R. Tijssen and L. de Galan, *J. Chromatogr.*, 149 (1978) 519.
11 L. R. Snyder, J. W. Dolan and J. R. Gant, *J. Chromatogr.*, 165 (1979) 3.
12 M. A. Stadalius, H. S. Gold and L. R. Snyder, *J. Chromatogr.*, 296 (1984) 31.
13 M.-I. Aguilar, A. N. Hodder and M. T. W. Hearn, *J. Chromatogr.*, 327 (1985) 115.
14 J. W. Dolan, J. R. Gant and L. R. Snyder, *J. Chromatogr.*, 165 (1979) 31.
15 M. T. W. Hearn and M. I. Aguilar, *J. Chromatogr.*, 352 (1986) 35.
16 B. L. Karger, L. R. Snyder and Cs. Horváth, *An Introduction to Separation Science*, Wiley, New York, 1973, pp. 278, 279.

Journal of Chromatography, 512 (1990) 325–335
Elsevier Science Publishers B.V., Amsterdam

CHROMSYMP. 1902

Peptide mapping of HIV polypeptides expressed in *Escherichia coli*

Quality control of different batches and identification of tryptic fragments containing residues of aromatic amino acids or cysteine

STAFFAN RENLUND* and ING-MARIE KLINTROT
Pharmacia LKB Biotechnology, S-751 82 Uppsala (Sweden)
MICHAEL NUNN and JEFFREY L. SCHRIMSHER
Pharmacia Genetic Engineering Inc., La Jolla, CA (U.S.A.)
and
CHRISTER WERNSTEDT and ULF HELLMAN
Ludwig Institute for Cancer Research, Uppsala Branch, Uppsala (Sweden)

ABSTRACT

Peptide mapping was used for the quality control of different batches of the recombinant HIV proteins p24 core and p24–gp41, expressed in *Escherichia coli*. These proteins comprise *gag* and *env* region polypeptides of the virus and may serve as suitable components in the diagnosis of HIV infections. The proteins were digested with trypsin and the mixtures were subjected to peptide mapping to prove batch equivalence of p24–gp41 and to isolate fragments of the p24–gp41 digest that differ from those of the p24 core digest. The proteins were reduced with dithiothreitol and the cysteine residues were derivatized by addition of 4-vinylpyridine. Peptide mapping was performed by means of reversed-phase high-performance liquid chromatography. Batch equivalence was proved by comparison of the maps. Peaks present in one map but not in the other were considered to be due to sequence differences or variability in digestion.

INTRODUCTION

The outer membrane of the human immunodeficiency virus (HIV) contains a glycoprotein gp41[1–3] which is important in the attachment of the virus to the surface of the host. The core, which carries the RNA, contains a 232-residue polypeptide, p24 (refs. 1–3). A fusion protein, consisting of p24 core and part of gp41, was produced using the recombinant DNA technique (Fig. 1). This polypeptide, called p24–gp41, may be a suitable reagent in the diagnosis of HIV-1 infections.

0021-9673/90/$03.50

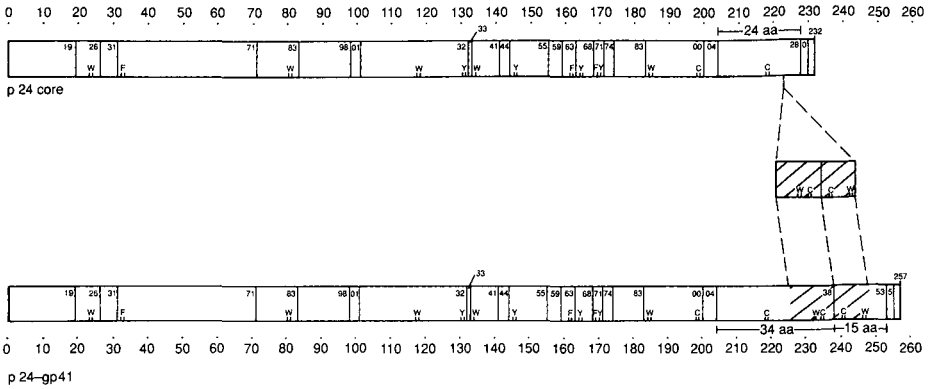

Fig. 1. General structures of p24 core and p24–gp41. The figures in the boxes indicate the positions of the Lys and Arg residues and thus the fragments produced by complete tryptic digestion. The aromatic amino acid residues and the cysteine residues are indicated with one-letter symbols.

Peptide mapping has been used for fragmentation in protein sequencing[4–7] and to detect lot-to-lot variations in recombinant proteins[8,9]. The aim of this study was to perform a quality control of different batches of p24–gp41 by means of peptide mapping of their tryptic digests.

The reduced and unfolded polypeptides were derivatized using 4-vinylpyridine[10,11], generating pyridylethylated cysteine residues with an absorbance maximum at 254 nm. Tentative assignments were made by multiple-wavelength detection at 215, 254 and 280 nm. Sequence analysis confirmed those fragments that differed in the tryptic fingerprints of p24 and p24–gp41.

EXPERIMENTAL

Chemicals and reagents

Acetic acid (No. 55), acetonitrile (No. 14291), tris(hydroxymethyl)aminomethane (Tris) (No. 8382), EDTA (No 8418), 4-vinylpyridine (No. 808513) and water (LiChrosolv No. 15333) were obtained from E. Merck (Darmstadt, F.R.G.), ammonium hydrogencarbonate (No. 10302) and guanidine hydrochloride (No. 45208) from BDH (Poole, U.K.), triethylamine (TEA) (No. 25108) and trifluoroacetic acid (TFA) (No. 28902) from Pierce (Rockford, IL, U.S.A.), dithiothreitol (DTT) (No. D-0632) and N-tosyl-L-phenylalanyl chloromethyl ketone (TPCK)-treated trypsin (No. T-8642) from Sigma (St. Louis, MO, U.S.A.) and anhydrous calcium chloride (No. 4132) from Mallinckrodt (St. Louis, MO, U.S.A.). All chemicals were of highest available purity.

Samples

The HIV-derived polypeptides p24–gp41 and p24 core were produced using the recombinant DNA technique. p24 core is coded by the *gag* gene of the HIV and contains 232 amino acid residues[1]. p24–gp41 constitutes a fusion of p24 and part of gp41, a glycoprotein found in the outer membrane or envelope of the HIV[1–3], making the non-glycosylated fusion protein 257 residues long.

The purification of the two polypeptides from *Escherichia coli* included

suspension and lysis of the cells in 0.1 mol/l sodium phosphate buffer (pH 7.0) containing 0.17% (w/w) lysozyme, centrifugation of the homogenate, resuspension of the pellet in Tris buffer containing urea and dithiothreitol, centrifugation, stirring of the supernatant with guanidine hydrochloride and DTT and overnight dialysis. The solution was then centrifuged and the supernatant desalted by gel filtration. The p24 polypeptides were obtained from the desalted protein fraction by cation-exchange

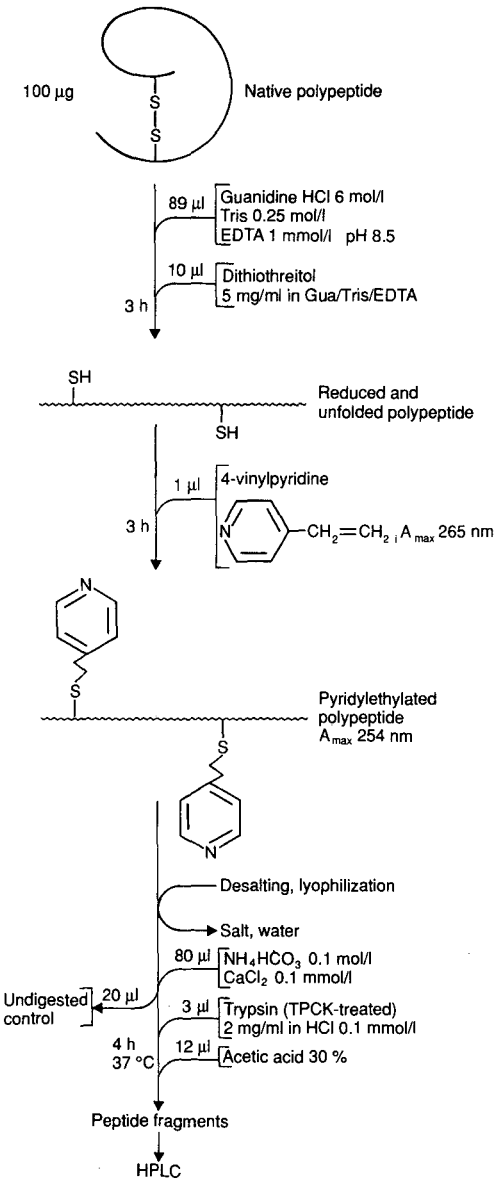

Fig. 2. Protocol used for reduction, derivatization and tryptic digestion of the polypeptides.

chromatography (CM-Sepharose® CL-6B; Pharmacia LKB Biotechnology, Uppsala, Sweden) and dried using a vacuum centrifuge.

Reduction, derivatization and tryptic digestion

The polypeptides (4 nmol; 40 μmol/l, containing cysteine residues corresponding to 80 or 160 μmol/l) were reduced with DTT (3 mmol/l) in Tris (0.25 mol/l, pH 8.5) containing guanidine hydrochloride (6 mol/l) and EDTA (0.25 mol/l) and the SH groups were derivatized using 4-vinylpyridine (94 mmol/l) as shown in Fig. 2.

Desalting. NAP™-10 columns (Pharmacia LKB Biotechnology) were equilibrated with TEA (20 mmol/l, adjusted to pH 8.35 with acetic acid). Each polypeptide sample was diluted to 1.0 ml with the TEA solution and applied to the column. The polypeptide was eluted with 1.5 ml of TEA solution and dried in a vacuum centrifuge.

Tryptic digestion. Trypsin was dissolved in hydrochloric acid (0.1 mmol/l) to an enzyme concentration of 2 μg/μl. The incubation buffer used was ammonium hydrogencarbonate (100 mmol/l) containing calcium chloride (0.1 mmol/l).

The polypeptide (100 μg, 4 nmol) was dissolved in 80 μl of incubation buffer. An aliquot (20 μl; 25 μg) was removed to serve as an undigested control, 3 μl (6 μg) of trypsin solution were added to the remaining 60 μl (75 μg) of peptide sample and 1 μl of incubation buffer was added to the undigested control. Both mixtures were incubated for 4 h at 37°C and stirred every 30 min. The digestion was terminated by adding 12 μl of 30% acetic acid to the digested sample and 4 μl to the undigested control to give a final peptide concentration of 1 μg/μl for both samples.

Equipment

All the instruments and software for the chromatographic procedures were from Pharmacia LKB Biotechnology. The equipment included HPLCmanager™ software for instrument and gradient control, a Solvent Conditioner 2156, two HPLC pumps 2248, High Pressure Mixer for solvent delivery and gradient formation and an Autosampler 2157 for sample injection. The column used was a SuperPac™ Pep-S C_2/C_{18} (5 μm, 100 Å) (250 × 4 mm I.D.) equipped with a precolumn (10 × 4 mm I.D.) packed with the Pep-S material. The column temperature was maintained at 38°C by means of Column Oven 2155.

All measurements were monitored at 215, 254 and 280 nm using Variable Wavelength Monitor 2141. Data were converted to Nelson chromatography software for evaluation.

Peptide mapping: chromatographic procedures

The solvents, balanced to the same absorbance, were (A) 0.15% TFA in water and (B) 0.144% TFA in acetonitrile–water (60:40). The samples (2 nmol) were eluted at a flow-rate of 1 ml/min in a gradient composed of four linear sections as follows: 0% B for 2 min, 0–25% B in 30 min, 25–35% B in 58 min, 35–60% B in 46 min and 60–100% B in 10 min.

Amino acid sequence analysis

Amino acid sequences were determined with an Applied Biosystems (Foster City, CA, U.S.A.) Model 470A protein/peptide sequencer equipped with an on-line detection system, Applied Biosystems Model 120A phenylthiohydantoin (PTH)

analyser. The apparatus was operated according to the manufacturer and the sequencer performed at a *ca.* 90–92% repetitive yield. The initial yield was not determined. PTH standards, including pyridylethyl cystine-PTH, were purchased from Applied Biosystems.

RESULTS AND DISCUSSION

Comparison of different batches of p24–gp41

The tryptic maps of three batches of p24–gp41 are shown in Fig. 3. The two upper chromatograms (batches 17 and 23) match well, but the lower trace (batch 34) exhibits conspicious differences from the former chromatograms. Batch 34 exhibits three peaks between 120 and 130 min in proportions which are different from those of the other batches. This may be due to variability in digestion.

Tentative identification of fragments

The general structures of p24 core and p24–gp41 are shown schematically in Fig. 1. The boxes indicate the fragments produced by tryptic cleavage. The position of tryptophan (W), tyrosine (Y), phenylalanine (F) and cysteine residues (C) are indicated with one-letter symbols.

The tryptic maps of p24–gp41 monitored at three different wavelengths are shown in Fig. 4. At 215 nm we detect peptide fragments in general, at 254 nm fragments containing pyridylethylated cysteine residues and at 280 nm fragments containing aromatic amino acid residues. Ratios of the peak areas (PA) taken from the different traces are given in Table I. A PA280/PA215 > 0 shows that the fragment contains

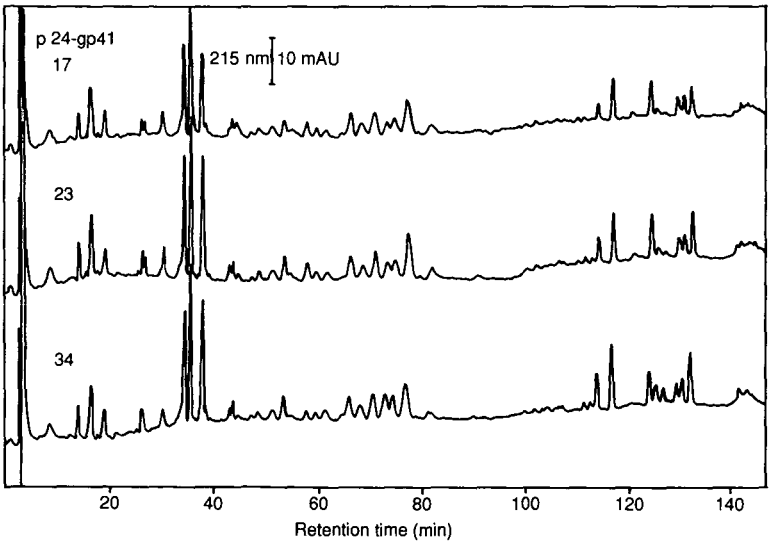

Fig. 3. Tryptic maps of three batches (Nos. 17, 23 and 34) of p24–gp41. The samples (1 nmol) were injected into a SuperPac Pep-S, C_2/C_{18} (5 μm) column (250 × 4 mm I.D.) and eluted in a gradient running from 100% A (0.15% TFA) to 100% B [0.144% TFA in acetonitrile–water (60:40)] in 146 min. The gradient rates of the different segments of the gradient were 0.50, 0.10, 0.33 and 2.4% min acetonitrile, respectively.

TABLE I

HIV POLYPEPTIDES p24–gp41 AND p24 CORE WERE DIGESTED WITH TRYPSIN AND SUBJECTED TO PEPTIDE MAPPING, THE PEAK AREAS (PA) MONITORED AT 215, 254 AND 280 nm WERE CALCULATED AND THE PA280/PA215, PA254/PA215, PA254/PA280 RATIOS WERE CALCULATED FOR THE FRAGMENTS ELUTED AT THE DIFFERENT RETENTION TIMES (V_t)

Ratios indicated by > are calculated from peaks which were off-scale in the 254-nm trace. Fragments that differed in the two peptide maps were identified by amino acid sequence analysis (amino acid residues in italics).

V_t (min)	*Polypeptide*						*Fragments identified by amino acid sequence analysis*	
	p24–gp41			*p24 core*			*Residue numbers*	*Amino acid sequence*
	PA280/PA215	*PA254/PA215*	*PA254/PA280*	*PA280/PA215*	*PA254/PA215*	*PA254/PA280*		
14.0	0	0	–	0	0	–		
16.6	0.65	0.42	0.65	0.63	0.51	0.80		
19.7	0	0	–	0	0	–		
26.2	0	0	–	0	0	–		
30.2	1.0	**2.0**	**2.0**	0	0	–		
34.3	0	0	–	0	0	–		
35.4	1	1	1	1	1	1		
36.0	0.28	0	0	0	0	–		
37.6	1.1	1.1	1.0	0.92	0.91	1.0		
43.4	0.79	**2.0**	**2.6**	←— No fragment —→			239–253	*LICTTAVPW*NGPGHK

44.3	0.55	0.65	1.2	–	–	–		
50.3	0.20	0	0	0.30	0	–		
53.0	0	0	–	0	0	–		
57.5	0	0	–	0	–	–		
59.0	0	0	–	0.18	–	–		
67.6	0.64	0.66	1.0	0.49	–		–	
70.0	0.95	1.0	1.1	2.1	>0.34	–		
72.5	0.94	1.1	1.2	0.93	>0.20	>0.21		
76.1	0.80	**2.1**	**2.6**	0.84	>1.4	>**1.7**	184–200	*NWMTETLLVQNANPDCK*
108	← No fragment →			0	>0.67	>**2**	205–228	*ALGPAATLEEMMTA*CQGVGGPGHK
112	0.70	0.18	0.26	0.69	–	–		
114	0.61	0	–	0.65	0	–		
116	0.62	0.61	0.98	0.56	>0.05	>0.09		
118	← No fragment →			0.45	>0.10	>0.22	184–200 205–228	*NWMTETLLVQNANP*DCK/ *ALGPAATLEEMMTA*CQGVGGPGHK
124	0.57	**2.2**	**3.9**	← No fragment →			205–238	*ALGPAATLEEMMTACQGVG*GPDQQ LLGIWGCSGK
125	0.71	**2.5**	**3.5**	–	–	–		
129	0	0	–	0	0	–		
130	0	0	–	0	0	–		
132	0	0	–	0	0	–		

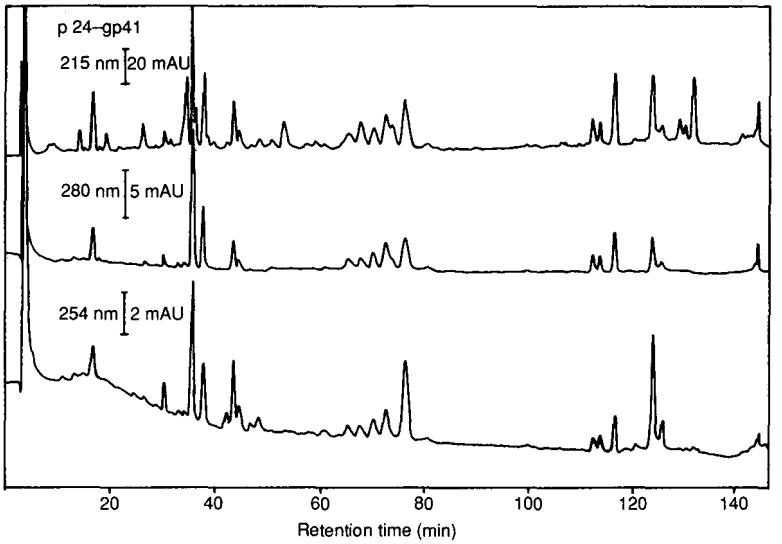

Fig. 4. Tryptic maps of p24–gp41 (2 nmol) monitored at 215, 254 and 280 nm. For chromatographic conditions, see text and Fig. 3.

aromatic amino acid residue(s), while PA254/PA215 or PA254/PA280 > 1.5 indicate that the fragment has a pyridylethylated cysteine content.

In p24–gp41 there should be eleven fragments having no aromatic amino acid residue (Fig. 1). There are ten peaks in the 215-nm trace which have no corresponding peaks in the 280-nm trace and which therefore have PA280/PA215 = 0 (Table I). These peaks should correspond to non-aromatic fragments and the others should represent fragments containing aromatic residues.

In the tryptic digest of p24–gp41 there should be three cysteine-containing fragments, one containing two cysteine residues and two containing one cysteine residue. By comparing the PA280/PA215 and PA254/PA280 ratios in Table I with the corresponding peaks in Fig. 4 we can identify these.

The digest of p24–gp41 gives five peaks having PA254/PA215 or PA254/PA280 ratios > 1.5 (Table I). Three of these peaks are dominant among the five (Fig. 4) (43.4, 76.1 and 124 min) and therefore most likely represent the pyridylethylated cysteine-containing fragments of the p24–gp41 digest. The PA254/PA280 ratio of the peak at 124 min is significantly higher (50%) than that of the others. (Table I). This peak could therefore be predicted to represent the fragment containing two cysteine residues, *i.e.*, the fragment represented by residues 250–238. The fragments eluted at 43.4 and 76.1 min should thus contain one cysteine residue each, *i.e.*, should be the fragments represented by residues 184–200 and 239–253. Without further information we cannot tell which of these peaks represents which fragment. However, it is possible to make a prediction in this respect by comparing the digests of p24–gp41 and p24 core.

Comparisons of p24–gp41 and p24 core

The digest of p24 core should produce two pyridylethylated cysteine-containing fragments. One should be common to the digests of both p24 core and p24–gp41

(residues 184–200) and the other should be unique to p24 core (residues 205–228) (Fig. 1). It has already been concluded that the peak at 76.1 min should represent a fragment containing one cysteine residue. Since that peak is common to both maps (Fig. 5), it should represent the fragment containing residues 184–200.

The peak at 43.4 min of the p24–gp41 peptide map should therefore represent the second fragment of the p24–gp41 digest containing only one cysteine residue, *i.e.*, the fragment composed by residues 239–253.

The fragments discussed above, *i.e.*, those eluted at 43.4, 76.1 and 124 min, were identified by amino acid sequence analysis. The predictions of their cysteine contents were thereby confirmed (Table I).

Two further fragments of the p24–gp41 digest (at 30.2 and 125 min) had PA254/PA215 and PA254/PA280 ratios > 1.5 (Table I). The PA254/PA280 ratio of the former indicates a content of one cysteine residue of the fragment, whereas the PA254/PA280 ratio of the latter indicates that the fragment should contain two cysteine residues. The fragments were considered to be incompletely reduced or incompletely digested polypeptide material and were therefore not subjected to sequence analysis.

Sequencing of non-identical parts of p24 core and p24–gp41

The digest of p24–gp41 should contain two fragments (residues 205–238 and 239–253) which cannot be produced by p24 core. Candidates are the fragments eluted at 43.4 and 124 min, since they have no corresponding fragments in the digest of p24 core (bottom map in Fig. 5). Their identities were discussed above.

The digest of p24 core should produce one unique 24-residue fragment (residues 205–228) with no corresponding fragment in the digest of p24–gp41. However, the

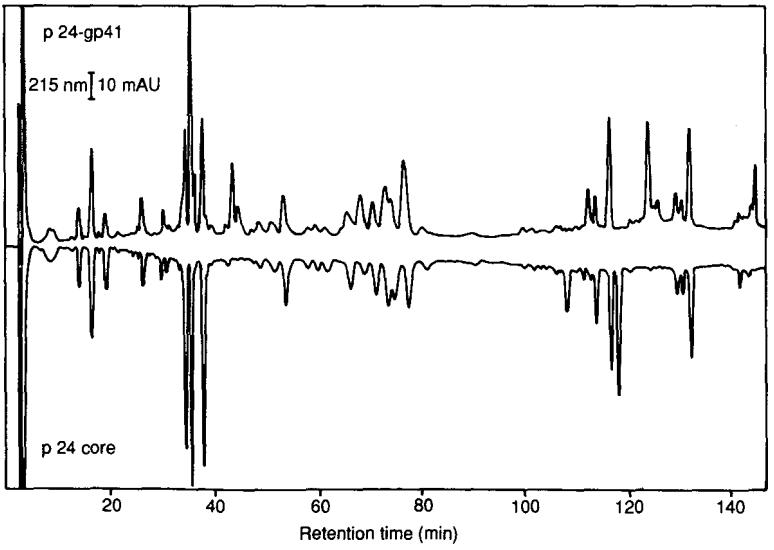

Fig. 5. Tryptic maps of p24–gp41 (2 nmol) and p24 core inverted (2 nmol). For chromatographic conditions, see text and Fig. 3.

tryptic map of p24 core contains two peaks having no corresponding peaks in the map of p24–gp41, one at 108 and the other at 118 min.

Comparisons of the different absorbances at 254 and 280 nm of the fragments eluted with these peaks makes identification possible. The fragment eluted at 118 min absorbs almost equally at both wavelengths (chromatograms not shown) and should therefore contain no pyridylethylated cysteine residue but presumably one (or several) tryptophan residues. This precludes its identity with the fragment composed of residues 205–228, which contains no aromatic amino acid residue but a cysteine residue. However, the fragment eluted at 108 min has a PA280/PA215 ratio = 0 but a PA254/PA280 ratio > 2 and should therefore have no aromatic residue but a pyridylethylated cysteine residue. This fragment is therefore a perfect candidate for the unique 24-residue fragment of the p24 digest (Fig. 1).

Amino acid sequence analysis confirmed these predictions (Table I). The fragment eluted at 118 min turned out to be a double sequence composed of residues 184–200 and 205–228, presumably connected by an unreduced disulphide bridge. Thus, as predicted, the fragment contained no pyridyl group although it contained two cysteine residues and, also as predicted, one tryptophan residue.

CONCLUSIONS

The three different batches of p24–gp41 gave rise to equivalent peptide maps indicating identical contents of the batches. To prove this sequence analysis of every single fragment produced in the different digests, amino acid analysis or fast atom bombardment mass spectrometry would be required, which is impractical for quality control purposes.

When comparing the structures of different polypeptides it is of great help to be able to identify fragments containing aromatic amino acid residues or cysteine residues. The usefulness in this respect of comparing the absorbances of a peptide at 215 and 280 nm is well known, primarily for the identification of fragments containing tryptophan and to some extent fragments containing tyrosine and phenylalanine. Less known is the ease by which cysteine residues can be detected after reduction and pyridylethylation. We have clearly demonstrated that both the occurrence and amounts of cysteine residues in separate fragments can be predicted by comparing their absorbances at 280 and 254 nm. To us, this way of identifying such fragments seems both economical and efficient.

REFERENCES

1 L. Ratner, W. Haseltine, R. Patarca, K. J. Livak, B. Starcich, S. F. Josephs, E. R. Doran, J. A. Rafalski, E. A. Whitehorn, K. Baumeister, L. Ivanoff, S. R. Petteway, Jr., M. L. Pearson, J. A. Lautenberger, T. S. Papas, J. Ghrayeb, N. T. Chang, R. C. Gallo and F. Wong-Staal, *Nature (London)*, 313 (1985) 277.
2 R. M. Thorn, G. A. Beltz, C.-H. Hung, B. F. Fallis, S. Winkle, K.-L. Cheng and D. J. Marciani, *J. Clin. Microbiol.*, 25 (1987) 1207.
3 R. C. Gallo, *Sci. Am.*, 256 (1987) 39.
4 V. M. Ingram, *Methods Enzymol.*, 6 (1963) 831.
5 J. C. Bennett, *Methods Enzymol.*, 11 (1967) 330.
6 H. V. J. Kolbe, F. Jaeger, P. Lepage, C. Roitsch, G. Lacaud, M.-P. Kieny, J. Sabatie, S. W. Brown, J.-P. Lecocq and M. Girard, *J. Chromatogr.*, 476 (1989) 99.

7 R. C. Chloupek, R. J. Harris, C. K. Leonard, R. G. Keck, B. A. Keyt, M. W. Spellman, A. J. S. Jones and W. S. Hancock, *J. Chromatogr.*, 463 (1989) 375.
8 R. L. Garnick, M. J. Ross and C. P. du Mée, in J. Swarbrick and J. C. Boylan (Editors), *Encyclopedia of Pharmaceutical Technology, Absorption of Drugs to Biovailability of Drugs and Bioequivalence,* Vol. 1, Marcel Dekker, New York and Basel, 1988, p. 253.
9 R. L. Garnick, N. J. Solli and P. A. Papa, *Anal. Chem.*, 60 (1988) 2546.
10 J. F. Cavins, and M. Friedman, *Anal. Biochem.*, 35 (1970) 489.
11 M. Friedman, L. H. Krull and J. F. Cavins, *J. Biol. Chem.*, 245 (1970) 3868.

Journal of Chromatography, 512 (1990) 337–343
Elsevier Science Publishers B.V., Amsterdam

CHROMSYMP. 1942

Synthetic antibody fragment as ligand in immunoaffinity chromatography

GJALT W. WELLING*, TON GEURTS, JUDITH VAN GORKUM, RIA A. DAMHOF and JAN WOUTER DRIJFHOUT

Laboratorium voor Medische Microbiologie, Rijksuniversiteit Groningen, Oostersingel 59, 9713 EZ Groningen (The Netherlands)

W. BLOEMHOFF

Organische Chemie, Gorlaeus Laboratoria, Rijksuniversiteit Leiden, P.O. Box 9502, 2300 RA Leiden (The Netherlands)

and

SYTSKE WELLING-WESTER

Laboratorium voor Medische Microbiologie, Rijksuniversiteit Groningen, Oostersingel 59, 9713 EZ Groningen (The Netherlands)

ABSTRACT

The possibility that a fragment of an antibody molecule may interact with a protein antigen was tested by studying the binding properties of a thirteen-residue synthetic peptide with an amino acid sequence similar to part of a hypervariable segment of a monoclonal antibody directed against lysozyme. Affinity adsorbents were prepared with this peptide and with non-related peptides as ligand. Non-specific interactions could be abolished by washing the column with 0.05 *M* sodium thiocyanate in 20 m*M* Tris–HCl (pH 7.4). Lysozyme was only bound to the antilysozyme adsorbent and could be eluted with 1 *M* sodium thiocyanate. The results show that immunoaffinity chromatography with synthetic peptide ligands which mimic the antigen-binding site may be a useful tool in the selective purification of proteins.

INTRODUCTION

One of the most selective biological interactions is that between antigen and antibody. Multiple non-covalent forces, hydrogen bonding, electrostatic, hydrophobic and Van der Waals forces are responsible for the antigen antibody reaction.

The aim of this study was to exploit the recognition potential of an antibody for the purification of a particular protein by using a peptide ligand which mimics the antigen-binding site of a monoclonal antibody molecule directed against this protein. Immunoglobulin G molecules are large (M_r = 150 000). A relatively small section of the molecule (see Fig. 1a), consisting of three hypervariable segments of the L chain

0021-9673/90/$03.50

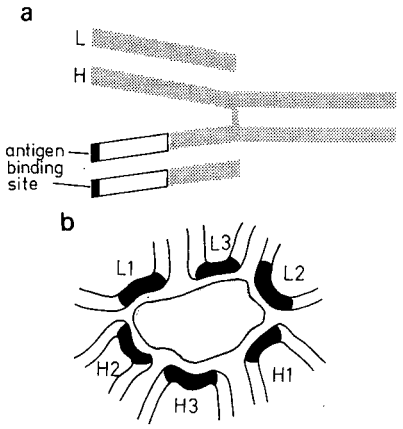

Fig. 1. (a) Schematic representation of an immunoglobulin G molecule. Open blocks indicate the variable regions of the heavy (H) and light (L) chains. One antigen-binding site is composed of three hypervariable polypeptide segments (indicated in black) of the L chain and three of the H chain [see (b)]. (b) Schematic representation of the antigen-binding site [perpendicular to the view in (a)]. The hypervariable segments L1, L2, L3, H1, H2 and H3 are indicated in black. The antigenic determinant is shaded.

and three of the H chain (Fig. 1b), binds to the antigen, often with high affinity ($K_{diss} = 10^{-8}$–10^{-12} M). For this reason, severe conditions are often required for elution of the protein antigen in conventional immunoaffinity chromatography. Other parts of the immunoglobulin molecule may show aspecific interactions with contaminating proteins, which may interfere with the purification of the protein antigen. When the antibody molecule is reduced to its smallest possible biologically active size, *i.e.*, still showing antigen-binding properties, the aforementioned aspecific interactions will no longer occur. Binding will be less strong, especially when only part of the antigen-binding site is used as a ligand. However, this may also be favourable as the protein can then be eluted under relatively mild conditions.

To test this hypothesis, we used a model of an antigen–antibody complex, *i.e.*, a lysozyme–anti-lysozyme complex[1–3]. The antibody segment with the largest number of contact residues was selected for synthesis. This synthetic thirteen-residue anti-lysozyme peptide was immobilized and used to purify lysozyme from a mixture of proteins.

EXPERIMENTAL

Peptide selection and synthesis

An anti-lysozyme (anti-LY) peptide was selected (Table I) using the modelling studies of complexes of monoclonal antibodies and lysozyme[2,3]. A peptide with as many contact residues as possible in a linear sequence was synthesized by the solid-phase methodology[4]. Boc-Cys-3-nitro-2-pyridinesulphenyl-OH [Boc-Cys-(NPys)-OH] was coupled as an N-terminal residue to the resin-linked peptide to allow specific coupling to its N-terminus[5]. After deprotection and cleavage from the resin, the NPys-cysteinyl peptide (6 μmol = 10.4 mg) was added to thiopropyl-Sepharose 6B

TABLE I

AMINO ACID SEQUENCE AND CHARGE OF SYNTHETIC PEPTIDES AT NEUTRAL pH

Peptide	*Amino acid sequence*	*Charge*
Anti-LY	Glu–Ile–Phe–Pro–Gly–Asn–Ser–Lys–Thr–Tyr–Tyr–Ala–Glu	−1
P7	Ala–Val–Leu–Glu–Arg–Ala–Ala–Arg–Ser–Val–Leu–Leu–Asn–Ala–Pro[a]	+2
P26	Ser–Thr–Leu–Leu–Pro–Pro–Glu–Leu–Ser–Glu–Thr–Pro–Asn–Ala–Thr[a]	−1
P36	Glu–Leu–Ala–Pro–Glu–Asp–Pro–Glu–Asp–Ser–Ala–Leu–Leu–Glu–Asp[a]	−6

[a] C-terminal amide group.

(Pharmacia, Uppsala, Sweden) converted into the free thiol form by removing the 2-thiopyridyl protecting groups by treatment with dithiothreitol according to the instructions of the manufacturer. Four equal portions of the NPys-cysteinyl peptide were added to a column with 50 mg of thiopropyl-Sepharose containing 3.75 μmol of SH groups. The liberation of the yellow reaction product, 3-nitro-2-thiopyridone, was monitored after each addition. The eluate was colourless after the fourth addition, indicating that an excess of peptide had been used and that coupling of 6.5 mg of Cys(NPys) anti-LY peptide had been achieved. The column material was mixed with Sepharose 4B to give a column volume of 1.6 ml.

Three other peptides (analogous to the amino acid sequence of herpes simplex glycoprotein D) were synthesized as peptide amides (see Table I) according to the method of Houghten[6] and were used to prepare control affinity adsorbents. Peptides (2 mg) were coupled to 0.4 g of Tresyl-activated Sepharose 4B (Pharmacia, Uppsala) in 0.1 *M* $NaHCO_3$–Na_2CO_3 (pH 8.5) containing 1 *M* sodium chloride according to the instructions of the manufacturer. The percentage coupling was determined by reversed-phase (RP) HPLC of the peptide solution before coupling and the eluate after coupling. Peptides P7, P26 and P36 were coupled for 35, 55 and 63%, respectively.

Chromatography

Affinity chromatography was carried out at room temperature at a flow-rate of 9 ml/h during application of samples and 18 ml/h during chromatography. Columns were eluted with 0.05*M* sodium thiocyanate in 20 m*M* Tris–HCl (pH 7.4) followed by 1 *M* sodium thiocyanate in the same buffer. The absorbance was measured at 280 nm.

RP-HPLC was performed with a system from LKB (Bromma, Sweden) consisting of a Model 2150 HPLC pump, Model 2152 LC controller, Model 11300 Ultrograd mixer driver, a Rheodyne Model 7125 injector, Model 2151 variable-wavelength monitor and a Model 2210 recorder. The column (25 × 4.6 mm I.D.) contained Nucleosil 10 C_{18} (Macherey-Nagel, Düren, F.R.G.). Proteins and peptides were eluted with a 20-min gradient from 10% acetonitrile in 0.1% TFA to 60% acetonitrile in 0.09% TFA. The absorbance was monitored at 214 nm.

Proteins

Hen egg-white lysozyme and bovine ribonuclease A were obtained from Boehringer (Mannheim, F.R.G), bovine serum albumin, ovalbumin and carbonic anhydrase from Sigma (St. Louis, MO, U.S.A.) and foetal calf serum from Gibco (Paisley, U.K.).

RESULTS AND DISCUSSION

Lysozyme is a relatively basic protein with an isoelectric point of 11. It may show interaction with hydrophilic groups present in Sepharose. Initial experiments showed that such interactions could be abolished by using 0.05 *M* sodium thiocyanate in the

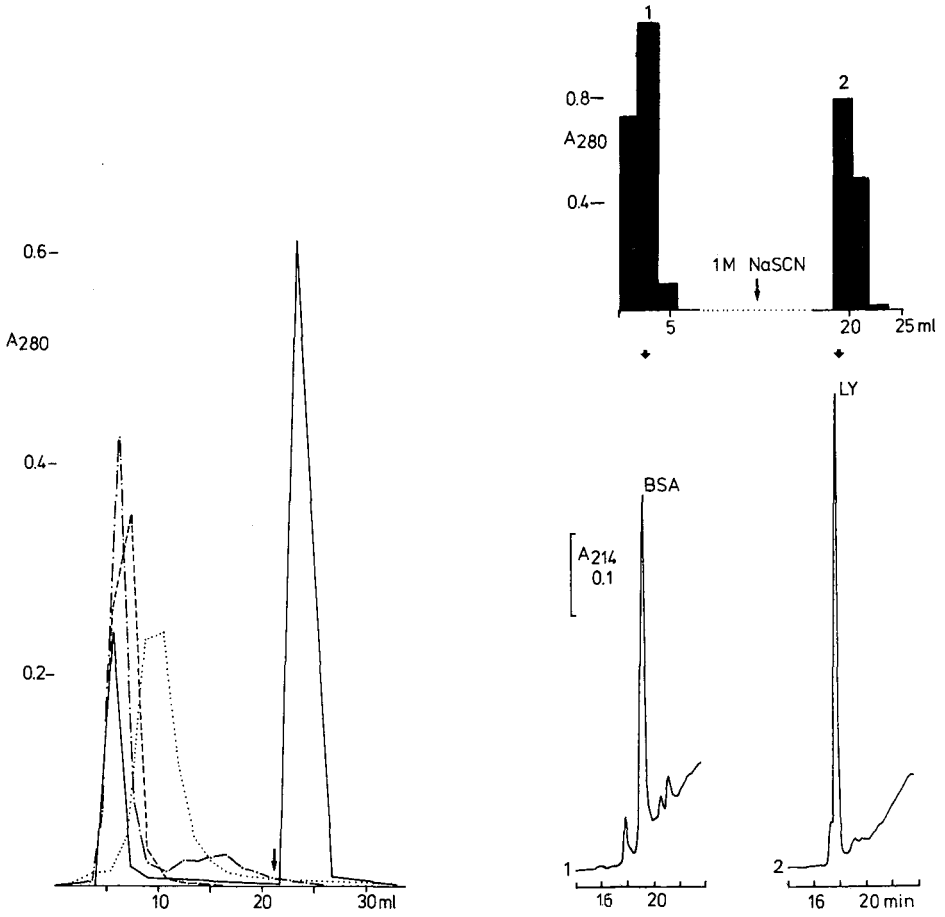

Fig. 2. Affinity chromatography of lysozyme on adsorbents with different peptide ligands. Synthetic peptides(Table I) were coupled either to thiopropyl-Sepharose (the anti-LY peptide) or to Tresyl-activated Sepharose (three herpes simplex virus glycoprotein D peptides). Amounts of 0.8 and 1.6 mg of lysozyme were applied to the herpes virus peptide adsorbents and the anti-LY adsorbent, respectively. The columns were eluted with 0.05 *M* sodium thiocyanate in 20 m*M* Tris–HCl (pH 7.4). The arrow indicates the start of the elution with 1 *M* sodium thiocyanate in the same buffer. The flow-rate was 9 ml/h during application of the sample and 18 ml/h during chromatography. The absorbance was measured at 280nm. ——— = Anti-LY; — · — · — = P7; ---- = P26; ..... = P36. The charge and the amino acid sequence of the peptides are given in Table I.

Fig. 3. Affinity chromatography with the anti-LY adsorbent. A 1.6-mg amount of lysozyme in 10-fold diluted foetal calf serum was applied to the column. Elution conditions as in Fig. 2. Volumes of 100-μl of the indicated fractions 1 and 2 were analysed by RP-HPLC (bottom). BSA = Bovine serum albumin; LY = lysozyme.

starting buffer. Under these conditions, lysozyme did not bind to Sepharose, deprotected thiopropyl-Sepharose or deactivated Tresyl-Sepharose. Fig. 2 shows the elution pattern obtained after application of 1.6 mg of lysozyme to the anti-LY column and 0.8 mg of lysozyme to three control columns. Lysozyme was slightly retarded on the acidic column (P36; peptide charge before coupling, −6) and not at all on the other two control columns (P26 and P7; peptide charge, −1 and +2, respectively). Elution with 1 *M* sodium thiocyanate did not result in further peaks. In contrast, most of the lysozyme (77%) was specifically eluted by 1 *M* sodium thiocyanate from the anti-LY column (solid line, Fig. 2). Further experiments showed that lysozyme could be eluted between 0.15 and 0.25 *M* sodium thiocyanate from this column.

Fig. 3 shows the elution pattern when lysozyme in 10-fold diluted foetal calf serum was applied to the anti-LY column. Fractions were analysed by RP-HPLC (Fig. 3, bottom). The results show that the main component of the serum, bovine serum albumin, did not bind to the column and that lysozyme was specifically eluted by 1 *M* sodium thiocyanate.

In Fig. 4 the elution pattern is shown after affinity chromatography of a mixture of reference proteins including lysozyme. RP-HPLC analysis of fractions that were eluted with the starting buffer containing 0.05 *M* sodium thiocyanate showed that bovine serum albumin, carbonic anhydrase, ovalbumin and a small amount of

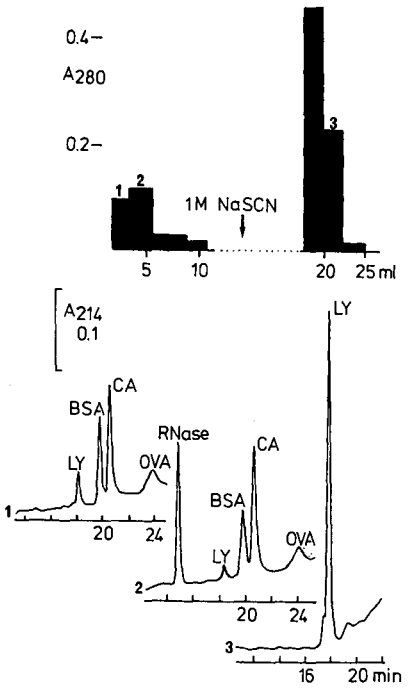

Fig. 4. Affinity chromatography with the anti-LY adsorbent. A mixture of 0.8 mg of lysozyme (LY) and 0.05 mg of pancreatic ribonuclease (RNase), bovine serum albumin (BSA), carbonic anhydrase (CA) and ovalbumin (OVA) was applied to the column. Elution conditions as in Fig. 2. Aliquots of 100 μl of the indicated fractions 1, 2 and 3 were analysed by RP-HPLC (bottom).

lysozyme did not bind to the column. Ribonuclease was slightly retarded and was eluted together with other proteins in fraction 2. Most of the lysozyme (95%) was eluted with 1 *M* sodium thiocyanate (*e.g.*, fraction 3).

The relatively small amounts of lysozyme which were eluted with 0.05 *M* sodium thiocyanate (Figs. 2–4) were not the result of overloading, as the capacity of the anti-LY column was at least 4.7 mg of lysozyme. Whether the presence of bound and unbound lysozyme can be explained by a pseudoequilibrium[7] between lysozyme and anti-LY remains to be investigated. Earlier studies[8,9] showed that after reduction of an immunoglobulin molecule by protein engineering to the variable region of the H and L chain, antigen binding properties could be retained. In the study by Huston *et al.*[8], a biosynthetic antibody incorporating the variable domains of an anti-digoxin monoclonal antibody in a single polypeptide chain (M_r = 26 354) did bind digoxin a factor of 6 less strongly than the intact monoclonal antibody. In the study by Bird *et al.*[9], similar single-chain constructs were made directed against bovine growth hormone and fluorescein. Recently, Ward *et al.*[10] showed that single variable regions, especially those from the H chain, could bind the antigen with good affinity. Williams and co-workers[11,12] showed that further reduction of the size of the variable domains was possible with retention of antigen-binding properties. They were studying the reovirus–reovirus receptor system. Antibodies were produced against reovirus and thereafter antibodies were made against the anti-reovirus antibodies. The amino acid sequence of the latter antibody was determined and peptides were synthesized with the amino acid sequence of the hypervariable segments. One of these peptides showed reovirus receptor-binding properties.

In our study we were aided by the availability of a model of the complex between an anti-lysozyme monoclonal antibody (Gloop 2) and lysozyme[3]. The variable segment of Gloop 2 with the largest number of contact residues with lysozyme was selected for synthesis. To avoid coupling to the ε-NH_2 of lysine at position 8 of the anti-LY peptide, it was coupled after elongation with NPys-Cys with its N-terminus to thiopropyl-Sepharose using the 3-nitro-2-pyridinesulphenyl protection–activation method of Drijfhout *et al.*[5]. This allowed contact of the amino acid residues of the anti-LY peptide with lysozyme, resulting in a sufficient number of interactions, *i.e.*, in binding of lysozyme.

These results show that immunoaffinity chromatography with a synthetic peptide ligand which mimics part of the antigen-binding site is possible. In this particular instance the selection of the peptide was aided by the availability of a tertiary structure model of the protein antigen and the amino acid sequence of monoclonal antibodies directed against the antigen. In general, less information would be sufficient in order to design a peptide ligand for the purification of a particular protein. The amino acid sequence of the variable regions of a monoclonal antibody can be determined by sequencing of immunoglobulin mRNA[13] and, as the variable regions do contain a number of invariant residues, the hypervariable segments can be located easily. A set of overlapping synthetic peptides from these antigen-binding regions should then be tested for the ability to bind the protein antigen. Immunoaffinity adsorbents based on this principle may be a useful tool in the selective purification of a protein.

ACKNOWLEDGEMENTS

This study was supported by the Technology Foundation (STW), grant GGN 88.1609, to G.W.W. and S.W.-W.

REFERENCES

1 M. J. Darsley and A. R. Rees, *EMBO J.*, 4 (1985) 393.
2 M. J. Darsley and A. R. Rees, *EMBO J.*, 4 (1985) 383.
3 P. de la Paz, B. J. Sutton, M. J. Darsley and A. R. Rees, *EMBO J.*, 5 (1986) 415.
4 E. A. Atherton and R. C. Sheppard, *J. Chem. Soc., Chem. Commun.*, (1985) 165.
5 J. W. Drijfhout, E. W. Perdijk, W. J. Weijer and W. Bloemhoff, *Int. J. Pep. Protein Res.*, 32 (1988) 161.
6 R. A. Houghten, *Proc. Natl. Acad. Sci. U.S.A.*, 82 (1985) 5131.
7 J. R. Sportsman, J. D. Liddll and G. S. Wilson, *Anal. Chem.*, 55 (1983) 771.
8 J. S. Huston, D. Levinson, M. Mudgett-Hunter, M.-S. Tai, J. Novotny, M. N. Margolies, R. J. Ridge, R. E. Bruccoleri, E. Haber, R. Crea and H. Oppermann, *Proc. Natl. Acad. Sci. U.S.A.*, 85 (1988) 5879.
9 R. E. Bird, K. D. Hardman, J. W. Jacobson, S. Johnson, B. M. Kaufman, S.-M. Lee, T. Lee, S. H. Pope, G. S. Riordan and M. Whitlow, *Science (Washington, D.C.)*, 242 (1988) 423.
10 E. S. Ward, D. Güssow, A. D. Griffiths, P. T. Jones and G. Winter, *Nature (London)*, 341 (1989) 544.
11 W. V. Williams, D. B. Weiner, J. C. Cohen and M. I. Greene, *Bio/Technology*, 7 (1989) 471.
12 W. V. Williams, D. A. Moss, T. Kieber-Emmons, J. A Cohen, J. N. Myers, D. B. Weiner and M. I. Greene, *Proc. Natl. Acad. Sci. U.S.A.*, 86 (1989) 5537.
13 F. C. Grant, A. D. Levin and W. Kindsvogel, *Nucleic Acids Res.*, 15 (1987) 5496.

Journal of Chromatography, 512 (1990) 345–363
Elsevier Science Publishers B.V., Amsterdam

CHROMSYMP. 1953

Immobilization of Protein A at high density on azlactone-functional polymeric beads and their use in affinity chromatography

PATRICK L. COLEMAN*, MARGARET M. WALKER, DEAN S. MILBRATH and DARLENE M. STAUFFER
Biosciences Laboratory, Building 270-3S-06, 3M Corporation, 3M Center, St. Paul, MN 55144 (U.S.A.)
and
JERALD K. RASMUSSEN, LARRY R. KREPSKI and STEVEN M. HEILMANN
Corporate Research Technology Development Laboratory, 3M Corporation, 3M Center, St. Paul, MN 55144 (U.S.A.)

ABSTRACT

This paper presents the results of the use of highly cross-linked, porous, hydrophilic copolymer beads with protein immobilized on their surface for affinity chromatography. Copolymer beads composed of vinyldimethyl azlactone (oxazolone) and methylene-bis-acrylamide in various ratios, with up to 3.5 mequiv./g azlactone functionality, will undergo nucleophilic attack by amines, as well as by thiols and alcohols. The ring-opening reaction of a nucleophile-containing ligand (*e.g.*, a protein) resulted in covalent attachment to the support. The reaction was rapid, half-complete in about 5 min, yielding proteins immobilized at very high densities, recombinant Protein A at 397 mg/g, and human immunoglobulin G at 225 mg/g. The reaction proceeded at significant levels from pH 4 to 9. There was a marked enhancement in the amount of protein coupled, its rate of reaction, and its biological activity when Protein A was made to react in the presence of high concentrations of sodium sulfate. Evaluation of affinity columns, prepared with Protein A immobilized at over 200 mg/g, gave molar ratios of immunoglobulin G to immobilized Protein A of 1:1 or greater. Up to 56 mg of immunoglobulin G was recovered per ml of column bed volume. The support combined high flow-rates with low back-pressures and no bed-volume changes upon changing mobile phases, including highly ionic aqueous solvents and ethanol.

INTRODUCTION

There is an extensive literature documenting the coupling of proteins to matrices. Scouten[1] thoroughly reviewed ligand immobilization and affinity chromatography in a 1981 monograph. Much of the recent literature has been reviewed by Katchalski-

0021-9673/90/$03.50

Katzir[2], with special emphasis on immobilizing enzymes, and by Jervis[3], who focused on affinity chromatographic applications. The reviews summarized the numerous methods of immobilization and critically evaluated the advantages and disadvantages of each. Jervis[3] outlined several characteristics of an ideal activation/coupling chemistry which included: (1) rapid, efficient formation of a stable, uncharged, covalent bond under mild conditions with no side reactions; (2) easy blocking of residual activated groups with simple, hydrophilic, uncharged groups; and (3) use of inexpensive, non-toxic reagents in procedures which could be scaled up. A deficiency in at least one of these categories was exhibited by each method reviewed.

The synthesis and chemistry of azlactones (oxazolones), cyclic anhydrides of N-acylamino acids, have been subjects of an extensive recent review by Rao and Filler[4]. An important reaction is the ring-opening addition which occurs with various nucleophiles, RNH_2, RSH and ROH (Fig. 1). Reaction with a primary amine results in formation of an amide bond between the azlactone and the amine (*e.g.*, lysyl group on a protein) and a rearrangement such that the ligand is tethered to the polymer through two amide bonds, which should provide both separation of the ligand from the backbone of the polymer, and a linkage which is stable in most biological solutions. Three of the authors have reviewed the extensive literature of azlactones in polymers[5], and we have synthesized new polymeric beads of azlactones with acrylamides and other hydrophilic monomers and investigated them as potential supports for immobilizing biochemicals, especially proteins, with particular applications in the area of affinity separations[6–8].

We report here results which show that polymeric beads containing azlactone functionality have exceedingly high capacities for coupling proteins while retaining their biological activity. Several proteins have been coupled at greater levels than 100 mg of protein per g of polymeric bead. The coupling reaction is rapid, with more than half of the reaction occurring in the first 5 min, and efficient, with 60 to 100% of the protein being immobilized. Furthermore, these protein-derivatized beads, with a high density of an immobilized active ligand, *e.g.*, Protein A, are especially useful supports for high-performance liquid affinity chromatography. Protein A, immobilized at over 200 mg of protein per g of bead, maintained its ability to bind human immunoglobulin G (IgG) in a 1:1 molar ratio.

EXPERIMENTAL

Materials

Vinyldimethyl azlactone (VDM) was purchased from SNPE, (Princeton, NJ, U.S.A.). Methylene-bis-acrylamide (MBA) and all other organic reagents were obtained from Aldrich (Milwaukee, WI, U.S.A.). Recombinant Protein A (rProtA) was

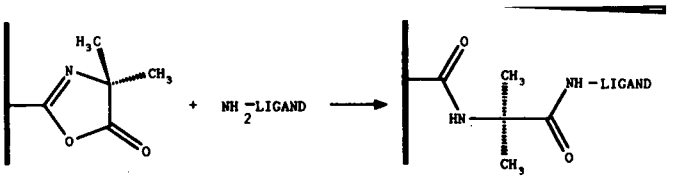

Fig. 1. The ring-opening reaction of dimethyl azlactone, as part of a polymer, with an amine.

purchased from Repligen (Cambridge, MA, U.S.A.). The best available grades of the other proteins were purchased from Sigma (St. Louis, MO, U.S.A.) Molecular weight standards were purchased as a kit prepared for electrophoretic use from Bio-Rad (Richmond, CA, U.S.A.). Na ^{125}I was purchased from DuPont NEN (Billerica, MA, U.S.A.). Iodo-beads™ and bicinchoninic acid reagents were purchased from Pierce (Rockford, IL, U.S.A.). Electrophoresis gels were purchased from Pharmacia (Piscataway, NJ, U.S.A.).

Polymer synthesis

The polymeric beads were prepared by an inverse-phase polymerization process, as described by Rasmussen *et al.*[6]. Briefly, a water–dimethylformamide phase, containing the monomers, was suspended in a density-balanced heptane–carbon tetrachloride phase, using copoly[isooctylacrylate–acrylic acid] 90:10 (%, w/w) as a suspending agent. Binary polymers were prepared by ammonium persulfate–tetramethylethylene diamine-initiated polymerization with varying ratios of VDM and MBA. The given ratio of polymer (*e.g.*, 20:80 or 42:58) is understood to be the % (w/w) ratio of VDM to MBA monomers in the reaction. After polymerization, the beads were given sequential washes with acetone, water and acetone, dried to constant mass in a vacuum oven, and stored in a desiccator at ambient temperature until used. Table I lists the properties of the polymers used in this study, and Fig. 2 shows a scanning electron micrograph of a preparation of 42:58 beads.

Surface areas of beads were determined by the BET method of nitrogen adsorption. The mercury porosimetry method was used to determine pore sizes. Bead diameter measurements were made following hydration, using a Coulter counter Model TA2. Azlactone functionality was measured by complete reaction with an excess of ethanolamine (0.1 *M*), followed by back-titration with 0.1 *M* HCl with a Radiometer RTS822 Autotitrator.

Protein iodination

Proteins were radiolabeled with ^{125}I by the chloramine-T reaction using Iodo-beads. The typical reaction contained 0.5 mg of protein (rProtA, human immunoglobulin or bovine serum albumin) and 100 μCi of ^{125}I-labeled sodium iodide in 100 m*M* sodium phosphate, 100 m*M* NaCl buffer (pH 7.5) and 2 Iodo-beads in a total volume of 500 μl. The reaction was terminated after 30–60 min by removal of the solution from the beads. Protein was separated from unreacted radioisotope on PD-10 col-

TABLE I

SUMMARY OF SOME PHYSICAL AND CHEMICAL PROPERTIES OF AZLACTONE POLYMERIC BEADS

Polymer	*Azlactone functionality (mequiv./g)*	*Particle size (μm)*	*Pore size (Å)*	*Surface area (m^2/g)*
20:80	1.12	54	–	221
30:70	1.54	72	–	170
42:58	2.06	–	555	186

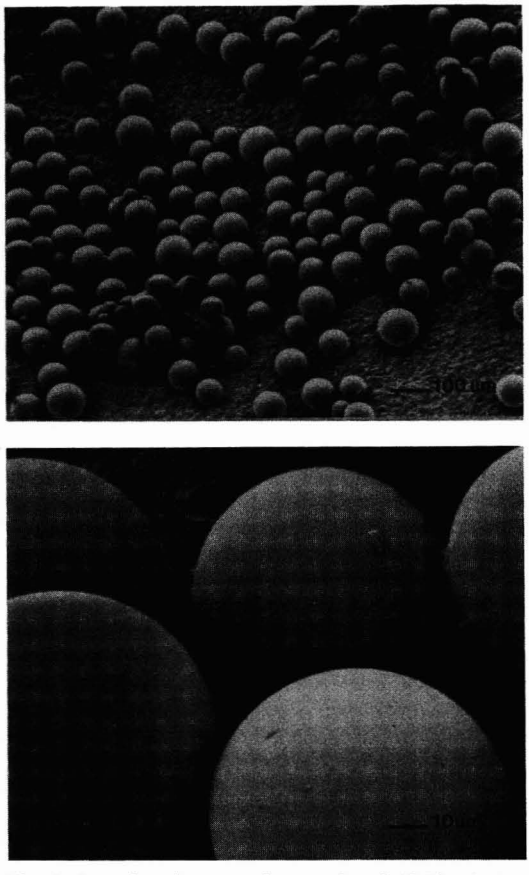

Fig. 2. Scanning-electron micrographs of 42:58 azlactone-functional beads. Dried, underivatized beads were prepared for electron microscopy by mounting them on a stage with conducting carbon cement, followed by sputter-coating with gold. The Model SX 30 scanning-electron microscope of International Scientific Instruments, (Pleasanton, CA, U.S.A.) was used. The magnification scale is indicated on each micrograph.

umns (Pharmacia). Typically 50% or more of the isotope was incorporated into the protein for a specific radioactivity of 0.10—0.15 μCi/μg of protein. Radioiodinated protein solutions were stored frozen and used up to a month after preparation.

Protein coupling

The typical protein coupling reaction consisted of 10 mg of polymeric beads suspended in 200 μl of 25 m*M* sodium phosphate, 150 m*M* NaCl (pH 7.5) containing a variable amount of protein (20 μg to 5.0 mg). In some experiments up to 1.5 *M* Na_2SO_4 was substituted for the NaCl. The suspension was continuously rocked for the duration of the reaction. After the standard coupling time of 60 min, the reaction was terminated by the addition of the blocking reagent, 1.0 ml of 1.0 *M* ethanolamine in 25 m*M* sodium pyrophosphate, which had been titrated to pH 9.0 with HCl. After 5 min of continuous rocking, the sample was centrifuged, the supernatant solution

was removed, and fresh ethanolamine solution was added to continue the blocking of the residual azlactone functional groups. After 60 min of additional reaction, the beads were centrifuged and resuspended several times in the pH 7.5 phosphate–NaCl buffer. In time-course experiments protein coupling was allowed to proceed from 5 min to 24 h, with "zero" time points established by first blocking the azlactone functionality, as described above, then allowing reaction with the protein.

The amount of bound radiolabeled protein was determined in a Packard γ scintillation counter (Model 5230). The specific radioactivity of the protein to be coupled was adjusted prior to each experiment by addition of unlabeled protein and ranged from 100 to 2000 cpm/μg of protein. After the initial determination of bound radiolabeled protein, the amount which was covalently linked to the polymeric beads was determined following incubation of the beads with 1.0% sodium dodecyl sulfate (SDS) for 4 h at 37°C with intermittent mixing, followed by centrifugation, removal of the supernate, and several additional wash cycles with SDS.

In those experiments performed without radiotracers, bound protein was determined by measuring both the amount bound to the beads and the residual protein in the supernatant solution by the bicinchoninic acid method[9].

In the pH profile experiments a ternary buffer of acetate, phosphate and pyrophosphate (50 m*M* each) was titrated to the final pH indicated (pH 4–9) with either HCl or NaOH. The lowest pH tested in the presence of sulfate was pH 4.5, since each protein began to precipitate in the presence of sulfate at pH 4.0. All other procedures were the same as those described above except that the reaction was allowed to proceed for 30 rather than 60 min.

Activity of immobilized rProtA

The biological activity of immobilized rProtA was determined by using excess amounts of radiolabeled human IgG. The amount of rProtA binding was determined with the radiolabeled rProtA, as described above. Unlabeled rProtA, coupled under identical conditions, was used to bind radiolabeled IgG. Amounts of 1.25 to 8.75 mg of radiolabeled IgG were added to 10 mg of 20:80 beads, containing 3–120 μg of rProtA and incubated at ambient temperature in 25 m*M* sodium phosphate, 25 m*M* sodium pyrophosphate buffer (pH 9.0), containing 1.0 *M* $(NH_4)_2SO_4$, for 60 min with continuous rocking. The beads were washed several times with the binding buffer, and the residual radioactivity was determined. The beads were then treated for 1 h with 1.0 *M* glycine (pH 2.0), washed several times, and this was followed by determination of residual radioactivity. To substantiate that the IgG was binding through the immobilized rProtA and not through residual azlactone functionality, beads were incubated with 1% SDS for 4 h at 37°C. In these experiments and the chromatographic experiments described below the stoichiometry of IgG:rProtA was calculated from the amount of radioactivity or absorbance at 280 nm eluted with the glycine treatment and 150 000 dalton for the molecular weight and 1.3 cm^2/mg for the extinction coefficient of human IgG and 45 000 dalton for rProtA.

Affinity chromatography

Immobilized rProtA for affinity chromatography was prepared by 60-min reactions of 250 mg of 20:80 beads with 1.25 to 25 mg of rProtA in a total volume of 5.0 ml of 25 m*M* sodium phosphate (pH 7.5), containing either 150 m*M* NaCl or 1.5 *M*

sodium sulfate. Residual azlactone functionality was inactivated by two treatments with ethanolamine, followed by washings with phosphate buffers and 1.0 *M* NaCl to remove adsorbed protein. Derivatized beads were stored at 4°C in 20% ethanol until used.

Chromatography was performed on a Pharmacia fast protein liquid chromatography (FPLC) system controlled by the FPLC Manager™ software (Pharmacia). Protein A affinity chromatography was performed with purified human IgG or human serum and either a 10 × 0.3 cm (0.70 ml) Omni column (Rainin, Woburn, MA, U.S.A.) or a 10.0 × 0.5 cm (2.0 ml) column (Pharmacia). IgG was dissolved in 25 m*M* sodium phosphate, 150 m*M* NaCl (pH 7.5). The protein concentration and flow-rate varied according to the experiment. Human serum was diluted with an equal volume of the phosphate buffer. All samples were filtered through a 0.2-μm filter immediately prior to injection into the column.

After the sample was loaded, the column was eluted first with the phosphate–150 m*M* NaCl buffer, followed by a step gradient to the same phosphate buffer with 1.0 *M* NaCl, to remove any non-specifically bound protein, except where otherwise indicated. After the column was returned to the low-chloride buffer the specifically bound IgG was eluted by a step gradient to 0.1 *M* glycine–2.0% acetic acid buffer (pH 2.2).

Recovery of protein from the column was determined by measurement of the absorbance at 280 nm of each fraction, since, at high protein concentrations (>2 mg/ml) the flow cell optical readings are unreliable. Purity of recovered IgG was monitored by electrophoretic analysis, performed on samples of each of the eluates from the Protein A affinity columns. The protein-containing fractions obtained from each elution of the affinity column were pooled and dialyzed against deionized water. Pools low in protein (high-salt elution) were lyophilized and redissolved in a smaller volume of water. All samples were prepared for electrophoresis by heating to 100°C for 5 min in SDS–mercaptoethanol reagent[10] and electrophoresed on Pharmacia 10–15% acrylamide gradient PhastGels™ at 250 V for 70 "accumulated V h" (about 25 min), using a PhastSystem electrophoresis instrument (Pharmacia). Gels were stained with 0.04% Coomassie Brilliant Blue in 10% acetic acid for 15 min and destained with methanol–acetic acid.

RESULTS

Protein coupling

An initial survey experiment in which rProtA was coupled to beads of varying azlactone content (bead formulations varied from 10:90 to 70:30) showed that the amount of protein coupled was not significantly dependent on the effective azlactone functionality between 1 and 3 mequiv./g (Fig. 3). The percentage of protein remaining bound after the SDS treatment, a measure of the amount of binding which was covalently coupled, ranged from 77 to 90%, suggesting a high degree of covalent coupling of rProtA.

In a second survey experiment, designed to measure the maximum binding capacity as a function of amount of available azlactone, we measured the concentration-dependency (0.1–10 mg/ml) of rProtA coupling to three beads: 20:80, 42:58, and 60:40. A plot of coupled protein *vs.* concentration (not shown) suggested a saturation

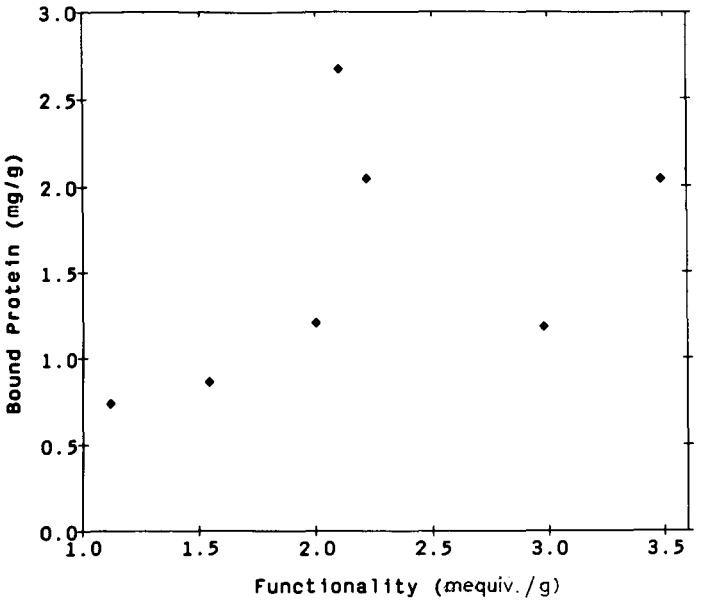

Fig. 3. The amount of rProtA coupled as a function of the titratable azlactone content. Azlactone functionality of the various VDM–MBA copolymers (10:90, 20:80, 30:70, 42:58, 60:40, and 70:30) was determined by alkali titration, as described in the text. Protein coupling was determined with radiolabeled rProtA (0.25 mg/ml) under the standard conditions described in the text, using the chloride-containing buffer.

effect, and a double reciprocal plot gave the following maximum protein coupling density estimates: 20:80, 248 mg protein per g of polymer; 42:58, 245; 60:40, 227. At the maximum observed protein couplings the percentages of residual bound protein following the SDS treatments were 99–100%, and the lowest value for the experiment was 91%. Based on these results, we concluded that there was little difference in the maximum amounts of protein which these beads could couple, and chose to use 20:80 and 30:70 beads for our subsequent studies, since greater azlactone density was not necessary for increased protein density.

We measured the coupling capacity of azlactone-functional beads for several proteins by varying the protein concentration (1–25 mg/ml) and allowing the reaction to progress for 60 min. rProtA and human IgG were coupled in 25 mM sodium phosphate buffer–150 m*M* NaCl (pH 7.5); however, since concanavalin A (Con A) tends to aggregate at this pH it was coupled using the same buffer at pH 6.0 (Fig. 4A). The efficiency of protein coupling (the percent of the available protein which was immobilized) was 6–38% for rProtA, 20–100% for IgG, and 52–100% for Con A. Although the efficiency of coupling decreased with increasing concentrations, the actual density of immobilized protein continued to increase. 91–99% (rProtA) and 60–65% (IgG) remained bound following the SDS treatment.

Sulfate effect

It has been previously reported that some activated polymeric supports will bind more protein under highly ionic coupling conditions[11–14]. The phenomenon has

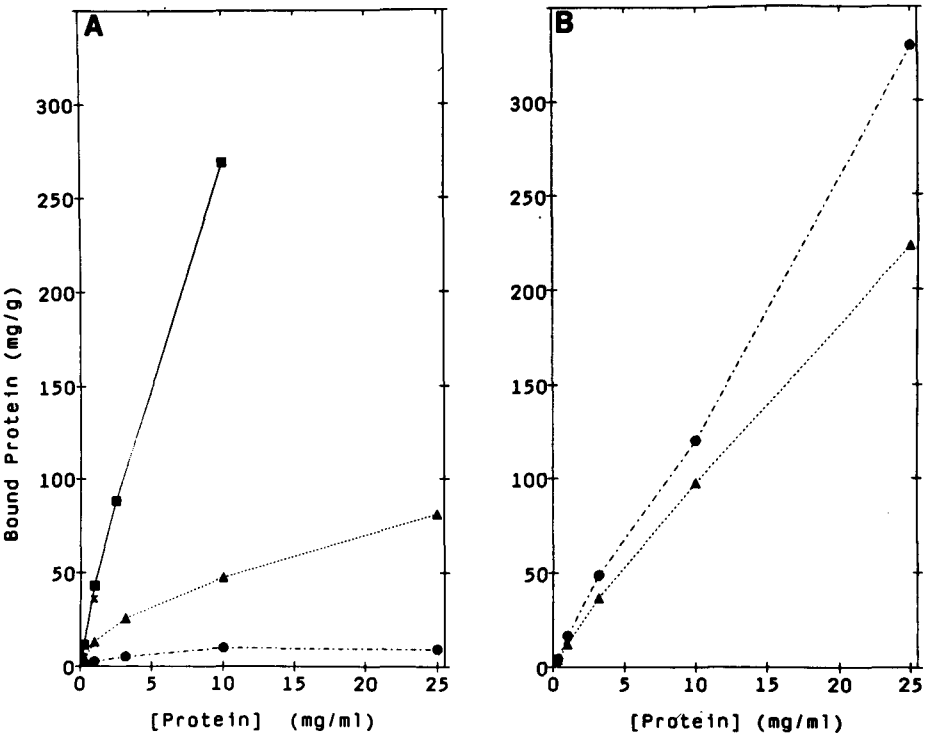

Fig. 4. The concentration dependency of the coupling of various proteins to azlactone-functional beads. 20:80 Beads were used, except for the Con A studies, which were with 30:70 beads. Protein concentrations varied from 0.1 to 25 mg/ml. Reaction conditions were the standard conditions described in the text in either 150 m*M* NaCl (A) or 1.5 *M* Na_2SO_4 (B), except that Con A was coupled at pH 6.0 rather than pH 7.5. ▲ = IgG; ● = rProtA; ■ = Con A. Note that the single Con A concentration (1.0 mg/ml) for which sulfate data were collected is indicated in A by ×.

been likened to the effect of high concentrations of sulfate or phosphate on the adsorption of protein on hydrophobic-interaction columns[14]. Fig. 5 depicts the effect of the concentration of sodium sulfate on the coupling density of rProtA. Coupling increases above 0.15 *M* sulfate and continues to increase up to the solubility limit, about 1.5 *M*. The effect is more apparent at 5 mg of rProtA/ml than at 0.25 mg/ml. There is also a significant effect of sulfate on the covalent coupling. In the absence of sulfate, the residual bound after the SDS treatment was 70–76%; in the presence of 1.5 *M* sulfate, 98% remained bound at 0.25 mg/ml rProtA and 100% at 5 mg/ml.

In the concentration-dependency experiments (Fig. 4B), IgG and rProtA showed enhanced coupling in the presence of sulfate, two-fold for IgG and more than ten-fold for rProtA. (It should be noted that sulfate had to be reduced to 0.75 *M* for IgG to prevent its precipitation.) Although the coupling densities are very high (225 mg/g for IgG and 325 mg/g for rProtA), from the shapes of the curves neither appears to have fully saturated the bead. In contrast to the sulfate enhancement of IgG and rProtA coupling, there was no effect on Con A. At 1.0 mg/ml of Con A 38.6 ± 1.8 mg of protein bound per g of polymer with sulfate and 42.0 ± 2.7 without sulfate. (Note

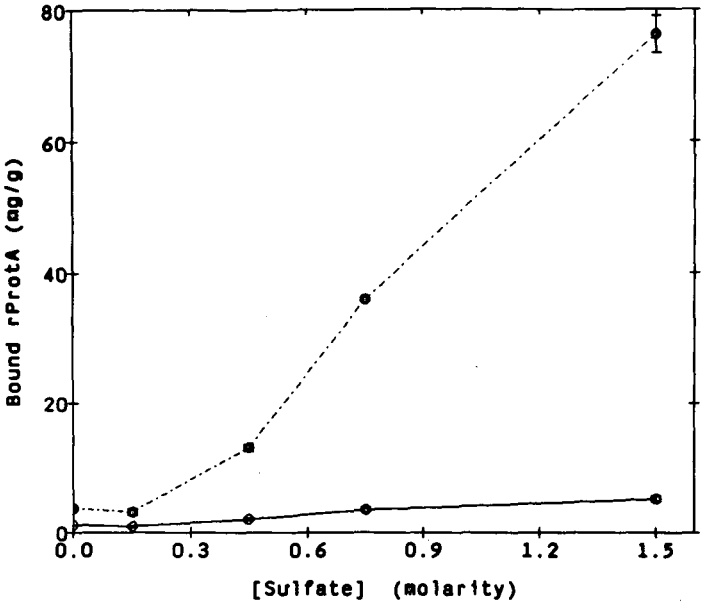

Fig. 5. The effect of sodium sulfate on the coupling of rProtA to azlactone-functional beads. 20:80 Beads and standard coupling conditions were used. Sulfate was varied as indicated from 0.0 to 1.5 *M*. In those experiments without sulfate the reaction medium contained 150 m*M* NaCl. Experiments performed at 5 mg/ml (●) and at 0.25 mg/ml (○) rProtA.

that the sulfate point is indicated by the × in Fig. 4A.) The coupling efficiencies for rProtA were 66–93% and 43–71% for IgG. In additional experiments we have observed that the enhanced binding of rProtA in 1.0 *M* sodium phosphate is 80% of that in 1.5 *M* sodium sulfate, while the effect of 3.0 *M* NaCl is only 8% of the sulfate effect.

In other experiments in the presence of sulfate (not shown) we have also immobilized trypsin, ovalbumin, and bovine serum albumin (BSA) at densities greater than 100 mg/g. Trypsin (102 mg/g) remained enzymically active, and ovalbumin (217 mg/g) was able to bind anti-ovalbumin antibodies[15].

Immobilization time course

The time courses for the coupling of rProtA and Con A to azlactone-functional beads (Fig. 6A) showed that the reaction is very rapid. More that 50% of the final binding density is achieved in the first 5 min. Fig. 6B shows the comparison of the time course for the binding of rProtA with and without sulfate. The 24-h coupling in the absence of sulfate (2.6 mg/ml) is less than 10% of the 5-min reaction in the presence of sulfate. In another time course at 25 mg/ml (not shown), 397 mg of rProtA bound per g of 20:80 polymer in 24 h. In this and all other cases studied, there was a slight increase in coupling by extending the reaction time to 24 h, but the immobilizations were essentially complete in 1-2 h.

pH profile

Since there was a marked pH effect on Con A coupling (Fig. 6A) which might

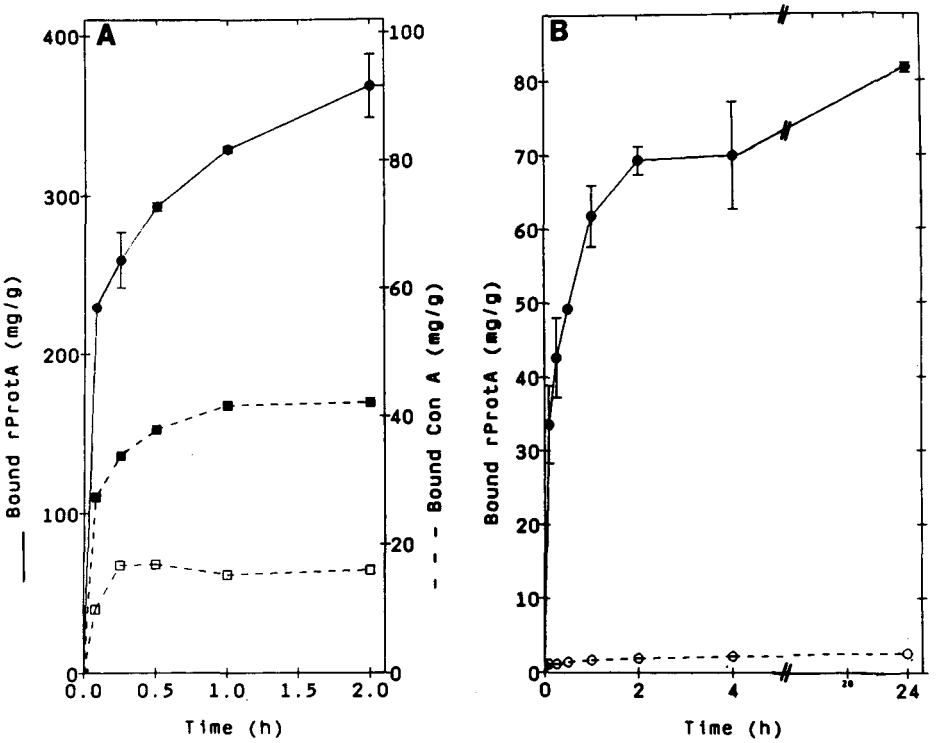

Fig. 6. The time course for the coupling of rProtA and Con A to azlactone-functional beads. (A) rProtA (●) (25 mg/ml) was coupled to 20:80 beads under the standard conditions in the presence of sulfate. Con A (1.0 mg/ml) was coupled to 30:70 beads at pH 6.0 (■) and pH 7.0 (□) in 150 m*M* NaCl. "Zero" time was determined by allowing the beads to react first with the 1.0 *M* ethanolamine blocking agent, followed by reaction with the protein, followed by another blocking step. Only the first 2 h of the 16-h course of the rProtA experiment are illustrated, since less than 10% increase was observed over the remainder of the experiment. (B) rProtA (5 mg/ml) was coupled as in (A) to 20:80 beads for 24 h in the presence of chloride (○) or sulfate (●).

be attributable to its known insolubility at high pH[16], we conducted a study of rProtA and BSA binding in the pH range 4–9. The shape of the pH profiles (Fig. 7) depends on whether sulfate is present. When it is present, the optimum is pH 8–9 with a steady, almost linear, increase in bound protein from pH 4.5–8.0. Without sulfate (*i.e.*, in 150 m*M* NaCl) the pH profile is characterized by a minimum at pH 5–7 with considerably greater activity at both the acid and alkali extremes of the tested range. 94% and 92% of rProtA and BSA, respectively, are resistant to solubilization by the SDS treatment at pH 4 (or 4.5), an effect independent of sulfate. Such high percentages indicate that the proteins are actually coupled to the support and not interacting ionically, as might be expected if the azlactone ring were opened by water hydrolysis to form a carboxyl group. Furthermore, these percentages are consistently 91% or higher across the pH range studied, if sulfate is present; however, in the absence of sulfate there is a minimum at pH 6.0 where the values are 73% for rProtA and 56% for BSA.

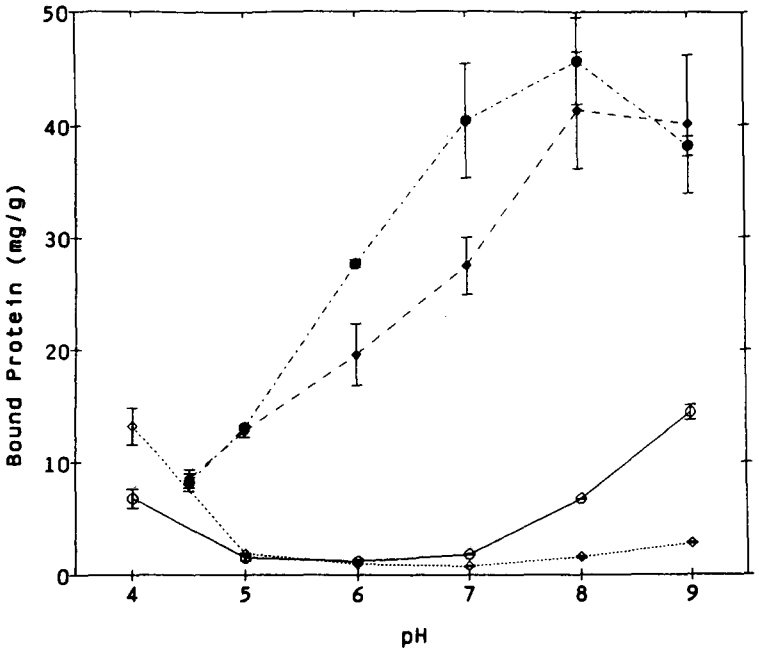

Fig. 7. The pH dependency for the reaction of rProtA and BSA in the presence of sulfate or chloride. The buffering agent in each experiment was 50 m*M* each of acetate, phosphate and pyrophosphate plus either 150 m*M* NaCl or 1.5 *M* Na_2SO_4, titrated to the designated pH. Protein concentrations were 2.5 mg/ml for rProtA (○) and BSA (◇). (The filled symbols indicate that sulfate was present.) The standard coupling conditions were followed with 20:80 beads, except that there was only a 30-min coupling reaction prior to the blocking step.

Activity of immobilized rProtA

The activity of immobilized rProtA was first evaluated in small-scale "batch" experiments with radiolabeled human IgG. Molar ratios were calculated on the basis

TABLE II

ANTIBODY-BINDING ACTIVITY OF IMMOBILIZED rProtA

Derivatized beads with rProtA immobilized at the density indicated in the table were incubated with radiolabeled IgG sufficient to provide at least a two-fold molar excess of IgG over rProtA according to the procedures detailed in the text. The molar ratio was calculated on the basis of the amount of radioactivity specifically eluted by the acid step. Each value is an average of duplicates. The second value in each pair represents an identical experiment in which BSA was substituted for ethanolamine as the blocking agent after the rProtA coupling step.

rProtA density (mg/g)	*Ratio eluted IgG–bound rProtA*
2.7	0.5, 0.8
16.7	0.2, 0.2
40	0.5, 0.4
120	0.3, 0.5

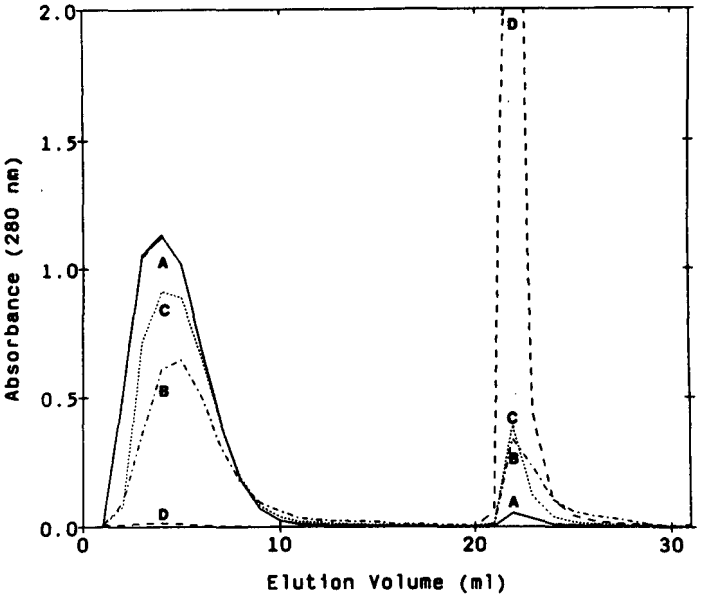

Fig. 8. The effect of coupling conditions on the efficiency of IgG binding to rProtA immobilized to azlactone beads. rProtA was coupled to 20:80 azlactone-functional beads with the standard conditions described in the text, using either 0.25 or 5.0 mg of rProtA/ml in the presence of either 150 m*M* NaCl or 1.5 *M* Na_2SO_4. The resulting rProtA densities are given in Table III. The beads were packed into 10.0 × 0.3 cm (0.70 ml) columns. Human IgG [4.5 ml of 1.0 mg/ml in 25 m*M* sodium phosphate, 150 m*M* NaCl (pH 7.5)] was injected into each column, and unbound protein was eluted with 14.5 ml of the same buffer. Antibody release was effected by eluting the column with 7.0 ml of 0.1 *M* glycine–2% (v/v) acetic acid (pH 2.2). The flow-rate for all steps was 0.5 ml/min, a linear flow of 7.1 cm/min. Fractions were collected, and the absorbance of each at 280 nm was determined and plotted as a function of elution volume. The amounts of IgG eluted from each column and the molar ratios of specifically bound and eluted IgG to coupled rProtA are listed in Table III.

of the amount of IgG which could be specifically eluted at 1.0 *M* glycine (pH 2.0). The modest levels of antibody binding which were obtained (Table II) might be expected when macromolecules must diffuse from a solution into the relatively small volume of a porous matrix in a limited amount of time.

Affinity chromatography

rProtA was immobilized to 20:80 beads under varying protein and salt concentrations to determine how its IgG-binding activity in an affinity column varies with the density of bound protein and with the presence of sulfate in the immobilizing medium. Affinity chromatograms of human IgG (Fig. 8) demonstrate that the amount of IgG recovered from the column is roughly proportional to the density of immobilized rProtA, even at a rProtA density (6 mg/ml) where the resulting IgG capacity is 26 mg/ml. However, on closer inspection, there is an improved correlation between high ratio of IgG to rProtA immobilized in the presence of sulfate ion in the coupling medium (Table III). The two preparations in chloride produced a molar ratio of 0.5, and the two in sulfate were 1.3. Reports in the scientific literature of such

TABLE III

EFFECT OF SULFATE AND rProtA DENSITY ON IgG RECOVERY FROM AN AZLACTONE AFFINITY COLUMN

rProtA was coupled to 20:80 beads, blocked, and packed into 0.70-ml columns as detailed in the text. For columns A and B 0.25 mg/ml rProtA were coupled to 250 mg of beads in a final volume of 5.0 ml. For C and D the protein concentration was 5.0 mg/ml, and other conditions were the same. A and C were used with chloride; B and D with sulfate. IgG (4.5 ml, 1.0 mg/ml) was injected into the column in 25 m*M* sodium phosphate–150 m*M* NaCl (pH 7.5), and eluted at 0.5 ml/min. Coupled densities were determined by radiometric experiments. Values of IgG bound are in units of mg IgG eluted from the column per ml of column bed volume. The IgG–rProtA ratio is a molar ratio calculated as described in the text. Values of replicate experiments are given for the sulfate-enhanced couplings.

Column	*Sulfate present*	*rProtA density mg/ml*	*IgG bound mg/ml*	*Ratio Eluted IgG–bound rProtA*
A		0.072	0.12	0.49
B	+	0.25	0.92	1.11
			0.99	1.20
			1.22	1.47
C		0.40	0.72	0.54
D	+	5.91	26.0	1.32
			26.4	1.34

molar ratios for immobilized Protein A have been rare, although manufacturers regularly give such information in their product literature. Muramatsu *et al.*[17] reported a ratio of 0.4; however, vendors (Genzyme and InFerGene, for example) generally indicate values of 0.8–1.4 for commercially available columns. Uhlen[18] has demonstrated that Protein A has five binding domains for IgG, all of which are independently functional; however, the maximum binding ratio observed in free solution was 2 mol of IgG per mol of Protein A.

Passage of 2.25 ml of human serum through the highest-density column (column D in Table III) resulted in the specific elution of 15 mg of human IgG (Fig. 9A), corresponding to a molar ratio of 1.1. SDS–polyacrylamide gel electrophoretic analysis (not shown) revealed that the heavy- and light-chain bands for the IgG completely disappeared from the flow-through fraction and appeared as clean bands in the acid-eluted fraction. Fig. 9A also shows the results of subjecting 3 mg of BSA to the same fractionation procedure; 99% of the albumin was recovered in the flow-through fraction and less than 1% in the acid-eluted fraction.

Fig. 9B presents results from similar experiments with a larger column (10 × 0.5 cm, 2 ml) containing beads derivatized to a higher rProtA density (214 mg/g, 16 mg/ml). As before, all of the IgG was removed from the human serum sample (compare Fig. 10, lane 2, injected serum sample, with lane 3, the flow-through fraction) and was recovered in the acid-eluted fraction (lane 6), where it appears as pure as the commercially available human IgG (lane 7). Despite the high density of rProtA, we observed none in the high-salt or acid-eluted fractions (compare lanes 4 and 5 with rProtA in lane 8). Lane 4 shows that albumin is probably the major non-specifically bound protein eluted by the high salt wash. After this experiment a control chroma-

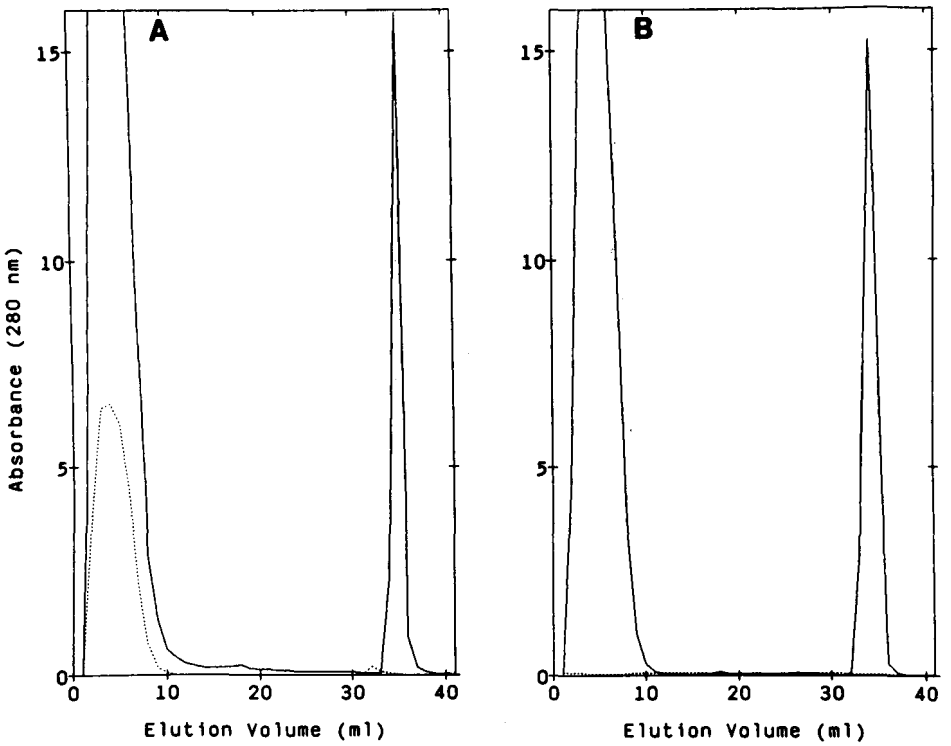

Fig. 9. Affinity purification of IgG from human serum on rProtA coupled to azlactone-functional beads. The chromatograms represented in A are from column D described in Fig. 8 and Table III. Those in B were obtained from a 10 × 0.5 cm (2.0 ml) column, packed with rProtA-azlactone beads, in which the rProtA density was 16 mg/ml. The derivative was prepared by allowing 250 mg of 20:80 beads to react with 84 mg of rProtA in 5.0 ml of sulfate-containing buffer for 60 min under the standard coupling conditions described in the text. In both A and B the solid line represents the elution profile following injection of 2.25 ml of human serum, diluted to 4.5 ml with elution buffer (25 m*M* sodium phosphate–150 m*M* NaCl, pH 7.5). The dashed line in A represents the elution profile following injection of 4.5 ml of BSA (0.7 mg/ml). The dashed line in B represents the elution profile of a "blank" chromatographic experiment immediately following the serum chromatogram (injecting 4.5 ml of buffer). Elution conditions for all columns were: 15 ml of the phosphate buffer, followed by 9.0 ml of the phosphate with 1.0 *M* NaCl (except for the BSA experiment), followed by return to the low-salt phosphate (7.0 ml), followed by 7.0 ml of the 0.1 *M* glycine–2% acetic acid buffer (pH 2.2), all at 0.5 ml/min. Fractions were collected and diluted as necessary to record absorbances at 280 nm.

togram was obtained by injecting starting buffer into the column, followed by the standard salt and acid steps in an attempt to find a "ghost" peak, *i.e.*, residual IgG which had remained bound from a previous experiment. The chromatogram (Fig. 9B) demonstrates that none was found. In subsequent experiments with this column (not shown) we were also unable to find a "ghost" peak after the column was saturated with specifically-bound IgG from which 112 mg of IgG was eluted.

Flow properties of azlactone-functional beads were examined in a 10 × 0.5 cm column in which the flow-rate was incrementally increased from 0.25 ml/min to 15 ml/min (the limit of the system). The increase in back pressure was a linear function of

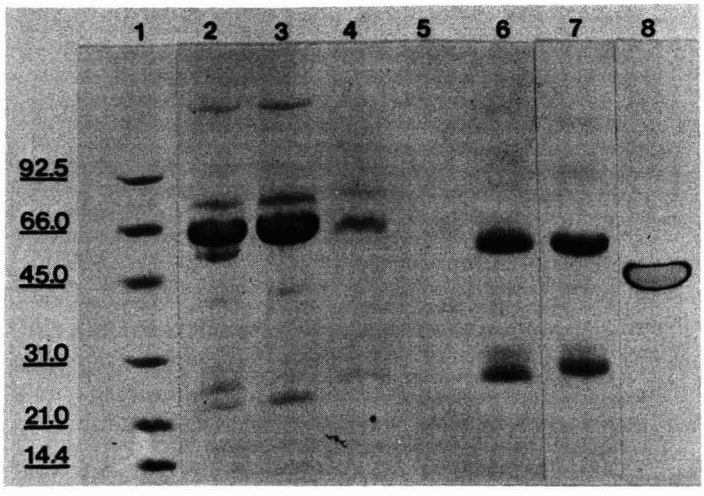

Fig. 10. Electrophoretic analysis of the chromatographic fractions from the rProtA-azlactone bead affinity column shown in Fig. 9B. The lanes contained the following samples (*ca.* 5 μg of protein per lane): 1 = molecular weight standards, given in kilodalton (phosphorylase *b*, 92:5; BSA, 66; ovalbumin, 45; carbonic anhydrase, 31; soybean trypsin inhibitor, 21; lysozyme, 14.4); 2 = unfractionated serum; 3 = flow-through fraction; 4 = fraction eluted at high salt concentration; 5 = fraction eluted with low-salt buffer between high-salt and acid elutions; 6 = acid-eluted fraction; 7 = human IgG; 8 = rProtA.

the flow-rate, *ca.* 0.1 MPa at 0.25 ml/min and 1.4 MPa (210 p.s.i.) at 15 ml/min. There was a slight compacting above 10 ml/min; however, this is understandable, since the column had been packed at 2 ml/min. At the highest flow-rate the linear flow-velocity was 76 cm/min. In another experiment at 7 cm/min linear flow, 100% of a 5-mg IgG sample was bound by the column used in Fig. 9A above, and 98% of it was recovered in the acid elution step.

Standard storage conditions for the column were 20% ethanol in water, 4°C. After 4 months' storage under these conditions or short-term storage (1–3 days) at higher ethanol concentrations (50, 70 and 100%) we observed no loss in biological activity. In addition, there were no solvent effects on the column bed volume.

DISCUSSION

A wide variety of chemical reactions has been proposed for the coupling of proteins to solid supports, indicative of the general inadequacy of each in one or more important respects[1–3]. Among the most important requirements are speed of coupling, density of immobilized ligand, and retention of the biological activity of the immobilized protein. With these priorities in mind we have investigated the utility of the azlactone functionality for the immobilization of proteins.

Azlactone copolymer beads have a high capacity for immobilizing protein, and this capacity is largely independent of the degree of azlactone functionality within the range of 1–3 mequiv./g. Thus one may choose a formulation based primarily on considerations other than degree of functionality, *e.q.*, bead size, flow properties, and ease of preparation.

Protein coupling to azlactone-functional beads is very rapid, typically reaching half of the maximum in 5 min and completion in about 1 h. This compares very favorably with other forms of activated supports, such as oxirane (epoxide), cyanogen bromide, activated thiol, aldehyde and hydrazide, which have reaction times of 16–72 h[19–24]. Thus, azlactone supports could prove valuable in situations requiring very short coupling times.

The coupling of many of the proteins which we have investigated is enhanced in the presence of sulfate or phosphate ion. This effect was first noted in reference to oxirane-functional methacrylate copolymers[11–13]. Further investigations with an hydroxyethyl methacrylate polymer[14] suggested that the effect of sulfate (or other ion in the Hofmeister series) was similar to its effect in hydrophobic-interaction chromatography, where these ions are believed to promote a weak affinity between the more hydrophobic portions of the protein surface and the matrix by promoting the imminent precipitation of the protein[25]. In our investigations the effect was maximal at the solubility limit of sodium sulfate (about 1.5 *M*) and influenced both the amount of protein which was immobilized and the rate of immobilization. Unexpectedly, it also enhanced the resultant antibody-binding activity of immobilized rProtA, increasing the molar IgG–rProtA ratio from about 0.5 to 1.0–1.3.

The amounts of protein directly immobilized on supports which we have reported here (397 mg rProtA/g, 31 mg/ml) are higher than we have found reported elsewhere. For example, Taylor[19] reported an extensive study in which he coupled four proteins to nine supports at five pH values. The highest IgG density was 3 mg/g (only binding 25% of the protein offered for coupling) and only one-third of it was biologically active. His highest reported protein binding was 23 mg/g for alkaline phosphatase to cyanogen bromide-activated Sepharose™, only half of which was active.

In an extensive study of leakage problems associated with N-hydroxysuccinimide (NHS) ester-activated supports, Wilchek and Miron[26] show that the relatively high density yield of these supports (up to about 100 mg/g) is accompanied by very high leakage rates. They recommend a variation which greatly reduces the leakage rate but also reduces the density to about 20 mg/g and conclude that 'for very high capacity columns, alternative methods should be developed." The azlactone-functional beads we have studied couple protein at densities higher than those reported for NHS supports[26], and, to the limited extent which we have studied loss of ligand from the support, the leakage rate is considerably reduced compared to NHS supports.

The pH optimum, as measured in this study, is primarily a measure of the reactivity of the available nucleophiles. The reactivities in the presence of chloride at pH 6–9 are consistent with the free (unprotonated) ε-amine of lysine as the attacking nucleophile. The results in the presence of high concentrations of sulfate are consistent with the sulfate-induced perturbance of the apparent pK for the deprotonation of the ε-amine of lysine by at least one pH unit.

The reactivities in the acidic region are more difficult to interpret. A review of the literature revealed five reports of pH effects on azlactone reactivity[27–31], none of which could verify our observation. In the only study under acidic conditions, Baranowski *et al.*[27] reported on the reaction of a monomeric azlactone derivative of *p*-nitrobenzoyl valine with gelatin at pH 3, 7.4, and 10. On the acidic side they report-

ed a 20-fold *decrease* in reactivity (pH 7.4 to 3), in marked contrast to the 4- to 20-fold *increase* we observed (pH 7 to 4). Additionally, Chuaqui *et al.*[32], using a 2-phenyl azlactone, have shown that there is an acetic acid-catalyzed azlactone ring-opening reaction with various amino acids in CCl_4 resulting in the formation of an amide bond. They suggested that one of two possible cyclic intermediates involving proton transfers could account for the reaction. We speculate that Baranowski *et al.*[27] did not observe acid catalysis because the more strongly electron-withdrawing *p*-nitrophenyl group at the 2-position on the azlactone ring destabilized the proposed intermediates. This would not be expected with the 2-phenyl of Chuaqui or the polymer backbone we used.

Affinity chromatography

The affinity chromatography experiments demonstrate the utility of the high protein densities which we have reported. Even at the highest density of rProtA which we have tested for biological activity, 214 mg/g (16 mg/ml), the amount of IgG recovered (56 mg/ml) yields a ratio of 1.0. This unexpectedly high binding activity at such high ligand coupling densities is not only counter-intuitive, it is also opposite to the effect reported by Eveleigh and Levy[33], *i.e.*, continuously decreasing ratio as antibody coupling density increased from 1 to 22 mg/ml. Although they were coupling an antibody which is considerably larger than Protein A, the size of its final binding complex with albumin (218 000 dalton) is comparable to the rProtA-IgG complex we have used (195 000 dalton).

Despite the wide interest in antibody purification by Protein A, few studies are reported in the scientific literature of IgG yields from immobilized Protein A. A study by Lee *et al.*[34] details their experience with purifying a monoclonal antibody on Protein A–Sepharose. They routinely obtained 4–8 mg of antibody per ml of column bed. Other studies with immobilized Protein A reported recoveries of 1.8 mg IgG per ml[35] and 5 mg/ml[36]. An immobilized Protein G investigation reported a yield of 2–5 mg/ml[37]. Immobilization of Protein A onto an azlactone support, which has yielded as much as 56 mg of IgG per ml of column bed, is clearly a substantial improvement.

Such high biological activity at high density means that the sizes of affinity columns can be scaled down, providing a great time and cost advantage in large scale purification processes. In very-small-scale analytical uses, such as described by Janis and Regnier[38], a reduction in the volume of the affinity column means a shorter cycle time and greater efficiency.

This increase in capacity is obtained at no loss in the quality of the affinity separation. Electrophoresis shows that the IgG is depleted from the serum and that there is little or no contaminant in the recovered IgG fraction. Back-pressures are consistently low (<0.3 MPa), and, under the usual flow conditions, we have seen no changes in bed volume.

We have immobilized almost 400 mg of rProtA per gram of 20:80 bead. This means that the resultant graft polymer is over 25% protein. Chromatographic results with a preparation containing 214 mg rProtA per g of polymer indicated that it bound an additional 700 mg of IgG per g, so that the final protein mass approximated the mass of azlactone–acrylamide copolymer.

In his review, Jervis[3] outlined several characteristics of an ideal activation/coupling method. The results presented here support azlactone copolymer beads as

closely approximating his model. Azlactone reacts rapidly and efficiently to form stable, uncharged, amide linkages between the ligand and the polymeric backbone. If there are any hydrolytic side reactions which form carboxylates or other groups, they do not interfere in the affinity applications we have investigated. Excess sites are easily blocked with ethanolamine resulting in an uncharged, hydrophilic ligand. In addition, there is no need for toxic reagents in either the activation, the coupling, or the blocking steps. Finally, a great benefit of the ring-opening nature of the azlactone reaction which is especially useful for production-scale applications is that there are no by-products of the coupling reaction itself which would have to be removed.

ACKNOWLEDGEMENTS

We wish to thank Howell K. Smith II (Technology Development Laboratory) and Julie B. Stahl (Biosciences) for their excellent technical assistance in the preparation and evaluation of the azlactone-functional supports and Diane Frederick (Biosciences) for preparation of the scanning electron micrographs. We are also indebted to Professors Kathleen A. Parson (Macalester College) and Robert F. O'Dea (University of Minnesota) for their valuable comments during the preparation of this manuscript.

REFERENCES

1 W. H. Scouten, *Affinity Chromatography—Bioselective Adsorption on Inert Matrices*, Wiley, New York, 1981.
2 E. Katchalski-Katzir, *Angew. Makromol. Chem.*, 166/167 (1989) 227.
3 L. Jervis, in D. C. Sherrington and P. Hodge (Editors), *Syntheses and Separations using Functional Polymers*, Wiley, New York, 1988, p. 265.
4 Y. S. Rao and R. Filler, in I. J. Turchi (Editors), *Heterocyclic Compounds, Vol. 45, Oxazoles*, Wiley, New York 1986, p. 361.
5 J. K. Rasmussen, S. Heilmann and L. Krepski, in H. F. Marks, N. Bikales, C. G. Overberger and G. Menges (Editors), *Encyclo. Polym. Sci. Engineer.*, Vol. 11, Wiley, New York, 1988, p. 558.
6 J. K. Rasmussen, S. M. Heilmann, L. R. Krepski, H. K. Smith II, M. M. Walker, D. M. Stauffer, D. S. Milbrath and P. L. Coleman, *Polym. Prepr.*, 31 (1990) in press.
7 S. M. Heilmann, J. K. Rasmussen, L. R. Krepski, D. S. Milbrath and P. L. Coleman, *U.S. Pat.*, 4 737 560 (1988).
8 S. M. Heilmann, J. K. Rasmussen, L. R. Krepski, D. S. Milbrath and P. L. Coleman, *U.S. Pat.* 4 871 824 (1989).
9 P. K. Smith, R. I. Krohn, G. T. Hermanson, A. K. Mallia, F. H. Gartner, M. D. Provenzano, E. K. Fujimoto, N. M. Goeke, B. J. Olson and D. C. Klenk, *Anal. Biochem.*, 150 (1985) 76.
10 U. K. Laemmli, *Nature (London)*, 227 (1970) 680.
11 O. Hannibal-Friedrich, M. Chun and M. Sernetz, *Biotech. Bioengineer.*, 22 (1980) 157.
12 J. Turkova, K. Blaha, J. Horacek, J. Vajcner, A. Frydrychova and J. Coupek, *J. Chromatogr.*, 215 (1981) 165.
13 I. Zemanova, J. Turkova, M. Capka, L. A. Nakhapetyan, F. Svec and J. Kalal, *Enzyme Microb. Technol.*, 3 (1981) 229.
14 K. Smalla, J. Turkova, J. Coupek and P. Hermann, *Biotech. Appl. Biochem.*, 10 (1988) 21.
15 C. L. Astry, 3M Biosciences, St. Paul, MN, personal communication.
16 A. J. Kalb and A. Lustig, *Biochim. Biophys. Acta*, 168 (1968) 366.
17 H. Muramatsu, J. M. Dicks, E. Tamiya and I. Karube, *Anal. Chem.*, 59 (1987) 2760.
18 M. Uhlen, Royal Institute of Technology, Stockholm, Sweden, personal communication.
19 R. F. Taylor, *Anal. Chim. Acta*, 172 (1985) 241.
20 K. Burg, O. Mauz, S. Noetzel and K. Sauber, *Angew. Makromol. Chem.*, 157 (1988) 105.

21 G. Wehnert, A. Sauerbrei and K. Schugerl, *Biotech. Lett.*, 7 (1985) 827.
22 A. Santucci, P. Soldani, L. Lozzi, M. Rustici, L. Bracci, S. Petreni and P. Neri, *J. Immunol. Methods*, 114 (1988) 181.
23 K. Kurkijarvi and T. Korpela, *Biochimie*, 71 (1989) 439.
24 R. S. Matson and M. C. Little, *J. Chromatogr.*, 458 (1988) 67.
25 J. Porath, *Biopolymers*, 26 (1987) S193.
26 M. Wilchek and T. Miron, *Biochemistry*, 26 (1987) 2155.
27 T. Baranowski, M. Kochman, K. Nowak and I. Siemion, *Bull. Polan, Sci., Ser. Sci. Biol.*, 11 (1963) 107.
28 V. Daffe and J. Fastrez, *J. Chem. Soc., Perkin Trans. II*, (1983) 783.
29 V. Daffe and J. Fastrez, *J. Chem. Soc., Perkin Trans. II*, (1983) 789.
30 M. Narita, K. Ishikawa, K. Kudo and T. Endo, *Bull. Chem. Soc. Jpn.*, 58 (1985) 3125.
31 J. Suh, E. Lee, Y. C. Myoung, M. Kim and S. Kim, *J. Org. Chem.*, 50 (1985) 977.
32 C. Chuaqui, S. Atala, A. Marquez and H. Rodriguez, *Tetrahedron*, 29 (1973) 1197.
33 J. W. Eveleigh and D. E. Levy, *J. Solid-Phase Biochem.*, 2 (1977) 45.
34 S.-M. Lee, M. E. Gustafson, D. J. Pickle, M. C. Flickinger, G. M. Muschik and A. C. Morgan, Jr., *J. Biotechnol.*, 4 (1986) 189.
35 A. C. Kenney and H. A. Chase, *J. Chem. Tech. Biotech.* 39 (1987) 173.
36 C. Ploiesi, A. Tamanini, S. Ghielmi and A. Albertini, *J. Chromatogr.*, 465 (1989) 101.
37 S. Ohlson, R. Nilsson, U. Niss, B.-M. Kjellberg, C. Freiburghaus, *J. Immunol. Methods.*, 114 (1988) 175.
38 L. J. Janis and F. E. Regnier, *J. Chromatogr.*, 444 (1988) 1.

Journal of Chromatography, 512 (1990) 365–376
Elsevier Science Publishers B.V., Amsterdam

CHROMSYMP. 1868

Preparative high-performance liquid chromatography on a unique high-speed macroporous resin

LINDA L. LLOYD* and FRANK P. WARNER
Polymer Laboratories Ltd., Essex Road, Church Stretton, Shropshire SY6 6AX (U.K.)

ABSTRACT

The use of high-performance liquid chromatography (HPLC) for the analysis and purification of biological macromolecules has increased with the commercial availability of packing materials specifically designed for large-molecule analysis. However, the speed of analysis is limited as the efficiency of the HPLC columns for macromolecules has been significantly lower that that acheived for small molecule separations. One possible solution to the speed/capacity/resolution triangle experienced with large biological molecules is to increase the pore size of the HPLC matrix. A rigid macroporous polymer with a 4000 Å pore size has, therefore, been developed for evaluation as a high performance matrix for macromolecule HPLC separations. The mechanical stability of this polymer enables the material to be packed in conventional columns, 4.6 mm I.D., and operated under HPLC conditions of flow rate and pressure.

The high speed, fast flow matrices evaluated are for reversed-phase HPLC, PLRP-S 4000 Å, and for anion-exchange HPLC, PL-SAX 4000 Å. The matrices/columns have been assessed for stability, permeability, efficiency, selectivity and capacity with macromolecules and their suitability for analytical and preparative applications evaluated.

INTRODUCTION

As research workers continually strive for increased speed of analysis in the separation/fractionation of biological macromolecules much effort has been put into the optimization and design of chromatographic supports for high-performacne liquid chromatography (HPLC). This is reflected in the fact than HPLC is now one of the fastest growing techniques with a proliferation of column packings and instrumentation.

A suitable adsorbent for HPLC should have a controlled uniform pore geometry, mechanical stability, chemical resistance, clean homogeneous surface and narrow particle size distribution. In the 1970s silica became the base matrix of choice being commercially available in a range of pore and particle sizes and being easily derivatized to produce different functionalities, reversed-phase[1], ion-exchange[2], affin-

0021-9673/90/$03.50

ity[3] and for gel filtration chromatography[4]. However the silica-based packings have restricted chemical stability.

Although liquid chromatography of biopolymers, proteins, nucleic acids etc., was originally performed using polymer gels[5–7] these were microporous semi-rigid gels where the pore size is dependent upon the degree of swelling, hydration of the polymer chains. Unless operated at low pressure with low flow-rates these gels collapse, restricting the flow and so making them unsuitable for high speed separations. It was not until 1964[8] that rigid macroporous polymers were produced for liquid chromatography and in 1985 used for the HPLC analysis of proteins[9].

Even with these rigid macroporous, microparticulate HPLC packing materials the speed of macromolecule analysis is limited due to the reduced efficiency/resolution of large-molecule separations compared to those achieved with small molecule HPLC under similar conditions. This is attributed to both kinetic and thermodynamic factors. The diffusion coefficient of a solute decreases as its molecular size in solution increases so limiting its ability to rapidly diffuse in and out of the matrix pore structure. Large-molecule diffusion coefficients have been measured at 10^{-10} and 10^{-11} m^2/s (ref. 10) but these are further reduced by pore diffusion (solute diffusion into and out of the porous structure of the packing material). It has been shown that when the ratio of the solute diameter to pore diameter exceeds 0.2 the pore diffusion is restricted[11]. This leads to a reduction in efficiency/resolution as band-spreading increases at flow-rates normally used for small-molecule HPLC. In order to reduce band-spreading and improve efficiency the linear velocity must be reduced but this increases the sample residence time in the columns and hence contact time with potentially denaturating conditions. This is obviously undesirable for the analysis of biologically active molecules.

In order to improve intraparticle stagnant mobile phase mass transfer for macromolecules the pore size must be increased. However, the configuration of the molecule in solution and in contact with the stationary phase surface will determine the size of the pore required. One solution to the problem would be to have a non-porous matrix where stagnant mobile phase mass transfer would be eliminated. Unger and co-workers used 1.5-μm non-porous silica as a matrix for affinity chromatography in 1984[12] and subsequently for reversed-phase[13] and hydrophobic-interaction chromatography[14] non-porous polymers have also been used to produce high-speed matrices[15,16]. However, these materials, even when used in small particle form, have reduced capacity due to the loss of internal pore surface area compared with porous matrices. Therefore it is felt that a more general solution to the speed/capacity/resolution triangle is needed for high-load analytical separations and preparative fractionations.

This paper reports on the chromatographic characteristics of a unique highly porous polymer matrix which can be used for reversed-phase separations or in a derivatized form for ion exchange and which when operated at high flow-rates with rapid gradient development times maintains the resolution and capacity of the separation/fractionation.

EXPERIMENTAL

HPLC system

All chromatography and dynamic capacity measurements were carried out using a modular Knauer HPLC system (Knauer, Berlin, F.R.G.) equipped with two reciprocating high-pressure pumps, Model 64, a gradient former, Model 50B, static mixing chamber with a 20-μl internal volume, variable-wavelength UV detector, Model 87, fitted with a standard analytical cell of 10 mm pathlength/10 μl volume and twin-pen chart recorder. To improve mixing at high flow-rates whilst maintaining the minimum volume of mixing for the high speed separations a Lee Viso-Jet® micromixer with a 10 μl internal volume was inserted between the pumps and the static mixing chamber. (Lee Products, Gerrards Cross, U.K.). Sample introduction was achieved with a Rheodyne 7125 injection valve fitted with a 200-μl loop (supplied by HPLC Technology, Macclesfield, U. K.). A Trilab 2000 computer equipped with a liquid chromatography/gas chromatography data handling programme was used for peak detection, integration and data manipulation (Trivector, Sandy, U.K.).

Mobile phases and chemicals

Water used for sample and eluent preparation was purified using an Elgastat UHP system (Elga, High Wycombe, U.K.) and the buffer salts were of analytical or HPLC grade (FSA Laboratory Supplies, Loughborough, U.K.). Proteins used as chromatographic test probes were of high purity (Sigma, Poole, U.K.). Lyophilized bovine serum albumin (BSA), purified by chromatography to > 99% was used for the determination of dynamic loading capacity (Advanced Protein Products, Brierley Hill, U.K.).

Dynamic load capacity

Frontal analysis was used to determine the binding capacity of the 4000 Å high-speed macroporous resin[17]. The dynamic protein capacity for a medium-molecular-weight globular protein, BSA, was obtained by pumping a dilute solution of the protein in binding buffer through a 50 × 4.6 mm I.D. polyether ether ketone (PEEK) column at 1.0 ml/min (2.5 mg BSA/ml in 0.01 *M* Tris · HCl, pH 8.0). The column was first eluted with a cleaning buffer, 0.01 *M* Tris · HCl + 1.0 *M* NaCl, pH 8.0, followed by conditioning with the binding buffer, 0.01 *M* Tris · HCl, pH 8.0. The protein breakthrough curve was established by monitoring the column eluent at 256 nm and the volume of protein solution required to saturate the column was determined by dropping a perpendicular line from the front breakthrough boundary at 20% of the maximum UV adsorbance.

Chromatographic methods

Matrix permeability and mechanical rigidity was determined using the high-performance 150 × 4.6 mm I.D. stainless-steel hardware. Methanol–water (70:30, v/v) was pumped through the column at constant pressure using a Haskel (Sunderland, U.K.) air-driven pump Model MCP-71 and the flow-rate monitored using an analytical flowmeter (supplied by HPLC Technology).

Reversed-phase analysis of proteins under denaturing conditions was carried out using PLRP-S 300 Å 5 μm and PLRP-S 4000 Å 8 μm material packed in 50 × 4.6

mm I.D. stainless-steel hardware. The test proteins were dissolved in water containing 0.1% trifluoroacetic acid and eluted with a gradient of 0.1% trifluoroacetic acid in acetonitrile.

The resolution of a protein test mixture under non-denaturing conditions by anion exchange, was determined using PL-SAX 4000 Å 8 μm and PL-SAX 1000 Å 8 μm material packed in biocompatible PEEK hardware, 50 × 4.6 mm I.D. The proteins were dissolved in 0.01 *M* Tris · HCl, pH 8.0 and eluted with a gradient of increasing NaCl concentration.

The influence of flow-rate on the band spreading of non-retained solutes was investigated using a PL-SAX 4000 Å 8 μm 250 × 4.6 mm I.D. stainless-steel column. A 0.01 *M* Tris · HCl + 0.5 *M* NaCl, pH 8.0 eluent was used.

The preparative fractionations were carried out using the PL-SAX 4000 Å 8 μm material packed in the biocompatible PEEK hardware 50 × 4.6 mm I.D. The samples were diluted using 0.01 *M* Tris · HCl, pH 8.0 and chromatoghraphed using an increasing salt gradient, 0.01 *M* Tris · HCl + 0.5 *M* NaCl, pH 8.0.

RESULTS AND DISCUSSION

Column stability

The conventional wide pore poly(styrene–divinylbenzene) reversed-phase material, PLRP-S 1000 Å, and the high speed, fast flow poly(styrene–divinylbenzene) matrix, PLRP-S 4000 Å, were compared for permeability and stability. A plot of column pressure *vs.* flow-rate was carried out for each material using the same column dimensions, 150 × 4.6 mm I.D. and eluent, methanol–water (70:30, v/v). The nominal particle size for both materials was 8 μm although there were slight differences in the maxima of the number-average particle size distributions. This is reflected in the off-set of the curves and flow-rates at 2000 p.s.i. The PLRP-S 40000 Å being slightly larger with a flow-rate of 2.07 ml/min compared with the PLRP-S 1000 Å at 1.75 ml/min.

A linear relationship for both materials is achieved up to 3000 p.s.i., the column packing pressure, after which the bed is repacked resulting in deviation from linearity (Fig. 1). Comparing the mechanical rigidity and flow characteristics, permeability, of these two materials it is clear that the fast flow matrix, PLRP-S 4000 Å, is capable of operating at the high flow-rates and pressures necessary for HPLC without particle compression or fragmentation.

By changing the eluent polarity [*i.e.* so that it is more polar than the neutral non-polar poly(styrene–divinylbenzene) surface] it is possible to use this polymeric matrix for reversed-phase separations. Fig. 2 compares the resolution achieved for a representative selection of globular proteins on a conventional reversed-phase material, PLRP-S 300 Å 5 μm operated at 1.0 ml/min with a 20-min gradient development time and the fast flow matrix, PLRP-S 4000 Å 8 μm operated at 4.0 ml/min with a 1-min gradient development time. The separations were both carried out at ambient temperature. No deterioration in separation efficiency was observed for the fast flow matrix, PLRP-S 4000 Å when operated repeatedly with short gradient development times and high flow-rates. Rapid re-equilibration was achieved, 30 s, between the end of the first gradient run and the start of a second.

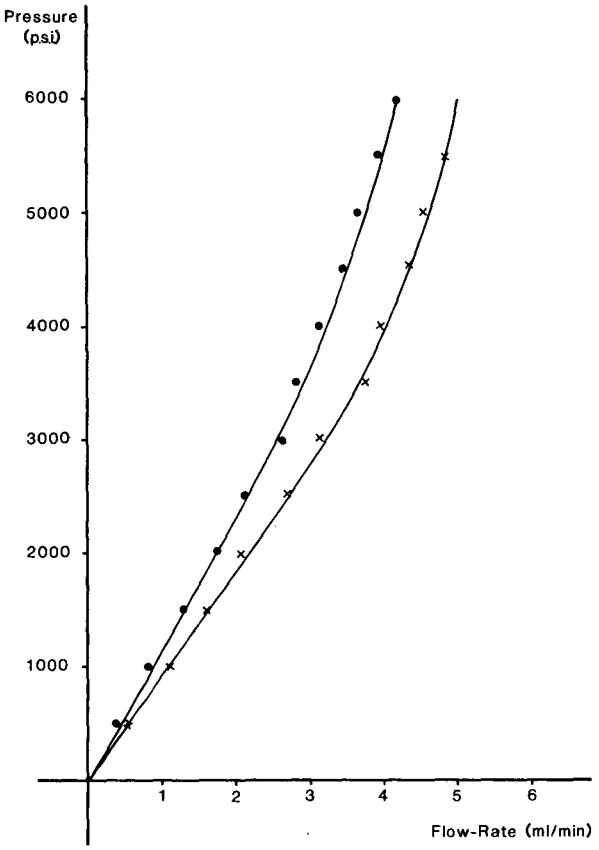

Fig. 1. Column pressure *vs.* flow-rate. Eluent, methanol–water (70:30, v/v); temperature, ambient; column 150 × 4.6 mm I.D.; particle size 8 μm. ● = PLRP-S 1000 Å; × = PLRP-S 4000 Å.

Adsorbent capacity

In order to evalutate the fast flow matrix in non-denaturing eluents for its suitability as a rapid purification system for biologically active molecules a strong anion exchanger was produced. The PLRP-S 1000 Å and 4000 Å materials were derivatized, coated with poly(ethyleneimine) and quaternized following the method published by Rounds *et al.*[18] to produce the strong anion exchangers PL-SAX 1000 Å and PL-SAX 4000 Å.

The influence of pore size on the chromatographic loading was determined by reference to the separation of the proteins ovalbumin and soybean trypsin inhibitor. The resolution factor, R_s as calculated from the difference in retention volume divided by the mean peak (base) volume was determined at various protein loadings.

$$R_s = \frac{t_{R(A)} - t_{R(B)}}{\frac{1}{2}(W_A + W_B)} \qquad \text{(ref. 19)}$$

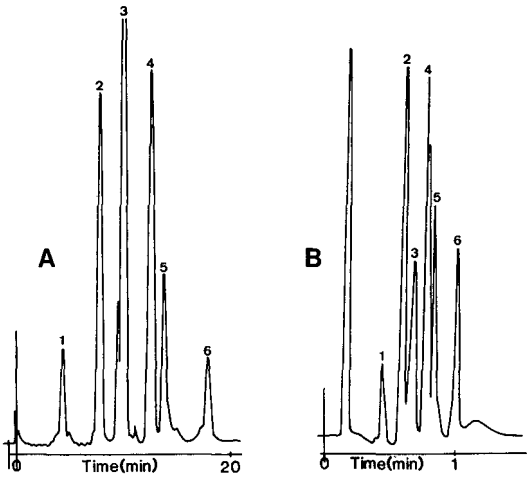

Fig. 2. Comparison of the resolution achieved for 6 globular proteins run under reversed-phase conditions. Proteins: 1 = ribonuclease A; 2 = cytochrome *c*; 3 = lysozyme; 4 = bovine serum albumin; 5 = myoglobin; 6 = ovalbumin. Detection, UV at 280 nm; temperature, ambient; eluent A, 0.1% trifluoroacetic acid in acetonitrile–water (5:95, v/v); eluent B, 0.1 % trifluoroacetic acid in acetonitrile–water (95:5, v/v). (A) column, PLRP-S 300 Å 5 μm 50 × 4.6 mm I.D.; gradient, linear 15–55% B in 20 min at a flow-rate of 1.0 ml/min. (B) Column, PLRP-S 4000 Å 8 μm 50 × 4.6 mm I.D.; gradient, linear 18–60% B in 1 min at a flow-rate of 4.0 ml/min.

where $t_{R(A)}$ and $t_{R(B)}$ are the retention volumes of soybean trypsin inhibitor and ovalbumin respectively and W_A and W_B are the respective peak volumes at the base.

Fig. 3, the plot of resolution factor R_s *vs.* protein load shows that at low loadings comparable resolution is achieved but that the resolution obtained with the

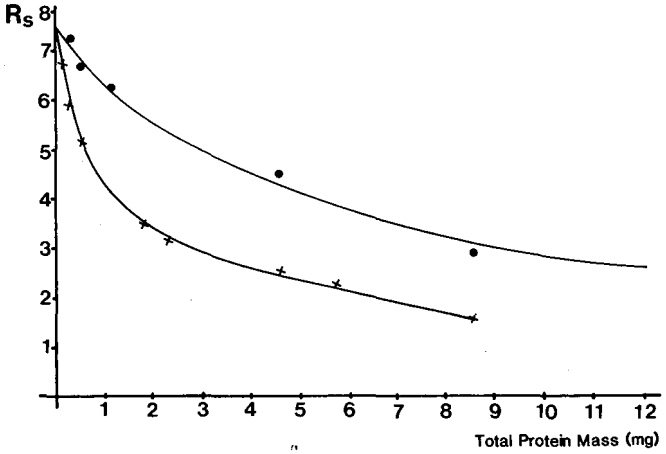

Fig. 3. Resolution factor, R_s, *vs.* total protein load for the anion-exchange separation of ovalbumin and soybean trypsin inhibitor. Eluent A, 0.01 *M* Tris · HCl, pH 8.0; eluent B, A + 0.35 *M* NaCl, pH 8.0; gradient, linear 0–100% B in 20 min; flow-rate, 1.0 ml/min; detection, UV at 280 nm. ● = PL-SAX 1000 Å 8 μm 50 × 4.6 mm I.D. PEEK hardware; × = PL-SAX 4000 Å 8 μm 50 × 4.6 mm I.D. PEEK hardware.

PL-SAX 4000 Å material is more dependent upon column load. Therefore, for high-resolution analytical separations of medium-molecular-weight globular proteins using the PL-SAX 4000 Å 50 × 4.6 mm I.D. column of 0.83 ml volume a typical protein load would be 100 μg. However, 8 mg of total protein can be loaded before the resolution factor drops to 2, the normal criteria for an excellent separation where for gaussian peaks there are 2 base widths between the peak maxima and one base width of near baseline[19].

This would be predicted due to a decrease in surface area with increasing pore size. The total surface area of the poly(styrene–divinylbenzene) 1000 Å and 4000 Å matrices being 267 m^2/g and 139 m^2/g respectively as determined using multipoint nitrogen adsorption, (Digisorb 2600, Coulter Electronics, Luton, U.K.). These values are higher than expected when compared with a silica-based material due to the lower density, 0.3 g/ml, and the presence of microporous structure within the polymer matrix which is accessible to nitrogen but not to an HPLC solute[20]. From the multipoint nitrogen adsorption measurements it is estimated that approximately 1/3 of the surface area is located in pores with an average diameter of less than 20Å. In order to compare available surface area for protein fractionation the dynamic loading capacity was determined by frontal analysis as detailed in the Experimental section. Values obtained were 93 mg BSA/ml of column volume for the PL-SAX 1000 Å and 34 mg/ml for the 4000 Å.

High-speed resolution

As both the PL-SAX 1000 Å and 4000 Å materials are rigid macroporous polymers and are, therefore, capable of operating at high flow-rates and pressures and have exceptionally rapid equilibration rates it is predicted that the packed columns would be stable for high speed operation. As would be expected with porous HPLC matrices a decrease in gradient development time, with a constant flow-rate leads to a decrease in resolution. However, when the flow-rate is increased with a short gradient development time, 2 min, a significant increase in the resolution factor is obtained for the fast flow-rate matrix, PL-SAX 4000 Å, from 4.80 to 7.30. This does not occur with the wide-pore material PL-SAX 1000 Å where the resolution factor increases from 3.25 to 4.00. This suggests that there is a difference in the intraparticle mass transfer of these two materials for large molecules at high flow as the protein peak width (band spreading) decreases for the 4000 Å matrix but not the 1000 Å.

Using an isocratic system and a high salt buffer to give a solute capacity factor (k') of 0 and peak symmetry factors of 1.3 (anion exchange, non-interactive conditions) plate count (efficiency) measurements were carried out for three solutes with increasing linear velocity. The probes used were adenosine 5′-monophosphate and two proteins of increasing molecular weight, myoglobin with a molecular weight of 16 950 daltons and ferritin of 470 000 daltons. As the molecular size in solution of a solute increases so the diffusion coefficient decreases. This significantly increases the band broadening and hence reduces the efficiency of macromolecule separation compared with small molecules at a given flow-rate. As seen in Fig. 4, the H *vs.* U plot, for the PL-SAX 4000 Å material there is a decrease in efficiency with increased molecular size. However, at a linear velocity of approximately 3.5 mm/s the decrease in efficiency for the three probes is halted. It would appear that with the high-speed/fast flow matrix above a critical linear velocity irrespective of solute size the efficiency

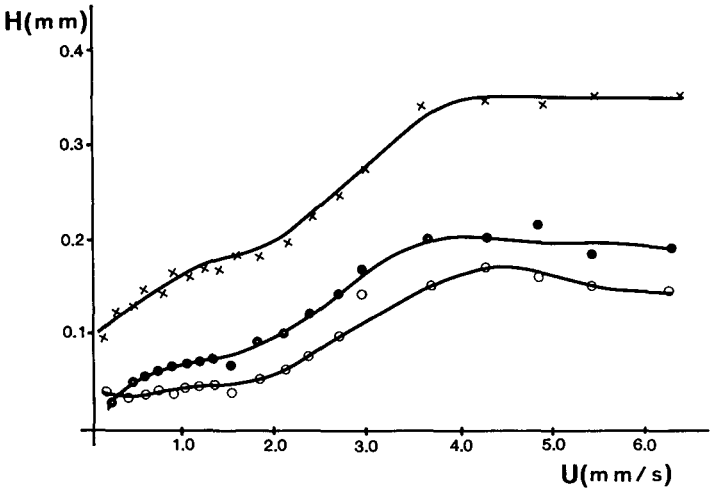

Fig. 4. Plate height (*H*) *vs.* linear velocity (*U*) for the PL-SAX 4000 Å 8 μm material run in a non-interactive mode. Eluent, 0.01 *M* Tris·HCl, 0.5 *M* NaCl, pH 8.0; detection, UV at 280 nm; column, 250 × 4.6 mm I.D. stainless-steel hardware. ○ = Adenosine 5′-monophosphate; **O** = myoglobin; × = ferritin.

starts to improve suggesting an apparent increase in the diffusion coefficient. This type of curve is not typical for porous materials although it has been observed with some non-porous packings.

High-speed capacity

If at high linear velocities the increase in efficiency is due to the matrix performing as a non-porous support then a decrease in dynamic protein capacity and an increased dependence of resolution on sample load would be observed as there would be a decrease in available suraface area.

The plot of resolution factor, R_s, *vs.* total protein load for the analytical separation of ovalbumin and soybean trypsin inhibitor demonstrated that there is no greater dependence of resolution on load at 4.0 ml/min than 1.0 ml/min. However, as would be predicted from the *H vs. U* plot there is an increase in resolution with increased flow-rate at similar protein loads. The dynamic loading capacity as determined by frontal loading was determined as 34 mg BSA/ml of column volume at 1.0 ml/min and 32 mg at 4.0 ml/min. The difference in shape of the two frontal loading curves (Fig. 5) is due to the differences in the flow path through the column. However, at flow-rates of 4.0 ml/min it would be possible to utilize over 80% of the column volume before valuable product is detected in the eluent system. It would, therefore, appear that although the efficiency of separation increases at high linear velocity suggesting a change in the intraparticle diffusion coefficients the high-speed/fast flow material is not performing as a non-porous matrix. There is no decrease in sample load at the increased linear velocities as would be observed if the internal pore surface area was no longer accessible. The surface area of non-porous packings being approximately two orders of magnitude lower than that of porous packings of the same particle size, 0.55 m^2/g for a 5-μm particle[21].

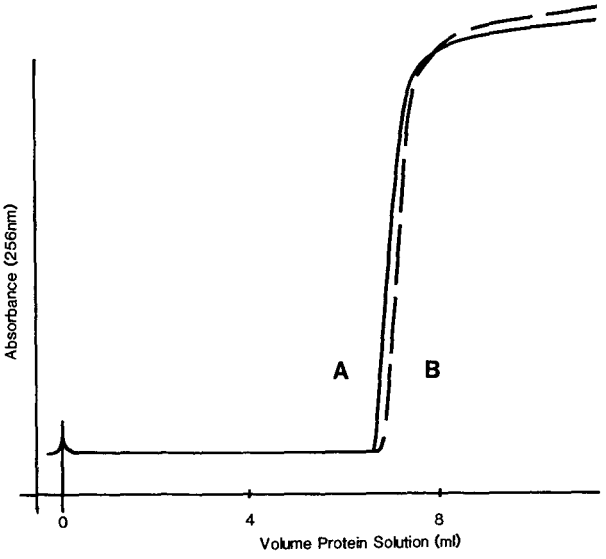

Fig. 5. BSA frontal loading curves. Eluent, 2.5 mg BSA/ml 0.01 *M* Tris·HCl, pH 8.0; detection, UV at 256 nm; column, PL-SAX 4000 Å 8 μm, 50 × 4.6 mm I.D.; PEEK hardware. (A) Flow-rate, 4.0 ml/min; (B) flow-rate, 1.0 ml/min.

Applications

The isolation of antibodies from complex biological matrices necessitates the use of several chromatographic stages if high purity is required. For the isolation of poly/monoclonal antibodies from serum where the composition is relatively well defined although the actual quantities of the various components will be species/individual dependent the antibodies would be expected to be 20% and albumin 60% of the total protein concentration. In order to selectively separate the group of antibodies from non-antibody proteins the first chromatographic step would be the use of immobilized Protein A. The serum was diluted with binding buffer, 0.01 *M* Tris · HCl, pH 8.0 in the ratio 1:5 (v/v) and filtered prior to pumping through the PL-AFC Protein A column. The polyclonal antibodies are selectively retained and after equilibrating the column with binding buffer eluted by reducing the pH, 0.1 *M* glycine, pH 2.5. Following the affinity separation the pH of the eluted polyclonal antibody fraction was adjusted to neutrality to maximise the recovery of biological activity. The purity of the bound fraction or the presence of antibodies in the unbound fraction can be determined using anion exchange or if high purity is required residual albumin and transferrin can be removed (Fig. 6). Using the high speed/fast flow PL-SAX 4000 Å material exposure to potentially deactivating conditions can be minimised as fractionation is accomplished in 90 s.

The enzyme amyloglucosidase was fractionated from *Aspergillus niger* cell culture filtrate which had a total protein concentration as determined by UV at 280 nm of 395 mg/ml. The crude cell culture filtrate was diluted with the low-strength component of the mobile phase, eluent A : 0.01 *M* Tris · HCl, pH 8.0, and filtered prior to the chromatographic fractionation. No other sample preparation was carried out. Using

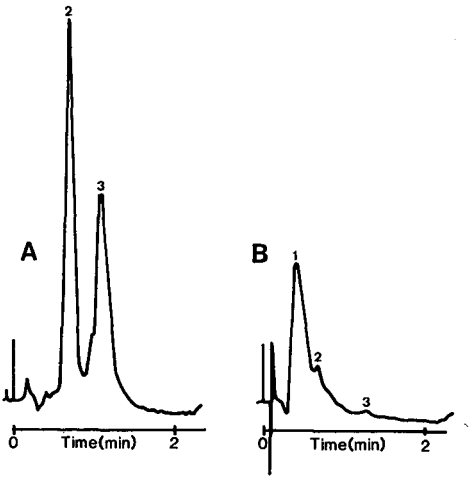

Fig. 6. Anion-exchange separation of the bound (B) and unbound (A) fractions from a Protein A antibody purification. Eluent A, 0.01 *M* Tris·HCl, pH 8.0; eluent B, A + 0.5 *M* NaCl, pH 8.0; gradient, linear 0–100% B in 2 min; flow-rate, 4.0 ml/min; detection, UV at 280 nm; column, PL-SAX 4000 Å 8 μm, 50 × 4.6 mm I.D.; PEEK hardware. Peaks: 1 = antibodies; 2 = transferrin; 3 = albumin.

an analytical column, PL-SAX 4000 Å 8 μm, 50 × 4.6 mm I.D. PEEK column and a total protein load of 36 μg baseline resolution of two components was achieved in less than 2 min. As it is known that the enzyme amyloglycosidase occurs in two forms with molecular weights of 99 000 daltons and 112 000 daltons of the same amino acid composition but with different carbohydrate content[22] an enzyme activity measure-

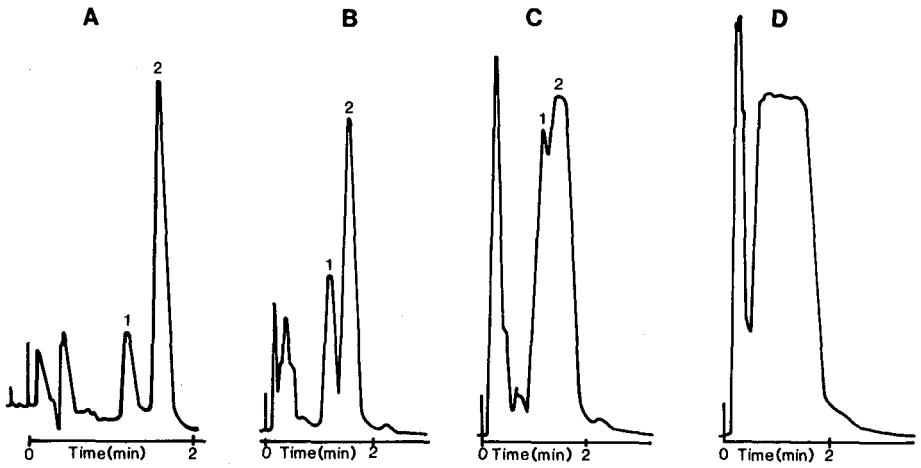

Fig. 7. Anion-exchange separation of two isoenzymes of amyloglucosidase from *Aspergillus niger* cell culture filtrate. (A) 36 μg of protein; (B) 3.6 mg of protein; (C) 10 mg of protein; (D) 20 mg of protein. Eluent A, 0.01 *M* Tris·HCl, pH 8.0; Eluent B, A + 0.5 *M* NaCl, pH 8.0; gradient, linear 0–100% B in 2 min; flow-rate, 4.0 ml/min; detection, UV at 280 nm; column, PL-SAX 4000 Å 8 μm, 50 × 4.6 mm I.D.; PEEK hardware.

ment was carried out on both peaks, by adding an aliquot of the fractions to a 1% starch solution heated to 60°C. After a 10-min hydrolysis the amount of glucose produced was determined using the dinitrosalicylic acid assay[23]. Enzyme activity was confirmed in both peaks 1 and 2. Using the analytical size column baseline resolution of the two isoenzymes can be achieved with loadings upto 1.4 mg; however, for the purification of total enzyme a column load of 20 mg can be chromatographed with a 2-min gradient development time and 30 s re-equilibration (Fig. 7). This would enable 480 mg of protein to be fractionated per hour with an analytical 50 × 4.6 mm I.D. column.

CONCLUSION

From this initial evaluation of the high-speed, fast flow matrix both as a reversed-phase material, PLRP-S 4000 Å and in the derivatized form as a strong anion exchanger, PL-SAX 4000 Å, it would appear to be a more universal solution to the speed/capacity/resolution triangle. When used with short gradient development times and high linear velocities resolution and loading are comparable to those achieved under conventional HPLC conditions for wide pore matrices.

The equipment requirements for the use of these materials are not as severe as with the non-porous matrices due to the higher loadings involved although the requirement on the pumping system and gradient former are similar. The work reported here was carried out using an unmodified analytical UV detector with a 10 μl cell volume and 10 mm path length.

It is anticipated that the main application areas for these material will be in the analysis of very large biomolecules under conventional HPLC conditions, the rapid preparative fractionation of biologically active molecules in mg–g quantities, high-speed purity determination of fractions from a large-scale LC process and the optimization of product yields from fermentation broths and process separation systems.

REFERENCES

1 K. Tsuji and J. H. Robinson, *J. Chromatogr.*, 112 (1976) 663.
2 S. H. Chang, K. M. Gooding and F. E. Regnier, *J. Chromatogr.*, 112 (1976) 103.
3 S. Ohlson, L. Hansson, P. O. Larssen and K. Mosbach, *FEBS Lett*, 93 (1978) 5.
4 F. E. Regnier and R. Noel, *J. Chromatogr. Sci.*, 14 (1976) 316.
5 H. A. Sober and E. A. Peterson, *J. Am. Chem. Soc.*, 76 (1954) 1711.
6 E. A. Peterson, *Cellulosic Ion Exchangers*, Elsevier, Amsterdam, 1970.
7 J. Porath and P. Flodin, *Nature (London)*, 183 (1959) 1657.
8 J. C. Moore, *J. Polym. Sci. Part A*, 2 (1964) 835.
9 T. N. Tweeten, K. A. Tweeten, F. P. Warner and L. L. Lloyd, *5th International Symposium on HPLC of Proteins, Peptides and Polynucleotiedes, Toronto, November 4–6, 1985.*
10 G. Guiochon and M. Martin, *J. Chromatogr.*, 326 (1985) 3.
11 K. K. Unger, R. Janzen and G. Jilge, *Chromatographia*, 24 (1987) 144.
12 B. Anspach, K. K. Unger, H. Giesche and M. T. W. Hearn, *4th International Symposium on HPLC of Proteins, Peptides and Polynucleotides, Baltimore, MD, December 10–12, 1984.*
13 G. Jilge, R. Janzen, H. Giesche, K. K. Unger, J. N. Kinkel and M. T. W. Hearn, *J. Chromatogr.*, 397 (1987) 71.
14 R. Janzen, K. K. Unger, H. Giesche, J. N. Kinkel and M. T. W. Hearn, *J. Chromatogr.*, 397 (1987) 91.
15 M. A. Rounds and F. E. Regnier, *J. Chromatogr.*, 443 (1988) 73.
16 D. J. Burke, J. K. Duncan, C. Siebert and G. S. Ott, *J. Chromatogr.*, 359 (1986) 533.

17 J. Jacobson, J. Frenz and Cs. Horváth, *J. Chromatogr.*, 316 (1984) 53.
18 M. A. Rounds, W. D. Rounds and F. E. Regnier, *J. Chromatogr.*, 397 (1987) 25.
19 P. A. Bristow, *LC In Practice,* hetp, Wilmslow, Cheshire, 1976, p. 41.
20 J. V. Dawkins and M. Hemming, *Makromol. Chem.*, 176 (1975) 1795.
21 G. Jilge, K. K. Unger, U. Esser, H. J. Schafer, G. Rathgeber and W. Muller, *J. Chromatogr.*, 476 (1989) 37.
22 J. H. Pazur and T. Ando, *J. Biol. Chem.*, 234 (1959) 1966.
23 M. F. Chaplin in M. F. Chaplin and J. F. Kennedy (Editors), *Carbohydrate Analysis*, IRL Press, Oxford, 1986, p. 3.

Journal of Chromatography, 512 (1990) 377–386
Elsevier Science Publishers B.V., Amsterdam

CHROMSYMP. 1872

Binding of lysozyme on the surface of entrapped phosphatidylserine–phosphatidylcholine vesicles and an example of high-performance lipid vesicle surface chromatography

QING YANG* and PER LUNDAHL
Department of Biochemistry, Biomedical Centre, University of Uppsala, P.O. Box 576, S-751 23 Uppsala (Sweden)

ABSTRACT

Phospholipid vesicles (liposomes) composed of phosphatidylserine (PS) and phosphatidylcholine (PC) in five different molar ratios were formed and entrapped in agarose gel beads (Sepharose 6B and Superose 6). For this purpose a previous dialysis–entrapment procedure was improved by use of an apparatus with continuous buffer flow and rotating dialysis cells. By rotary dialysis combined with a method of vesicles fusion with the aid of Ca^{2+} ions, the capacity of entrapped vesicles composed of 80–85% phosphatidylserine from bovine brain [denoted "PS (brain extract)"] was increased. The entrapment of PS–PC vesicles increased as the content of PS was increased. Lysozyme was applied to a PS–PC vesicle–Sepharose 6B column. The amount of bound lysozyme was about 9 nmol per μmole of lipids for entrapped PS–PC vesicles with 20 and 45 mol-% PS contents. The amounts of bound lysozyme increased to 29, 30 and 40 nmol per μmole of lipids as the fraction of PS in the vesicles was increased to 65, 80–85 and 100 mol-% PS, respectively. The lysozyme molecules thus closely packed on the surface of the vesicles with the higher PS contents. The losses of the entrapped vesicles in the first two chromatographic lysozyme-binding experiments were 5% for 80–85% PS (brain extract) vesicles, 10–12% for vesicles with 20 to 65 mol-% PS content and 23% for pure PS vesicles. PS (brain extract) vesicles were also formed and entrapped in Superose 6 gel beads (diameter 13 μm). Ribonuclease A, lysozyme and cytochrome *c* were well separated on this PS-vesicle–Superose column at an ionic strength of 0.05–0.15 *M*.

INTRODUCTION

Dialysis entrapment of lipid vesicles and protein lipid vesicles in gel beads without the use of hydrophobic ligands, *i.e.*, entrapment of vesicles (liposomes) in gel bead pores as the vesicles are formed on dialysis, has recently been developed in our

0021-9673/90/$03.50

laboratory[1]. Separation of bovine albumin monomers and dimers, for instance, can be done by anion-exchange chromatography on 20% stearylamine–egg yolk phospholipid vesicles entrapped in Sepharose 6B[2]. For chromatographic purposes it is of interest to know the effects of the ligand density of charged lipids in the entrapped vesicle bilayer on the capacity of binding of protein to the vesicles and on the reproducibility of the capacity values. For the separation of bound and unbound proteins and for the release of the bound proteins from the vesicle surfaces, chromatography of the proteins on the entrapped vesicles should be simpler than the ultracentrifugation method, which has been employed for binding studies heretofore[3–6]. Entrapped vesicles might provide a convenient and rapid method for investigating the binding of proteins and peptides to lipid vesicle surfaces, especially for testing the reversibility of the binding.

By the use of pure phosphatidylserine (PS) and pure phosphatidylcholine (PC) we studied the effects of the ligand density in the entrapped vesicle surfaces on the binding of lysozyme. Lysozyme, a basic protein, has been widely used in studies of interactions of protein with negatively charged phospholipid vesicles[4,7–9]. We have also carried out the high-performance ion-exchange chromatography of lysozyme, ribonuclease A and cytochrome *c* on anionic vesicles entrapped in a small-bead agarose gel (Superose 6). In this work we used a dialysis apparatus with a rotating cell surrounded by slowly flowing buffer in combination with a Ca^{2+}–EDTA chelation procedure for vesicle fusion in order to increase the entrapment capacity of the vesicles composed of PS. The Ca^{2+}–EDTA chelation method, previously reported by Papahadjopoulos *et al.*[10], was improved by Gould-Fogerite and Mannino[11], who employed an apparatus for rotary dialysis.

EXPERIMENTAL

Materials

Sepharose 6B and Sephacryl S-1000 gels as well as prepacked Mono S and Superose 6 columns were obtained from Pharmacia-LKB Biotechnology (Uppsala, Sweden). Lysozyme (chicken egg white, L-6876), ribonuclease A (bovine pancreas, type III-A, R-5125) and cytochrome *c* (horse heart type III, C-2506) were purchased from Sigma (St. Louis, MO, U.S.A.). Spectrapor dialysis membrane tubing with a nominal molecular weight cut-off of 6000–8000 and a diameter of 20.4 mm was bought from Spectrum Medical Industries (Los Angeles, CA, U.S.A.). Phosphatidylcholine (PC) from egg yolk and purified phosphatidylserine (PS) from bovine brain were purchased in the form of chloroform solutions in sealed ampoules from Avanti Polar Lipids (Birmingham, AL, U.S.A.) and were stored at −70°C. Brain extract containing 80–85% PS and other brain lipids [here denoted "PS (brain extract)"] (bovine brain type III, B-1627) and Tris (Trizma base) were bought from Sigma, $CaCl_2$, NaCl and EDTA were obtained from Merck (Darmstadt, F.R.G.) and 2-mercaptoethanol and cholic acid from Fluka (Buchs, Switzerland).

Rotary dialysis–entrapment

An appropriate amount of PC and PS in chloroform was transferred to a 5-ml glass vial fitted with a screw-cap lined with aluminium foil. The mixture was dried to a thin film under a stream of nitrogen, and nitrogen was passed over the lipid film for

10 min in order to remove the residual traces of chloroform. The lipid film was dissolved in 1.5 ml of dialysate solution (200 m*M* NaCl–1 m*M* 2-mercaptoethanol–5 m*M* Tris–HCl, pH 7.1) supplemented with 100 m*M* cholate under nitrogen at room temperature. The sum of the concentrations of PS and PC was 40 m*M*. A 1.2-ml volume of the lipid solution was pumped into a Sepharose 6B column (12 mm × 10 mm I.D.) or a Superose 6 column (50 mm × 5 mm I.D.) at a flow-rate of 15 ml/h. The gel bead diameters were 45–165 μm for Sepharose 6B and 13 ± 2 μm for Superose 6. The mixture of the gel and the lipid solution was then transferred from the column into a dialysis cell (see Fig. 1 in ref. 1) by use of the excess 0.3 ml of the lipid solution. To control the rate of detergent removal on vesicle formation and provide thorough mixing of the gel beads with the lipid–cholate solution during the dialysis–entrapment process, a rotary dialysis apparatus consisting of a magnetically driven Perspex rotor inside a 300-ml dialysate container was constructed. Two dialysis cells were fixed at opposite sides of the dialysis rotor and buffer was pumped slowly through the container, as detailed below. The cells containing the mixture of the gel and lipid solution (see above) were dialyzed with rotation, first for 12 h against dialysate solution in order to form vesicles (rotor speed 15 rpm), second against dialysate solution containing 5 or 50 m*M* $CaCl_2$ for 8 h to induce fusion of the vesicles and third against dialysate containing 10 m*M* EDTA (buffer E) for 15 h at a rotor speed of 40 rpm. The rate of buffer flow through the container was 120 ml/h. After dialysis the gel beads were washed three times with buffer E by centrifugation at 150 *g* for 5 min. The suspensions containing non-entrapped vesicles were collected and 200 μl of the suspension were applied to a Sephacryl S-1000 column for determination of the K_d value (for details see the legend to Fig. 1). The gel beads containing entrapped anionic vesicles were repacked into columns (sizes as above) and washed further by elution with 3–5 column volumes of buffer E before equilibration with starting buffer (see below).

Determination of lysozyme binding capacities of entrapped vesicles containing five different amounts of phosphatidylserine

A 5-mg amount of lysozyme in 2.5 ml of starting buffer was applied to an anionic vesicle–Sepharose 6B column (12 mm × 10 mm I.D.). This column was pre-equilibrated with starting buffer (50 m*M* NaCl–0.1 m*M* EDTA–5 m*M* Tris–HCl, pH 7.1) and connected to a UV monitor (UV-2; Pharmacia-LKB Biotechnology) and a recorder for monitoring the course of saturation of the entrapped vesicles. Following sample application the column was washed with ten bed volumes of the above buffer. The bound lysozyme was then released by elution with 0.3 *M* NaCl containing 0.1 m*M* EDTA and 5 m*M* Tris–HCl (pH 7.1). Two chromatographic experiments were done on each column. All of the effluent fractions from the rinsing, elution and equilibration were collected in tared tubes for weight determination and the amount of released phospholipids present in each was determined by phosphorus analyses according to the method of Bartlett[12]. The initial amount of entrapped phospholipids was calculated as the sum of the amount of lipids released during the chromatographic experiments and the amount of lipids solubilized with 100 m*M* cholate.

The amounts of desorbed lysozyme were determined by automated amino acid analysis following hydrolysis for 24 h in 6 *M* HCl. Owing to the presence of trace amounts of serine from PS, the amount of protein was calculated from the known

amino acid composition of lysozyme using the analysis values for a few stable amino acids.

High-performance ion-exchange chromatography

Superose 6 (cross-linked agarose gel beads of diameter 13 ± 2 μm) with entrapped PS (brain extract) vesicles was packed into a column (40 or 50 mm × 5 mm I.D.). This column, or a 55 mm × 5 mm I.D. column of Mono S (a strong cation exchanger with a gel bead diameter of 10 μm) used as a control, was connected to two precision pumps (P-500), a mixer, a sample injection valve (V-7) and UV monitor set at 280 nm (UV-1). This system was controlled by a liquid chromatography controller (LCC-500 Plus). All of these components were provided by Pharmacia-LKB Biotechnology.

RESULTS

Entrapment of negatively charged phospholipid vesicles

The capacity for entrapment of PS (brain extract) vesicles in Sepharose 6B was 2.0 μmol lipid/ml packed gel on rotary dialysis without addition of $CaCl_2$. On addition of 5 m*M* Ca^{2+} to a dialysate solution (see Experimental) to induce fusion of the vesicles, the capacity increased to 4.4 μmol lipid/ml packed gel, *i.e.*, by a factor of about two. The K_d value of the corresponding non-entrapped vesicles on Sephacryl S-1000 (see legend to Fig. 1) was 0 for the fused vesicles and 0.39 for the non-fused vesicles. The vesicles thus grow considerably in the fusion process. The effect of Ca^{2+} on the entrapment capacity may be due to this enlarged size of the vesicles on fusion. Under the same conditions of fusion and entrapment for PS–PC (molar ratio 82.5:17.5) vesicles the capacity was 2.2 μmol/ml packed gel and the K_d value was 0.41. Fusion of

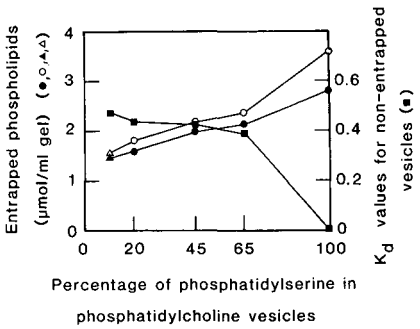

Fig. 1. Capacities for entrapment of PS–PC vesicles in Sepharose 6B gel beads. Formation of vesicles and simultaneous entrapment were done by dialysis of cholate-solubilized phospholipids in the presence of gel beads (see Experimental). (●, ○) Dialysis against dialysate solution in the presence of 50 m*M* Ca^{2+} (see Experimental); (▲, △) dialysis against dialysate solution without addition of Ca^{2+} ions; (○, △) calculated initial amounts of entrapped phospholipids before chromatography of lysozyme (see Experimental); (●, ▲) final amounts of entrapped phospholipids, determined after solubilization with 100 m*M* cholate following chromatographic experiments. K_d values (■) were obtained by chromatography on non-entrappd vesicles on Sephacryl S-1000 [column 60 cm × 1 cm I.D., flow-rate 6 ml/h (determined by weighing) and sample volume 0.2 ml]. The K_d value is defined as $(V_e - V_0)/(V_t - V_0)$, where V_0 and V_t are the void volume and total volume of the packed column, respectively, and V_e is the elution volume of non-entrapped vesicles (see Experimental).

the PS–PC vesicles at room temperature, which is above the phase transition temperature, was very limited compared with that observed with the PS (brain extract) vesicles, where fusion was enhanced by contamination with phosphatidylethanol amine[13–15]. It has been reported that for phosphatidylserine–dipalmitoylphosphatidylcholine (1:1) vesicle fusion was completely inhibited at 30°C and at 10 mM Ca^{2+} concentration (*cf.*, Fig 4 in ref. 16). Entrapped capacities of vesicles with five different molar ratios of PS to PC at a Ca^{2+} concentration of 50 mM are illustrated in Fig. 1 (○, ●). The amount of entrapped lipids increased with increasing content of PS. This may be consistent with an increase in vesicle size to different extents, which is reflected by the decreases in the K_d values of the corresponding non-entrapped vesicles (Fig. 1, ■).

The initial amount of entrapped phospholipid (Fig. 1, △, ○; see also Experimental) decreased by 23% for the pure PS vesicles and by 10–12% for entrapped PS–PC vesicles with lower PS contents (Fig. 1, ▲, ●) during the first two chromatographic lysozyme-binding experiments (see below) done after the entrapment. These losses seem to be related to protein effects on the lipid bilayers (see Discussion).

Effect of phosphatidylserine density

A basic protein, lysozyme (pI = 11), was used as a model protein in order to investigate the effect of ligand density on protein binding to vesicle surfaces. We found that the capacity of lysozyme binding to the PS–PC vesicles increased with increasing charge density of PS from 45 to 100 mol-%. Unexpectedly, the capacity was lower at 45

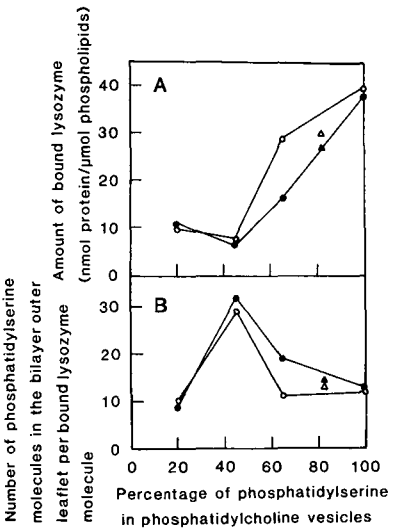

Fig. 2. (A) Binding of lysozyme to entrapped PS–PC vesicles (●, ○) and PS (brain extract) vesicles (▲, △) (see Experimental). An excess amount of lysozyme was applied to an entrapped vesicle–Sephadex 6B column for chromatographic binding experiments (see Experimental). (○, △) Amount of bound protein eluted during the first chromatographic run; (●, ▲) amount of protein eluted in the second chromatographic run. (B) Number of PS molecules in the outer lipid leaflet of the vesicles corresponding to one bound lysozyme molecule. The estimates were made by use of the data from (A) and the percentages of PS in PC vesicles. It is assumed that half of the total number of phospholipid molecules are in the outer leaflet of the bilayers. Symbols as in (A).

mol-% PS content than at 20 mol-% (Fig. 2A). Both of them showed lower protein binding capacities with respect to the capacities for the vesicles with higher PS contents (Fig. 2A). From these data we calculated the number of PS molecules in the outer phospholipid monolayer per bound lysozyme molecule (Fig. 2B). After each dialysis–entrapment the first chromatographic run showed 10–13 PS molecules per bound lysozyme molecule, except for the vesicles with 45 mol-% PS (Fig. 2B, △, ○). Not more than ten charges were therefore needed to bind each molecule of lysozyme on the vesicle surfaces on chromatography at an ionic strength about 50 m*M*.

The capacity for protein binding per μmole of lipids decreased by 41% from the first to the second chromatographic run on the PS–PC (65:35) vesicles (Fig. 2A). This decrease in protein capacity was accompanied by a phospholipid loss of only 7%. A possible explanation is that the released phospholipids in the eluted fractions may be enriched in PS. The charge density on the vesicle surfaces may therefore become decreased. For PS–PC (45:55) and PS–PC (20:80) vesicles the protein binding capacities were very similar in the first and second chromatographic runs (Fig. 2A). It seems that the charge density on the surface of the vesicles with lower PS contents was not changed much despite small losses of the entrapped vesicles (8% and 10%, respectively). The 80–85% PS vesicles entrapped in Sepharose 6B gel beads showed a high and nearly constant protein binding capacity (Fig. 2A) with a small loss of entrapped vesicles (about 5%) during two chromatographic experiments. For pure PS vesicles the loss of phospholipids on chromatography (Fig. 1) was higher (23%) compared with other PS–PC vesicles. This may be due to the extreme close-packing of protein molecules on the vesicle outer leaflet (see Discussion).

High-performance ion-exchange chromatography on entrapped-vesicle surfaces

PS (brain extract) vesicles were entrapped in Superose 6 gel beads. A mixture of ribonuclease A, lysozyme and cytochrome *c* was separated at an ionic strength below 0.15 *M* on the PS vesicle–Superose 6 column (Fig. 3A). A five-fold higher ionic strength was required for elution of the proteins from the commercial cation exchanger Mono S (Fig. 3C). For a control experiment the entrapped vesicles were solubilized and eluted from the Superose 6 column with 100 m*M* cholate. Chromatography of the protein mixture on the lipid-free Superose 6 column following equilibration of the column with starting buffer (see legend to Fig. 3) showed that most of the cytochrome *c* and ribonuclease A passed through the column on rinsing with starting buffer, whereas lysozyme was retarded in the column and was eluted as a very broad peak with increasing salt concentration (Fig. 3B). This may be due to both ionic and hydrophobic interactions of the protein(s) with the gel matrix. High-performance chromatography on the vesicle–Superose 6 column utilizing the entrapped vesicles was performed several times at room temperature over a period of 24 h in order to optimize the experimental conditions for separation. The total loss of lipids during the 24-h series was *ca.* 15%. Only the first elution profile was disturbed owing to the release of a small amount of entrapped vesicles from the column. To remove these unstable vesicles entrapped in Superose 6 gel beads one or two prechromatographic runs without application of proteins are recommended. Such a prechromatographic run caused a loss of entrapped vesicles of about 4% in a separate experiment. The amounts of entrapped lipids in Superose 6 gel beads were 2.5–3 μmol/ml packed gel.

We repeated the separation of the protein mixture on another PS vesicle–

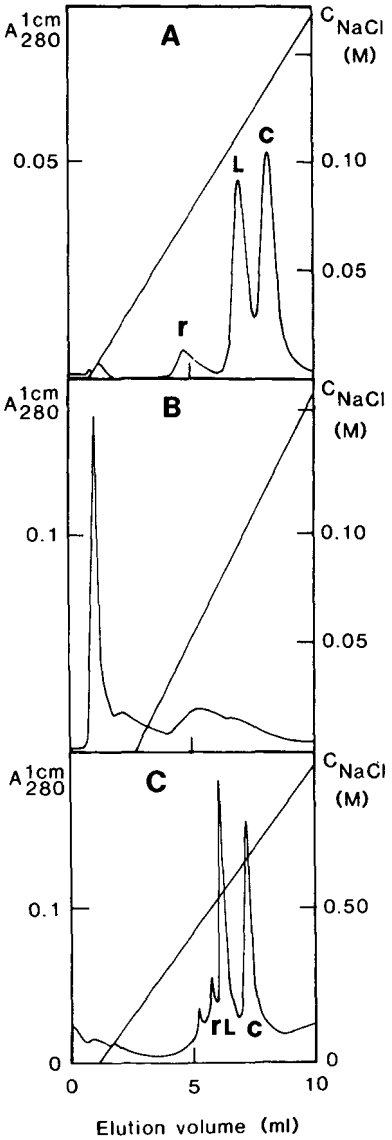

Fig. 3. High-performance ion-exchange chromatography of ribonuclease A (r), lysozyme (L) and cytochrome *c* (C). Sample: 25 μl of the protein mixture [protein concentrations are each 0.5 mg/ml for (A) and 1 mg/ml for (B) and (C)]. (A) Chromatography on PS vesicles entrapped in Superose 6 gel beads (column 40 mm × 5 mm I.D.). Flow-rate, 0.4 ml/min, except during sample application, when it was 0.1 ml/min. Starting buffer, 25 m*M* NaCl–0.1 m*M* EDTA–5 m*M* Tris–HCl (pH 7.0); end buffer, 0.2 *M* NaCl–0.1 m*M* EDTA–5 m*M* Tris–HCl (pH 7.0). (B) Chromatography on the lipid-free Superose 6 column. The entrapped vesicles were solubilized and eluted from the column in (A) with 100 m*M* cholate solution. This column was then equilibrated overnight with at least 100 column volumes of starting buffer to ensure complete removal of cholate, which may bind to the gel matrix. Flow-rate, 0.2 ml/min. Starting and end buffers as in (A). (C) Comparative experiment: chromatography on a Mono S column (55 mm × 5 mm I.D.). Flow-rate, 0.4 ml/min. 0.05 *M* NaCl for starting buffer and 1 *M* NaCl for end buffer in 5m*M* Tris–HCl (pH 7.1) containing 0.1 m*M* EDTA. Note the difference in ionic strength between (A) and (C).

Superose 6 column and obtained the same result as in Fig. 3A (not shown). The same result was also obtained after storage of this latter column at 7°C for about 72 h. When the entrapped vesicles were saturated with lysozyme and the protein was released by elution, 23% of the lipids were lost from the PS vesicle–Superose 6 column, much more than the corresponding loss of the same type of vesicles entrapped in Sepharose 6B gel beads. In other words, entrapped PS (brain extract) vesicles are more stable in Sepharose 6B than in Superose 6 gel beads. The reason for this is not clear.

DISCUSSION

Lysozyme is a basic protein with a p*I* value of 11 and the dimensions 45 × 30 × 30 Å. By use of the estimated cross-sectional areas of lysozyme (30 × 30 = 900 $Å^2$; *cf.*, Fig. 3 in ref. 7 and Fig. 5 in ref. 8) and of egg yolk phospholipid molecules (*ca.* 70 $Å^2$, ref. 17) we can estimate from the results shown in Fig. 2A that about 30% of the outer leaflet of the bilayer became occupied by the protein for PS–PC (20:80) vesicles and about 20% for PS–PC (45:55) vesicles. These values are consistent with the value reported previously[2] for ferritin binding: the area covered by ferritin was 30% on egg yolk phospholipid vesicles containing 20% stearylamine. These estimates of the protein-covered area of the vesicle surface imply that for charge densities corresponding to 20–50% PS, the area that may be covered by proteins on vesicle surfaces is limited to *ca.* 20–30%, presumably owing to spatial limitations, electrostatic repulsion between bound protein molecules and weak attraction between protein and the vesicle surface. The result shown in Fig. 2B for PS–PC (45:55) vesicles may therefore indicate that more than half of the PS molecules were not involved in binding of protein molecules. We propose that a 50% PS ligand density is a sort of threshold value for close packing of lysozyme onto the vesicle surfaces. Above this density the attraction between the protein and the vesicle surfaces may become the dominant force. Using the cross-sectional area of 900 $Å^2$ per lysozyme molecule, we obtained values of about 75%, 79% and 100% protein-covered area of the vesicle surface for 65% PS, 80–85% PS (brain extract) and 100% PS vesicles (data from Fig. 2A, ○, △), respectively. These values indicate that the packing of the protein molecules on the vesicle surface containing high PS contents is extremely compact.

It is interesting that the packing of cytochrome *c* reported in Table I in ref. 18 corresponds to about ten lipid molecules per bound protein molecule, similar to the values we have found for lysozyme binding on PS vesicles. As about ten PS molecules were available per bound lysozyme molecule (except at 45% PS) and as the net charge of lysozyme is about +10 at pH 7, we can possibly regard the protein as a type of multivalent counter ion to the vesicle surface charges. As the vesicle surface is flexible and the charged lipid molecules can diffuse laterally, optimum binding can always be attained, either between a few charges on the protein (at close packing) and many charges on the vesicle surface (at high charge density), or between several charges on the protein (at optimum protein orientation) and a limited number of vesicle surface charges (at low charge density). In most instances the total net charge of all bound protein molecules at saturation seems to correspond well with the total net charge of the vesicle surfaces.

The losses of entrapped phospholipid vesicles on saturation of the vesicles with protein followed by elution with increasing ionic strength were always higher than

those observed with gradient elution alone without application of protein (see Results). The same phenomenon was also observed in previous experiments (*cf.*, Fig. 1 in ref. 2). The fact that the loss of lipid vesicles was affected not only by increasing osmotic pressure but also by the binding and release of protein may be explained as follows: binding of lysozyme may form microdomains in the membrane bilayers with different "microviscosity"[18]. The bilayer may therefore have become pertubed by the surface-bound protein molecules[18,19]. Further, hydrophobic interaction between bound lysozyme and the lipid membrane may occur to some extent[4,7,8]. The entrapped vesicles containing microdomains on their surfaces may shrink more in response to increasing salt concentration than do those lacking the microdomains. Some of the shrunken vesicles became smaller than pore size of the gel beads in which they were formed and were thus released from the vesicle–gel column.

Pidgeon and Venkataram[20] reported the separation of proteins and peptides on a high-performance liquid chromatographic column of silica beads (7 μm in diameter) covered by phosphatidylcholine. Using entrapped PS vesicles in Superose 6 gel beads (13 μm in diameter), we succeeded in demonstrating the separation of model proteins on the vesicle surface by high-performance ion-exchange chromatography. The entrapped vesicles are relatively stable toward changes in osmotic pressure and on storage and, as expected, against higher pressures over the column. For the vesicle–Superose 6 column the ionic strength required for elution of the proteins was much lower than that required for the commercial Mono S column (see Fig. 3A and C). This is due to the low charge density and the uniform charge distribution on the vesicle surfaces and indicates that vesicle surface ion-exchange chromatography is a very mild method.

CONCLUSIONS

An increased capacity for the entrapment of negatively charged vesicles in gel beads can be obtained by a vesicle fusion procedure. Lipid vesicles entrapped in gel beads can be used for chromatographic studies of lipid bilayer–protein interactions. Close packing of lysozyme on PS–PC vesicles was observed at PS contents above 45%. Further, high-performance vesicle surface chromatography can be done under very mild experimental conditions, as exemplified by the ion-exchange chromatography of basic proteins on entrapped PS vesicles.

ACKNOWLEDGEMENTS

We thank Eva Greijer for valuable assistance and manuscript editing. We also appreciate help from Erik Mascher and David Eaker. We are grateful for financial support from the Swedish National Board for Technical Development (Grant No. 89-519P), the Swedish Natural Science Research Council and the O.E. and Edla Johansson Science Foundation.

REFERENCES

1 M. Wallstén, Q. Yang and P. Lundahl, *Biochim. Biophys. Acta*, 982 (1989) 47.
2 Q. Yang, M. Wallstén and P. Lundahl, *J. Chromatogr.*, 506 (1990) 379.
3 C. Sweet and J. E. Zull, *Biochim. Biophys. Acta*, 219 (1970) 253.

4 H. K. Kimelberg and D. Papahadjopoulos, *J. Biol. Chem.*, 246 (1971) 1142.
5 J. Gutowicz and T. Modrzycka, *Biochim. Biophys. Acta,* 512 (1978) 105.
6 J. Kim and H. Kim, *Biochemistry*, 25 (1986) 7867.
7 T. Gulik-Krzywicki, E. Shechter, Vittorio Luzzati and M. Faure, *Nature (London)*, 223 (1969) 1116.
8 T. Gulik-Krzywicki, E. Shechter, M. Iwatsubo, J. L. Ranck and Vittorio Luzzati, *Biochim. Biophys. Acta,* 219 (1970) 1.
9 G. Oshima, *J. Biochem.*, 94 (1983) 1615.
10 D. Papahadjopoulos, W. J. Vial, K. Jacobson and G. Poste, *Biochim. Biophys. Acta,* 394 (1975) 483.
11 S. Gould-Fogerite and R. J. Mannino, *Anal. Biochem.*, 148 (1985) 15.
12 G. R. Bartlett, *J. Biol. Chem.*, 234 (1959) 466.
13 R. R. Cullis and A. J. Verkleij, *Biochim. Biophys. Acta,* 552 (1979) 546.
14 P. R. Cullis and B. de Kruiff, *Biochim. Biophys. Acta,* 559 (1979) 399.
15 L. V. Chernomordik, M. M. Kozlov, G. B. Melikyan, G. B. Abidor, V. S. Markin and Y. A. Chizmadzher, *Biochim. Biophys. Acta,* 812 (1985) 643.
16 N. Düzgünes, J. Paiement, K. B. Freeman, N. G. Lopez, J. Wilschut and D. Papahadjopoulos, *Biochemistry*, 23 (1984) 3486.
17 M. Z. Atassi and F. S. A. Habeeb, *Methods Enzymol.*, 25 (1972) 546.
18 P. Mustonen, J. A. Virtanen, P. J. Somerharju and P. K. J. Kinnunen, *Biochemistry,* 26 (1987) 2991.
19 J. F. Faucon, J. Dufourcq, C. Lussan and R. Bernon, *Biochim. Biophys. Acta,* 436 (1976) 283.
20 C. Pidgeon and U. V. Venkataram, *Anal. Biochem.*, 176 (1989) 36.

Journal of Chromatography, 512 (1990) 387–394
Elsevier Science Publishers B.V., Amsterdam

CHROMSYMP. 1889

Isolation of anti-idiotypic antibodies by immunoaffinity chromatography on Affinichrom beads

TERRY M. PHILLIPS*
Immunochemistry Laboratory, The George Washington University Medical Center, Room 413 Ross Hall, 2300 Eye Street, N.W., Washington, DC 20037 (U.S.A.)
and
JAMES V. BABASHAK
Kontes Scientific Glassware, Vineland, NJ (U.S.A.)

ABSTRACT

Anti-idiotypic antibodies are important regulators of the immune system but they are difficult to isolate and monitor. We have developed a technique for isolating specific auto-anti-idiotypic antibodies by high-performance immunoaffinity chromatography using immobilized autologous anti-tumor antibodies as the affinity ligand. The isolated anti-idiotypes demonstrated the ability to react with the original anti-tumor antibodies and inhibit their reactivity against autologous tumor cells. This technique can be used to monitor regulatory antibodies in cancer patients receiving immune modulation therapy.

INTRODUCTION

Anti-idiotypic antibodies are part of the regulatory pathways of the immune system and are responsible for regulating both humoral and cellular immune responses[1–5]. They are actively involved in the down-regulation of the immune system in cancer patients and are thought to be responsible for the suppression of active immune surveillance against growing tumor cells[6–8]. This leads to a loss of host control over the growing neoplasm and is thought by some investigators to be the first step that leads to the metastatic spread of the cancer[6–9].

Anti-idiotypic antibodies react with sites in the hyper-variable or antigen-binding regions of the target antibody (idiotype) and inhibit it from reacting with the antigen[10]. In a similar manner, suppressive anti-idiotypic antibodies can interact with specific antigen receptors on activated T cells and suppress clonal expansion, even in the presence of antigen[11]. Although these inhibitory antibodies can be detected by antigen binding inhibition studies using the original idiotype and its reactive antigen, isolation and measurement of reactive anti-idiotypes is difficult. Affinity chromatography or immunoprecipitation techniques, using solid-phase or cross-linked im-

0021-9673/90/$03.50

munoglobulin G (IgG) molecules have been used to isolate anti-idiotypes, but these techniques have been shown to isolate other anti-antibodies, such as anti-F(Ab)$_2$ and rheumatoid factor[12].

In an attempt to study the involvement of inhibitory anti-idiotypes in the suppression of immune responses in cancer patients receiving immunomodulatory therapy, we developed a high-performance immunoaffinity chromatography (HPIAC) technique for isolating specific auto-anti-idiotypic antibodies in a biologically active form.

EXPERIMENTAL

Materials

Solid glass beads (diameter, 1 mm) were obtained from Kontes (Vineland, NJ, U.S.A.). Purified streptavidin was purchased as a lyophilized, pure product from Bethesda Research Labs (Gaithersburg, MD, U.S.A.) and reconstituted in 0.5 *M* carbonate buffer, pH 9.0. The hydrazine biotin and the laboratory chemicals including the 3-aminopropyltriethoxysilane and 1,1′-carbonyldiimidazole (CDI) were obtained from Sigma (St. Louis, MO, U.S.A.). All columns and column fittings were purchased from Alltech (Deerfield, IL, U.S.A.). Radiolabels (^{51}Cr and ^{125}I) were obtained from Amersham (Arlington Heights, IL, U.S.A.). Immunodiffusion plates and the human IgG standards were obtained from Kallestad (Austin, TX, U.S.A.).

Blood samples from 50 patients with malignant melanoma, on active immunotherapy were obtained weekly. Autologous tumor material was obtained following surgical resection and scissor-minced into a single cell suspension and following controlled-rate freezing, the suspensions were stored at −136°C in vapor-phase liquid nitrogen.

Detection and isolation of anti-tumor antibodies

The patients' serum samples were checked for the presence of cytotoxic anti-tumor antibodies by a chromium release assay[13], with use of ^{51}Cr-labeled autologous tumor cells. Samples which exhibited specific autologous anti-tumor activity were selected for further purification. Reactive anti-tumor antibodies were isolated by incubating the patients' serum overnight at 4°C with a pellet of autologous cells fixed in 50 ml of 2% glutaraldehyde. After extensive washing to remove unreacted serum, the tumor cells were incubated in 2 *M* sodium thiocyanate, for 30 min at room temperature, then centrifuged at 500 *g* for 20 min. The supernate was dialyzed overnight against 0.1 *M* phosphate buffer, pH 7.2 and further purified by cross-absorption against a panel of allogeneic melanoma cell lines. The isolated antibody preparations were checked by immunoelectrophoresis and the immunoglobulin content measured by radial immunodiffusion.

Western blot analysis of the anti-tumor antibodies

The specificity of the isolated anti-tumor antibodies was checked by performing a Western blot[14] against polyacrylamide gel maps of sodium dodecyl sulfate-solubilized autologous and allogeneic melanoma cell membranes. Briefly, 100 μl of each patient's anti-tumor antibodies were reacted against western blots, of the major protein bands of the patient's autologous tumor and against the 125 000-dalton band

isolated from two allogeneic tumors and from six melanoma cell lines, overnight at 4°C. The bound antibodies were detected by reacting the blot with ^{125}I-labelled anti-human IgG for 2 h at room temperature. Each band was cut from the nitrocellulose paper, washed in 0.1 *M* phosphate buffer and counted.

Affinichrom streptavidin immunoaffinity beads

The glass beads were cleaned, silanized and activated with carbonyldiimidazole as previously described[15–17]. The beads were air-dried and used immediately for immobilization of the streptavidin. A 10-g amount of the CDI-derivatized beads was suspended in 5 ml of doubly distilled water prior to the addition of 5 ml of 0.5 *M* carbonate buffer containing 2.5 mg of streptavidin. The mixture was placed into a 15-ml capped glass tube and incubated for 18 h at 4°C in an overhead mixer. Following this incubation, the beads were allowed to settle and washed ten times in 0.01 *M* phosphate buffer, pH 7.2 by sedimentation and decantation. Attachment of the streptavidin to the beads was checked by incubating a drop of the bead suspension, obtained from the last wash, with fluorescein-labelled biotin and examining 100 beads under a fluorescence microscope.

Construction of the immunoaffinity column

The idiotypic anti-tumor antibodies were biotinylated via their carbohydrate component of the fragment crystalline (Fc) portion by reacting them with hydrazide-derivatized biotin as previously described[15–18]. The biotinylated antibodies were immobilized on the streptavidin-coated glass beads by incubating 1 ml of the antibody solution (adjusted to 150 μg/ml in 0.5 *M* carbonate buffer, pH 8.5) with 10 g of the streptavidin-coated glass beads overnight at 4°C. The beads were then washed five times in 0.1 *M* phosphate buffer, pH 7.2 and slurry-packed into a 5 cm × 4.6 mm (I.D.) HPLC column and attached to the HPLC system.

HPIAC isolation of auto-anti-idiotypic antibodies

HPIAC was performed with a Beckman Model 340 isocratic high-performance liquid chromatography (HPLC) system (Beckman, Palo Alto, CA, U.S.A.), comprising a Model 112 pump, a Model 160 ultraviolet detector set at 280 nm and a Shimadzu C-R1B peak integrator (Shimadzu, Columbia, MD, U.S.A.). Elution control was performed by programming an Autochrom Model III OPG/S solvent selector (Autochrom, Milford, MA, U.S.A.).

A 100-μl volume of the patient's serum was injected into the system, through an Altex 210 injection port and the column isocratically developed at 1 ml/min for 15 min with 0.1 *M* phosphate buffer, pH 7.0 as the mobile phase. Throughout the entire run, the column temperature was maintained at 4°C by a glass column jacket, attached to a recycling ice-bath.

Following the initial 15-min run, during which the auto-anti-idiotypic antibodies reacted with the immobilized ligand, an elution recovery phase was started A chaotropic ion gradient was developed by adding 0 to 2.5 *M* sodium thiocyanate to the running buffer, over a further 15 min and maintained at the high level for 5 min before recycling the column back to the original running buffer. Fractions of the eluted material were collected in 500-μl Beckman Microfuge tubes, in a modified ISCO Cygnet fraction collector (ISCO, Lincoln, NB, U.S.A.) and dialyzed overnight at 4°C against 0.01 *M* phosphate, pH 7.2.

Inhibition studies

The specificity of the immunoaffinity purified anti-idiotypic antibodies was tested by studying their ability to inhibit the antigen-binding capacity of the original anti-tumor antibodies. The tumor cells were thawed at 37°C and following a cell count, adjusted to $1 \cdot 10^6$ cells/ml in RPMI 1640 medium prior to freezing and thawing three times. The disrupted cells were then sonicated for 2 min at maximum power. The sonicated pellet was resuspended in 2 ml of 0.01 *M* phosphate buffer and the membrane fraction was isolated by centrifugation of 100 000 *g* for 60 min. The membrane-enriched supernatant from the autologous tumor cells were labeled with ^{125}I by the lactoperoxidase technique[19] and incubated with either the anti-tumor antibody or a mixture (preincubated for 30 min at room temperature) of anti-tumor antibody and anti-idiotypic antibody. Samples collected after 0, 5, 10, 20, 40, 80 and 160 min of incubation were precipitated with 100% saturated ammonium sulfate and the precipitates were analyzed for the presence of radiolabelled antigen.

RESULTS

The presence of autologous cytotoxic anti-tumor antibodies was demonstrated in 41 of the 50 patients studied and was shown to be strongest at 21 days post-treatment. This anti-tumor activity was shown to last for five to six week before there was a sharp decline in the antibody concentrations. Repeat treatments produced a second peak of cytotoxic anti-tumor activity, that lasted for three to five weeks before returning to baseline.

Isolation of the anti-tumor antibodies from the positive samples, by absorption to fixed autologous tumor cells yielded an average IgG anti-tumor antibody concentration of 120–270 ng/ml but following cross-absorption against six melanoma cell lines resulted in a reduction of the anti-tumor antibody levels to 60–85 ng/ml. Western blot analysis demonstrated that the anti-tumor antibodies reacted only with

TABLE I

BINDING SPECIFICITY OF THE ANTI-TUMOR ANTIBODIES AGAINST WESTERN BLOTS OF TUMOR ANTIGENS

Blotted antigen	*Band (molecular weight, dalton)*	*^{125}I-labeled antibody binding (counts/min)*[a]
Autologous tumor	125 000	35199 ± 1587
Autologous tumor	92 000	305 ± 221
Autologous tumor	51 000	499 ± 515
Autologous tumor	21 000	428 ± 364
Allogeneic tumor I	125 000	914 ± 400
Allogeneic tumor II	125 000	1245 ± 704
Melanoma cell line 1	125 000	608 ± 627
Melanoma cell line 2	125 000	455 ± 309
Melanoma cell line 3	125 000	617 ± 300
Melanoma cell line 4	125 000	511 ± 363
Melanoma cell line 5	125 000	490 ± 388
Melanoma cell line 6	125 000	639 ± 426

[a] Counts expressed as mean minus backgroup ± standard error of the mean (n = 41).

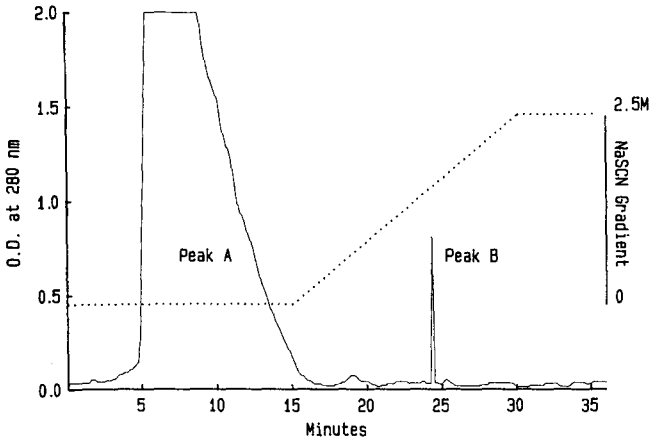

Fig. 1. HPIAC isolation of anti-idiotypic antibodies. Peaks: A = unreacted material; B = the anti-idiotypic antibody fraction. The dotted line represents the sodium thiocyanate gradient.

a 125 000-dalton band derived from the autologous tumor. The antibodies failed to react with any other blotted band, although several bands could be detected by silver staining of the membrane preparation. A lack of reactivity was also observed when the antibodies were reacted against Western blots of the membranes of the other patients tumor cells. These results are shown in Table I.

HPIAC isolation of the reactive anti-idiotypic antibodies produced the chromatogram shown in Fig. 1. Following the development of the primary peak (A) which contained non-specific serum products, the anti-idiotypic antibodies were isolated as a sharp, well-defined second peak (B), eluted at 24.5 min into the chromatography run. Immunoelectrophoretic and immunodiffusion studies demonstrated that only IgG was contained in the second peak at a concentration of 5–12 ng/ml. In twelve of the

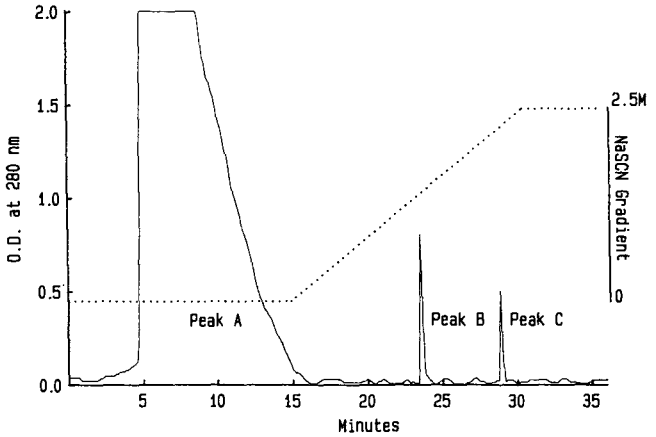

Fig. 2. HPIAC isolation of anti-idiotypic antibodies. Peaks: A = unreacted material; B = the anti-idiotypic antibody fraction; C = an anti-F(Ab)$'_2$ fraction. The dotted line represents the sodium thiocyanate gradient.

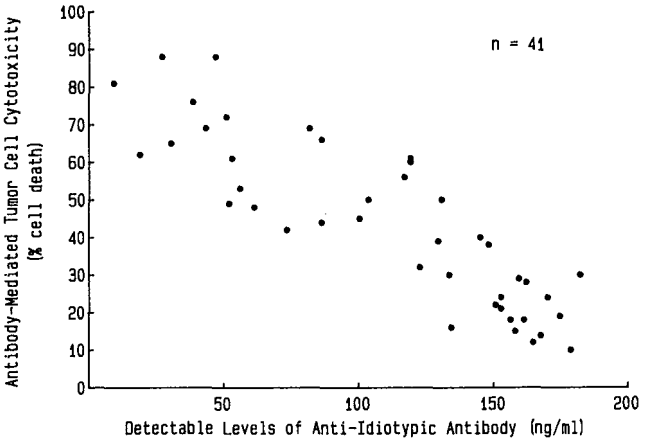

Fig. 3. Correlation between the concentrations of anti-idiotypic antibodies, as detected by immunoaffinity chromatography, and the concentrations of detectable anti-tumor antibody.

anti-tumor antibody positive patients, a different chromatographic pattern was seen (Fig. 2). Following the development of the primary peak (A), two distinct peaks were developed during the elution phase. The second peak (B) eluted at 24 min into the run and was followed by the third peak (C) at 28.5 min. Analysis of these two peaks demonstrated that both peaks contained IgG at concentrations of 5–15 ng/ml and 30–100 ng/ml, respectively.

Experiments on the effects of the isolated anti-idiotypes on the antigen-binding capacity of the original anti-tumor antibodies demonstrated that the antibodies isolated in the second peak (peak B) of the HPIAC runs possessed the ability to greatly reduce the activity of the anti-tumor antibodies. This effect could be shown to increase proportionally with the concentration of detectable anti-idiotype. The antibodies contained in the third peak (peak C) did not demonstrate any ability to inhibit the antigen-binding capacity of the original anti-tumor antibodies. Further studies, using Western blots of enzyme digests of the original antibodies demonstrated that the antibodies isolated in peak C reacted with the hinge region of the original anti-tumor antibodies and appears to be an anti-$F(Ab)'_2$ class of anti-antibodies.

The levels of anti-idiotype also correlated with a loss of cytotoxic anti-tumor activity in all of the patients monitored (Fig. 3). Chromium-release studies demonstrated that a decrease of 20–90% in the original cytotoxic reactivity of the anti-tumor antibodies could be demonstrated following incubation with the autologous anti-idiotype. This reduction in tumor cell kill was not present when the anti-tumor antibodies were pre-incubated with anti-idiotypes from other patients.

DISCUSSION

Several mechanisms have been put forward to explain the relative state of immunological unresponsiveness in cancer patients[20–22]. However, few studies have monitored the presence of regulatory idiotypic antibodies; possibly due to the difficulty involved in isolating and monitoring these highly specific antibodies. In an

attempt to overcome these difficulties, we have used the patient's autologous anti-tumor antibodies as immobilized ligands for isolating reactive anti-idiotypes by immunoaffinity chromatography. Isolation of reactive anti-idiotypes in an active form allows further investigation of their exact role in the suppression of the immune responses against growing tumors to be performed.

The presence of suppressive anti-idiotypes has been described in several different tumor systems, especially malignant melanoma[9,22,23] and lymphatic leukemia[24]. In the former case, the presence of anti-antibodies have been shown to correlate with the loss of active immune surveillance against the growing tumor. Studies on the effects of the anti-antibodies in the inhibition of tumoricidal activity has been shown to be proportional to the level of anti-antibodies detected in the patient serum[23]. In lymphatic leukemia, the use of laboratory-made anti-idiotypic antibodies, directed against idiotypic antibodies on the tumor cell membrane, has been suggested as a therapeutic procedure[24].

If the system forwarded by Jerne[25] is correct, then isolation of suppressive anti-idiotypes could have value in providing material for a vaccine capable of stimulating enhancing anti-idiotypes in cases where the immune monitoring demonstrates that a loss of the original idiotypic response is taking place. Animal studies have shown that anti-idiotypic antibodies can be elicited when a vaccine of idiotypic antibodies complexed with rheumatoid factor is injected into normal animals[26].

In this study we have demonstrated that specific anti-idiotypic antibodies can be isolated by HPIAC using the original idiotype as the ligand. Biotinylation of the original idiotypes by the hydrazine technique appeared to inhibit the binding of anti-Fc antibodies but could not inhibit the binding of anti-$F(Ab)'_2$ antibodies. However, the anti-idiotypic antibodies consistently eluted before the anti-$F(Ab)'_2$ antibodies, and this prevented contamination of the anti-idiotypic fractions with other types of anti-antibodies. In this way we feel that HPIAC is a reasonable technique for the isolation of regulatory anti-antibodies, especially when the ligand is coupled to streptavidin-coated glass beads. This form of attachment prevents binding of anti-Fc antibodies which are a major source of contamination in auto-anti-idiotypic antibody isolations. Streptavidin-coated Affinichrom solid glass beads[15–17] are a stable immunoaffinity packing media which can be used to immobilize antibodies for the immunoaffinity isolation of anti-antibodies. The packing is stable for 50–70 cycles and can be run at relatively high flow-rates with little deterioration. Immunoaffinity techniques using Affinichrom beads can isolate anti-idiotypes in under 30 min with no apparent loss of biological activity.

CONCLUSIONS

The use of HPIAC provides a technique which can detect, measure and isolate anti-idiotypic antibodies in under 30 min. This technique can be used in any facility that has a simple HPLC system and can be converted to batch isolations for research purposes. Once made, the immobilized antibody columns remain viable for 50–70 runs and are storable under refrigerated conditions for up to one year.

REFERENCES

1 H. G. Kunkle, H. Mannik and R. C. Williams, *Science (Washington, D.C.)*, 140 (1963) 1218.
2 H. Kohler, *Transplant. Rev.*, 27 (1975) 24.
3 H. Koher, *Immunol. Today*, 1 (1980) 18.
4 J. Urbain, C. Wuilmert and P. A. Cavenave, *Contemp. Top. Mol. Immunol.*, 8 (181) 113.
5 J. T. Nemazee and V. L. Sato, *Proc. Natl. Acad. Sci U.S.A.*, 79 (1982) 3828.
6 M. G. Lewis, T. M. Phillips, K. B. Cook and J. Blake, *Nature (London)*, 232 (1971) 52.
7 S. Dray, A Gilman-Sachs and W J. Hornig, *Ann. N.Y. Acad. Sci.*, 418 (1983) 84.
8 H. Koprowski, D. Herlyn, M. Lubeck, E. Defreitas and H. F. Sears, *Proc. Natl. Acad. Sci. U.S.A.*, 81 (1984) 216.
9 M. G. Lewis, *Curr. Top. Microbiol. Immunol.*, 63 (1974) 49.
10 C. A. Bona, C.-Y. Kang, H. Kohler and M. Monestier, *Immunol. Rev.*, 90 (1986) 115.
11 J. W. Moorhead, *J. Exp. Med.*, 155 (1982) 820.
12 M. Waller and K. Blaylock, *J. Immunol.*, 97 (1966) 438.
13 R. M. Thorn, J. C. Palmer and L. A. Manson, *J. Immunol. Methods*, 4 (1974) 301.
14 H. Towbin, T. Staehelin and J. Gordon, *Proc. Natl. Acad. Sci. U.S.A.*, 76 (1979) 4350.
15 J. V. Babashak and T. M. Phillips, *J. Chromatogr.*, 444 (1988) 21.
16 T. M. Phillips, in J. C. Giddings, E. Grushka and P. R. Brown (Editors), *Advances in Chromatography*, Vol. 29, Marcel Dekker, New York, 1989, Ch 3, p. 133.
17 T. M. Phillips, S. C. Frantz, J. V. Babashak and J. J. Chmielinska, *J. Chromatogr.*, 458 (1988) 185.
18 D. J. O'Shannessy and R. H. Quarles, *J. Immunol. Methods*, 99 (1987) 153.
19 J. J. Marchelonis, Biochem. J., 113 (1969) 299.
20 G. A. Currie, *Brit. J. Cancer*, 26 (1972) 141.
21 S. C. Bansal, B. R. Bansal and J. P. Boland, *Curr. Top. Microbiol. Immunol.*, 75 (1976) 45.
22 T. M. Phillips, T. V. Holohan, S. Korec, N. S. More and W. D. Queen, in F. Salinas and M. Hanna (Editors), *Contempory Topics in Immunobiology*, Vol. 15, Plenum, New York, 1985, Ch. 3, p. 111.
23 T. M. Phillips, *Clin. Chem.*, 34 (1988) 1689.
24 M. J. Glennie and G. T. Stevenson, in A. S. Darr (Editor), *Tumour Markers in Clinical Practice: Concepts and Applications*, Blackwell, Oxford, 1987, p. 362.
25 N. K. Jerne, *Ann. Immunol. (Paris)*, 125C (1974) 373.
26 T. M. Phillips, W. D. Queen, N. S. More and A. M. Thompson, *Ann. N.Y. Acad. Sci.*, 435 (1984) 475.

Journal of Chromatography, 512 (1990) 395–401
Elsevier Science Publishers B.V., Amsterdam

CHROMSYMP. 1946

Assay of cytosine and cytidine deaminases by means of reversed-phase high-performance liquid chromatography

PROBIR K. DUTTA*, MARK S. SHANLEY and GERARD A. O'DONOVAN
Department of Biological Sciences, University of North Texas, Denton, TX 76203-5218 (U.S.A.)

ABSTRACT

A rapid and sensitive high-performance liquid chromatographic assay for cytosine and cytidine deaminases, based upon the chromatographic separation and subsequent ultraviolet detection of enzymatically liberated uracil and uridine, was developed. Using cell-free extract from *Escherichia coli* the enzymes can be assayed with incubation times of 30 min or less. Reversed-phase separation of products from substrates was accomplished by isocratic elution with monobasic ammonium phosphate buffer at pH 3.5. The assay is fast and reproducible with little or no interference from competing reactions in cell extracts. It is sensitive and can concomitantly detect nanomole changes in the concentration of substrate and product. It is faster, more sensitive, and requires fewer sample manipulations than standard spectrophotometric and radiometric methods of analysis.

INTRODUCTION

Cytosine deaminase (cytosine aminohydrolase, EC 3.5.4.1) and cytidine deaminase (cytidine aminohydrolase, EC 3.5.4.5) catalyze the hydrolytic deamination of cytosine to uracil and cytidine to uridine, respectively. Both enzymes have been detected in a variety of organisms[1–4] and both play anabolic salvage roles in pyrimidine metabolism in that they supply exogenous pyrimidines *in lieu* of the *de novo* pyrimidine pathway. Both cytosine and cytidine deaminase activities can be determined by direct spectrophotometric assay from fall in absorbance at 285 nm, following conversion of the 4-amino to the 4-keto compounds[5]. When high levels of extraneous protein or certain nucleoside inhibitors are present, the background absorbance becomes too high at 285 nm, the reaction may then be followed at 295 nm. Cytidine deaminase can also be assayed by measuring the amount of labeled uridine formed by the deamination of 2-^{14}C-labeled cytidine[6].

Our laboratories have been examining cytosine deaminases from several bacterial genera including *Pseudomonas*, *Salmonella* and *Escherichia* for some time[1]. The assay for ring deamination at the 4 position based on the spectrophotometric detection of the products and the substrates has some limitations. Cytosine has an

0021-9673/90/$03.50

absorbance maximum at 267 nm while uracil has an absorbance maximum at 259 nm. However, both compounds absorb strongly over a broad range (200–290 nm). Previous assays[3,4] were based on the ability to separate the product from the substrate based on differences on their molar absorptivity at a particular wavelength. In this paper we describe an assay wherein the product and substrate of the reactions are physically separated by a reversed-phase C_{18} high-performance liquid chromatography (HPLC) method prior to measuring the absorbance. Since product and substrate absorb so strongly and since we are not measuring the difference in absorption but the total absorption, the assay is very sensitive and capable of measuring disappearance of substrate and appearance of product in the nanomolar range.

HPLC has been used to monitor enzyme reactions rapidly in a variety of systems[7–9]. There are various advantages for such assays[8]. The assay time is faster than the time course of the reaction, allowing for "real time" assaying of reaction mixture. HPLC methods allow the quantitation of both substrate disappearance (cytidine or cytosine) and product appearance (uridine or uracil) without interference from competing reactions. There is no need to terminate the assay or remove proteins from the assay mix because injection onto the HPLC column effectively terminates the reaction as well as removes and separates protein from the substrates. The enzymatic assay that we describe here overcomes limitations of existing methods while embodying all the above advantages.

EXPERIMENTAL

Chemicals and reagents

Cytidine, cytosine, uridine and uracil were obtained from Sigma (St. Louis, MO, U.S.A.). Monobasic ammonium phosphate was obtained from Mallinckrodt (Paris, MO, U.S.A.). All other chemicals were of analytical grade. Solutions were prepared with distilled deionized water obtained from a Milli-Q system (Millipore, Bedford, MA, U.S.A.).

Growth of cells

Escherichia coli TB2 (*pyrBl*, *argF*, *argl*) was grown in M9 minimal medium with 0.2% (w/v) glucose as carbon source[10]. The medium was supplemented with 0.4% casamino acids and uracil at 50 μg/ml. The turbidity was measured with a Klett-Summerson photoelectric colorimeter, using a green filter No. 54. Growth was measured at 37°C and recorded as Klett Units (KU), where 1 KU equals 10^7 cells/ml. Cultures of 1 l at a cell density of 100 KU were harvested and centrifuged at 8000 *g* for 2 min at 4°C. The supernatant was decanted and the cell pellet was used for enzyme extraction. The pellet was suspended in 10 m*M* Tris–HCl (pH 7.0) and broken by explosive decompression using a chilled French Pressure Cell (SLM/AMINCO, Urbana, IL, U.S.A.). The homogenate was centrifuged at 10 000 *g* at 4°C. The pellet was discarded and the supernatant was used for enzyme assay without any further purification. Protein content was determined by the method of Bradford[11], using crystalline bovine serum albumin, Fraction V, as standard.

Cytosine and cytidine deaminase assays

Assays were performed in 1.5-ml microcentrifuge tubes at 37°C in a shaking water bath. The assay mix contained in 1 ml: 10 m*M* Tris–HCl (pH 7.30), 20 μl of appropriately diluted cell extract, and varying concentrations of cytosine or cytidine, as given in the Results and Discussion section. The reaction was terminated after 15–60 min by filtering the entire assay mixture through a 0.45-μm ACRO LC13 filter (Gelman, Ann Arbor, MI, U.S.A.) into a tube stored on ice. A 10-μl volume of this reaction sample was injected onto the column for detection of substrates and products by HPLC. The entire procedure from filtration to injection took less than 30 s. Non-enzymatic oxidative deamination of cytosine or cytidine for the time periods and conditions of temperature and pH employed could not be detected by the subsequent methods of separation and detection described below.

Chromatographic apparatus and conditions

The concentrations of cytidine, cytosine, uridine and uracil were determined using reversed-phase HPLC. The chromatographic system (Waters Assoc., Milford, MA, U.S.A.) consisted of a Model 510 pump, a U6K injector and a variable-wavelength Model 481 LC spectrophotometer. Peaks were integrated manually by paper weighing copies of the output from a Cole Palmer (Chicago, IL, U.S.A.) strip chart recorder or more typically on a Waters Model 740 data module. Samples of 10 μl were injected onto an IBM C_{18} column (250 mm × 4.5 mm I.D.; particle size 5 μm; now supplied by I.I.I Supplies Co., Wallington, CT, U.S.A.). Compounds were separated using isocratic elution (5 m*M* $NH_4H_2PO_4$, pH 3.5) at a flow-rate of 1 ml/min. Compounds were detected by monitoring the column effluent at 254 nm with a sensitivity fixed at 0.1 absorbance units full scale (a.u.f.s.). Individual components of the reaction mixture were identified, using retention times relative to known standards and by injecting known internal standards.

Calculation of K_M values

Initial velocities (V) were measured as a function of substrate concentration (S). Michaelis constants (K_M) for cytosine and cytidine were evaluated from double reciprocal Lineweaver–Burk plots[12]. Uracil formation by cytosine deaminase or uridine formation by cytidine deaminase was linear over the course of the reaction.

RESULTS AND DISCUSSION

Several HPLC procedures have been described for separation of nucleic acid bases and nucleosides. Originally, ion-exchange HPLC[13–16] was used, but subsequently reversed-phase HPLC[17–24] has proven to be more suitable. The reversed-phase techniques included paired-ion chromatography[17], gradient elution[18–22], and isocratic conditions[23,24]. The effects of pH, ionic strength and type of buffer on the reversed-phase separation of nucleosides and bases have been described previously[25]. We have chosen isocratic elution at pH 3.5 to resolve cytosine, uracil, cytidine and uridine.

Typical chromatograms of aqueous standard solutions containing either cytosine and uracil or cytidine and uridine are shown in Fig. 1a and c, respectively. The chromatogram in Fig. 1b gives the results shown after incubation of cytosine with fresh

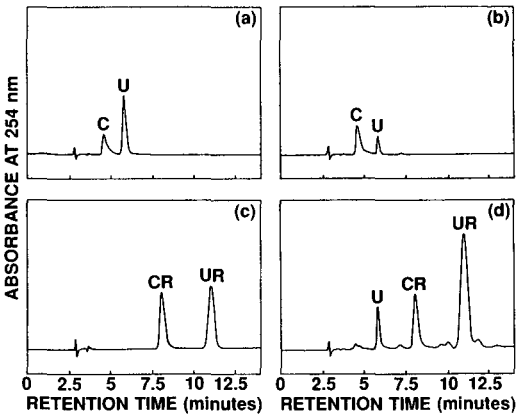

Fig. 1. Chromatograms of aqueous standard solutions of 0.5 m*M* cytosine and uracil (a) and of 0.5 m*M* cytosine after incubation with an enzyme preparation (b). Peaks identified as described in Experimental as cytosine and uracil are labeled C and U respectively. (c) Chromatogram of an aqueous standard solution, containing 1.0 m*M* cytidine and uridine. (d) The enzymatic conversion of cytidine (CR) to uridine (UR) and uracil (U). Graphic reproduction of the chromatogram in Panel D resulted in a change in scale from 0.1 to 0.02 a.u.f.s. The assay mixture contained 1 m*M* cytidine and was treatad as described.

cell extract. The conversion of cytosine to uracil by cytosine deaminase is readily apparent by the concomitant appearance of the uracil peak. The uracil peak was confirmed as pure by both retention time (5.92 *versus* 4.69 for cytosine), as well as inclusion of an internal uracil standard with cytosine. The conversion of cytidine to uridine by cytidine deaminase is shown in Fig. 1d. Incubation of cytidine with cell extract resulted in the appearance of uridine with a concomitant decrease in the cytidine concentration together with the appearance of a uracil peak. Many different organisms have the ability to further degrade uridine to uracil and this is seen in the Fig. 1d. In such cases enzyme activity can be determined by summing the two products or more conveniently by the rate of disappearance of the substrate cytidine. Confirmation of peak purity was made as before with retention times of 8.06 min for cytidine and 11.05 min for uridine. The chromatograms had no extraneous peaks.

The assay was highly reproducible. Assays of the enzymes from different cultures where the cells were grown, harvested, broken and assayed under identical conditions yielded coefficients of variation of less than 12% for cytosine deaminase and less than 11% for cytidine deaminase. Moreover, repeated assays (at least three times) on a single sample gave coefficients of variation of 2.0% or less for both cytosine deaminase and cytidine deaminase.

The reproducibility of the enzymatic reaction was investigated three times for the same cell extract and for different cell extracts of the same strain at 0.5 nmol (cytosine) and 1 nmol (cytidine) and 0.2 mg/ml protein concentrations. The coefficients of variation were 2 and 12% for cytosine deaminase and 2 and 11% for cytidine deaminase.

Thus the assay above, used to detect the presence of the enzymes in crude cell extracts is applicable also for kinetic characterization of cytosine and cytidine deaminases. At a relatively high fixed substrate concentration, the initial velocity

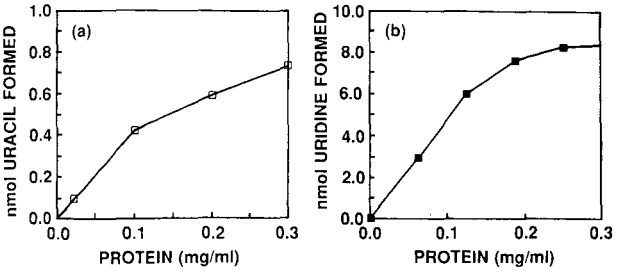

Fig. 2. Effect of enzyme concentration of the rate of the reaction. Cytosine deaminase initial velocity (a) plotted as a function of increasing enzyme concentration; rate of uridine production (b) at increasing enzyme concentration. The assays were performed at constant substrate concentrations of 0.5 m*M* cytosine and 1.0 m*M* cytidine for 30 min, as described in Experimental.

measured was proportional to the amount of enzyme or cell extract employed (Fig. 2). The optimal incubation time for initial velocity measurements was determined by a kinetic assay using a fixed enzyme concentration found to be on the linear portion of the curves shown in Fig. 3a and b. In the example shown, the rate of enzymatic conversion of substrates to products is linear for up to 60 min. Subsequent measurements for kinetic characterization of the enzymes employed sampling times of only 10 min. The incubation conditions, described in Experimental were empirically determined from the above data and represent appropriate linear responses for the variables of enzyme concentration and time of assay. Use of highly purified enzyme or cell extracts with significantly different specific activities may require modifications which are readily determined by additional "range finding" experiments.

To demonstrate the general validity of this assay, we used it to compare the results of our previous determinations of K_M and V_{max} (maximal velocity) for cytosine deaminase[1] that used conventional spectrophotometric assays. The effect of various concentrations of substrate (cytosine or cytidine) on the production of uracil or uridine by crude cell extracts was determined. The enzymes exhibited typical hyperbolic Michaelis–Menten kinetics allowing measurement of the K_M and V_{max} of the two enzymes. Lineweaver–Burk reciprocal plots (Fig. 4) of the experimental data were constructed to measure the effect of increasing substrate concentration on the initial veloc-

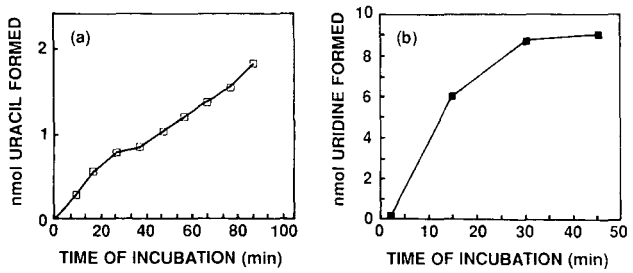

Fig. 3. Time course of the reaction for the production of uracil and uridine by a cell-free extract of *E. coli*. Cytosine deaminase activity (a) was determined at a substrate concentration of 0.5 m*M*. Cytidine deaminase (b) was assayed at a cytidine concentration of 1 m*M*. In every case, 20 μl of cell extract (4 μg protein) was used as described in Experimental.

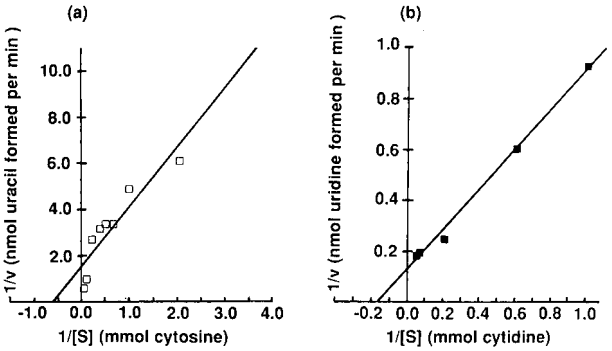

Fig. 4. Lineweaver–Burk plots for cytosine deaminase activity from *E. coli* (a) determined in unpurified preparations of the enzyme. Double reciprocal plot of the production of uridine by cytidine deaminase (b), determined in crude preparations of the enzyme from *E. coli*.

ity. Cytosine deaminase had a K_M of 1.6 m*M* cytosine using data derived from HPLC determinations of enzymatic activity (Fig. 4a) in comparison to a K_M of 1.5 m*M* cytosine for the same sample but determined spectrophotometrically as previously described[1]. Similarly, cytidine deaminase had a K_M of 6.6 m*M* cytidine determined using the assay described, but a K_M of 5.8 m*M* cytidine when assayed spectrophotometrically.

The reversed-phase HPLC determination of cytosine and cytidine deaminase activity described here offers several advantages over currently available assays. Sample preparation is minimal involving no precipitation of protein prior to chromatography. The analysis time, after incubation, is short and the separation is free from interfering substances. The enzymatically liberated uracil and uridine are separated from precursor and measured at 254 nm making detection highly sensitive. Though the results shown were obtained using bacterial cell extracts, the method can be applied to other biological samples.

ACKNOWLEDGEMENTS

This investigation was supported in part by a Research Initiation Grant to M.S.S. from the Office of Research and Academic Grants and by a Texas Advanced Technology Research Grant to G.A.O'D.

REFERENCES

1 T. P. West, M. S. Shanley and G. A. O'Donovan, *Biochim. Biophys. Acta*, 719 (1982) 251.
2 G. W. Camiener and C. G. Smith, *Biochem. Pharmacol.*, 14 (1965) 1405.
3 D. F. Wentworth and R. Wolfenden, *Biochemistry*, 14 (1975) 5099.
4 I. K. Rothman, V. G. Malathi and R. Silber, *Cancer Res.*, 31 (1971) 274.
5 P. L. Ipata, G. Cercignami and E. Balestreri, *Biochemistry*, 9 (1970) 3390.
6 I. K. Rothman, R. Silber, K. M. Klein and F. F. Becker, *Biochim. Biophys. Acta*, 228 (1971) 307.
7 J. L. Hodge and E. F. Rossomando, *Anal. Biochem.*, 102 (1980) 59.
8 E. G. E. Jahngen and E. F. Rossomando, *Anal. Biochem.*, 137 (1984) 493.
9 F. Broly, C. Libersa and M. Lhermitte, *J. Chromatogr.*, 431 (1988) 369.
10 E. H. Anderson, *Proc. Natl. Acad. Sci. U.S.A.*, 32 (1946) 120.

11 M. M. Bradford, *Anal. Biochem.*, 72 (1976) 248.
12 H. Lineweaver and D. Burk, *J. Am. Chem. Soc.*, 56 (1934) 658.
13 A. Floridi, C. A. Palmerini and C. Fini, *J. Chromatogr.*, 138 (1977) 203.
14 H. G. Schneider and A. J. Glazko, *J. Chromatogr.*, 139 (1977) 370.
15 H. G. Breter, G. Seibert and R. K. Zahn, *J. Chromatogr.*, 140 (1977) 251.
16 B. C. Pal, *J. Chromatogr.*, 148 (1978) 545.
17 M. Ehrlich and K. Ehrlich, *J. Chromatogr. Sci.*, 17 (1979) 531.
18 B. Bakay, E. Nissinen and L. Sweetman, *Anal. Biochem.*, 86 (1978) 65.
19 A. M. Krstulovic, P. R. Brown and D. M. Rosie, *Anal. Chem.*, 49 (1977) 2237.
20 P. R. Brown and A. M. Krstulovic, *Anal. Biochem.*, 99 (1979) 1.
21 R. A. Hartwick, S. P. Assenza and P. R. Brown, *J. Chromatogr.*, 186 (1979) 647.
22 H. K. Webster and J. M. Whaun, *J. Chromatogr.*, 209 (1981) 283.
23 G. A. Taylor, P. J. Dady and K. R. Harrap, *J. Chromatogr.*, 183 (1980) 421.
24 C. W. Gehrke, K. C. Kuo and R. W. Zumwalt, *J. Chromatogr.*, 188 (1980) 129.
25 R. A. Hartwick and P. R. Brown, *J. Chromatogr.*, 126 (1976) 679.

Journal of Chromatography, 512 (1990) 403–407
Elsevier Science Publishers B.V., Amsterdam

CHROMSYMP. 1947

Characterization of temperature-sensitive cytidine triphosphate synthase mutations in bacteria by high-performance liquid chromatography

ANDREA J. BAILEY, PROBIR K. DUTTA*, MARK S. SHANLEY and GERARD A. O'DONOVAN
Department of Biological Sciences, University of North Texas, Denton, TX 76203-5218 (U.S.A.)

ABSTRACT

Cytidine triphosphate (CTP) synthase catalyzes the last step in pyrimidine ribonucleotide synthesis, namely the formation of CTP from UTP, ATP, and glutamine. Mutants devoid of CTP synthase activity require cytidine for growth and have been designated *pyrG* in an obligate *cdd* background. Using a *ts* mutation blocked in the conversion of UTP to CTP at 43°C, it was demonstrated that the conversion occurs by growing cells at 33°C or below where UTP and CTP pools are normal. Growth at 43°C shuts off the enzyme, while UTP accumulates and CTP is decreased significantly. By now feeding exogenous cytidine the CTP pool can be restored to the level found at the permissive temperature.

Intracellular nucleoside triphosphates (CTP and UTP) were separated on a Partisil SAX10 cartridge, using a linear gradient of low buffer (7 m*M* ammonium dihydrogenphosphate, pH 3.8) to high buffer (250 m*M* ammonium dihydrogenphosphate, pH 4.5 with 500 m*M* potassium chloride).

Nucleoside triphosphates were also separated after enzymatic conversion of UTP to CTP in solution by cell extracts using ion-pair reversed-phase chromatography on a C_{18} cartridge eluted with a mixture of 95% buffer A (25 m*M* ammonium dihydrogenphosphate with 1 m*M* tetrabutylammonium phosphate, pH 7.0) and 5% buffer B (15% aqueous acetonitrile). Using the two different separation techniques, it was possible to monitor the level of UTP and CTP inside cells as well as the enzymatic conversion of UTP to CTP by the enzyme CTP synthase.

INTRODUCTION

High-performance liquid chromatography (HPLC) was used to identify and characterize a temperature-sensitive mutation in the pyrimidine pathway of *Salmonella typhimurium*. Because the temperature-sensitive mutant has a defective cytidine triphosphate (CTP) synthase (EC 6.3.4.2), which catalyzes the final step of the pathway [that converting uridine triphosphate (UTP) to CTP], it was also possible to monitor the normal flow through the pathway by growing the mutant at 33°C, the

0021-9673/90/$03.50

permissive temperature. Normal levels of UTP and CTP were obtained at 33°C. By shifting the organism to 43°C, no further CTP was produced from UTP. At this restricted temperature, the CTP concentration dropped sharply while the UTP concentration increased three-fold. Thus, it was possible (a) to confirm that the metabolic block in this mutant was in the final step of the pathway, the step catalyzed by CTP synthase, (b) to show the effect of temperature on nucleotide changes in a temperature-sensitive mutant, (c) to show the precise temperature at which the block is absolute (43°C) or at which no effect (33°C) is seen, and (d) since UTP and CTP are known repressing metabolites of the pyrimidine pathway[1] and since in this mutant the concentration of these two nucleotides could be changed independently, it was also possible to study the regulation of a primary biosynthetic pathway. This was achieved by adding cytidine to growing cells to swell the CTP pool independently of the UTP pool at the restrictive temperature (43°C)[2]. Accordingly, it is suggested that HPLC is an ideal method for studying single, multiple and consecutive reactions and their control in cellular metabolism *in vivo* and *in vitro*.

EXPERIMENTAL

Chemicals and reagents

CTP and UTP were obtained from Sigma (St. Louis, MO, U.S.A.). Monobasic ammonium phosphate was obtained from Mallinckrodt (Paris, MO, U.S.A.). All other chemicals were of analytical grade. Solutions were prepared with distilled deionized water obtained from a Milli-Q system (Millipore, Bedford, MA, U.S.A.).

Growth of cells

Salmonella typhimurium KR1530 (*pyrA81*, *pyrG1611*, *cdd-7*, *udp-2*) was graciously provided by Dr. R. A. Kelln, University of Regina, Saskatchewan, Canada. The strain was grown in minimal medium A with 0.2% (w/v) glucose as carbon source[3]. This strain requires arginine and uracil at all temperatures. In addition, it requires cytidine when the cells are grown at temperatures above 33°C with an absolute requirement when the cells are grown above 43°C. All supplements were added at 50 μg/ml. The turbidity was measured with a Klett-Summerson photoelectric colorimeter, using a green filter No. 54. Growth was measured at 33°C and at 43°C and recorded as Klett Units (KU), where 1 KU equals 10^7 cells/ml.

Extraction of intracellular UTP and CTP

Bacterial cultures were grown to a density of 100 KU, harvested and centrifuged at 12 000 *g* for 3 min at 4°C. The supernatant was decanted and the cell pellet washed once in minimal medium. Cells were extracted with 1.0 ml of 6% (w/v) trichloroacetic acid (TCA), shaken on a vortex mixer and allowed to stand at 4°C for 30 min before being centrifuged at 12 000 *g* for 10 min at 4°C. The acid extract containing the nucleotides was removed and neutralized with an equal volume of ice-cold freon/amine solution. The freon–amine solution contained 0.7 *M* tri-*n*-octylamine in Freon-113 (ref. 4). Samples were shaken on a vortex mixer for 2 min and the phases were allowed to separate for 15 min at 4°C. The top aqueous layer, containing the nucleotides, was removed, filtered through a 0.45-μm ACRO LC13 filter (Gelman, Ann Arbor, MI, U.S.A.), and frozen at −20°C until separated by ion-exchange chromatography as described below.

Assay for CTP synthase

Cultures of 1 l at a cell density of 100 KU were harvested and centrifuged at 8000 *g* for 2 min at 4°C. The supernatant was decanted and the cell pellet was used for enzyme extraction. The pellet was suspended in 10 ml 10 m*M* Tris–HCl (pH 7.0) and broken by explosive decompression, using a chilled French Pressure Cell (SLM/AMINCO, Urbana, IL, U.S.A.). The homogenate was centrifuged at 10 000 *g* at 4°C. The pellet was discarded and the supernatant was used for enzyme assay without further purification. Protein content was determined by the method of Bradford[5], using crystalline bovine serum albumin, Fraction V, as standard.

Assays were performed in 1.5-ml microcentrifuge tubes at 33°C in a shaking water-bath. The assay mix was prepared as described previously[6] and contained in 1 ml: 10 m*M* imidazole-acetate (pH 7.2), 20 μl of appropriately diluted cell extract, 10 m*M* glutamine, 1 m*M* $MgCl_2$, 1 m*M* ATP and 1 m*M* UTP. The addition of the substrate UTP initiated the reaction. The reaction was terminated after 30 min by filtration through a 0.45-μm ACRO LC13 filter into a tube on ice and immediately injected onto the column as described below. The rate of product formation was linear with respect to time and protein concentration.

Chromatographic apparatus and conditions

The chromatographic system (Waters Assoc., Milford, MA, U.S.A.) consisted of two Model 510 pumps, a Model 680 automated gradient controller, a U6K injector and a variable-wavelength Model 481 LC spectrophotometer. Nucleotides were detected by monitoring the column effluent at 254 nm with a sensitivity fixed at 0.05 absorbance units full scale (a.u.f.s.). A Waters radial compression Z-module system was employed that held 100 mm × 8 mm I.D. cartridges.

Separations of nucleotides in cell extracts for quantitation of endogenous nucleotide pools were performed on a Waters Radial-Pak Partisil SAX cartridge in the Z-module system. As previously described[7–9], the elution buffer consisted of eluent A, 7 m*M* ammonium dihydrogenphosphate (pH 3.8), and eluent B, 250 m*M* ammonium dihydrogenphosphate (pH 4.5) with 500 m*M* potassium chloride. A linear gradient of eluent A to eluent B was applied for 20 min followed by an isocratic period of 10 min with eluent B. The column was regenerated by washing with 30 ml of eluent A (pH 3.8) buffer. The flow-rate was maintained at 4 ml/min. Peaks were integrated, using a Waters 740 data module.

Quantitation of the enzymatic conversion of UTP to CTP by CTP synthase was by HPLC separation using the apparatus described above, except that a C_{18} cartridge was substituted in the Z-module system. In this case, the elution buffer consisted of 95% buffer A (25 m*M* ammonium dihydrogenphosphate with 1 m*M* tetrabutylammonium phosphate, pH 7.0) and 5% buffer B (15% aqueous acetonitrile) at a flow-rate of 2 ml/min. The effluent was monitored at 250 nm at a sensitivity of 0.1 a.u.f.s. and the peaks integrated as above. The isocratic separation on reversed-phase column allowed for much more rapid analysis of UTP and CTP levels in solution than the previously described gradient ion exchange separation necessary for the analysis of nucleoside triphosphates in cell extracts.

RESULTS AND DISCUSSION

Our laboratory has been involved in the regulation of CTP synthase for some time and has sought a more direct method to monitor changes in the enzyme activity and in attendant changes in the intracellular pyrimidine nucleotide pools[6,10]. This becomes particularly important for temperature-sensitive mutants of the *pyrG* gene encoding CTP synthase. Strains carrying such mutations are typically employed to independently manipulate pyrimidine nucleotide pools. The pyrimidine nucleotides UTP and CTP are repressing metabolites for a number of genes[1,2,6,10,11]. However, alterations in the pools as well as the enzyme's activity are extremely difficult to quantify. Appropriate mutant strains have not been isolated. The genotype of putative mutants may not be verified, since the CTP synthase enzyme assay is difficult and the metabolic effects of mutation can only be followed by quantitation of endogenous nucleoside triphosphates. Previously, this required tedious radioactive labeling and thin layer chromatographic techniques[1,2].

By exploiting HPLC it is now possible to quickly achieve our goal of mutant characterization by two means. First, CTP synthase activity can be monitored *in vivo* by alterations in the intracellular levels of its immediate substrate (UTP) and product (CTP). Upon starvation of a *pyrG* strain, at the restrictive temperature, the intra-

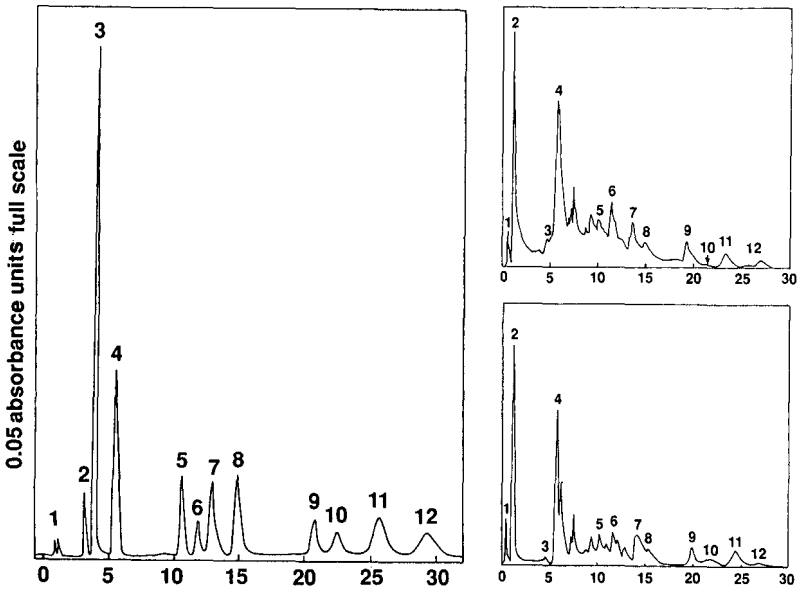

Fig. 1. Chromatogram of aqueous standard ribonucleotide mixture (left panel) separated on an anion exchange Radial-Pak Partisil SAX cartridge. A 100-μl sample consisting of 10^{-5} *M* of each nucleotide was injected. The numbered peaks correspond to: 1 = CMP; 2 = AMP; 3 = UMP; 4 = GMP; 5 = UDP; 6 = CDP; 7 = ADP; 8 = GDP; 9 = UTP; 10 = CTP; 11 = ATP; 12 = GTP. Under these conditions it is possible to detect 0.1 nmol of nucleotide. Nucleotide profile of *S. typhimurium* cells grown at 42°C (top right panel). Numbered peaks correspond to those given above. The CTP peak, nearly absent in this sample, is denoted by the arrow under number 10. Nucleotide profile of *S. typhimurium* cells grown at 33°C (bottom right panel). At this temperature the strain synthesizes CTP (peak 10) from UTP (peak 9) and the levels of CTP increase. Time axis in min.

cellular level of CTP drops to near zero (Fig. 1). Under permissive conditions, the UTP concentration was 2.2 μmol/g dry weight while the CTP concentration was 1.2 μmol/g dry weight. After a shift to the restrictive temperature of 43°C, in 1 h, the level of CTP dropped to 0.2 μmol/g dry weight. With CTP synthase presumably inactivated at the restrictive temperature, its substrate UTP increased approximately three-fold to 6.4 μmol/g dry weight.

Second, the activity of CTP synthase in sonicated cell extracts can be quickly monitored *in vitro*. At 33°C or lower the enzyme is active in converting UTP to CTP as determined by enzymatic assay using HPLC. Under the conditions described in Experimental, the enzyme had a specific activity of 0.9 nmol per min per mg protein. When the assay was performed at the restrictive temperature of 43°C using crude sonicated extracts from cells grown at 33°C, no detectable conversion of UTP to CTP was observed. As expected, there was no detectable CTP synthase activity in cells grown (in cytidine supplemented medium) at the restrictive temperature of 43°C even when assayed at the permissive temperature.

CTP pools in these *pyrG* mutant strains can be maintained in two ways. First, if the cells are grown at the permissive temperature, CTP synthase is active and therefore the UTP and CTP pools are maintained at wild type physiological levels. This is shown by the presence of both peaks 9 and 10 in the bottom right panel of Fig. 1. Since *pyrG* mutants must be isolated in a *cdd* background[12] it is possible to add exogenous cytidine to growing cultures of *pyrG*, *cdd* mutants and restore the levels of CTP to those found in wild type strains. The addition of exogenous cytidine gives an identical result to that obtained by growing the cells at the permissive temperature (Fig. 1). Using HPLC we can both monitor changes in the levels of enzyme activity and their control by intracellular levels of pyrimidine nucleotides. Additionally we can measure changes in the intracellular concentrations of the uridine and cytidine nucleotides themselves.

ACKNOWLEDGEMENTS

This investigation was supported in part by a Research Initiation Grant to M.S.S. from the Office of Research and Academic Grants and by a Texas Advanced Technology Research Grant to G.A.O'D.

REFERENCES

1 R. A. Kelln, J. J. Kinahan, K. F. Foltermann and G. A. O'Donovan, *J. Bacteriol.*, 124 (1975) 764.
2 G. A. O'Donovan, S. Herlick, D. E. Beck and P. K. Dutta, *Arch. Microbiol.*, 153 (1989) 19.
3 B. D. Davis and E. S. Mingioli, *J. Bacteriol.*, 60 (1950) 17.
4 J. X. Khym, *Clin. Chem.*, 21 (1975) 1245.
5 M. M. Bradford, *Anal. Biochem.*, 72 (1976) 248.
6 T. P. West and G. A. O'Donovan, *J. Gen. Microbiol.*, 128 (1982) 895.
7 A. L. Pogolotti, Jr. and D. L. Santi, *Anal. Biochem.*, 126 (1982) 335.
8 P. K. Dutta and G. A. O'Donovan, *J. Chromatogr.*, 385 (1987) 119.
9 I. Dutta, G. A. O'Donovan and D. W. Smith, *J. Chromatogr.*, 444 (1988) 183.
10 T. P. West, S. A. Herlick and G. A. O'Donovan, *FEMS Microbiol. Lett.*, 18 (1983) 275.
11 G. A. O'Donovan and J. Neuhard, *Bacteriol. Rev.*, 34 (1970) 278.
12 J. Neuhard and J. L. Ingraham, *J. Bacteriol.*, 95 (1968) 2431.

Journal of Chromatography, 512 (1990) 409–414
Elsevier Science Publishers B.V., Amsterdam

CHROMSYMP. 1838

Preparation of ethylenediaminephosphoramidates of nucleotides and derivatization with fluorescein isothiocyanate

AMR NOUR AL-DEEN
Department of Biochemistry, Alexandria University, Alexandria (Egypt)
DOUGLAS C. CECCHINI and SAMY ABDEL-BAKY
Department of Medicinal Chemistry, College of Pharmacy and Allied Health Professions, and Barnett Institute of Chemical Analysis and Materials Science, Northeastern University, Boston, MA 02115 (U.S.A.)
NEHAD M. ABDEL MONEAM
Department of Biochemistry, Alexandria University, Alexandria (Egypt)
and
ROGER W. GIESE*
Department of Medicinal Chemistry, College of Pharmacy and Allied Health Professions, and Barnett Institute of Chemical Analysis and Materials Science, Northeastern University, Boston, MA 02115 (U.S.A.)

ABSTRACT

Fluorescence post-labeling of nucleotides is a potentially useful technique for the detection of trace amounts of damaged DNA (DNA adducts). Towards this goal, we have studied a derivatization procedure starting with the four major 5′-deoxynucleotides as model compounds. The 5′-phosphate group was first labeled with ethylenediamine via a phosphorimidazolide intermediate in methanol with an organic-soluble carbodiimide. The resulting ethylenediaminephosphoramidate products were reacted in turn with fluorescein isothiocyanate. The reaction sequence has been characterised at all stages by high-performance liquid chromatography.

INTRODUCTION

In order to label a nucleic acid with a reporter group, the nucleic acid often is first prepared in a form which contains one or more aliphatic amine substituents. For example, Chu *et al.*[1] labeled nucleotides and polynucleotides at the terminal 5′-phosphate group with ethylenediamine.The reaction took place in imidazole buffer using a water-soluble carbodiimide. In turn, the amino-DNA product has been labeled with biotin[2,3], peroxidase and amplifiable reporter RNA[4]. Kelman *et al.*[5] utilized the same chemistry for the fluorescent labeling and high-performance liquid chromatography (HPLC) detection of damaged nucleotides (DNA adducts) derived from irradiated calf thymus DNA. As the authors pointed out, this approach could potentially be used for the assay in general of DNA adducts produced *in vivo*.

We are similarly interested in fluorophore labeling of DNA adduct nucleotides.

0021-9673/90/$03.50

Our goal is to use this technique to facilitate the detection and isolation of DNA adducts for subsequent structural elucidation by mass spectrometry. In the present work, we have investigated the conditions for fluorophore labeling. Some improvements are presented especially for the initial coupling of ethylenediamine to nucleotides.

MATERIALS AND METHODS

Chemicals and reagents

2′-Deoxyadenosine 5′-monophosphate (5′-dAMP), 2′-deoxycytosine 5′-monophosphate (5′-dCMP), 2′-deoxyguanosine 5′-monophosphate (5′-dGMP), thymidine 5′-monophosphate (5′-TMP), 1-ethyl-3-(3-dimethylaminopropyl)carbodiimide, ethylenediamine and fluorescein isothiocyanate (FITC) were purchased from Sigma (St. Louis, MO, U.S.A.). Imidazole, 2,6-lutidine, N,N′-dicyclohexylcarbodiimide and acetic acid were from Aldrich (Milwaukee, WI, U.S.A.). Silylation-grade dimethyl sulfoxide (DMSO), triethylamine (sequanal grade) and ninhydrin were from Pierce (Rockford, IL, U.S.A.). Sodium carbonate, sodium bicarbonate, HPLC-grade monobasic potassium phospate, ammonium hydroxide, 0.22-μm MSI Cameo, 3-mm diameter filters and HPLC solvents were from Fisher (Bedford, MA, U.S.A.).

HPLC

The analytical HPLC comprised a Series 4 LC system from Perkin-Elmer (Norwalk, CT, U.S.A.), a Brownlee RP C_{18}, Spheri-5, 150 × 4.6 mm I.D. cartridge column (Rainin, Woburn, MA, U.S.A.), a 9060 Polychrom diode array detector (Varian, Walnut Creek, CA, U.S.A.), a FS970 fluorescence detector (Schoeffel, Westwood, NJ, U.S.A.), a Cl-10B Integrator (LDC/Milton Roy, Bloomfield, CT, U.S.A.) and a Timberline column oven (Boulder, CO, U.S.A.). The fluorescence and diode array detector were connected in series. Ultraviolet spectra were saved on an IBM personal computer using the Polysoc program from Varian. Solvent A was 0.1 *M* potassium dihydrogen phosphate (pH 4.6) and solvent B was acetonitrile. The flow-rate was 1 ml/min. The column was equilibrated for at least 15 min with the starting solvent composition for each gradient prior to sample injection. At the end of each gradient elution, the solvents were returned to their starting compositions over a 2-min period and then the column was equilibrated for 15 min prior to the next injection. The deoxynucleotide-5′-monophosphates were separated with a 20-min gradient from 0-20% B. A 20-min, 0–30% B gradient was used for the nucleotide-phosphorimidazolide reaction mixtures. The nucleotide–ethylenediaminephosphoramidate reaction mixtures were separated with a 0–10% B gradient in 15 min. For all of the above, the column temperature was maintained at 30°C. The nucleotide-fluorescein derivatives were subjected to HPLC with a 20-min, 0–70% B gradient at 30°C, or with a 40-min, 10–20% B gradient at a column temperature of 80°C. Preparative HPLC was carried out (as described below) on the same equipment using a Rainin 25 × 1.0 cm RP-18, 5-μm Microsorb cartridge column (Rainin).

Synthesis

Deoxynucleotide-5′-ethylenediaminephosphoramidates (5′-dNMP-EDP). Three μmol of 5′-dAMP, 5′dGMP or 5′-TMP were dissolved in 20 μl of DMSO and added to

300 μl of a methanol solution of N,N-dicyclohexylcarbodiimide (DCC) and imidazole (1 *M* each). A 3-μmol amount of 5′-dCMP was dissolved in 32 μl of water and added to 600 μl of the same DCC–imidazole solution. (The 5′-dCMP was not soluble in DMSO, and the larger volume of the DCC–imidazole solution was necessary to prevent precipitation of the DCC in the presence of water.) In parallel, 20 μl of each of the four nucleotide solutions were combined and added to 600 μl of the DCC–imidazole solution. After 1 h at room temperature, one-half of each sample was added to an equal volume (200 or 300 μl) of 0.63 *M* aqueous ethylenediamine that had been adjusted to pH 7.5 with hydrochloric acid. The precipitate which formed (from DCC) was removed by centrifugation (2000 *g*) or by filtration through a 0.22-μm nylon filter. Each reaction mixture was heated to 55°C for 2 h and then kept at −20°C until further use.

The samples were evaporated to dryness with a Speed-Vac concentrator (Savant, Farmingdale, NY, U.S.A.), redissolved in 200 μl of water and purified by preparative HPLC. The mobile phase buffer was 0.005 *M* acetic acid, adjusted to pH 4.6 with triethylamine. The 5′-dCMP-EDP was purified isocratically with 100% buffer, 5′-TMP-EDP with a 10-min linear gradient from 0 to 5% acetonitrile and 5′-dGMP-EDP as well as 5′-dAMP-EDP with a 10-min gradient from 0 to 10% acetonitrile at a flow-rate of 5 ml/min. The purity of each compound was then determined by analytical HPLC. The 5′-dCMP-EDP required a second purification, which was done on the 22 × 0.46 cm I.D. Brownlee RP C_{18} column using 100% buffer. The pure products were evaporated to dryness in a Speed-Vac concentrator and stored at −20°C until further use.

FITC conjugates

Each 5′-dNMP-EDP (0.2 μmol) was dissolved in 0.1 ml of sodium carbonate–bicarbonate buffer, 0.1 *M*, pH 9.5. FITC (0.8 mg, 2 μmol) was added in 4 μl of dimethylformamide and the reaction was kept for 18 h at room temperature in the dark, followed by freezing at −20°C until further use.

The 5′-dNMP-FITC derivatives were purified by preparative gradient HPLC, 10 to 70% acetonitrile over 30 min in 0.01 *M* acetic acid–triethylamine (pH 4.6) at 5 ml/min.

RESULTS AND DISCUSSION

Deoxynucleotide-5′-ethylenediaminephosphoramidates (5′-dNMP-EDP)

In order to label nucleotides, we initially followed the procedure of Chu *et al.*[1] developed for labeling the 5′-terminus of oligodeoxynucleotides. The 5′-dNMP-phosphorimidazolides (5′-dNMP-PIs) were prepared in an aqueous solution (pH 6) of imidazole and water-soluble carbodiimide. These products were then treated with an excess of ethylenediamine buffered with lutidine–HCl (pH 7.5) and the reactions were monitored by HPLC. The UV spectra of the 5′-dNMPs and their corresponding PI and EDP products were identical as expected (Fig. 1). Based on measurements of the relative peak areas of the products and starting materials for each reaction, the yields of the 5′-dNMP-EDPs were 80–90%.

We intend to use this reaction to facilitate the detection and isolation of nucleotide adducts obtained from enzymatic hydrolysates of DNA. These nucleotide

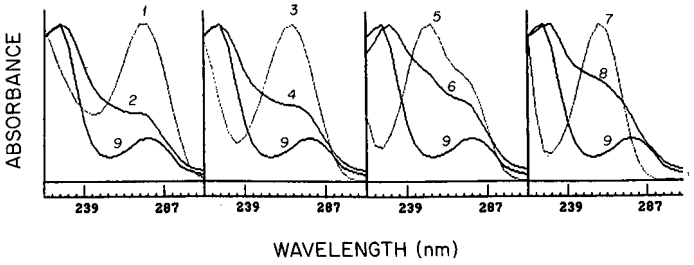

Fig. 1. Diode array UV spectra of HPLC peaks of the 5′-dNMPs and their corresponding FITC derivatives. 1 = 5′-dCMP; 2 = 5′-dCMP-FITC; 3 = 5′-TMP; 4 = 5′-TMP-FITC; 5 = 5′-dGMP; 6 = 5′-dGMP-FITC; 7 = 5′-dAMP; 8 = 5′-dAMP-FITC; 9 = FITC. The spectra were normalized to give full-scale absorbance at the UV maximum.

adducts occur at extremely low levels[6]. It is therefore desirable to optimize the reaction in every respect. In order to improve the reaction yields, we varied the conditions of the first step of the reaction sequence, the formation of the phosphorimidazolide. However, under aqueous conditions we could not achieve greater than 90–95% conversion of starting nucleotides to the corresonding 5′-dNMP-PI intermediate products based on HPLC analysis. The remaining 5–10% could be seen by HPLC as

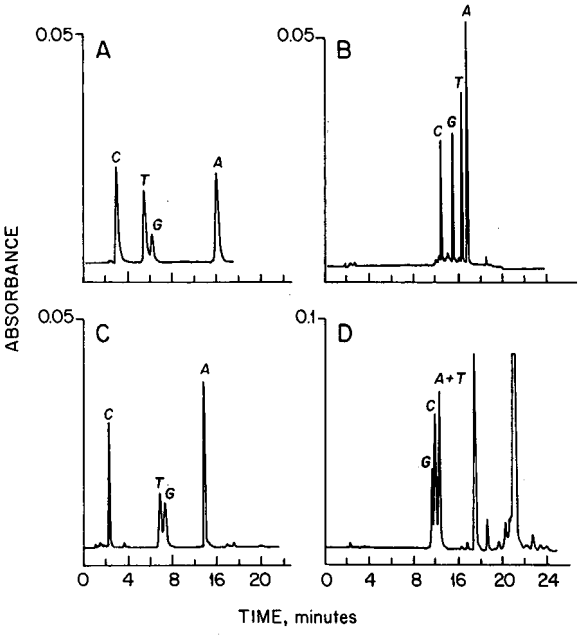

Fig. 2. Reversed-phase HPLC chromatograms of 5′-dNMP starting materials and their subsequent PI, EDP and FITC reaction mixtures. From each reaction mixture, a 2–15-μl sample was injected without prior purification containing *ca.* 1 nmol of each nucleotide or modified nucleotide. The HPLC solvent was a gradient of acetonitrile in 0.1 *M* potassium phosphate, pH 4.5. (A) 5′-dNMPs, 0–20% acetonitrile in 20 min, (B) 5′-dNMP-PIs, 0–30% acetonitrile in 20 min, (C) 5′-dNMP-EDPs, 0–10% acetonitrile in 15 min, (D) 5′-dNMP-FITCs, 0–70% acetonitrile in 20 min. Detection was at 263 nm.

the 5′-dNMP starting materials (data not shown). At pH 6, it is known that 5′-dNMP-PIs slowly hydrolyze back to the 5′-dNMPs[1]. This could account for the presence of the residual starting nucleotides. Since our interest is in the detection of nucleotides rather than oligonucleotides it was not necessary to maintain aqueous conditions. By changing the starting solvent to methanol along with a change to an organic-soluble carbodiimide, we were able to form the PI intermediates in a quantitative yield based on HPLC (Fig. 2B). Under these conditions, the 5′-dNMP-PIs were significantly stabilized: the reaction mixtures could be stored for weeks at 4°C with no change in the amount of 5′-dNMP-PIs. The use of the organic-soluble carbodiimide may also have been advantageous since side reactions are known to occur when a positively charged, water-soluble carbodiimide is reacted with a nucleotide[7].

The PI intermediates were then reacted directly with an aqueous solution of ethylenediamine adjusted to pH 7.5 with hydrochloric acid. The lutidine buffer was eliminated since it seemed to be unnecessary and tended to overload the column during preparative HPLC of the 5′-dNMP-EDPs. With these modifications, a quantitative conversion of the 5′-dNMPs to the corresponding 5′-dNMP-EDPs was obtained (Fig. 2C).

5′-dNMP-FITC

The 5′-dNMP-EDPs were purified by preparative HPLC and reacted, both separately and combined, with an excess of FITC at pH 9.5. An HPLC chromatogram of a combined reaction mixture (Fig. 2D) shows complete disappearance of the

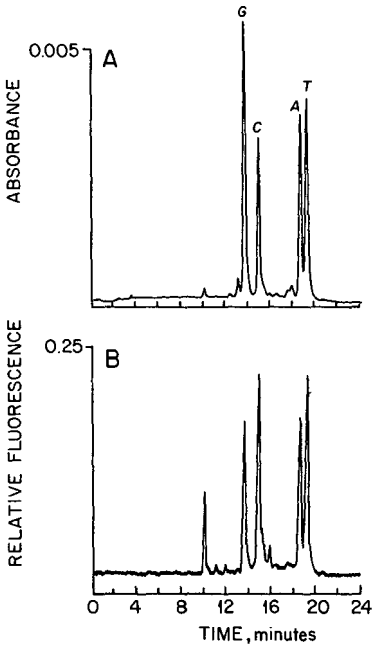

Fig. 3. Reversed-phase HPLC chromatogram of the HPLC-purified 5′-dNMP-FITCs with simultaneous UV (263 nm, A) and fluorescence (480 nm excitation, 520 nm emission filter, B) detection. The separation was performed at 80°C using a 20-min, 10–20% acetonitrile gradient in 0.1 *M* potassium phosphate, pH 4.5.

5′-dNMP-EDPs and the appearance of the 5′-dNMP-FITC derivatives. The later eluting peaks are the hydrolysis products of FITC. These peaks are also present when a reaction blank is tested that contains no 5′-dNMP-EDPs (data not shown).

As seen in Fig. 2D, sharp peaks are obtained for the 5′-dNMP-FITCs, but the resolution is poor. In fact, 5′-dAMP-FITC and 5′-TMP-FITC coelute. This separation was achieved by reversed-phase HPLC using a steep gradient. When a less steep gradient is employed, the latter two peaks remain unresolved, and all 5′-dNMP-FITC peaks tail severely (data not shown).

In order to investigate this separation in more detail, we isolated the 5′-dNMP-FITCs from the separate reaction mixtures by preparative HPLC and prepared a combined sample free of the FITC hydrolysis products. The 5′-dNMP-FITCs could be fully separated by analytical reversed-phase HPLC at 80°C as shown in Fig. 3. Although this elevated temperature dramatically improved the peak shape, it will undoubtedly reduce the column lifetime. Thus, other approaches to this separation need to be investigated. The diode array UV spectra for the 5′-dNMP-FITCs (Fig. 1) correspond exactly to the composite spectra derived from FITC and the 5′-dNMP's. Both UV (Fig. 3A) and fluorescence (Fig. 3B) detection were performed.

The two chromatograms in Fig. 3 show some unidentified, small peaks in addition to the four major peaks for the 5′-dNMP-FITCs. These peaks are either previously unresolved side products formed during the FITC conjugation reaction, or decomposition products generated during the isolation of the 5′-dNMP-FITC.

CONCLUSION

Nucleotide ethylenediaminephosphoramidate derivatives (5′-dNMP-EDPs) can be formed in a quantitative yield, stored without decomposition and labeled efficiently with a fluorophoric reagent such as FITC. In our future work, we will investigate the formation, stability and separation properties of the fluorescein derivatives in more detail and also explore the use of other fluorescent labeling reagents. These studies should lead to a practical method for detecting and isolating DNA adducts.

ACKNOWLEDGEMENTS

The research described in this article was supported by Grant CA 35843 from the National Cancer Institute and by funding from the Channel Program of the Egyptian Government. Contribution No. 415 from the Barnett Institute.

REFERENCES

1 B. C. F. Chu, G. M. Wahl and L. E. Orgel, *Nucleic Acids Res.*, 11 (1983) 6513.
2 A. Chollet and E. H. Kawashima, *Nucleic Acids Res.*, 13 (1985) 1529.
3 B. C. F. Chu and L. E. Orgel, *DNA*, 4 (1985) 327.
4 B. C. F. Chu and L. E. Orgel, *Nucleic Acids Res.*, 16 (1988) 3671.
5 D. J. Kelman, K. T. Lilga and M. Sharma, *Chem.-Biol. Interact.*, 66 (1988) 85.
6 A. M. Jeffery, in D. Grunberger and S. Goff (Editor), *Mechanisms of Cell Transformation by Carcinogenic Agents*, Pergamon Press, New York, 1987, p. 33.
7 P. T. Gilham, *J. Am. Chem. Soc.*, 84 (1962) 687.

Journal of Chromatography, 512 (1990) 415–431
Elsevier Science Publishers B.V., Amsterdam

CHROMSYMP. 1829

Convenient purification of tritylated and detritylated oligonucleotides up to 100-mer

TONYA L. HILL* and JAMES W. MAYHEW
Beckman Instruments, Altex Division, 4550 Norris Canyon Road, P.O. Box 5101, San Ramon, CA 94583 (U.S.A.)

ABSTRACT

Oligomers from crude phosphoramidite synthesis mixtures have been purified by reversed-phased high-performance liquid chromatography by exploiting the chromatographic variables of stationary phase pore size, chain length, and gradient shape. Chromatography was performed on oligomers up to 100-mer with mobile phases containing triethylammonium acetate/acetonitrile mixtures. Convenient guidelines are offered to enrich or purify synthetic oligomers.

Tritylated oligomers up to 25 bases in length are best purified on C_8 or C_{18}, 80 Å columns with moderate strength mobile phases using a combination of isocratic delays and shallow gradients. For oligomers longer than 25-mer, C_3, 300 Å columns provide adequate fast purification in as little as 5 min, while 300 Å, C_8 columns with long, slow gradients gave substantially increased purity.

Chromatography of detritylated oligomers requires a modified approach. Up to 25-mer they are best purified on 80 Å, C_{18} columns with much lower organic concentrations and shallower gradients than those used for tritylated oligomers. Detrytilated oligomers greater than 25-mer can be enriched on both C_3 and C_8, 300 Å columns using the same conditions described for shorter detritylated oligomers.

INTRODUCTION

Successful oligonucleotide chromatography requires a thoughtful assessment of analytical choices in light of experimental goals. Before the synthesis is even begun, the scientist chooses the oligomer base sequence and length, and whether the products of synthesis are to be recovered in the tritylated or detritylated form. Other variables affect the separation of the products during the chromatographic purification. These include pore size, ligand chain length, gradient shape and selection of solvent type and ion-pairing agent[1–4]. Both the synthesis and chromatographic variables are interactive. An understanding of these interactions is important so that the required level of product purity can be achieved conveniently.

The base sequence and length of the oligomer are of course defined before synthesis. The effect of base sequence on the purification of oligomers has been previ-

ously studied, and no absolute relation was found between oligomer length or base sequence and capacity factor (k') (ref. 5). The choice of whether to recover the oligomers in the tritylated or detritylated form is determined by the degree of purity and speed of analysis required. Generally, the scientist will choose the detritylated form if he is interested in isolating an enriched fraction containing his oligomer, requires a fast clean-up, or desires a quality assurance check on a routine synthesis.

The tritylated from will be chosen for the separation of very-high-purity product, or for preparative work[6,7]. Such applications will require the removal of some or all of the following impurities: synthesis by-products, truncated chains, base modified chains and chain cleavages[8]. If purified in the trityl-on form, the trityl group must be hydrolyzed and extracted after chromatographic purification. An additional purification step may even be required for some specific applications[9].

Pore size, ligand chain length and gradient shape are the primary tools for the reversed-phase high-performance liquid chromatography (HPLC) of synthetic oligonucleotides. Our studies include the chromatography of both tritylated and detritylated oligomers over the range 16- to 100-mer. Studies were performed on stationary phases with 80 Å pore diameters (C_8 and C_{18}) as well as 300 Å stationary phases (C_3 and C_8). Convenient guidelines are offered to enrich or purify:

(1) tritylated oligomers up to 25-mer;
(2) tritylated oligomers greater than 25-mer;
(3) detritylated oligomers up to 25-mer; and
(4) detritylated oligomers greater than 25-mer.

EXPERIMENTAL

Instrumentation

HPLC analysis was performed with a Beckman System Gold™ for Methods Development consisting of a Model 126 programmable solvent module, a Model 167 programmable scanning detector module monitoring at 254 nm, a Model 210A injection valve with a 20-μl loop, and an IBM-AT personal computer with System Gold software.

Chemicals

Acetonitrile was HPLC grade from J. T. Baker (Phillipsburg, PA, U.S.A.). Sequanal grade triethylamine used for preparation of the buffers was purchased from Pierce (Rockford, IL, U.S.A.). Buffers were prepared from high-purity water (Milli-Q). Glacial acetic acid was obtained from Mallinkrodt (Paris, KY, U.S.A.).

Chromatographic conditions

Gradient elution was used for the reversed-phase separations. Gradient profiles are given on each chromatogram. Various gradients and isocratic delay times were used for the separations as described below.

The aqueous buffer was 0.1 *M* triethylammonium acetate (TEAA), pH 7.0. The working solutions were prepared by dilution of a 0.5 *M* stock. The stock was prepared as follows: 27 ml of glacial acetic acid was added to 850 ml of HPLC-grade water. A 70 ml volume of sequanal-grade triethylamine was added with stirring. The pH was adjusted to 7.0 ± 0.05 with glacial acetic acid, and then the solution was brought up to 1.0 l.

The flow-rate was always 1.0 ml/min. Mobile phases for all chromatography are: (A) 0.1 *M* TEAA, pH 7.0; (B) 0.1 *M* TEAA in 70% acetonitrile.

A description of the methods follows.

Method 1: 3 min at 15% B, increase to 33% B over 11 min, isocratic for 29 min, then to 100% B over 4 min.

Method 2: increase from 15% B to 29% B over 10 min, isocratic for 20 min, then to 100% B over 4 min.

Method 3: increase from 15% B to 29% B over 3.3 min, isocratic for 6.6 min, then to 100% B in 1.32 min.

Method 4: 1 min at 15% B, increase to 57% B over 1.6 min, isocratic for 3.65 min, then to 15% B in 0.66 min.

Method 5: 3 min at 15% B, increase to 40% B over 5 min, isocratic for 4 min, then to 57% B over 2 min.

Method 6: increase from 0% B to 29% B over 40 min.

Method 7: increase from 0% B to 29% B over 12 min.

Method 8: increase from 0% B to 21% B over 60 min.

Samples

All oligomers were chromatographed in their crude form and were not extracted or desalted in any way before analysis. All oligomers were gifts and were synthesized by the phosphoramidite method. The sequences of the crude oligomers follow.

16-mer 5′ TGC TCT TGT TGA GCA G 3′
17-mer 5′ TGC TCT TGT TGA GCA GT 3′
29-mer 5′ GGC CAG TGC CAA GCG TGC TAG CCT GCA GG 3′
33-mer 5′ GAT CCC AGA AGT AGT TTT GAT GCA CAT GCA ACG
36-mer 5′ GCT TAG AAA GGA GGT GAT CCA GGT TTT GAA TTC ACA 3′
37-mer 5′A GCT TAG AAA GGA GGT GAT CCA GGT TTT GAA TTC ACA 3′
76-mer 5′CCT TCA GTT CAG GGG ACA GCT CCT TGG TTC TTC CAT ACA GGG TAA TTT TGA AGT ATT GCT TGT TTT CAG TTC AGA A 3′
100-mer 5′ AGC AGC AAG CTT GGT CGA CAG ATC CAG GAG AGG TCA ACC TGT CTG GTC TGA CTG TCT GCT CCC TTC TGA TCA ACC TAG GTT TGG GGC AGA GTT TGA TCT G 3′

Sample load was 5 to 50 μg of each oligomer in an injection volume of 5–20 μl. All samples were diluted to the same composition as the starting mobile phase of the gradient to be used.

When necessary, certain oligomers were detritylated. These samples were reduced to dryness under vacuum, then resuspended in 1.0 ml of 80% acetic acid. The solution was held at room temperature for 45 min and was then dried under vacuum. The residues were resuspended in the starting mobile phase. No further extraction or desalting steps were performed.

RESULTS AN DISCUSSION

Tritylated oligomers

The purification of tritylated oligomers will be discussed before the purification of detritylated oligomers. In each case we will illustrate the contributions of three chromatographic tools to the purification of crude synthetic oligomers: (1) pore size, (2) ligand chain length, and (3) gradient shape.

Figs. 1 and 2 show the chromatography of tritylated oligomers on C_8 stationary phases with pore diameters of both 300 and 80 Å. In general, oligomers greater than 25-mer are best purified on 300 Å packing, and those less than 25 are best purified on 80 Å packing. A mixture of two crude synthetic oligomers less than 25 bases in length were analyzed on 80 Å (Fig. 1A) and 300 Å (Fig. 1B) C_8 columns using the same mobile phases and gradients. The 16-mer and 17-mer differ only by a single thymidine at the 3′ end, and the 16-mer would be a likely failure contaminant in the synthesis of the 17-mer.

Although both columns are able to resolve the two oligomers and separate them from synthesis by-products and detritylated failures, the 80 Å column shows improved resolution of the 16-mer from the 17-mer. The 80 Å column also shows improved resolution of the 16- and 17-mers from suspected depurinated-mers. The oligomers have increased retention times on the 80 Å column as compared to the 300 Å column. The improved resolution and increased retention times correlate with the increased surface area available on the 80 Å as compared to the 300 Å column.

In our experience on reversed-phase HPLC with triethylammonium phosphate (TEAP) (pH 7.0), purines as free bases, nucleotides and 5′ mono- and diphosphates elute faster than pyrimidines (data not shown). Similar results have been reported by Ip *et al.*[10] using triethylammonium bicarbonate (TEAB) (pH 7.4).

The relative hydrophobic character of the exposed terminal base on the 3′ end of the oligomers appears to influence the reversed phase elution. In this case the 16-mer containing the less hydrophobic pyrimidine elutes before the 17-mer containing the more hydrophobic purine.

A mixture of two crude synthetic oligomers longer than 25 bases were chromatographed on both the 80 Å (Fig. 2A) and 300 Å (Fig. 2B) C_8 columns. The 36- and 37-mers differ only by a single adenosine residue at the 5′ end. Baseline resolution of the two oligomers is demonstrated on both columns, but the resolution of the 36- and 37-mers is favored on the 300 Å column.

The 300 Å packing also shows improved resolution of the suspected depurinated-mers from the products. A contaminant peak which co-elutes with the 37-mer on the 80 Å column is well resolved from the 37-mer on the 300 Å column. The more efficient purification of the 36- and 37-mers on the 300 Å column is the result of the increased ability of these oligomers to access the surface area within the pores on the 300 Å as compared to the 80 Å column. Most of the surface area available for the resolution of compounds is contained within the pores of the packing. The 36- and 37-mers, for example, have little access to the surface area within the 80 Å pores, while polymers less than 25-mer can be included in the pore volume.

The purification of tritylated oligomers on stationary phases having different ligand chain lengths are presented in Figs. 3 and 4. Oligomers less than 25 bases show little difference in resolution when run on the C_8 and C_{18}, 80 Å stationary phases.

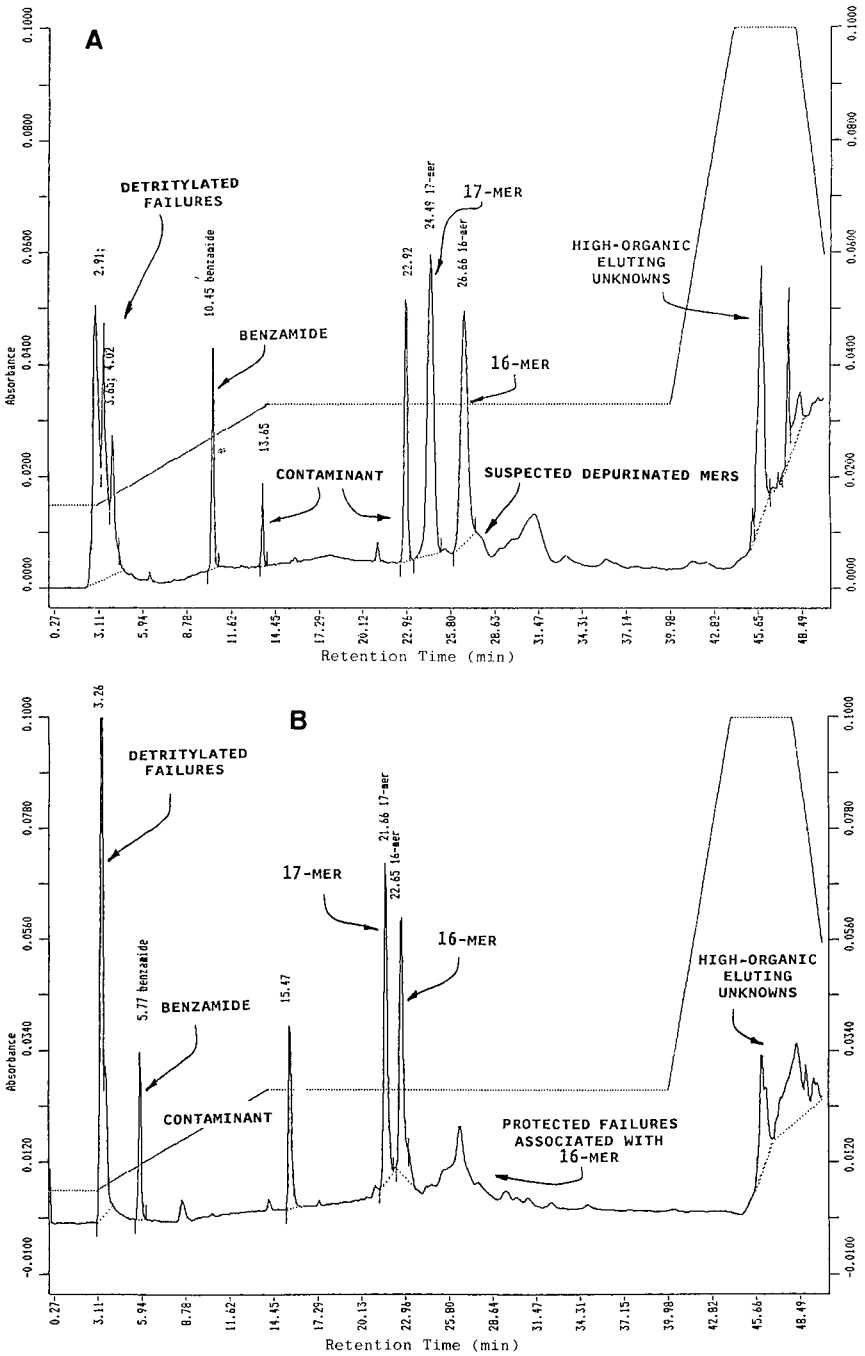

Fig. 1. Contribution of pore size to the separation of tritylated oligomers <25-mer. (A) Beckman Ultrasphere™ C_8, 80 Å (250 × 4.6 mm I.D.) column; (B) Beckman Ultrapore™ C_8, 300 Å (250 × 4.6 mm I.D.) column. Method 1.

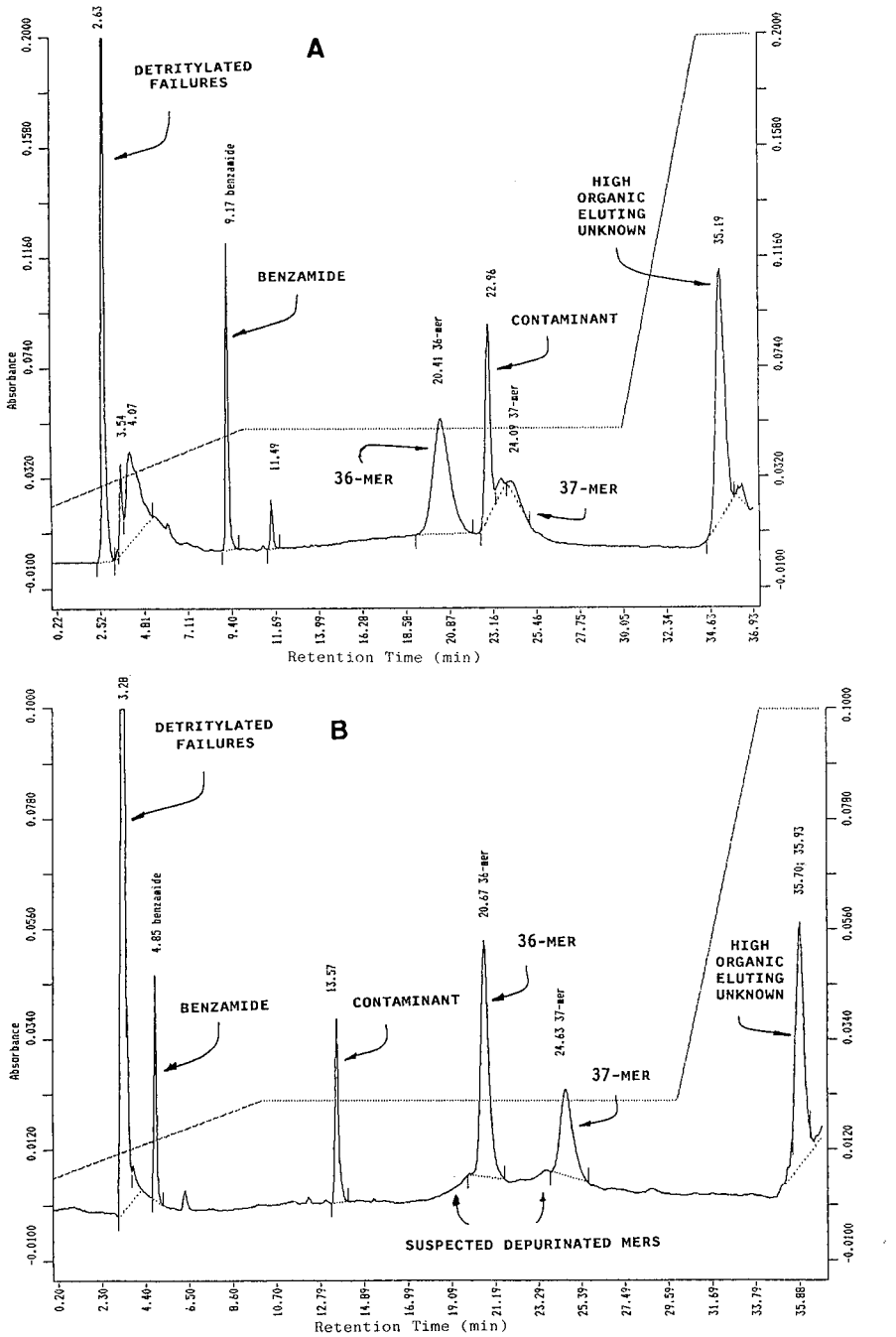

Fig. 2. Contribution of pore size to the separation of tritylated oligomers >25-mer. (A) Beckman Ultrasphere C_8, 80 Å (250 × 4.6 mm I.D.) column; (B) Beckman Ultrapore C_8, 300 Å (250 × 4.6 mm I.D.) column. Method 2.

However, oligomers greater than 25-mer were better resolved on the C_8, 300 Å as compared to the C_3, 300 Å column.

A mixture of crude synthetic 16- and 17-mers were analyzed on both C_8 (Fig. 3A) and C_{18} (Fig. 3B) 80 Å columns using identical mobile phases and gradients. Both C_8 and C_{18} columns provided baseline resolution of the 16- and 17-mers in the isocratic portion of the gradient. The 16- and 17-mers are retained approximately one minute longer on the C_{18} column and the peak widths are slightly larger than those on the C_8 column. In this case there is no real difference in resolution on C_8 and C_{18} columns. However, a contaminating substance found in both the 16- and 17-mers is better resolved from the 17-mer on the C_{18} column. The C_{18} column, therefore, may have an advantage for the purification of product oligomers from closely eluting contaminants.

The purification of a mixture of crude synthetic oligomers greater than 25 bases is shown in Fig. 4. The 36- and 37-mers are being separated on both C_3 (Fig. 4A) and C_8 (Fig. 4B) 300 Å columns. The C_8 column shows significantly increased resolution of the 36- and 37-mers as compared to the C_3 column.

Gradient shape can be manipulated to control the balance between the degree of purification and the speed of the analysis required. The contribution of gradient shape to oligomer separation is illustrated in Figs. 5 and 6. All chromatography is carried out on a C_8, 300 Å column (75 × 4.6 mm I.D.) with identical mobile phases and variations in gradient shape. Fig. 5A shows the purification of the 36- and 37-mer with an initial gradient of 3% acetonitrile per min followed by an isocratic hold at 20% acetonitrile. With this gradient, the 36- and 37-mers are well resolved from one another, as well as from the contaminant, the synthesis by-products, and detritylated oligomers. In Fig. 5B, the gradient was changed to consist of a 1-min isocratic hold followed by a gradient of 17% acetonitrile per min. Under these stronger eluting conditions, the 36-, 37-mer and contaminating compound co-elute. However, the gradient permits the purification of the product oligomers from both the synthesis by-products and detritylated-mers in less than 5 min.

Similar gradients consisting of a 3-min isocratic hold followed by a 3.5% increase in acetonitrile content per min were used in Fig. 6 to purify a 76-mer and a 100-mer. The product oligomers are cleanly separated from the synthesis by-products and detritylated oligomers. Often oligomers for gene constructs or mutagenic studies are in the range of 20–80 bases or more in length. Purity requirements for these products may be very stringent. A single purification step may not be sufficient to provide product of the required purity[11].

Detritylated oligomers

The principles discussed for selection of stationary phase pore diameter hold for detritylated oligomers as well as tritylated oligomers. Oligomers >25 in length are best analyzed on the wide-pore 300 Å packing, and oligomers <25 are best run on 80 Å packing.

The separation of detritylated oligomers on stationary phases having different ligand chain lengths is presented in Figs. 7–9. Oligomers less than 25 bases were better resolved on C_{18}, 80 Å as compared to C_8, 80 Å columns. However, oligomers greater than 25 showed no difference in resolution when run on the C_3 and C_8, 300 Å phases.

Fig. 7A shows the separation of a mixture of two detritylated 17-mers on the

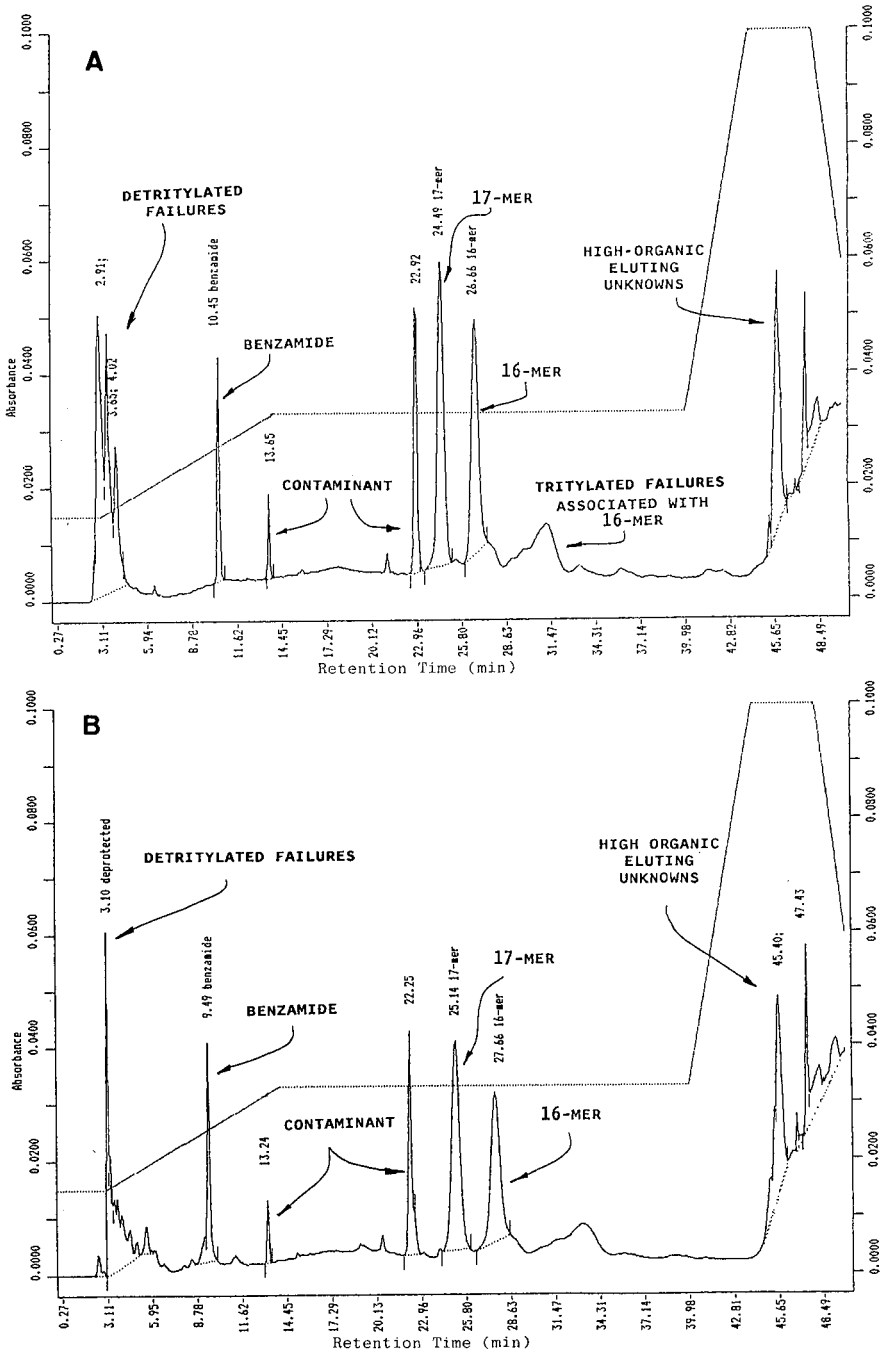

Fig. 3. Contribution of ligand chain length to the separation of tritylated oligomers <25-mer. (A) Beckman Ultrasphere C_8, 80 Å (250 × 4.6 mm I.D.) column; (B) Beckman Ultrasphere C_{18}, 80 Å (250 × 4.6 mm I.D.) column. Method 1.

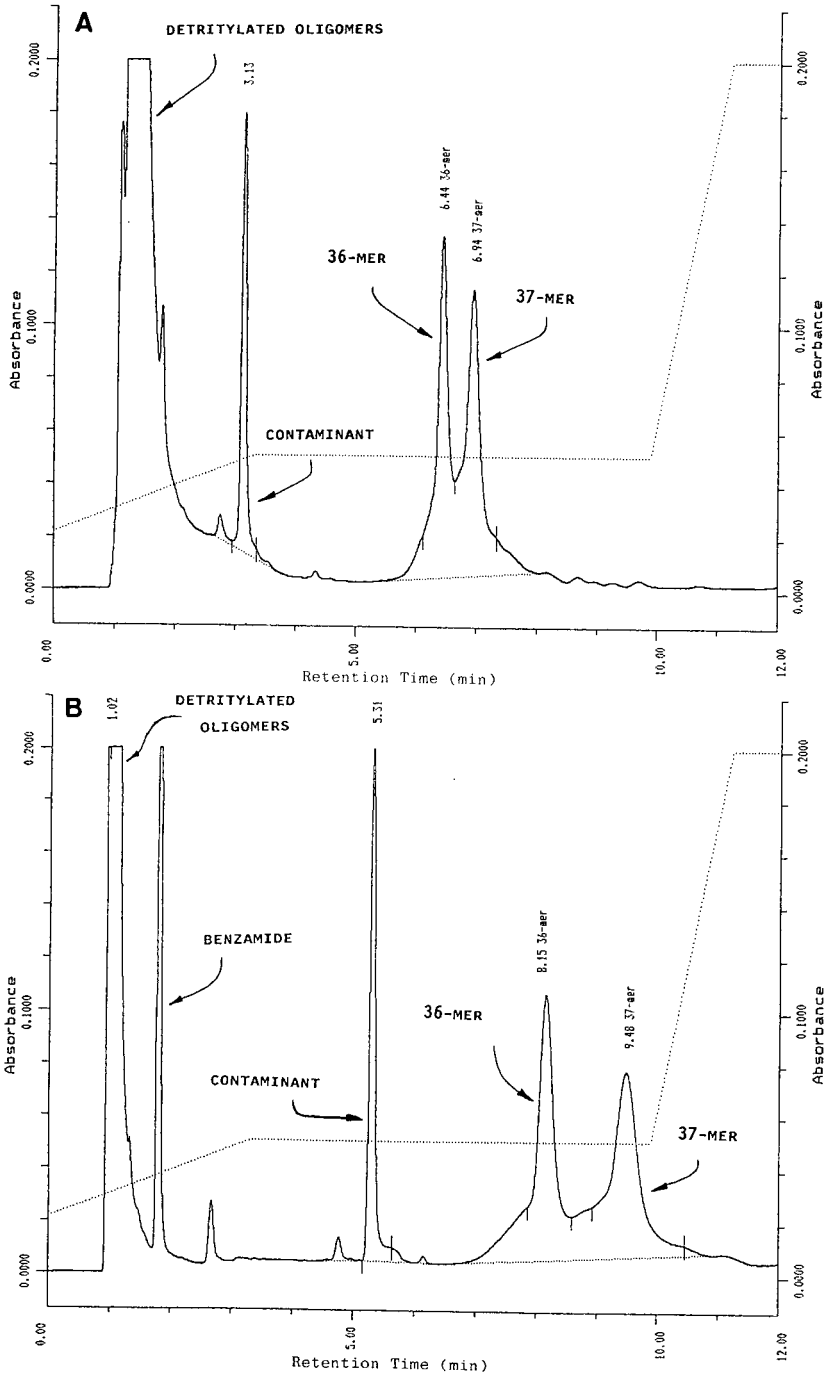

Fig. 4. Contribution of ligand chain length to the separation of tritylated oligomers >25-mer. (A) Beckman Ultrapore C_3 300 Å (75 × 4.6 mm I.D.) column; (B) Beckman Ultrapore C_8, 300 Å (75 × 4.6 mm I.D.) column. Method 3.

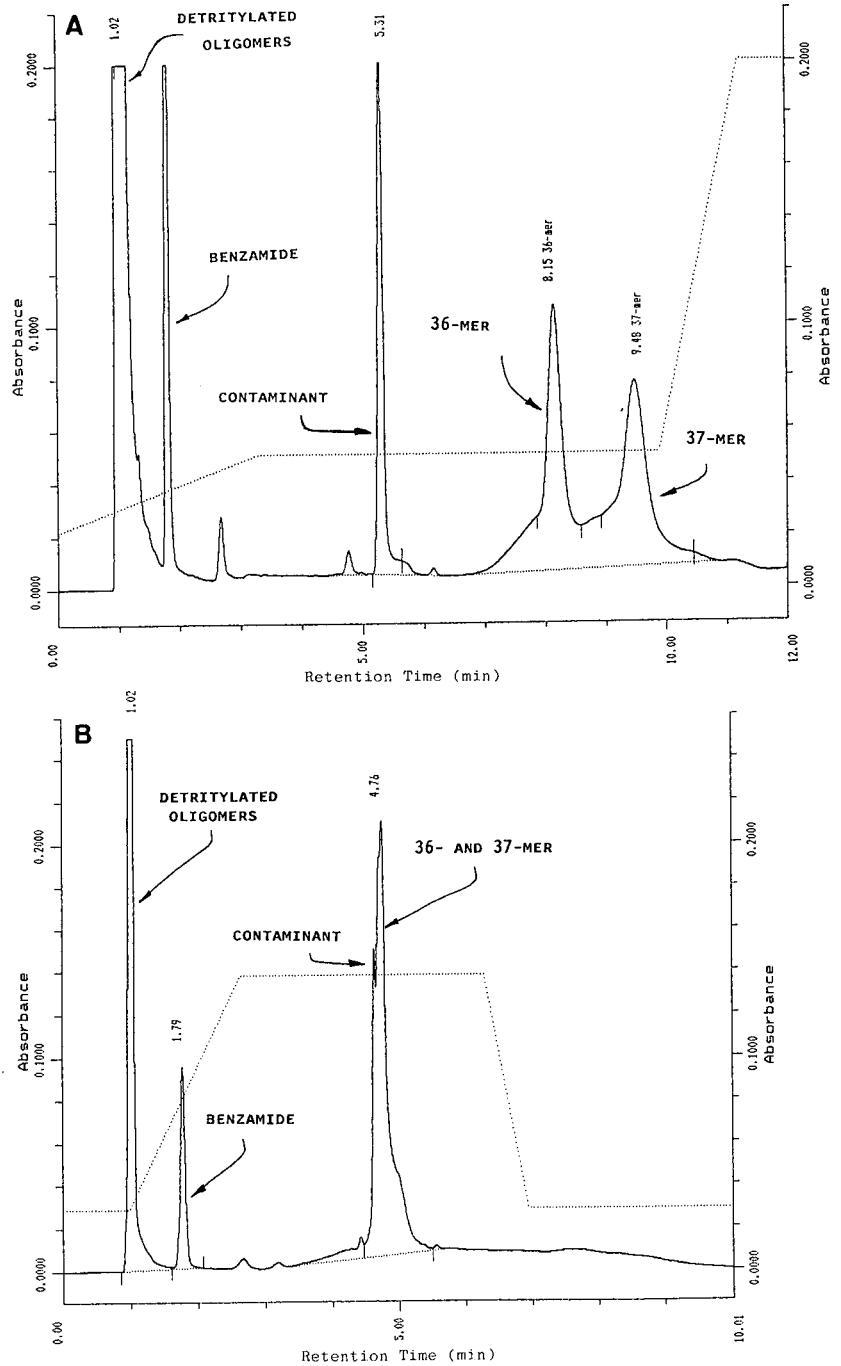

Fig. 5. Dependence of the separation of tritylated oligomers on the gradient shape. (A) Shallow gradient (method 3); (B) steeper gradient (method 4). Column: Beckman Ultrapore C_8, 300 Å (75 × 4.6 mm I.D.).

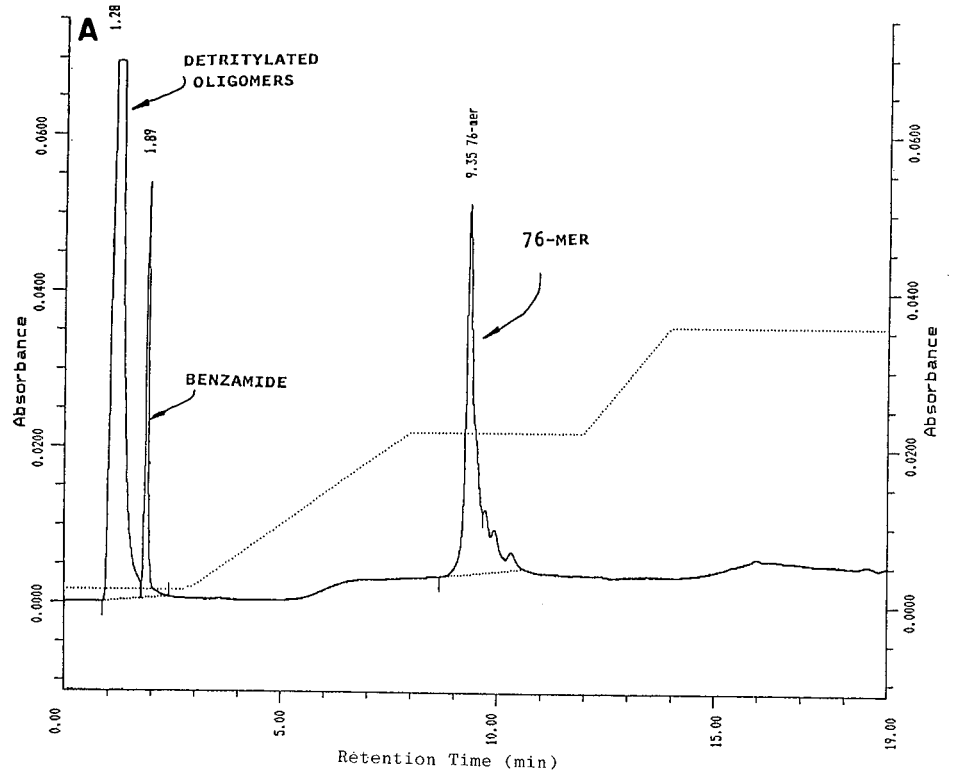

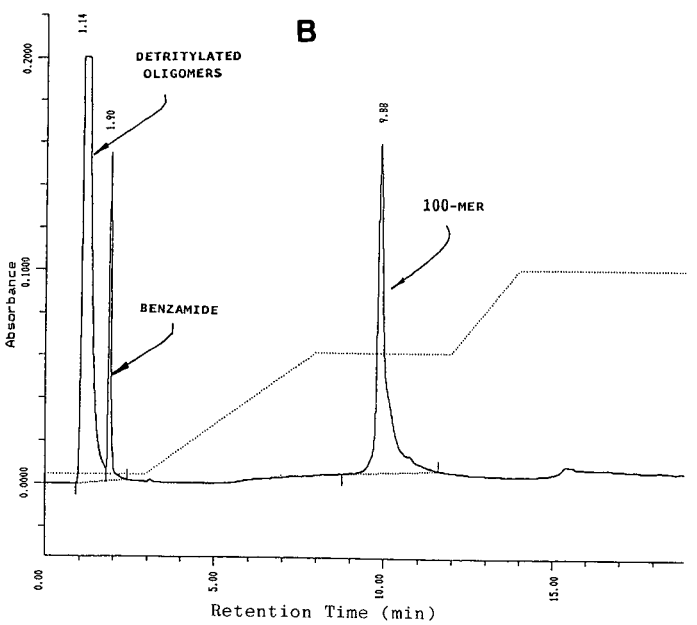

Fig. 6. Fast reversed-phase separation of tritylated oligomers >25-mer by gradient modification. (A) 76-mer; (B) 100-mer. Column: Beckman Ultrapore C_8, 300 Å (75 × 4.6 mm I.D.). Method 5.

C_8, 80 Å column. The two 17-mers have similar GC/AT ratios but very different sequences. The two oligomers are separated by 2.1 min on the C_8 column. Fig. 7B shows the same detritylated oligomers run on the C_{18} column, with a separation of 2.5 min. The C_{18} column provides improved separation of oligomers having similar base composition.

Oligomers greater than 25-mer were run on both C_3 and C_8, 300 Å columns using identical gradients and mobile phases. The 29- and 33-mer differ by both base sequence and composition. The GC/AT ratio for the 29-mer is 2.2 and for the 33-mer is 0.83. Fig. 8A shows the separation of the oligomers on the C_3, 300 Å column. The oligomers are separated by 0.62 min. Fig. 8B shows chromatography on the C_8, 300 Å column, and the separation is 0.51 min. The retention time is approximately 1 min longer on the C_8 column than on the C_3 column, but the increased retention time does not improve the resolution of the oligomers.

Gradient shape can be adjusted to further enrich detritylated oligomers. A shallower gradient offers increased resolution of similar composition oligomers, as well as a slight improvement in resolution from other compounds present in the reaction mixture. Fig. 9 illustrates two different gradients to separate oligomers less than 25-mer and Figs. 10 and 11 illustrate alteration of gradient shape for oligomers longer than 25.

Fig. 9A shows the separation of two 17-mers on a C_{18} column with a 0.5%/min acetonitrile gradient. Fig. 9B shows the same oligomers on the same column with a 0.25%/min acetonitrile gradient. As the retention time increases from approximately 26 min to 48 min with the shallower gradient, the separation increases from 2.5 min to 4.3 min. In addition, the 17-mers appear to be better resolved from other compounds present in the reaction mixture.

Fig. 10 shows the chromatography of a 76-mer using a gradient of 0.5% acetonitrile per min. Fig. 11 contains chromatographs of the same oligomer using a 0.25%/min acetonitrile gradient. The separation of the oligomer from failures and reaction by-products is slightly improved by the slower gradient. As the length of the oligomer increases, the number of failure sequences increases, and the difficulty of purification also increases[12].

CONCLUSIONS

Convenient purification guidelines are offered for the reversed-phase HPLC of crude synthetic oligonucleotides:

(1) Tritylated oligomers up to 25-mer are best purified on C_8 or C_{18} 80 Å columns. A combination of isocratic delays and shallow gradients with moderate strength mobile phases permits the simultaneous resolution of oligomers differing by as little as one base pair from suspected depurinated-mers as well as reaction by-products and detritylated-mers.

(2) Tritylated oligomers greater than 25-mer are best purified on 300 Å columns. The C_8 columns gave substantially increased purity as compared to the C_3 phase. Steeper gradients permitted oligomers up to 100-mer to be quickly separated from detritylated-mers and reaction by-products in as little as 10 min. A combination of shallower gradients and isocratic regions permitted the resolution of oligomers differing by as little as one base pair as well as the separation of depurinated-mers.

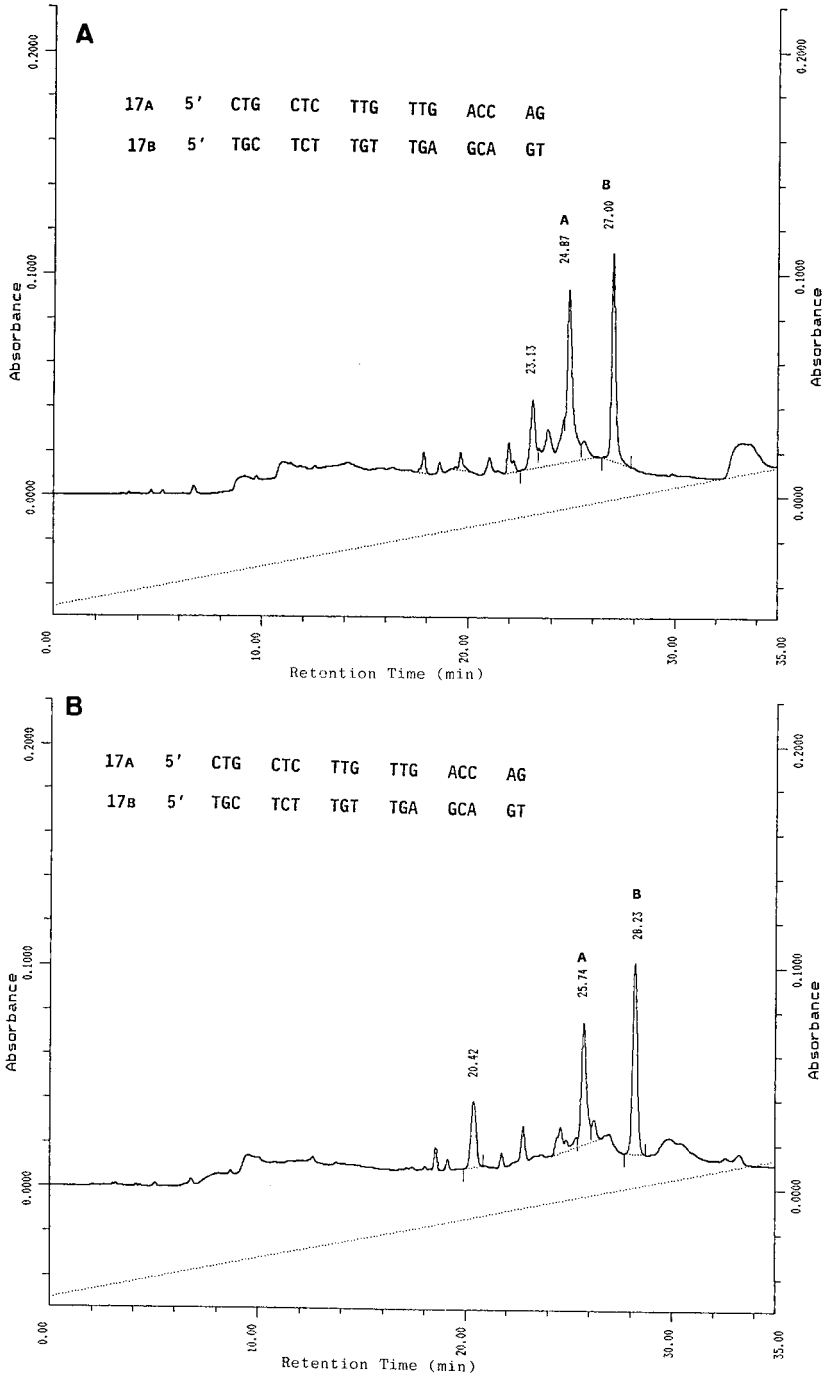

Fig. 7. Contribution of ligand chain length to the enrichment of detritylated oligomers <25-mer. (A) Beckman Ultrasphere C_8, 80 Å (250 × 4.6 mm I.D.) column; (B) Beckman Ultrasphere C_{18}, 80 Å (250 × 4.6 mm I.D.) column. Method 6.

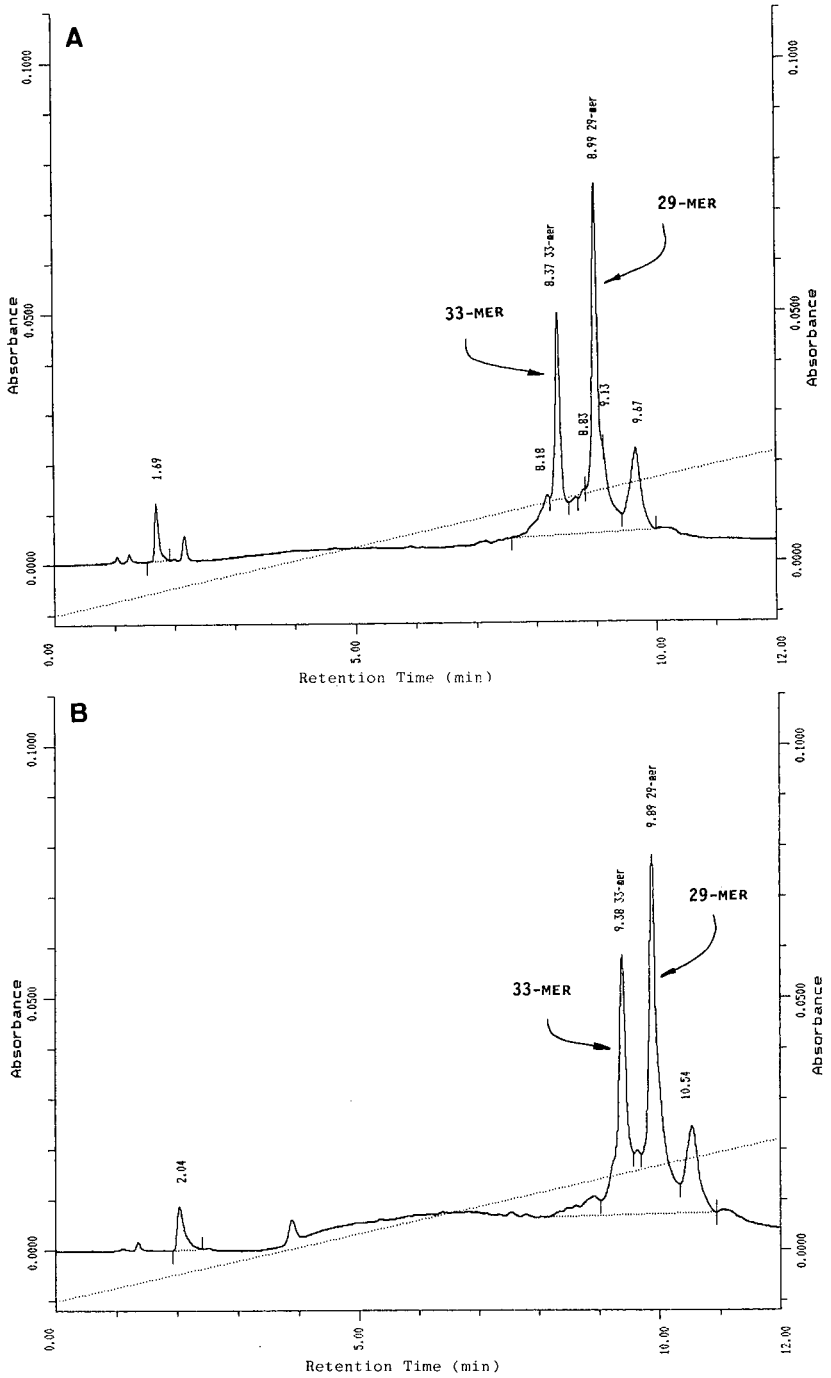

Fig. 8. Contribution of ligand chain length to the enrichment of detritylated oligomers >25-mer. (A) Beckman Ultrapore C_3, 300 Å (75 × 4.6 mm I.D.) column; (B) Beckman Ultrapore C_8, 300 Å (75 × 4.6 mm I.D.) column. Method 7.

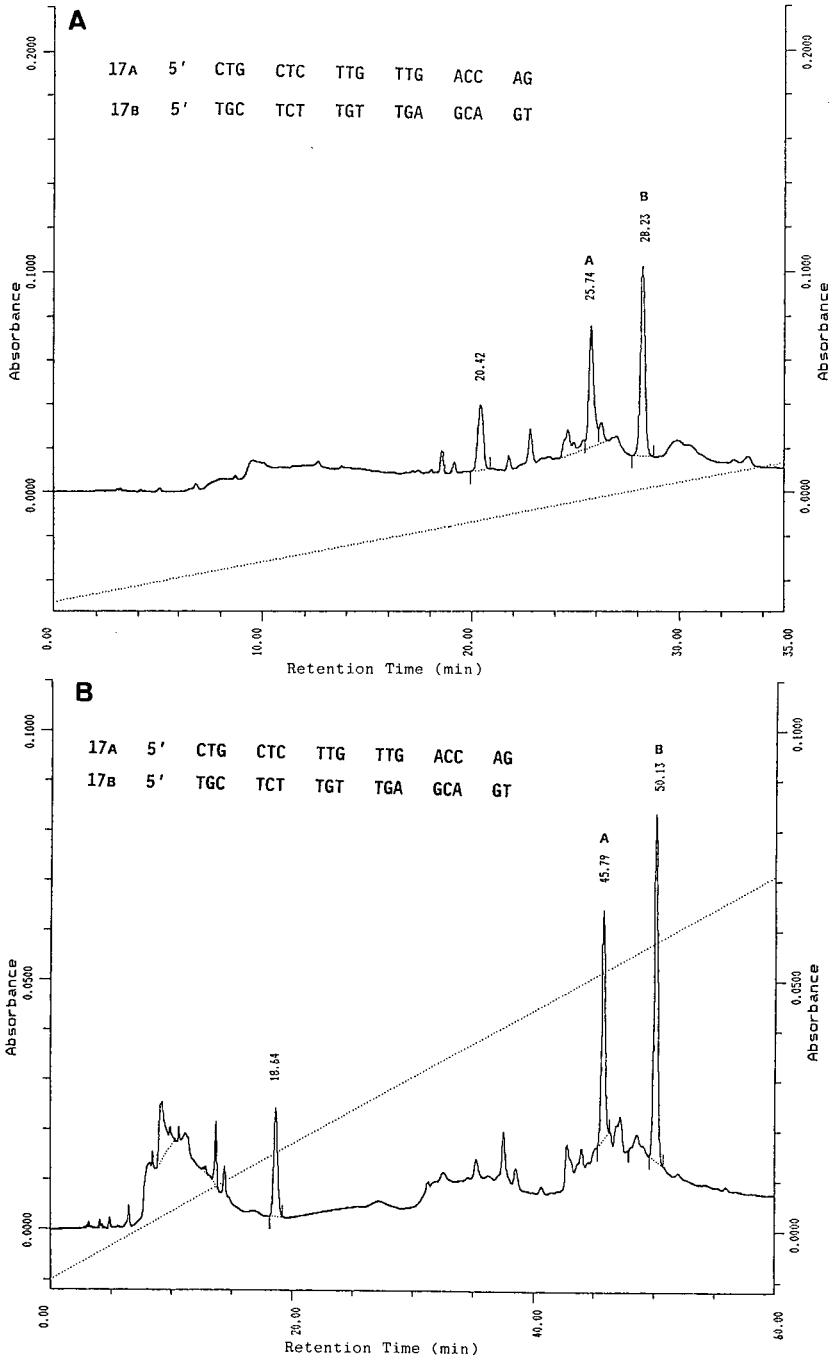

Fig. 9. Dependence of the enrichment of detritylated oligomers on gradient shape. (A) 0.5% acetonitrile per min, method 6; (B) 0.25% acetonitrile per min, method 8. Column: Beckman Ultrasphere C_{18}, 80 Å (250 × 4.6 mm I.D.).

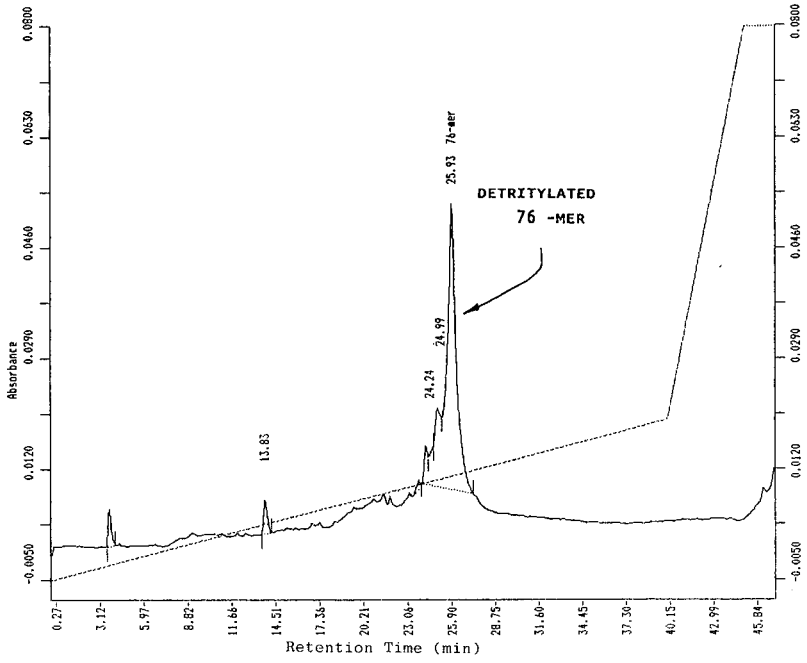

Fig. 10. Chromatography of a 76-mer with 0.5%/min actonitrile gradient. Column: Beckman Ultrapore C_8, 300 Å (250 × 4.6 mm I.D.). Method 6.

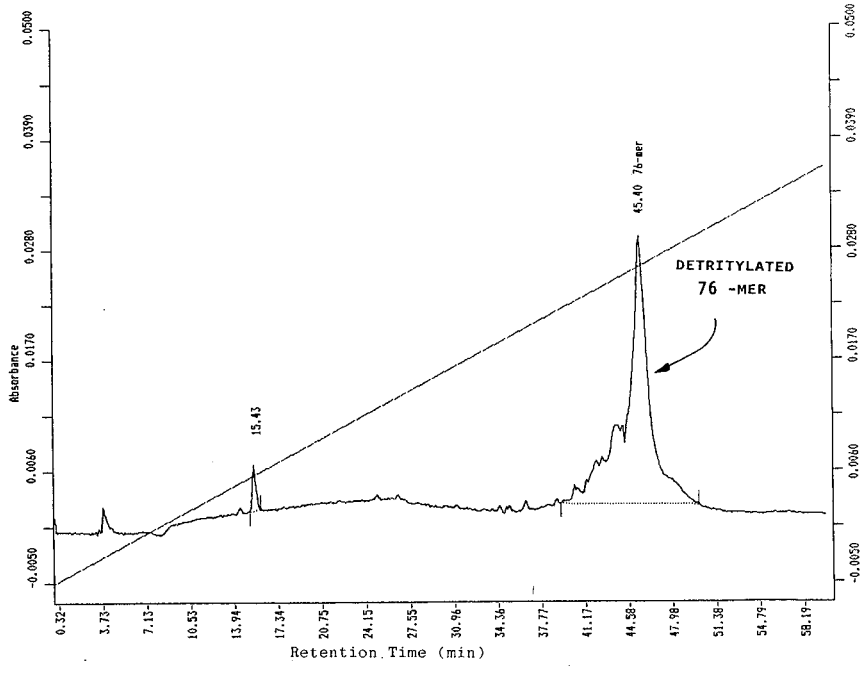

Fig. 11. Chromatography of a 76-mer with 0.25%/min acetonitrile gradient. Column: Beckman Ultrapore C_8, 300 Å (250 × 4.6 mm I.D.). Method 8.

(3) Detritylated oligomers require a modified approach. Up to 25-mer, they are best purified on C_{18}, 80 Å columns with much lower organic concentrations and shallower gradients than used for tritylated oligomers. Similar oligomers differing by base composition can also be separated under these conditions.

(4) Using methods described for shorter detritylated oligomers, 25- to 100-mer polymers can be enriched on both C_3 and C_8, 300 Å columns. Longer, shallower gradients will increase the purity of the collected oligomer. Chromatography of detritylated oligomers is best used for enrichment rather than for true purification.

ACKNOWLEDGEMENTS

We would like to thank Mr. Jack Ohms, Teresa Cash, and Karen Wert of the Beckman Spinco Division in Palo Alto, CA, U.S.A. for synthesizing many of the oligomers used in this study and for their helpful discussions. The contribution of various oligomer samples from Dr. Manfred von Wilm at the Beckman International Division in Nyon, Switzerland and Dr. Bill Lazar at the Stanford Research Institute in Palo Alto, CA, U.S.A. are gratefully acknowledged.

REFERENCES

1 C. R. Becker, J. W. Efcavitch, C. R. Heiner and N. F. Kaiser, *J. Chromatogr.*, 326 (1985) 293.
2 J. H. Hegeman and M. Linscheid, *J. Chromatogr.*, 348 (1985) 286.
3 H. Moriyama and Y. Kato, *J. Chromatogr.*, 445 (1988) 225.
4 P. A. Perrone, in P. R. Brown (Editor), *HPLC in Nucleic Acid Research: Methods and Applications*, Vol. 28, Marcel Dekker, New York, 1984, p. 161.
5 G. D. McFarland and P. N. Borer, *Nucleic Acid Res.*, 7 (1979) 1067.
6 H. Eckstein and H. Schott, *Chromatographia*, 19 (1984) 236.
7 H. J. Fritz, R. Belagaje, E. L. Brown, R. H. Fritz, R. A. Jones, R. G. Lees and H. G. Khorana, *Biochemistry*, 17 (1978) 1257.
8 M. J. Gait, in M. J. Gait (Editor), *Oligonucleotide Synthesis*, IRL Press, Washington, DC, 1984, p. 17.
9 J. B. Crowther, in P. R. Brown (Editor), *HPLC in Nucleic Acid Research: Methods and Applications*, Vol. 28, Marcel Dekker, New York, 1984, p. 210.
10 C. Y. Ip, D. Ha, P. W. Morris, M. L. Puttemans and D. L. Venton, *Anal. Biochem.*, 147 (1985) 180.
11 F. M. Ausubel, R. Brent, R. E. Kingston, D. D. Moore, J. G. Seidman, J. A. Smith and K. Struhl (Editors), *Current Protocols in Molecular Biology*, Vol. 1, 1989, pp. 8.2.5–8.2.13.
12 T. R. Floyd, J. B. Crowther and R. A. Hartwick, *LC, Mag. Liq. Chromatogr. HPLC*, 3 (1985) 508.

Journal of Chromatography, 512 (1990) 433–444
Elsevier Science Publishers B.V., Amsterdam

CHROMSYMP. 1955

Rapid separation, quantitation and purification of products of polymerase chain reaction by liquid chromatography

ELENA D. KATZ* and LAWRENCE A. HAFF
Perkin-Elmer, 761 Main Avenue, Norwalk CT 06859 (U.S.A.)
and
ROY EKSTEEN
TosoHaas, 82 Cummings Park, Woburn, MA 01801 (U.S.A.)

ABSTRACT

The polymerase chain reaction (PCR), a new, powerful method for rapid enzymatic amplification of specific DNA fragments, has gained tremendous popularity in molecular biology. This paper describes the successful application of liquid chromatography to the analysis of products of the PCR. Efficient separation of both DNA restriction fragments and amplified PCR products were achieved in 10–12 min on a new ion-exchange column, DEAE-NPR, packed with 2.5-μm non-porous particles. The PCR products were quantitated with a reproducibility within 10%. Use of liquid chromatography was demonstrated for separation and quantitation of PCR products in amounts below those required for direct analysis by ethidium bromide gel electrophoresis or a Hoechst 33258 dye-based fluorescence assay. Liquid chromatography was also demonstrated to be effective for quick optimization of PCR procedures.

INTRODUCTION

The polymerase chain reaction (PCR)[1,2] is an *in vitro* enzymatic amplification of specific DNA sequences directed by two oligonucleotide primers chosen to complement opposite strands of the target sequence of a DNA molecule. After annealing the two primers to the complementary sequences of the denatured DNA, extension of the annealed primers proceeds with a thermostable DNA polymerase. This cycle is commonly repeated 20–30 times. Since the product of primer extension essentially doubled after each cycle, exponential accumulation of target DNA is expected to take place. Parameters, such as melting, annealing, and extension temperatures, primer and enzyme concentrations, and initial concentration of DNA template must be considered in achieving amplified PCR products with high yields[2]. Generally, a 10^5-fold DNA amplification can easily be generated in 3 h. Speed, specificity and automation make the PCR technology extremely attractive for use in genetic analysis and detection of infectious diseases. Following the PCR process, amplified DNA must be detected

0021-9673/90/$03.50

and characterized. However, many post-PCR detection techniques, such as ethidium bromide gel electrophoresis, are time-consuming and complicated, often requiring considerable manual dexterity, and cannot be easily automated.

During the last ten years, liquid chromatography (LC) has become a well-established analytical technique, permitting very rapid separations and sensitive detection of complex mixtures of low-molecular-weight compounds. A better understanding of solute dispersion phenomena has increased sample throughput and detection sensitivity by optimizing column length, column radius and particle size of the packing material[3]. In recent years high-performance LC (HPLC) has also become the dominant method for the purification of biopolymers, even though these separations are not as efficient or rapid as those provided by other analytical techniques, such as high-voltage gel electrophoresis. However, new stationary phases that allow much faster and more efficient separations of biomolecules have recently become available.

Two decades ago, Horváth and co-workers[4,5] developed columns packed with fluid-impermeable (non-porous) spheres, coated with ion-exchange resin, and applied them to the fast analysis of nucleic acid fragments. The authors demonstrated improved column efficiency due to the reduced pathlength of diffusion within the solid phase. The disadvantage of these originally developed non-porous particles was their greatly reduced surface area and limited sample capacity.

Recently, Anspach *et al.*[6] returned to the concept of non-porous particles, mainly to test their hypothesis that non-porous particles would improve mass recovery of proteins. They synthesized 1-μm spherical non-porous silica particles for use in affinity chromatography. Due to their small size, the surface area of the beads is only about an order of magnitude smaller than that of 10-μm macroporous particles, thereby reducing the loss of retention associated with non-porous particles, while still taking advantage of higher mass recoveries due to the absence of pores. An increase in the retentive capacity of non-porous media has also been considered by Khalghatgi and Horváth[7] who prepared micropellicular (C_8-bonded) silica particles for the fast analysis of tryptic digests. Subsequent work by them and others has demonstrated the advantages of non-porous media for the analysis of proteins and peptides in almost all modes of liquid chromatography[8,9].

Non-porous resin columns were first described by Burke *et al.*[10]. They developed 7-μm polymethacrylate beads which were subsequently marketed for separations of monoclonal antibodies. In 1987, Kato *et al.*[11] demonstrated that use of 2.5-μm non-porous ion exchangers resulted in a 5- to 10-fold decrease in protein analysis times compared to chemically equivalent 10-μm porous ion exchangers.

The above-described trend towards the use of small, non-porous particles has also benefited the separation of DNA fragments. Following their work on oligonucleotides[12], Kato *et al.*[13] recently described highly efficient and rapid separations of typical DNA restriction fragments by anion-exchange chromatography. Using a column packed with 2.5-μm diethylaminoethyl-bonded non-porous resin particles (DEAE-NPR), the authors demonstrated the separation of practically all 22 restriction fragments in a pBR322-Hae III digest in less than 15 min, and the separation of a λDNA-Hind III digest in approximately 5 min. Their results suggest that the use of non-porous resin-based anion exchangers may complement or replace the use of traditional electrophoretic techniques.

Many PCR applications require isolation of an amplified DNA segment in solution for subsequent post-PCR analyses. Since the reaction products are typically purified by gel electrophoresis, an amplified product must be recovered from a gel that requires additional experimental steps to remove contaminants introduced from the gel[14,15]. However, LC can be successfully utilized for this purpose[16].

Modern LC appears to be ideally suited for fast separation and quantitation of amplified PCR products in solution in a single step. The goal of the present work, therefore, was to explore the feasibility of using an anion-exchange column, DEAE-NPR, for rapid separation and quantitation of PCR-amplified DNA fragments. Of primary importance were the stability and maintenance of the column when the samples were chromatographed without any sample preparation prior to injection.

EXPERIMENTAL

PCR amplifications

Reagents and PCR method. Amplifications were carried out with the Perkin-Elmer Cetus GeneAmp™ PCR reagent kit (Norwalk, CT, U.S.A.). A 500-nucleotide segment of bacteriophage λDNA (nucleotides 7131 to 7630) was used as a target, the initial concentration of which was 10 pg/100 μl or $3 \cdot 10^{-13}$ *M*. Two 25-base pair oligonucleotides, PCR01 and PCR02, were employed as primers, and Perkin-Elmer Cetus native Taq DNA Polymerase or AmpliTaq™ DNA Polymerase as the thermostable enzymes. Also, Tth DNA polymerase (Finnzymes, Finland) was used as another thermostable enzyme. The standard GeneAmp PCR Reagent Kit procedure, recommended by the manufacturer, was employed for amplifications of a 500-base pair product, unless otherwise indicated: three-temperature PCR was carried out for 1 min at 94°C, 2 min at 37°C and 3 min at 72°C for 25 cycles, using the Perkin-Elmer Cetus DNA Thermal Cycler.

To amplify a 4170-base pair segment of the λDNA, the primers used were PCR01 and a 24-mer synthesized using a custom-made DNA synthesizer. The sequence of the 24-mer was as follows: 5′-AATCTGCTCCGCCGACACGTTATG-3′ (nucleotides 7131 to 11 300). Two-temperature PCR was carried out for 1 min at 94°C and for 10 min at 70°C for 25 cycles.

Analysis. A 10-μl volume of amplified 500- and 4170-base pair products were electrophoresed on a 1% agarose gel (International Biotechnologies, New Haven, CT, U.S.A.), mixed with a 3% NuSieve™ agarose (FMC, Rockland, ME, U.S.A.), and on a 1.6% agarose gel, respectively, in Tris–borate electrophoresis buffer at 10 V/cm. DNA was detected by staining with 0.1 μg/ml ethidium bromide.

pBR322-Hae III, λDNA-Hind III and λDNA-EcoR I, Hind III digests (Sigma, St. Louis, MO, U.S.A.) were used as the molecular-weight markers. pBR322 DNA, completely digested by Hae III, yields 22 fragments: 587, 540, 504, 458, 434, 267, 234, 213, 192, 184, 124, 123, 104, 89, 80, 64, 57, 51, 21, 18, 11 and 8 base pairs. λDNA digested by Hind III yields the following fragments: 23 130, 9416, 6557, 4361, 2322, 2027, 564 and 125 base pairs. A λDNA-EcoR I digest, digested by Hind III, yields 13 fragments: 21 226, 5148, 4973, 4277, 3530, 2027, 1904, 1584, 1330, 983, 831, 564 and 125 base pairs.

Yields of PCR amplifications were quantitated by a fluorescence assay, employing Hoechst 33 258 dye (Behring Diagnostics, La Jolla, CA, U.S.A.)[17].

Liquid chromatography analysis

Apparatus. The system consisted of a Perkin-Elmer Series 410 BIO pump, a Model LC-90 BIO UV detector and a Rheodyne Model 7125Ti injection valve, equipped with a 10-μl loop. To check the purity of amplified DNA samples, a Perkin-Elmer LC-235 diode-array detector was also employed. Chromatographic data were collected, using an LCI-100 laboratory integrator.

A polymer-based TSK DEAE-NPR column (Perkin-Elmer), 35 mm × 4.6 mm I.D., packed with 2.5-μm particles, was used. A scavenger C_{18} column was placed between the pump and the injector.

Reagents and methods. HPLC-grade water (Brand-Nu Labs., Meriden, CT, U.S.A.) was employed for the mobile phase. The mobile phase was prepared as follows: reservoir A contained 0.25 *M* NaCl and 20 m*M* Tris–HCl (Boehringer Mannheim, Indianapolis, IN, U.S.A.) (pH 7.7); reservoir B contained 1 *M* NaCl and 20 m*M* Tris–HCl (pH 7.7). Two gradient programs were employed: (1) the mobile phase was linearly changed from 0 to 25% B in 0.1 min, then from 25 to 30% B in 2.9 min, and from 30 to 60% B in 20 min (method 1); (2) the mobile phase was changed from 20 to 30% B in 0.1 min (concave curve with steepness of 2); then linearly from 30 to 45% B in 2.9 min, and from 45 to 50% B in 9 min (method 2). In both gradient programs, 100% B was used for clean-up before reequilibration of the column with the initial mobile-phase composition for the next injection. The column was operated at 1 ml/min at room temperature, and the LC-90 UV detector was set at 260 nm throughout the experimental work.

RESULTS AND DISCUSSION

Chromatography of PCR product

Use of a DEAE-NPR column packed with non-porous 2.5-μm particles for the separation of oligonucleotides has been described recently by Kato and co-workers[12,13]. A separation of a pBR322-Hae III digest, obtained on a DEAE-NPR column by method 1 is shown in Fig. 1A. It is seen that adequate separation of almost all DNA fragments in this sample was achieved in 22 min. It should be noted that an optimized separation and identification of the peaks were beyond the scope of this work, since parameters such as temperature, ionic strength and mass load on column efficiency have already been investigated[12]. However, some of the DNA fragments that are of interest for the separation of PCR products amplified in this work are identified in the chromatogram, following the assignment of the peaks given by Kato *et al.*[13].

One of the important aspects of the PCR is that the reaction generates relatively simple mixtures of amplified products since selective amplification of a specific sequence generally takes place. Furthermore, if the conditions of the reaction are optimized, PCR will often amplify only the targeted sequence. It follows that, depending on the nature of amplified samples, the gradient profile can be adjusted to minimize the analysis time. Method 2 was tailored to the separation of 500-base pair products from smaller size products. A separation of a pBR322-Hae III digest, obtained by method 2, is shown in Fig. 1B. It is seen that the DNA fragments were separated in less than 15 min, while a very good resolution of the peaks was still maintained. Chromatograms of 500-base pair products from two different amplifications are shown in Fig. 2. Chromatogram A demonstrates an example of a PCR

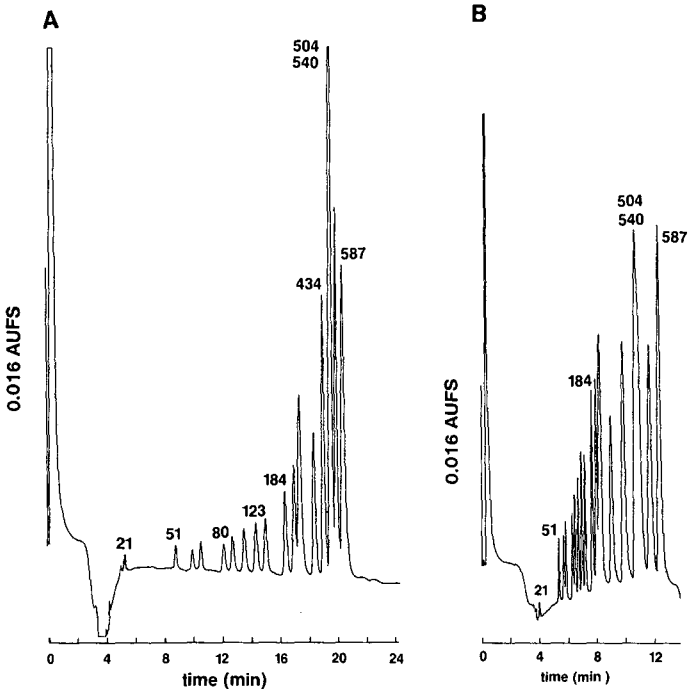

Fig. 1. (A) Separation of pBR322-Hae III digest. Sample size 20 μl of 50 μg/ml; method 1. (B) Separation of pBR322-Hae III digest. Sample size 10 μl of 50 μg/ml; method 2. Numbers at peaks indicate numbers of base pairs.

amplification where only one peak, attributed to the 500-base pair product, was generated. Chromatogram B demonstrates the separation of a PCR mixture obtained after an amplification during which a non-specific product, primer dimer, together with the 500-base pair product, was generated. In both chromatograms, identification was on the basis of the retention of appropriate DNA fragments in the pBR322-Hae III digest and confirmation by the electrophoretic separation of both the digest and 500-base pair products on 1% agarose gel.

For the PCR mixture chromatographed in Fig. 2B a very high enzyme concentration was employed, since the effect of the AmpliTaq DNA Polymerase concentration on the yield of the PCR process was studied. However, it is known that PCR amplifications in which high concentrations of primers or enzyme are employed can lead to the formation of primer dimer[18]. Also, high levels of primers and enzyme are likely to cause amplification of non-specific sequences when low concentrations of target, long annealing and extension times, and high cycle numbers are used. In these cases, simple quantitation procedures, such as a Hoechst 33 258 dye-based fluorescence assay, cannot be utilized, since they do not discriminate between responses from different DNA molecules. Therefore, a separation method must be employed to detect the amplified DNA target. Agarose gel electrophoresis can be used for the separation of amplified products, but if needed for further manipulations, these products cannot easily be recovered from the gel. In the chromatograms shown in Fig. 2A and B, the

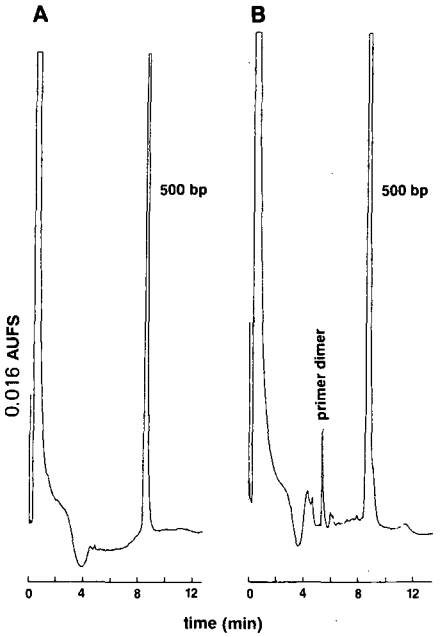

Fig. 2. Separation of 500-base pair (bp) PCR products. Sample size 10 μl; method 2, except pH 9.1 was used and the mobile phase was changed from 45 to 50% B in 7 min (step 3). PCR amplifications: three-temperature PCR. (A) Primer concentration, 0.2 μM, Taq DNA polymerase, 5 U/100 μl, 500-base pair product was amplified to 1800 ng/100 μl. (B) Primer concentration, 0.2 μM, AmpliTaq DNA polymerase, 17.5 U/100 μl, 500-base pair product was amplified to 3300 ng/100 μl.

500-base pair fragment was separated from all components of the mixture and, furthermore, the fraction corresponding to the 500-base pair product could be collected simply either manually or with a fraction collector.

For LC to be a useful technique for purification of PCR products, the chromatographic column must provide quantitative DNA recovery. The recovery of a 500-base pair product from the DEAE-NPR column was measured by injecting the undiluted 500-base pair sample in triplicate into the column. The column was then replaced with a PTFE tube, and injections of the same mixture were repeated. The total peak area of the PCR mixture eluted from the column was 57 950 (arbitrary units) *versus* 59 210; thus, 98% of the sample was recovered. It follows that not only can the amplified DNA fragments be separated and quantitated in less than 10 min, but also they can be quantitatively recovered from the column, all in a single step.

Purity of PCR product

PCR mixtures to be amplified generally contain proteins. For example, in the case of amplification of the 500-base pair target from λDNA, the samples contained Taq DNA polymerase and 0.001% gelatin. Consequently, the purity of the peak attributed to the 500-base pair product must be established. Peak confirmation and purity determination data can be conveniently obtained from diode-array UV spectra. The methods that can be used to ascertain peak purity include the determination of

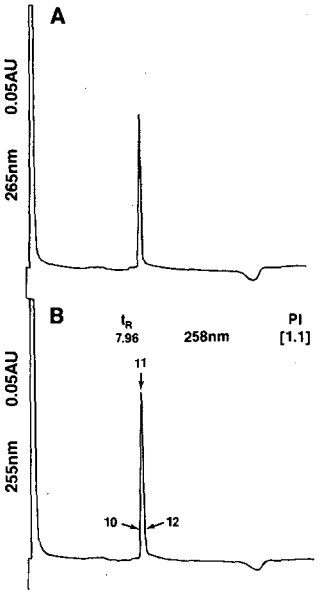

Fig. 3. Elution profiles of 500-base pair product obtained with the diode-array detector. Chromatography conditions as in Fig. 3. PCR amplification: three-temperature PCR; primer concentration, 0.1 μM; AmpliTaq DNA polymerase, 10 U/100 μl; 500-base pair product was amplified to 1900 ng/100 μl (A) 265 nm; (B) 255 nm.

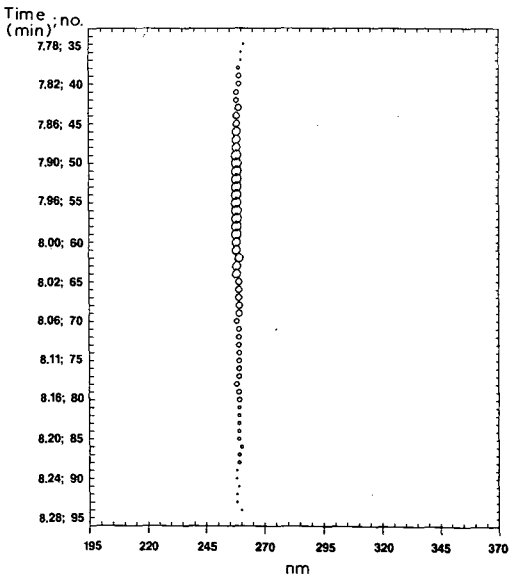

Fig. 4. Absorbance profile map of 500-base pair product. The sample is the same as in Fig. 3.

maximum absorbance wavelength, absorbance ratio plot, spectral overlay, and numerical spectral comparison (purity index). Chromatograms of a 500-base pair sample obtained with the LC-235 diode-array detector are shown in Fig. 3. It should be noted that the format of Fig. 3 is similar to the report generated by the detector software. Chromatograms A and B demonstrate the separation monitored at 265 and 255 nm, respectively. In chromatogram B, the peak eluted at 7.96 min (retention time, t_R) was scanned from 195 to 365 nm at three points, marked 10, 11 and 12. A Purity Index (*PI*) value of 1.1 was obtained by numerically comparing spectra 10 and 12 of the peak. This value, being close to 1.0, indicates that the peak was homogeneous. Also, the peak maximum at 258 nm (spectrum 11) was obtained. These results suggest that the peak represents a DNA peak not contaminated by proteins. To validate this further, an absorbance profile map can be constructed from the stored spectral data acquired during the chromatographic separation. The spectra of the same peak (t_R = 7.96 min), collected every 0.01 min, are graphically represented in Fig. 4. The collection time and spectrum number are given on the y axis, and the wavelength at which each absorbance maximum occurs is given on the x axis. The diameter of each circle corresponds to the absorbance intensity of each maximum. It is clearly seen that a straight vertical line at 258 nm was generated, and that no circles at 280 nm were observed, indicating the absence of protein contamination.

Quantitation of PCR products

It is often necessary to quantitate amplified PCR products. Using LC, a calibration curve can easily be produced for quantitation of unknown samples. Since no appropriate standards are commercially available, an LC calibration curve was generated with a 500-base pair DNA sample, amplified by the described PCR method. The specificity of the amplification was checked using the DEAE-NPR column, and

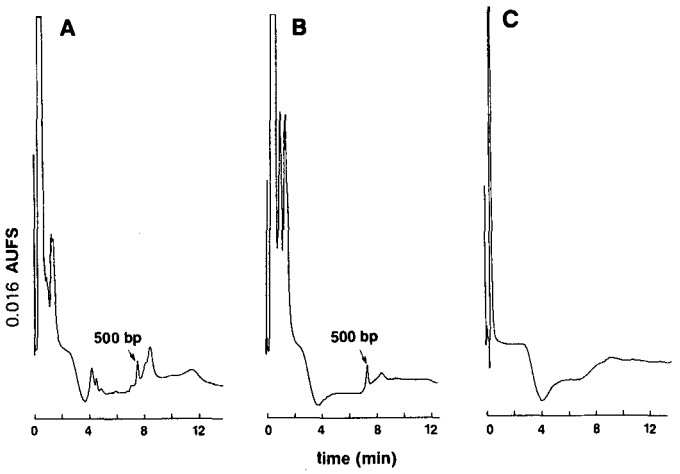

Fig. 5. Chromatograms of 500-base pair (bp) products, amplified with a thermostable enzyme. Chromatography and PCR conditions as used previously. (A) 500-Base pair product amplified to 46 ng/100 μl; primer concentration, 0.2 μM; Tth DNA polymerase, 2.5 U/100 μl. (B) 500-Base pair product amplified to 40 ng/100 μl; primer concentration, 0.2 μM; Tth DNA polymerase, 1.75 U/100 μl. (C) Blank chromatogram.

since the reaction yielded only one product, the Hoechst 33 258 dye-based fluorescence assay[17] was employed to determine the yield of the 500-base pair product. The DNA sample had been amplified to 2400 ng/100 μl, a typical value obtained with the standard amplification procedure and PCR conditions. The sample was then successively diluted to cover a range of concentrations from 0.24 to 24 ng/μl. A 10-μl volume of each diluted sample was injected into the column. The relative standard deviation (R.S.D.) in peak height (peak area) measurements was less than 10%. Reproducibility of the retention time was very good, the R.S.D. for 24 measurements being within 4%. The linear calibration curve with the correlation coefficient of 0.998 was obtained, which can be used for quantitation of other amplified samples.

The calibration curve was employed to quantitate PCR yields when 500-base pair products were amplified with the same standard procedure, but instead of Taq DNA polymerase, another commercially available thermostable enzyme was employed. The chromatograms are shown in Fig. 5. Distinct 500-base pair peaks were obtained in chromatograms A and B. Chromatogram C represents a blank run for comparison. Using the calibration curve, it was estimated that the yields of the 500-base pair fragments in samples A and B were 46 and 40 ng/100 μl, respectively. These values are too low for detection by the fluorescence assay and gel electrophoresis. To confirm this, both methods were applied. The fluorescence response of these products was commensurate with that of blank samples, and no visible bands on ethidium bromide-stained agarose gel could be observed.

Reproducible column performance is one of the requirements for carrying out quantitative analysis by chromatographic techniques. The small particles with which highly efficient LC columns are packed induce high inlet pressures. Therefore, some care must be taken to maintain their performance. Simple steps, such as using high-quality grade reagents, filtering mobile phases, and flushing columns with appropriate solvents, are generally recommended. In our work, HPLC-grade water and a scavenger C_{18} column were employed. The analytical column was regularly flushed with 2–3 ml of 0.2 *M* NaOH to prevent possible contamination by impurities in the mobile phase and the injected samples. These precautions allowed the retention times to be reproducible and the column inlet pressure to be kept at *ca.* 2000 p.s.i. with a flow-rate of 1 ml/min.

Although the peak area reproducibility was quite acceptable, the background level was found to increase with time, indicating accumulation of poorly eluted compounds. This could be due to the presence of large proteins in matrices of the PCR samples. It should be noted that this phenomenon did not interfere with the measurements carried out in the present work, but for very high column stability, some precautions, such as use of an appropriate guard column or organic solvent mixtures (*e.g.*, 20% aq. acetonitrile) for cleaning the column should be considered.

Optimization of PCR amplifications

One of the attractive features of the use of LC in post-PCR analysis is rapid evaluation of reaction products during tedious optimization procedures. PCR is now employed in a large number of applications in molecular biology. General guidelines for a typical reaction that can serve as a starting procedure have recently been outlined by Saiki[19] and Williams[20]. But each specific application will require that a number of different parameters affecting the PCR process be examined and controlled. Gel

electrophoresis is widely used to validate the specificity of amplifications. Fig. 6 exemplifies the electrophoresis of a targeted 4170-base pair product, amplified as described in the Experimental section, and a λDNA-Hind III digest, obtained on a 1.6% agarose gel. Electropherograms of a 500-base pair fragment and a pBR322-Hae III sample, used as control samples, are given for comparison. An additional band is seen in lane 5, corresponding to an approximately 1100-base pair product. This product was identified on the basis of the electrophoretic separation of the λDNA-EcoR I, Hind III fragments (data not shown). By changing the conditions of

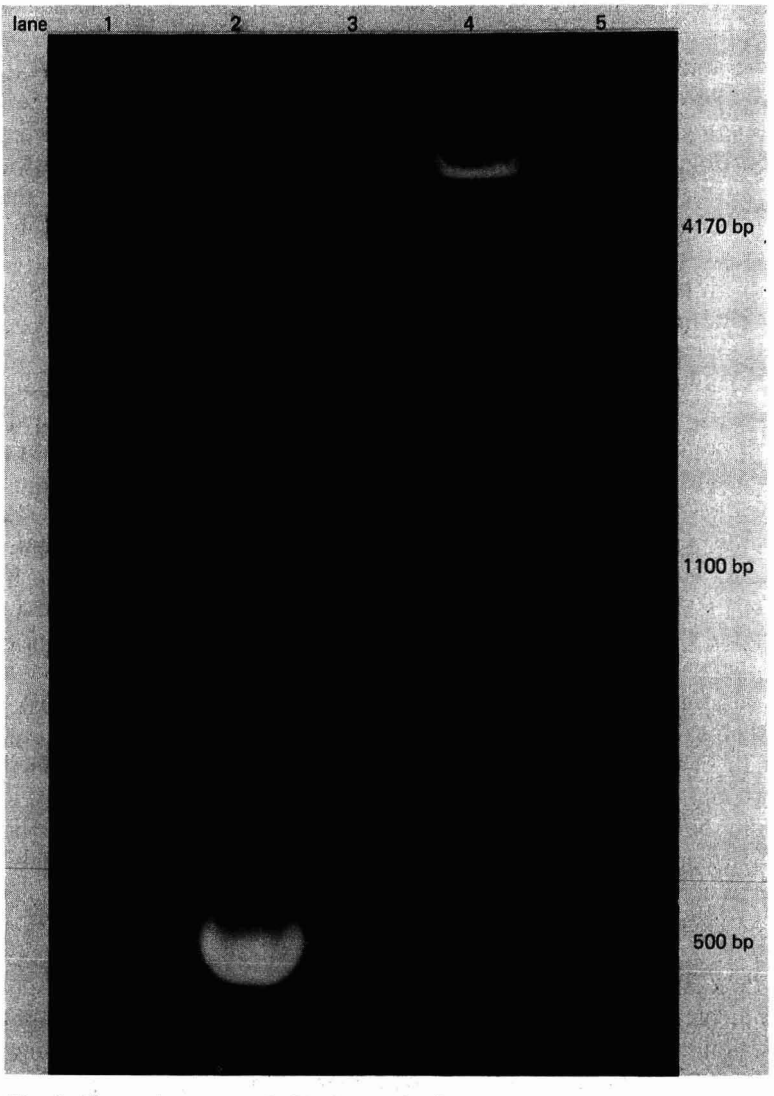

Fig. 6. Electropherogram of 4170-base pair (bp) product. PCR conditions: two-temperature; primer concentration, 0.2 μM; AmpliTaq DNA polymerase, 2.5 U/10 μl. Lanes: 1 = pBR322-Hae III (5 μl of 50 μg/ml); 2 = 500-base pair product (10 μl of 1900 ng/100 μl); 3 = λDNA-Hind III (5 μl of 50 μg/ml); 4 = 4170-base pair product (10 μl).

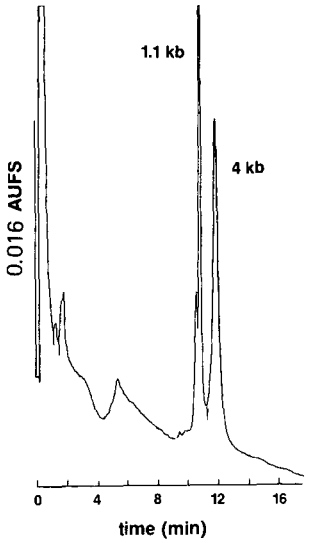

Fig. 7. A chromatogram of 4170-base pair product. Sample size 10 μl; chromatographic conditions as in Fig. 2, except pH 9.1 was used and the mobile phase was changed from 45 to 100% B in 20 min (step 3). kb = Kilobase pairs.

the PCR, the yield of this non-specific product was either enhanced or suppressed. Using 95°C for the denaturation step and 67°C for both the annealing and extension steps, only the 4170-base pair fragment was generated.

Electrophoresis of a single PCR product generally takes 1 or 2 h. Obviously, the capability of gel electrophoresis to process 16–24 samples simultaneously is not attractive during the optimization process when one parameter at a time must be changed. LC can be more efficient technique for this purpose. Fig. 7 shows a chromatographic separation of the same 4170-base pair product on the DEAE-NPR column by a modified method 2. It is clearly seen that the elution of the sample was achieved in less than 15 min, with both the 1100- and 4170-base pair fragments well separated. It follows that the next step of the optimization procedure can be initiated in a matter of minutes, not hours. Furthermore, the reaction can be monitored as it proceeds by injecting aliquots of a PCR sample during its amplification.

CONCLUSIONS

Using a DEAE-NPR anion-exchange column, the separation and quantitation of mixtures of amplified DNA fragments up to at least 4000 base pairs can be achieved in less than 15 min. At the same time, pure DNA product can be isolated from the column with quantitative recovery. Although PCR samples were injected without any sample preparation prior to injection, both the retention time and peak height (area) were reproducible, provided the column was regularly cleaned with 0.2 *M* NaOH. It follows that the LC method described can be employed successfully for rapidly separating, quantitating and purifying products of the PCR in a single run. Furthermore, the method allows much faster optimization of PCR amplifications by

replacing the gel electrophoresis method currently employed to monitor the conditions of the reaction.

REFERENCES

1 R. K. Saiki, S. Scharf, F. Faloona, K. B. Mullis, G. T. Horn, H. A. Erlich and N. Arnheim, *Science (Washington, D.C.)*, 230 (1985) 1350.
2 R. K. Saiki, D. H. Gelfand, S. Stoffel, S. J. Sharf, R. Higuchi, G. T. Horn, K. B. Mullis and H. A. Erlich, *Science (Washington, D.C.)*, 239 (1988) 487.
3 E. D. Katz, K. L. Organ and R. P. W. Scott, *J. Chromatogr.*, 289 (1984) 65.
4 Cs. Horváth, B. A. Preiss and S. R. Lipsky, *Anal. Chem.*, 39 (1967) 1422.
5 Cs. Horváth and S. R. Lipsky, *J. Chromatogr. Sci.*, 7 (1969) 109.
6 B. Anspach, K. K. Unger, H. Giesche and M. T. W. Hearn, presented at the *4th International Symposium on HPLC of Proteins, Peptides and Polynucleotides, Baltimore, MD, December 1984*, paper 103.
7 K. Kalghatgi and Cs. Horváth, *J. Chromatogr.*, 398 (1987) 355.
8 R. Janzen, K. K. Unger, H. Giesche, J. N. Kinkel and M. T. W. Hearn, *J. Chromatogr.*, 397 (1987) 91.
9 M. W. Dong, J. R. Gant and B. R. Larsen, *BioChromatogr.*, 4 (1989) 19.
10 D. J. Burke, J. K. Duncan, L. C. Dunn, L. Cummuings, C. J. Siebert and G. S. Ott, *J. Chromatogr.*, 353 (1986) 425.
11 Y. Kato, T. Kitamura and T. Hashimoto, *J. Chromatogr.*, 398 (1987) 327.
12 Y. Kato, T. Kitamura, A. Mitsui, Y. Yamasaki, T. Hashimoto, T. Murotsu, S. Fukushige and K. Matsubara, *J. Chromatogr.*, 447 (1988) 212.
13 Y. Kato, Y. Yamasaki, A. Onaka, T. Kitamura, T. Hashimoto, T. Murotsu, S. Fukushige and K. Matsubara, *J. Chromatogr.*, 478 (1989) 264.
14 R. C. A. Yang, J. Lis and R. Wu, *Methods Enzymol.*, 68 (1979) 176.
15 A. V. Vorndam and J. Kerschner, *Anal. Biochem.*, 152 (1986) 221.
16 Y. Kato, M. Sasaki, T. Hashimoto, T. Murotsu, S. Fukushige and K. Matsubara, *J. Biochem.*, 95 (1984) 83.
17 L. A. Haff and L. M. Mezei, *Amplifications*, 1 (1989) 8.
18 R. Watson, *Amplifications*, 2 (1989) 5.
19 R. K. Saiki, in H. A. Erlich (Editor), *PCR Technology —Principles and Applications for DNA Amplification*, Stockton Press, New York, 1989, Ch. 1.
20 J. F. Williams, *BioTechniques*, 7 (1989) 762.

Author Index

Selective Sample Handling and Detection in High-Performance Liquid Chromatography

Journal of Chromatography Library, 39

part A

edited by **R.W. Frei†**, *Free University, Amsterdam, The Netherlands, and* **K. Zech**, *Byk Gulden Pharmaceuticals, Konstanz, FRG*

Part A of this two-volume project attempts to treat the sample handling and detection processes in a liquid chromatographic system in an integrated fashion. The need for more selective and sensitive chromatographic methods to help solve the numerous trace analysis problems in complex samples is undisputed. However, few workers realize the strong interdependence of the various steps - sample handling, separation and detection - which must be considered if one wants to arrive at an optimal solution. By introducing a strong element of selectivity and trace enrich- ment in the sample preparation step, fewer demands are placed on the quality of the chromatography and often a simple UV detector can be used. By using a selective detection mode, i.e. a reaction detector, the sample handling step can frequently be simplified and more easily automated. The impact of such a "total system" approach on handling series of highly complex samples such as environmental specimens or biological fluids can be easily imagined.

Contents: 1. On-line sample handling and trace enrichment in liquid chromatography. The determination of organic compounds in water samples. 2. Determination of drugs and their metabolites in biological samples by fully automated HPLC with on-line solid-liquid extraction and pre-column switching. 3. Immobilization of compounds for selective interaction with analytes in liquid chromatography. 4. Design and choice of suitable labelling reagents for liquid chromatography. 5. Photodiode array detection and recognition in high-performance liquid chromatography. 6. Electrochemical techniques for detection in HPLC. 7. Solid-phase reactors in high-performance liquid chromatography. 8. Commercial aspects of post-column reaction detectors for liquid chromatography. Subject Index.

1988 xii + 458 pages
US$ 123.00 / Dfl. 240.00
ISBN 0-444-42881-X

part B

edited by **K. Zech**, *Byk Gulden Pharmaceuticals, Konstanz, FRG, and* **R.W. Frei†**, *Free University, Amsterdam, The Netherlands*

Part B completes the treatment of the handling, separation and detection of complex samples as an integrated, interconnected process. On the basis of this philosophy the editors have selected those contributions which demonstrate that optimal sample preparation leads to a simplification of detection or reduced demands on the separation process. Throughout the book emphasis is on chemical principles with minimum discussion of the equipment required - an approach which reflects the editors' view that the limiting factor in the analysis of complex samples is an incomplete knowledge of the underlying chemistry rather than the hardware available. This lack of knowledge becomes more evident as the demands for lower detection limits grow, as solving complex matrix problems requires a greater understanding of the chemical interaction between the substance to be analysed and the stationary phase.

Contents: I. Preconcentration and Chromatography on Chemically Modified Silicas with Complexation Properties. II. Sample Handling in Ion Chromatography. III. Whole Blood Sample Clean-Up for Chromatographic Analysis. IV. Radio-Column Liquid Chromatography. V. Modern Post-Column Reaction Detection in High-Performance Liquid Chromatography. VI. New Luminescence Detection Techniques. VII. Continuous Separation Techniques in Flow-Injection Analysis. Subject Index.

1989 xii + 394 pages
US$ 136.00 / Dfl. 265.00
ISBN 0-444-88327-4

Written by experienced practitioners, these volumes will be of interest to investigators in many areas of application, including environmental scientists and those active in the clinical, pharmaceutical and bioanalytical fields.

For more information, please write to:

Elsevier Science Publishers

P.O. Box 211, 1000 AE Amsterdam, The Netherlands
P.O. Box 882, Madison Square Station, New York, NY 10159, USA

PUBLICATION SCHEDULE FOR 1990

Journal of Chromatography and Journal of Chromatography, Biomedical Applications

MONTH	J	F	M	A	M	J	J	A	S
Journal of Chromatography	498/1 498/2 499	500 502/1	502/2 503/1 503/2 504/1	504/2 505/1	505/2 506 507 508/1	508/2 509/1 509/2 510	511 512 513	514/1 514/2 515	The publication schedule for further issues will be published later
Cumulative Indexes, Vols. 451–500		501							
Bibliography Section		524/1		524/2		524/3		524/4	
Biomedical Applications	525/1	525/2	526/1	526/2 527/1	527/2	528/1 528/2	529/1	529/2 530/1	530/2

INFORMATION FOR AUTHORS

(Detailed *Instructions to Authors* were published in Vol. 478, pp. 453–456. A free reprint can be obtained by application to the publisher, Elsevier Science Publishers B.V., P.O. Box 330, 1000 AH Amsterdam, The Netherlands.)

Types of Contributions. The following types of papers are published in the *Journal of Chromatography* and the section on *Biomedical Applications:* Regular research papers (Full-length papers), Notes, Review articles and Letters to the Editor. Notes are usually descriptions of short investigations and reflect the same quality of research as Full-length papers, but should preferably not exceed six printed pages. Letters to the Editor can comment on (parts of) previously published articles, or they can report minor technical improvements of previously published procedures; they should preferably not exceed two printed pages. For review articles, see inside front cover under Submission of Papers.

Submission. Every paper must be accompanied by a letter from the senior author, stating that he is submitting the paper for publication in the *Journal of Chromatography*. Please do not send a letter signed by the director of the institute or the professor unless he is one of the authors.

Manuscripts. Manuscripts should be typed in double spacing on consecutively numbered pages of uniform size. The manuscript should be preceded by a sheet of manuscript paper carrying the title of the paper and the name and full postal address of the person to whom the proofs are to be sent. Authors of papers in French or German are requested to supply an English translation of the title of the paper. As a rule, papers should be divided into sections, headed by a caption (*e.g.*, Summary, Introduction, Experimental, Results, Discussion, etc.). All illustrations, photographs, tables, etc., should be on separate sheets.

Introduction. Every paper must have a concise introduction mentioning what has been done before on the topic described, and stating clearly what is new in the paper now submitted.

Summary. Full-length papers and Review articles should have a summary of 50–100 words which clearly and briefly indicates what is new, different and significant. In the case of French or German articles an additional summary in English, headed by an English translation of the title, should also be provided. (Notes and Letters to the Editor are published without a summary.)

Illustrations. The figures should be submitted in a form suitable for reproduction, drawn in Indian ink on drawing or tracing paper. Each illustration should have a legend, all the *legends* being typed (with double spacing) together on a *separate sheet*. If structures are given in the text, the original drawings should be supplied. Coloured illustrations are reproduced at the author's expense, the cost being determined by the number of pages and by the number of colours needed. The written permission of the author and publisher must be obtained for the use of any figure already published. Its source must be indicated in the legend.

References. References should be numbered in the order in which they are cited in the text, and listed in numerical sequence on a separate sheet at the end of the article. Please check a recent issue for the layout of the reference list. Abbreviations for the titles of journals should follow the system used by *Chemical Abstracts*. Articles not yet published should be given as "in press" (journal should be specified), "submitted for publication" (journal should be specified), "in preparation" or "personal communication".

Dispatch. Before sending the manuscript to the Editor please check that the envelope contains three copies of the paper complete with references, legends and figures. One of the sets of figures must be the originals suitable for direct reproduction. Please also ensure that permission to publish has been obtained from your institute.

Proofs. One set of proofs will be sent to the author to be carefully checked for printer's errors. Corrections must be restricted to instances in which the proof is at variance with the manuscript. "Extra corrections" will be inserted at the author's expense.

Reprints. Fifty reprints of Full-length papers, Notes and Letters to the Editor will be supplied free of charge. Additional reprints can be ordered by the authors. An order form containing price quotations will be sent to the authors together with the proofs of their article.

Advertisements. Advertisement rates are available from the publisher on request. The Editors of the journal accept no responsibility for the contents of the advertisements.

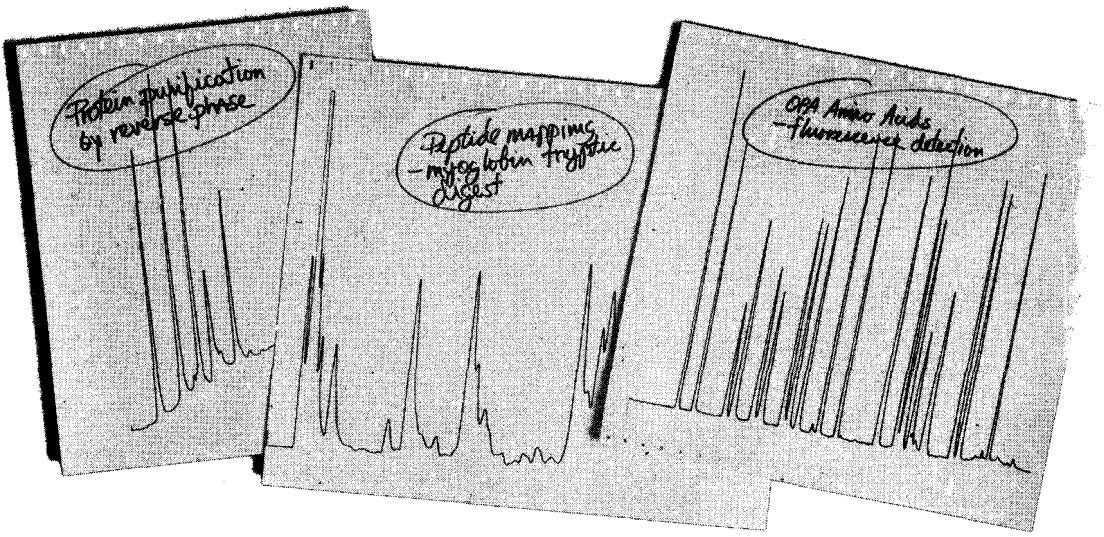

Here are three ways to record success in your biochromatography

Proteins

Isco ProTeam™ LC with proven high-performance macroporous columns offers outstanding speed and flexibility for your protein separations. Choose from a comprehensive selection of columns for SEC, ion exchange, reverse phase, and hydrophobic interaction modes. ProTeam SynChropak columns are available for any separation scale and any molecular size, with a broad range of phases for optimum selectivity. And for added assurance of active protein recovery, Isco ProTeam LC systems are available with fully biocompatible inert construction.

Peptides

For high-resolution peptide mapping by reverse-phase LC, you need precise gradient elution and the right bonded phase for optimum selectivity. ProTeam LC gives you both, with a choice of binary and ternary solvent delivery and packings from C1 to C18. And for sample-limited analyses such as synthetic peptides, you can get the same packings in Isco 2 mm and 1 mm columns.

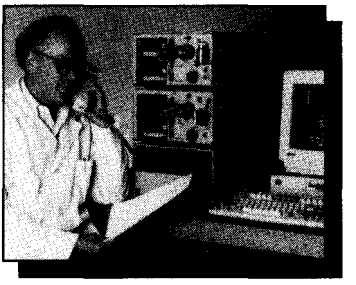

Amino acids

The same ProTeam LC system can also handle your amino acid analyses—in hydrolysates, physiological fluids, media, or for sequencing. Modular system design makes it easy to incorporate automated pre-column derivatization. Choose absorbance detection for picomole sensitivity with PITC, dabsyl, or OPA derivatives; or fluorescence for trace analysis with OPA and dansyl derivatives.

Ask today for details.

Isco, Inc., P.O. Box 534
Lincoln NE 68505, U.S.A.
Tel: **(800)228-42**
Isco Europe AG, Brüschst
CH8708 Männedorf, Switzerl
Fax **(41-1)920 62**

Distributors • **Australia:** Australian Chromatography Co. • **Austria:** INULA • **Belgium:** SA HVL NV • **Canada:** Canberra Packard Canada, Ltd. • **Denmark:** Mikrolab Aar
Finland: ETEK OY • **France:** Ets. Roucaire, S.A. • **Germany:** Colora Messtechnik GmbH • **Hungary:** Lasis Handelsges. mbH • **Italy:** Analytical Control Italia S.p.A. •
Japan: JSI Co. Ltd. • **Korea:** Sang Chung, Ltd. • **The Netherlands:** Beun-de Ronde B.V. • **Norway:** Dipl. Ing. Houm A.S. • **Spain:** CHEMICONTROL, S.L. •
Sweden: SAVEN AB • **Switzerland:** IG Instrumenten-Gesellschaft AG • **U.K.:** Life Science Laboratories, Ltd. •